ISSN 0021-9673

VOL. 668 NO. 2 MAY 13, 1994

THIS ISSUE COMPLETES VOL. 668

9th Danube Symposium on Chromatography Budapest, August 23–27, 1993

JOURNAL OF CHROMATOGRAPHY A

INCLUDING ELECTROPHORESIS AND OTHER SEPARATION METHODS

SYMPOSIUM VOLUMES

ELSEVIER

JOURNAL OF CHROMATOGRAPHY A

INCLUDING ELECTROPHORESIS AND OTHER SEPARATION METHODS

Scope. The *Journal of Chromatography A* publishes papers on all aspects of **chromatography, electrophoresis** and related methods. Contributions consist mainly of research papers dealing with chromatographic theory, instrumental developments and their applications. In the *Symposium volumes*, which are under separate editorship, proceedings of symposia on chromatography, electrophoresis and related methods are published. *Journal of Chromatography B: Biomedical Applications* —This journal, which is under separate editorship, deals with the following aspects: developments in and applications of chromatographic and electrophoretic techniques related to clinical diagnosis or alterations during medical treatment; screening and profiling of body fluids or tissues related to the analysis of active substances and to metabolic disorders; drug level monitoring and pharmacokinetic studies; clinical toxicology; forensic medicine; veterinary medicine; occupational medicine; results from basic medical research with direct consequences in clinical practice.

Submission of Papers. The preferred medium of submission is on disk with accompanying manuscript (see *Electronic manuscripts* in the Instructions to Authors, which can be obtained from the publisher, Elsevier Science B.V., P.O. Box 330, 1000 AH Amsterdam, Netherlands). Manuscripts (in English; *four* copies are required) should be submitted to: Editorial Office of *Journal of Chromatography A*, P.O. Box 681, 1000 AR Amsterdam, Netherlands, Telefax (+31-20) 5862 304, or to: The Editor of *Journal of Chromatography B: Biomedical Applications*, P.O. Box 681, 1000 AR Amsterdam, Netherlands. Review articles are invited or proposed in writing to the Editors who welcome suggestions for subjects. An outline of the proposed review should first be forwarded to the Editors for preliminary discussion prior to preparation. Submission of an article is understood to imply that the article is original and unpublished and is not being considered for publication elsewhere. For copyright regulations, see below.

Publication information. *Journal of Chromatography A* (ISSN 0021-9673): for 1994 Vols. 652–682 are scheduled for publication. *Journal of Chromatography B: Biomedical Applications* (ISSN 0378-4347): for 1994 Vols. 652–662 are scheduled for publication. Subscription prices for *Journal of Chromatography A*, *Journal of Chromatography B: Biomedical Applications* or a combined subscription are available upon request from the publisher. Subscriptions are accepted on a prepaid basis only and are entered on a calendar year basis. Issues are sent by surface mail except to the following countries where air delivery via SAL is ensured: Argentina, Australia, Brazil, Canada, China, Hong Kong, India, Israel, Japan, Malaysia, Mexico, New Zealand, Pakistan, Singapore, South Africa, South Korea, Taiwan, Thailand, USA. For all other countries airmail rates are available upon request. Claims for missing issues must be made within six months of our publication (mailing) date. Please address all your requests regarding orders and subscription queries to: Elsevier Science B.V., Journal Department, P.O. Box 211, 1000 AE Amsterdam, Netherlands. Tel.: (+31-20) 5803 642; Fax: (+31-20) 5803 598. Customers in the USA and Canada wishing information on this and other Elsevier journals, please contact Journal Information Center, Elsevier Science Inc., 655 Avenue of the Americas, New York, NY 10010, USA, Tel. (+1-212) 633 3750, Telefax (+1-212) 633 3764.

Abstracts/Contents Lists published in Analytical Abstracts, Biochemical Abstracts, Biological Abstracts, Chemical Abstracts, Chemical Titles, Chromatography Abstracts, Current Awareness in Biological Sciences (CABS), Current Contents/Life Sciences, Current Contents/Physical, Chemical & Earth Sciences, Deep-Sea Research/Part B: Oceanographic Literature Review, Excerpta Medica, Index Medicus, Mass Spectrometry Bulletin, PASCAL-CNRS, Referativnyi Zhurnal, Research Alert and Science Citation Index.

US Mailing Notice. *Journal of Chromatography A* (ISSN 0021-9673) is published weekly (total 52 issues) by Elsevier Science B.V., (Sara Burgerhartstraat 25, P.O. Box 211, 1000 AE Amsterdam, Netherlands). Annual subscription price in the USA US$ 4994.00 (US$ price valid in North, Central and South America only) including air speed delivery. Second class postage paid at Jamaica, NY 11431. **USA POSTMASTERS**: Send address changes to *Journal of Chromatography A*, Publications Expediting, Inc., 200 Meacham Avenue, Elmont, NY 11003. Airfreight and mailing in the USA by Publications Expediting.

See inside back cover for Publication Schedule, Information for Authors and information on Advertisements.

0021-9673/94/$07.00

Printed in the Netherlands

For Contents see p. 251.

SYMPOSIUM ISSUE

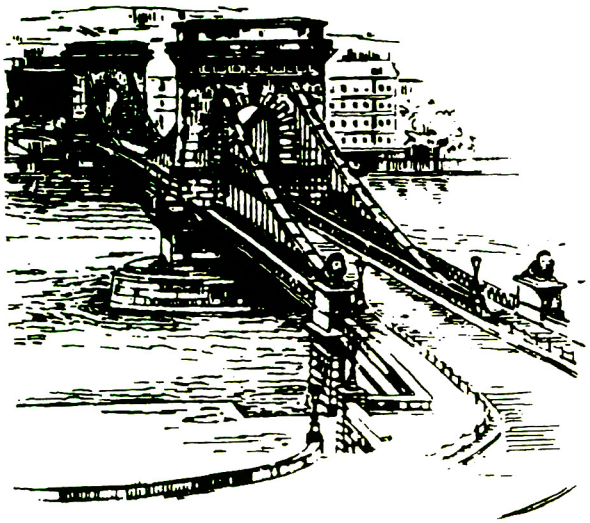

9TH DANUBE SYMPOSIUM ON CHROMATOGRAPHY

Budapest (Hungary), August 23–27, 1993

Guest Editor

L. SZEPESY

(Budapest, Hungary)

VOL. 668, NO. 2 JOURNAL OF CHROMATOGRAPHY A MAY 13, 1994

CONTENTS

9TH DANUBE SYMPOSIUM ON CHROMATOGRAPHY, BUDAPEST, AUGUST 23–27, 1993

ELSEVIER

Journal of Chromatography A, 668 (1994) 253–254

JOURNAL OF CHROMATOGRAPHY A

Foreword

The *9th Danube Symposium on Chromatography* organized by the Chromatography Group of the Hungarian Chemical Society in cooperation with the Chromatographic Committee of the Hungarian Academy of Sciences was held in Budapest from August 23rd to 27th, 1993. During that week, over 280 participants from 26 countries, 120 foreigners and 160 Hungarians, met in the Conference and Educational Centre in Villányi Street.

The series of Danube Symposia was started in 1977 in Szeged, Hungary, and since that time it has been organized every second year in one of the so-called "socialist" countries (1979, Karlovy Vary, Czechoslovakia; 1981, Siófok, Hungary; 1983, Bratislava, Czechoslovakia; 1985, Yalta, USSR; 1987, Varna, Bulgaria; 1989, Leipzig, GDR; 1991, Warsaw, Poland). The participation of East European scientists at the alternating West European symposia was always limited and only a few workers were able to be privileged to attend. The main idea of the Danube Symposium was to give East European workers the opportunity to make personal contacts with internationally recognized experts known only by name through the literature, and to introduce them to the unique atmosphere of an international forum. The name "Danube" was essentially a symbolic one. As this mighty artery traverses and connects many European countries irrespective of their social and economic systems, so also should the Danube Symposia bring together scientists without the barriers of frontiers, language and beliefs in order to promote and encourage the free exchange of ideas and information to achieve the development and application of separation science.

During the five days of the *9th Danube Symposium*, 43 oral lectures and 144 posters were presented. The keynote oral lectures were presented by internationally recognized scientists giving an overview of recent developments and new achievements in chromatography and related techniques. The poster presentations covered many of the most important applications of chromatography. The most abundant subjects were separations of biomolecules, pharmaceuticals and food products, environmental analysis, development of packings and columns, development and application of classical and forced-flow planar techniques and coupled techniques.

Twenty-one foreign and Hungarian companies participated in the instrument exhibition, showing a fine display of chromatographic equipment and materials. In addition, several companies presented seminars to introduce their latest developments.

The social events included a Welcome Reception on the terrace of the Conference Centre, a boat excursion on the Danube to Szentendre with sightseeing and a Cocktail Party.

I would like to express my gratitude to my colleagues on the organizing committee and the secretariat of the Hungarian Chemical Society for their cooperation and assistance in the successful arrangement of the Symposium.

Finally, some farewell words on the Danube Symposia on Chromatography are appropriate. Following the invitation of the organizers of the Western biennial International Symposium on

SSDI 0021-9673(93)E1060-D

Chromatography, the International Scientific Committee of the Danube Symposia has decided not to continue the series in its present form in order to harmonize the international symposia in Europe in the area of separation science. My colleagues and I have taken this decision with considerable regret. However, we look forward to the opportunity to contribute to the development of high-quality international meetings on chromatography and related topics in Europe.

Budapest (Hungary) László Szepesy

ELSEVIER

Journal of Chromatography A, 668 (1994) 255–284

JOURNAL OF CHROMATOGRAPHY A

Electrostatic retention model of reversed-phase ion-pair chromatography

Ákos Bartha[a], Jan Ståhlberg*[,b]

[a]Astra Production Liquid Products AB, Analytical Control, S-151 85 Södertälje, Sweden
[b]Astra Production Tablets AB, Analytical Control, S-151 85 Södertälje, Sweden

Abstract

The theoretical foundation of the electrostatic theory of ion-pair chromatography derives from colloid and surface chemistry. In the first part of this paper, the basic concepts of the theory are discussed with emphasis on the physical principles. The theory can predict retention changes of a charged solute when varying experimental parameters in ion-pair chromatographic systems. However, because of the interplay between the different parameters, such a prediction is only feasible when using iterative numerical procedures. Therefore, a simplified theory is developed in the second part where a relationship is derived which separates the contributions of various parameters, such as type and concentration of ion-pairing reagent, ionic strength, concentration of organic modifier and eluent pH. At high surface concentrations of the ion-pairing reagent, competition between the solute and ion-pairing reagent for the limited area of the stationary phase available may occur. It is shown in the third part of the paper that this results in a maximum in the relationship between capacity factor and concentration of ion-pairing reagent in the eluent. In the final section, an extended version of the electrostatic theory is developed. It accounts for the effect of accumulation of solute ions in the electrical double layer on the capacity factor. The extended form of the electrostatic theory provides the most complete treatment of the retention of charged solutes. However, this is achieved at the cost of developing a complex mathematical formulation.

1. Introduction

Reversed-phase ion-pair chromatography (RP-IPC) is a popular separation mode of HPLC [1]. It is primarily used for the separation of mixtures of ionic and/or ionizable compounds, often in the presence of neutral solutes. The technique is based on the addition of amphiphilic (surface-active) ions to the mobile phase in order to enhance the retention of ionic sample components. Other important application areas of IPC include the separation of inorganic ions, detection enhancement with UV-active ionic additives and the separation of enantiomers.

Although a number of alternative names exist (*e.g.*, ion-interaction chromatography, dynamic ion-exchange chromatography), ion-pair chromatography is the most commonly used name for the technique, and it derives from the historical application of ion-pair extraction principles to liquid chromatography by Schill [2]. Without implications for the actual mechanism of this chromatographic mode, we shall use the term IPC for the technique and pairing ion (IP reagent) for the amphiphilic ion throughout this paper.

* Corresponding author.

0021-9673/94/$07.00
SSDI 0021-9673(93)E1041-W

In IPC systems, numerous mobile phase variables (pairing ion type and concentration, ionic strength, eluent pH, organic solvents) can be used to control solute retention and separation selectivity. The broad choice and combination of these variables allow for the separation of complex sample mixtures containing ionic/ionizable and neutral solutes.

However, method development in IPC is often difficult owing both to the uncertainties concerning the interpretation of the underlying retention processes and to the large number of variables. In spite of many mechanistic studies, the theory of ion-pair chromatography has remained a subject of debate over many years. In order to develop a better understanding of ion-pair chromatographic systems, the physical background of the different theories must be examined.

Historically, two groups of retention theories can be distinguished, stoichiometric and non-stoichiometric [3]. At the introduction of the technique, stoichiometric theories were developed. These suggested that solute ions and pairing ions form stoichiometric complexes either in the mobile phase (ion-pair model) or at the stationary phase (dynamic ion-exchange model). The ion-pairing adsorption model assumes the formation of an ion pair in the polar mobile phase followed by the adsorption of this uncharged complex on the hydrophobic stationary phase. The dynamic ion-exchange model presumes that the amphiphilic IP reagent molecules adsorb together with their inorganic counter ions on the stationary phase and cause the column to behave as a dynamically generated ion exchanger. The retention of solute ions is then assumed to be due to ion exchange with the inorganic counter ions. In a fundamental study on stoichiometric models, Knox and Hartwick [4] pointed out that formally both models lead to identical retention equations. Many variants and combinations of such stoichiometric models have been published. They have provided an easy-to-understand qualitative picture of solute retention for many analysts and promoted the practical use of IPC. The reader is referred to a number of review papers for a more extensive discussion of stoichiometric models [3–7].

The common feature of stoichiometric models is to derive retention relationships from a number of equilibria between the mobile phase constituents. In chemical thermodynamics, stoichiometric relationships describe the behaviour of a system fairly well when the concentrations are low and the interactions are short range, *e.g.*, Van der Waals forces and London forces. In this case, the standard free energy of adsorption (ΔG_t^0) for the retention process is independent of the concentrations of the reactants and products in the system. However, this does not apply to electrostatic interactions resulting from long-range forces implying multi-body interactions. In Fig. 1 we illustrate the long-range nature of forces operating in typical ion-pair chromatographic systems. The electrostatic attraction and the electrostatic repulsion forces between molecules of pairing ions, solute ions and inorganic counter ions are represented by simple arrows, although more rigorously they result from the potential fields of all these ions. These forces are effective over a long range, which implies multi-body interactions, and they cannot be described by stoichiometric relationships. Therefore, the long-range nature of the electrostatic interactions

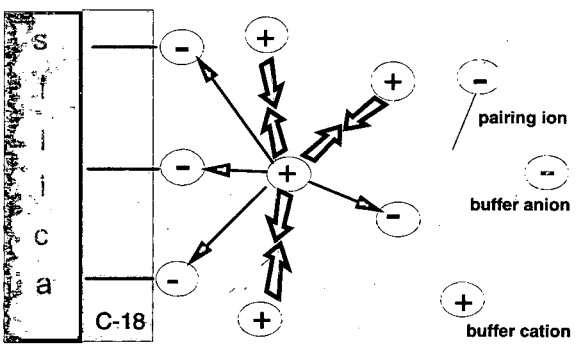

Fig. 1. Schematic illustration of the long-range nature of electrostatic forces between ions in typical ion-pair chromatographic systems. Open and full arrows represent electrostatic repulsion and attraction forces, respectively. See text for details.

makes the stoichiometric models fundamentally limited in interpreting electrostatic interactions involved in IPC systems. The remedy to describe the interaction between charged species is to turn to electrostatics and statistical thermodynamics which form the basis of the Poisson–Boltzmann equation.

Non-stoichiometric models describe the retention of ionic analytes without the formation of chemical complexes. These models assume that the retention of solute ions is partly determined by their interaction with the electric field created by the adsorbed pairing ion. Therefore, the effect of the pairing ion is assumed to be indirect and acts through establishing a certain electrostatic surface potential. The development of non-stoichiometric theories was largely stimulated by experimental evidence of the adsorption of the IP reagent on the hydrophobic stationary phase.

A qualitative description of electrostatic interactions in IPC systems was given by Bidlingmeyer [8] in the ion-interaction theory. According to this hypothesis, the pairing ion is adsorbed on the stationary phase surface forming a primary ion layer. The electrolytic (inorganic) counter ions form a secondary ion layer between the charged surface and the bulk eluent. The analyte ions are attracted or repelled by the primary ion layer depending on the sign of their charge and that of the layer. This simple qualitative picture, which did not assume the formation of complexes (ion pairs), has become popular and the term "ion-interaction" chromatography is still used at the time of writing [9]. A number of attempts have been made to formulate the model quantitatively [10,11]. However, none of them provided a rigorous description of the system, and some [9,12] even reduced to a stoichiometric model.

A theory based on two retention processes, *i.e.*, ion exchange and interaction with the electrical double layer, has been proposed by Cantwell and co-workers [13–15]. Based on their experimental results they suggested that the main process that determines retention is ion exchange between solute ions and inorganic counter ions in the diffuse part of the electrical double layer. Testing and application of the model are not straightforward and require the simultaneous measurement of the adsorption of the solute ion and the pairing ion [15] at different eluent concentrations. Further discussion of this model is given at the end of this paper.

Qualitatively, the electrostatic retention model as suggested by Ståhlberg [16] is similar to all these non-stoichiometric models. It assumes the formation of a surface potential between the bulk mobile phase and the hydrophobic stationary phase, resulting from the selective adsorption of amphiphilic pairing ions. The retention of ionic solutes depends on both their hydrophobicity and the electrical surface potential. The surface potential is obtained from solving the Poisson–Boltzmann equation. A theory based on similar concepts and on the solution of the Poisson–Boltzmann equation has been developed for the electrostatic interaction chromatography of proteins [17] and most recently for the ion-exchange chromatography of inorganic ions [18].

The major advantage of the electrostatic retention model for ion-pair chromatography is that it is well founded in physical chemistry and also that it provides equations for practical tests and retention prediction. It assumes that the primary contribution to the retention of ionic analytes is their increased (attraction) or decreased (repulsion) adsorption at the electrically charged surface. Therefore, it accounts for the retention behaviour of both oppositely and similarly charged solute ion–pairing ion combinations. Since it was introduced, the electrostatic model has been thoroughly tested [19,20] to describe the adsorption of the pairing ion and its effects on solute retention [21,22]. Based on this model, Ståhlberg and Hägglund [23] were able to explain the effects of different mobile phase electrolytes; Bartha and co-workers have extended the model to include the effect of organic solvent [24] and eluent pH [25]. However, the model has been considered to be too complex for practical work [1].

In this paper, we discuss and illustrate the basic concepts of the electrostatic retention

theory, especially that involving the electrostatic double layer and surface potential, and their effects on the adsorption isotherm of the pairing ion and on the capacity factor of charged solute ions.

We present a full framework to predict retention in ion-pair chromatographic systems based on a simplified form of the electrostatic model. A retention equation is developed to include the charges of solute and pairing ions and to provide an explicit expression for the effect of the ionic strength. This form of the model separates and delineates the contributions of solute charges, pairing ion concentration and hydrophobicity, organic solvent concentration, pH and ionic strength of the mobile phase, and also that of the reversed-phase packing material. In order to reach a practically useful equation, a number of simplifications have necessarily been made. These include the use of a solution of a linearized form of the Poisson–Boltzmann equation and a linearized form of the potential modified adsorption isotherm of the pairing ion. The simplified theoretical equations will therefore be applicable when the electrical surface potential (and the surface concentration of the adsorbed pairing ion) is relatively low (*i.e.*, less than ±50 mV). In practice, this corresponds to an approximately tenfold change in the capacity factor of analyte ions. The theoretical equations are accompanied by illustrations and comparison with experimental data both from the literature and our own work. The discussion of the simplified retention model aims to provide the information required to understand the basic features of the electrostatic theory and to utilize or test its predictions in practical work.

A more rigorous version of the retention model is also discussed when the surface concentration of the adsorbed pairing ion is high and solute retention is affected by competition for the adsorption sites. This extension of the model includes a full form of the potential-modified adsorption isotherm of the pairing ion. It considers the possible effects of competition for the adsorption sites of the stationary phase and uses the non-linear form of the Poisson–Boltzmann equation. Finally, we discuss the possible contributions of the diffuse part of the electrical double layer to the retention of analyte ions. This extended version of the electrostatic model, however, results in mathematically complex expressions and requires numerical evaluation.

2. Theory

2.1. General introduction

The addition of an ion-pairing (IP) reagent to the mobile phase has a characteristic influence on the retention of ionic analytes; it increases the retention of analytes with the opposite charge to that of the IP reagent, decreases the retention when the charges are of the same sign and has a negligible effect when the analyte is uncharged. The electrostatic theory for ion-pair chromatography (IPC) gives a quantitative and consistent physico-chemical explanation for this general behaviour by applying well known principles from colloid and surface chemistry. Its quantitative formulation is useful for prediction and optimization purposes. In this section, a brief introduction of some key concepts of the theory is outlined, while a more detailed discussion of the interplay between various parameters is presented in the following sections.

Consider a reversed-phase chromatographic system with an aqueous mobile phase in which a sodium phosphate buffer and octylsulphonate are dissolved and equilibrated with the stationary phase surface. As the octylsulphonate ions are more hydrophobic than their corresponding counter ions, *i.e.*, the sodium ions, they have a higher affinity for the hydrophobic surface and will therefore be bound to the surface in higher concentrations than the counter ions. It is a well established fact that in such a case the sodium ions are not bound to the IP reagent as stoichiometric 1:1 complexes, but are distributed in a layer close to the surface, the so-called diffuse double layer. The distribution of the sodium ions in the double layer is a result of the balance between the electrostatic attraction to the charged surface, the way the sodium ions shield

each other and the (smearing out) effect of thermal motion (entropy).

A well known consequence of the double layer is the electroosmotic flow in CZE, which of course would not exist if there were a complete formation of "ion pairs" between the surface charges and the counter ions. The important point is that a higher concentration of negatively charged octylsulphonate ions than of sodium ions at the hydrophobic surface implies that the surface carries a negative net charge. The argument may be put in a generalized form: when there is a difference in adsorption tendency between the IP reagent and its counter ions, a net surface charge is created. It is important to realise that this does not violate the principle of electroneutrality because the number of charges on the surface is balanced by an equivalent number of sodium ions located in a layer close to the surface (see Fig. 2).

Qualitatively, the effect of the negative net surface charge created by octylsulphonate ions on the retention of charged analytes is very simple: positively charged analytes are attracted to the negatively charged surface, while negatively charged analytes are repelled, resulting in an increase or decrease, respectively, in retention. The principle will, of course, hold irrespective of the charge of the IP reagent; a positively charged IP reagent will repel positively charged analytes from the surface and attract negatively charged analytes. This intuitive view of the effect of the IP reagent on retention is a useful starting point for a preliminary understanding of ion-pair chromatography. However, in order to formulate a theory for ion-pair chromatography it must be complemented with a quantitative formulation of the influence of the physical parameters which are of importance. Answers are sought to questions such as the following. How is the strength of attraction and repulsion affected by the nature and surface concentration of ion-pairing reagent on the surface? What is the relationship between the surface concentration of IP reagent and its concentration in the mobile phase? What is the effect of the concentration of organic modifier in the mobile phase? What is the effect of ionic strength and pH in the mobile phase? These questions must be answered quantitatively in physically consistent and realistic terms. In the rest of this paper they will be answered within the framework of the electrostatic theory of ion-pair chromatography and illustrated with experimental data. Although the mathematical treatment of the theory is awkward, it is possible to make some well defined, reasonable approximations and to obtain simple relationships which are useful in practical work. The complete theory, however, is readily evaluated by a computer.

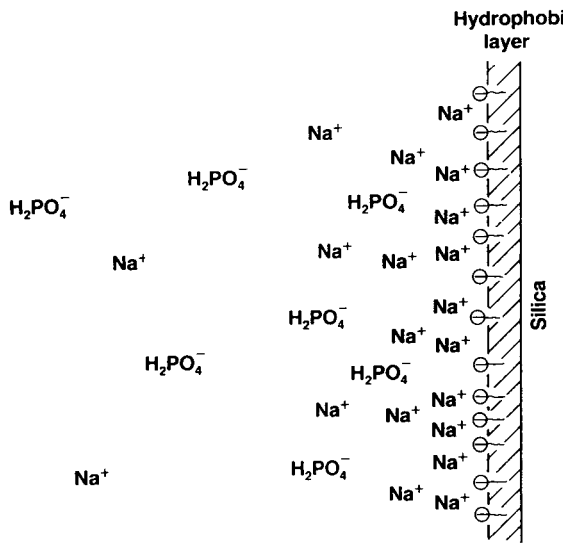

Fig. 2. An idealised picture of the electrical double layer in reversed-phase ion-pair chromatography.

2.2. Concept of electrostatic surface potential

As a first step to formulate a quantitative theory of ion-pair chromatography, the concept of electrostatic surface potential and its role in the determination of the magnitude of retention must be understood. From physics we know that a charged body creates an electrical field which causes similarly charged bodies to repel and oppositely charged bodies to attract each other. The electrical field around a charged body is a vector but it can also be described by a scalar quantity, the electrostatic potential. The electro-

static potential difference between two points is equal to the amount of work needed to move a positive unit test charge between these points.

In ion-pair chromatography, a difference in electrostatic potential is created between the bulk of the mobile phase, which is electroneutral, and the net charged surface. The difference is a result of the separation of charges in space originating from the difference in adsorption characteristics of the IP reagent and its counter ions. The electrostatic repulsion and attraction of analytes to the charged stationary phase surface are quantified as the amount of work (*i.e.*, free energy) needed to transport the charge of the analyte ion from the bulk of the mobile phase to the surface. If this work is positive the surface repels the analyte, whereas if it is negative it attracts it. There are several factors that determine the work of transporting a charge between two phases; we shall discuss only the surface potential changes caused by the adsorption of IP reagent, because the other factors are, to a first approximation, constant. The electrostatic work is, however, only one part of the total work involved in the process of transporting the analyte from the bulk of the mobile phase to the stationary phase surface. As will be discussed in the next section, it is the total work that ultimately determines the magnitude of the retention.

2.3. Preliminary discussion of the capacity factor in ion-pair chromatography

The thermodynamic interpretation of the capacity factor in ion-pair chromatography can be discussed on several theoretical levels. The first level discussed in this section is valid under most practical conditions. The complexity of the arguments will then gradually increase in subsequent sections.

The assumption at this level is that the capacity factor is a measure of the distribution of the analyte between the mobile phase and the surface of the stationary phase. Basic chromatographic theory relates the capacity factor to the equilibrium constant for adsorption according to

$$k_B = \phi K_{t,B} = \phi e^{-\frac{\Delta G^0_{t,B}}{RT}} \quad (1)$$

where ϕ is the column phase ratio and $K_{t,B}$ is the equilibrium constant for adsorption. As is known from thermodynamics, this equilibrium constant depends on the change in free energy of adsorption of the solute, $\Delta G^0_{t,B}$, which is equal to the work needed to transfer the molecule from the bulk of the mobile phase to the stationary phase surface. As discussed for the electrostatic surface potential, the electrostatic work involved in the transfer of a charged analyte to the charged surface constitutes one part of the total work, $\Delta G^0_{t,B}$, which is quantitatively expressed as a difference in electrostatic potential between the surface and the bulk of the mobile phase. We can therefore define the electrostatic contribution in $\Delta G^0_{t,B}$,

$$\Delta G^0_{t,B} = \Delta G^0_B + \Delta G^0_{el,B} = \Delta G^0_B + z_B F \Delta \Psi_0 \quad (2)$$

where z_B is the charge of the analyte ion, F the Faraday constant and $\Delta\Psi_0$ is the difference in electrostatic potential between the bulk of the mobile phase and the stationary phase surface, induced by adsorption of the IP reagent. The sign of $\Delta\Psi_0$ is the same as the sign of the IP reagent, so that the product $z_B\Delta\Psi_0$ is positive when the analyte and the IP reagent are of the same sign and negative when they are of opposite sign. Physically this means that the adsorption of the analyte is enhanced when the IP reagent is of opposite sign and decreases when they are of the same sign.

As indicated in Eq. 2, the electrostatic part of the free energy change constitutes only one part of the total free energy change of adsorption, $\Delta G^0_{t,B}$, of the charged analyte. The other part is usually called the "chemical" part, ΔG^0_B, of the total free energy change and in RP chromatography it is a measure of the hydrophobicity of the analyte. The physical meaning of this latter term corresponds to the free energy of adsorption of the analyte in the absence of IP reagent in the chromatographic system, and is related to the capacity factor of the analyte (Eq. 1) in an IP reagent-free mobile phase. A chromatographic

system without IP reagent is therefore a suitable reference point from which IP reagent-induced changes in the capacity factor of the analyte can be studied. Bearing in mind that all changes in capacity factor are related to a reference point, we can set the electrostatic potential in the bulk of the mobile phase to zero so that the difference in electrostatic potential between the bulk and the surface, $\Delta\Psi_0$, becomes numerically identical with Ψ_0, the electrostatic surface potential.

Fig. 3 (left-hand side) illustrates the thermodynamic relationships for one positively and one negatively charged analyte in the absence and presence of ion-pairing reagent. The capacity factor measured in the absence of IP reagent represents a reference point to which changes induced by the addition of IP reagent are related. When the IP reagent is added to the mobile phase, the stationary phase surface becomes electrically charged, as is illustrated on the right-hand side of Fig. 3 for a positively charged IP reagent. The capacity factor is related to the total free energy of adsorption, which also includes the free energy (=work) required to transfer the charge of the charged analyte to the charged surface. For positively and singly-charged analytes the capacity factor in the presence of a positively charged IP reagent is

$$k_{cB^+} = k_{0B^+} e^{-\frac{F\Psi_0}{RT}} \quad (3a)$$

and for negatively and singly-charged analytes the corresponding equation is

$$k_{cB^-} = k_{0B^-} e^{\frac{F\Psi_0}{RT}} \quad (3b)$$

where k_{0B} is the capacity factor of the respective analyte for the reference composition of mobile phase, *i.e.*, in the absence of IP reagent.

A generalisation of these equations can be obtained by combining Eqs. 1 and 2:

$$k_{cB} = k_{0B} e^{-\frac{z_B F\Psi_0}{RT}} \quad (4a)$$

bearing in mind that the electrostatic surface potential is positive when a positively charged IP reagent is used and negative when the IP reagent is negatively charged. The equation is therefore consistent with the fact that when the IP reagent and analyte ions are of opposite (or the same) charge, the retention increases (decreases). A

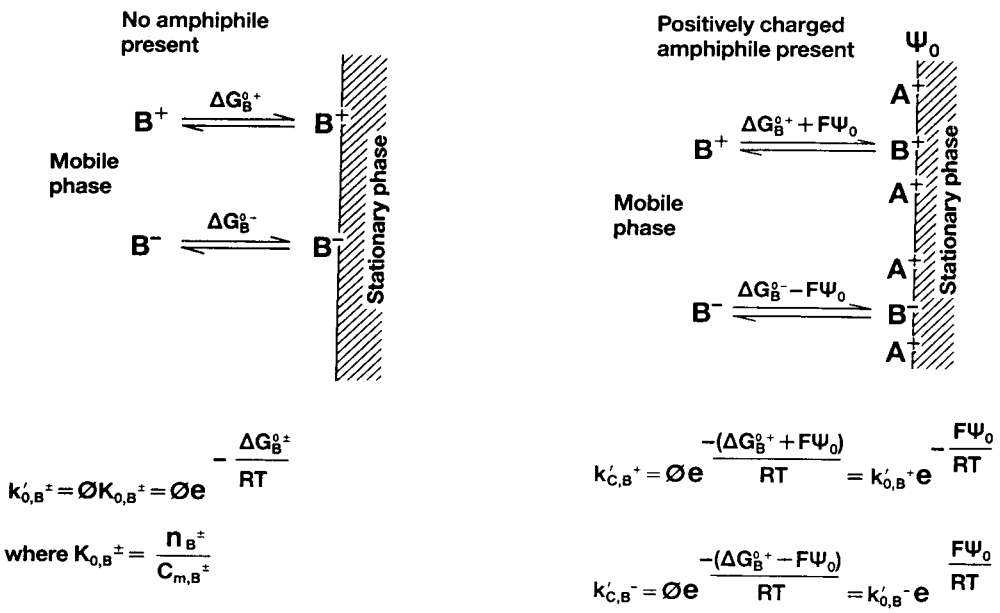

Fig. 3. Schematic illustration of the thermodynamics of the electrostatic theory applied to the distribution of analytes between the mobile phase and the stationary phase.

practical consequence of this equation is that the factor by which oppositely (or similarly) charged solutes increase (decrease) its capacity factor is the same for all oppositely (similarly) charged analytes. For example, if the capacity factor doubles for a solute on adding IP reagent, all other solutes with opposite charge to the IP reagent will also double their capacity factor. Further, all solutes with the same charge as that of the IP reagent will halve their capacity factor. Some of the experimental evidence of this symmetrical behaviour is given in ref. 19, where the theoretical implications of the equation are discussed. As discussed later, Eq. 4a is often limited to low surface concentrations of IP reagent.

By using Eq. 4a, it is possible to estimate the magnitude of the surface potential created by the IP reagent solely from the capacity factor data for a fully ionized solute, a feature that is used in the discussion of the adsorption isotherm of the IP reagent. By rearranging Eq. 4a we obtain

$$\Psi_0 = -\frac{z_B F}{RT} \cdot \ln \frac{k_{cB}}{k_{0B}} \tag{4b}$$

2.4. Gouy–Chapman theory of the electrical double layer

We have seen that it is the electrostatic surface potential created by the IP reagent that causes the changes in retention of charged analytes. The logical question is therefore: What factors influence the magnitude of the electrostatic surface potential? The answer is found in the theory for the electrical double layer, the Gouy–Chapman theory, and its coupling to the adsorption isotherm for the IP reagent. In this section a brief discussion of relevant parts of the Gouy–Chapman theory is presented.

From the discussion of the physical background of the electrostatic surface potential, it is intuitively clear that its magnitude *inter alia* is dependent on the concentration of charges at the surface. A rigorous theoretical treatment for a planar surface gives the following relationship:

$$\Psi_0 = \frac{2RT}{F} \ln \left\{ \frac{n_A z_A F}{\left(8\varepsilon_0 \varepsilon_r RT \sum_i c_{0i}\right)^{\frac{1}{2}}} + \left[\frac{(n_A z_A F)^2}{8\varepsilon_0 \varepsilon_r RT \sum_i c_{0i}} + 1 \right]^{\frac{1}{2}} \right\} \tag{5}$$

where n_A is the surface concentration of the charged species in mol/m^2, ε_0 is the electrical permittivity of vacuum, ε_r is the dielectricity constant of the mobile phase and Σc_{0i} is the mobile phase concentration of electrolyte ions, which are assumed to be singly charged. This equation shows that the electrostatic surface potential primarly depends on two parameters: the surface concentration of the IP reagent and the electrolyte concentration in the mobile phase. For low surface potentials its value is linearly dependent on the surface concentration and in this region Eq. 5 can be approximated by

$$\Psi_0 = \frac{z_A n_A F}{\kappa \varepsilon_0 \varepsilon_r} \tag{6}$$

where κ is called the inverse Debye length and is given by

$$\kappa = F \left[\frac{\sum_i (z_i^2 c_{0i})}{\varepsilon_0 \varepsilon_r RT} \right]^{1/2} \tag{7}$$

An interesting consequence of this theory is that it is the surface concentration and not the type of IP reagent that is of importance for retention. This was also found experimentally for alkylsulphate [4] and alkylsulphonate [26] pairing ions at a constant ionic strength of the mobile phase. In Fig. 4 the capacity factor of positively charged adrenaline is shown as a function of the experimentally measured surface concentration of butyl-, hexyl- and octylsulphonate pairing ions at a constant ionic strength (0.175 *M*) of the mobile phase [26]. It can be seen that pairing ions having different chain lengths result in identical

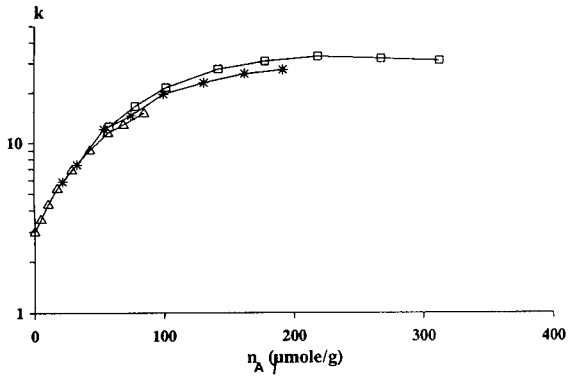

Fig. 4. Capacity factor (k) data for adrenaline *vs.* stationary phase concentration (n_A) of sodium (△) butyl-, (*) hexyl- and (□) octylsulphonate pairing ions measured at constant ionic strength (175 m*M* Na^+) of the phosphate buffer (pH 2.1) mobile phase on an ODS-Hypersil column. See ref. 26 for experimental details.

solute retention at the same surface concentration (electrostatic surface potential).

2.5. Adsorption isotherm of the IP reagent

In practical chromatographic work, the experimenter can choose the mobile phase concentration of the IP reagent and not its surface concentration. These two parameters are related through the adsorption isotherm of the IP reagent.

Thermodynamically, the adsorption is determined by the change in free energy of adsorption, which at low surface concentrations is divided into an electrostatic part and a chemical part, analogously to the treatment described earlier for the adsorption of an analyte. Physically this means that the electrostatic potential created by the IP reagent must be included in its own adsorption isotherm. The adsorbed IP reagent will electrostatically "repel itself" from the surface so that a non-linear relationship between mobile phase concentration and surface concentration is obtained. Another factor that influence the adsorption isotherm is the limited surface area or the monolayer capacity of the stationary phase surface. As the surface concentration increases, the area accessible for additional molecules on the surface decreases and the molecule will find it more and more difficult to find an adsorption site. This effect forms the background to the Langmuir adsorption isotherm, which, combined with the effect of the electrostatic surface potential, forms the basis of the surface potential modified Langmuir isotherm:

$$n_A = \frac{n_0 K_A C_A e^{-\frac{z_A F \Psi_0}{RT}}}{1 + K_A c_A e^{-\frac{z_A F \Psi_0}{RT}}} \quad (8)$$

where n_A is the surface concentration of IP reagent, n_0 the monolayer capacity, c_A its concentration in the mobile phase and K_A the adsorption constant, given by

$$K_A = e^{-\frac{\Delta G_A^0}{RT}} \quad (9)$$

where ΔG_A^0 is the "chemical" part of the free energy of adsorption, in an analogous fashion to the chemical free energy of adsorption for the analyte in Eq. 2. The non-linearity of the adsorption isotherm due to limited monolayer capacity is in practice not detected for surface concentrations lower than $0.3n_0$. On the other hand, the non-linearity caused by the electrostatic repulsion is usually noticeable for much lower surface concentrations, a point addressed later in this paper.

Substituting the expression for Ψ_0 as a function of n_A (Eq. 5) into Eq. 8 and solving for n_A should in principle give the desired adsorption isotherm for the IP reagent. However, because of the complex algebraic form of the resulting equation, this has not been accomplished without introducing the approximations discussed in the next section.

On the other hand, Ψ_0 data determined from the capacity factor of fully ionized solutes (*cf.*, eqn 4b) can be used to interpret the adsorption data of pairing ions. In Fig. 5a two adsorption isotherms are shown for butylsulphonate on a

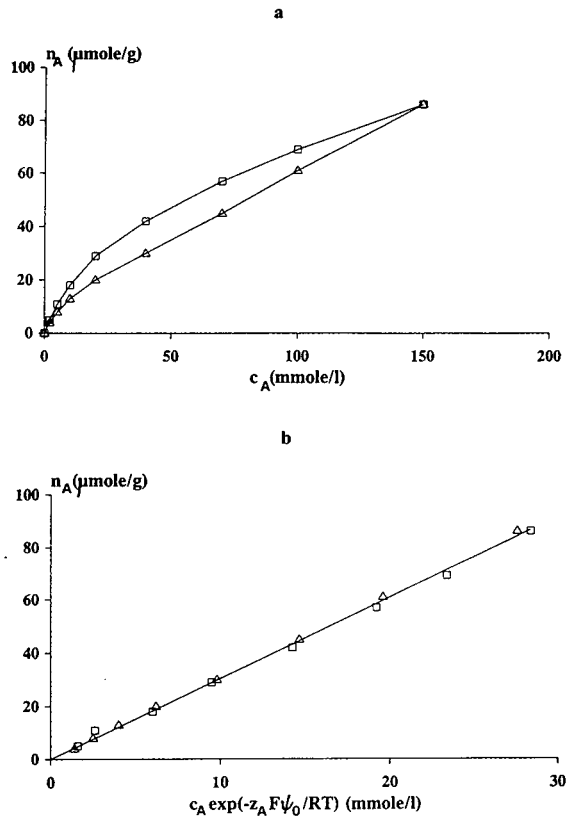

Fig. 5. Adsorption isotherms of sodium butylsulphonate pairing ion on an ODS-Hypersil (5 μm) reversed-phase column from a phosphate buffer at (△) varying (25–175 m*M* Na^+) and (□) constant ionic strength (175 m*M* Na^+): (a) without correction and (b) with correction for the surface potential. See ref. 21 for experimental details.

reversed-phase packing. The lower isotherm was obtained at a varying ionic strength (0.025–0.175 *M*), whereas higher adsorption is obtained for a constant ionic strength (0.175 *M*). As the surface concentration is relatively low, the linearized form of Eq. 8 can be used (the denominator is taken as 1). After correcting the mobile phase concentration with the electrical surface potential term (see Fig. 5b), calculated from simultaneously measured capacity factor data for adrenaline, the two isotherms coincide. This means that the effect of ionic strength on the adsorption data is fully accounted for by the induced variations in the surface potential (see refs. 21 and 23 for more details).

3. Simplified electrostatic model

3.1. Simplified treatment of the capacity factor as a function of mobile phase variables in ion-pair chromatography

The interplay between the surface concentration of IP reagent and the created electrostatic surface potential makes it difficult to obtain a rigorous yet simple relationship between the capacity factor and mobile phase concentration of IP reagent. However, by making a series of well defined approximations it is possible to obtain an equation (see Appendix for details of the derivation) which is of interest in practical work. For $c_A > 0$:

$$\ln k_{cB} = \ln k_{0B} + \left(\frac{-z_A z_B}{z_A^2 + 1}\right)\left[\ln\left(\frac{n_0 K_A c_A}{\kappa}\right) + \ln\left(\frac{F^2}{RT\varepsilon_0\varepsilon_r}\right) + 1\right] \quad (10)$$

The most important feature of this equation is that the different contributions to the capacity factor of a fully ionized analyte are separately identified:

(i) the capacity factor of the analyte in absence of IP reagent, k_{0B}, which is determined mainly by the hydrophobicity of the solute and the concentration of the organic modifier;

(ii) the effect of the charges of the solute ion and the pairing ion (z_B and z_A);

(iii) the influence of the mobile phase concentration of the IP reagent, c_A;

(iv) the influence of the electrolyte concentration in the mobile phase, included in the inverse Debye length, κ (see Eq. 7);

(v) the monolayer capacity of the stationary phase, n_0, and the free energy of adsorption of the IP reagent, $K_A = \exp(-\Delta G_A^0/RT)$, which depend on the type of IP reagent and the organic modifier concentration of the mobile phase.

The explicit expression makes it possible to

discuss and understand the contributions of different chromatographic variables in physicochemically meaningful terms, bearing in mind the limitations of this simplified treatment.

Eq. 10 can be used at relatively low electrostatic surface potentials (from 5 to about 50 mV) where the approximations of using linearized solutions for the Poisson–Boltzmann Eq. (6) and for the surface potential modified adsorption isotherm of the pairing ion, as well as the series expansion discussed in the Appendix, are applicable. This corresponds to *ca.* 0.08–0.8 μmol/m^2 surface concentration of adsorbed pairing ion on regular reversed-phase packings with surface areas of 150–200 m^2/g and ionic strengths of 0.05–0.1 *M*. Further, in order to use Eq. 6 for the approximation of the surface potential, the pore diameter of the stationary phase should be at least 100 Å and the electrolyte concentration of the mobile phase should exceed *ca.* 50 m*M*. As a first approximation, it is also assumed that the reversed-phase retention of solute *B* (k_{0B}), *i.e.*, the chemical part of the free energy adsorption, is not influenced by the presence of the pairing ion. The retention equations for the organic modifier were derived assuming that both ΔG^0_A and ΔG^0_B are linear functions of the concentration of the organic modifier, and that variations in the dielectric constant due to changing mobile phase conditions can be neglected.

Within the framework of these assumptions, the addition of the ion-pairing reagent usually results in a tenfold change in retention. Owing to the extensive linearization of the relationships, retention predicted from Eq. 10 may have a relative error up to 15–25%. In terms of the surface concentration of the pairing ion, Eq. 10 corresponds to the earliest and steepest part of solute retention curve (see Fig. 4). At high surface concentrations of the pairing ion (comparable to the monolayer capacity of the stationary phase), the retention curve levels off, which can be (at least partly) accounted for the competition of solute and pairing ion molecules for the hydrophobic surface, as discussed later. In the following subsections we discuss the retention-modifying effect of the individual chromatographic variables. Several examples of the utility of Eq. 10 in practical chromatographic work are presented.

3.2. Effect of electrical charge of the solute ion and the pairing ion

The sign of the ionic charge of the adsorbing pairing ion determines the sign of the electrostatic surface potential. Analyte ions with opposite charge are attracted whereas ions with identical charge are repelled by the charged surface. When the eluent (and surface) concentration of the pairing ion increases, the retention of analyte ions decreases for identical charges and increases for opposite charges. The steepness of this change is, however, determined by the actual number of charges on the solute and the pairing ion. Qualitatively, multiply charged ions would be expected to show larger changes than singly charged ions. In accordance with this qualitative picture, Eq. 10 predicts steeper changes for multiply charged ions if any of the mobile phase parameters (pairing ion concentration, ionic strength or organic modifier concentration) is varied.

At a given constant ionic strength and organic modifier concentration, Eq. 10 can be simplified as

$$\ln k_{cB} = K_2 - \left(\frac{z_A z_B}{z_A^2 + 1}\right) \cdot \ln c_A \qquad (11)$$

where K_2 is a constant depending on the hydrophobicity and the charge of solute and pairing ion, organic modifier and ionic strength. According to this equation, $\ln k_{cB}$ is a linear function of $\ln c_A$ with a slope and sign determined by the charge of solute and pairing ions. A simplified version of this equation for singly charged pairing ions has been published earlier [22]. The theoretical slope values for a few singly and doubly charged solute ion–pairing ion combinations are given in Table 1.

Predictions for singly charged pairing ions and singly and doubly charged solute ions based on this equation agree well with experimental data. Over a moderate concentration range of common octylsulphonate and tetrabutylammonium

Table 1
Theoretical slope values for the ln k_{cB} *versus* ln c_A relationship at different solute ion (z_B)–pairing ion (z_A) charges

z_A	z_B	$-z_A z_B/(z_A^2+1)$
+1	−1	+1/2
+1	+1	−1/2
+1	−2	+1
+1	+2	−1
+2	−1	+2/5
+2	+1	−2/5
+2	−2	+4/5
+2	+2	−4/5

pairing ions, experimental data for singly and doubly charged solute ions are characterized by the theoretical slopes of ±1/2 and ±1, respectively [22].

An interesting prediction of Eq. 11 is that the combination of a singly charged solute with a doubly charged pairing ion only gives a slope of 0.4, compared with a slope value of 1 for a doubly charged solute with a singly charged pairing ion. Experimental data for multiply charged solutes and pairing ions at constant ionic strength are scarce in the literature. In Fig. 6, we replotted retention data from Pettersson and Schill [27] for some naphthalene sulphonates and disulphonates against the eluent concentration of doubly charged hexamethonium ion as a pairing ion. The theoretical slope is shown by the solid lines (+0.4 for singly and +0.8 for doubly charged solutes) for the experimental data. No attempt was made to fit the data to the theoretical behaviour, rather the agreement between the predicted and experimental retention change for the differently charged solutes is interesting. The retention at low pairing ion concentrations was higher than expected (not shown on the plot). In fact, non-linear behaviour is expected at both low and high pairing ion concentrations where Ψ_0 is outside the range 5–50 mV (*cf.*, discussion for Eq. 10). However, the qualitative agreement between the predicted and experimental behaviour supports the applicability of Eq. 11 not only in interpreting but also in approximating the retention for multiply charged

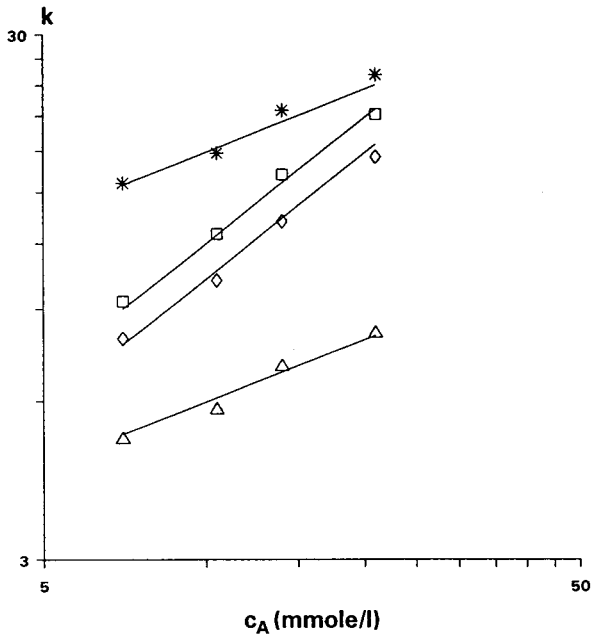

Fig. 6. Capacity factor (k) data for singly (△ = 1-naphthylamine-4-sulphonic acid; ∗ = 6-naphthol-2-sulphonic acid) and doubly charged sulphonic acids (□ = 2-naphthol-6,8-disulphonic acid; ◇ = naphthalene-2,7-disulphonic acid) as a function of eluent concentration (c_A) of a doubly charged pairing ion, hexamethonium bromide ($z_A = +2$). Data were measured by Petterson and Schill [27] using a phosphate buffer (pH 5.5) at constant ionic strength (0.1 *M*) on a LiChrosorb RP-18 column.

solute–pairing ion combinations. It must be pointed out that owing to the theoretical limitations of using the Poisson–Boltzmann equation for multiply charged ions, retention estimates may result in larger errors than for singly charged solutes.

Recently, Zhang *et al.* [28] have reported on the correlation between retention data measured in a reversed-phase mode (ln k_{0B}) and in the ion-pairing mode (ln k_{cB}). They found a linear correlation between retention data for sulphonic acids in the two modes of chromatography. The intercept parameters of the correlation were strongly dependent on the number of negative charges (from 1 to 3) of the solute ions, which is theoretically to be expected according to Eqs. 10 and 11.

3.3. Effect of pairing ion hydrophobicity

One of the important parameters to control retention in ion-pair chromatography is the hydrophobicity of the pairing ion. Generally, the retention of oppositely charged solutes increases with increasing hydrophobicity of the pairing ions when they are used at identical mobile phase concentrations. The retention change can be attributed to the higher adsorption of more hydrophobic pairing ions and a corresponding higher electrostatic surface potential, at a constant value of the ionic strength and other chromatographic variables. In terms of the electrostatic model, the hydrophobicity of the pairing ion influences the free energy of adsorption (ΔG^0_A), and the size of the paring ion affects the monolayer capacity (n_0), *i.e.*, it changes the factor $n_0 K_A(\Delta G^0_A)$ (which will be referred to as the "adsorption term" for convenience) in the adsorption isotherm of the pairing ion. At constant ionic strength and organic modifier concentration, Eq. 10 can be rewritten as

$$\ln k_{cB} = K_3 - \left(\frac{z_A z_B}{z_A^2 + 1}\right) \cdot \ln (n_0 K_A) - \left(\frac{z_A z_B}{z_A^2 + 1}\right) \cdot \ln c_A \quad (12)$$

where K_3 is a constant.

Eq. 12 predicts similar retention behaviour for ionic analytes as a function of the eluent concentration of the pairing ion (c_A), as long as the number and sign of the charges of the pairing ions are identical. Any change in pairing ion hydrophobicity results in an incremental change of its adsorption term ($\ln n_0 K_A$), *i.e.*, it causes a parallel shift of $\ln k_{cB}$ *vs.* $\ln c_A$ curves of the analyte ions. The more hydrophobic the pairing ion, the larger is the retention increase (oppositely charged solutes) or decrease (similarly charged solutes). Examples are shown in Fig. 7a and b for both positively (dopamine) and negatively (naphthalene-2-sulphonic acid) charged solute ions, respectively, with different alkylsulphonate pairing ions [26]. Note that the sign of the retention shift (due to increasing hydrophobicity of the pairing ion) depends on the combination of charges are predicted by Eq. 12.

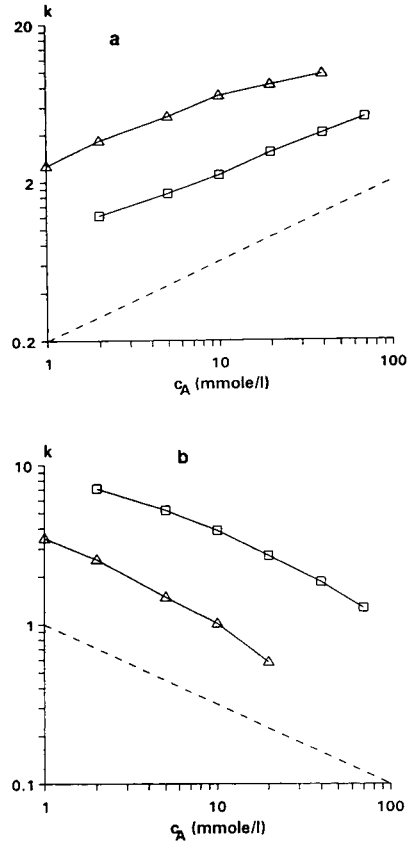

Fig. 7. Capacity factor (k) data for (a) dopamine and (b) naphthalene-2-sulphonic acid as a function of the eluent concentration of sodium (□) hexyl- and (△) octylsulphonate pairing ions. Measurements were made in methanol–aqueous phosphate buffer (pH 2.1) (10:90, v/v) eluents of constant ionic strength (175 m*M* Na^+, adjusted with sodium bromide) on an ODS-Hypersil column. The dashed line is the theoretical slope. See ref. 26 for experimental details.

The adsorption term $\ln n_0 K_A$ depends both on the hydrophobicity of the pairing ion and the concentration of the organic modifier. In practice, when using higher organic modifier concentrations one needs to use more hydrophobic pairing ions to reach a high enough retention. In other words, one has to select a pairing ion which can establish a sufficiently high electrostatic surface potential. Recommendations based

on measured adsorption data have been published by Bartha *et al.* [29] for the practical selection of the most common pairing ions (alkylsulphonates and tetraalkylammonium ions) and their eluent concentration in combination with increasing concentration of the organic modifier.

3.4. Effect of type and concentration of organic modifier in the mobile phase

In reversed-phase chromatography, the logarithm of the capacity factor for an uncharged analyte is often described as a linear function of the concentration of organic modifier in the mobile phase (φ):

$$\ln k_B(\varphi) = \ln k_{wB} - S_B\varphi \quad (13)$$

where k_{wB} is the capacity factor for analyte B in water and S_B is a constant for a given analyte–solvent combination. The physical interpretation of this relationship is that the free energy of adsorption is a linear function of the organic modifier concentration. For an uncharged analyte ($z_B = 0$) there is no electrostatic term in the total free energy of adsorption (Eq. 2), and by applying Eq. 1 we can rewrite Eq. 13 as

$$-\frac{\Delta G_B^0(\varphi)}{RT} = -\frac{\Delta G_B^0(\varphi = 0)}{RT} - S_B\varphi \quad (14)$$

For IP chromatography this relationship therefore means that the "chemical" part of the free energy of adsorption for the analyte (Eq. 2) decreases linearly with increasing concentration of organic modifier in the mobile phase. An analogous linear relationship for the "chemical" component of the free energy of adsorption for the pairing ion as a function of organic modifier concentration in the mobile phase is therefore to be expected.

$$\ln K_A(\varphi) = -\frac{\Delta G_A^0(\varphi)}{RT} = -\frac{\Delta G_A^0(\varphi = 0)}{RT} - S_A\varphi \quad (15)$$

The electrostatic component of the free energy of adsorption is, as before, governed by the electrostatic surface potential. We have shown earlier [24] from the analysis of adsorption isotherm data for alkylsulphonate pairing ions that this assumption is reasonable. A major advantage of the simplified equation (Eq. 10) for the capacity factor is that it separates the contributions from electrostatics, type of analyte and IP reagent from each other. After applying Eqs. 14 and 15 to Eq. 10, the following equation is obtained when $c_A > 0$:

$$\ln k_{cB}(\varphi) = \ln k_{0B}(\varphi = 0) - S_B\varphi + \left(\frac{-z_A z_B}{z_A^2 + 1}\right) \times \left[\ln K_A(\varphi = 0) - S_A\varphi + \ln\left(\frac{n_0 c_A}{\kappa}\right) + \ln\left(\frac{F^2}{RT\varepsilon_0\varepsilon_r}\right) + 1\right] \quad (16)$$

Although this equation relates the capacity factor for the analyte at a given concentration of organic modifier, φ, to its capacity factor in a mobile phase in which $\varphi = 0$, the relationship can equally well be applied to estimate the changes in k_{cB} fro any starting concentrations of organic modifier.

Assuming constant ionic strength and neglecting the effect of variations in the dielectric constant on the surface potential (note that the inverse Debye length, κ, also contains the dielectric constant), Eq. 16 can be rearranged for φ:

$$\ln k_{cB}(\varphi) = K_4 + \ln k_{0B}(\varphi = 0) - \left(S_B - \frac{z_A z_B}{z_A^2 + 1} \cdot S_A\right)\varphi + \left(\frac{-z_A z_B}{z_A^2 + 1}\right) \times \{\ln [n_0 K_A(\varphi = 0)] + \ln c_A\} \quad (17)$$

where K_4 is a constant depending on the charges, ionic strength and the dielectric constant. According to this equation, the reversed-phase retention dependence for ionized solutes on the organic modifier concentration (*i.e.*, slope of the $\ln k_{0B}$ *vs.* φ relationship, S_B) is modified in ion-pair chromatography by the dependence of the adsorption of the pairing ion (S_A) on φ and by the actual number of ionic charges. When the sample ion is oppositely charged to the pairing ion, the slope of the $\ln k_{cB}$ *vs.* φ relationship becomes steeper ($S_B + 0.5\ S_A$, for singly charged ions). If they have identical charges, the slope

becomes less steep ($S_B - 0.5\ S_A$, for singly charged ions) compared with the original reversed-phase slope (S_B).

Fig. 8a and b show the ln k_{cB} *vs.* φ plots for a positively charged (phenylalanine) and a negatively charged (naphthalene-2-sulphonic acid) solute ion in the absence (dashed lines) and presence (solid lines) of a negatively charged octylsulphonate (5 mmol/l) pairing ion [24]. It can be seen that the shifts of the slopes are in agreement with predictions from Eq. 17.

The polarity of the organic modifier influences the slope values for the dependence of solute retention (S_B) and pairing ion adsorption (S_A) as a function of φ. Generally, the less polar is the organic modifier, the steeper are the slopes

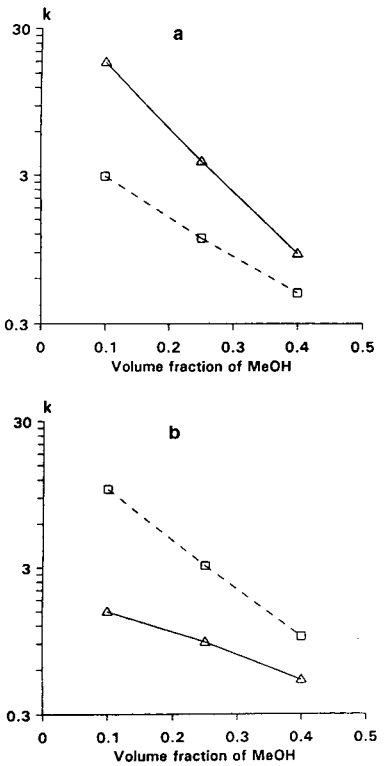

Fig. 8. Capacity factor (k) data for (a) phenylalanine and (b) naphthalene-2-sulphonic acid as a function of the methanol concentration (φ) in the phosphate buffer (pH 2.1, constant ionic strength, 175 mM Na^+) mobile phase in (□) the absence and (△) the presence (5 mM) of sodium octylsulphonate ion-pairing reagent. See ref. 24 for experimental details.

(larger absolute value). Further discussion of the organic modifier effects in IPC can be found in refs. 24 and 32.

A practical consequence of the above observation is that under IPC conditions the slope of the ln k_{cB} *vs.* φ relationship becomes steeper for oppositely charged solute ion–pairing ion combinations and the separation is less robust (while the opposite is expected for similarly charged solutes and pairing ion combinations). Further, the size of this effect is amplified by higher number of charges of the solute ions.

3.5. *Effect of mobile phase electrolyte*

Changing the mobile phase ionic strength induces effects that partly cancel each other out with respect to the capacity factor. The influence of ionic strength can be understood on the basis of the thermodynamic principles involving the adsorption isotherm of the IP reagent and the capacity factor of the analyte.

The free energy of adsorption of the analyte and of the IP reagent can be partitioned into a "chemical" free energy and an electrostatic free energy component. The influence of moderate variation in the ionic strength on the "chemical" component is usually very small and can be neglected in relation to the changes in the electrostatic part of the free energy of adsorption, *i.e.*, changes in the electrostatic surface potential. Assuming that there are no specific interactions, *i.e.*, no ion pairing or adsorption of the counter ions, Eq. 5 can be used to determine the influence of ionic strength on the surface potential at fixed concentration of charges on the surface. As the mobile phase salt concentration term appears in the denominator of the equation, an increase in salt concentration for this case results in a decrease in the magnitude of the electrostatic surface potential. On the other hand, when the magnitude of the surface potential decreases the adsorption of the IP reagent increases owing to there being less electrostatic "self"-repulsion, *i.e.*, the surface concentration of charges increases. The net effect is to lower the magnitude of the electrostatic surface potential, but because of the increased surface

concentration of the IP reagent the decrease is less than that simply predicted from Eq. 5. As discussed for the adsorption isotherm of the pairing ion, the effect of ionic strength on the adsorption data can be fully accounted for by the variations induced in the surface potential [21,23].

Another important question is the effect of the nature of the electrolyte ions. In the ideal case only the amphiphilic pairing ion (*e.g.*, tetrabutylammonium) adsorbs to the surface, thereby creating the surface potential. However, electrolytic counter ions with slight hydrophobic properties (*e.g.*, bromide, acetate) can also adsorb on the surface layer, thus reducing the effective surface charge concentration. Ståhlberg and Hägglund [21] studied the adsorption of tetrabutylammonium ion in the presence of different electrolytic counter ions. They concluded that the effect can be described by a term in the "chemical" component of the free energy of adsorption, which is added to the non-specific electrostatic energy (see ref. 21 for details), *i.e.*, by applying the same principles as for the adsorption of analyte and IP reagent, respectively.

In conclusion, the concentration of the electrolyte influences the retention of ionic analytes through modifying the surface potential established by the adsorbing pairing ion. The higher the ionic strength, the lower is the surface potential. With increasing ionic strength both the attraction of oppositely charged analytes and the repulsion of similarly charged analytes decreases.

When the surface concentrations are relatively low and no specific adsorption of the electrolytic counter ions occurs, Eq. 10 can be used to predict the effect of the ionic strength on the capacity factor. The ionic strength effect on the surface potential and the capacity factor is embedded in the inverse Debye length (κ). Therefore, by substituting Eq. 7 into Eq. 10 for κ, one can obtain an expression for the capacity factor which is explicit for the ionic strength (I):

$$\ln k_{cB} = K_5 + \frac{1}{2} \cdot \left(\frac{z_A z_B}{z_A^2 + 1} \right) \cdot \ln I - \left(\frac{z_A z_B}{z_A^2 + 1} \right) \cdot \ln c_A \quad (18)$$

where K_5 is a constant depending on the respective charges and hydrophobicity of the solute and the pairing ion and on the organic modifier concentration. According to Eq. 18, with increasing ionic strength the retention of oppositely (similarly) charged solute ions decreases (or increases) at a given pairing ion concentration. The slope of the $\ln k_{cB}$ *vs.* $\ln I$ relationship depends on the number of charges of the solute and pairing ions. The retention of singly charged analyte ions that are opposite in charge to the pairing ion is expected to *decrease* with a slope of $-1/4$. The retention of similarly charged ions is expected to *increase* with a slope of $+1/4$.

A typical experimental example is shown in Fig. 9, where retention data from Van de Venne *et al.* [31] are plotted for negatively charged hydroxybenzoic acids as a function of ionic strength (varying concentration of phosphate buffer in the eluent) as a constant mobile phase concentration of the positively charged ion-pairing reagent (5 m*M* hexylamine). There is generally good agreement between the theoretical slope (shown by the dashed line) and the experimental behaviour. Many other examples can

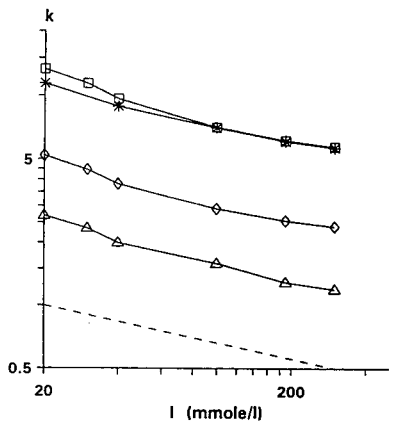

Fig. 9. Capacity factor (k) data for dissociated carboxylic acids as a function of ionic strength (I) of the phosphate buffer (pH 7) mobile phase at a constant concentration (9.2 m*M*) of hexylamine as ion-pairing reagent. Data were measured by Van de Venne *et al.* [31] using a LiChrosorb RP-18 column. Solutes: △ = 3,5-dihydroxybenzoic acid; ◇ = 4-hydroxymandelic acid; ∗ = 2,4-dihydroxybenzoic acid; □ = mandelic acid. The dashed line is the theoretical slope. For other conditions, see ref. 31.

be found in the literature for decrease (and increase) in retention of oppositely (and similarly) charged solutes and pairing ions with the addition of inorganic salts (*e.g.*, [26,32]).

Another interesting feature of Eq. 18 is its prediction of the simultaneous effect of the pairing ion concentration and the ionic strength. When the eluent concentration of the pairing ion is varied, the ionic strength can either be kept constant by the addition of an inorganic salt or can be left to vary. In the first case, the slope of the $\ln k_{cB}$ *vs.* $\ln c_A$ relationship is constant and proportional to the charges as shown above. In the second case the ionic strength becomes a function of the concentrations of the initial buffer and the pairing ion and the slope of the $\ln k_{cB}$ *vs.* $\ln c_A$ will vary between 1/2 and 1/4 for singly charged ions. A special case when there is no buffer, or where its concentration is negligible compared with the concentration of the pairing ion, and the ionic strength will be practically equal to c_A, so that Eq. 18 simplifies to

$$\ln k_{cB} = K_5 - \frac{1}{2} \cdot \left(\frac{z_A z_B}{z_A^2 + 1} \right) \cdot \ln c_A \qquad (19)$$

According to Eq. 19, the slope of the $\ln k_{cB}$ *vs.* $\ln c_A$ relationship will be only half of the values given in Table 1. Some experimental data taken from Jandera *et al.* [33] and theoretical slope values predicted from Eq. 16 for multiply charged solutes are given in Table 2. Only strong acids (naphthalenesulphonic acids) were selected as examples as these are fully ionized and have a well defined number of charges.

Although the concentration range of the pairing ion (and the ionic strength) is fairly low, the experimental slopes show relatively good agreement with those predicted from theory. Again one must remember that quantitative predictions from the model are expected to agree within 10–25% and are mainly applicable in the concentration ranges discussed in connection with Eq. 10.

An important consequence of the above analysis is that (as for all other parameters discussed) the effect of the ionic strength is amplified by the number of charges on the solute and the pairing ions. Zhang *et al.* [28,34] recently published capacity factor *vs.* salt concentration data for multiply charged solutes. Their data show good qualitative agreement with predictions from Eq. 18, *i.e.*, the retention of oppositely and multiply charged analyte ions decreases more steeply than that for singly charged ions.

3.6. Effects of the stationary phase

Pore size of the reversed-phase packing

The stationary phase in RP-IPC typically consists of porous particles. The adsorbed pairing ion establishes an electrostatic potential both in the pores and on the outside of the particles. The simplified treatment of the capacity factor (*cf.*,

Table 2
Experimental (fitted by linear regression, $r > 0.98$) and theoretical (calculated from Eq. 19) slope values of the $\ln k_{cB}$ *versus* $\ln c_A$ relationship for some differently charged naphthalenesulphonic acids ($z_B = -1$ to -3) in the presence of 1.5–4.0 m*M* tetrabutylammonium bromide IP reagent ($z_A = +1$) in methanol–water (35:65, v/v) as mobile phase on an octadecylsilica column

Compound	z_B	Experimental slope	Theoretical slope
2-Naphthalenesulphonic acid	−1	0.298	0.25
1,5-Naphthalenedisulphonic acid	−2	0.497	0.50
1,6-Naphthalenedisulphonic acid	−2	0.582	0.50
2,6-Naphthalenedisulphonic acid	−2	0.454	0.50
2,7-Naphthalenedisulphonic acid	−2	0.532	0.50
1,3,5-Naphthalenetrisulphonic acid	−3	0.800	0.75
1,3,6-Naphthalenetrisulphonic acid	−3	0.687	0.75
1,3,7-Naphthalenetrisulphonic acid	−3	0.721	0.75

See ref. 33 for more details.

Eq. 10) is based on the solution of the linearized Poisson–Boltzmann equation for planar surfaces (see Eq. 6) rather than in the pores. In order to examine the possible effect of pores, they may be considered as a cylindrical surface. For such surfaces the relationship between the surface potential, Ψ_0, and the concentration of surface charge, n_A, can be obtained [20] as

$$\Psi_0 = \frac{z_A n_A F I_0(\kappa r)}{\kappa \varepsilon_0 \varepsilon_r I_1(\kappa r)} \quad (20)$$

where $I_0(\kappa r)$ and $I_1(\kappa r)$ are modified Bessel functions of the first kind (of order zero and one), r is the pore radius of the stationary phase and κ is the inverse Debye length. The solution of the Poisson–Boltzmann equation for planar and cylindrical surfaces differs in the factor of $I_0(\kappa r)/I_1(\kappa r)$. When the Debye length ($1/\kappa$) is relatively small compared with the pore radius, this factor becomes a constant close to unity and Eq. 20 reduces to that for planar surfaces. Table 3 gives some typical data for ionic strength and the corresponding Debye length, in addition to nominal pore sizes for reversed-phase packings.

It can be seen that if the ionic strength is at least 10 mM (which is a minimum requirement for buffer concentration in IPC [4]) and the pore diameter of the reversed-phase packing material is at least 100 Å, the ratio $I_0(\kappa r)/I_1(\kappa r)$ changes less steeply with ionic strength and converges to unity. This conclusion is supported by calculations by Weber [35], who determined the theoretical potential profile from an analytical solution of the Poisson–Boltzmann equation for idealized (200 Å diameter) pores of the stationary phase. The results showed that the pore geometry plays a significant role below 10 mM electrolyte concentration.

Table 3
Typical values of $I_0(\kappa r)/I_1(\kappa r)$ as a function of ionic strength and pore radii

Ionic strength (mM)	$1/\kappa$ (Å)	r (Å)	κr	$I_0(\kappa r)/I_1(\kappa r)$
1	97	50	0.52	4.01
5	43	50	1.15	2.01
10	31	50	1.63	1.63
25	19	50	2.58	1.29
50	14	50	3.60	1.18
100	9.7	50	5.15	1.11

Calculations were made assuming a pore diameter of 100 Å and a dielectric constant of $\varepsilon_r = 80$ for the aqueous mobile phase and room temperature (25°C).

In conclusion, under realistic experimental conditions when the ionic strength and pore size of the stationary phase are reasonably large, the ratio $I_0(\kappa r)/I_1(\kappa r)$ can be considered as constant, and therefore the simplified retention model (Eq. 10) can be used for the discussion of stationary phase effects.

Adsorption capacity of the reversed-phase packing

The use of stationary phases with higher hydrophobicity (*e.g.*, longer alkyl chains or higher bonded-phase ligand density) influences the retention of ionic analytes by providing higher $-\Delta G_A^0$ and $-\Delta G_B^0$ values. Increased adsorption of the pairing ion results in higher electrostatic surface potentials and consequently larger changes in solute retention.

At constant ionic strength and organic modifier concentration, a simplified equation can be derived from Eq. 10:

$$\ln k_{cB} = K_6 + \ln k_{0B} - \left(\frac{z_A z_B}{z_A^2 + 1}\right) \cdot \ln (n_0 K_A) - \left(\frac{z_A z_B}{z_A^2 + 1}\right) \cdot \ln c_A \quad (21)$$

where K_6 is a constant depending on the charge of the solute and the pairing ions, ionic strength and organic modifier of the eluent.

Stationary phases with different hydrophobicities and monolayer capacities will influence both the second and third terms of Eq. 21, *i.e.*, the adsorption of the solute without pairing ion ($\ln k_{0B}$) and the adsorption term (monolayer capacity, n_0, and adsorption constant, K_A) of the pairing ion. Therefore, the retention of ionic solutes, $\ln k_{cB}$, should be a linear function of the mobile phase concentration of the pairing ion, $\ln c_A$, on any of the reversed-phase columns at constant ionic strength and organic modifier

concentration (provided that the pairing ion surface concentration is well below the monolayer capacity of the respective stationary phase). In similar fashion to the effect of the pairing ion hydrophobicity, changing the reversed-phase packing material will influence only the position of the ln k_{cB} *vs.* ln c_A plot but not its slope.

In Fig. 10a and b, the retention dependence of dopamine ($z_B = +1$) and 2-naphthalenesulphonic acid ($z_B = -1$) is shown as a function of the eluent concentration of sodium octylsulphonate ($z_A = -1$) as pairing ion on seven different reversed-phase columns at constant ionic strength (0.175 *M*) [30]. The theoretical slopes (+1/2 and −1/2) are indicated by dashed lines. Generally, good agreement is found between the theoretically expected and the experimental behaviour irrespective of the silica base or ligand chain length of the packings.

A practical consequence of this behaviour is that solute retention changes with pairing ion concentration can be easily predicted on any of the stationary phases (without a knowledge of the actual adsorption isotherm data) after measuring the capacity factor at only one pairing ion concentration. Differences in the adsorption of the pairing ion do not influence the slope (robustness) of the logarithmic retention plot. This interesting observation can be expected to have profound practical implications for methodological design in RP-IPC.

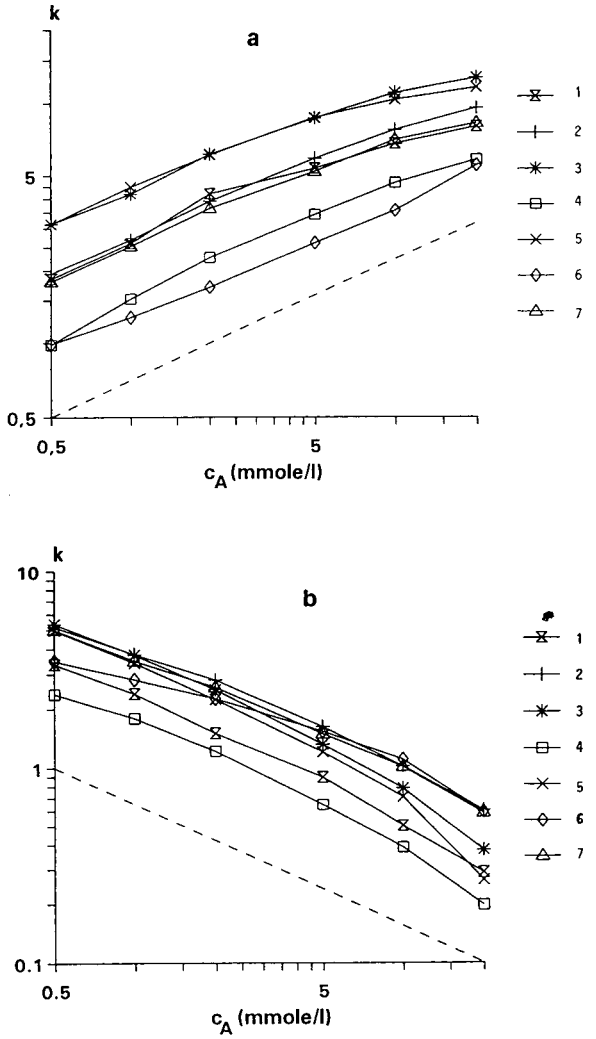

Fig. 10. Capacity factor (k) data for (a) dopamine and (b) naphthalene-2-sulphonic acid as a function of the mobile phase concentration (c_A) of sodium octylsulphonate on seven reversed-phase columns: 1 = LiChrosorb RP-18; 2 = Nucleosil C_{18}; 3 = Dimethyl-ODS; 4 = LiChrosorb RP-8; 5 = Supelco S C_{18}; 6 = BST-C_{18}; 7 = ODS-Hypersil. All measurements were made in methanol–aqueous phosphate buffer (pH 2.1) (10:90, v/v) eluents of constant ionic strength (175 m*M*, adjusted with sodium bromide). The theoretical slope predicted from the electrostatic model is shown by the dashed line.

Dissociation of silanol groups

The retention data of acids and especially bases measured on different silica-based reversed-phase columns often show large variations. Deviations are usually accounted for by the effect of silanol groups remaining on the silica surface after the chemical bonding process. The largest effect on the retention of basic (positively charged) substances usually occurs in buffers at pH values higher than the pK_a value of the silica gel, where the residual silanol groups become partly ionized, so that the negatively charged silanol groups establish a certain (negative) surface potential even in the absence of amphiphilic ions. This means that the reference point for the capacity factor (k_{0B}) in the electrostatic model corresponds to non-zero surface potential and in the ion-pair chromatographic

mode the adsorbing amphiphilic pairing ion meets a negatively charged surface.

When the pairing ion is negatively charged, its adsorption will add to the negative potential. When positively charged pairing ions adsorb on the negatively charged surface, the surface potential will be determined by the net surface concentration of charges ($[n_{A^+}] - [n_{SiO^-}]$). Therefore, the adsorption of the positively charged pairing ion has first to counterbalance this negative potential, before the surface can become positively charged.

As Eq. 21 is based on relative surface potential, it will probably be applicable as a first approximation for low and moderate concentrations of dissociated silanols. However, further experimental data are needed to clarify the effect of dissociated silanol groups on the adsorption isotherm of the ion-pairing reagents.

3.7. Effect of eluent pH

In the discussion so far, we have assumed a constant eluent pH and fully ionized solute (and pairing) ions. However, variation of the eluent pH can introduce large changes in the degree of ionization and consequently in the retention of weak acids and bases in both the regular reversed-phase and the ion-pair chromatographic modes. In reversed-phase chromatography, the capacity factor of partly ionized analytes, k_B, is the weighted sum of the capacity factor for the charged, k_{iB}, and the uncharged, k_{uB}, species, respectively

$$k_B = (1-f)k_{uB} + fk_{iB} \quad (22)$$

where f is the fraction of charged analyte at the given pH value. At a constant pH the addition of IP reagent influences only the retention of the ionized fraction of the analyte. Retention in the ion-pair chromatographic mode can be expressed by substituting Eq. 4a for the capacity factor in the presence of the IP reagent into Eq. 22:

$$k_B = (1-f)k_{uB} + fk_{0iB}e^{-\frac{z_i F \Psi_0}{RT}} \quad (23)$$

where k_{0iB} is the capacity factor of the fully ionized form of the analyte in the absence of IP reagent. Expressing the fraction of the charged analyte as a function of the hydrogen ion concentration ($[H^+]$) and the dissociation constant(s) (K_a), one can derive retention equations for weak acids and bases [25].

It has been demonstrated that expressions analogous to those used in RP chromatography can be obtained, and the experimental retention data agreed reasonably well with model predictions both for weak and strong acids and bases [25]. In order to use the model for predictive purposes, one needs the pK value, the k values of the charged and uncharged forms of the solute ion, and the retention or the value of the surface potential at a given pairing ion concentration (the latter can be obtained from Eq. 4b by measuring the retention of one fully ionized solute in the absence and in the presence of the pairing ion). As a result, measurements in three eluents provide a starting point to estimate the magnitude of retention shifts at other eluent compositions. As the retention estimates have an error margin of 10–20%, the above equations can be utilized in estimating the initial mobile phase conditions which provide reasonable retention for certain solute ion–pairing ion combinations, rather than for describing collected retention data.

3.8. Summary of the simplified electrostatic model

The major advantage of the simplified electrostatic model is that it allows us to discuss and understand the contributions of different chromatographic variables in physico-chemically meaningful terms. While the limitations of this simplified treatment must be kept in mind (*cf.*, discussion of Eq. 10), the explicit expression for the capacity factor can be utilized to predict the magnitude and direction of retention changes brought about by the major variables in ion-pair chromatographic systems. To conclude the discussion of individual parameters, Eq. 10 can be rewritten in the following form, at constant pH and organic modifier concentration:

$$\ln k_{cB} = \ln k_{0B} + \left(\frac{-z_A z_B}{z_A^2 + 1}\right) \cdot \left[\ln (n_0 K_A) + \ln c_A - \frac{1}{2} \cdot \ln I + \ln \left(\frac{e^2 F^2}{RT\varepsilon_0 \varepsilon_r}\right)^{1/2}\right] \quad (24)$$

or by including the effect of the organic modifier concentration:

$$\ln k_{cB}(\varphi) = \ln k_{0B}(\varphi = 0) - \left(S_B - \frac{z_A z_B}{z_A^2 + 1} \cdot S_A\right)\varphi + \left(\frac{-z_A z_B}{z_A^2 + 1}\right) \cdot \left[\ln (n_0 K_A(\varphi = 0) + \ln c_A - \frac{1}{2} \cdot \ln I + \ln \left(\frac{e^2 F^2}{RT\varepsilon_0 \varepsilon_r}\right)^{1/2}\right] \quad (25)$$

where the temperature (T) and the dielectric constant of the mobile phase (ε_r) are collected in the last logarithmic term together with other constants. The effect of the chromatographic variables on the capacity factor of ionized solutes is shown in Table 4.

It must be pointed out that throughout this discussion we have concentrated on understanding and predicting retention and not separation selectivity in ion-pair chromatographic systems. One must realize that often very small differences in the chemical structure of the solutes can result in specific interactions with the different components of the chromatographic system. Prediction of small changes in retention (and selectivity) would require more sophisticated retention models, both for the underlying reversed-phase system and for the IPC system.

4. Capacity factor when competition with IP reagent for the limited surface area occurs

It was stated earlier that there are several theoretical levels at which the capacity factor of the analyte can be described. In the first discussion, the effect of the chemical and electrostatic free energies of adsorption of the analyte are considered. After discussion of the adsorption isotherm of the IP reagent, the effect of the limited monolayer capacity of the stationary phase can be included.

A theoretical analysis shows [21] that when there is a one-to-one competition between the analyte and the IP reagent for the limited area accessible, the following expression is obtained for the capacity factor:

$$k_{cB} = \frac{k_{0B} e^{-\frac{z_B F \Psi_0}{RT}}}{1 + K_A c_A e^{-\frac{z_A F \Psi_0}{RT}}} \quad (26)$$

where the definitions of the symbols are as before. The degree of competition between the analyte and IP reagent for the surface area may, however, depend on the type of IP reagent and analyte used. The capacity factors of *p*-toluenesulphonate and adrenaline were found to follow this equation with a series of alkylsulphonates as IP reagents [21]. On the other hand, the simpler Eq. 4 could be used over the entire surface concentration range when tetrabutylammonium ion was used [23]. This difference in behaviour can be explained by the difference in the adsorbed layer: the alkylsulphonate ions adsorb so that the charged polar sulphonate group is oriented towards the polar mobile phase and thereby the hydrophobic contact area between these two phases is reduced, whereas the symmetrically placed alkyl chains of tetrabutylammonium ion intermingle with the alkyl chains of the stationary phase.

An often debated phenomenon in the literature of ion-pair chromatography is the parabolic concentration dependence of retention, *i.e.*, with increasing concentration of IP reagent the capacity factor of an oppositely charged analyte increases to a maximum followed by a decrease at higher concentrations of IP reagent [3]. The understanding of such behaviour is straightforward if micelle formation has occurred in the mobile phase. If the ionic strength is not kept constant when increasing the IP reagent concentration, it can also counteract the retention increase (see earlier discussion). However, a maximum in k'_{cB} may still occur for concentrations of IP reagent below the critical micelle formation concentration (CMC) even when the ionic strength is kept constant, although it is not as pronounced as under non-constant conditions.

Table 4
Effect of increasing the value of different chromatographic variables in reversed-phase ion-pair chromatographic systems according to the simplified electrostatic model

Variable	Effect	k (oppositely charged solute)	k (similarly charged solute)
Charge of analyte ion ($z_B = \pm 1, 2, \ldots$)	Amplifies the effect of all parameters below	Increasing number of charges of the solute ion increases the absolute slope of the ln k_{cB} *vs.* ln c_A relationship	
Charge of pairing ion ($z_A = \pm 1, 2, \ldots$)	Determines the sign of the electrostatic surface potential	Increasing number of charges of the pairing ion slightly decreases the absolute slope of the ln k_{cB} *vs.* ln c_A relationship	
Concentration of pairing ion (c_A)	Increases the absolute value of the electrostatic surface potential through the adsorption of pairing ion molecules on the hydrophobic stationary phase	Increases owing to attraction to the charged surface	Decreases owing to repulsion from the charged surface
Hydrophobicity of pairing ion (K_A)	The adsorption constant of the pairing ion increases with increasing hydrophobicity. The more hydrophobic the IP reagent, the higher is its adsorption under identical eluent conditions	Increases owing to higher electrostatic surface potential	Decreases owing to higher electrostatic surface potential
Concentration of organic modifier (φ)	Decreases both the adsorption of the pairing ion (lower surface potential) and the reversed-phase retention of the analyte (lower polarity of the mobile phase)	Decreases. The slope of the ln k_{cB} *vs.* φ relationship becomes steeper compared with the regular RP slope	Decreases. The slope of the ln k_{cB} *vs.* φ relationship becomes less steep compared with the regular RP slope
Type of organic modifier (S_A, S_B)	Less polar organic modifiers lead to larger decreases in both pairing ion adsorption and solute retention	The slope of the ln k_{cB} *vs.* φ relationship becomes even steeper	The slope of the ln k_{cB} *vs.* φ relationship becomes even less steep
Ionic strength (I)	The adsorption of the pairing ion slightly increases while the electrostatic surface potential decreases	Decreases owing to lower electrostatic surface potential	Increases owing to lower electrostatic surface potential
Type of stationary phase	The higher the adsorption capacity of the stationary phase, the higher are the surface concentration of the pairing ion and the electrostatic surface potential. It affects the RP retention of the solute (k_{0B}) and the adsorption term ($n_0 K_A$) of the pairing ion	A parallel shift of the ln k_{cB} *vs.* c_A relationship occurs for both positively and negatively charged analytes when using different columns	
Eluent pH	Influences the ionization of solute (and pairing) ions. If the solute becomes more ionized, the retention contribution of the electrostatic interactions increases	Retention of the ionized form increases; it can become even larger than the regular RP retention of the non-ionized form	Retention of the ionized form decreases

One major reason for this retention behaviour is the competition for available surface area as described by Eq. 26.

In Fig. 11, the experimentally found capacity factor of adrenaline is shown as a function of the eluent concentration of octylsulphonate [26] at two different (constant) ionic strengths, 0.095 and 0.175 *M*. Model calculations were performed by a numerical computation solving simultaneously the Gouy–Chapman equation (Eq. 5) for the electrostatic surface potential and Eq. 26 for the capacity factor using Mathcad ver. 3.0. In order to obtain a reasonable fit to the experimental values, the previously reported value for n_0 ($1.81 \cdot 10^{-6}$ mol/m^2) [21] and a slightly adjusted value of K_A (2.5 m^3/mol) were used. Note that the same set of values is used for both data series and that the value of K_A agrees well with that obtained for the adsorption isotherm of octylsulphonate, as reported in ref. 21. It can be seen that the extended model (indicated by the lines) predicts the experimentally observed fold

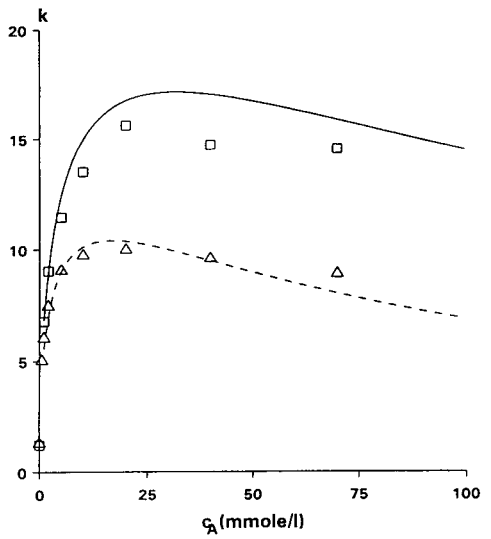

Fig. 11. Capacity factor (k) data for adrenaline as a function of the mobile phase concentration (c_A) of sodium octylsulphonate at two different (constant) ionic strengths, (□) 95 m*M* and (△) 175 m*M*. Other conditions as in ref. 26. The lines were calculated from the electrostatic model for high pairing ion surface concentrations (see text) using as parameter values $k_{0B} = 1.2$, $n_0 = 1.81 \cdot 10^{-6}$ mol/m^2 and $K_A = 2.5$ m^3/mol. See text for details.

over of the capacity factor at high pairing ion concentrations, while using realistic (experimental) values for the monolayer capacity and the adsorption constant.

One of the simplifications made in the derivation of this model is the assumption that the analyte ion and the pairing ion require approximately the same surface area for their adsorption. According to Eq. 26, the ratio k_{cB}/k_{0B} for two different solutes having the same charge should be constant (*i.e.*, the ln k_{cB} *vs.* ln c_A plots should run parallel). Whereas at low surface concentrations of the pairing ion this assumption proved to be reasonable [21,22], at high concentrations solutes (even with similar charge and chemical structure [36]) can show different retention behaviour [37]. Recently, Narkiewicz-Michalek [37] suggested that such behaviour can be accounted for by differences in the required surface area for adsorption of the analyte ion and the pairing ion, and extended the electrostatic model by including a multi-site occupancy model for adsorption.

In conclusion, according to the extended electrostatic model, competition for the available surface area on the stationary phase between the analyte ions and pairing ions will decrease the overall retention when the surface concentration of the pairing ion is high (*ca.* $n_A > 0.3n_0$). For oppositely charged solute ion–pairing ion combinations, this will result in a fold over of the ln k_{cB} *vs.* ln c_A plots. For similarly charged solute ion–pairing ion combinations it will decrease retention even further. A better fit to retention data can be obtained by refining the model with the different surface area requirements of solute ion and pairing ion adsorption.

5. Extended theory of ion-pair chromatography

5.1. Discussion of the distance-dependent capacity factor

The theory presented so far has treated the capacity factor as a result of the distribution between the mobile phase and the stationary phase surface. Close to the charged stationary

phase there is the double layer in which oppositely charged ions (both analytes and bulk electrolyte ions) are accumulated and similarly charged ions are depleted. The effect of accumulation (or depletion) on the capacity factor of analyte ions is not considered in the original version of the theory and is usually of minor importance for organic analyte ions. There are, however, conditions under which this effect cannot be neglected and it is therefore pertinent to include it to complete the treatment.

For porous packing materials the contribution to the capacity factor from the small fraction of the surface that lies outside the particle can be neglected. The retention of analyte ions is mainly due to the adsorption of ions at the pore surface and, to a certain extent, to accumulation in the double layer extending from the pore surface into the pore volume, where the mobile phase is stagnant. The mathematical relationship between the excess (or deficiency) of analyte in the stagnant mobile phase in the pores and its capacity factor has recently been formulated and applied to the ion-exchange chromatography of proteins [17] and small ions [18]. The detailed derivation of the final equation is complex and can be found in ref. 17; the final result is

$$k_{DL} = \frac{A_s}{V_0} \cdot \int_0^{x'} \{\exp[-\Delta G_t(x)/RT] - 1\}\, dx \quad (27)$$

where A_s is the area of the stationary phase and V_0 the column dead volume. The integral represents the sum of surface excesses of the analyte over the distance, x, from the surface. $\Delta G_t(x)$ represents the total free energy change in moving the analyte from the bulk of the mobile phase to a point at a distance x from the stationary phase surface. In ion-pair chromatography, $\Delta G_t(x)$ is entirely due to the change in electrostatic potential between the bulk of the mobile phase and the point x, $\Delta\Psi(x)$. Since the convention is that the electrostatic potential is zero in the bulk of the mobile phase, we can substitute $\Delta\Psi(x)$ by $\Psi(x)$ so that $\Delta G_t(x) = z_B F\Psi(x)$ in Eq. 27. The measured capacity factor, k_{cBt}, is the sum of contributions from surface adsorption, k_{cB} (Eq. 26), and accumulation in the double layer, k_{DL}:

$$k_{cBt} = k_{cB} + k_{DL} = \frac{k_{0B} e^{-\frac{z_B F\Psi_0}{RT}}}{1 + K_A c_A e^{-\frac{z_A F\Psi_0}{RT}}} + \frac{A_s}{V_0} \cdot \int_0^{x'} \{\exp[z_B F\Psi(x)/RT] - 1\}\, dx \quad (28)$$

For a planar geometry the potential at a point situated a distance x from the surface is approximately $\Psi(x) = \Psi_0 \exp(-\kappa x)$, which can be used in Eq. 27. The resulting integral can only be solved by numerical methods but, as discussed in the Appendix, after making the series expansion $\exp(-\kappa x) \approx (1 - \kappa x)$, the integral can be solved approximately:

$$k_{DL} = \frac{A_s}{V_0} \cdot \int_0^{x'} (e^{-\frac{z_B F\Psi_0 e^{-\kappa x}}{RT}} - 1)\, dx \approx \frac{A_s}{V_0} \cdot \frac{1}{\kappa} \left[\frac{RT(1 - e^{-\frac{z_B F\Psi_0}{RT}})}{z_B F\Psi_0} - 1 \right] \quad (29)$$

The final approximate equation for the capacity factor is obtained by substituting Eq. 29 into Eq. 28:

$$k_{cBt} = k_{cB} + k_{DL} = \frac{k_{0B} e^{-\frac{z_B F\Psi_0}{RT}}}{1 + K_A c_A e^{-\frac{z_A F\Psi_0}{RT}}} + \frac{A_s}{V_0} \cdot \frac{1}{\kappa} \left[\frac{RT(1 - e^{-\frac{z_B F\Psi_0}{RT}})}{z_B F\Psi_0} - 1 \right] \quad (30)$$

From this equation it is inferred that the contribution from accumulation in the double layer becomes of primary importance when k_{0B} is very small, *e.g.*, for inorganic ions, or for low ionic strengths, *i.e.*, when $1/\kappa$ is large.

The contribution of the accumulations of ions in the double layer to the final capacity factor as a function of mobile phase ionic strength or its κ value is shown in Fig. 12a and b for analyte ions with two different k_{0B} values (0.1 and 0.3) (for a constant surface potential of 50 mV, neglecting any competition for available surface area), *i.e.*, the denominator in the first term is equal to unity. For each k_{0B} value (using a constant

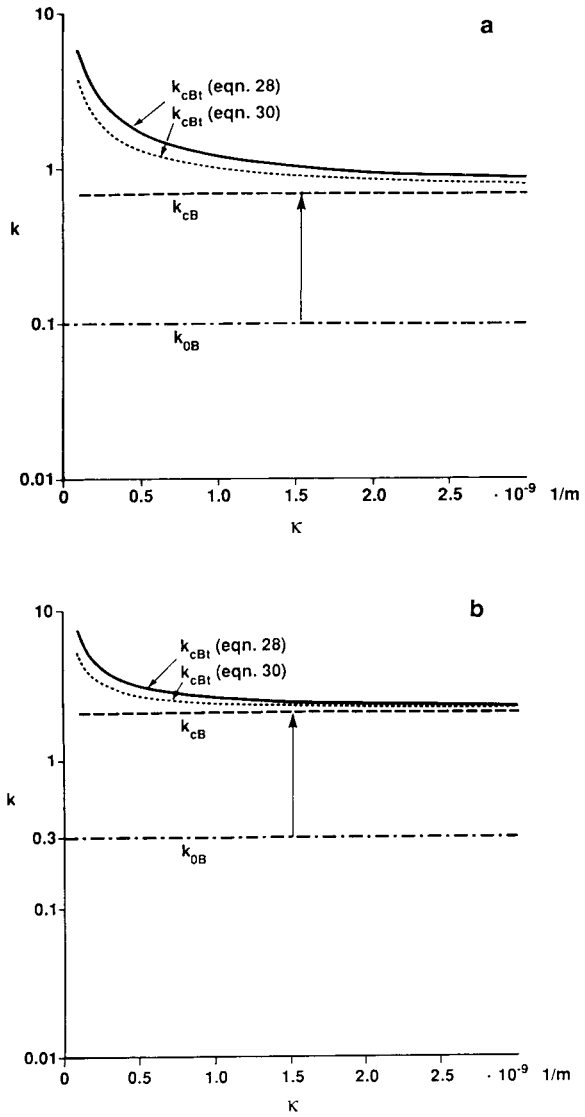

Fig. 12. Contribution of the accumulation of ions in the double layer to the capacity factor (k) at a constant surface potential (50 mV) as a function of the inverse Debye length (κ) (or ionic strength). Retention of hypothetical positively charged analyte ions with a reversed-phase retention (k_{0B}) of (a) 0.1 and (b) 0.3. Other parameters: phase ratio (A_s/V_0), $\phi = 1.5 \cdot 10^8$ m^2/m^3; $z_A = -1$; $z_B = +1$; temperature, $T = 300$ K. See text for discussion.

surface potential of 50 mV), the resulting k_{cB} value was calculated and connected to the respective k_{0B} value with an arrow as shown. The term k_{cB} corresponds to the capacity factor calculated from the simple version of the theory, calculated from Eq. 4a. The resulting k_{cBt} value as a function of the inverse Debye length (κ) was calculated by numerical integration of Eq. 28. The difference between the lines of k_{cBt} and k_{cB} in Fig. 12 is equal to k_{DL} as a function of κ. To compare the values of k_{cBt} obtained by the numerical evaluation of the integral in Eq. 28 with those obtained from the approximate analytical solution in Eq. 30, both sets of data are plotted in Fig. 12 using the same set of calculation parameters.

Fig. 12 shows that, under these conditions, the influence of accumulation in the double layer can be neglected when the k_{0B} value is larger than 0.3 (Fig. 12b). It can be seen that for lower k_{0B} values the effect of accumulation becomes increasingly important and dominates the retention for k_{0B} values lower than 0.1 (Fig. 12a). It is found that the approximate Eq. 30 underestimates the contribution of double-layer accumulation, but that it can be used to make a first estimate of its importance relative to the surface adsorption term, k_{cB}. For practical applications of Eq. 30 a value for the column phase ratio is needed and, unless it is well known, any calculation of k_{DL} becomes approximate. When using Eq. 30 it should also be borne in mind that it is based on an assumption of planar geometry. If the pore radius is smaller than about three times the Debye length, the effect of overlapping double layers and surface curvature must be considered. Inclusion of such effects follows the same principles as used above, but becomes mathematically more complex and is therefore omitted in this presentation. An illuminating study of the combined effect of pore radius and salt concentrations has been made by Weber [35].

5.2. Brief comparison with the model for RP-IPC developed by Cantwell

A retention theory based on an ion-exchange process in the diffuse double layer combined with surface adsorption, which includes electrostatic interactions, has been developed by Cantwell and co-workers [13–15]. Without going into

detail, we shall briefly discuss two crucial points where the Cantwell model differs from that discussed in this paper.

(i) The basic assumption made by Cantwell in both the theoretical and experimental analysis is that a constant activity of the IP reagent in the mobile phase results in a constant electrostatic potential at the stationary phase surface. The argument for this assumption derives from the Nernst equation for an ion that determines the potential and Cantwell consequently uses the term potential-determining ion for the IP reagent. In this context it is appropriate to cite the discussion of potential determining ions in the AgI–water system in the classical book by Hunter ([38], p. 19):

"The important assumption in deriving Eq. 4" (*i.e.* the Nernst equation) "is that ... when the bulk activity of Ag^+ is altered, the surface activity remains constant. The justification for this assumption is that the surface of the AgI crystals contains a large number of Ag^+ and I^- ions and the few extra ions which are adsorbed in order to establish the potential Ψ_0 are not likely to affect the activity of those surface ions. The special role of the crystal lattice ions is recognized by referring to them as the *potential-determining ions* for the system, to distinguish them from ions like K^+ and NO_3^- which are not expected to enjoy a special interaction with the surface. These latter are called *indifferent ions*. Intermediate between these extremes are ions which appear to interact in some special (*e.g.*, chemical) way with the surface and these are referred to as *specifically adsorbed ions*".

When discussing the theoretical implications of the Nernst equation, Hunter [38] writes (p. 238): "For the silver halide–solution interface we shall assume the validity of the Nernst equation: ... and a similar equation should hold for any system in which the potential-determining ions are themselves constituents of the crystal lattice (*e.g.*, $BaSO_4$) so that the assumption in deriving ..." (*i.e.*, the Nernst equation) "can be assumed to hold ... *In all other cases it will be necessary to set up a more elaborate expression for* Ψ_0, *and indeed this will prove to be one of the more difficult aspects of the problem*" (present authors' italics).

In the electrostatic theory as presented in this paper, the IP reagent is treated as specifically adsorbed ions (in contrast to Cantwell and co-workers, who used the potential-determining ion concept) and Ψ_0 is calculated from the Gouy–Chapman theory or related theories describing the relationship between surface concentration of the IP reagent and Ψ_0.

(ii) Cantwell and co-workers assign a stoichiometric constant for the exchange of ions between the bulk of the mobile phase and the diffuse part of the double layer and obtained numerical values for this constant as high as 900 for the exchange between *p*-nitrobenzenesulphonate and chloride ions [39]. From their investigations, they conclude that this ion-exchange process is the dominant contribution to retention at low ionic strengths or high surface potentials. As the exchange constant is a measure of differences in solvent–analyte interactions (*i.e.*, no electrostatic interactions are included) between the bulk phase and the "double-layer phase", Cantwell and co-workers' description is tantamount to a transfer of ions between two different phases.

In the theory described in this paper, the role of the double layer in the retention process is only accounted for in the extended version, where it is considered as an accumulation of ions in the diffuse layer. It is also possible, however, to introduce an exchange constant in this treatment, which then takes the value of unity. For the moment there are no physical reasons to believe that the value of this constant should depart significantly from unity.

6. Conclusions

The retention of organic ions in RP-IPC is influenced by the choice of mobile phase parameters such as concentration of organic modifier, ionic strength, pH and type and concentration of ion-pairing reagent. The electrostatic theory of IPC offers a physically consistent and quantitative description of retention when varying these

parameters. The theoretical foundation of the electrostatic theory has its origin in surface and colloid chemistry and the basic principles may therefore fall outside the customary expertise of chromatographers. In the first section the elementary concepts of the theory are presented, focusing on a qualitative understanding of the physical principles.

The complete theory, as discussed in the theoretical sections, is mathematically complex and can only be solved using numerical methods; consequently, it is less useful for practical work. To provide a relationship that is easy to use in practice, an equation has been developed that separates the originally complicated interdependence between the chromatographic parameters into its constituent components. The limitations of the simplified theory and its usefulness have been thoroughly discussed and illustrated by using many practical examples. From these examples it can be concluded that the simplified theory is an effective tool for the understanding and prediction of the retention of solute ions of differing type and charge when the mobile phase composition is varied. The generality of the simplified theory with respect to different stationary phases has also been illustrated.

At high surface concentrations of the ion-pair reagent, competition between the solute ion and the ion-pair reagent for the limited surface area of the stationary phase occurs. As a result of this competition there is a maximum in the plot of capacity factors *versus* ion-pair reagent concentration in the mobile phase. This was illustrated for octylsulphonate as IP reagent and keeping the ionic strength constant at 0.095 and 0.175 *M*.

When the solute ion has a small adsorption constant to the stationary phase, *i.e.*, $k_{0B} < 0.3$, the contribution of accumulation in the electrical double layer to its capacity factor in the presence of the IP reagent cannot be neglected. The ion-pair chromatography of inorganic ions is a typical example for such systems. An extended version of the electrostatic theory has been presented where this contribution to the capacity factor is included. Although the extension is based on the Gouy–Chapman theory for a planar surface, the principles presented can in fact be used for any suitable geometry, *e.g.*, if the stationary phase pores are approximated by cylinders.

7. Symbols

A	ion pair reagent
(A^-)	concentration of weak acid
A_s	surface area of the stationary phase, m^2/g
B	analyte ion
c_A	concentration of ion pair reagent in the mobile phase, mol/m^3 (=m*M*)
$c_{i,0}$	bulk concentration of electrolyte ion *i*, mol/m^3 (=m*M*)
f	fraction of ionized weak acid or base analyte
F	Faraday constant, C/mol
G	Gibbs free energy, J/mol
$G(x)$	Gibbs free energy at a point located a distance x from the stationary phase surface
I	ionic strength of the mobile phase
I_0	modified Bessel functions of the first kind of zero order
I_1	modified Bessel functions of the first kind of first order
k_{0B}	capacity factor for analyte B at zero concentration of ion pair reagent
k_{cB}	capacity factor for analyte B at a non-zero concentration of ion pair reagent in the mobile phase due to surface adsorption of the analyte
k_{cBt}	capacity factor for an analyte due to both surface adsorption and accumulation in the diffuse double layer, *i.e.*, $k_{cBt} = k_{cB} + k_{DL}$
k_{DL}	capacity factor for an analyte due to accumulation in the diffuse double layer
K_A	binding constant for the binding of the ion pair reagent to the surface, m^3/mol
K_B	binding constant for the binding of the analyte ion *i* to the surface, m^3/mol
K_n	numerical constant, $n = 1–6$
n_A	surface concentration of ion pair reagent, mol/m^2

n_0 monolayer capacity of the stationary phase surface for the ion-pair reagent, mol/m^2
R gas constant, $J/mol \cdot K$
S_A slope of a log $(n_0 K_A)$ *vs.* percentage of organic modifier (in the mobile phase) plot
S_B slope of a log k' *vs.* percentage of organic modifier (in the mobile phase) plot
T temperature, K
V_0 column dead volume $(=V_s + V_m)$, m^3
x distance from the stationary phase surface, m
z_A charge of ion pair reagent ion
z_B charge of analyte ion B
z_i charge of the mobile phase electrolyte ions

Greek letters

ε_0 permittivity of vacuum, F/m
ε_r dielectricity constant of the mobile phase
κ inverse Debye length, m^{-1}
σ surface charge density on the stationary phase, C/m^2
φ percentage of organic modifier in the mobile phase
ϕ column phase ratio, m^2/m^3
Ψ_0 electrostatic potential of the surface relative to the bulk of the electrolyte, V
$\Psi(x)$ electrostatic potential at distance x from the stationary phase surface, V

8. Appendix

8.1. Derivation of Eq. 10

The capacity factor of the analyte B, k_{cB}, when the IP reagent concentration in the mobile phase is c, is related to its capacity factor at zero concentration of IP reagent, k_{0B}, through the relationship

$$k_{cB} = k_{0B} e^{-\frac{z_B F \Psi_0}{RT}} \quad \text{(A1)}$$

where z_B is the charge of the analyte and Ψ_0 is the electrostatic surface potential. According to the Debye–Hückel approximation, Ψ_0 is a linear function of the surface concentration of IP reagent, n_A (mol/m^2);

$$\Psi_0 = \frac{z_A n_A F}{\kappa \varepsilon_0 \varepsilon_r} \quad \text{(A2)}$$

where κ is the inverse Debye length defined in Eq. 7 and z_A is the charge of the IP reagent. For moderate surface concentrations of the IP reagent, n_A is related to the mobile phase concentration, c_A, through the equation

$$n_A = n_0 K_A c_A e^{-\frac{z_A F \Psi_0}{RT}} \quad \text{(A3)}$$

Substituting Eq. A1 into the right-hand side of Eq. A3 and Eq. A2 into the left-hand side and rearranging gives

$$\Psi_0 = \frac{z_A F}{\kappa \varepsilon_0 \varepsilon_r} \cdot n_0 K_A c_A \cdot \left(\frac{k_{cB}}{k_{0B}}\right)^{\frac{z_A}{z_B}} \quad \text{(A4)}$$

The value for Ψ_0 is also obtained by rewriting Eq. A1:

$$\Psi_0 = -\frac{RT}{z_B F} \cdot \ln\left(\frac{k_{cB}}{k_{0B}}\right) \quad \text{(A5)}$$

which is substituted into Eq. A4, giving

$$\left(\frac{k_{cB}}{k_{0B}}\right)^{\frac{-z_A}{z_B}} \cdot \frac{-1}{z_A z_B} \cdot \ln\left(\frac{k_{cB}}{k_{0B}}\right) = \frac{F^2}{RT\varepsilon_0\varepsilon_r} \cdot \frac{n_0 K_A c_A}{\kappa} \quad \text{(A6)}$$

After taking the natural logarithm of Eq. A6, we obtain

$$\ln\left(\frac{k_{cB}}{k_{0B}}\right)^{\frac{-z_A}{z_B}} + \ln\left[\ln\left(\frac{k_{cB}}{k_{0B}}\right)^{\frac{-1}{z_A z_B}}\right] = \ln\left(\frac{n_0 K_A c_A}{\kappa}\right) + \ln\left(\frac{F^2}{RT\varepsilon_0\varepsilon_r}\right) \quad \text{(A7)}$$

The double logarithmic term on the left-hand side is series expanded using the expression $\ln(x+1) = x$ for small x values, where

$$x = \ln\left(\frac{k_{cB}}{k_{0B}}\right)^{\frac{-1}{z_A z_B}} - 1 \quad \text{(A8)}$$

or

$$\ln\left\{\left[\ln\left(\frac{k_{cB}}{k_{0B}}\right)^{\frac{-1}{z_A z_B}}-1\right]+1\right\}\approx\ln\left(\frac{k_{cB}}{k_{0B}}\right)^{\frac{-1}{z_A z_B}}-1 \quad (A9)$$

which is substituted into Eq. A7 for the double logarithmic term. The final equation is obtained after rearrangement of the exponents containing z_A and z_B terms:

$$\ln k_{cB}=\ln k_{0B}+\left(\frac{-z_A z_B}{z_A^2+1}\right)\cdot\left[\ln\left(\frac{n_0 K_A c_A}{\kappa}\right)+\ln\left(\frac{F^2}{RT\varepsilon_0\varepsilon_r}\right)+1\right] \quad (A10)$$

When the capacity factor ratio k_{cB}/k_{0B} varies between 2 and 10, approximating the double logarithmic term results in a relative error below 15% when the whole Eq. A10 is compared with Eq. A7. Keeping this in mind, Eq. A10 can be used to estimate the influence of different parameters on the capacity factor of a completely ionized analyte.

8.2. Derivation of Eq. 27

The electrostatic surface potential as a function of the distance from a planar surface in contact with an electrolyte solution is approximately

$$\Psi(x)=\Psi_0\,e^{-\kappa x} \quad (A11)$$

The change in free energy when transporting an ion from the bulk of the mobile phase, where $\Psi=0$, to a point located at a distance x from the surface is

$$\Delta G^0_{t,B}(x)=z_B F\Psi(x) \quad (A12)$$

The capacity factor for a distance-dependent interaction is described by the following equation, into which Eqs. A11 and A12 are substituted:

$$k_{DL}=\frac{A_s}{V_0}\cdot\int_0^{x'}\left[\exp(-z_B F\Psi_0\,e^{-\kappa x}/RT)-1\right]dx \quad (A13)$$

where x' is formally chosen so that

$$A_s\cdot\int_0^{x'}dx=V_p \quad (A14)$$

where V_p is the pore volume. In the ensuing numerical evaluation of the integral in Eq. A13 it is assumed that the Debye length is much smaller than the pore radius, so that the actual value of x' becomes unimportant as long as it is larger than about three Debye lengths. The integral A13 has no closed-form solution and is therefore evaluated numerically in Fig. 12a and b. The approximate closed-form solution shown in Eq. 30 is obtained by straightforward integration after using the series expansion $\exp(-kx)\approx 1-\kappa x$ in Eq. A13 and consequently changing the upper integral limit to $1/\kappa$:

$$k_{DL}=\frac{A_s}{V_0}\cdot\int_0^{\frac{1}{\kappa}}\{\exp[-z_B F\Psi_0(1-\kappa x)/RT]-1\}dx=\frac{A_s}{V_0}\cdot\frac{1}{\kappa}\left[\frac{RT(1-e^{-\frac{z_B F\Psi_0}{RT}})}{z_B F\Psi_0}-1\right] \quad (A15)$$

9. References

[1] C.F. Poole and S.K. Poole, *Chromatography Today*, Elsevier, Amsterdam, 1991, p. 411.
[2] G. Schill, in J.A. Marinsky and Y. Marcus (Editors), *Ion-Exchange and Solvent Extraction*, Vol. 6, Marcel Dekker, New York, 1974.
[3] M.T.W. Hearn (Editor), *Ion-Pair Chromatography —Theory and Biological and Pharmaceutical Applications*, Marcel Dekker, New York, 1985.
[4] J.H. Knox and R.A. Hartwick, *J. Chromatogr.*, 204 (1981) 3.
[5] Cs. Horváth (Editor), *High Performance Liquid Chromatography —Advances and Perspectives*, Vols. 1 and 2, Academic Press, New York, 1980.
[6] M.T.W. Hearn, *Adv. Chromatogr.*, 18 (1980) 59.
[7] R.H.A. Sorel and A. Hulshoff, *Adv. Chromatogr.*, 21 (1983) 87.
[8] B.A. Bidlingmeyer, *J. Chromatogr. Sci.*, 18 (1980) 525.
[9] P.R. Haddad and P.E. Jackson, *Ion Chromatography: Principles and Applications* (*Journal of Chromatography Library*, Vol. 46), Elsevier, Amsterdam, 1990, Ch. 6.
[10] R.C. Kong, B. Sachok and S.N. Deming, *J. Chromatogr.*, 199 (1980) 307.

[11] S.N. Deming and J.J. Stranahan, *Anal. Chem.*, 54 (1982) 1540.
[12] J. Zou, S. Motozimu and H. Fukotomi, *Analyst*, 116 (1991) 1399.
[13] F.F. Cantwell, *J. Pharm. Biomed. Anal.*, 2 (1984) 153.
[14] H. Liu and F.F. Cantwell, *Anal. Chem.*, 63 (1991) 993.
[15] H. Liu and F.F. Cantwell, *Anal. Chem.*, 63 (1991) 2032.
[16] J. Ståhlberg, *J. Chromatogr.*, 356 (1986) 231.
[17] J. Ståhlberg, B. Jönsson and Cs. Horváth, *Anal. Chem.*, 63 (1991) 1867.
[18] J. Ståhlberg, *Anal. Chem.*, in press.
[19] J. Ståhlberg and A. Furangen, *Chromatographia*, 24 (1987) 783.
[20] J. Ståhlberg, *Chromatographia*, 24 (1987) 820.
[21] J. Ståhlberg and A. Bartha, *J. Chromatogr.*, 456 (1988) 253.
[22] A. Bartha and J. Ståhlberg, *J. Chromatogr.*, 535 (1990) 181.
[23] J. Ståhlberg and I. Hägglund, *Anal. Chem.*, 60 (1988) 1958.
[24] A. Bartha, Gy. Vigh and J. Ståhlberg, *J. Chromatogr.*, 506 (1990) 85.
[25] A. Bartha, J. Ståhlberg and F. Szokoli, *J. Chromatogr.*, 552 (1991) 13.
[26] A. Bartha, Gy. Vigh, H.A.H. Billiet and L. de Galan, *J. Chromatogr.*, 303 (1984) 29.
[27] C. Pettersson and G. Schill, *Chromatographia*, 28 (1989) 437.
[28] Y.K. Zhang, H.F. Zou, M.F. Hong and P.C. Lu, *Chromatographia*, 32 (1991) 538.
[29] A. Bartha, Gy. Vigh and Z. Varga-Puchony, *J. Chromatogr.*, 499 (1990) 423.
[30] A. Bartha, J. Ståhlberg and Z. Varga-Puchony, in preparation.
[31] J.L.M. Van de Venne, J.L.H.M. Hendrikx and R.S. Deelder, *J. Chromatogr.*, 167 (1978) 1.
[32] A. Bartha, Gy. Vigh, H.A.H. Billiet and L. de Galan, *J. Chromatogr.* 291 (1984) 91.
[33] P. Jandera, J. Churacek and B. Taraba, *J. Chromatogr.*, 262 (1983) 121.
[34] Y.K. Zhang, H.F. Zou, M.F. Hong and P.C. Lu, *Chromatographia*, 32 (1991) 329.
[35] S.G. Weber, *Talanta*, 36 (1989) 99.
[36] A. Bartha, Gy. Vigh and J. Ståhlberg, *J. Chromatogr.*, 485 (1989) 403.
[37] J. Narkiewicz-Michalek, *Chromatographia*, 35 (1993) 527.
[38] R.J. Hunter, *Zeta Potential in Colloid Science: Principles and Applications*, Academic Press, New York, 1981.
[39] S. Afrashtehfar and F.F. Cantwell, *Anal. Chem.*, 54 (1982) 2422.

ELSEVIER

Journal of Chromatography A, 668 (1994) 285–291

JOURNAL OF CHROMATOGRAPHY A

Sample preparation by supercritical fluid extraction for quantification
A model based on the diffusion-layer theory for determination of extraction time

T. Veress

Institute of Forensic Sciences, P.O. Box 314/4, H-1903 Budapest, Hungary

Abstract

A mathematical model based on the diffusion-layer theory was elaborated in order to calculate the extraction time in dynamic supercritical fluid extraction required to reach a predefined level of extraction recovery. The goodness of the model is demonstrated by application to the extraction of the main neutral cannabinoids from marihuana and hashish samples. For monitoring of the cannabinoid content of extracts normal-phase HPLC was applied. To obtain reliable quantitative results, the extraction time ensuring a predefined level of recovery should be calculated for each individual sample according to the model because the extraction recovery depends on the sample matrix. The systematic error caused by the unextracted compounds can be eliminated by correction of the experimental data. For semi-quantitative determinations, where a knowledge of the correct value of the extraction recovery is not important, as a rule of thumb the extraction of marihuana with carbon dioxide of density 0.9 g/ml at 40°C for 34 min and of hashish for 18 min can be suggested. The application of the proposed extraction times ensured at least a 95% recovery for the main neutral cannabinoids.

1. Introduction

Supercritical fluid extraction (SFE) is a versatile method for sample clean-up and trace enrichment. For qualitative analysis the selection of suitable conditions to extract a given analyte even from a complex matrix is not so difficult, because the selectivity and solubility can easily be controlled by the composition, density and temperature of the extraction fluid [1–6]. However, the determination of the conditions required for reliable quantification is much more complicated because the efficiency of extraction is dependent on both the properties of the sample (water content, matrix, particle size, etc.) and also the operating parameters (void volume, flow-rate, extraction time) [1–3,7,8].

The effect of the sample properties on the extraction efficiency will not be discussed here. The scope of this study was the investigation of the operating parameters, especially the extraction time, in dynamic SFE in order to select the optimum values required for reliable chromatographic quantification.

Among the operating parameters, the volume of extractor chamber is determined by the instruments commercially available. It is advisable to keep the void volume of the extractor as low as

0021-9673/94/$07.00
SSDI 0021-9673(93)E1221-K

possible [7]. The density of the extraction fluid required for sufficient solubility can be calculated by Chrastil's method [9]. Logic predicts that a higher flow-rate of the extraction fluid will give a more rapid extraction. In practical analytical-scale SFE the range 1–4 ml/min is generally accepted. However, a convenient method for the determination of the extraction time required for a predefined level of recovery of the analyte from a given matrix using a particular instrument and extraction fluid at a selected flow-rate has not yet been developed. It is well known that a 100% extraction recovery cannot be achieved theoretically but the extraction of 95–98% of the analyte is possible even within 1 h, which is acceptable for analytical work. Different models [10] have been reviewed for the description of the kinetics of the SFE of various substrates. An approach developed by Newman [11] according to Fick's second law is applicable for the calculation of the extraction time needed to reach a predefined level of recovery. Andersen *et al.* [3] demonstrated the applicability of Newman's method for the prediction of extraction time, *e.g.*, assuming a diffusivity value of the order of $1 \cdot 10^{-10}$ m^2/s, particle sizes averaging 0.5 mm diameter should provide a 99% recovery in a 5-min dynamic extraction, which seems to be unlikely.

The aim of this study was to develop a procedure for the prediction of the extraction time required to reach a predefined level of extraction recovery with dynamic SFE of compounds to be determined chromatographically. The procedure elaborated is based on a mathematical model created according to the diffusion-layer theory [12,13], which was successfully applied to the description of the dissolution process of solids in liquids [14]. To demonstrate the applicability of the proposed model to the prediction of extraction time, the extraction of some neutral cannabinoids from hashish and marihuana was studied. These illicit preparations contain more than 400 compounds of different polarities [15], representing sufficiently complex matrices to use them for demonstration purposes as real samples.

2. Theoretical

It is assumed that during dynamic SFE two processes occur simultaneously: transport of the analyte from the matrix to the bulk of the extraction fluid by dissolution and the flushing out of the dissolved analyte from the extractor by the extraction fluid. For the description of the process of dissolution of a solid in a liquid, one of the simplest models is the diffusion-layer theory, which is based on Fick's first law. According to this theory, the dissolution rate is controlled by the rate of diffusion of the solute molecules across a diffusion layer of thickness h. The dissolution rate (dm/dt), *e.g.*, the mass of solute dissolved per unit time, is given by the following equation:

$$dm/dt = (AD/h)(c_s - c_b) \quad (1)$$

where A is the surface area of the solid, D is the solute diffusivity, c_s is the concentration of the dissolving solute, which is equal to the solubility, and c_b is the concentration in the bulk solution.

To describe the flushing out process, assuming a solute concentration c_0 at the beginning of the extraction without mass transfer from the matrix to the fluid and total mixing inside the extractor chamber, the time dependence of concentration can be represented by with the following differential equation:

$$dc/dt = (F/V)(c_0 - c) \quad (2)$$

where c is the actual concentration at time t, F is the flow-rate of the extraction fluid and V is the void volume of the extraction chamber.

Omitting the detailed derivatization according to Eq. 1 and 2, the concentration profile in dynamic SFE can be represented by the expression

$$c = \frac{M\beta}{\beta V - F}(e^{-Ft/V} - e^{-\beta t}) \quad (3)$$

where β is a constant relating to the analyte transport from the matrix to the fluid, defined to be proportional to the term AD/h, M is the mass

of analyte to be extracted and present in the matrix and F, V, c and t are as in Eq. 1 and 2.

The equation describing the time dependence of the recovery in dynamic SFE can be derived from the integral of the product of c and F by taking into consideration that total recovery could only be achieved after an infinite time of extraction. According to this, the recovery r can be expressed in terms of the previously used variables as follows:

$$r = 1 - \frac{\beta F}{\beta V - F}\left(\frac{V}{F}\cdot e^{-Ft/V} - \frac{1}{\beta}\cdot e^{-\beta t}\right) \quad (4)$$

In Eq. 4, V and F are known, as measurable operating parameters. The term β, representing the analyte transport from the matrix to the fluid, is assumed to be constant for a given matrix–analyte–extraction fluid system. By knowing β the extraction time required to reach a predefined level of extraction recovery can be calculated according to Eq. 4.

3. Experimental

3.1. Materials and equipment

The organic solvents *n*-hexane and ethanol were of LiChrosolv grade (Merck, Darmstadt, Germany). The carbon dioxide extraction agent was of 99.996% purity (Union Carbide, Westerlo, Belgium).

The cannabinoid standards Δ^9-tetrahydrocannabinol (THC) and cannabidiol (CBD) were obtained from the UN Narcotic Laboratory Section, (Vienna, Austria). Marihuana and hashish, applied as test materials, were samples seized by the Hungarian drug enforcement agencies. Cannabinoid-free, blank plant matrices were prepared by removing the cannabinoids from a marihuana sample by multiple extraction.

SFE experiments were performed on a Hewlett-Packard (Avondale, PA, USA) Model 7680T supercritical fluid extractor controlled by a Hewlett-Packard Vectra 386/16N personal computer. For the extraction, 7-ml thimbles were used as extractor chambers. The void volume of the extractor was decreased by filling the empty space with 2-mm diameter nickel balls, which resulted in an interstitial volume of 4.6 ml. The void volume was measured by adding a known volume of *n*-hexane to fill the interstices inside the extractor. For analyte trapping, a Hypersil ODS octadecylsilica (d_p 30–40 μm) (Shandon Scientific, Runcorn, UK) packed column was used.

The HPLC separation and chromatographic data handling were performed on a Kontron (Milan, Italy) HPLC System 400 liquid chromatograph with the following configuration: two Model 420 HPLC pumps, a Model 460 autosampler, a Model 480 column oven, a Model 430 rapid-scanning UV–Vis detector and an IBM/AT-compatible Model 450 data system. For evaluation of experimental data, SigmaPlot Scientific Graphing System V.4.02 software (Jandel Scientific, San Rafael, CA, USA) was applied.

3.2. Supercritical fluid extraction

The air-dried marihuana and hashish samples chosen as test materials were ground in an electric grinder. Fractions from the particle size range 0.4–0.6 mm were used for the experiments. From marihuana 50-mg and from hashish 10-mg amounts were weighed on to 75 mm × 30 mm filter-papers. The papers were folded to hinder the plugging of extractor frits with solid particles and inserted into the thimbles. The extractions were made with carbon dioxide of density 0.9 g/ml at 40°C. The flow-rate of the extraction fluid was 1.5 ml/min. The total extraction time was 100 min and within this period the fractions extracted serially for 5, 5, 7, 8, 10, 15, 20 and 30 min were trapped at 25°C and then eluted with 1.5 ml of *n*-hexane at 40°C. Each experiment was run at least in duplicate. The main neutral cannabinoid contents of the fractions obtained from the different intervals of extraction were monitored by HPLC in the normal-phase mode, as described previously [16].

3.3. Recovery experiments

In order to investigate the extraction recovery, 50-mg amounts of cannabinoid-free marihuana were spiked with known amounts of cannabinoids in the range 40–611 μg by adding 0.2 ml of *n*-hexane solutions of the compounds. The solvent was left to evaporate at ambient temperature and the spiked samples were extracted. The re-extracted cannabinoids were determined by HPLC [16].

Both the dependence of the recovery on the amounts of cannabinoids, applying a 30-min extraction time, and the time dependence of cannabinoid recovery, applying the same extraction time programme as detailed in Section 3.2, were studied. In the latter experiments 540 μg of CBD and 416 μg of THC were added to the blank plant matrices.

4. Results and discussion

Typical results for the dynamic SFE of a marihuana sample for THC and CBD are shown in Figs. 1 and 2, respectively. The percentage recoveries calculated from experimental data and percentage recoveries calculated according to Eq. 4, as detailed below, are plotted against the extraction time. To calculate the percentage recoveries from experimental data, the cumulative values were determined within the total extraction time interval by summing the appropriate cannabinoid contents obtained by consecutive extractions and these values were normalized to the highest cumulative value. The latter, which relates to the total extraction time, was assumed to be equal to the maximum extractable amount of cannabinoid from the given matrix. As Figs. 1 and 2 show, these maximum values could be approached 30–50 min before the total extraction time. Fig. 1 shows that after extraction for 70 min the increase in THC recovery is negligible. The results in Fig. 2 indicate that CBD can be extracted faster than THC, *e.g.*, the previously mentioned limit could be reached after extraction for 50 min.

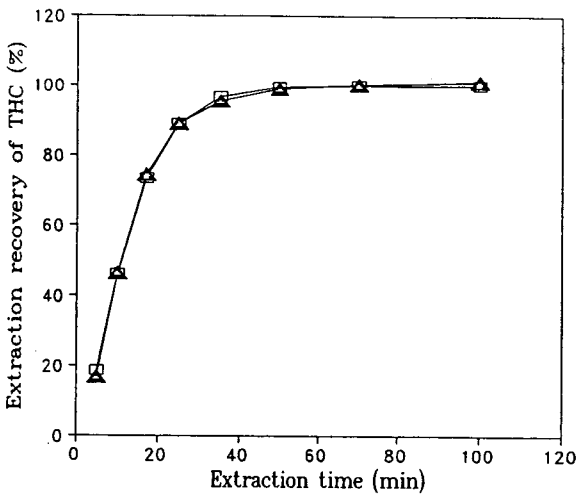

Fig. 1. Typical plot of extraction recovery of THC *versus* extraction time. For extraction conditions, see text. ▲ = Measured; □ = calculated.

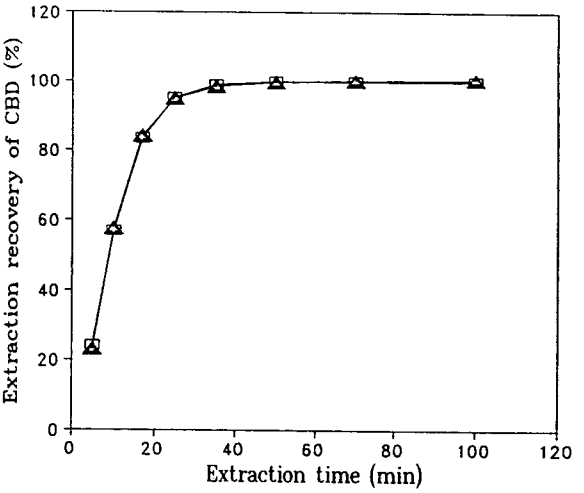

Fig. 2. Typical plot of extraction recovery of CBD *versus* extraction time. For extraction conditions, see text. ▲ = Measured; □ = calculated.

In order to determine the term β in Eq. 4, required for the calculation of the extraction time needed for a predefined level of extraction recovery, the experimental data were fitted to Eq. 4 by using the SigmaPlot software. The calculated results for six marihuana and two hashish samples are given in Table 1, together with the standard deviations of the calculated β values. The good quality of the curve fitting can

Table 1
β Values of THC and CBD, calculated[a] according to Eq. 4 and their standard deviations for six marihuana and two hashish samples

Sample	No.	β_{THC} (min^{-1})	β_{CBD} (min^{-1})
Marihuana	1	0.168 ± 0.005	0.280 ± 0.006
	2	0.118 ± 0.003	0.172 ± 0.004
	3	0.118 ± 0.003	0.176 ± 0.003
	4	0.100 ± 0.003	0.152 ± 0.002
	5	0.124 ± 0.004	0.191 ± 0.003
	6	0.119 ± 0.007	0.170 ± 0.009
Hashish	1	0.243 ± 0.011	0.347 ± 0.007
	2	0.229 ± 0.009	0.363 ± 0.008

[a] Number of data pairs used for the calculation = 8.

be observed in Figs. 1 and 2, where the recoveries recalculated according to eq. 4 by using the β values are very close to data obtained experimentally. It can be seen in Table 1 for both THC and CBD that the β values for hashish samples are nearly double those for marihuana samples. The higher β values obtained for hashish samples mean that the transfer of cannabinoids from hashish to the extraction fluid is faster than that from marihuana. This finding can easily be understood by considering that hashish is a preseparated material, which consists mainly of resinous matrix obtained from the surface of the plant, whereas marihuana is a plant material containing resin with compounds to be extracted both inside and outside the plant. As the same compounds were extracted under the same extraction conditions from different matrices, the differences between the calculated β values are obviously due to the different matrix effects, so β mirrors the effect of the matrix. According to the data in Table 1, it can also be seen that the β values for CBD are higher than those for THC, indicating that supercritical carbon dioxide dissolves CBD more effectively than THC.

The relative standard deviation of the β values calculated by using data obtained from five parallel extractions of a marihuana sample did not exceed 9%.

In Table 2 the calculated extraction times required to reach 95% and 99% recoveries of cannabinoids are shown for the samples listed in Table 1. The calculation was done according to Eq. 4 for each sample by using the β values given in Table 1. It can be seen in Table 2 that 95% of THC can be extracted from most of the marihuana samples within 30 min, whereas a 99% recovery requires about 45 min. The corresponding extraction times for CBD are *ca.* 20 and 30 min, respectively. Owing to the high β values for hashish samples, the cannabinoid

Table 2
Calculated extraction times required for 95% and 99% recoveries of THC and CBD according to Eq. 4 using β values listed in Table 1

Sample	No.	Extraction time (min)			
		THC		CBD	
		95% Recovery	99% Recovery	95% Recovery	99% Recovery
Marihuana	1	22	32	16	22
	2	29	43	22	31
	3	29	43	21	31
	4	34	50	24	34
	5	28	41	20	29
	6	29	43	22	31
Hashish	1	17	24	14	20
	2	18	25	14	19

content can be extracted exhaustively within 30 min. The shorter extraction time for hashish compared with marihuana is in accordance with the previous considerations regarding the matrix quality.

4.1. Recovery experiments

The results of recovery experiments at different levels of added cannabinoids are given in Table 3. It can be seen that for levels of added cannabinoids >100 μg the recovery is 95–98%, whereas with a level of *ca.* 40 μg the recovery is only 90–91%. The lower recovery in the lower concentration range might be due to the constant error probably caused by the irreversible adsorption inside the extraction system, which causes a higher relative error in the lower than in the higher concentration range.

The β values calculated according to Eq. 4 using the experimental data obtained from the sequential extraction of spiked samples for different times are higher by a factor of 5 than those listed in Table 1, *e.g.*, $\beta_{THC} = 0.538$ min^{-1} and $\beta_{CBD} = 1.081$ min^{-1}. These significant differences between β values obtained for spiked and non-spiked natural samples indicate that the mass transfer of cannabinoids from spiked samples to the extraction fluid is quicker than that from natural samples. A possible explanation of this phenomenon could be that by spiking the cannabinoid-free blank marihuana with solutions of cannabinoids the compounds cannot be placed in the same matrix environment as the original non-spiked sample. Consequently, the interactions between the added compounds and the matrix differ from those acting in the original sample, resulting in a change in the kinetics of component transport. According to these results, it should be noted that the determination of systematic errors of the extraction procedure must not be based on measurements of spiked samples.

Table 3
Recoveries and standard deviations[a] obtained for extractions of spiked marihuana

THC		CBD	
Spiked amount (μg)	Recovery (%)	Spiked amount (μg)	Recovery (%)
40	90 ± 12	45	91 ± 9
122	97 ± 6	131	97 ± 7
376	98 ± 5	420	95 ± 6
581	97 ± 5	611	97 ± 4

For the extraction conditions, see text.
[a] Number of parallel measurements = 5.

5. Conclusions

The elaborated mathematical model based on the diffusion-layer theory is suitable for the description of the concentration profile of dynamic supercritical fluid extraction using pure carbon dioxide as the extraction fluid. According to the model the extraction times to extract either 95% or 99% of the main neutral cannabinoids from hashish and marihuana samples were calculated. The extraction times calculated for six different marihuana samples were scattered with a relative standard deviation of more than 10%, which indicates that the matrix has a significant effect on the extraction recovery. According to the equation describing the concentration profile of dynamic SFE, the effect of the matrix is taken into account by the term β. As β is a constant regarding the analyte transport from the matrix to the fluid, the magnitude of β represents the effect of matrix quality on the extraction recovery, *e.g.*, under constant extraction conditions the higher is β the greater is the extraction recovery per unit time. These previous statements were experimentally verified for hashish and marihuana samples; for hashish samples the β values obtained were nearly double those for marihuana samples, indicating that owing to the different matrix effects of marihuana and hashish the transport of cannabinoids from hashish to the extraction fluid is faster than that from marihuana. According to the experimental results obtained for hashish and marihuana, it can be seen that an increase in β by a factor of two resulted in a decrease in the time required for extraction by *ca.* 30%. Because

the quality of the sample matrix might be different from sample to sample, in order to obtain reliable quantitative results the extraction time should be calculated for each individual sample according to the model. The systematic error caused by the unextracted proportion of the analyte can then be eliminated by the correction of the experimental data. It was also found in the extraction of cannabinoids that the determination of systematic errors of the extraction procedure must not be based on measurements of spiked samples because by spiking blank matrices with the analytes to be extracted the compounds cannot be placed in the same matrix environment as the original non-spiked sample.

For semi-quantitative determinations, where the correct value of the extraction recovery is not of interest, as a rule of thumb the extraction of marihuana with carbon dioxide of density 0.9 g/ml at 40°C for 34 min and of hashish for 18 min can be suggested. The application of the proposed extraction times ensured at least a 95% recovery of the main neutral cannabinoids.

It should be emphasized that for application of the proposed procedure to unknown samples, the appropriate extraction conditions should previously be determined experimentally to ensure the dissolution of the analyte from the given matrix. Then the concentration profile of the extraction should be determined experimentally and the β value should be calculated by using the experimental data as described previously. The validity of the model for the actual extraction system should be checked either graphically or by other methods (*e.g.*, by analysis of residuals). For a valid model the calculated β value can be used to determine the extraction time required to reach a predefined level of recovery.

As the samples of natural origin have different matrix qualities with unknown composition and with unknown interactions between the matrix components, the extraction conditions required for a particular level of recovery cannot be predicted theoretically. Therefore, the steps of the developed procedure described above should be followed for each individual sample in order to obtain reliable quantitative results.

6. References

[1] T.P. Zhuze, G.N. Jushkevich and J.E. Gekker, *Maslo-Zhir. Promst.*, 24 (1958) 34.
[2] E. Stahl and W. Schilz, *Talanta*, 26 (1979) 675.
[3] M.R. Andersen, J.T. Swanson, N.L. Porter and B.E. Richter, *J. Chromatogr. Sci.*, 27 (1989) 371.
[4] T.S. Oostdyk, R.L. Grob, J.L. Snyder and M.E. McNally, *Anal. Chem.*, 65 (1993) 596.
[5] J.C. Giddings, M.N. Myers, L. McLaren and R.A. Keller, *Science*, 162 (1968) 67.
[6] J.J. Langenfeld, S.B. Hawthorne, D.J. Miller and J. Pawliszyn, *Anal. Chem.*, 65 (1993) 338.
[7] S.B. Hawthorne, *Anal. Chem.*, 62 (1990) 633A.
[8] W. Pipkin, *LC·GC Int.*, 5, No. 1 (1992) 8.
[9] J. Chrastil, *J. Phys. Chem.*, 86 (1982) 3016.
[10] M.L. Lee and K.E. Markides (Editors), *Analytical Supercritical Fluid Chromatography and Extraction*, Chromatography Conferences, Provo, UT, 1990, p. 324.
[11] A.B. Newman, *Trans. Am. Inst. Chem. Eng.*, 27 (1931) 203.
[12] W. Nerst, *Z. Phys. Chem.*, 47 (1904) 52.
[13] E. Brunner, *Z. Phys. Chem.*, 47 (1904) 56.
[14] D.J.W. Grant and T. Higuchi, in A. Weisberger and W.H. Saunders (Editors), *Solubility Behavior of Organic Compounds*, Wiley, Toronto, 1990, p. 478.
[15] C.E. Turner, *Marihuana Research Findings: 1980*, National Institute on Drug Abuse, Rockville, MD, 1980, p. 81.
[16] T. Veress, J.I. Szántó and L. Leisztner, *J. Chromatogr.*, 520 (1990) 339.

ELSEVIER

Journal of Chromatography A, 668 (1994) 293–299

JOURNAL OF CHROMATOGRAPHY A

Influence of eluent composition on retention and selectivity of alkylamide phases under reversed-phase conditions

B. Buszewski[☆], M. Jaroniec*, R.K. Gilpin

Department of Chemistry, Kent State University, Kent, OH 44242, USA

Abstract

The sorption properties of alkylamide phases have been studied under reversed-phase conditions using different compositions of methanol–water as eluents. These studies have revealed that the specific structural properties of the alkylamide phases have a greater influence on solute retention and selectivity than is observed for conventional alkyl bonded phases. Also, it has been demonstrated that the composition of solvents in the stationary phase can be changed significantly by the presence of a specific interaction site in the bonded ligands.

1. Introduction

A variety of chemically bonded phases (CBP) have been used as packing materials in reversed-phase high performance liquid chromatography (RP-HPLC) [1–3]. Their selectivity is determined by many factors, such as: chemical nature of bonded ligands, their coverage density, and surface properties of the solid support. These factors influence strongly the retention mechanism and selectivity of chemically bonded phases under RP-HPLC conditions [4–6].

In many of the earlier RP-HPLC models it was assumed that the retention mechanism was controlled by the specific and nonspecific solute–solvent interactions in the mobile phase, whereas the bonded alkyl chains were passive acceptors of the solute [7,8]. Recent studies of chemically bonded phases, especially phases of specific functionality and structural properties [9–11], have shown that the type, structure and density of the CBP are important factors which control the solute's retention. Moreover, it has been suggested that alkylamide (AA) phases with incorporated solvent molecules have a more ordered structure than conventional alkyl phases [11].

Homologs are often used as test solutes to evaluate the relative hydrophobicity of different CBPs under RP-HPLC conditions [12–14]. The nonspecific or hydrophobic selectivity for adjacent members in a homologous series is defined as follows:

$$\alpha_c = k'_{n+1}/k'_n \quad (1)$$

where k'_{n+1} and k'_n are respectively the capacity factors for solutes with $n+1$ and n carbon atoms in their alkyl chains [12]. In many cases the natural logarithm of α_c is nearly constant over a range of homolog pairs were steric effects do not

* Corresponding author.

☆ Permanent address: Department of Chemical Physics, Faculty of Chemistry, Maria Curie-Sklodowska University, Pl-20 031 Lublin, Poland.

0021-9673/94/$07.00
SSDI 0021-9673(93)E1090-M

play a role [12]. Further, the $\ln \alpha_c$ is proportional to the free energy of transfer of a methylene group ($-CH_2-$) between the mobile and stationary phases [6,13] and it can be determined from the slope of the plot of $\ln k'_n$ *vs.* n_c measured at a constant composition of hydro–organic mobile phase:

$$s = d(\ln k'_n)/dn_c = \ln \alpha_c \quad (2)$$

For binary mixtures of water–methanol the dependence of s on the volume fraction of water (φ_w^1) is nearly linear over the entire range of solvent compositions [12,13,15–22]. However, for other hydro–organic mobile phases (*e.g.* water–acetonitrile, water–tetrahydrofuran, water–isopropanol, etc.) the plots of s *vs.* φ_w^1 are non-linear [15–22].

In the current work, chemically bonded alkylamide phases were studied under reversed-phase conditions using different compositions of methanol–water as the eluent. These studies have revealed that the specific and structural properties of the alkylamide phases have a greater affect on the solute's retention and selectivity than is observed for conventional alkyl bonded phases. The sorption properties of the alkylamide phases were evaluated on the basis of retention measurements for alkylbenzene homologs. It has been shown that the composition of solvents in the stationary phase can be changed significantly by the presence of a specific interaction site in the bonded ligands.

2. Experimental

2.1. Materials

LiChrospher Select B (Merck, Darmstadt, Germany) with a mean particle diameter of 5 μm and with a BET specific surface area (S_{BET}) of 570 m^2/g has been used to prepare the chemically bonded phases. Two types of packings were synthesized: conventional C_{18} phases and alkylamide (AA) phases with alkyl chains of different length ($-CH_3$, $-C_5H_{11}$ and $-C_{17}H_{35}$). The AA phases were synthesized in a sealed glass reactor by a two-step process [9–11], in which an initial aminopropyldimethylsilyl phase was prepared under environmentally isolated conditions and subsequently reacted with either acetyl, hexanoyl and stearoyl chlorides. For instance, the amino phase modified with acetyl chloride contain the following bonded ligands: $-Si(CH_3)_2 - CH_2 - CH_2-CH_2 - NH - CO - CH_3$ (methylamide chains) and $-Si(CH_3)_2-CH_2-CH_2-CH_2-NH_2$ (aminopropyl residuals). In addition, each silica-based chemically bonded phase contains unreacted surface silanols. Listed in Table 1 are the coverage data for the materials based on elemental carbon and nitrogen analysis. Additional information (obtained from solid-state NMR, porosimetry and secondary-ion mass spectrometry) about these packings as well as the unmodified silica have been reported elsewhere [10,11].

Solvents

Methanol and acetonitrile (HPLC grade purity) were purchased from Fisher Scientific (Fairlawn, NJ, USA). The hydro–organic mobile phases were prepared from deionized water purified in-house using a Milli-Q reagent water system (Millipore, El Paso, TX, USA).

Table 1
Surface coverages of the aminopropyl ($SG-NH_2$), alkylamide (AA) and octadecyl (C_{18}) phases

Phase	R [a]	Total %C	c_{RP} [b]	c_{NH_2} [c]
$SG-NH_2$	–	6.9	–	2.33
AA_1	$-CH_3$	8.3	1.38	0.95
AA_2	$-C_5H_{11}$	9.9	0.98	1.35
AA_3	$-C_{17}H_{35}$	19.7	1.59	0.74
C_{18}	$-C_{18}H_{37}$	23.2	2.42	–

For the AA phases c_{RP} denotes only the concentration of alkylamide ligands and c_{NH_2} represents the concentration of unreacted (residual) aminopropyl groups; the total coverage density is the sum of the surface concentrations of alkylamide ligands and aminopropyl residuals. Note that for the aminopropyl phase c_{NH_2} denotes the total coverage density because this phase has only one type of bonded ligands.

[a] R-alkyl chain attached to the amide group.

[b] c_{RP}-concentration of bonded alkyl-ended ligands expressed in [$\mu mol/m^2$].

[c] c_{NH_2}-concentration of aminopropyl groups expressed in [$\mu mol/m^2$].

The modified materials were packed into 60 × 2.1 mm I.D. stainless-steel tubes purchased from Supelco (Bellefonte, PA, USA) according to procedures described elsewhere [3,4].

2.2. Chromatographic studies

Retention measurements were carried out at 298 K using a liquid chromatograph which consisted of a Spectra-Physics (San Jose, CA, USA) Model SP-8810 precision isocratic pump, a Model Spectra 100 variable UV detector (λ = 254 nm), and a Chromjet integrator. Solutes were injected using a Rheodyne (Berkeley, CA, USA) Model 7125 sampling valve with 20-μl sample loop. In all chromatographic investigations the flow rate (1 ml/min) was monitored with a Phase Separations (Queensberry, Clwyd, UK) Model FLOSO A1 flow meter connected to the detector outlet.

3. Results and discussion

Shown in Figs. 1 and 2 are the retention data for the alkylbenzenes plotted as the natural logarithm of the capacity ratio (k') *vs.* the number of carbon atoms (n_c) in the chain segment of the solute. These data were measured on both the alkylamide and C_{18} phases (*cf.*, Table 1) using different mixtures of water–methanol as the mobile phase. The ($\ln k'$ *vs.* n_c) dependencies for the AA_1, AA_2 and AA_3 phases are presented in Figs. 1a, 1b and 1c, respectively, and the data for the C_{18} phase are plotted in Fig. 2. Except for the data shown in Fig. 1a for the totally aqueous conditions, the remaining Figs. contain a series of ($\ln k'$ *vs.* n_c) plots measured for different compositions of the binary mobile phase.

A comparison of the plots presented in Figs. 1 and 2 shows that their slopes change systematically with the composition of the mobile phase. In all cases the dependence of $\ln k'$ on the number of carbon atoms in alkyl chain of the successive homologs is linear as has been reported [12,13,15–22]. For the longer alkylamide phases the retention data could be measured

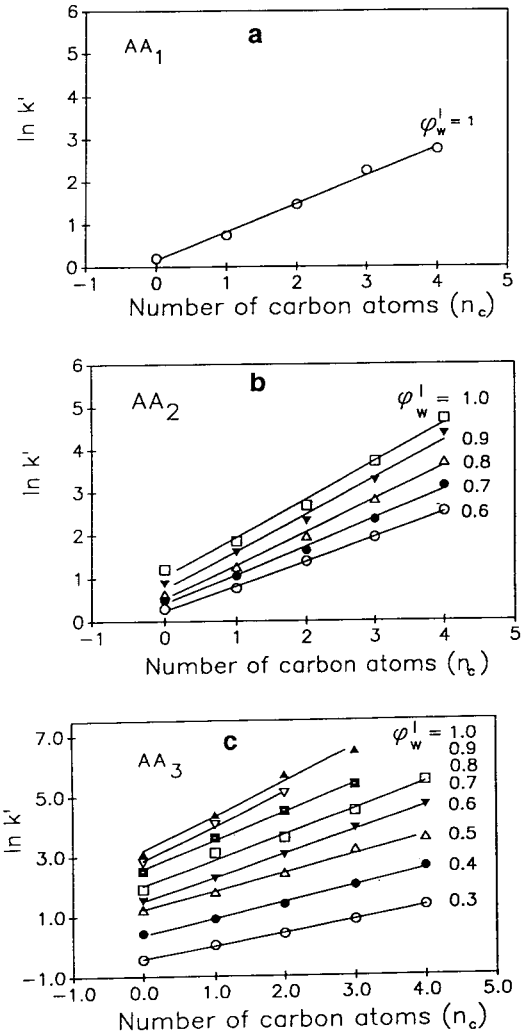

Fig. 1. Experimental dependencies of the natural logarithm of the capacity ratio ($\ln k'$) on the number n_c of carbon atoms in the alkyl chain of homologous alkylbenzenes in the water–methanol mobile phase on (a) AA_1, (b) AA_2 and (c) AA_3 packings at 298 K measured at different volume fractions of water in the mobile phase.

over a wider range of the mobile phase concentrations. For example, a satisfactory separation of alkylbenzenes could be achieved on the methylamide phase with almost totally aqueous eluents, whereas in the case of the longer AA phases the same solutes were separable over a wide range of the mobile phase concentrations. The length of alkyl chain in the bonded

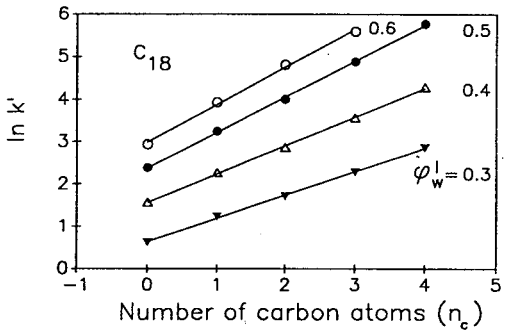

Fig. 2. Experimental dependencies of the natural logarithm of the capacity ratio ($\ln k'$) on the number n_c of carbon atoms in the alkyl chain of homologous alkylbenzenes in the water–methanol mobile phase on the C_{18} packing at 298 K measured at different volume fractions of water in the mobile phase.

alkylamide ligands had a significant influence on the methylene selectivity (defined by the slope of the $\ln k'$ *vs.* n_c plot, which characterizes quantitatively the separation of homologue solutes).

The slopes of the linear dependencies shown in Figs. 1 and 2 were plotted against the volume fraction of water in the mobile phase, φ_w^l (*cf.*, Fig. 3). Unfortunately, construction of the (*s vs.* φ_w^l) plot for the AA_1 packing was impossible because the alkylbenzenes could be separated only over a very limited concentration range of the mobile phases (*i.e.*, $\varphi_w^l \sim 1$). It can be seen from Fig. 3 that the relationships between *s* and φ_w^l were linear for both the AA and C_{18} phases when water–methanol mobile phases were used. These results agree with earlier reports on the

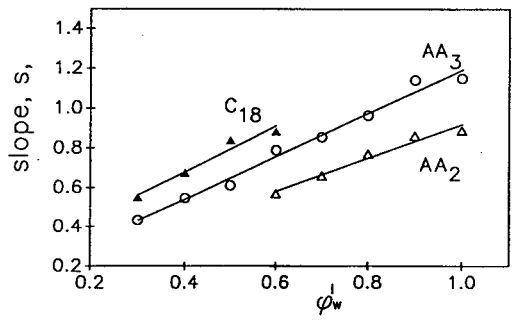

Fig. 3. The natural logarithm of the methylene selectivity plotted against the volume fraction of water in water–methanol eluent for the AA and C_{18} phases at 298 K.

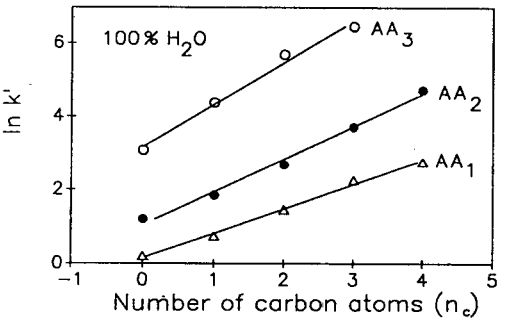

Fig. 4. Experimental dependencies of the natural logarithm of the capacity ratio ($\ln k'$) on the number n_c of carbon atoms in the alkyl chain of homologous alkylbenzenes for 100% water on the AA packings at 298 K.

concentration dependence of the methylene selectivity [12,13,15–22].

The (*s vs.* φ_w^l) plots shown in Fig. 3 were used to estimate the *s* value under fully aqueous conditions (*i.e.*, the s_w value). The quantity s_w was determined graphically by linear extrapolation of the (*s vs.* φ_w^l) plot to the volume fraction $\varphi_w^l = 1.0$. In contrast to the C_{18} phase, the s_w values for the AA phases could be evaluated from the ($\ln k'$ *vs.* n_c) plots measured under fully aqueous conditions (*cf.*, Fig. 4). The extrapolated values of s_w are summarized in Table 2 as well as the s_w values measured using 100% water. As can be seen from Table 2, the extrapolated and measured values of s_w for the AA phases differ only about 3%.

A comparison of the data summarized in Table 2 shows that the s_w values for the AA phases with short alkyl chains are smaller than those for the C_{18} packings. Moreover, the s_w

Table 2
Values of K_{wo} and s_w for the systems studied

Phase	K_{wo}	$s_{w(ext)}$ [a]	$s_{w(me)}$ [b]
AA_1	–	–	0.66
AA_2	4.13	0.92	0.89
AA_3	0.87	1.19	1.15
C_{18}	0.81	1.38	-
C_{18} [c]	1.08	1.19	-

[a] $s_{w(ext)}$ denotes extrapolated s_w-values.
[b] $s_{w(me)}$ denotes measured s_w-values.
[c] Data from ref. 21.

values for the AA phases increase with increasing length of the alkyl chain attached to the amide group. Thus, either an extension of the bonded ligands hydrophobic segments and/or an increase in the coverage density of the alkyl ligands increases the probability of the non-specific methylene–ligand interactions, which results in an increase in the s_w value. In addition, differences in the conformational behavior of the bonded ligands and their ability to screen the residual silanols and aminopropyl groups alter the chain–chain interactions. For instance, an increase in the concentration of alkyl bonded ligands (compare the C_{18} phases in Table 2) reduces the total number of residual silanols which causes an increase in the s_w value. In the case of AA phases an increase in the concentration of alkylamide ligands reduces the total number of residual aminopropyl groups (c_{NH_2}), however, the amount of residual silanols is not changed. A change in the ratio of alkylamide ligands to residual aminopropyl groups can change both the structure and composition of the stationary phase. Alkylamide and aminopropyl ligands as well as residual silanols control the intercalation (competitive sorption) process of solvent molecules into the chemically bonded phase, which alter their physicochemical properties.

If the s_w value is known, the methylene selectivity data shown in Fig. 3 can be plotted against the ratio of the volume fractions of water and methanol in the mobile phase [19,21]:

$$(s_w - s)^{-1} = (s_w - s_o)^{-1} + K_{wo}\,(s_w - s_o)^{-1}\,\varphi_w^1/\varphi_o^1 \quad (3)$$

where K_{wo} is the equilibrium constant that describes the displacement process between molecules of water and organic solvent for ideal mobile and surface phases, and s_w represents a hypothetical methylene increment which characterizes retention for the pure aqueous mobile phase. According to Eq. 3, which was derived by assuming a partition–displacement model for the solute's retention [22,23], the dependence of $(s_w - s)^{-1}$ on the $(\varphi_w^1/\varphi_o^1)$ ratio should be linear. Fig. 5 demonstrates that Eq. 3 is a good representation of the selectivity data measured on the AA and C_{18} phases. From the slopes of the linear dependencies shown in Fig. 5 the K_{wo} equilibrium constants can be calculated for the phases studied; K_{wo} characterizes the competitive sorption of water and methanol into the chemically bonded phase. The K_{wo} values for the systems studied are summarized in Table 2. For purposes of comparison, the values of K_{wo} and s_w reported in ref. 21 for the LiChrosorb Si-60 with a specific surface area of 550 m^2/g and modified with the low-density C_{18} phase (the carbon loading was 11.1%) are included.

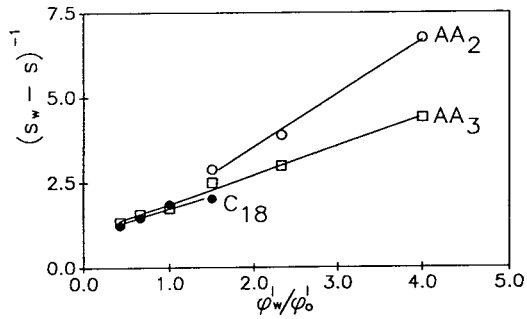

Fig. 5. Dependence of $(s_w - s)^{-1}$ on φ_w^1/φ_o^1 for alkylbenzenes chromatographed in the water–methanol mobile phases on the AA and C_{18} columns at 298 K.

The K_{wo} values summarized in Table 2 provide information about the composition of solvents that are incorporated into the stationary phase. In the case of the octadecyl phases the K_{wo} values decrease with increasing carbon loading, *e.g.*, $K_{wo} = 1.08$ for the C_{18} phase with 11.1% C and 0.81 for the phase with 23.2% C. Based on the model of competitive adsorption for ideal solutions on energetically homogeneous solids [23], when $K_{wo} > 1$ water is preferentially intercalated into the bonded phase, whereas for $K_{wo} < 1$ organic solvent is preferentially sorbed. Thus, since for the high coverage density C_{18} packing the K_{wo} value is smaller than unity, the data indicate that methanol is preferentially intercalated into the chemically bonded phase. However, the preferential sorption of water can occur for octadecyl phases with lower coverage densities.

A comparison of the K_{wo} values for the

alkylamide and octadecyl phases with similar carbon loadings show that although methanol is preferentially intercalated into both these phases, its sorption is slightly smaller for the AA_3 packing. The later effect is probably due to the presence of the specific interaction site in alkylamide phases, which has a stronger interaction with water molecules. It is logical to expect that this effect should be greater in the case of the AA_2 phase, which contains a shorter (C_5H_{11}) alkyl chain attached to the amide group; for this phase $K_{wo} = 4.13$.

The K_{wo} values calculated using Eq. 3 refer to an ideal stationary phase, the composition of which is described by the following relationship [20,21]:

$$\varphi_w^\sigma = \frac{K_{wo}\varphi_w^l}{\varphi_o^l + K_{wo}\varphi_w^l} \quad (4)$$

Eqn. 4 expresses the volume fraction (φ_w^σ) of water in the stationary phase in terms of the mobile phase's composition (*i.e.*, the volume fraction of water in the mobile phase, φ_w^l). Since Eq. 4 was derived for ideal phases, it does not predict an azeotropic point on the excess sorption isotherm (*i.e.*, the value of the volume fraction, φ_w^l, at which $\varphi_w^\sigma = \varphi_w^l$). The probability for azeotropic behavior is greater for systems with K_{wo} close to unity and has been reported for alkyl bonded phases in contact with water–methanol eluents [18,21].

Shown in Fig. 6 are the individual sorption isotherms of water on the AA_2, AA_3 and C_{18} phases calculated using Eq. 4. In the case of the C_{18} and AA_3 phases, the sorption excesses of water in the stationary phase (which are proportional to $\varphi_w^\sigma - \varphi_w^l$), are similar and both are negative. Thus, the excess of sorbed methanol in the stationary phase must be positive because the sum of the excesses for all compounds must be equal to zero [23]. In contrast to the AA_3 phase, the sorption excess of methanol for the AA_2 packing was negative. In addition, for the AA_2 packing the difference in the compositions of solvents in the stationary and mobile phases is much greater than that for the C_{18} and AA_3 phases.

A significant excess of water in the AA phases with short alkyl chains strongly affects their chromatographic selectivity (*cf.*, Fig. 7). Shown in Fig. 7 are separations of derivatives of aniline under totally aqueous conditions on the AA phases. The best resolution between individual peaks was obtained for the AA phases with longer alkyl chains, *i.e.*, for the AA_3 and AA_2 packings. However, an extension of the alkyl chain resulted in an increase in the analysis time. Thus, the alkylamide phases with medium length alkyl chains seem to be especially attractive for separation of polar compounds such as amines and amides. An advantage of the AA phases in comparison to the conventional alkyl packings is

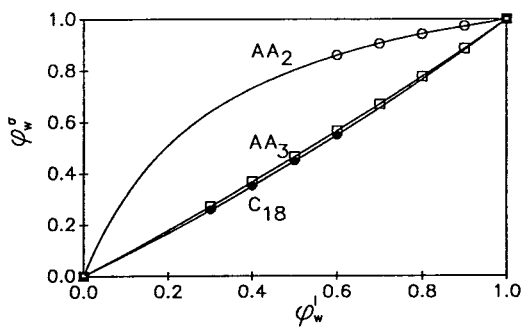

Fig. 6. Dependence between the volume fractions of water in the stationary and mobile phases for the AA and C_{18} packings at 298 K.

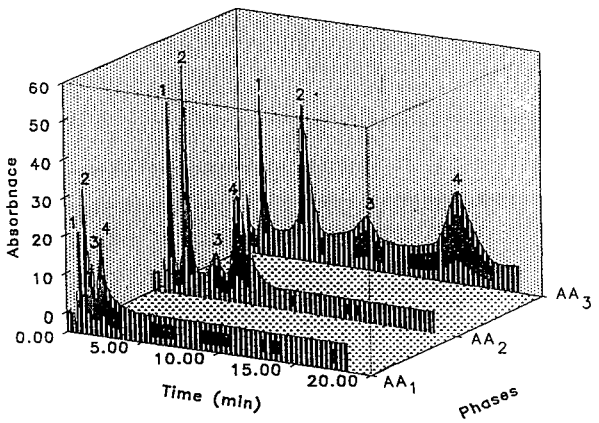

Fig. 7. Separations of alkylanilines under fully aqueous conditions on the AA phases at 298 K. Peaks: 1 = aniline, 2 = methylaniline, 3 = dimethylaniline and 4 = diethylaniline.

that good resolution can be achieved under fully aqueous conditions. A possible important use for such packings is to separate biomolecules such as: peptides, polypeptides and proteins.

4. Acknowledgement

This work was supported by U.S. Army Research Office, grant No. DAAL 03-90-G-0061.

5. References

[1] L.C. Sander and S.A. Wise, *CRC Crit. Rev. Anal. Chem.*, 18 (1987) 299.
[2] K.K. Unger, *Packings and Stationary Phases in Chromatographic Techniques*, Marcel Dekker, New York, 1990.
[3] B. Buszewski, *Preparation, Properties and Application of Chemically Bonded Phase in Chromatographic Analysis*, Sc.D. Thesis, Slovak Technical University, Bratislava, 1992.
[4] B. Buszewski, Z. Suprynowicz, P. Staszczuk, K. Albert, B. Pfleiderer and E. Bayer, *J. Chromatogr.*, 499 (1990) 305.
[5] J.G. Dorsey and K.A. Dill, *Chem. Rev.*, 59 (1989) 331.
[6] M. Jaroniec, *J. Chromatogr.*, 656 (1993) 37.
[7] H. Colin, G. Guiochon and P. Jandera, *Chromatographia*, 17 (1983) 83.
[8] P. Jandera, *J. Chromatogr.*, 314 (1984) 13.
[9] B. Buszewski, J. Schmid, K. Albert and E. Bayer, *J. Chromatogr.*, 552 (1991) 415.
[10] B. Buszewski, R.K. Gilpin and M. Jaroniec, *44th Pittsburgh Conference on Analytical Chemistry and Applied Spectroscopy, Atlanta, GA, 1993*, Abstracts, p. 477bP.
[11] B. Buszewski, P. Staszczuk, M. Jaroniec and R.K. Gilpin, *17th International Symposium on Column Liquid Chromatography, Hamburg, Germany, 1993*, Abstracts, p. I-176.
[12] H. Colin, G. Guiochon, Z. Yun, J.C. Diez-Masa and P. Jandera, *J. Chromatogr. Sci.*, 21 (1983) 179.
[13] P.C. Sadek, P.W. Carr and M.J. Ruggio, *Anal. Chem.*, 59 (1987) 1032.
[14] S. Héron and A. Tchapla, *Chromatographia*, 36 (1993) 11.
[15] B.P. Johnson, M.G. Khaledi and J.G. Dorsey, *J. Chromatogr.*, 384 (1987) 221.
[16] J.G. Dorsey and B.P. Johnson, *J. Liq. Chromatogr.*, 10 (1987) 2695.
[17] B.L. Karger, J.R. Gant, A. Hartkopf and P.H. Weiner, *J. Chromatogr.*, 128 (1976) 65.
[18] R.K. Gilpin, M. Jaroniec and S. Lin, *Anal. Chem.*, 62 (1990) 2092.
[19] R.K. Gilpin, M. Jaroniec and S. Lin, *Chromatographia*, 30 (1990) 393.
[20] M. Jaroniec, S. Lin and R.K. Gilpin, *Chromatographia*, 32 (1991) 13.
[21] R.K. Gilpin, M. Jaroniec and S. Lin, *Anal. Chem.*, 63 (1991) 2849.
[22] M. Jaroniec and R.K. Gilpin, *J. Liq. Chromatogr.*, 15 (1992) 1431.
[23] M. Jaroniec and R. Madey, *Physical Adsorption on Heterogeneous Solids*, Elsevier, Amsterdam, 1988.

ELSEVIER

Journal of Chromatography A, 668 (1994) 301–312

JOURNAL OF CHROMATOGRAPHY A

Characterization of stationary phases used in reversed-phase and hydrophobic interaction chromatography

Géza Rippel*[,a], Edit Alattyani[a], László Szepesy[b]

[a]Department of Agricultural Chemical Technology, Technical University of Budapest, H-1521 Budapest, Hungary
[b]Department of Chemical Technology, Technical University of Budapest, H-1521 Budapest, Hungary

Abstract

Nine prepacked columns used in reversed-phase and in hydrophobic interaction chromatography were studied. The stationary phases investigated were widely different with respect not only to the type and surface concentration of the ligands but also to the material and geometry of the support and the extent of previous usage. In order to characterize the columns, measurements were made under isocratic conditions with three different homologous series. From the retention behaviour of the components some descriptors were calculated according to four characterization methods described in the literature. On the basis of the intercept of the ln k–methanol content relationship, a rough estimate of the hydrophobicity of the stationary phases could be given. More realistic results were obtained with the polar–apolar characterization suggested by Hetem and co-workers, but some discrepancies were also found. The use of the isopotential eluent composition as a descriptor resulted in the most acceptable characterization. Two-dimensional mapping along the parameters of the slope–intercept relationships summarizes the results obtained with the other techniques.

1. Introduction

With continuing developments in high-performance liquid chromatography (HPLC), an increasing variety of stationary phases are commercially available. Improvements are aimed at increasing the selectivity and the efficiency of the columns, but the number of the tailor-made stationary phases suitable for specific separations is also increasing [1,2]. The most commonly used technique in routine laboratory practice is reversed-phase liquid chromatography (RPLC), which is usually performed with n-octadecyl-modified silica packings. As the ligands are chemically bonded to the surface of the support, these packings are stable with time, providing selective and reproducible separations. With a better understanding of the phenomenon of "selectivity" in RPLC practice and the need for sophisticated and fully optimized solutions to separation problems [3–5], interest in RP stationary phases with various type of ligands and geometry has grown. Even if only these "reversed-phase-like" packings are considered, the number of the applicable columns is tremendous and the choice amongst them is not at all straightforward.

The separation of biologically active compounds, especially proteins, needs stationary phases of different types. The ligands in RPLC packings are very hydrophobic and are distributed very densely. The interaction between the proteins and the stationary phase is strong, and addition of an organic modifier is therefore

* Corresponding author.

0021-9673/94/$07.00
SSDI 0021-9673(93)E1274-4

needed for elution. As a consequence of these conditions, dehydration, conformational changes, partial or complete unfolding of the components and significant losses of amount and biological activity could occur [6–8]. For the separation of proteins, hydrophobic interaction chromatography (HIC) is an alternative to RPLC. The functional groups in HIC packings are less hydrophobic and their surface concentration is low, producing moderately hydrophobic stationary phases and mild hydrophobic interactions. Protein-stabilizing salts are used to promote the retention, and protein purity can therefore be obtained while retaining the biological activity [6,9–13]. More recently, a wide variety of stationary phases suitable for HIC have become available [1,2,14]. The selection of the most applicable packing material for a certain protein separation is even more difficult than in RPLC as the HIC columns have greater diversity as regards type and geometry of the support and the ligands.

It is well known that the retention of a solute measured at a specific mobile phase composition varies widely between stationary phases having the same type of ligands but originating from different manufacturers [15,16]. Even packings from the same source differ between batches of the same material [17]. Several reasons for these batch-to-batch variations have been given. One of the major causes is the regions of the support uncovered by the ligands which can also interact with the solutes, *i.e.*, the retention can be greatly affected by the properties of the accessible parts of the support [18]. This means that preliminary characterization of the stationary phases is necessary when new columns are to be used or when the possibilities of new types of columns are investigated.

To study the properties of chemically bonded phases, a broad range of characterization techniques have been reported. These procedures can be divided into two categories: non-chromatographic and chromatographic methods. The techniques belonging to the first group were summarized, discussed and investigated by Claessens *et al.* [19] and Hetem and co-workers [20–22], so here only a brief summary is given. These methods can be further subdivided.

(i) The determination of bulk properties such as specific surface area, volume and size distribution of the pores and of the particles. The procedures applicable for the purpose (*e.g.*, BET and Coulter Counter techniques) are well known.

(ii) The characterization of the surface structure of the packing materials considering the concentration, conformation and mobility of the ligands and the structure, chemistry and accessibility of the support. The procedures could be destructive or non-destructive. In the former instance, the packing material is subjected to some modification, such as titration, chemical reactions or solvolysis, pyrolysis and fragmentation, and the reaction products are analysed so as to obtain information about the properties investigated. The latter group involves instrumental analysis such as fluorescence and infrared spectroscopy or NMR techniques of different kinds. These methods leave the packing material intact and are also suitable for direct chromatographic characterization.

The chromatographic characterization of the stationary phases utilizes the information obtained from the retention behaviour of some selected components. These methods can also be subdivided.

(i) The characterization of the efficiency properties of the packings, which reflect mainly the kinetics of the separation in a packed chromatographic bed but some physico-chemical aspects such as secondary interactions must also be considered. For commercially available columns a test chromatogram is usually provided from which some efficiency characteristics (*e.g.*, theoretical plate number, asymmetry factor) can also be calculated. However, in most instances these token chromatograms are not applicable to comparing different columns as neither the sample components nor the eluent composition are the same.

(ii) The characterization of some specific properties of the stationary phase such as silanophilic or polar capacity and hydrophobicity. On the basis of the type and number of the test components and the eluent conditions, three groups of methods can be distinguished. (a) Only a few solutes with different molecular properties

are applied, usually at one eluent composition. From the retention order of the components the polar–apolar character of the packing could be qualified [23]. (b) Homologous series are used and the behaviour of the components is modelled over a wider range of eluent composition. From the constants of the regression equations the above characteristics can be calculated (see Results and Discussion). (c) Application of retention indices: the idea of using retention indices calculated from the retention behaviour of homologous series also in RPLC originates from the well known Kováts retention indices used in gas chromatography. The aim is to obtain "phase-system-independent" retention parameters. Most of these techniques have been reviewed [24]. However, it is also revealed that the retention indices vary with the properties of the stationary phase [17] and of the eluent [25]. (Note that these procedures are transient from method (b) above to the following methods.)

(iii) Calibration of the stationary phase. Here usually a set of components are chromatographed at several eluent compositions and an abstract model of retention is built by using the techniques of multivariate data analysis such as factor analysis [26], principal component analysis [27] and related techniques [28,29]. The basic aim of this type of investigation is the accurate prediction of retention. When columns with the same or similar stationary phases are used these techniques give adequate results [26–29] but the applicability for different packing materials has not been completely revealed.

As outlined above, RPLC and HIC are the same in nature. In both techniques hydrophobic functional groups are bound to the support and the driving force of the separation, hydrophobic interaction, is considered identical. However, the features of the packings can be unique. The use of homologous series for the characterization of RPLC phases has been extensively investigated [19–22,30–34] on *n*-alkyl-modified silica substrates but we are not aware of any application for comparison of stationary phases with widely different characteristics.

In this work, homologous series were used to characterize stationary phases used in RPLC and HIC with different characteristics. First, the validity of the underlying retention models of the methods was checked, then the characterization of the columns was performed on the basis of some calculated descriptors.

2. Experimental

2.1. Materials

The test components used for characterization were all of analytical-reagent grade and were obtained from different sources: set I = benzene homologues (I): benzene (B), toluene (T), *m*-xylene (mX) and *p*-isopropyltoluene (*p*-cymene, pC); set II = dialkyl phthalates (II): dimethyl (DMP), diethyl (DEP), dipropyl (DPP) and dibutyl phthalate (DBP); set III = *n*-alkyl *p*-hydroxybenzoates (III): methyl (MP), ethyl (EP), *n*-propyl (PP) and *n*-butyl *p*-hydroxybenzoate (BP). Methanol was of reagent grade (Reanal, Budapest, Hungary). Water was freshly prepared by double distillation in the laboratory.

2.2. Columns

The characteristics of the columns used are listed in Table 1. The symbols RPLC and HIC in parentheses reflect the operational mode recommended by the manufacturers.

2.3. Chromatography

A Merck–Hitachi (Merck, Darmstadt, Germany) fully automated chromatograph was used, consisting of an L-4250 UV–Vis programmable detector operated at 254 nm, L-6200 programmable pumps and an autoinjector (Rheodyne, Cotati, CA, USA) with a 10-μl loop. System control, data acquisition and evaluation were performed with HPLC Manger software (Merck) running on an IBM PC AT-compatible computer.

Measurements were made under isocratic conditions with methanol–water mixtures. The composition of the eluent was always adapted to the components, *i.e.*, it was varied so as to obtain 5–7 retention values in the range $-1 < \ln k < 3$ for all the test components on all the

Table 1
Characteristics of the columns used

Material	Source	Ligand type	Support material	Column dimensions (mm × mm I.D.)	Particle size (μm)	Pore size (Å)	Abbreviation
LiChrospher 100 RP-8	Merck (Darmstadt, Germany)	C_8	Silica	125 × 4.0	5	100	MC8 (RPLC)
Bakerbond WP C18	J.T. Baker (Deventer, Netherlands)	C_{18}	Silica	250 × 4.6	5	300	BWP (RPLC)
LiChrospher 500 CH-8	Merck	C_8	Silica	250 × 4.0	10	500	MHB (RPLC)
Synchropak RP-4	Synchrom (Lynden, IN, USA)	C_4	Silica	250 × 4.1	6.5	300	SC4 (RPLC)
Hypersil C_8 WP-300	Shandon Southern Products (Runcorn, UK)	C_8	Silica	120 × 4.6	5	300	HPS (RPLC)
Separon Hema-BIO 1000 Phenyl	Tessek (Prague, Czech Republic)	Phenyl	HEMA[a]	80 × 8.0	10	1000	HEMA (HIC)
TSK PHENYL 5-PW	Beckman Instruments (San Ramon, CA, USA)	Phenyl	SDVB[b]	75 × 7.5	5	1000	TSK (HIC)
OR C_3-OH	Dr. Ohmacht POTE (Pécs, Hungary)	C_3-OH	Silica	250 × 4.6	6	300	OR (HIC)
Synchropak propyl	Synchrom	C_3	Silica	250 × 4.1	6.5	300	SC3 (HIC)

[a] Hydroxyethyl methacrylate.
[b] Styrene–divinylbenzene copolymer.

columns. The hold-up time was also measured at all compositions with an aqueous solution of sodium nitrite. All the measurements were repeated at least twice and the average values were used for the calculations.

3. Results and discussion

After the completion of the measurements it was immediately revealed that the RPLC and HIC columns were similar in nature. On the basis of the raw data, the columns cannot be divided into two definite sets as is done by the manufacturers, but rather they form a series regarding strength. The retention values obtained on the HEMA and TSK columns were nearly the same as those on some RPLC columns.

If the same components are used in the same eluent but on different columns, the deviations in retention should reflect the alteration of the properties of the stationary phases and therefore at a reference eluent composition comparison of the columns can be performed. In our case direct comparison cannot be performed without further evaluation as the compositions of the eluents used were not the same for the columns (see section 2.3). For such a comparison, the most straightforward selection is $\ln k_w$ ($\ln k$ extrapolated to 100% water), as this parameter is not affected by the type of organic modifier used and additionally water is the eluent that usually provides the largest differences in the retentions

of the components. Although this parameter cannot be measured in most instances, it can be calculated from the data measured.

The retention of a solute under RPLC conditions can be described as a function of the eluent composition [19–22,30–34]

$$\ln k = \ln k_w - Sx \quad (1)$$

where x is the methanol content of the eluent, ln k_w and S (constants) are the intercept and the slope of the profile, characteristic of the components and the type of the stationary and mobile phases used. Eq. 1 was fitted to the measured retention data and a very good correlation was obtained for all the components on all columns ($r > 0.998$ for RPLC and $r > 0.992$ for HIC columns), *i.e.*, the retention can be described by Eq. 1 also on the HIC columns operating under RPLC conditions.

Comparison of the columns on the basis of the calculated ln k_w values is shown in Fig. 1a–c (note that the lines in this and other figures of the same type have no physical meaning; they are used only to connect the related points). The overall picture corresponds well with the order expected from the retention data measured. The RPLC and HIC columns cannot be divided sharply, rather they form a set with gradually decreasing strength. The HEMA and TSK columns were very similar to the RPLC columns. It was also surprising that SC4 was as strong as most of the C_8 columns.

The order of the set for the RPLC columns is II > I > III, which fits the hydrophobicity of these components. For the HIC columns the order is III > II > I, *i.e.*, the retention of the most polar set is the highest, which could be an indication of the higher polarity of these stationary phases. It is also clear that the ranges spanned by the ln k_w values obtained are always wider for the RPLC columns. This means that the characterization of the columns with only this parameter is ambiguous as the order of the columns depends not only on the type of set used but also on the member of the set which is taken into account. On the other hand, the information relating to the nature of the components (homologous series) is neglected.

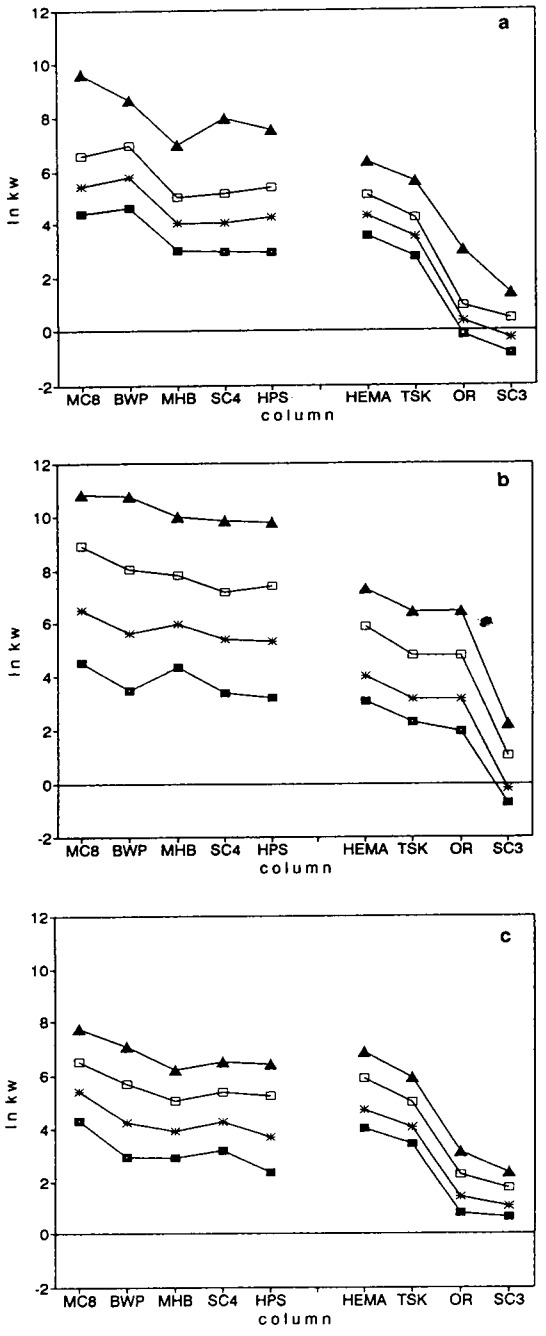

Fig. 1. Ln k_w values of the test components obtained on the different columns with (a) benzene homologues, (b) dialkyl phthalates and (c) *n*-alkyl *p*-hydroxybenzoates. (a) ■ = B; * = T; □ = mX; ▲ = pC. (b) ■ = DMP; * = DEP; □ = DPP; ▲ = DBP. (c) ■ = MP; * = EB; □ = PB; ▲ = BB (for abbreviations, see Experimental).

The characterization of apolar phases with homologous series is based on the work of Jandera [30–32] and Smith [33,34]. For such components

$$\ln k_w = a_0 + a_1 n_c \quad (2a)$$

$$S = m_0 + m_1 n_c \quad (2b)$$

and further

$$p = m_1/a_1 \quad (3a)$$

$$q = m_0 - a_0 p \quad (3b)$$

where n_c is the incremental carbon number of the homologous series and a_0, a_1, m_0 and m_1 are constants. The parameters m_0 and a_0 are the characteristic constants (slope and intercept) of the molecular residue of the homologous series ($n_c = 0$). After elimination of n_c from Eqs. 2a and 2b, we obtain

$$S = m_0 - a_0(m_1/a_1) + a(m_1/a_1) = q + p \ln k_w \quad (4)$$

The parameters of Eqs. 2–4 are not purely formal and an interpretation can be given on the basis of interaction indices [30,31].

The validity and applicability of the above model has been extensively investigated [19–22] on *n*-alkyl-modified silica phases with water–methanol eluents and the following conclusions were drawn. The selectivity of the separation system can be readily described by the parameters m_0 and q; m_0 reflects the apolar/hydrophobic selectivity and q gives the polar selectivity of the stationary phases. Hetem *et al.* [21] used *n*-alkylbenzenes, *n*-alkyl aryl ketones and *n*-alkyl *p*-hydroxybenzoates as test components on *n*-alkyl (C_1–C_{18}) phases with known surface characteristics. It was found that m_0 calculated for *n*-alkylbenzenes showed a good correlation with the hydrophobicity of the packings, *i.e.*, with the increasing carbon number of the ligands at identical surface coverage. As a measure of polar selectivity, q calculated for *n*-alkyl *p*-hydroxybenzoates was recommended because it showed a good correlation with the uncovered silica surface.

Eq. 2 was also fitted to our data and good correlations were found ($r > 0.963$) even for the HIC columns. The largest deviations were obtained for Set I, which was caused by *p*-cymene (pC). This component is not a "real" member of the homologous series; the apparent n_c is between 3 and 4. After re-evaluating the data of this set without pC, the correlation was significantly improved ($r > 0.984$).

As the model proved to be valid on the columns investigated, the characteristics were calculated according to Eqs. 2 and 3. The hydrophobicity and polarity of the stationary phases calculated for all the three sets are shown in Fig. 2a and b. It is clear that the parameters are highly dependent on the type of test components

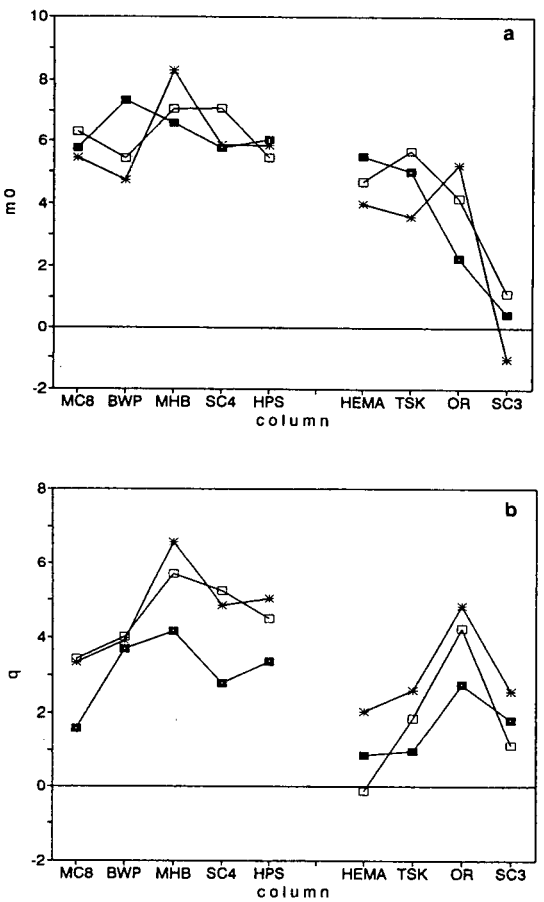

Fig. 2. Values of (a) hydrophobic and (b) polar selectivity obtained on the different columns. ◘ = Set I; ∗ = Set II; □ = Set III.

used, which is in agreement with the literature [19–22,30–34]. The hydrophobicity of the stationary phases measured by $m_0(I)$ (m_0 calculated for Set I) corresponds well with that expected from the retention data and that indicated by the order of ln k_w values. (All further parameters derived from or relating to measurements with Sets I–III will be designated by the number of the set in parentheses.) This parameter is the slope in Eq. 1 for the molecular residue of Set I, which is benzene. As this component was included, the measured and calculated values were compared and a very good correlation was obtained ($r = 0.991$). The result is shown in Fig. 3. This means that this parameter can be measured directly with good accuracy.

Judging the polarity indicated by q(III) is not straightforward because the information concerning the surface properties of the stationary phases is deficient; nevertheless, the values obtained for the RPLC packings are in the range reported in the literature [19–22,30–34]. It is interesting that the order of polarity is more or less the same for all sets. This is also in accordance with the literature [21], where deviations were only obtained for columns having very short alkyl ligands (C_1, C_2). This means that for comparison any of these sets (or those used in the studies cited) could be used, and the polarity order of the columns is not affected as much by the type of the compounds as is the hydrophobicity.

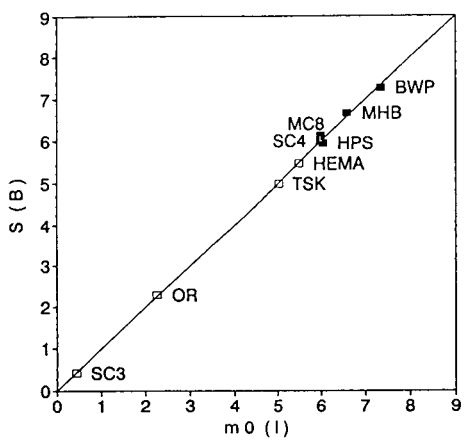

Fig. 3. Comparison of the calculated [m_0(I)] and measured [S(B)] slopes for benzene. ■ = RPLC; □ = HIC.

However, the overall picture seems to be slightly contrary to the recommendations of the manufacturers and to the order that could be expected from the ligand type and geometry of the packings. The largest deviations appear with HEMA, TSK and SC4. The HIC columns are intended for use in protein separations but stationary phases as strong as calculated cannot be operated under HIC conditions. A possible explanation of this behaviour may be the nature of the support. The stationary phases of these columns are formed by moderately hydrophobic phenyl (Ph) groups with low surface concentrations suited to protein separations and therefore low-molecular-mass components could have access to the uncovered part of the support having a similar hydrophobic character. Increased retention could result from this composite interaction. Another reason for this behaviour could be the specific affinity of these phases towards the aromatic components, *i.e.*, the increased retention could have been caused by Ph–Ph interactions. However, none of these explanations can hold true for SC4. In this case, possibly the lower hydrophobicity of the ligand was compensated for by an increased surface coverage. However, it seems that this sort of characterization of the hydrophobicity is applicable only for stationary phases with longer alkyl ligands (C_8 or larger) and for other types of ligand or support material it tends to overestimate the apolar character of the packings.

Another equation describing the behaviour of the homologous series under RPLC conditions was given by Bidlingmeyer *et al.* [35]:

$$\ln k = c_0 + c_1(c_2 - x)(c_3 - n_c) \quad (5)$$

where c_0–c_3 are constants. Although this equation was purely empirical, it described well the retention of some *n*-alkylsulphonates. In Eq. 5, c_2 was called the isopotential eluent composition (x_{ip}) because in this eluent ($x = c_2$) there is no difference between the retentions of the components. The ln k–x profiles converge to this point, *i.e.*, at this composition the retention is

independent of n_c. The retention corresponding to x_{ip} is c_0 ($\ln k_{ip}$). It was presumed [35] that the isopotential eluent composition could be a measure of the overall polarity of the stationary phases because the higher is x_{ip} the lower is the polarity of the stationary phase.

As Eqs. 1–5 are consistent, the parameters of Eq. 5 can be readily formulated by the parameters of Eqs. 1–4:

$$c_0 = a_0 - m_0(a_1/m_1) = -q/p = \ln k_{ip} \quad (6a)$$

$$c_1 = m_1 \quad (6b)$$

$$c_2 = a_1/m_1 = 1/p = x_{ip} \quad (6c)$$

$$c_3 = -m_0/m_1 = n_{c,ip} \quad (6d)$$

The polarity of the stationary phases (x_{ip}) calculated for all sets is shown in Fig. 4. The values obtained for the RPLC columns are not realistic (the isopotential eluent content is >100%) but are applicable for comparison purposes. A value >1 means that even pure methanol is not strong enough to reach isopotential conditions. It is seen that the value of x_{ip} is dependent on the type of components used. The order indicated by x_{ip}(I) is very similar to that obtained with m_0(I) but the presumed lower hydrophobicity of the HIC and SC4 columns is clearly shown and the differences between the columns seem to be more acceptable. On the other hand, the order given by x_{ip}(II) and x_{ip}(III) is similar to that of q(II) and q(III) but, again, the values are more realistic. This means that x_{ip} acts as m_0 and q, and it is applicable to measure the polar–apolar character of the stationary phases. A two-dimensional mapping along x_{ip}(I) as hydrophobic and x_{ip}(III) as polar descriptors is shown in Fig. 5. The RPLC and HIC columns are clearly separated (they spread over different regions) but it is also seen that the HIC columns are, from a practical point of view, "weakened" RPLC columns, as indicated above, and the main difference is in the overall strength of the columns.

Inserting x_{ip} into Eq. 1 and rearranging gives

$$\ln k_w = \ln k_{ip} + x_{ip}S \quad (7)$$

which is the inverse of Eq. 4. Earlier, Eq. 4 was considered as a general function [36], valid for all RPLC stationary phases. Further studies [37] revealed some deviations from the suggested values. The differences were high for q but low for p. This seems to be in agreement with the literature [20,31], where p was postulated as a constant. The variations of the parameters were explained by the error of measurement and/or by the "incompleteness" of the sample set used, and less attention was paid to these results, because they do not cause serious errors in the

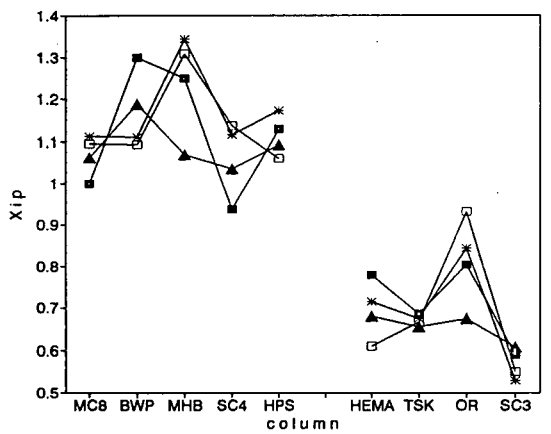

Fig. 4. Isopotential eluent composition obtained on the different columns with (■) (I) benzene homologues, (*) (II) dialkyl phthalates, (□) (III) *n*-alkyl *p*-hydroxybenzoates and (▲) (all) all the components.

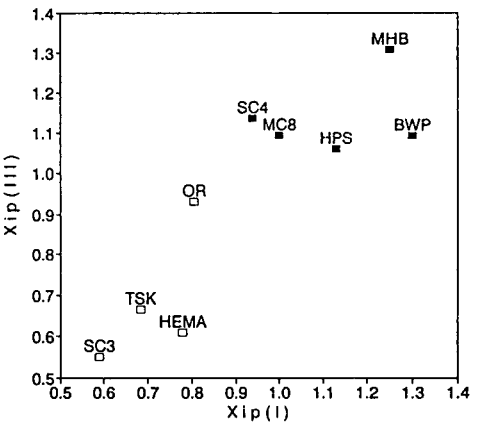

Fig. 5. Two-dimensional mapping of the columns. The axis x_{ip}(I) corresponds to the hydrophobicity and x_{ip}(III) to the polarity of the stationary phases. ■ = RPLC; □ = HIC.

prediction of retention on the most commonly used C_{18} columns [38,39]. However, on the basis of the model described, the parameters of the ln k_w–S or the S–ln k_w function should be characteristic for the stationary phases.

The slope and intercept values calculated for the RPLC columns are shown in Fig. 6a and those for the HIC columns in Fig. 6b. When the data were fitted to Eqs. 4 and 7, the correlations for Sets I–III were good ($r > 0.967$) on all columns but the parameters (q, p) were different. When all the data obtained on a column were fitted the correlation was lower ($r > 0.921$). This is the result of the diverse behaviour of Sets I–III, which is shown in Fig. 7a (RPLC) and 7b

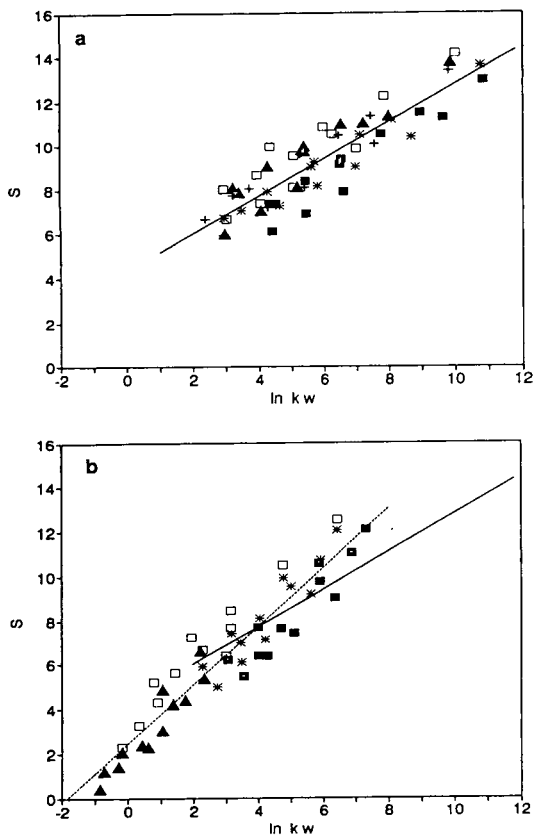

Fig. 6. Slope (S) and intercept (ln k_w) values obtained on the different (a) RPLC and (b) HIC columns. (a) ■ = MC8; * = BWP; □ = MHB; ▲ = SC4; + = HPS. (b) ■ = HEMA; * = TSK; □ = OR; ▲ = SC3. Solid line = RPLC; dashed line = HIC.

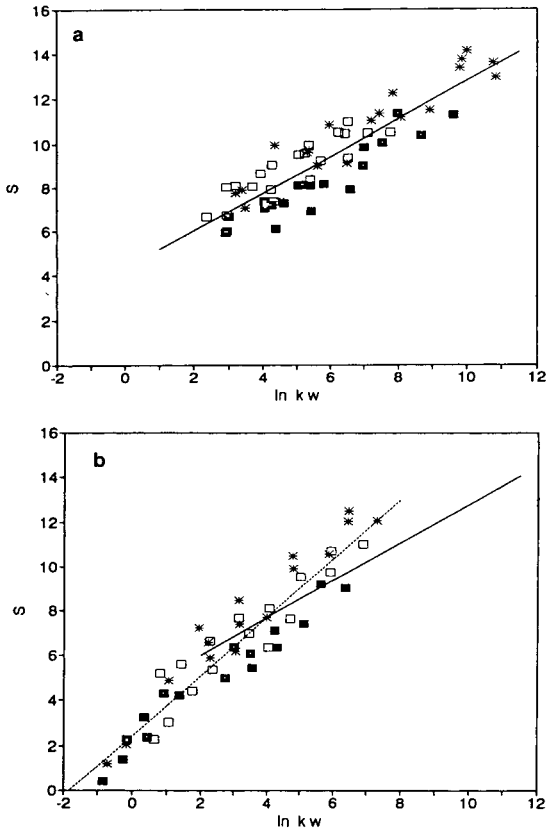

Fig. 7. Slope (S) and intercept (ln k_w) values obtained with (■) (I) benzene homologues, (*) (II) dialkyl phthalates and (□) (III) *n*-alkyl *p*-hydroxybenzoates on the (a) RPLC and (b) HIC columns. Solid line = RPLC; dashed line = HIC.

(HIC). In this instance p corresponds to a general x_{ip} value (see Eq. 6c), which is also shown in Fig. 4 [x_{ip}(all), triangles]. The order obtained with this parameter is the same as with x_{ip}(I), but the differences between the columns are smaller. For the HIC columns this order seems to be the most realistic. In our earlier studies [40,41] it was shown that the difference between TSK and SC3 when used under HIC conditions is small, which corresponds to the relationship indicated by x_{ip}(all) or x_{ip}(I) and x_{ip}(III) or q(III).

It is also seen in Figs. 6 and 7 that the ranges spanned by the values are different for the RPLC and HIC columns. When all the data obtained on the RPLC and HIC columns were

fitted to Eq. 4, two different functions were obtained. These are indicated by the lines in Figs. 6 and 7. The correlation was acceptable ($r > 0.941$ for RPLC and $r > 0.901$ for HIC). The "RP-like" behaviour of HEMA and TSK is clearly indicated. The parameters obtained on these columns fall in the range for RPLC columns but the direction of their spread is that of HIC columns. These results indicate that the discrimination of RPLC and HIC columns is arbitrary.

In Fig. 8 all the S–ln k_w values are shown. It is seen that the overall function relating to all points is curved, *e.g.*, logarithmic or square root type. Within this profile the columns span different regions (the strongest RPLC columns are located at the top right and the weakest HIC columns at the bottom left) which can be approximated with a linear function. The two-dimensional mapping of the columns along the parameters of these functions (p, q) is shown in Fig. 9. The order of the stationary phases along the q axis reflects polarity and the order along the p axis is inversely proportional to hydrophobicity. The values suggested in the literature [36,37] are also included for comparison. The small variation in p mentioned above can be attributed to the similar hydrophobicities of the stationary phases investigated (all were well conditioned C_{18} packings).

Possibly the scale of hydrophobicity would be more realistic with x_{ip}(I) and that of the polarity with q(III) or x_{ip}(III) (*cf.*, Fig. 5), but we think that a more appropriate selection of the test components is needed. The investigation of some possible test mixture is in progress. On the other hand, these parameters [p(all), q(all)] are very practicable because they can be directly inserted into an optimization process [38,39,42] while this type of application of m_0(I), q(III) or any of the x_{ip} values is not trivial. Further, thorough characterization of the HIC columns under HIC conditions is also needed to judge the applicability of these types of descriptors for the design and optimization of HIC separations. This work has begun [40,41,43] and the available data seem to be in accordance with the results outlined above.

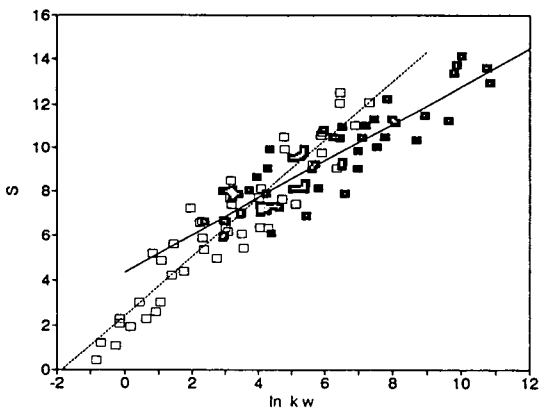

Fig. 8. Slope (S) and intercept (ln k_w) values obtained on the different columns. ■ (solid line) = RPLC; □ (dashed line) = HIC.

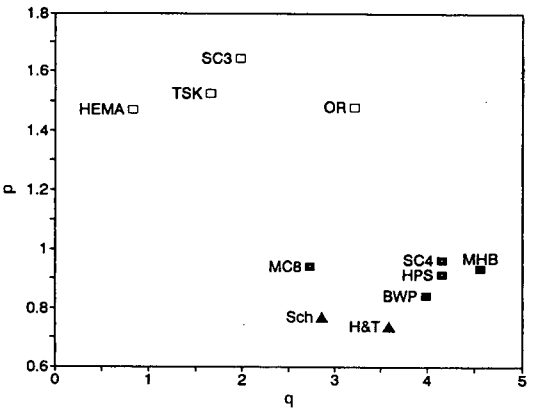

Fig. 9. Two-dimensional mapping of the stationary phases using the parameters of Eq. 4 obtained on the different columns and suggested in the literature [37–39]. ■ = RPLC; □ = HIC; ▲ = literature.

4. Conclusions

Nine commercially available prepacked columns used in RPLC and HIC with different characteristics concerning the type of ligands and the type and geometry of the support material were studied. Three homologous series were chromatographed under isocratic conditions with water–methanol as eluent. From the retention behaviour of the components, different characterizations of the stationary phases were performed according to the literature.

On the basis of ln k_w (the intercept of the ln

k–methanol content relationship), a rough estimate of the hydrophobicity of the stationary phases could be given. Some conclusions could also be drawn concerning the polarity of the packings, but the characterization was ambiguous.

More realistic results can be obtained with the polar–apolar characterization suggested by Hetem and co-workers [20–22], but some discrepancies were also found. It seems that this sort of characterization is applicable only for n-alkyl-modified silica packings with ligand chain length greater than C_4 and with a relatively high surface concentration. For columns of different types this method could give misleading results.

The use of the isopotential eluent composition as a descriptor resulted in the most acceptable characterization. From the parameters obtained for the different type of homologous series the polar–apolar nature of the stationary phases can be described.

Two-dimensional mapping along the parameters of the slope–intercept relationship seems to summarize the results obtained with other techniques. This type of representation reveals the polar and hydrophobic character of the stationary phases and also has practical relevance, *i.e.*, these parameters can be used directly in the design and optimization of separations.

5. Acknowledgements

This work was supported by the Hungarian Academy of Sciences under grant OTKA-1998. Special thanks are due to Dr. Jan Plicka (UVVVR, Prague), Dr. Robert Ohmacht (Medical University of Pécs) and Mr. Dietrich Brügel (Baker Chemikalien, Gross-Gerau) for donating the Separon HEMA, OR C_3-OH and Bakerbond WP columns, respectively.

6. References

[1] R.E. Majors, *LC·GC Int.*, 6 (1993) 196.
[2] R.E. Majors, *LC·GC Int.*, 6 (1993) 276.
[3] P.J. Schoenmakers, *Optimization of Chromatographic Selectivity*, Elsevier, Amsterdam, 1986, pp. 47, 116.
[4] K.A. Dill, *J. Phys., Chem.*, 91 (1987) 1980.
[5] P. Coenegracht, H. Metting, A Smilde and P. Coenegracht-Lamers, *Chromatographia*, 27 (1989) 135.
[6] J.L. Fausnaugh, L.A. Kennedy and F.E. Regnier, *J. Chromatogr.*, 317 (1984) 55.
[7] F.E. Regnier, *Science*, 238 (1987) 319.
[8] J. Frenz, W.S. Hancock, W.J. Henzel and Cs. Horváth, in K.M. Gooding and F.E. Regnier (Editors), *HPLC of Biological Macromolecules*, Marcel Dekker, New York, 1990, p. 145.
[9] W. Melander and Cs. Horváth, *Arch. Biochem. Biophys.*, 183 (1977) 200.
[10] D.R. Nau, *Biochromatography*, 4, No. 2 (1989) 62.
[11] K.-O. Eriksson, in J.-K. Janson and L. Ryden (Editors), *Protein Purification*, VCH, New York, 1989, p. 207.
[12] R.E. Shansky, S-L. Wu, A. Figueroa and B.L. Karger, in K.M. Gooding and F.E. Regnier (Editors), *HPLC of Biological Macromolecules*, Marcel Dekker, New York, 1990, p. 95.
[13] L. Szepesy and G. Rippel, *LC·GC Int.*, 5, No. 11 (1992) 24.
[14] N. Cooke, P. Shieh and N. Miller, *LC·GC Int.*, 3, No. 1 (1990) 9.
[15] J.G. Atwood and J. Goldstein, *J. Chromatogr. Sci.*, 18 (1980) 650.
[16] L. Hansson and L. Trojer, *J. Chromatogr.*, 207 (1981) 1.
[17] R.M. Smith, T.G. Hurdley, R. Gill and A.C. Moffat, *Chromatographia*, 19 (1984) 407.
[18] E. Bayer and A. Paulus, *J. Chromatogr.*, 400 (1987) 1.
[19] H.A. Claessens, J.W. de Haan, L.J.M. van de Ven, P.C. de Bruyn and C.A. Cramers, *J. Chromatogr.*, 436 (1988) 345.
[20] M.J.J. Hetem, L.J.M. van de Ven, J.W. de Haan, C.A. Cramers, K. Albert and E. Bayer, *J. Chromatogr.*, 479 (1989) 269.
[21] M.J.J. Hetem, J.W. de Haan, H.A. Classens, L.J.M. van de Ven, C.A. Cramers and J.N. Kinkel, *Anal. Chem.*, 62 (1990) 2288.
[22] M.J.J. Hetem, J.W. de Haan, H.A. Classens, L.J.M. van de Ven, C.A. Cramers, P.W.J.G. Wijnen and J.N. Kinkel, *Anal. Chem.*, 62 (1990) 2296.
[23] C.F. Poole and S.K. Poole, *Chromatography Today*, Elsevier, Amsterdam, 1991, p. 357.
[24] R.M. Smith, *Adv. Chromatogr.*, 26 (1987) 277.
[25] R.M. Smith, G.A. Murilla, T.G. Hurdley, R. Gill and A.C. Moffat, *J. Chromatogr.*, 384 (1987) 259.
[26] C.H. Lochmüller, S.J. Breiner, C.E. Reese and M.N. Koel, *Anal. Chem.*, 61 (1989) 367.
[27] P. Karsnas and T. Lindblom, *J. Chromatogr.*, 599 (1992) 131.
[28] A.K. Smilde, C.H.P. Bruins, P.M.J. Coenegracht and D.A. Doornbos, *Anal. Chim. Acta*, 212 (1988) 95.
[29] A.K. Smilde, P.M.J. Coenegracht, C.H.P. Bruins and D.A. Doornbos, *J. Chromatogr.*, 485 (1989) 169.
[30] P. Jandera, *Chromatographia*, 19 (1984) 101.
[31] P. Jandera, *J. Chromatogr.*, 314 (1984) 13.
[32] P. Jandera, *J. Chromatogr.*, 352 (1986) 91.

SUBSCRIBER!

Please cut out and paste on page 312 of Vol. 668, No. 2

Erratum

Characterization of stationary phases used in reversed-phase and hydrophobic interaction chromatography [*Journal of Chromatography A*, 668 (1994) 301–312]

G. Rippel, E. Alattyani, L. Szepesy

Page 312 of this article was erroneously left blank. The text on this page should read:

[33] R.M. Smith, *J. Chromatogr.*, 236 (1982) 313.
[34] R.M. Smith, *Anal. Chem.*, 56 (1984) 256.
[35] B.A. Bidlingmeyer, S.N. Deming, W.P. Price, B. Sachok and M. Petrusek, *J. Chromatogr.*, 186 (1979) 419.
[36] P.J. Schoenmakers, H.A.H. Billiet and L. de Galan, *J. Chromatogr.*, 185 (1979) 179.
[37] T.L. Hafkenscheid and E. Tomlinson, *J. Chromatogr.*, 264 (1983) 47.
[38] P.J. Schoenmakers, *Optimization of Chromatographic Selectivity*, Elsevier, Amsterdam, 1986, p. 64.
[39] P.J. Schoenmakers, A. Bartha and H.A.H. Billiet, *J. Chromatogr.*, 550 (1991) 425.
[40] L. Szepesy and G. Rippel, *Chromatographia*, 34 (1992) 391.
[41] G. Rippel and L. Szepesy, *J. Chromatogr. A*, 664 (1994) 27.
[42] A. Drouen, J.W. Dolan, L.R. Snyder, A. Poile and P.J. Schoenmakers, *LC · GC Int.*, 5, No. 2 (1992) 28.
[43] L. Szepesy and G. Rippel, *J. Chromatogr. A*, 668 (1994) 337.

ELSEVIER

Journal of Chromatography A, 668 (1994) 313–321

JOURNAL OF CHROMATOGRAPHY A

Binaphthyl-based amphiphile as a reagent for dynamically modified silica and fluorescence detection in high-performance liquid chromatography

Bernard Juskowiak

Faculty of Chemistry, A. Mickiewicz University, Grunwaldzka 6, 60-780 Poznan, Poland

Abstract

The modification of bare silica with a binaphthyl-containing surfactant is described. The effects of several factors on the amount of binaphthyl amphiphile adsorbed on the silica surface are reported and the retention mechanisms of solutes are discussed. The separation of non-ionic aromatic compounds shows a clear reversed-phase mechanism, even at very low coverage of silica (below 10 nmol m^{-2}, 3 μmol g^{-1}), which indicates an extremely strong interaction between binaphthyl moieties of the adsorbed surfactant and aromatic rings of the solutes. The ion-pair reversed-phase mechanism appears to be major process responsible for the retention of anionic solutes, especially at higher amphiphile concentrations in mobile phase. The concept of the application of fluorescent amphiphiles in liquid chromatography is discussed, and an example of the detection of non-fluorescent analytes using the "visualization effect" is also presented.

1. Introduction

Surfactants or amphiphilic compounds are valuable mobile phase additives in high-performance liquid chromatography (HPLC). In reversed-phase ion-pair chromatography, separations of ionic compounds are achieved due to the presence of relatively low concentrations of surfactant in the mobile phase [below the critical micelle concentration (CMC)] [1–5]. The use of aqueous surfactant solutions at concentrations above the CMC provides a new separation technique, micellar liquid chromatography [6–10]. The third approach to the use of surfactants in HPLC is the dynamic modification of bare silica with surfactant solutions, giving chromatographic separations similar to those obtained with chemically bonded reversed-phase (RP) materials. It has been shown that these RP-HPLC systems exhibit an excellent reproducibility of selectivity and also superior peak shapes of amine solutes [11–13].

Surprisingly, only a very limited number of surfactants have been applied in such chromatographic separations, mainly conventional, such as cetyltrimethylammonium bromide (CTAB), sodium dodecyl sulphate (SDS), Tweens and Brij 35 [13–15]. The reason for the application of alkyl chain-type surfactants exclusively is limitations with regard to the spectrophotometric detection widely used in HPLC, which needs an optically transparent mobile phase. However, one can take advantage of the presence of light-absorbing surfactants in mobile phase, *e.g.*, monitoring of "transparent" species by an indirect technique used in ion-pair chromatography [16].

We are trying to introduce into analytical

0021-9673/94/$07.00
SSDI 0021-9673(93)E1085-E

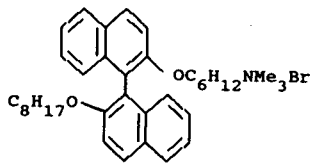

C_8BNC_6N

practice functionalized surfactants bearing a fluorescent aromatic moiety. The binaphthyl-based cationic amphiphile C_8BNC_6N has been successfully used for monitoring iodine in the indirect determination of ascorbic acid [17]; the aggregates of the amphiphile show a high affinity for hydrophobic solutes, especially polycyclic aromatic hydrocarbons (PAHs), and can serve as efficient collective energy donors. The sensitized emission of a particular PAH is then observed [18].

The concept of the application of C_8BNC_6N in chromatographic techniques takes advantages of the presumably strong interactions of the surfactant with the silica surface, which allows surface modification at low surfactant concentrations in the mobile phase; additionally, the presence of a fluorescent amphiphile in the mobile phase can be exploited for indirect detection.

In this paper, the modification of bare silica with the binaphthyl-containing surfactant C_8BNC_6N is reported. The effects of the content of methanol in the mobile phase, pH, buffer concentration and temperature on the amount of amphiphile adsorbed on the silica surface were studied. The retention mechanism of solutes is discussed, and an example of the detection of non-fluorescent analytes using the "visualization effect" is presented.

2. Experimental

2.1. Apparatus

The chromatographic system was composed of a Model 1440 liquid chromatograph (ISCO, Lincoln, NB, USA) and an RF 5000 spectrofluorimeter (Shimadzu, Kyoto, Japan) equipped with a sample flow cell. The solutes were detected as follows ($\lambda_{ex}/\lambda_{em}$): naphthalene and 1,2-dimethylnaphthalene, 260/320 nm; anthracene and benzo[*a*]pyrene, 380/400 nm; and 3-hydroxynaphthoate and quinine, 380/450 nm.

Separations were performed on 100 × 4.6 mm I.D. columns which were packed with LiChrosorb Si 100 (Merck, Darmstadt, Germany), $d_p = 10$ μm, by the slurry technique at 300 bar with a Knauer pneumatic high-pressure pump.

A precolumn packed with silica gel (35–40 μm) (Merck) was located between the pump and sample injector, in order to saturate the mobile phase with silica. The analytical column was thermostated at 25°C unless stated otherwise.

2.2. Reagents

The amphiphile compound, C_8BNC_6N, was prepared and purified as described elsewhere [19]. A stock standard solution of C_8BNC_6N ($5 \cdot 10^{-3}$ *M*) was prepared by dissolving the weighed sample in methanol. All other chemicals were of analytical-reagent grade and were used as received. Water filtered through a Milli-Q system (Millipore, Bedford, MA, USA) was used throughout.

2.3. Procedures

The adsorption isotherms were determined from the breakthrough curves recorded with the spectrofluorimeter (λ_{ex} = 340 nm, λ_{em} = 380 nm). The concentration of C_8BNC_6N in the eluates was determined spectrophotometrically at 340 nm using a Specord M 40 instrument (Carl Zeiss, Jena, Germany).

The columns were modified by two methods:

(i) two-step modification, the column initially being washed (conditioning) with 100 ml of mobile phase containing buffer, but without amphiphile additive, followed by modification with amphiphile-containing mobile phase without buffer;

(ii) conventional, one step modification, with mobile phase containing buffer solution and appropriate amounts of amphiphile.

2.4. Determination of critical micelle concentration (CMC)

The CMC of C_8BNC_6N in methanol–water was measured in the presence of varied amounts of phosphate by the method based on energy transfer [20] using perylene as an energy acceptor.

3. Results and discussion

3.1. Adsorption isotherms

In order to examine factors governing amphiphile adsorption, modifications of silica gel were performed by two general procedures as indicated under Experimental, varying the pH of the "conditioning mobile phase" and the content of methanol in the mobile phase in the two-step procedure, and changing the composition of the mobile phase in the one-step procedure. The results are presented in Fig. 1.

The pH of the "conditioning mobile phase" during the initial treatment of silica is a crucial factor governing surface coverage by the amphiphile in the two step-procedure (Fig. 1A). The adsorption isotherms do not show Langmuir behaviour, and exhibit saturation at higher amphiphile concentrations. The amount of amphiphile adsorbed increases as the pH of the mobile phase during the washing step increases. As expected, higher surface coverages were obtained for columns pretreated at pH 8.5 (curve 4, Fig. 1A), even when a higher content of methanol in the mobile phase was used [methanol–water (5:5, v/v)]. The courses of the isotherms reflect the two-step procedure applied. The washing step is responsible for the initial amount of ionized silanols accessible for ion-pair formation with amphiphile molecules. The modification step, with mobile phase without buffer, causes the gradual protonation of silanols, yielding a final surface coverage that depends on the pH of initial washing and the duration of the modification step.

The curves in Fig. 1B represent adsorption isotherms obtained by the one-step procedure.

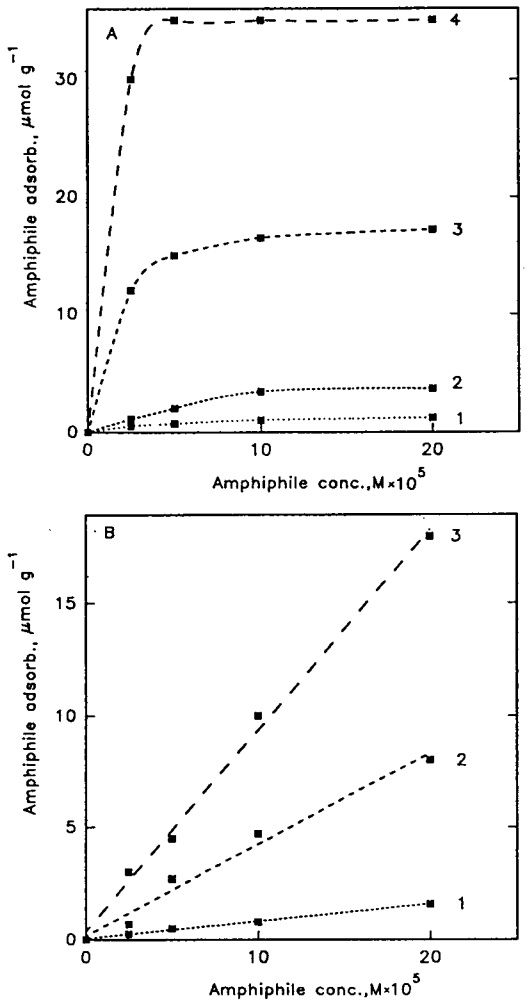

Fig. 1. Adsorption of C_8BNC_6N amphiphile by LiChrosorb Si 100 as a function of C_8BNC_6N concentration in the mobile phase for different modification procedures. (A) Two-step procedure. Eluent, methanol–water (1)–(3) (30:70) and (4) (50:50); pH of conditioning mobile phase, (1) 0.1 *M* H_3PO_4, (2) 5.0, (3) 6.4 and (4) 8.5. (B) One-step procedure. Mobile phase, methanol–water–0.2 *M* phosphate buffer, (1), (2) (30:65:5) and (3) (30:20:50); pH of buffer, (1) 5.0, (2) 6.4 and (3) 2.1.

As expected, an increase in the pH of the mobile phase causes an enhancement of the adsorption of the surfactant on the silica gel, but the unexpected efficient adsorption at pH 2.1 (curve 3) should be noted. In pure methanol–water (3:7, v/v), one would expect domination of

monomeric molecules of the amphiphile, but the presence of a high concentration of counter ions (phosphate) should improve micelle formation. Indeed, the determined CMC value at 0.1 *M* phosphate buffer concentration is $1 \cdot 10^{-4}$ *M*, which indicates the presence in the mobile phase (pH 2.1) at least of premicellar aggregates. The low pH decreases the ionization of silanols, thus making them inaccessible for ion-pair interactions with cationic amphiphile molecules. Taking into account the dissociation constant of silanols, $pK = 7.1$ [21], one can calculate that only 1% of silanols is dissociated at pH 5.0, and markedly less at pH 2.1. The abnormally high adsorption of the amphiphile at low pH can be explained in the terms of micellar phenomena, by the formation of multilayers of amphiphile on the silica surface.

From the comparison of two modification procedures, the significant effect of the presence of phosphate buffer in the mobile phase is clear. Buffer at a concentration of $1 \cdot 10^{-2}$ *M* decreases the adsorption of the amphiphile by about 50%, probably as the result of competitive interaction of buffer cations with silanols, which has been reported by Hansen *et al.* [22], and also competitive ion-pair equilibria of phosphate ions with amphiphile molecules. The two-step procedure seems to be more convenient for the flexible regulation of the amount of C_8BNC_6N adsorbed on silica, because by changing the pH of the washing phase, and the composition of mobile phase used for modification, one can obtain reproducible surface coverages below 10 nmol m^{-2} ($pH < 5$) and highly coated silica, containing above 600 nmol m^{-2} (column washed with the mobile phase containing $2 \cdot 10^{-2}$ *M* ammonia). Moreover, the absence of buffer ions in the mobile phase will be advantageous for the indirect detection of ionic solutes.

3.2. Retention studies

The columns modified under different conditions were tested by retention studies, using solutes chosen to represent anionic [3-hydroxynaphthoic acid (3HNA)], cationic [quinine (Q)] and non-ionic [naphthalene (N), 1,2-dimethylnaphthalene (DMN) and anthracene (A)]. The dependences of capacity factors (k') as a function of C_8BNC_6N concentration are presented in Fig. 2.

The clear correlation between the retention of non-ionic solutes and the amount of adsorbed C_8BNC_6N can be seen in all instances. The concentration of C_8BNC_6N in the mobile phase and the presence of buffer solution play a negligible role for non-polar solutes. Approximately the same k' value is observed for different columns and different mobile phase compositions, providing similar amounts of C_8BNC_6N adsorbed. The separations show a clear reversed-phase mechanism even for low coverages of silica (Fig. 2B and C), which indicates an extremely strong adsorptive interaction between binaphthyl moieties of the adsorbed surfactant and aromatic rings of the solutes. Quinine is not retained over the full range of amphiphile concentrations used (Fig. 2A); in contrast, 3-hydroxynaphthoic acid shows a strong dependence on the concentration of the amphiphile in the mobile phase. The mechanism of the retention of anionic solutes seems to be more complex, and results should be discussed considering a reversed-phase ion-pair mechanism as an additional process. The ion-pair reversed-phase mechanism appears to be major process at higher C_8BNC_6N concentrations in the mobile phase, which is reflected by an abrupt increase in k'. This effect is the most clearly seen in Fig. 2D, where despite the constant amount of amphiphile adsorbed, k' still increases with increasing surfactant concentration.

An increase in the amount of organic modifier, methanol, in the mobile phase causes a normal decreasing effect on retention, as indicated from a comparison of Fig. 2C and D.

The retention of all solutes decreases at elevated temperature (Fig. 3), as would be expected considering the effect of temperature on partition equilibria and the decrease in surface coating by amphiphiles.

The pH effect on k' for non-ionic solutes is simply related to the amount of adsorbed C_8BNC_6N, but with 3HNA the strong increase in retention at higher pH region indicates more

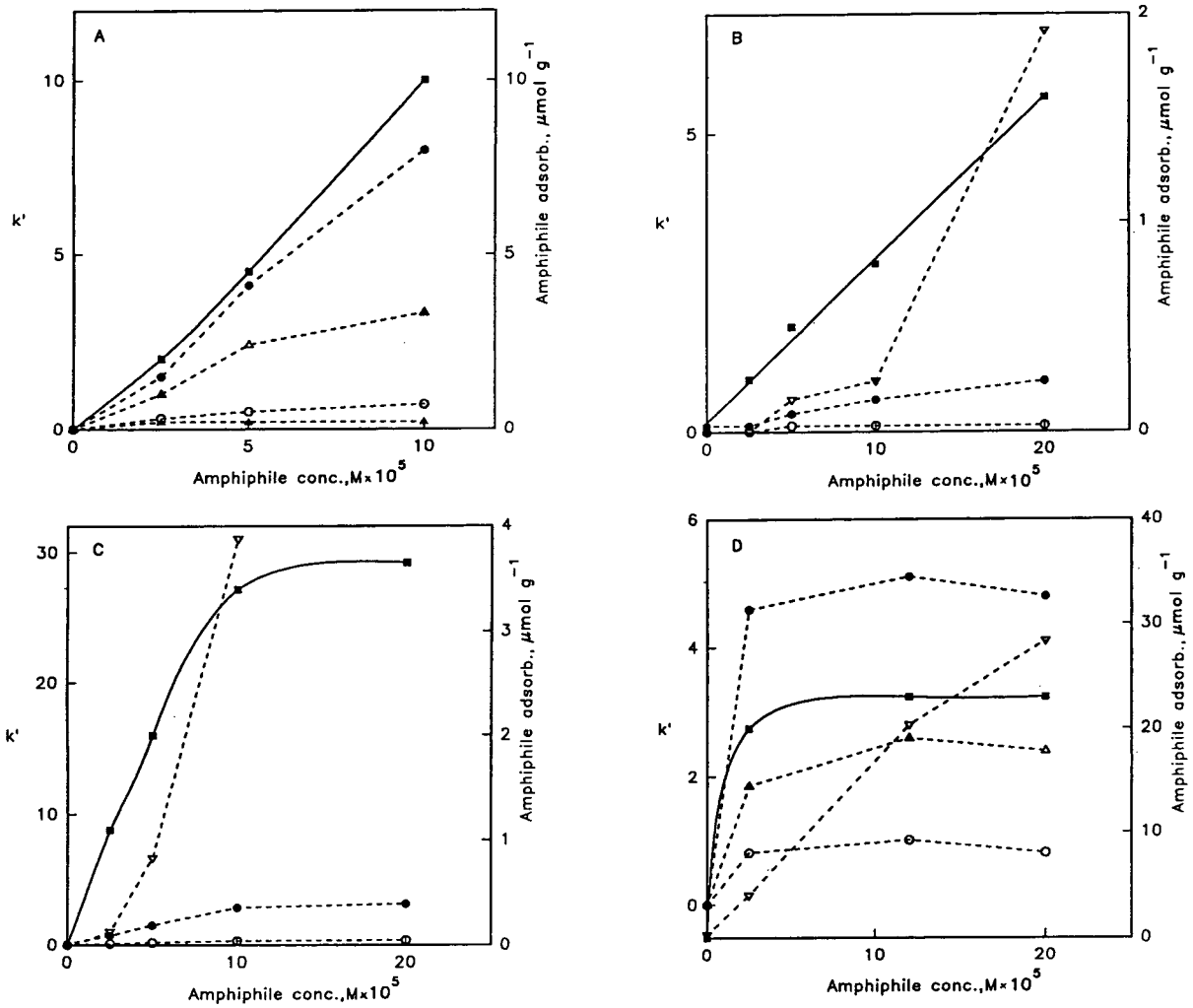

Fig. 2. Relationship between the concentration of C_8BNC_6N in the mobile phase and retention (k' values) for the test solutes: ○ = naphthalene; △ = DMN; ● = anthracene; ▽ = 3HNA; ▲ = quinine; □ = adsorption isotherm for different experimental conditions. One-step procedure: (A) pH = 2.1, eluent = methanol–water–0.2 *M* buffer (30:20:50); (B) pH = 5.0, eluent = methanol–water–0.2 *M* buffer (30:65:5). Two-step procedure; (C) pH = 5, eluent = methanol–water (30:70); (D) pH = 8.5, eluent = methanol–water (50:50).

complete ionization of the solute, and thus the significance of reversed-phase ion-pair interactions (Fig. 4).

3.3. Retention mechanism

The generally high retention observed for both non-ionic and anionic solutes indicates strong interaction with the adsorbed binaphthyl amphiphiles. Assuming the simple reversed-phase interaction for non-polar solutes, the partition coefficient (P) can be simply calculated from the fundamental chromatographic equation

$$k' = \phi P \quad (1)$$

where k' is capacity factor, and $\phi = v_{ads}/v_m$ is the phase ratio.

The volumes of surfactant adsorbed (v_{ads}) were calculated from breakthrough curves, using a molar volume of the amphiphile of 900 Å^3 [18],

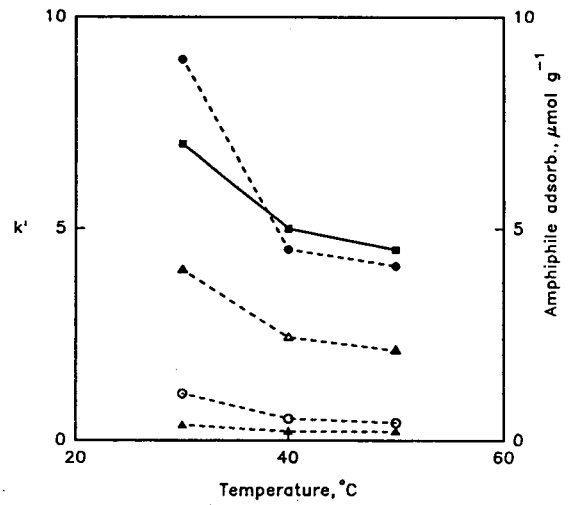

Fig. 3. Effect of temperature on C_8BNC_6N adsorption and retention (k' values). Eluent, methanol–water–0.2 M buffer (30:20:50); pH = 2.1. Symbols as in Fig. 2.

and the dependence of the capacity factor (k') on ϕ for $v_m = 0.85$ ml was plotted. The partition coefficients obtained for particular solutes and mobile phase compositions are given in Table 1. The value for benzo[a]pyrene (BaP) was obtained from two experimental points, as in most instances BaP was completely retained on the columns.

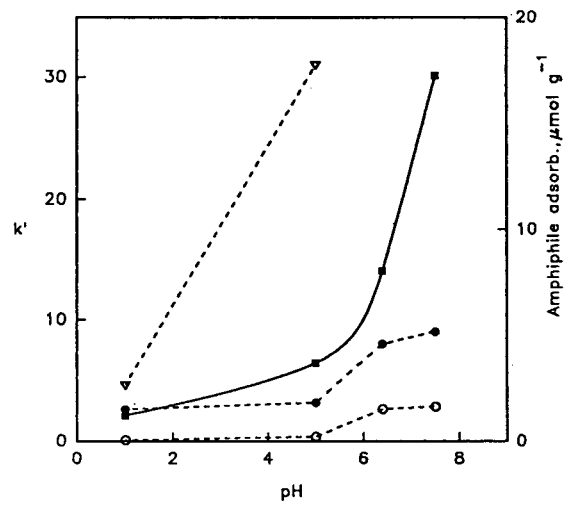

Fig. 4. Effect of pH on C_8BNC_6N adsorption and retention (k' values). Two-step procedure: conditioning solution, methanol–water–0.2 M buffer (30:65:5); eluent, methanol–water (30:70) containing $1 \cdot 10^{-4}$ M C_8BNC_6N. Symbols as in Fig. 2.

An increase in elution power of the mobile phase [methanol–water (5:5)] causes a decrease in the interaction of all non-ionic solutes with the adsorbed surfactant. The addition of methanol should decrease the polarity of the bulk phase without affecting the polarity of the surface coating [23], which in addition to the retention effect, should result in increased mass transfer, this in turn resulting in improved efficiency. As expected, the values of the partition coefficients reflect the hydrophobicity of the solutes, reaching a very high value, $3.1 \cdot 10^3$, for benzo[a]pyrene.

With the anionic solute, 3-hydroxynaphthoic acid, ion-pair equilibria should be considered. From the general rules of ion-pair extraction, the following fundamental equilibria were taken into account:

$$R^+S^- \rightleftharpoons \overline{R^+S^-} \qquad P = \frac{\overline{[R^+S^-]}}{[R^+S^-]} \tag{2}$$

$$R^+ + S^- \rightleftharpoons R^+S^- \qquad K = \frac{[R^+S^-]}{[R^+][S^-]} \tag{3}$$

$$R^+ + S^- \rightleftharpoons \overline{R^+S^-} \qquad E = \frac{\overline{[R^+S^-]}}{[R^+][S^-]} \tag{4}$$

where a bar denotes concentration in the stationary phase, concentrations without a bar refer to the mobile phase, P is the partition coefficient, K is the association constant in the mobile phase and E is the extraction constant. These equilibria are not independent, as

$$E = PK \tag{5}$$

An expression for the capacity factor of S^- can be then obtained, considering

$$k' = \phi \frac{\Sigma \overline{R^+S^-}}{\Sigma S^-} = \phi \frac{\overline{[R^+S^-]}}{[R^+S^-] + [S^-]} + k'_0 \tag{6}$$

where k'_0 is the term for the amphiphilic ion independent retention. Eq. 6 can be rewritten as

$$k' - k'_0 = \phi \frac{PK[R^+]}{K[R^+] + 1} \tag{7}$$

Table 1
Partition coefficients (P) calculated from Eq. 1 for C_8BNC_6N-modified LiChrosorb Si 100

Eluent: MeOH–H_2O (v/v)	Partition coefficient, $P \cdot 10^{-2}$			
	Naphthalene	Anthracene	DMN	Benzo[a]pyrene
3:7	1.4	16	–	–
5:5	0.70	3.7	1.7	31

and after rearrangement

$$\frac{\phi}{k' - k'_0} = \frac{1}{P} + \frac{1}{E[R^+]} \quad (8)$$

Assuming that $k'_0 \ll k'$, Eq. 8 simplifies to

$$\frac{\phi}{k'} = \frac{1}{P} + \frac{1}{E[R^+]} \quad (9)$$

This equation is similar to simplified equations proposed by Horváth *et al.* [2], Westerlund and Theodorsen [24] and Knox and Hartwick [25].

A plot of ϕ/k' versus $[R^+]^{-1}$ should result in a straight line. Further, the constants describing the equilibria (K, P and E) can be calculated from the intercept and slope values. Unfortunately, it appeared that calculation of association constant (K) and partition coefficient (P) cannot be performed, as negative intercepts of the plots were obtained. The extraction constant values (E) obtained for methanol–water (3:7 and 5:5, v/v) mobile phases are $5 \cdot 10^7$ and $2 \cdot 10^6$, respectively. Considering the improving effect of a less polar mobile phase on the ion-pair formation equilibria (K), one can suspect a far greater decrease in the partition coefficient (P) than calculated for non-ionic solutes (Table 1).

The negative intercepts indicate contributions from other equilibria, probably connected with the competing effect of counter anions, Br^-, present in the mobile phase, or interactions of the solute with cationic head groups of the surfactant adsorbed on the silica gel and not fully neutralized by ionized silanols. Similar problems with negative intercepts have been observed in micellar chromatography for sparingly soluble solutes, and it was explained by the slow mass transport in the bulk phase [26,27].

The restricted mass transfer between the mobile and stationary phases is reflected by broadening of the chromatographic bands. Large peak widths were observed especially for 3HNA and anthracene. In order to elucidate the effect of entrance–exit rate constants on retention, the random-walk model [28] was applied. The values for the desorption rate constant, k_d, were obtained from the measured chromatographic parameters, substituted into the equation

$$H = \frac{2k'}{(1 + k')^2} \frac{\nu}{k_d} \quad (10)$$

where H is the height equivalent to a theoretical plate and ν is the linear velocity. The adsorption rate constant, k_a, was calculated using the basic chromatographic expression $k' = k_a/k_d$. If both the adsorption and desorption rate constants of a solute with the stationary phase were large, mass transfer would not limit the efficiency, but the rate constants can vary greatly.

The values of k_d and k_a were calculated using Eq. 10 for a flow rate of 1.54 mm s^{-1} (0.8 ml min^{-1}). The results are given in Table 2. The k_a values were normalized to the same amount of C_8BNC_6N adsorbed, in order to compare two mobile phases. The values of k_a are surprisingly low (*e.g.*, $k_a = 322$ s^{-1} has been reported for β-naphthol in the presence of SDS below the CMC on an ODS column [29]). Moreover, a higher content of methanol in the mobile phase causes a lowering of the adsorption rate, which is unexpected as the adsorption is diffusion controlled. The very low values of k_a may indicate interaction of the solute with the surfactant in the mobile phase; even below the CMC the formation of premicellar, cluster-like aggregates

Table 2
Adsorption and desorption rate constants for C_8BNC_6N-modified LiChrosorb Si 100

Eluent: MeOH–H_2O (v/v)	Rate constant	Naphthalene	Anthracene	Benzo[*a*]pyrene
3:7	k_a (s^{-1})	6.6	20.4	–
	k_d (s^{-1})	1.81	1.03	–
5:5	k_a (s^{-1})	2.81	10.1	11.6
	k_d (s^{-1})	2.72	1.98	0.27

has been reported [30]. On the other hand, the increase in k_d on going to a methanol-rich mobile phase is in accordance with expectation. This means that a solute with a higher k_d value can return to the bulk phase frequently, and thereby is closer to equilibrium, whereas a much smaller k_d values results in solutes remaining in the stationary phase much longer. As both effects act in the same direction, a marked improvement in efficiency is observed in a methanol-rich mobile phase. It should be noted that the elution of benzo[*a*]pyrene with methanol–water (3:7, v/v) mobile phase was virtually impossible owing to the substantial peak broadening, which was not the case with methanol–water (5:5, v/v).

3.4. Application

As the main reason for undertaking these studies was the application of fluorescent amphiphiles in chromatographic practice, mainly taking advantage of the fluorescence characteristics of the amphiphile, we checked the usefulness of the system for the fluorescence detection of non-fluorescent solutes. Taking into account the ion-pair reversed-phase mechanism of retention of anionic solutes (S^-), one can expect an increase in the fluorescent signal when the $C_8BNC_6N^+S^-$ ion pair is eluted. Pilot studies performed with heptanesulphonate ($C_7SO_3^-$) and pentanesulphonate ($C_5SO_3^-$) appeared to be promising. Fig. 5 shows an example of a chromatogram obtained for these two non-fluorescent solutes injected into an eluent containing the fluorescent C_8BNC_6N amphiphile (ion-pair reagent).

The next approach to be examined is the construction of a sensing energy transfer system, consisting of acceptor molecules incorporated in donor fluorescent aggregates, for monitoring non-fluorescent solutes (spatial perturbation of sensitized emission of acceptor). Benzo[*a*]pyrene and perylene are good candidates for efficient acceptors, as sensitized emission of these solutes in binaphthyl aggregates [18,20] and decreased entrance–exit rate constants have been observed. These studies will be continued, as the system seems to be promising for the separation

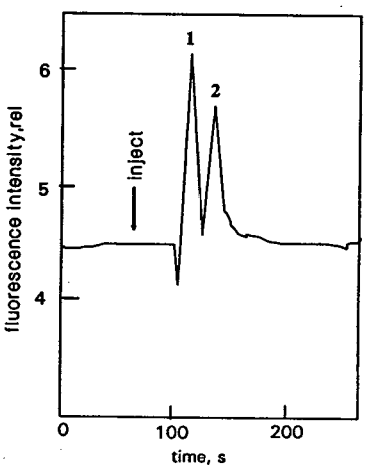

Fig. 5. Separation of alkylsulphonates on LiChrosorb Si 100 modified with C_8BNC_6N amphiphile with fluorescence detection. Excitation and emission wavelengths, 330 nm and 380 nm, respectively; mobile phase, methanol–water (50:50, v/v) containing $1 \cdot 10^{-4}$ *M* C_8BNC_6N; flow-rate, 0.8 ml min^{-1}. Peaks: 1 = pentanesulphonate and 2 = heptanesulphonate (0.5 μg each).

and detection of amino acids, peptides and other bioactive substances.

4. Acknowledgement

The work was partially supported by the KBN Grant No. 2 07639101.

5. References

[1] J.H. Knox and G.R. Laird, *J. Chromatogr.*, 122 (1976) 17.
[2] C. Horváth, W. Melander, I. Molnár and P. Molnár, *Anal. Chem.*, 49 (1977) 2295.
[3] J.L.M. van de Venne, J.L.H.M. Hendrik and R.S. Deelder, *J. Chromatogr.*, 167 (1978) 1.
[4] B.A. Bidlinmeyer, *J. Chromatogr. Sci.*, 18 (1980) 525.
[5] R.M. Cassidy and S. Elchuk, *Anal. Chem.*, 54 (1982) 1558.
[6] D.W. Armstrong and S. Henry, *J. Liq. Chromatogr.*, 3 (1980) 657.
[7] D.W. Armstrong and F. Nome, *Anal. Chem.*, 53 (1981) 1662.
[8] W.L. Hinze, *Ann. Chim. (Rome)*, 77 (1987) 167.
[9] F.P. Tomasella, J. Fett and L.J. Cline Love, *Anal. Chem.*, 63 (1991) 474.
[10] G.L. McIntire, *CRC Crit. Rev. Anal. Chem.*, 21 (1990) 257.
[11] Y. Ghaemi and R.A. Wall, *J. Chromatogr.*, 174 (1979) 51.
[12] S.H. Hansen, *J. Chromatogr.*, 209 (1981) 203.
[13] P. Helboe, S.H. Hansen and M. Thomsen, *Adv. Chromatogr.*, 28 (1989) 196.
[14] R.A. Wall, *J. Chromatogr.*, 194 (1980) 353.
[15] Y. Ghaemi and R.A. Wall, *J. Chromatogr.*, 198 (1980) 397.
[16] H. Small and T.E. Miller, *Anal. Chem.*, 54 (1982) 54.
[17] B. Juskowiak and W. Szczepaniak, *Anal. Chim. Acta*, 262 (1992) 79.
[18] B. Juskowiak, M. Takagi and S. Takenaka, *Bull. Chem. Soc. Jpn.*, in preparation.
[19] B. Juskowiak, S. Takenaka and M. Takagi, *Bull. Chem. Soc. Jpn.*, in preparation.
[20] B. Juskowiak and W. Szczepaniak, *Anal. Chim. Acta*, in press.
[21] M.L. Hair and W. Hertl, *J. Phys. Chem.*, 74 (1970) 91.
[22] S.H. Hansen, P. Helboe and U. Lund, *J. Chromatogr.*, 270 (1983) 77.
[23] P. Stilbs, *J. Colloid Interface Sci.*, 89 (1982) 547.
[24] D. Westerlund and A. Theodorsen, *J. Chromatogr.*, 144 (1977) 23.
[25] J.H. Knox and R.A. Hartwick, *J. Chromatogr.*, 204 (1981) 3.
[26] D.W. Armstrong, T. Ward and A. Berthod, *Anal. Chem.*, 58 (1988) 579.
[27] W.L. Hinze and S.G. Weber, *Anal. Chem.*, 63 (1991) 1808.
[28] J.C. Giddings, *Dynamics of Chromatography, Part I*, Marcel Decker, New York, 1965.
[29] P. Yarmchuk, R. Weinberger, R.F. Hirsch and L.J. Cline Love, *J. Chromatogr.*, 283 (1984) 47.
[30] J.E. Desnoyers, R. De Lisi, C. Ostigny and G. Perron, in K.L. Mittal (Editor), *Solution Chemistry of Surfactants*, Vol. 1, Plenum Press, New York, 1979, p. 221.

ELSEVIER

Journal of Chromatography A, 668 (1994) 323–329

JOURNAL OF CHROMATOGRAPHY A

Stability of *o*-phthalaldehyde–sulfite derivatives of amino acids and their methyl esters: electrochemical and chromatographic properties

György Turiák[☆,a], Ladislav Volicer*[,a,b]

[a]*Department of Pharmacology, Boston University School of Medicine, 80 East Concord Street, Boston, MA 02118, USA*
[b]*Geriatric Research, Education and Clinical Center, 182B, E.N. Rogers Memorial Veterans Hospital, 200 Springs Road, Bedford, MA 01730, USA*

Abstract

RP-HPLC coupled with 16-channel coulometric electrode array detection was used to monitor the decomposition of five amino acid *o*-phthalaldehyde (OPA)–sulfite derivatives (Ala, Arg, Glu, Ser, Tyr) and their methyl ester derivatives as well. At fixed OPA and sulfite concentrations inclusion of methanol and EDTA in the derivatization media has increased most effectively the room temperature stability of both derivatives measured at pH 9.2 (amino acids) and pH 8.2 (methyl esters). Decreases in product concentrations by 6% have occured after more than 15 h for amino acid derivatives and 8 h for methyl ester derivatives.

The oxidation potential maxima for OPA–sulfite derivatives of amino acids were found at 600 mV while the same methyl ester derivatives had 60–120 mV higher maxima with the exception of tyrosine. The detector responses were found to be linear in the studied 0.1–10 μM concentration range for both derivative forms and their detection limit was 100–200 fmol injected on the column.

The RP-HPLC retention of amino acid methyl ester OPA–sulfite derivatives was very similar to the amino acid OPA–2-mercaptoethanol ones while the more polar amino acid OPA–sulfite derivatives were eluted earlier ($k' < 1$) under the same chromatographic conditions.

1. Introduction

o-Phthalaldehyde (OPA) reacts with primary amines in the presence of a suitable thiol compound to produce fluorescent and electrochemically active 1-alkylthio-2-alkyl-substituted isoindoles [1,2]. This rapid and sensitive derivatization has become widely used in conjunction with HPLC to analyze common amino acids. However the instability of isoindoles limits the utility of the precolumn derivatization method. Careful timing of the reaction or even instrumental automation is required to ensure acceptable analytical precision [3].

Recently various thiol compounds and thiol substitutes have been used to gain more stable primary amine derivatives (reviewed in ref. 4). Among them the well defined sodium sulfite appeared to be a good candidate unlike the volatile and malodorous organic thiols [5]. With the exceptions of few application notes [6,7] no

* Corresponding author. Address for correspondence: Geriatric Research, Education and Clinical Center, 182B, E.N. Rogers Memorial Veterans Hospital, 200 Springs Road, Bedford, MA 01730, USA.
☆ On leave from Semmelweis University of Medicine, Institute of Pharmacognosy.

0021-9673/94/$07.00
SSDI 0021-9673(93)E1228-R

detailed and systematic study has been performed yet to characterize the OPA–sulfite derivatives of amino acids.

The investigate OPA-sulfite derivatizations, five amino acids (Ala, Arg, Glu, Ser, Tyr) representing five different amino acid groups and their methyl esters (AlaMe, ArgMe, SerMe, TyrMe and glutamate dimethyl ester, GluDiMe) were selected for this study. Our present objectives have been to calculate the long term stability of OPA–sulfite derivatives of amino acids and their methyl esters and to examine the effect of the organic modifier and EDTA on the concentration decrease. In addition, other properties of the derivatives (electrochemical detectability and RP-HPLC retention) which could affect the general liquid chromatographic utility of these products were also investigated.

2. Experimental

2.1. Chemicals

OPA, 2-mercaptoethanol (2-ME), amino acid and methyl ester standards were purchased from Sigma (St. Louis, MO, USA), sodium sulfite, buffer constituents, HPLC-grade water and methanol were from Fisher Scientific (Fair Lawn, NJ, USA) All chemicals were used as received.

2.2. HPLC procedure

Gradient HPLC system equipped with autosampler and IBM Model 286 computer was used in this study (Neurochemical Analyzer, ESA, Bedford, MA, USA). The coulometric electrode array consisted of 16 porous graphite electrodes in series, the oxidation potentials were set from 0 to 960 mV in 60-mV increments. The analytical column used was an Ultracarb (20) ODS, 5 μm, 150 × 4.6 mm (Phenomenex, Torrance, CA, USA) and its temperature was set 35°C. Mobile phase A consisted of 29 m*M* phosphate buffer (pH 7.1) and 0.1 m*M* EDTA while mobile phase B had 65 parts A and 35 parts methanol. The separations were run at 1 ml/min flow-rates, mobile phase B was used to resolve the amino acid methyl ester OPA–sulfite derivatives and to compare the retention and electrochemical properties of all derivatives. Linear gradient (0 min: 8% B; 4 min: 8% B; 22 min: 70%B) was run to separate the amino acid OPA–sulfite derivatives. Hold-up time for k' calculations was determined by injection of 0.05 *M* borate buffer.

2.3. Derivatization procedure

The OPA–2-ME derivatizations were performed as described earlier [8]. OPA (0.15 mg/ml) and 0.1 mg/ml sodium sulfite in 0.05 *M* borate buffer (pH 9.2 for amino acids and pH 8.2 for methyl esters) were used for sulfite derivatizations, and 20% (v/v) methanol and/or 4 μg/ml EDTA was used for stability studies. Typically 10 μl of standard mixtures (individual amino acid and methyl ester concentrations of approximately 0.15 mg/ml) were combined with 990 μl derivatization mixtures and were vortexed for 30 s. The amber glass vials were kept at 20°C on the autosampler rack and 10-μl aliquots were injected onto the HPLC column at different time intervals.

3. Results

Our first experiments studied the RP-HPLC retention and separation of the OPA–sulfite derivatives of the model compounds. As a starting point we selected a mobile phase solvent strength which is used to separate the amino acid OPA–2-ME derivatives [8] and we have used them for the comparisons of these derivatives as well. The underivatized, electrochemically active tyrosine and tyrosine methyl ester were also investigated and the results are summarized in Table 1.

As we expected the amino acid OPA–2-ME derivatives were eluted in the 0.7–8.49 capacity factor range, while the same sulfite derivatives did not retain at all with the k' values less than 0.68. The methyl ester OPA–2-ME derivatives proved to be very non-polar and had high k' values while the OPA–sulfite derivatives had a

Table 1
k' values for native and derivatized (OPA–2-ME, OPA–sulfite) amino acids and methyl esters

	Amino acids			Methyl esters		
	Native	Derivatives		Native	Derivatives	
		2-ME	Sulfite		2-ME	Sulfite
Alanine		8.08	0.37		69.31	2.97
Arginine		4.03	0.44		27.81	2.09
Glutamate		0.70	0.17		94.84[a]	5.72[a]
Serine		2.12	0.27		18.38	1.09
Tyrosine	0.32	8.49	0.68	1.97	>115	11.90

See Experimental section for HPLC conditions.
[a] Dimethyl ethers.

reasonable retention at this solvent strength between 1.09 and 11.9. This capacity factor range was about the same for the amino acid OPA–2-ME derivatives. In general the OPA–sulfite derivatives were essentially more polar than the OPA–2-ME ones and the methyl ester derivatives were retained longer on RP-HPLC than the corresponding amino acid ones. In certain cases the relative retention order was also affected by the different derivatizations or esterification (Table 1). Besides the model compounds other amino acids were also detected with the OPA-sulfite derivatizations. We could observe single, uniform peaks for Asn, Asp, Gln, Gly, His, Ile, Leu, Lys, Met, Phe, Ser, Tau, Thr, Trp, Val, γ-amino-*n*-butyric acid as well as for cysteic acid and dipeptides carnosine and homocarnosine. Most of these amino acid OPA–sulfite derivatives were identified from the 0.1 *M* perchloric acid extracts of different monkey brain tissues as well.

Parallel with the retention studies the electrochemical behaviour of the same derivatives was also investigated (Table 2). Each derivative had a characteristic electrochemical pattern, a dominant oxidation potential where the strongest signal occured and other subdominant potentials with weaker signals. The peak height ratios of the different potentials were highly reproducible if the mobile phase composition was kept constant. The peak heights of the dominant electrodes were considered 100% and the other subdominant signals were expressed as a fraction of it. Ala, Arg, Ser had the same electrochemical behaviour. Their OPA–2-ME derivatives were oxidized at the lowest potentials, while their methyl ester derivatives had 60–120 mV higher oxidation potential maxima. The sulfite derivatives of these amino acids were oxidized at 180 mV higher than the corresponding 2-ME ones, in case of methyl esters this difference has increased by 60 mV. These results indicate that esterification resulted in a slight increase in the oxidation potential maxima for the same derivatives, while the products of the sulfite derivatizations were more difficult to oxidize than the corresponding 2-ME ones. The Glu OPA–2-ME derivative had higher oxidation maximum than expected while the inherent electrochemical activity of Tyr and TyrMe was affected less by the different derivatizations.

Because of the lack of any information on the pH dependent formation of sulfite derivatization of amino acids and their methyl esters we also investigated the suitable derivatization pH range (Fig. 1). Standard mixtures were derivatized at different pH in phosphate and borate buffers and the maximum electrochemical responses were determined by repeated injections at different time intervals from the beginning of derivatization. In the case of amino acids the electrochemical signals of the sulfite derivatives were increased at alkaline pH, and were approximately the same between pH 8 and 10. The increased

Table 2
Comparative electrochemistry of native and derivatized (OPA–2-ME, OPA–sulfite) amino acids and their methyl esters

		Electrode array oxidation potentials in mV							
		300	360	420	480	540	600	660	720
Alanine	2-ME		41.3	*100*	27.0				
	Sulfite					43.7	*100*	29.4	
Methyl ester	2-ME			76.9	*100*	68.1			
	Sulfite						35.2	*100*	88.5
Arginine	2-ME	71.3	*100*	34.4					
	Sulfite			26.2	20.3	93.2	*100*	12.0	
Methyl ester	2-ME			29.6	*100*	42.2			
	Sulfite						87.2	*100*	31.7
Glutamate	2-ME		25.0	78.0	46.8	*100*	66.9		
	Sulfite					34.8	*100*	69.1	
Dimethyl ester	2-ME				53.7	*100*	13.0		
	Sulfite						21.4	86.3	*100*
Serine	2-ME		43.2	*100*	40.3	39.8			
	Sulfite					47.2	*100*	61.5	
Methyl ester	2-ME			83.3	*100*	80.6			
	Sulfite						57.3	*100*	29.3
Tyrosine	Native					20.6	*100*	64.2	
	2-ME		36.2	*100*	44.6	61.7	69.0	47.4	
	Sulfite					61.5	*100*	37.5	
Methyl ester	Native					33.3	*100*	33.1	
	2-ME				68.0	*100*	68.0		
	Sulfite					30.2	*100*	28.1	

The specific oxidation potentials are presented, where the peaks appeared on the electrode array. *100* represents the maximum peak height at the leading channel; peak heights at subdominant channels are expressed as a percentage of the peak height. See Experimental section for HPLC conditions.

isoindole formation in alkaline media is in good agreement with earlier data obtained with organic thiols [1] but we have not experienced considerable differences between the phosphate and borate buffers at the same pH value. The pH-dependent plot for the amino acid methyl ester sulfite derivatives shows a different shape. In the neutral pH range the derivative formation was not complete while the strongly alkaline media saponified the methyl ester groups. The formation of serine methyl ester at pH 8.2 in phosphate buffer was less than in borate buffer and it was best formed under weak acidic condition. On the basis of these results, we decided to derivatize the amino acids at pH 9.2 and the methyl esters at pH 8.2 both in borate buffer.

Before the stability studies the linearity of the electrochemical responses was also investigated. Five different dilutions of amino acid or methyl ester standard mixtures were derivatized the same way and the average peak area values of duplicate determinations were plotted against the concentrations. Linear correlation coefficients of at least 0.999 were obtained for each derivative in the investigated 0.1–10 μM concentration range. Further dilutions were made to establish the detection limit. Although at this point of our research the separations were not optimized, we could identify the sulfite derivatives in the 100–200 fmol range ($S/N = 2$). The same experiments were performed with the amino acid OPA–2-ME derivatizations as well and similar linear correlation coefficients (>0.999) and range of detection limits were established.

The long term stability of amino acid and methyl ester OPA–sulfite derivatives was determined by monitoring their decomposition for a 23-h period. In Fig. 2 arginine and arginine methyl ester serve as a typical example. Usually the first samples, 1 h following the derivatization were considered 100% and the later injections

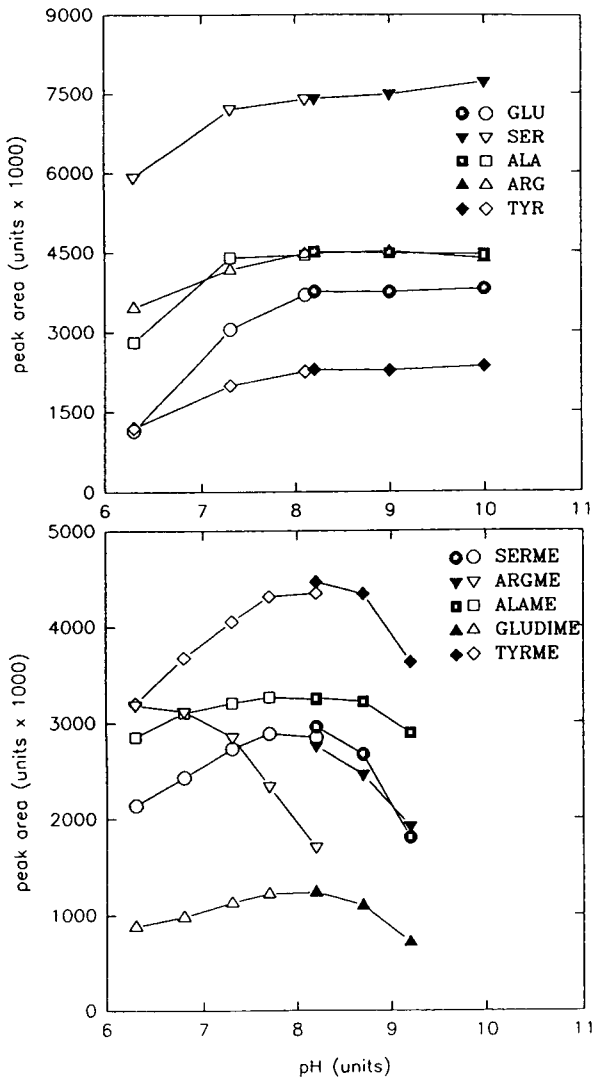

Fig. 1. pH-dependent formation of OPA–sulfite derivatives of amino acids and their methyl esters in phosphate (opened labels) and borate (filled labels) buffers. Each point represents the average of three measurements.

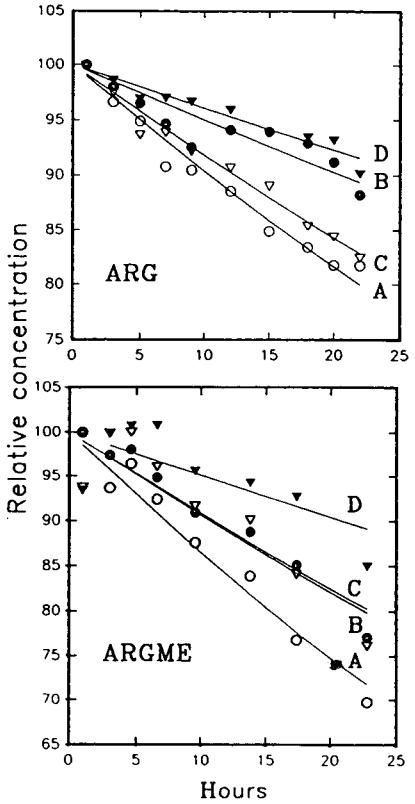

Fig. 2. Long term degradation of OPA–sulfite derivative of arginine and arginine methyl ester (see Table 3 for differences in A, B, C and D derivatizations).

were related to these values. The derivative formation of ArgMe, GluDiMe, SerMe and TyrMe was not complete in 1 h if 20% methanol was involved and in these cases the second time (3 h) point was considered 100%. Earlier observations on the decomposition of primary amine isoindole sulfonates [5] suggested a pseudo-first-order kinetics, and we have calculated and plotted the ideal lines according to this relationship.

To characterize and compare the stability of each derivative we decided to calculate the times required for 6% decrease ($t_{6\%}$) in product concentration (Table 3). Even in the aqueous, buffered derivatization media the amino acid OPA–sulfite derivatives exhibited good stability at room temperature and the $t_{6\%}$ values were several hours. Involvement of EDTA or 20% methanol in the derivatization media has increased the stability. Tyrosine was less affected by these changes while glutamate showed extremely good stability. When both EDTA and methanol were involved, more than 15 h were needed even for the tyrosine concentration to decrease by 6%. We have also calculated the theoretical X values from the A, B and C

Table 3
Long-term stability of OPA–sulfite derivatives of amino acids and their methyl esters in four derivatization mixture

	D. mix.	Amino acids			Methyl esters		
		n	$t_{6\%}$	S.D.	*n*	$t_{6\%}$	S.D.
Alanine	A	10	9.25	0.56	8	11.01	0.57
	B	10	14.39	1.35	8	15.10	0.58
	C	10	12.14	0.53	8	16.29	0.95
	D	10	21.34	1.01	8	>25	
	X		17.28			20.38	
Arginine	A	10	6.09	0.19	8	4.26	0.22
	B	10	12.07	0.94	8	6.28	0.37
	C	10	7.24	0.21	7	6.43	0.71
	D	10	15.44	0.72	7	12.26	2.20
	X		13.22			8.45	
Glutamate	A	10	23.24	2.50	8	11.01	0.50
	B	10	>25		8	>25	
	C	10	>25		7	>25	
	D	10	>25		7	>25	
	X						
Serine	A	10	9.97	0.69	8	2.26	0.09
	B	10	11.84	0.97	8	2.83	0.16
	C	10	9.42	0.49	7	7.60	0.51
	D	10	16.33	0.99	7	8.74	0.66
	X		11.29			8.17	
Tyrosine	A	10	12.58	1.02	8	17.99	1.01
	B	10	13.14	1.05	8	>25	
	C	10	12.63	0.91	7	24.37	1.80
	D	10	15.55	0.95	7	>25	
	X		13.19				

$t_{6\%}$ = 6% Drop in the initial product concentration (h); *n* = number of observations between 1 and 23 h; SD = standard deviation; D. mix. = derivatization mixture; A = aqueous; B = 0.01 m*M* EDTA included; C = 20% (v/v) methanol; D = both EDTA and methanol included; *X* = calculated theoretical value (B − A + C).

experiments. First we subtracted the $t_{6\%}$ values of A experiments (derivatizations performed in aqueous media) from the B ones (derivatizations in the presence of EDTA) with the difference representing the contribution of EDTA on stability increase. These values were added to the $t_{6\%}$ values of C experiments (20% methanol in the derivatization mixture) representing the theoretical addition of EDTA and methanol effect on the stability. These theoretical values were always less than the measured ones (D experiments, both EDTA and methanol in the derivatization mixture) suggesting an enhancement effect between the EDTA and methanol. The same results were found with the methyl ester derivatives. Compared to the amino acids, TyrMe was more stable than Tyr unlike SerMe which had poorer stability than Ser. The other amino acid and methyl ester pairs had approximately the same stability range.

4. Discussion

Our results indicate that very stable amino acid and methyl ester OPA–sulfite derivatives are formed in the presence of 0.01 m*M* EDTA and 20% methanol. Earlier the formation of 1-isoindole sulfonate structure was proposed for this derivatization using isopropylamine as reactant [5].

Expensive and complex instrumentation is not

needed for the derivatizations because the derivatives are stable at room temperature. The measured stability range is competitive or even better than the recently introduced isoindole derivatizations when naphthalene-2,3-dicarboxaldehyde and cyanide [9] or OPA and N-acetyl-L-cysteine were used [10].

Earlier experiments suggested stability enhancement effect of organic solvents [11,12] on the OPA–organic thiol derived isoindoles and our results showed the same effect on the sulfite ones as well. However, care should be taken to choose the proper organic solvent concentrations because high proportions or anhydrous conditions can slow down the rate of derivative formation.

No reports were found on the influence of EDTA or other metal chelator on the isoindole stability. It is possible that EDTA acts by extracting metals because its concentration was more than one magnitude less than that of the other reactants. The autoxidation process which is thought to be responsible to some extent for the isoindole degradation [13,14] is dependent on the amount of contaminating metal ions in the reagents [15]. The extraction of trace metals would slow down the autoxidation process and improve the overall stability.

The OPA–sulfite derivatives of amino acids and their methyl esters, similar to other isoindoles, are good subjects for electrochemical detections and approximately 180 mV increase in the oxidation potential maxima was established compared to the traditional 2-ME derivatives. The same shift was earlier observed when primary amines were used instead of amino acids [5]. The coulometric electrode array proved to be sensitive and accurate for the identification and the quantification of these compounds.

The pH-dependent formation of OPA–sulfite derivatives of amino acids showed a maximum plateau above pH 8, which was independent from the type of buffers. The same methyl ester derivatives had a maximum at pH 8 with the exception of serine methyl ester which was best formed under weak acidic conditions.

Interestingly the amino acid methyl ester OPA–sulfite derivatives had the same retention range on the RP-HPLC column as the amino acid OPA–2-ME ones. We could identify the neurotransmitter amino acid OPA–sulfite derivatives from the perchloric acid extracts of monkey brain tissues as well. Our latest efforts to separate the full amino acid spectrum suggest that the highly polar amino acid OPA–sulfite derivatives can be separated after complex optimization procedures at weak acidic conditions in the presence of ion pairing reagents and these results will be published later.

5. Acknowledgements

This work was supported by USPAS grants A60001-17A2 and HD22539 and by the Department of Veteran Affairs.

6. References

[1] M. Roth, *Anal. Chem.*, 43 (1971) 880.
[2] M.H. Joseph and P. Davies, *J. Chromatogr.*, 277 (1983) 125.
[3] P. Fürst, L. Pollack, T.A. Graser, H. Godel and P. Stehle, *J. Chromatogr.*, 499 (1990) 557.
[4] M.C. García Alvarez-Coque, M.J. Medina Hernández, R.M. Villaneuva Camañas and C. Mongay Fernández, *Anal. Biochem.*, 178 (1989) 1.
[5] W.A. Jacobs, *J. Chromatogr.*, 392 (1987) 435.
[6] S.J. Pearson, C. Czudek, K. Mercer and G.P. Reynolds, *J. Neural Transm. (Gen. Sect.)*, 86 (1991) 151.
[7] S. Smith and T. Sharp, *Br. J. Pharmacol.*, 107 (1992) 210p.
[8] B.A. Donzanti and B.K. Yamamoto, *Life Sci.*, 43 (1988) 913.
[9] P. de Montigny, J.F. Stobaugh, R.S. Givens, R.G. Carlson, K. Srinivasachar, L.A. Sternson and T. Higuchi, *Anal. Chem.*, 59 (1987) 1096.
[10] M.C. García Alvarez-Coque, M.J. Medina Hernández, R.M. Villaneuva Camañas and C. Mongay Fernández, *Anal. Biochem.*, 180 (1989) 172.
[11] R.F. Chen, C. Scott and E. Trepman, *Biochim. Biophys. Acta*, 576 (1979) 440.
[12] S.S. Simons and D.F. Johnson, *Anal. Biochem.*, 82 (1977) 250.
[13] R. Bonnett and S.A. North, *Adv. Heterocycl.*, 29 (1981) 341.
[14] J.F. Stobaugh, A.J. Repta and L.A. Stearnson, *J. Pharm. Biomed. Anal.*, 4 (1986) 341.
[15] B. Halliwell, *Acta Neurol. Scand.*, 126 (1989) 23.

ELSEVIER

Journal of Chromatography A, 668 (1994) 331–335

JOURNAL OF CHROMATOGRAPHY A

Monitoring of optical isomers of some conformationally constrained amino acids with tetrahydroisoquinoline or tetraline ring structures

Antal Péter*[,a], Géza Tóth[b], Dirk Tourwé[c]

[a]*Department of Inorganic and Analytical Chemistry, Attila József University, P.O. Box 440, H-6701 Szeged, Hungary*
[b]*Hungarian Academy of Sciences, Biological Research Centre, Isotope Laboratory "B" Level, P.O. Box 521, H-6721 Szeged, Hungary*
[c]*Eenheid Organische Chemie, Vrije Universiteit Brussel, Pleinlaan 2, B-1050 Brussels, Belgium*

Abstract

Conformationally constrained amino acids were synthesized in optically pure or racemic forms: D- and L-1,2,3,4-tetrahydroisoquinoline-3-carboxylic acid, its *erythro*-D,L-4-methyl analogue, D- and L-1,2,3,4-tetrahydro-7-hydroxyisoquinoline-3-carboxylic acid, D- and L-1,2,3,4-tetrahydro-7-hydroxy-6,8-dibromo- and -6,8-diiodo-isoquinoline-3-carboxylic acid and D,L-6-hydroxy-2-aminotetraline-2-carboxylic acid. A method was developed for the separation and identification of optical isomers using precolumn derivatization with chiral derivatization reagents: 1-fluoro-2,4-dinitrophenyl-4-L-alaninamide and 2,3,4,6-tetra-O-acetyl-β-D-glucopyranosyl isothiocyanate. The effects of pH, eluent composition and different buffers on the separation were also investigated.

1. Introduction

Diastereomeric peptides, isomers in which one or more asymmetric centres have opposite configurations, may have similar or different physico-chemical or biological properties. The biological activities often exhibit antagonistic or agonistic properties which differ greatly from each other.

In the synthesis of receptor-selective peptides, unusual racemic amino acids are often used, or the originally pure amino acid can racemize to some extent in the course of protection and synthesis. It is therefore very important to develop effective chromatographic methods for the separation of racemic amino acids and for the characterization and identification of optically pure products.

Several papers and reviews have been published on the development of enantioselective separations. High-performance liquid chromatographic (HPLC) methods can be divided into three main groups: direct separation on chiral columns [1–3], separation on achiral columns with chiral mobile-phase additives [3–5] and separation of the diastereoisomers formed by precolumn derivatization with chiral reagents [3,6–17].

Some conformationally constrained aromatic amino acids have been synthesized in our laboratory for the design of receptor-selective opioid

* Corresponding author.

0021-9673/94/$07.00
SSDI 0021-9673(93)E1036-Y

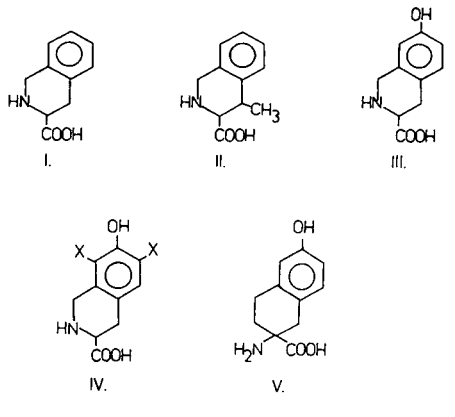

Fig. 1. I = Tic, D- and L-1,2,3,4-tetrahydroisoquinoline-3-carboxylic acid; II = β-Me-Tic [*erythro*, (*SS*, *RR*)], D,L-1,2,3,4-tetrahydro-4-methylisoquinoline-3-carboxylic acid; III = HOTic, D- and L-1,2,3,4-tetrahydro-7-hydroxyisoquinoline-3-carboxylic acid; IVa = Br_2HOTic and IVb = I_2HOTic, D- and L-1,2,3,4-tetrahydro-7-hydroxy-6,8-dihaloisoquinoline-3-carboxylic acid; V = Hat, D,L-6-hydroxy-2-aminotetraline-2-carboxylic acid.

peptides (Fig. 1). This paper describes the separation of isomers of these unusual amino acids. For this purpose, an HPLC method was applied, using precolumn derivatization with 1-fluoro-2,4-dinitrophenyl-5-L-alaninamide (FDAA, Marfey reagent) and 2,3,4,6-tetra-O-acetyl-β-D-glucopyranosylisothiocyanate (GITC). The effects of the eluent composition and of the nature of the buffer on the separation of D- and L-isomers were investigated under isocratic conditions.

2. Experimental

2.1. Chemicals and reagents

The amino acids in Fig. 1 were prepared by literature methods: in optically pure form I [18], III [19] and IV [19], and in racemic form II [20] and V [21]. All compounds were checked by melting point determination, ^{1}H NMR spectrometry, fast atom bombardment MS and chiral TLC [22].

FDAA and L-amino acid oxidase were purchased from Sigma (St. Louis, MO, USA), GITC from Aldrich-Chemie (Steinhem, Germany) and trifluoroacetic acid, sodium acetate, potassium dihydrogenphosphate of analytical-reagent grade, HPLC-grade solvents (acetonitrile and methanol) and other reagents of analytical-reagent grade from Merck (Darmstadt, Germany). Buffers were prepared with doubly distilled water and further purified by pumping through a 0.45-μm CA filter (Paraplan, Budapest, Hungary). The pH was adjusted with phosphoric acid (phosphate buffer), acetic acid (acetate buffer) or sodium hydroxide.

Chiral TLC was performed on Chiralplates (Macherey–Nagel, Düren, Germany) with detection using 0.1% ninhydrin spray reagent.

2.2. Apparatus

The HPLC system consisted of an L-6000 liquid chromatographic pump (Merck–Hitachi, Tokyo, Japan), a Model 7125 injector with a 20-μl loop (Rheodyne, Cotati, CA, USA), a variable-wavelength UV 308 spectrophotometric detector (Labor MIM, Budapest, Hungary) and an HP 3395 integrator (Hewlett-Packard, Waldbroun, Germany). The columns used were Vydac 218 TP 104 C_{18} (250 × 4.6 mm I.D., 10 μm particle size) (Separations Group, Hesperia, CA, USA) and Nucleosil 10C_{18} (250 × 4.6 mm I.D., 10 μm particle size) (Macherey–Nagel).

^{1}H NMR spectroscopy was performed on an AM 400 spectrometer (Brucker, Zug, Switzerland).

2.3. Derivatization of amino acids

Amino acids (0.5–1 mg) were derivatized with FDAA or GITC by the method of Marfey [12] or Nimura *et al.* [9].

2.4. Enzymatic digestion of *erythro*-D,L-β-MeTic

erythro-D,L-β-MeTic (0.3 mg) was dissolved in 0.1 *M* Tris buffer (pH 7.2) in a test-tube and 0.3 mg of L-amino acid oxidase was added. The test-tube was filled with oxygen, tightly closed and incubated for 24 h at 37°C. The reaction mixture was used for derivatization reactions.

The configuration of D,L-Hat could not be determined directly with L-amino acid oxidase because of the lack of an α-hydrogen. The sequence of isomers was presumed by analogy with other amino acids.

3. Results and discussion

3.1. Separation of FDAA derivatives

The HPLC separation of the derivatized amino acids was carried out in the three different aqueous buffer systems containing acetonitrile as organic modifier: 0.1% trifluoroacetic acid, 0.01 *M* potassium dihydrogenphosphate (pH 3) and 0.01 *M* sodium acetate (pH 3); pH 3 was chosen on the basis of preliminary experiments and our earlier work on D,L-β-methylphenylalanine separations [23]. The k' values at low buffer pH were very high, probably because of the total protonation of the amino acids. At higher pH, the R_s values decreased.

It is interesting to compare the effects of the organic modifier content of the eluent and of different buffers on the separation of the isomers. With a decrease in the organic content of the mobile phase from 50% to 40–35%, k' increased and the separation of the L- and D-forms improved. In some instances an acceptable separation was attained (Table 1). A further decrease in the acetonitrile concentration to 30% improved the resolution of the L- and D-forms of I, II and III (Figs. 2–4), whereas only a partial resolution of V was observed even at 20% acetonitrile. IVa and b exhibited large values of k' (>30) at 30% acetonitrile, and the use of a high concentration of organic modifier is therefore favourable (Fig. 5).

Investigation of the effects of the buffers on the separation showed that the TFA systems have high k' values compared with the phosphate and acetate systems, probably because the pH of the eluent was lower than 3. In the sodium acetate system, the k' values (except that for II) were lower and the resolution and peak shape also seemed better (Figs. 2–5).

Table 1
Dependence of capacity factor (k'), separation factor (α) and resolution (R_s) of FDAA derivatives on eluent composition

Amino acid	Eluent[a]	k'_L	k'_D	α	R_s
I	TFA	11.00	18.00	1.64	3.88
	KH_2PO_4	9.55	15.53	1.61	2.15
	NaOAc	5.50	8.50	1.54	3.33
II	TFA	20.66	25.53	1.23	1.60
	KH_2PO_4	17.17	22.50	1.31	2.34
	NaOAc	22.66	28.22	1.24	3.64
III	TFA	5.86	9.00	1.54	2.24
	KH_2PO_4	5.20	8.00	1.54	2.15
	NaOAc	3.82	5.66	1.48	2.36
IVa	TFA (40:60)	15.05	17.50	1.16	1.02
	KH_2PO_4 (35:65)	11.00	14.96	1.30	1.23
	NaOAc (35:65)	8.86	12.50	1.41	1.30
IVb	TFA (35:65)	21.13	22.61	1.07	0.98
	KH_2PO_4 (35:65)	15.66	17.53	1.12	1.07
	NaOAc (35:65)	15.11	21.20	1.40	2.20
V	TFA (20:80)	8.33	8.91	1.07	0.43
	KH_2PO_4 (20:80)	6.67	7.27	1.09	0.42
	NaOAc (20:80)	6.27	6.77	1.08	0.49

Column, Vydac 218 TP 104 C_{18} (250 × 4.6 mm I.D.); flow-rate, 1 ml/min.
[a] CH_3CN–buffer (30:70). Buffer: TFA = 0.1% trifluoroacetic acid; KH_2PO_4 = 0.01 *M* KH_2PO_4 (pH 3); NaOAc = 0.01 *M* CH_3COONa (pH 3).

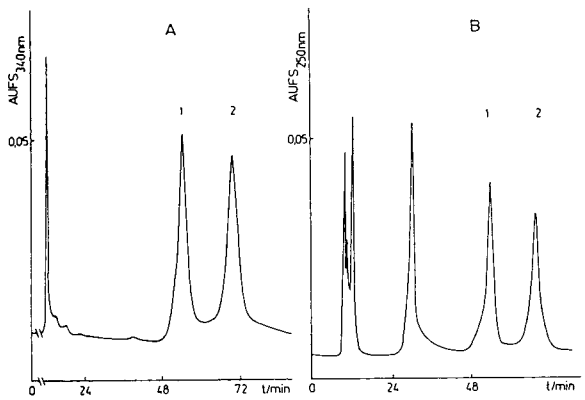

Fig. 2. Chromatograms of Tic derivatives. Column: Vydac 218 TP 104 C_{18} (250 × 4.6 mm I.D.); flow-rate, 1 ml/min; eluent, acetonitrile–0.01 *M* sodium acetate (pH 3) (30:70); derivatization reagent, (A) FDAA and (B) GITC. Peaks: 1 = L-Tic; 2 = D-Tic.

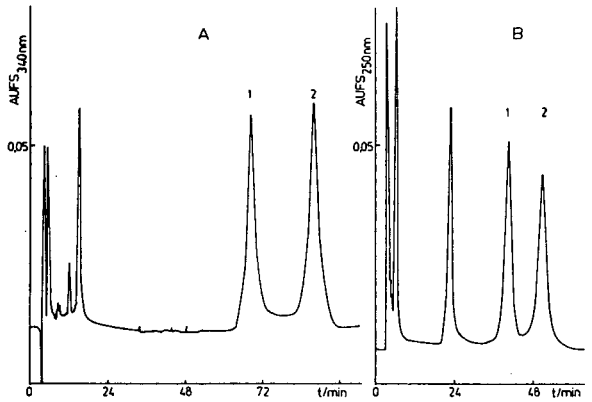

Fig. 3. Chromatograms of β-Me-Tic derivatives. Conditions as in Fig. 2. Peaks: 1 = L-β-MeTic; 2 = D-β-MeTic.

3.2. Separation of GITC derivatives

The separations were carried out with the same eluent systems and the results are summarized in Table 2. The GITC derivatives of amino acids had lower k' values than those of the FDAA derivatives. Good separations were achieved for I, II and III at 30% acetonitrile (Figs. 2–4). IVa and b had lower k' values than those of the FDAA derivatives and the peaks remained somewhat overlapped. Surprisingly, the high k' values for V were not accompanied by good resolution. When the organic modifier was changed from acetonitrile to methanol, a good resolution with low k' values was observed with the sodium acetate buffer system (Fig. 6).

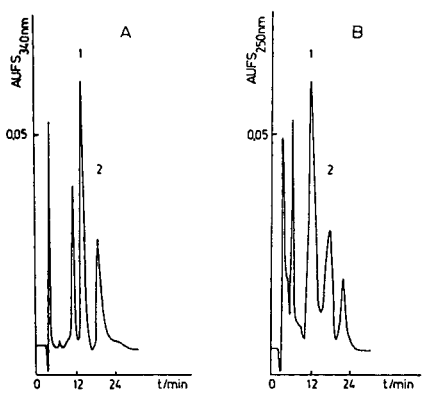

Fig. 4. Chromatograms of HOTic derivatives. Conditions as in Fig. 2. Peaks: 1 = L-HOTic; 2 = D-HOTic.

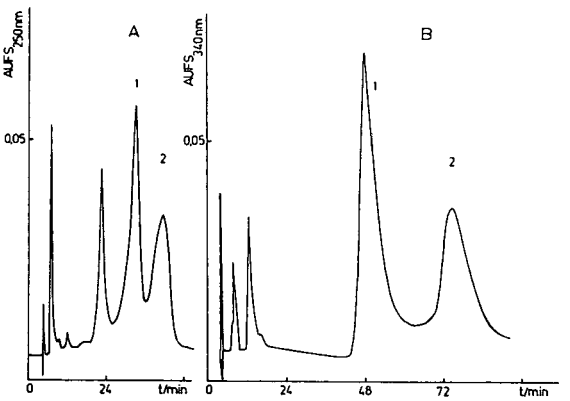

Fig. 5. Chromatograms of Br_2HOTic and I_2HOTic derivatives. Column, Vydac 218 TP 104 C_{18} (250 × 4.6 mm I.D.); flow-rate, 1.0 ml/min; eluent, (A) acetonitrile–0.01 *M* sodium acetate (pH 3.0) (30:70) and (B) acetonitrile–0.01 *M* sodium acetate (pH 3.0) (35:65). (A) Br_2HOTic + GITC; (B) I_2HOTic + FDAA. Peaks: 1 = L-isomer; 2 = D-isomer.

4. Conclusions

The described procedures can be applied to the separation and identification of conformationally constrained unusual aromatic amino acids. The acetonitrile–sodium acetate systems are generally more efficient than TFA or phosphate systems in the separation of isoquinoline

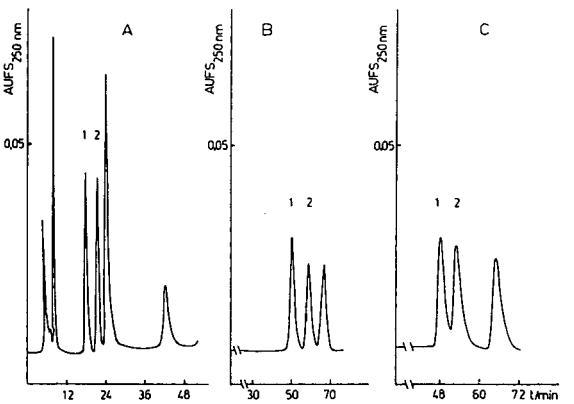

Fig. 6. Chromatograms of Hat derivatives. Column: Vydac 218 TP 104 C_{18} (250 × 4.6 mm I.D.); flow-rate, 1.0 ml/min; eluent, (A) methanol–0.01 *M* sodium acetate (pH 3) (40:60), (B) methanol–0.01 *M* potassium dihydrogenphosphate (pH 3) (35:65) and (C) methanol–0.1% trifluoroacetic acid (35:65); derivatization reagent, GITC. Peaks 1 = L-Hat; 2 = D-Hat.

Table 2
Dependence of capacity factor (k'), separation factor (α) and resolution (R_s) of GITC derivatives on eluent composition

Amino acid	Eluent[a]	k'_L	k'_D	α	R_s
I	TFA	11.48	15.53	1.35	1.83
	KH_2PO_4	9.56	12.33	1.29	2.50
	NaOAc	6.78	10.00	1.59	4.11
II	TFA	17.20	2.08	1.33	1.66
	KH_2PO_4	15.47	20.11	1.30	3.10
	NaOAc	12.74	16.23	1.27	2.18
III	TFA	4.07	6.27	1.53	1.16
	KH_2PO_4	4.01	6.22	1.55	1.34
	NaOAc	3.08	4.66	1.52	1.32
IVa	TFA	12.11	14.77	1.22	0.92
	KH_2PO_4	14.23	17.08	1.20	1.19
	NaOAc	10.00	12.77	1.28	1.32
IVb	TFA (35:65)	9.44	10.95	1.16	0.89
	KH_2PO_4 (35:65)	11.27	13.41	1.19	1.08
	NaOAc (35:65)	6.86	8.37	1.22	1.33
V	TFA (20:80)	23.00	25.33	1.11	0.96
	KH_2PO_4 (20:80)	22.33	25.33	1.13	0.85
	NaOAc (20:80)	14.80	16.86	1.14	0.73
V[b]	TFA (35:65)	15.33	16.94	1.10	1.12
	KH_2PO_4 (35:65)	15.83	18.43	1.16	1.49
	NaOAc (35:65)	4.72	5.88	1.25	1.78

Column, Vydac 218 TP 104 C_{18} (250 × 4.6 mm I.D.).
[a] CH_3CN–buffer (30:70). Buffer: TFA = 0.1% trifluoroacetic acid; KH_2PO_4 = 0.01 *M* KH_2PO_4 (pH 3); NaOAc = 0.01 *M* CH_3COONa (pH 3).
[b] Organic modifier: CH_3OH.

ring-containing amino acids. GITC derivatives have lower k' values than those of FDAA derivatives. Dibromo- and diiodohydroxy-Tic exhibit large k' values with characteristic band broadening. The optical isomers of hydroxy-aminotetralincarboxylic acid could only be analysed in the methanol-containing system.

5. Acknowledgement

This work was supported by grants from the Hungarian Research Foundation (OTKA 71/91 and OTKA 2993/91).

6. References

[1] W.H. Pirkle and J. Finn, in J. Morrison (Editor), *Asymmetric Synthesis, Vol. I, Analytical Methods*, Academic Press, New York, 1983, Ch. 6.
[2] W.F. Lindner and C. Petterson, in I. Wainer (Editor), *Liquid Chromatography in Pharmaceutical Development: an Introduction*, Part 1, Aster, Springfield, VA, 1985, p. 63.
[3] D.W. Armstrong and S.M. Han, *CRC Crit. Rev. Anal. Chem.*, 19 (1988) 175.
[4] V.A. Davankov, A.A. Kurganov and A.S. Bochkov, *Adv. Chromatogr.*, 22 (1983) 71.
[5] C. Petterson, *Trends Anal. Chem.*, 7 (1988) 209.
[6] W.F. Lindner, in L. Crane and B. Zief (Editors), *Chromatographic Chiral Separations*, Marcel Dekker, New York, 1987, p. 91.
[7] W.F. Lindner, in J.F. Lawrence and R.W. Frei (Editors), *Chemical Derivatization in Analytical Chemistry*, Vol. 2, Plenum Press, New York, 1982, p. 145.
[8] T. Nambara, in W.S. Hancock (Editor), *CRC Handbook of HPLC for the Separation of Amino Acids, Peptides and Proteins*, Vol. I, CRC Press, Boca Raton, FL, 1984, p. 383.
[9] N. Nimura, H. Ogura and T. Kinoshita, *J. Chromatogr.*, 202 (1980) 375.
[10] T. Kinoshita, Y. Kasahara and N. Nimura, *J. Chromatogr.*, 210 (1981) 77.
[11] N. Nimura, A. Toyama and T. Kinoshita, *J. Chromatogr.*, 316 (1984) 547.
[12] P. Marfey, *Carlsberg Res. Commun.*, 49 (1984) 591.
[13] S. Einarsson, B. Josefsson, P. Möller and D. Sanchez, *Anal. Chem.*, 59 (1987) 1191.
[14] H. Brückner and C. Gah, *J. Chromatogr.*, 555 (1991) 81.
[15] H. Brückner, R. Wittner and H. Godel, *Chromatographia*, 32 (1991) 383.
[16] H. Brückner and B. Strecker, *Chromatographia*, 33 (1992) 586.
[17] S. Einarsson and G. Hansson, in C.T. Mant and R.S. Hodges (Editors), *High Performance Liquid Chromatography of Peptides and Proteins*, CRC Press, Boca Raton, FL, 1991, p. 369.
[18] A. Pietet and T. Spengler, *Chem. Ber.*, 44 (1911) 2030.
[19] K. Verschueren, G. Tóth, D. Tourwé, M. Lebl, G. Van Binst and V.J. Hruby, *Synthesis*, (1992) 458.
[20] M. Lebl, G. Tóth, I. Slaninova and V.J. Hruby, *Int. J. Pep. Protein Res.*, 40 (1992) 148.
[21] T. Deeks, D.A. Crooks and R.D. Waigh, *J. Med. Chem.*, 26 (1983) 762.
[22] G. Tóth, M. Lebl and V.J. Hruby, *J. Chromatogr.*, 504 (1990) 450.
[23] A. Péter, G. Tóth, E. Cserpán and D. Tourwé, *J. Chromatogr.*, 660 (1994) 283.

ELSEVIER

Journal of Chromatography A, 668 (1994) 337–344

JOURNAL OF CHROMATOGRAPHY A

Effect of the characteristics of the phase system on the retention of proteins in hydrophobic interaction chromatography

László Szepesy*,[a], Géza Rippel[b]

[a]Department of Chemical Technology, Technical University of Budapest, Budafoki u. 8, H-1521 Budapest, Hungary
[b]Department of Agricultural Chemical Technology, Technical University of Budapest, Budafoki u. 8, H-1521 Budapest, Hungary

Abstract

In contrast to reversed-phase chromatography (RPC), where the stationary phases available show only minor differences as regards the retention and selectivity of separation, in hydrophobic interaction chromatography (HIC) the various stationary phases may show different effects depending on the type of support and ligand applied. In this work, the data obtained on four commercially available HIC columns with five standard proteins using salts of different types were investigated. It was found that the slope–intercept plot derived from the ln k *vs.* salt molality relationship can furnish a useful characterization of the hydrophobic interaction chromatography of proteins. A new hydrophobicity index introduced in RPC can also be applied as an overall parameter to characterize hydrophobic interaction. By using the above parameters the effects of both the column type and salt can be evaluated. Characterization of the HIC columns can be of considerable assistance in the selection of the appropriate column for a given separation.

1. Introduction

In the last decade, high-performance hydrophobic interaction chromatography (HIC) has developed into a powerful and popular technique for the analytical and preparative separation of proteins and other biopolymers [1–16]. Although the molecular interaction involved, London-type dispersion, is similar to that operating in reversed-phase liquid chromatography (RPLC), there are substantial differences as regards the separation of biologically active materials. Table 1 shows the main characteristics of the two techniques.

In RPLC packings the functional groups are long alkyl chains, very densely distributed, producing strongly hydrophobic surfaces. As a result, organic solvents must be used to desorb the proteins. As a consequence of the strong interaction and the organic solvent used, most of the proteins are subjected to unfolding and could loose some or all of their biological activity.

In contrast, in HIC packings there are short alkyl or cyclic functional groups, much more sparsely distributed, producing moderately hydrophobic surfaces and resulting in mild hydrophobic interaction. As a result, elution can be accomplished by buffers without addition of organic solvents. Proteins are retained at high initial salt concentrations (1–3 M) and eluted

* Corresponding author.

0021-9673/94/$07.00
SSDI 0021-9673(93)E0040-2

Table 1
Comparison of RPLC and HIC

Parameter	RPLC	HIC
Interaction	Dispersion	Dispersion
Stationary phase:		
Ligand type	Long alkyl chains (C_8–C_{18})	Short alkyl chains (C_2–C_4), phenyl, CH_x
Ligand density	High	Low
Hydrophobicity	Strong	Moderate
Mobile phase:		
Type	Aqueous–organic (CH_3OH, CH_3CN)	Solution of different salts
Operation	Gradient	Reverse gradient
Protein:		
Structure on the stationary phase	Unfolded	Native (folded, three-dimensional)
Dominant feature (retention)	Overall hydrophobicity (primary sequence)	Surface hydrophobicity
Loss of biological activity	Considerable	Small

selectively by decreasing the salt concentration using reverse gradients under conditions that promote the preservation of the biological activity of most proteins [3,4].

In recent years, several stationary phases have been developed for HIC on various matrices with different functional groups and with widely different retention characteristics [1,2,5,10–12]. In addition, various mobile phase parameters (type of salt, initial salt concentration, gradient time, flow-rate, temperature, pH, addition of organic modifiers) are applicable for the modulation of retention and selectivity [3–9,13–16].

In our laboratory, measurements have been carried out under gradient conditions on four commercially available HIC columns with different types of salts [17–19]. By comparison and evaluation of the data obtained, it was demonstrated that the retention and selectivity of protein separations depend on both the type of stationary phase and the salt used [17,19,20]. In contrast to RPLC, where the stationary phases show only minor differences as regards the absolute and relative retentions of various solutes [21–25], in HIC the stationary phases may show different effects depending on the type of support and ligand applied [4–12].

In this study, we investigated the characteristics that can be used to describe the hydrophobic interaction and retention of proteins on HIC columns of different types and using different types of salts in the mobile phase.

2. Experimental

The experimental approach used in this study was taken from the papers of Szepesy and Rippel [17,19], where exact descriptions of the materials and the chromatographic conditions are given. The data obtained under gradient conditions were evaluated according to the linear solvent strength (LSS) model of gradient elution with a program written in C and run on the computer used as a part of the chromatographic system. (For the theory of the LSS model and for the details of the evaluation procedure see ref. 19 and references cited therein.)

2.1. Columns [17,19]

TSK-Phenyl 5-PW (PHE) (Beckman, San Ramon, CA, USA), Synchropak-Propyl (PRO) (Synchrom, Linden, IN, USA), Spherogel CAA-HIC (CAA) (Beckman) and Alkyl-Superose HR 10/10 (ALK) (Pharmacia–LKB, Uppsala, Sweden) columns were used.

2.2. Proteins [17]

Cytochrome *c* (CYT), ribonuclease A (RNA), ovalbumin (OVA), lysozyme (LYS), α-chymotrypsinogen A (CHY) were obtained from Sigma (St. Louis, MO, USA).

3. Results and discussion

Users often find the behaviour of proteins on HIC media to be unpredictable. Generally it is difficult to identify the characteristics of a protein, *e.g.*, its hydrophobicity, that will predict its interaction with the HIC packing. The significance of hydrophobicity in stabilizing protein structure has been recognized and is amply reviewed in the literature. However, a quantitative description and understanding of hydrophobic interaction and its exact role, *e.g.*, in the folding of proteins, is still being investigated.

In the literature over 80 more or less different set of parameters have been reported to describe the hydrophobicity of amino acids [26]. These parameters were used to predict the overall hydrophobicity of the proteins or to characterize their surface regions, on the basis of the primary amino acid sequence. In several studies it was found that very few of these descriptors derived for hydrophobicity correlate well. In addition, most of the widely used set of hydrophobicity parameters show very poor correlation with the retention behaviour of the proteins [26,27]. According to the most recent theory suggested, the hydrophobicity is not constant and is closely related to the hydration of amino acids in a changing environment [28,29]. For this reason, we tried to find some parameters derived directly from the chromatographic measurements with standard proteins to characterize interactions in HIC.

Several models have been suggested to describe the retention of proteins under HIC conditions. The theoretical backgrounds of these models are different, *e.g.*, preferential interaction [30,31], displacement model of chromatography [32] or a combination of the hydrophobic and electrostatic interactions existing in an HIC phase system [33], and none of them has gained general acceptance. It was found that at the higher salt concentrations regularly used in HIC the retention of solutes can be readily described with a two-parameter linear function:

$$\ln k = \ln k_w + S m_s \quad (1)$$

where m_s is the molality of the salt used, $\ln k_w$ is the intercept, *i.e.*, the hypothetical retention in pure water, and S is the slope of the function. We have found that our data correlate well with Eq. 1 [19], and we therefore studied the influence of the operating parameters on the retention of proteins according to this relationship.

This type of equation is very similar to that used in RPLC to describe the retention behaviour of the solutes and characterize their hydrophobicity [24,25,35]. The S index for a particulate solute was observed to be nearly constant on different C_{18} packing materials [34]. On the other hand, $\ln k_w$ was suggested as a descriptor of hydrophobicity for various solutes [24,25].

In HIC, both parameters of Eq. 1 have also been suggested to describe hydrophobic interaction. Fausnaugh and Regnier [6] presented $\ln k_w$ as the "strength of hydrophobic interaction". Horváth and co-workers [7,33] introduced S as a "hydrophobic interaction parameter". However, none of these parameters has been found adequate to describe the hydrophobic interaction of various proteins under different operating conditions. The retention characteristic of a protein depends on both the intercept and slope. For this reason, these parameters should be combined, *e.g.*, by plotting the slope as a function of the intercept, which can be given as

$$S = p + q \ln k_w \quad (2)$$

where p and q are constants for a given stationary phase in a given salt solution. Gehas and Wetlaufer [35] investigated this relationship for dansylamino acids. They found that a good correlation existed between the slope and intercept values, which suggests that both are dependent variables. Whereas the slope depends on the contact surface area of the molecule, the intercept seems to characterize the strength of

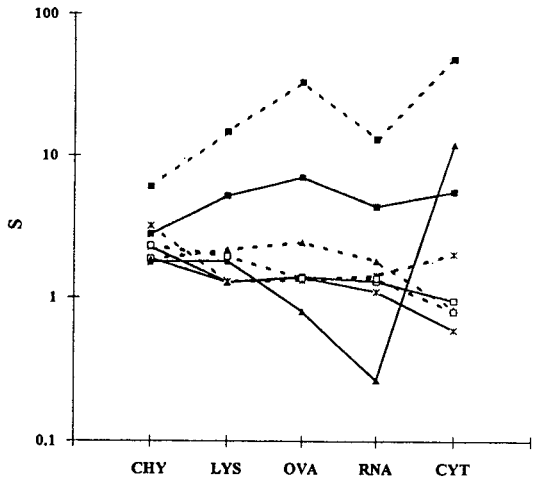

Fig. 1. Slopes of the ln k *vs.* salt molality relationship obtained in ammonium sulphate (solid lines) and in sodium citrate (dashed lines) for the columns and proteins investigated. Column: ◘ = ALK; ▲ = CAA; * = PHE; □ = PRO.

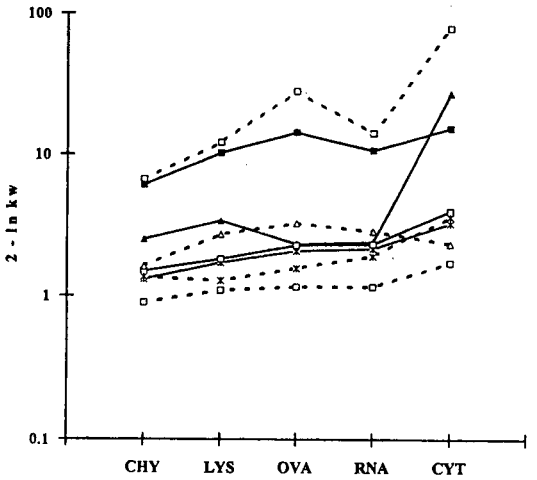

Fig. 2. Intercepts of the ln k *vs.* salt molality relationship obtained in ammonium sulphate (solid lines) and in sodium citrate (dashed lines) for the columns and proteins investigated. Column: ◘ = ALK; ▲ = CAA; * = PHE; □ = PRO.

the interaction between the solute and stationary phase [6,7,33,35].

In Fig. 1, the slopes of the ln k *vs.* salt molality relationships obtained in ammonium sulphate (AS) and sodium citrate (SC) for the columns and proteins investigated are shown. With both salts the S values are very close on the PHE and PRO columns, reflecting the similar characteristics of these columns [17]. The S values obtained on the CAA column are different and the largest deviations are observed on the ALK column [19].

Fig. 2 shows the intercept values in AS and in SC for the columns and proteins investigated. In order to present all the data on the same figure, the scale has been transformed as indicated, *i.e.*, inverse scaling is used. The courses of these plots are very similar to those presented in Fig. 1. The PHE column produces similar values for all proteins, the PRO and CAA columns slightly different values and the deviations on the ALK column are the largest.

The effect of the salt type on the parameters can be evaluated by plotting the values obtained in the different salt solutions against each other. Fig. 3a shows a comparison of the slope values and Fig. 3b that of the intercept values for the two salts investigated. The data obtained on the PHE column are on or around the diagonals, indicating a minor effect of the salt change. On the PRO column the impact is more pronounced on the intercepts and lower on the slopes. The data obtained on the CAA and ALK columns show considerable changes in the characteristics when using SC instead of AS. On all columns the extent of effect is highly dependent on the type of protein, *i.e.*, it is not the same for the different proteins.

Fig. 4 shows the slope–intercept relationships obtained on the various columns. (Note that the lines on the figure do not cover the values relating to the proteins; they only demonstrate the effect of salt change. The markers are not real values but are used only for designation.) On the PHE column the regression lines almost coincide, *i.e.*, the salts affect the retentions similarly. On the PRO column the positions of the lines are very different. The slopes (q in Eq. 2) are positive on both of these columns. On the CAA and ALK columns the change of salt results in distinctly different courses of the data. On these columns the slopes in Eq. 2 are negative and the spread of the points indicates an opposite tendency of modifications. The extent of the changes on the CAA column is similar to those on the PRO column but in the opposite direction. The largest changes were

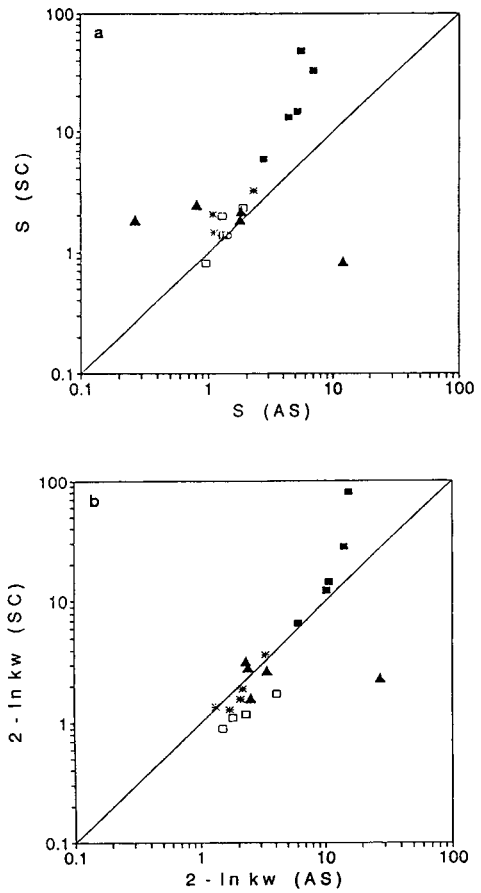

Fig. 3. Comparison of (a) the slope and (b) the intercept values obtained in ammonium sulphate (AS) and those obtained in sodium citrate (SC) on the columns investigated. Column: ◘ = ALK; ▲ = CAA; * = PHE; □ = PRO.

obtained on the ALK column (cf. Figs. 1 and 2). This column was also tested with sodium acetate [19] and the results are also presented.

The intercepts of the regression lines (p in Eq. 2) also show different courses. On the PHE and PRO columns the intercept decreased, whereas on the CAA and ALK columns it increased on replacing AS with SC. This indicates that the characteristics of the phase system are not modified in the same way on changing the type of salt in the eluent.

Most recently Valkó and Slégel [36] suggested a new hydrophobicity index (φ_0) of solutes under RPLC conditions which can be calculated as the

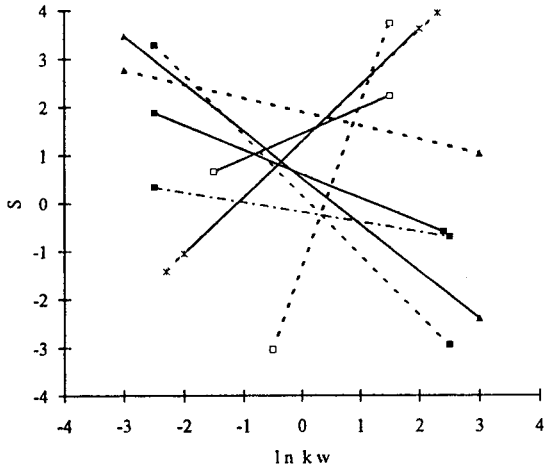

Fig. 4. Slope–intercept relationships obtained in ammonium sulphate (solid lines), in sodium citrate (dashed lines) and in sodium acetate (dot-dashed lines) on the columns investigated. Column: ◘ = ALK; ▲ = CAA; * = PHE; □ = PRO. The lines do not cover the region of the values obtained experimentally; they only represent the fit of Eq. 2. For more details, see text.

ratio of the intercept and the slope values obtained from the log k *vs.* φ (volume fraction of the organic modifier) relationship. Under HIC conditions this parameter can be designated by m_0:

$$m_0 = -\ln k_w / S \quad (3)$$

As m_0 is the salt molality, where $\ln k = 0$ (*cf.* Eq. 1), this means that when using this eluent the molar concentrations of the related compound are identical in the stationary and mobile phases. This parameter can also be used as a descriptor similar to $\ln k_w$. With $\ln k_w$ the mobile phase composition is fixed ($m = 0$) and the extent of retention is used for the characterization. With m_0 the reference condition is a fixed retention ($\ln k = 0$) and the salt concentration of the mobile phase in which it is obtained is taken into consideration.

In Fig. 5, the m_0 values determined in AS and in SC are shown for all the columns and proteins investigated. In some instances the values obtained are fictitious as m_0, *i.e.*, the characteristic concentration of the salt, is lower than zero. This means that in these instances the reference

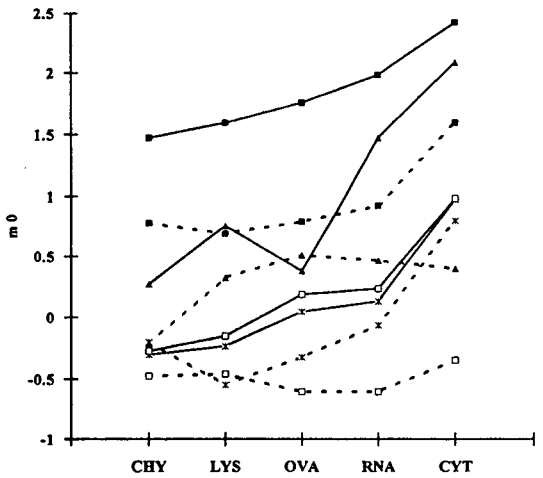

Fig. 5. m_0 values determined in ammonium sulphate (solid lines) and in sodium citrate (dashed lines) for the columns and proteins investigated. Column: ■ = ALK; ▲ = CAA; * = PHE; □ = PRO.

condition cannot be maintained under real conditions, *i.e.*, the ln k_w values of the related components are higher than zero. However, the value are applicable for comparison.

The plots obtained are very similar to those presenting the slope and intercept values (Figs. 1 and 2), but as m_0 involves both of these values it can be regarded as an overall parameter reflecting the "retentive strength" of the related phase system. The positions of the markers for the individual columns indicate the relative strength of the hydrophobic interaction between the stationary phase and the proteins investigated because the larger is m_0 the weaker is the interaction.

As regards the strength of the stationary phases, in AS the PHE and PRO columns are the strongest and they are very similar. The CAA column is weaker and the ALK column has the lowest strength. In SC the strength of the interaction is increased (the m_0 values are lower), *i.e.*, the retention on the same column is always higher in SC than in AS. The order of the columns seems to remain the same but the differences between the columns are smaller.

In order to evaluate the effect of salt on the columns the m_0 values obtained with the different salts can be plotted against each other. Fig. 6 shows the m_0 values obtained with AS and SC for the four columns. The spread of the points indicates that some correlation exists within the two sets. A straight line could have been fitted to the data with a good correlation. The values relating to the different columns are located in different regions along this line. These regions for the PHE and PRO columns are partly overlapped, which is an indication of the similarity of these stationary phases, but the effects of the salt change are different. The slope of the regression line equals the rate of the molal surface tension increments of the two salts. As regards the behaviour of the proteins on the columns, the larger is the distance of the points from the diagonal, the greater is the effect of the salt change.

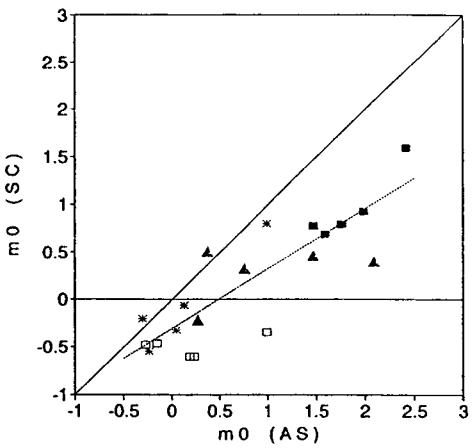

Fig. 6. Comparison of the m_0 values determined in ammonium sulphate (AS) and in sodium citrate (SC) on the columns investigated. Column: ■ = ALK; ▲ = CAA; * = PHE; □ = PRO. Dashed line = fit. For details, see text.

4. Conclusions

The slope–intercept relationship derived from the ln k *vs.* salt molality plot can furnish a useful characterization of the hydrophobic interaction chromatography of proteins. The new hydrophobicity index (φ_0) introduced in RPLC can

also be applied in HIC, providing an overall parameter to describe hydrophobic interaction. By using this parameter the effects of both the column type and salt can be evaluated.

On the PHE and PRO columns, which furnish data with positive slopes of the slope *vs.* intercept plot, the change of salt has a minor effect on the retention of proteins although the relative retention, *i.e.*, the selectivity, may change considerably. These phase systems can be designated as stationary phase controlled.

In contrast, on the CAA and ALK columns, the data produce negative slopes of the slope–intercept plot. The change of salt type has a large effect on the retention of proteins and on the selectivity of separation. These phase systems can be termed mobile phase or salt controlled.

In contrast to RPLC, where the stationary phases show only minor differences as regards the retention and selectivity of separation for various solutes, in HIC the stationary phases may show different effects depending on the type of support and ligand applied. For this reason it is of practical importance to characterize every HIC column in order to predict the performance to be expected in a given separation. If sufficient separation of a sample cannot be achieved in a stationary phase-controlled system, it is expedient to try a column of the salt-controlled type.

As regards the prediction of retention of the individual proteins under different HIC conditions, especially a theoretical framework remains to be developed that can adequately describe the conformation and surface properties of proteins under various operating conditions. For the time being the selection of the phase system in HIC is carried out by trial and error. For this process the above characterization of the stationary phases can provide considerable assistance.

5. Acknowledgements

We gratefully acknowledge the financial support given by the Hungarian Academy of Sciences under grants OTKA No. 1998/1991 and OTKA No. F7634/1993.

6. References

[1] Y. Kato, T. Kitamura and T. Hashimoto, *J. Chromatogr.*, 266 (1983) 49.
[2] Y. Kato, T. Kitamura and T. Hashimoto, *J. Chromatogr.*, 360 (1983) 260.
[3] J.L. Fausnaugh, L.A. Kennedy and F.E. Regnier, *J. Chromatogr.*, 317 (1984) 141.
[4] J.L. Fausnaugh, E. Pfannkoch, S. Gupta and F.E. Regnier, *Anal. Biochem.*, 137 (1984) 464.
[5] N.T. Miller and B.L. Karger, *J. Chromatogr.*, 326 (1985) 45.
[6] J.L. Fausnaugh and F.E. Regnier, *J. Chromatogr.*, 359 (1986) 131.
[7] A. Katti, Y.F. Maa and Cs. Horváth, *Chromatographia*, 24 (1987) 646.
[8] D.R. Nau, *BioChromatography*, 4, No. 2 (1989) 62.
[9] D.J. Gisch and T.S. Reid, *BioChromatography*, 4, No. 2 (1989) 74.
[10] J.A. Smith and M.O'Hare, *J. Chromatogr.*, 496 (1989) 71.
[11] N. Cook, P. Shieh and N.T. Miller, *LC · GC Int.*, 3, No. 1 (1990) 8.
[12] P. Smide, J. Kleinmann, J. Plicka and V. Svoboda, *J. Chromatogr.*, 523 (1990) 131.
[13] W.R. Melander, D. Corradini and Cs. Horváth, *J. Chromatogr.*, 317 (1984) 67.
[14] J.P. Chang, Z.El Rassi and Cs. Horváth, *J. Chromatogr.*, 396 (1985) 399.
[15] M.L. Heinitz, L.A. Kennedy, W. Kopaciewicz and F.E. Regnier, *J. Chromatogr.*, 443 (1988) 173.
[16] L. Szepesy and Cs. Horváth, *Chromatographia*, 26 (1988) 13.
[17] L. Szepesy and G. Rippel, *Chromatographia*, 34 (1992) 391.
[18] L. Szepesy and G. Rippel, *LC · GC Int.*, 5, No. 11 (1992) 24.
[19] G. Rippel and L. Szepesy, *J. Chromatogr. A*, 664 (1994) 27.
[20] L. Szepesy and G. Rippel, presented at the *19th International Symposium on Chromatography, 13–18 September 1992, Aix-en-Provence.*
[21] H.H. Freiser and K.M. Gooding, *BioChromatography*, 2, No. 4 (1987) 186.
[22] D. Guo, C.T. Mant, A.K. Taneja and R.S. Hodges, *J. Chromatogr.*, 359 (1986) 499 and 519.
[23] R. Steffens and J.J. Anderson, *BioChromatography*, 2, No. 4 (1987) 85.
[24] Th. Braumann, H.G. Genieser, C. Lüllmann and B. Jastorff, *Chromatographia*, 24 (1987) 777.
[25] A. Kaibara, C. Hohda, N. Hirata, M. Hirose and T. Nakagawa, *Chromatographia*, 29 (1990) 275.
[26] J.M.R. Parker and R.S. Hodges, in C.T. Mant and R.S. Hodges (Editors), *HPLC of Peptides and Proteins*, CRC Press, Boca Raton, FL, 1991, p. 737.
[27] C.C. Bigelow, *J. Theor. Biol.*, 16 (1967) 187.

[28] D.W. Urry, R.D. Harris and K.V. Prasad, *J. Am. Chem. Soc.*, 110 (1988) 3303.
[29] D.W. Urry, *J. Protein Chem.*, 7 (1988) 1.
[30] S.L. Wu, K. Benedek and B.L. Karger, *J. Chromatogr.*, 359 (1986) 3.
[31] S.L. Wu, A. Figueroa and B.L. Karger, *J. Chromatogr.*, 371 (1986) 3.
[32] X. Geng, L. Guo and J. Chang, *J. Chromatogr.*, 507 (1990) 1.
[33] W.R. Melander, Z.El Rassi and Cs. Horváth, *J. Chromatogr.*, 469 (1989) 3.
[34] N. Chen, Y. Zhang and P. Lu, *J. Chromatogr.*, 603 (1992) 35.
[35] J. Gehas and D.B. Wetlaufer, *J. Chromatogr.*, 511 (1990) 123.
[36] K. Valkó and P. Slégel, *J. Chromatogr.*, 631 (1993) 49.

ELSEVIER

Journal of Chromatography A, 668 (1994) 345–351

JOURNAL OF CHROMATOGRAPHY A

Chromatographic characterization of HSV-1 gD 268–284 and IL-6 179–185 synthetic oligopeptides by reversed-phase high-performance liquid chromatography, automated Edman degradation and mass spectrometric analysis

Szilvia Bősze[a], Marianna Mák[b], Hedvig Medzihradszky-Schweiger[a], Ferenc Hudecz*,[a]

[a]*Research Group of Peptide Chemistry, Hungarian Academy of Sciences, Eötvös L. University, P.O. Box 32, H-1518 Budapest 112, Hungary*

[b]*Central Institute of Chemistry, Hungarian Academy of Sciences, Budapest, Hungary*

Abstract

Two groups of synthetic oligopeptides ($n_{\text{amino acid}} = 7$ and 17) were prepared by solid-phase peptide synthesis using the Boc–polystyrene strategy. After deprotection, cleavage and gel permeation, the crude products were analysed by conventional RP-HPLC methods. Separation and isolation of major components were performed on a semi-preparative RP-HPLC column. In order to clarify the primary structure of these products, amino acid analysis, Edman degradation sequence determination and analytical RP-HPLC characterization were applied. The isolated fractions were further assessed by direct molar mass investigation utilizing the fast atom bombardment and ^{252}Cf plasma desorption mass spectrometry. The results with an interleukin-6 oligopeptide corresponding to the ^{179}LRALRQM^{185} sequence indicate that the single peak product obtained by RP-HPLC separation contains only one component, as verified by amino acid analysis and mass spectrometry. In contrast, the analysis of ^{268}LAPEDPEDSALLEDPVG^{284}-NH_2 from HSV-1 gD protein suggests that this large peptide amide showing a single peak after repeated purification by RP-HPLC contains microheterogeneities as revealed by mass spectrometry and sequencing, but not by amino acid analysis.

1. Introduction

During development, activation and functioning of the immune system, the cytokines play a prominent part in the realization of the cell to cell communication. Interleukin-6 (IL-6) as a multifunctional cytokine is produced by different cells (*e.g.*, monocytes, macrophages, fibroblasts, B- and T-lymphocytes) after appropriate stimulation. Further, IL-6 is the major regulator of the acute phase protein synthesis in human hepatocytes and in haematopoiesis. Several secondary structure prediction analyses of IL-6 and epitope mapping studies with IL-6 specific monoclonal antibodies and deletion mutants indicated that the C-terminal region (178–185 amino acids) is essential for biological activity [1–4]. Considering this observation, a number of C-terminal peptides including ^{179}LRALRQM^{185} were synthesized in our laboratory.

Herpes simplex virus (HSV), with two closely

* Corresponding author.

0021-9673/94/$07.00
SSDI 0021-9673(94)00022-2

related serotypes, HSV-1 and HSV-2, is one of the most frequent infectious agents in humans. Glycoprotein D (gD) represents a major immunogenic glycoprotein component of the human virion envelope [5]. It is, therefore, a logical target for the construction of subunit vaccines against HSV infection. It has been shown that peptides from the N-terminal region of HSV-1 gD are able to induce both B- and T-cell responses [6–8]. Another epitope region has been predicted in our laboratory [9,10] and partially characterized by HSV gD specific monoclonal antibodies [11,12]. For inhibition studies and structural investigations, a peptide amide, ^{268}LAPEDPEDSALLEDPVG^{284}-NH_2, covering this sequence has been synthesized.

This study was aimed at verifying the primary structure of the ^{179}LRALRQM^{185} peptide and ^{268}LAPEDPEDSALLEDPVG^{284}-NH_2 peptide amide produced by solid-phase synthesis (SPS) and to compare the efficacy of routinely used (amino acid analysis, RP-HPLC) and newly introduced (mass spectrometry, automatic Edman degradation) analytical methods. These techniques and their combinations have been applied to the characterization of peptide mixtures from natural tissues [13,14] and for homogeneity studies of synthetic peptides derived from SPS strategy [13,15,16]. Both types of studies indicated that preparations showing a single RP-HPLC peak are not necessarily pure, single substances. In reported cases the chromatographic separation alone was found to be inadequate [13,15]. Our results suggest that with large peptides reliable results could be achieved only by a combination of analytical techniques including HPLC, sequencing and mass spectrometry.

2. Experimental

2.1. Materials

Abbreviations for amino acids follow the revised recommendations of the IUPAC–IUB Committee on Biochemical Nomenclature, entitled *Nomenclature and Symbolism for Amino Acids and Peptides* (recommendations of 1983). The IL-6 fragment ^{179}LRALRQM^{185} (H–^{179}Leu–Arg–Ala–Leu–Arg–Gln–Met^{185}–OH) and the HSV-1 gD fragment amide ^{268}LAPEDPEDSALLEDPVG^{284}–NH_2 (H–Leu–Ala–Pro–Glu–Asp–Pro–Glu–Asp–Ser–Ala–Leu–Leu–Glu–Asp–Pro–Val–Gly–NH_2) were synthesized manually by a solid-phase technique on Merrifield resin (Bachem, Bubendorf, Switzerland) with the Boc–polystyrene strategy in our laboratory. The solvents acetonitrile, methanol, acetic acid and trifluoroacetic acid (TFA) were of HPLC grade and others were of analytical-reagent grade from Chemolab (Budapest, Hungary). Chemicals were purchased from Reanal (Budapest, Hungary).

2.2. Gel permeation

After deprotection and cleavage from the resin, the crude products were first purified on a Sephadex G-25M (Pharmacia, Uppsala, Sweden) column using acetic acid–water (50:50) as eluent. A Bio-Rad, (Richmond, CA, USA) Econo instrument was applied and the peaks were detected by ninhydrin spot assay on Whatman (Maidstone, UK) paper.

2.3. High-performance liquid chromatography

After gel permeation, ^{179}LRALRQM^{185} was further purified by RP-HPLC. Analytical RP-HPLC was performed on a laboratory-assembled Knauer, (Bad Homburg, Germany) HPLC system using a Delta-Pak C_{18} column (300 × 3.9 mm I.D.) with 15-μm silica (300 Å pore size) (Milligen, Milford, MA, USA) as the stationary phase and linear gradient elution with eluent A = 0.1% TFA in water and eluent B = 0.1% TFA in acetonitrile–water (80:20, v/v) as the mobile phase at a flow-rate of 1 ml/min at ambient temperature and detection at 220 nm. A 20-μl volume of a solution of crude and purified peptide or peptide amide (1 mg/ml in eluent A) was injected.

Separation of major components was performed on a Delta-Pak C_{18} semi-preparative column (300 × 19 mm I.D.) with 15-μm silica

(300 Å pore size) (Milligen) as the stationary phase and linear gradient elution with eluent A = 0.1% TFA in water and eluent B = 0.1% TFA in acetonitrile–water (80:20, v/v) as the mobile phase and detection at 220 nm. The gradients were developed from 15 to 45% eluent B in 45 min for ^{179}LRALRQM^{185} and from 25 to 40% eluent B in 30 min for ^{268}LAPEDPED-SALLEDPVG^{284}–NH_2 with a flow-rate of 3 ml/min and the peptides were applied at a 40 mg/ml concentration. After collection of all the peaks, the relevant fractions were freeze-dried.

2.4. Amino acid analysis

The primary sequence of products from the peaks separated by RP-HPLC were investigated by amino acid analysis using a Beckman (Fullerton, CA, USA) Model 6300 amino acid analyser. Prior to analysis samples were hydrolysed in 6 *M* HCl in sealed and evacuated tubes at 110°C for 24 h.

2.5. Edman degradation of HSV-1 gD fragment

The sequence analysis of purified peptide samples was carried out on a Knauer (Bad Homburg, Germany) Model 910 sequencer equipped with an on-line HPLC gradient system to separate and determine the phenylthiohydantoin (PTH) amino acids at 269 nm. The peptide samples (about 300 pmol each) were applied on a poly(vinylidene difluoride) (PVDF) membrane. For HPLC, buffer A was 5% tetrahydrofuran–0.4% 3 *M* sodium acetate solution (pH 3.8)–0.025% 3 *M* sodium acetate solution (pH 4.6)–0.02% glacial acetic acid in water and buffer B was acetonitrile. The flow-rate was 280 μl/min and the gradient was developed from 15 to 45% B in 23 min.

2.6. Mass spectrometry

Fast atom bombardment mass spectrometry (FAB-MS)

FAB mass spectra were obtained on a VG-ZA-2SEQ tandem mass spectrometer (Fisons, Loughborough, UK) equipped with a caesium ion gun (25 keV). For analysis, the peptide samples were dissolved in a 0.05 *M* NH_4HCO_3 buffer containing 1% of trifluoroacetic acid (TFA) and mixed with glycerol matrix.

Plasma desorption mass spectrometry (PD-MS)

PD-MS measurements were carried out using a Bioion 20 mass spectrometer (Applied Biosystems, Warrington, UK). A ^{252}Cf source was applied to ionize the molecules. The molar masses of the peptides were calculated by the time-of-flight technique. Thin layer chromatography was carried out on nitrocellulose (Mylar foil) which was wetted with 5 μl of a solution of

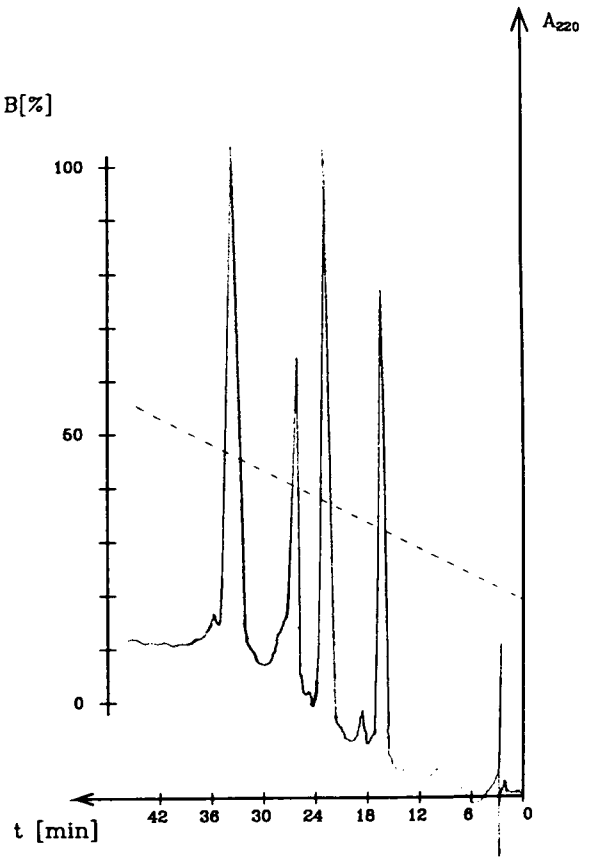

Fig. 1. Analytical RP-HPLC profile of the crude LRALRQM. Elution was performed at a flow-rate of 1 ml/min using a linear gradient from 15 to 55% eluent B in 45 min [eluent A = 0.1% TFA in water, eluent B = 0.1% TFA in acetonitrile–water (80:20, v/v)]. Detection at 220 nm. A 20-μl volume of a solution of crude peptide (2 mg/ml in eluent A) was injected.

1% TFA in methanol–water (50:50). The sample solution was applied to the wetted layer.

3. Results and discussion

3.1. Purification of the peptide and peptide amide

After gel permeation, the deprotected and cleaved material was analysed by analytical RP-HPLC. The chromatogram of the crude ^{179}LRALRQM^{185} preparation is shown in Fig. 1. Four major, easily separable peaks were detected by UV measurement at 220 nm after gradient elution. Fractions corresponding to these four peaks were collected, combined and isolated by freeze-drying after semi-preparative-scale separation. The first two peaks [LRALRQM/a, $R_F = 16$ min (Fig. 2a), and LRALRQM/b, $R_F = 22$ min] corresponded to

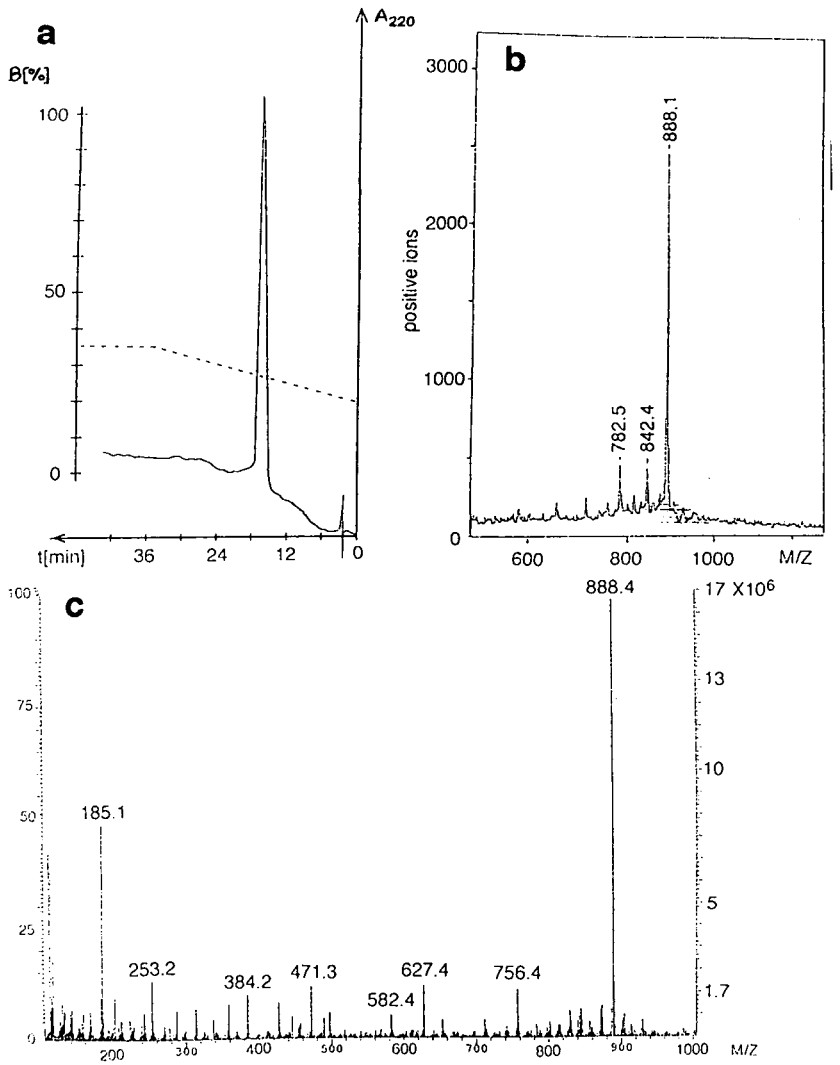

Fig. 2. (a) Analytical RP-HPLC profile and (b) ^{252}Cf PD and (c) monoisotopic FAB mass spectra of the purified LRALRQM/a peak of crude LRALRQM. RP-HPLC elution was performed at a flow-rate of 1 ml/min using a linear gradient from 15 to 35% eluent B in 30 min (eluents as in Fig. 1). Detection at 220 nm. A 20-μl volume of a solution of the purified first peak of the crude preparation (1 mg/ml in eluent A) was injected.

the required peptide sequence while the third and fourth peaks showed compounds with aberrant sequences. All four components were characterized by amino acid analysis and to check their purity were re-chromatographed by analytical RP-HPLC.

For the crude peptide amide ^{268}LAPEDPEDSALLEDPVG^{284}–NH_2 six different peaks were observed in RP–HPLC after gel permeation. The chromatogram of the crude peptide amide is shown in Fig. 3. After semi-preparative chromatography on the same packing material all peak-related material was characterized by analytical RP-HPLC, amino acid analysis and Edman degradation.

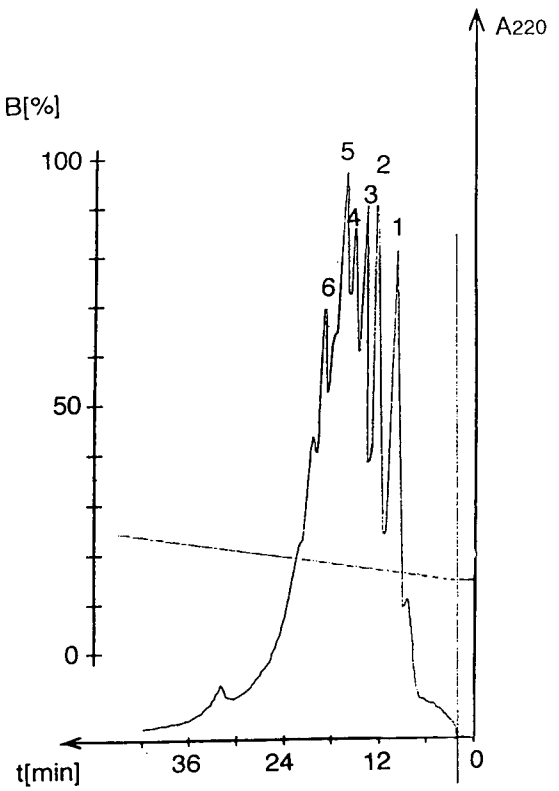

Fig. 3. Analytical RP-HPLC profile of crude LAPEDPEDSALLEDPVG–NH_2 peptide amide. RP-HPLC elution was performed at a flow-rate of 1 ml/ml using a linear gradient from 25 to 40% eluent B in 30 min (eluents as in Fig. 1). Detection at 220 nm. A 20-μl volume of a solution of crude peptide amide (1 mg/ml in eluent A) was injected.

3.2. Identification of the peptide and peptide amide

The amino acid composition of the isolated LRALRQM/a (R_F = 16 min, first peak in Fig. 1) and LRALRQM/b peptide (R_F = 22 min, second peak in Fig. 1) (Table 1) was essentially the same, but the R_F value of the LRALRQM/b peptide was much higher than that of the LRALRQM/a peptide (Fig. 2a). In order to understand this result, these two compounds were analysed by ^{252}Cf PD-MS and FAB-MS.

The relative molar mass (887.1) of the LRALRQM/a peptide (Fig. 2b and c) matches the calculated value (886.34) for ^{179}LRALRQM^{185}. In contrast, the mass spectrum of the LRALRQM/b peptide indicates the presence of an additional oxygen atom at the Met residue. This difference between the LRALRQM/a and LRALRQM/b peptide peaks was confirmed by both MS methods (Fig. 2b and c).

Results of the amino acid analysis of the peptide amide ^{268}LAPEDPEDSALLEDPVG^{284}–NH_2 peaks are given in Table 2. The analytical RP-HPLC profile of the first separated product (HSV/a) (Fig. 4a) shows only one peak but both PD-MS and FAB-MS show three components (Fig. 4b and c). The main peak (HSV/a) corresponds to the expected sequence of the 17-mer amide (calculated molar mass was 1765.93, observed mass 1766.2). The second and third components match the calculated values for the truncated derivatives of native or dehydrated peptide amides beginning either with ^{270}Pro or

Table 1
Amino acid analysis of ^{179}LRALRQM^{185} peptide

Amino acid	Calculated	Found[a]
Leu (L)	2	2.00
Arg (R)	2	1.93
Ala (A)	1	0.97
Gln (Q)	1	1.03[b]
Met (M)	1	0.87

[a] Acid hydrolysis (6 *M* HCl, 110°C, 24 h). The amino acid analysis was carried out on a Beckman Model 6300 analyser.

[b] The Q residue after acid hydrolysis was measured as E.

Table 2
Amino acid analysis of the ^{268}LAPEDPEDSALLEDPVG^{284}–NH_2 peptide amide fractions

Amino acid	Calculated	Found[a]					
		HSV/a	HSV/b	HSV/c	HSV/d	HSV/e	HSV/f
Leu (L)	3	3.03	2.98	2.98	3.02	2.94	2.85
Ala (A)	2	1.96	1.99	1.98	2.00	2.00	1.46
Pro (P)	3	2.88	2.89	2.93	2.92	2.89	2.89
Glu (E)	3	3.22	3.19	3.20	3.19	3.17	3.01
Asp (D)	3	2.98	2.98	2.92	2.92	2.91	3.41
Ser (S)	1	1.03	1.01	0.98	0.97	1.02	1.31
Val (V)	1	0.94	0.94	0.97	0.97	0.97	0.89
Gly (G)	1	1.04	1.02	1.02	1.02	1.10	1.18

[a] Acid hydrolysis (6 *M* HCl, 110°C, 24 h). The amino acid analysis was carried out on a Beckman Model 6300 analyser.

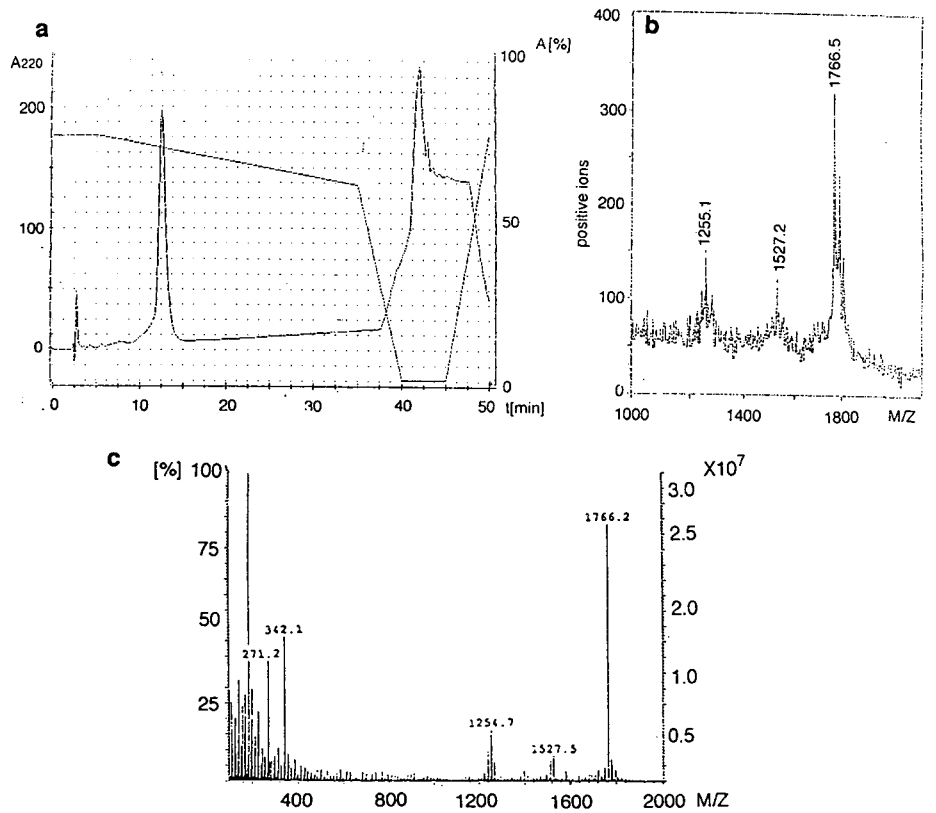

Fig. 4. (a) Analytical RP-HPLC profile and (b) ^{252}Cf PD and (c) monoisotopic FAB mass spectra of the purified HSV/a (first) peak of the crude LAPEDPEDSALLEDPVG–NH_2 peptide amide. Elution was performed at a flow-rate of 1 ml/min using a linear gradient from 25 to 40% eluent B in 30 min (eluents as in Fig. 1). Detection at 220 nm. A 20-μl volume of a solution of the purified first peak of the crude preparation (1 mg/ml in eluent A) was injected.

with ^{273}Pro [observed mass for 270–284–NH_2 1582.5 and for 273–284–NH_2 1240.2 and their derivatives, dehydrated (three times dehydrated 1527.2 and otherwise modified species)] (Fig. 4b and c).

Results from MS analysis correspond to the data obtained by the Edman degradation, which indicated the presence of all three sequences (each *ca.* 10% of the total amount) (data not shown).

The other five separated peaks were also characterized by analytical RP-HPLC, PD-MS, FAB-MS and Edman degradation. These fractions proved to be heterogenic even by analytical RP-HPLC and in most instances more than one peak was detected (data not shown).

All these results indicate that in certain instances it is necessary to investigate even the RP-HPLC-purified product by different MS methods (PD-MS, FAB-MS) and possibly by Edman degradation because sometimes the perfect-looking results of the analytical RP-HPLC and amino acid analyses do not guarantee that the synthetic peptide or peptide derivative is entirely pure.

4. Acknowledgements

This study was supported by grants from the Hungarian National Science Fund (OTKA) No. F-5324 and T-4217. We thank Mr. John Keyte (Biopolymer Unit, Department of Biochemistry, University of Nottingham) for the PD-MS measurements, Professor M. Szekerke, Dr. Gy. Szókán, Dr. G. Mezö and K. Uray for their comments and advice and Ms. A. Vörös for excellent technical assistance with the HPLC studies.

5. References

[1] J.F. Bazan, *Proc. Natl. Acad. Sci. U.S.A.*, 87 (1990) 6934.
[2] J.F. Bazan, *Immunol. Today*, 11 (1990) 350.
[3] S.C. Bischof, *Lymphokine Cytokines Res.*, 11 (1992) 33.
[4] J.P.J. Brackenhoff, *J. Immunol.*, 145 (1990) 561.
[5] M.J. Hall and K. Katrak, *Vaccine*, 4 (1986) 138.
[6] B. Dietzschold, R.J. Eisenberg, M. Ponce de Leon, E. Gulob and F. Hudecz, *J. Virol.*, 52 (1984) 431.
[7] E. Heber-Katz, M. Hollósi, B. Dietzschold, F. Hudecz and G.D. Fasman, *J. Immunol.*, 135 (1985) 1385.
[8] W.J. Weijer, J.W. Drijfhout, H.J. Geerlings, W. Bloemhoff, M. Feijbrief, A.B. Cees, P. Hoogerhout, K.E.T. Keerling, T. Popken-Boer, K. Slopsema, J.B. Wilterdrink, G.W. Welling and S. Welling-Wester, *J. Virol.*, 62 (1988) 501.
[9] G. Mezö, M. Szekerke, I. Kurucz and F. Hudecz, in E. Bayer and G. Jung (Editors), *Peptides 1988*, Walter de Gruyter, Berlin, 1989, p. 701.
[10] F. Hudecz, A. Hilbert, G. Mezö, I. Mucsi, J. Kajtár, Sz. Bösze, I. Kurucz and É. Rajnavölgyi, *Pept. Res.*, 6 (1993) 263.
[11] R.J. Eisenberg, D. Long, M. Ponce de Leon, J.T. Matthews, P.G. Spear, M.G. Gibson, L.A. Lasky, P. Berman, E. Gulob and G.H. Cohen, *J. Virol.*, 53 (1985) 634.
[12] V.J. Isola, R.J. Eisenberg, G.H. Siebert, C.J. Heilman, W.C. Wilcox and G.H. Cohen, *J. Virol.*, 63 (1989) 2325.
[13] G. Grübler, E. Yildiz, H. Zimmermann, M. Mihelic, H. Echner, S. Stoeva, S. Spyropoulos and W. Voelter, in N. Yanaihara (Editor), *Peptide Chemistry*, ESCOM, Leiden, 1993, p. 208.
[14] E. Wünsch, in W. Voelter and G. Weitzel (Editors), *Structure and Activity of Natural Peptides*, Walter de Gruyter, Berlin, 1981, p. 3.
[15] E. Bayer, W. Rapp and L. Zhang, in G. Jung and E. Bayer (Editors), *Peptides 1988*, Walter de Gruyter, Berlin, 1989, p. 390.
[16] G. Jung, A.G. Beck-Sickinger, N. Zimmermann, J. Metzger, R. Spohn, S. Stevanovic, K. Deres and K.-H. Weismuller, in R. Epton (Editor), *Innovation and Perspectives in Solid Phase Synthesis*, Intercept, Andover, 1992, p. 227.

ELSEVIER

Journal of Chromatography A, 668 (1994) 353–358

JOURNAL OF CHROMATOGRAPHY A

Gas chromatographic–mass spectrometric determination of α-phenylcinnamic acid isomers: practical and theoretical aspects

B. Török[a], I. Pálinkó*[,a], Gy. Tasi[b], L. Nyerges[c], F. Bogár[d]

[a]Department of Organic Chemistry, József Attila University, Dóm tér 8, H-6720 Szeged, Hungary
[b]Applied Chemistry Department, József Attila University, Rerrich B. tér 1, H-6720 Szeged, Hungary
[c]Department of Medicinal Chemistry, Szent-Györgyi Albert University, Dóm tér 8, H-6720 Szeged, Hungary
[d]Theoretical Physics Department, József Attila University, Aradi Vértanúk tere 1, H-6720 Szeged, Hungary

Abstract

The Perkin condensation of benzaldehyde and phenylacetic acid was performed in the presence of acetic anhydride and triethylamine. After silylation, the resulting mixture was analysed with a Hewlett-Packard gas chromatograph equipped with a mass-selective detector. Excellent baseline separation was achieved for the α-phenylcinnamic acid trimethylsilyl ester (2,3-diphenylpropenoic acid trimethylsilyl ester) isomers. The fragments were identical in the mass spectra of the isomers; however, the relative intensities differed appreciably. The identification of most peaks was straightforward; nevertheless, non-trivial fragments were also formed via bond scissions and subsequent rearrangements of the McLafferty type. Semi-empirical quantum chemical calculations were also performed and bond orders were determined for the fully optimized geometries of various silyl ester derivatives of the neutral molecules and of the parent ions. These were aimed at mapping the strength of bonds expected to break in the mass-selective detector. It was found that the bond orders in the isomers do not differ significantly, hence the fragmentation patterns would be essentially the same, irrespective of the silylating agent. Major cleavage routes could be predicted, however. Predictions based on calculations were verified experimentally.

1. Introduction

Cinnamic acid derivatives are important building blocks in the production of lignins in higher plants. They derive from the shikimic acid metabolic pathway and their mechanism of formation is complex [1]. Nevertheless, the key reactions in this scheme are condensations (mostly of the Claisen type), just as in their laboratory-scale synthesis (mostly of the Perkin type). This latter reaction, a modified Perkin condensation leading to a mixture of (*E*)- and (*Z*)-α-phenylcinnamic acids (2,3-diphenylpropenoic acids) [2] was studied, with the aim of following and influencing isomeric distribution [3]. A high-resolution method was needed to monitor the accumulation products. GC–MS analysis was considered because of its simplicity, speed and the small amount of material required. It may be worth mentioning that *in situ* analysis was not performed in previous work on these compounds; the products were first isolated and their UV or IR spectra were recorded and evaluated [2,4,5] instead.

During this work several additional questions arose, such as (i) whether the mass spectra of the isomeric acid derivatives differ from each other, (ii) whether it is possible to identify fragments

* Corresponding author.

0021-9673/94/$07.00
SSDI 0021-9673(93)E1182-Y

with significant abundances and suggest reaction pathways for non-trivial ones and (iii) whether there is any chance of obtaining differing mass spectra for the isomers by the application of various silylating agents. The results of this work, and possible answers to the above questions, are reported in this paper.

2. Experimental

Synthesis was based on the recipe of Fieser [6]. It involved heating a mixture of benzaldehyde (2 cm^3), phenylacetic acid (2.5 g), acetic anhydride (2 cm^3) and triethylamine (2 cm^3). Varying the duration of reflux varied the isomeric composition. To obtain reasonable amounts of both isomers, refluxing for 35 min was necessary.

2.1. Method

The following measurements were performed: (i) GC–MS analysis of the silyl esters of the pure acids, (ii) GC analysis of their mixture and (iii) GC analysis of silylated samples withdrawn from the reaction mixture. Silylation was necessary, as the pure acids were not volatile enough for GC measurements.

2.2. Silylation

The silylating agents were N,N-diethyltrimethylsilylamine and N - methyl - N - (*tert.* - butyldimethylsilyl)trifluoroacetamide (Fluka). Both compounds were applied to the pure isomers, but only N,N-diethyltrimethylsilylamine was used for silylating the mixture of the two pure acids and the withdrawn samples from the reaction mixture. The samples (10 mg) were dissolved in N,N-dimethylformamide (100 μl) and an excess of the silylating agent (500 μl) was added at room temperature. The reaction was complete within 5 min. A 5-μl volume of this mixture was used for analysis.

2.3. Instruments and conditions

A Hewlett-Packard (HP) Model 5890 gas chromatograph equipped with a quadrupole mass-selective detector was used to measurements. Data analysis was performed on an HP 5997 Chemstation attached to the GC–MS apparatus. A 50-m HP-1 capillary column was used; the solvent delay was 7 min, the column temperature was programmed from 250 to 350°C at 4°C min^{-1} and the electron impact (EI) ionization energy was 70 eV.

3. Theoretical calculations

To explore the bond strengths in the isomers, semi-empirical quantum chemical calculations were carried out with the AM1 method, included in the PcMol package [7]. Full geometric optimization was performed for the neutral molecules and for the parent ions of the isomers of the trimethylsilyl (**1**) and *tert.*-butyldimethylsilyl (**2**) esters (Fig. 1). Bond orders were taken as a measure of bond strength, hence they were calculated for the optimized geometries and compared for the respective isomeric pairs.

4. Results and discussion

In the following, experimental results obtained with the trimethylsilyl esters are detailed, as preliminary measurements with the more expensive *tert.*-butyldimethylsilyl esters showed essentially identical behaviour.

4.1. GC–MS measurements

First, the trimethylsilyl ester derivatives of the pure isomers were analysed and the mass spectra of both isomers were recorded (Figs. 2 and 3). It can be seen that GC peaks corresponding to the isomers are distinct, allowing the convenient separation of the isomeric mixture. This was confirmed by the analysis of a mixture of isomers, and also a silylated sample withdrawn from the Perkin condensation mixture, showing

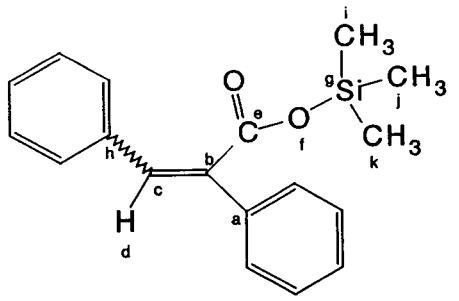

1

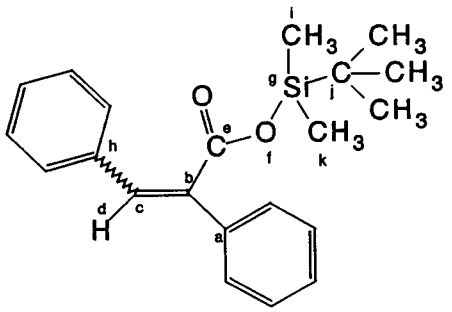

2

Fig. 1. Structure **1**, α-phenylcinnamic acid trimethylsilyl esters; structure **2**, α-phenylcinnamic acid *tert.*-butyldimethylsilyl esters.

excellent baseline separation in a reasonable time (Figs. 4 and 5).

The ease of preparation of the silyl esters combined with the high resolution of GC gives

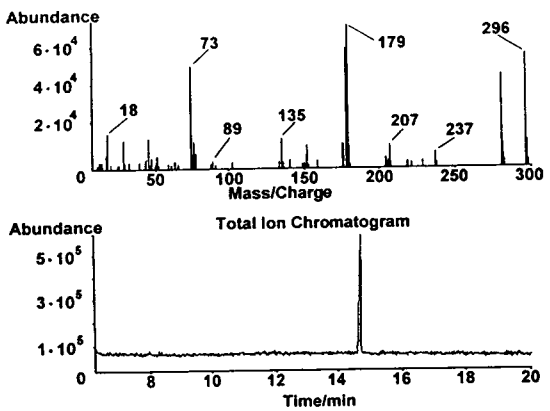

Fig. 2. Total ion chromatogram and mass spectrum of the *E* isomer of compound **1**.

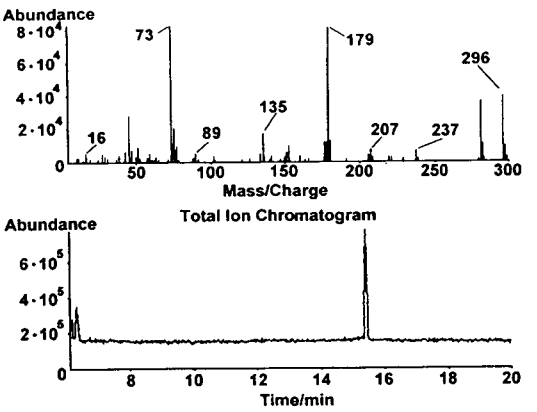

Fig. 3. Total ion chromatogram and mass spectrum of the *Z* isomer of compound **1**.

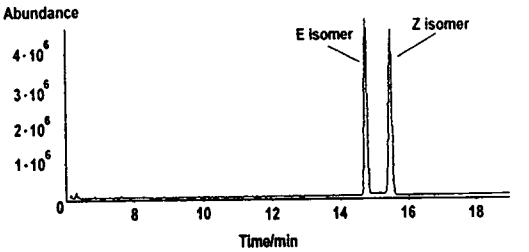

Fig. 4. Total ion chromatogram of the isomeric mixture of compound **1**.

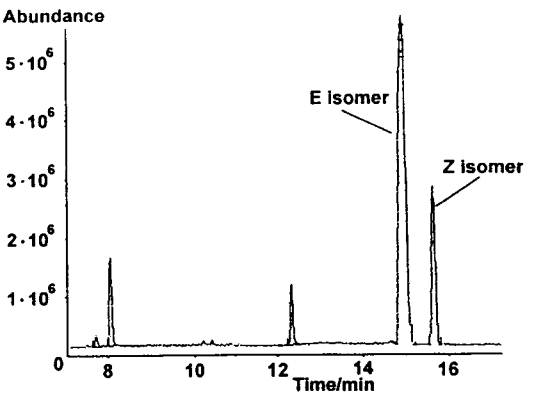

Fig. 5. Total ion chromatogram of the trimethylsilyl derivatives of the product mixture after a 35-min reflux of benzaldehyde, acetic anhydride, phenylacetic acid and triethylamine.

an excellent method for following the isomeric distribution in the Perkin reaction.

4.2. Analysis of mass spectra

Recording the EI mass spectra of the isomers, in addition to identifying the compounds, gives an insight into the bond strength distribution of the isomers. Moreover, secondary reactions, such as rearrangements after fragmentation, can also be studied [8,9].

Unfortunately, the mass spectra alone (Figs. 2 and 3) were not suitable for distinguishing between the isomers in an isomeric mixture, as the fragments were identical. Nevertheless, the relative intensities were significantly (an reproducibly) different (Table 1, columns 3 and 4), allowing the identification of the pure isomers without a known sample for comparison.

As far as the fragmentation pattern is concerned, the most abundant fragments and the molecular ion could be easily identified (Table 1). They were formed via the scission of the O–Si, Si–C and C–O bonds or decarboxylation occurring with the subsequent loss of the olefinic hydrogen. These last two processes were the most important fragmentation pathways.

However, there were fragments that underwent complicated secondary reactions in the mass spectrometer. These reactions involved the scission of several bonds and subsequent rearrangements of the McLafferty type [10,11]. For instance, the suggested route to the fragment of m/z 237 involved the scission of the olefinic hydrogen and then rearrangement to a coumarin or benzopyrilium derivative, resulting in ion **4**. This ion rearranged by losing the $Si(CH_3)_3$ but acquiring one of its CH_3 substituents, ending up with ion **5** (Fig. 6).

The formation of the fragment of m/z 135 may be explained by the rupture of the O–Si and, most interestingly, the olefinic double bond and the scission and subsequent rearrangement of a hydrogen from the α-phenyl group, ending up with a coumaran or benzofuran derivative (Fig. 7).

Table 1
The most abundant fragments, their m/z values and relative peak intensities in the EI mass spectra of (*E*)- and (*Z*)-α-phenylcinnamic acid trimethylsilyl ester isomers (structure **1** in Fig. 1)

Fragment[a]	m/z	Relative intensity (%)	
		E	*Z*
$M^{+\cdot}$	296	78.2	48.6
$[M - CH_3]^+$	281	64.1	43.2
5[b]	237	11.5	8.1
$[M - OSi(CH_3)_3]^+$	207	16.7	9.5
$[M - CO_2Si(CH_3)_3]^+$	179	100.0	100.0
$[M - H - CO_2Si(CH_3)_3]^+$	178	82.1	81.1
Unidentified	152	15.4	12.2
6[c]	135	20.5	21.6
$[(CH_3)_3SiO]^+$	89	5.1	8.1
$[(CH_3)_2SiOH]^+$	75	19.2	24.3
$[(CH_3)_3SI]^+$	73	70.5	100.0
$[SiOH]^+$	45	20.5	33.8

[a] $M^{+\cdot}$ represents the parent ion, *i.e.*, the ion which is formed with the loss of an electron.
[b] see Fig. 6.
[c] see Fig. 7.

4.3. Theoretical aspects

AM1 semi-empirical quantum chemical calculations with full geometric optimization resulted in the minimum energy structures in the gas phase of the two pairs of neutral molecules (**1** and **2**) and their (positively charged) parent ions.

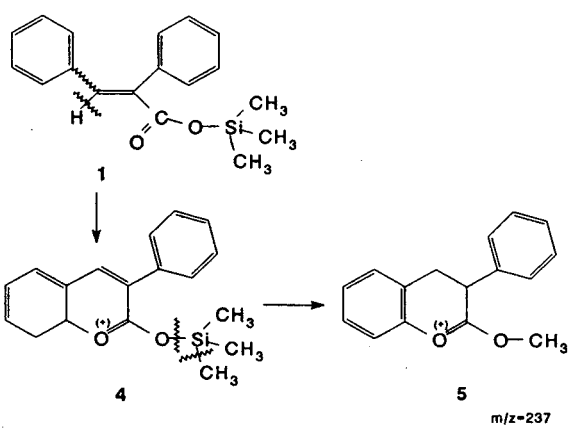

Fig. 6. Route to fragment of m/z 237.

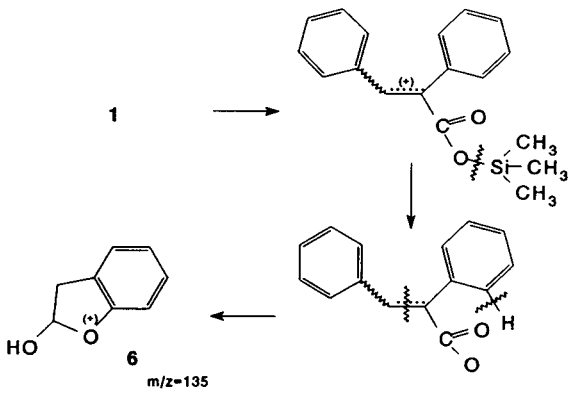

Fig. 7. Route to fragment of m/z 135.

Table 2
Enthalpy of formation for the E and Z isomers of the parent ions and the neutral molecules of α-phenylcinnamic acid silyl ester derivatives (structures **1** and **2** in Fig. 1) calculated by AM1 semi-empirical quantum chemical method after full geometric optimization

Compound	$\Delta H_{f,298}$ (kJ mol^{-1})			
	Parent ion		Neutral molecule	
	E	*Z*	*E*	*Z*
1	647.7	650.2	−320.7	−319.2
2	581.6	584.9	−360.9	−355.9

The calculated standard enthalpies of formation are given in Table 2.

Bond orders were calculated for the optimized geometries. Data for bonds expected to break in the mass spectrometer are displayed in Table 3. It is obvious that bond orders of the parent ions are of relevance to mass spectrometry, as fragmentation and other side-reactions are derived from the parent ion. Nevertheless, bond orders for the neutral molecules are included in Table 3 in italics in order to examine the changes in bond strength due to ionization.

It can be seen that for compound **1**, the experimentally found major routes of bond scission coincide with theoretical calculations. Bond order calculations predict that the most abundant fragments should form via the cleavage of C_b–C_e, O–Si, Si–C or the olefinic C–H bonds and, indeed, this was found experimentally. The loss of the β-phenyl group only occurred in the more complicated scission, the subsequent rearrangement of which was a remarkably important pathway with relative intensities above 20% (fragment **6**; for the mechanism, see Fig. 7).

Comparison of the bond orders of the neutral molecules and their cations revealed that the olefinic double bonds (b–c) became significantly weaker in the parent ions than they were in the neutral molecules. It is highly probable that an electron form the olefinic π-bond was removed

Table 3
Bond orders in the parent ions (roman type) and the neutral molecules (italic type) of the silyl ester derivatives of stereoisomeric α-phenylcinnamic acids (structures **1** and **2** in Fig. 1) determined for geometries optimized by the AM1 semi-empirical quantum chemical method

Bond	**1**				**2**			
	E		*Z*		*E*		*Z*	
a–b	1.14	*0.99*	1.15	*0.99*	1.13	*0.99*	1.16	*0.99*
b–c	1.45	*1.82*	1.44	*1.84*	1.46	*1.82*	1.46	*1.85*
b–e	0.94	*0.94*	0.94	*0.92*	0.95	*0.94*	0.95	*0.92*
c–d	0.93	*0.94*	0.93	*0.94*	0.93	*0.94*	0.93	*0.94*
c–h	1.20	*1.02*	1.20	*1.02*	1.19	*1.02*	1.18	*1.02*
e–f	1.04	*1.12*	1.04	*1.11*	1.04	*1.11*	1.04	*1.11*
f–g	0.67	*0.65*	0.67	*0.65*	0.68	*0.65*	0.67	*0.66*
g–i	0.88	*0.87*	0.89	*0.87*	0.91	*0.88*	0.90	*0.87*
g–j	0.88	*0.88*	0.88	*0.88*	0.87	*0.83*	0.87	*0.84*
g–k	0.91	*0.88*	0.91	*0.88*	0.88	*0.88*	0.89	*0.88*

by electron bombardment in the mass-selective detector and the resulting three-electron bond grew appreciably weaker, facilitating the rupture of the bond in further reactions. The C–O bond (e–f) also weakened, accounting for the relative importance of fragment of m/z 207. Bonds a–b and c–h (the bonds between the olefinic carbons and the phenyl groups) grew stronger, however, explaining the experimental finding that the relative intensity of **5** (direct removal of the α-phenyl group) was lower than that of **6** (indirect removal of the β-phenyl group) in both isomers.

Calculated bond orders for the two pairs of different silyl esters revealed that the major cleavage routes remained the same irrespective of the silylating agent. Experiments with compound **2** verified this finding. It was also predicted that routine EI mass spectrometry could not differentiate between the isomeric esters, again irrespective of the silylating agent. This was also verified experimentally with compounds **1** and **2**.

5. Conclusions

A convenient and rapid GC–MS method was developed for the analysis of the complex reaction mixture leading to an α-phenylcinnamic acid isomeric mixture. Analysis of the mass spectra resulted in the identification of the major cleavage pathways. Bond scission and subsequent rearrangement reaction sequences were suggested to explain the formation of some unusual fragments. Bond order calculations for the optimized geometries of the parent ions were found to be able to predict major cleavage routes. Finally, calculations and experiments revealed that a routine mass spectrometer with an EI source cannot distinguish between the isomers, irrespective of the silylating agent.

6. Acknowledgements

This work was financed by the National Science Foundation of Hungary through grant F4297/1992, and the work was completed at the University of Sussex, Brighton, where one of us (I.P.) held a three-month fellowship funded by the Commission of the European Communities, under the East–West Mobility Scheme for Scientists (grant 12009). This support is gratefully acknowledged.

7. References

[1] J. Mann, *Secondary Metabolism*, Oxford Science Publications, Clarendon Press, Oxford, 1987.
[2] H. Zimmermann and L. Ahramjian, *J. Am. Chem. Soc.*, 81 (1959) 2086.
[3] B. Török, I. Pálinkó, Gy. Tasi and F. Bogár, in preparation.
[4] Y. Ogata and M. Tsuchida, *J. Org. Chem*, 24 (1959) 78.
[5] R. Ketcham and D. Jambotkar, *J. Org. Chem.*, 28 (1963) 1034.
[6] L. Fieser, *Experiments in Organic Chemistry*, Heath, Boston, 1955.
[7] G. Tasi, I. Pálinkó, G. Náray-Szabó and J. Halász, *PcMol 3.1, Semiempirical Calculations on Microcomputers*, Chemicro Budapest, 1992.
[8] H. Gusten, L. Klassinc, V. Kramer and J. Marsel, *Org. Mass Spectrom.*, 8 (1974) 323.
[9] K.P. Madhusudan, V.S. Murthy, D. Fraisse and M. Becchi, *Org. Mass Spectrom.*, 26 (1991) 505.
[10] F.W. McLafferty (Editor), *Mass Spectrometry of Organic Ions*, Academic Press, New York, 1963.
[11] F.W. McLafferty, *Interpretation of Mass Spectra*, Benjamin, New York, 1973.

ELSEVIER

Journal of Chromatography A, 668 (1994) 359–363

JOURNAL OF CHROMATOGRAPHY A

Determination of thiamine (vitamin B_1) and riboflavin (vitamin B_2) in meat and liver by high-performance liquid chromatography

Éva Barna*, Ernő Dworschák

Department of Food Chemistry, National Institute of Food Hygiene and Nutrition, Gyáli út 3/a, Budapest 1097, Hungary

Abstract

HPLC methods described so far for the determination of thiamine and riboflavin in meat samples have used mostly fluorescence detection. The aim of this work was to elaborate a suitable method with UV detection for this purpose and to compare the thiamine and riboflavin contents obtained for meat and liver samples from various pig groups. Homogenized spare rib, chop, ham and liver samples were treated with acid and heated (at 121°C, 30 min), followed by enzymatic digestion to release the vitamins. After a clean-up procedure the simultaneous determination of thiamine and riboflavin was performed with a Nucleosil ODS (3 μm) packed column at 45°C. The mobile phase was phosphate buffer (pH 3.0)–acetonitrile (84:16, v/v) containing 5 m*M* sodium heptanesulphonate. The relative standard deviation was 5% for thiamine and 12% for riboflavin in meat and 8% for thiamine and 5% for riboflavin in liver for four parallel determinations.

1. Introduction

During the last 20 years numerous HPLC methods have been published concerning the determination of water-soluble vitamins in foods or enriched foods. UV detection was used successfully with enriched cereals and cereal products for the determination of their thiamine and riboflavin contents [1] and also with rice and rice products for the determination of thiamine, riboflavin and niacin [2], but in meat samples thiamine and riboflavin have been determined mainly by applying fluorescence detection [3–6]. The type of food sample has to be emphasized because the nature and amount of various components other than vitamins may influence the effectiveness of the separation system.

Our aim was to elaborate a suitable HPLC method with UV detection after a clean-up procedure for the parallel determination of thiamine and riboflavin in meat and liver samples because thiamine has no natural fluorescence so it needs a pre- or postcolumn derivatization when applying fluorescence detection. Measuring UV absorbance, the procedure was simpler and the levels of thiamine in meat and liver samples were sufficient for this less sensitive detection. We applied this method to various pig groups in order to establish whether there is a difference in the vitamin contents, besides other important components, between the groups.

2. Experimental

The enzymes used in the sample preparation

* Corresponding author.

0021-9673/94/$07.00
SSDI 0021-9673(93)E0008-I

were papain (Cat. No. 7147; Merck, Darmstadt, Germany), taka-diastase (Cat. No. 86250; Fluka, Buchs, Switzerland) and clara-diastase (Cat. No. 27540; Fluka). The clean-up columns (Nucleosil C_{18} cartridge of 500 mg) and the analytical column were purchased from BST (Budapest, Hungary). Acetonitrile and methanol were of chromatographic grade (Merck). Heptanesulphonic acid sodium salt, thiamine and riboflavin were obtained from Fluka.

2.1. Sample preparation

Spare rib, chop, ham and liver were separated from each animal (twelve animals in both groups) and the meat and liver samples were minced twice in a mincer and stored at −18°C before the analysis.

A 5-g amount of homogenized sample was suspended with 35 ml of 0.01 *M* hydrochloric acid and then autoclaved at 121°C for 30 min. After cooling to room temperature, 2.0 ml of taka-diastase suspension (2.5 g per 100 ml of 2.5 *M* sodium acetate solution), 2 ml of clara-diastase suspension (1 g per 100 ml of water) and 2 ml of papain suspension (5 g per 100 ml of water) were added to the meat sample. For liver, the concentration of clara-diastase suspension was increased to 2 g per 100 ml of water because of the higher riboflavin content of the liver sample. The pH was adjusted to 4.5 and the samples were submitted to enzymatic digestion for 16–18 h at 37°C in order to release the vitamins from the bound forms. Then the samples were filtered through paper (Faltenfilter, Macherey–Nagel No. 615), the pH was adjusted to 6.5 and after a second filtration the volume was brought to 50 ml with water.

2.2. Sample clean-up

Purification of the extracts was carried out on the clean-up columns mentioned above. The procedure used was similar to the method published by Wills *et al.* [5], applying another ion-pair reagent and changing the ratio of methanol in the washing mixture and also in the eluent in order to decrease the amount of interfering substances. The columns were preconditioned by washing with methanol (2 ml), then methanol solution (2 ml) containing 5 m*M* sodium heptanesulphonate, an ion-pair reagent, followed by doubly distilled water (twice, 2 ml). Sample solutions of 4 ml were applied to the columns. At the same time thiamine and riboflavin standard solutions were added to one sample of each batch at three levels before the clean-up procedure. The columns were then washed with 2 ml of water–methanol (80:20) containing 0.005 *M* sodium heptanesulphonate. The components of interest were eluted with 2 ml of water–methanol (50:50) containing 0.005 *M* sodium heptanesulphonate. The volumes of the solutions collected were recorded. Samples were protected from light during the whole procedure because of the light sensitivity of riboflavin.

2.3. Chromatographic conditions

Chromatographic separation was performed on a Liquochrom Model 2010 HPLC system (Labor MIM, Budapest, Hungary) equipped with a UV detector operating at 254 nm. Chromatographic separation was achieved on a Nucleosil C_{18} column (150 × 4.6 mm I.D.) with 3-μm diameter particles and a guard column (20 × 4.6 mm I.D.) packed with Nucleosil C_{18}, particle size 10 μm. The eluent used was 0.01 M potassium dihydrogenphosphate buffer (pH 3.0)–acetonitrile (84:16, v/v) containing 5 m*M* sodium heptanesulphonate for meat samples and the same components in a ratio of 85:15 for liver samples. The volume of sample solution injected was 50 μl and the temperature of the column and the eluent was maintained at 45°C.

At the end of the daily work the column was washed with water–acetonitrile (80:20) to remove the water-soluble components and then stored in acetonitrile.

2.4. Calculation

Quantification was based on the peak height of the vitamins in the samples and in spiked samples using a calibration graph obtained at three levels of vitamin addition and the peak height of

the original sample. The peak height was measured from the line connecting the start point and the end point of the peak (valley to valley).

2.5. Microbiological method

The results of HPLC determination were compared with those obtained by microbiological determination of thiamine and riboflavin [7].

3. Results

A combination of sample clean-up and modification of the mobile phase used by Kamman *et al.* [1] gave appropriate chromatograms for meat and liver samples with UV detection. Figs. 1 and 2 show some examples of the chromatographic separation of spare rib and liver samples. For liver a change in sensitivity was necessary between the peaks of thiamine and riboflavin because of the great differences in the absorbances.

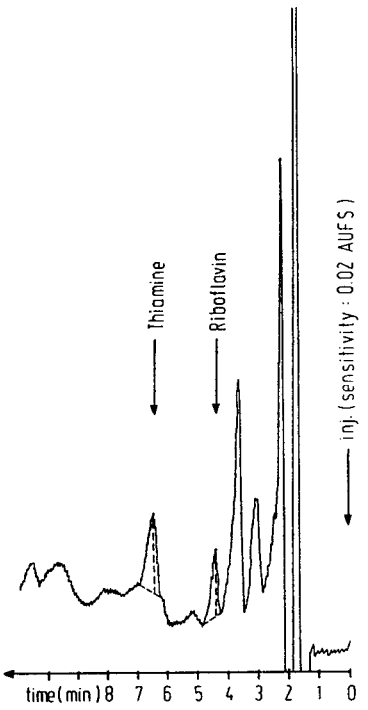

Fig. 1. HPLC of a spare rib sample from group 1. Mobile phase, 0.01 *M* phosphate buffer (pH 3.0)–acetonitrile (84:16, v/v) containing 5 m*M* sodium heptanesulphonate; UV detection at 254 nm, 0.02 AUFS.

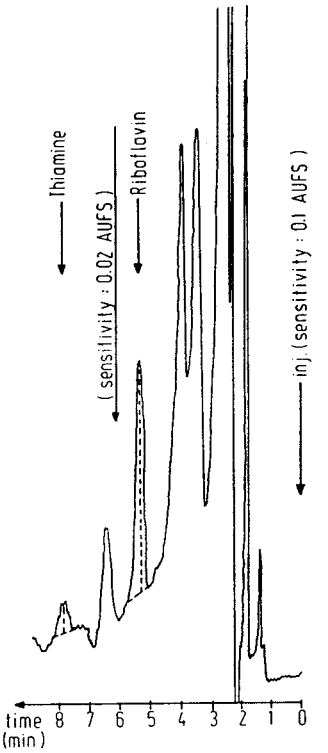

Fig. 2. HPLC of a liver sample from group 1. Mobile phase, 0.01 *M* phosphate buffer (pH 3.0)–acetonitrile (85:15, v/v) containing 5 m*M* sodium heptanesulphonate; UV detection at 254 nm. The sensitivities had to be changed between the peak of thiamine and riboflavin from 0.1 to 0.02 AUFS because of the large differences in the absorbances.

In the HPLC determination of thiamine, the presence of an acidic ion-pair reagent is important. For meat and liver samples heptanesulphonate resulted in the best separation from the interfering substances. The retention time of thiamine was shorter with hexanesulphonate than with heptanesulphonate, but the former resulted in co-elution of the thiamine with another compound. With octanesulphonate the retention time increased, giving shorter and wider peaks.

The concentration ranges for calibration for meat samples were 1.0–4.0 μg/ml of thiamine and 0.2–1.0 μg/ml of riboflavin and for liver

Table 1
Calibration graphs obtained by adding thiamine and riboflavin to the samples before sample clean-up

Sample	Thiamine		Riboflavin	
	Calibration equation[a]	Correlation coefficient (r)	Calibration equation[a]	Correlation coefficient (r)
Spare rib	$y = 5.77x + 3.21$	0.99897	$y = 19.62x + 1.80$	0.99976
Chop	$y = 5.18x + 3.78$	0.99961	$y = 16.14x + 2.23$	0.99963
Ham	$y = 5.04x + 4.17$	0.99891	$y = 18.48x + 4.61$	0.99998
Liver	$y = 5.36x + 1.95$	0.99950	$y = 18.08x + 84.20$	0.99962

[a] y = peak height (cm); x = concentration (μg/ml).

samples 0.4–2.0 μg/ml of thiamine and 2.0–10.0 μg/ml of riboflavin according to their vitamin contents. Calibration graphs obtained with spiked samples (spiking before clean-up) are presented in Table 1. The slopes of the lines are similar in the various samples in spite of the differences in disturbing compounds. The intercepts on the ordinate depend on the original vitamin contents of the samples.

The limits of detection were 0.1 μg/ml of thiamine and 0.03 μg/ml of riboflavin using a signal-to-noise ratio of 3. This means that 50 μg of thiamine and 16 μg of riboflavin in a 100-g sample can be determined.

The average recoveries of thiamine and riboflavin were 85% and 71%, respectively, in meat samples and 83% and 89%, respectively, in liver samples with addition of vitamin standard solutions before the extraction at the same level as present in the sample originally. The relative standard deviation was 6% for thiamine and 12% for riboflavin in meat and 8% for thiamine and 5% for riboflavin in liver for four parallel determinations.

A comparison between the HPLC and microbiological methods is given in Table 2. The concentrations of thiamine and riboflavin in meat samples measured by HPLC were lower than those determined by the microbiological method (10% and 40%, respectively). For liver the two methods gave approximately identical results.

The results obtained for the various samples are given in Table 3.

4. Conclusions

In the determination of B-group vitamins in biological materials the extraction and release of the free vitamins from the coenzymes are very

Table 2
Comparison of the HPLC and microbiological methods

Parameter	Vitamin	HPLC method		Microbiological method	
		Meat	Liver	Meat	Liver
Recovery (%)[a]	Thiamine	85	83	94	97
	Riboflavin	71	89	95	98
Reproducibility (%)[a]	Thiamine	6	8	17	18
	Riboflavin	12	5	16	15

[a] $n = 4$.

Table 3
Thiamine and riboflavin contents of the samples

Sample	Group 1		Group 2	
	Thiamine (μg per 100 g)	Riboflavin (μg per 100 g)	Thiamine (μg per 100 g)	Riboflavin (μg per 100 g)
Spare rib	382 ± 154	68 ± 18	312 ± 45	145 ± 21
Chop	395 ± 143	86 ± 10	404 ± 146	80 ± 21
Ham	507 ± 171	99 ± 21	482 ± 186	96 ± 21
Liver	210 ± 90	2347 ± 258	121 ± 24	1630 ± 231

Mean results ± S.D. (n = 12).

important steps in the method. A combination of acid and heat treatment and also enzyme digestion is necessary for this purpose. The most frequently used dephosphorylating enzyme preparations are taka-diastase and clara-diastase; the former proved more effective for thiamine and the latter for riboflavin. Digestion with papain resulted in chromatograms that were clearer and easier to evaluate with UV detection than that without a proteolytic treatment. The incomplete decomposition of the compounds related to the vitamin molecules may cause some discrepancy between the results of the HPLC and microbiological methods. This is a possible explanation of why the vitamin levels in meat samples were lower than would be expected.

The characteristics of the clean-up columns for the sample may change when they are used several times in the sample series. It cannot be determined in advance how many times they can be used with a selected sample type without considerable changes in retention.

By applying samples with vitamins added at the same levels in each batch the slight variations in the charge of the clean-up columns can be eliminated.

The purity of the peaks was confirmed by measuring the thiamine and riboflavin peaks of the standard and sample solutions at a different wavelength (268 nm) and was found to be acceptable.

5. References

[1] I.F. Kamman, T.P. Labuza and I.I. Warthesen, *J. Food. Sci.*, 45 (1980) 1497.
[2] R.B. Toma and M.M. Tabekhia, *J. Food. Sci.*, 44 (1979) 263.
[3] C.Y.W. Ang and F. Moseley, *J. Agric. Food. Chem.*, 28 (1980) 483.
[4] R.G. Skurray, *J. Food. Chem.*, 7 (1981) 77.
[5] R.B.H. Wills, P. Wimalasiri and H. Greenfield, *J. Micronutrient Anal.*, 1 (1985) 23.
[6] K.R. Dawson, N.F. Unklesbay and H.B. Hedrick, *J. Agric. Food. Chem.*, 36 (1988) 1176.
[7] P. György and W.N. Pearson, *The Vitamins*, Academic Press, New York, 1967, pp. 80–83 and 130–134.

ELSEVIER

Journal of Chromatography A, 668 (1994) 365–370

JOURNAL OF CHROMATOGRAPHY A

Chromatographic behaviour of triazine compounds

Giovanni Sacchero, Susanna Apone, Corrado Sarzanini*, Edoardo Mentasti

Department of Analytical Chemistry, University of Turin, Via P. Giuria 5, 10125 Turin, Italy

Abstract

A comparative study was made of the chromatographic behaviour of eight 1,3,5-triazine compounds, including Cl-triazines and S-triazines (Ametryne, Atrazine, Cyanazine, Prometryne, Propazine, Simazine, Terbutryne, Terbutylazine). The techniques investigated included liquid–liquid partitioning and ion interaction chromatography with UV detection. Capacity factors are discussed as a function of mobile phase parameters: pH, ionic strength and organic modifier and ion interaction reagent concentrations.

1. Introduction

The chromatographic determination of triazine herbicides is of great importance in environmental control. Generally, analytical methods deal with the simultaneous determination of different chemical families of pesticides [1]. The techniques usually used include gas chromatography (GC) [2] and liquid chromatography (LC) [3–11], the latter being preferable for polar or thermolabile analytes [12]. LC methods have been developed with particular attention to detection [3–7] and sample preconcentration [8,9]. In order to obtain high selectivity and lower detection limits, a method coupling LC with GC–MS has recently been developed [13]. A liquid–liquid partition study was reported by Günther and Kettrup [10] with reference to the retention time behaviour of these compounds, but the retention mechanism as a function of the eluent composition has received little attention.

The aim of this work was a comparison of the chromatographic behaviour and the separation mechanism for eight triazine species (Fig. 1), using liquid–liquid partitioning (LLC) and ion interaction (IIC) procedures.

2. Experimental

A Varian (Walnut Creek, CA, USA) LC 5000 liquid chromatograph equipped with a UV 100 spectrophotometric detector and a Vista 401 data system was used. Graphic representations were performed with an IBM PS/2 Model 57 SX desk-top PC and Sigma Plot version 5 software (Jandel Scientific). The analytical column was LiChrospher 100 RP-18 (5 μm) (250 × 4 mm I.D.), obtained from Merck (Darmstadt, Germany).

Acetonitrile (HPLC grade), phosphoric acid, sodium hydroxide, lithium perchlorate, tetrabutylammonium hydroxide (TBA-OH) and sodium dodecyl sulphate (SDS) were Merck analytical-reagent grade products.

Eluents were prepared with high-purity water obtained from a Milli-Q system (Millipore, Bedford, MA, USA), filtered and degassed under vacuum before use.

Reference standards for triazine compounds

* Corresponding author.

0021-9673/94/$07.00
SSDI 0021-9673(93)E1165-V

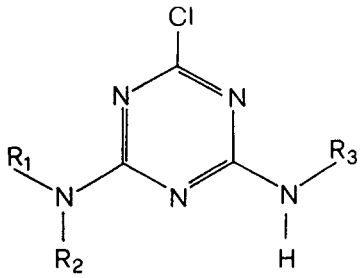

Names	R_1	R_2	R_3	pK_a
Simazine	H	Et	Et	1.7
Atrazine	H	Et	i-Pr	1.7
Propazine	H	i-Pr	i-Pr	1.7
Terbutylazine	H	Et	t-Bu	2.0
Cyanazine	H	Et	CH_3 | C-C=N | CH_3	1.0

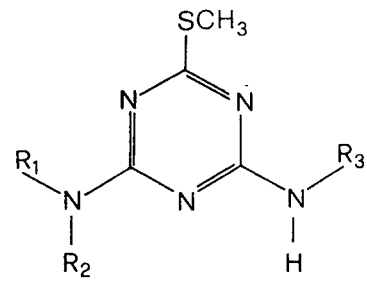

Names	R_1	R_2	R_3	pK_a
Ametryne	H	Et	i-Pr	4.1
Prometryne	H	i-Pr	i-Pr	4.1
Terbutryne	H	Et	t-Bu	4.3

Fig. 1. Structure and acid dissociation constants (pK_a) of the investigated triazine compounds. Et = Ethyl; i-Pr = isopropyl; t-Bu = *tert.*-butyl.

were obtained from Riedel-de Haën–Schering (Seelze, Germany) (98.0–99.9% purity). Stock standard solutions of the analytes (200 mg/l) were prepared in acetonitrile and stored in the dark at 4°C. Working standard solutions were obtained daily by diluting the stock standard solutions with acetonitrile. The amount of each analyte injected was 600 ng, unless stated otherwise.

The UV detector was set at 220 nm as a compromise between the maximum absorbance of the analytes and the reduced background of the eluents at this wavelength. Acetonitrile was chosen owing to its low absorbance background in the UV region.

Both reversed-phase LLC and IIC techniques were applied and the eluent flow-rate was 1.0 ml/min unless stated otherwise. Sample volumes injected were 100 μl. Chromatographic retention times (t_R) are the means of triplicate determinations and the dead time (t_0) was evaluated by injection of nitrate ion (1.0 m*M* $NaNO_3$), taken as the unretained peak in LLC, and by injection of water (water dip) in IIC. The capacity factors (k') were calculated from the retention times of the triazine compounds using the relationship $k' = (t_R - t_0)/t_0$.

The eluents were acetonitrile–water mixtures (see below) containing, depending on the chromatographic technique, the following components. For LLC studies, sodium phosphate buffer (15.0 m*M* H_3PO_4 + NaOH to adjust the pH) and, if stated, lithium perchlorate (0–1.2 *M*) or TBA-OH (0.25 m*M*) were used. After optimization, the system adopted was acetonitrile–water (45:55), 15 m*M* H_3PO_4 (pH 7.0) at a flow-rate of 1.5 ml/min. The pH values of all eluent mixtures were measured with reference to the actual medium (acetonitrile–water buffer) with the aid of a combined glass–calomel electrode. For IIC studies, SDS (0–1.0 m*M*) and sodium phosphate buffer (15.0 m*M* H_3PO_4 + NaOH to adjust the pH) were used. After optimization, the system adopted was acetonitrile–water (50:50), 1.0 m*M* SDS, 15 m*M* H_3PO_4 (pH 7.0) at a flow-rate of 1.0 ml/min.

3. Results and discussion

3.1. Liquid–liquid partition chromatography (LLC)

Experiments were performed, with respect to the mechanism acting in LLC, to evaluate the influence of organic modifier concentration, pH, ionic strength and modification of the stationary phase polarity. Fig. 2 shows, as an example, the

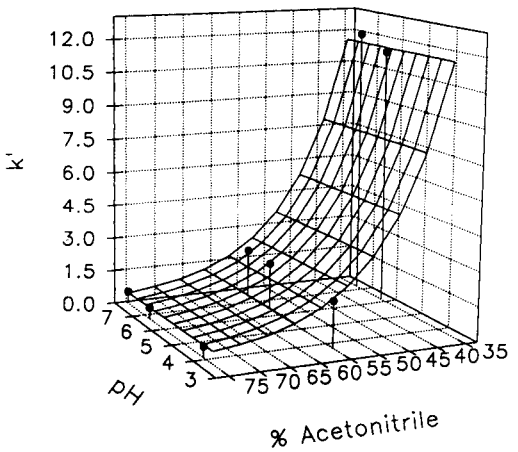

Fig. 2. Retention surface for ametryne in LLC. For experimental conditions, see text.

behaviour of k' for ametryne as a function of eluent composition (pH, acetonitrile concentration) in terms of the "retention surface". The dependence of the capacity factor on the concentration of the organic modifier is expressed by an exponential decrease corresponding to the increase in acetonitrile concentration. The retention time is not significantly affected by the eluent pH, which means that the variations in the partial charges on the nitrogen atoms do not change substantially the molecular lipophilicity. The same trend of the capacity factor was observed for all the triazines investigated, as a function of either pH or acetonitrile concentration. Nevertheless, the stronger inductive effect ($-I$) of the chloride atom in position 2 with respect to the $-SCH_2$ group generates an increase in the charge density on the triazine ring, in particular on the nitrogen atoms in positions 1 and 3, making such species more polar and with less affinity for the stationary phase.

Cl-triazines generally have lower retention times than S-triazines. This behaviour is observed with the exception of terbutylazine, for which the influence of the *tert.*-butyl group in position 4 prevails over the effect of chlorine in position 2, so that terbutylazine has a lower polarity, that is, a higher k', than the S-triazine ametryne. For a defined substituent in position 2, the k' value may be explained by considering the structure of the group in positions 4 and 6. The k' values for Cl-triazines show the sequence cyanazine < simazine < atrazine < propazine < terbutylazine, where cyanazine has the lowest k' value owing to the polar substituent group $-NHCH(CH_3)CN$.

Triazines are slightly basic compounds; the pK_a values (Fig. 1) show that significant protonation occurs at pH < 2 for Cl-triazines and at pH < 4 for S-triazines. As the dielectric constant of water–acetonitrile mobile phases is lower than that of water alone, the k' values are approximately constant at pH > 3. Anyway, the pH may influence other chromatographic parameters, such as the column resolution. Table 1 shows the number of theoretical plates $[N = 16(t_R/W)^2$, where W = peak width] evaluated for prometryne and propazine, which are representative of S- and Cl-triazines, respectively. According to the pK_a values, the pH effect is greater for S-triazines. This is also confirmed by the behaviour of the peak asymmetry factor (AF10), evaluated at 10% of the peak height; S-triazines show a tailed peak at acidic pH values of the mobile phase.

Fig. 3 shows an example of the separation obtained by LLC at neutral pH. Mobile phases containing perchlorate ion have been used [10]; this addition improves the resolution and chromatographic performance with a significant effect on the retention times. In our experiments, the lithium salt, which is more soluble, was preferred as the effect is evidenced only at very high concentrations. By increasing the perchlorate concentration the affinity between the eluent and the more polar species increases, resulting in lower k' values (pH 3.0). As expected, S-triazines show a greater deviation. The inversion of

Table 1
Effect of pH on the number of theoretical plates for propazine and prometryne (Cl- and S-triazine, respectively)

pH	Prometryne	Propazine
3	548	481
5	1118	510
7	1150	547

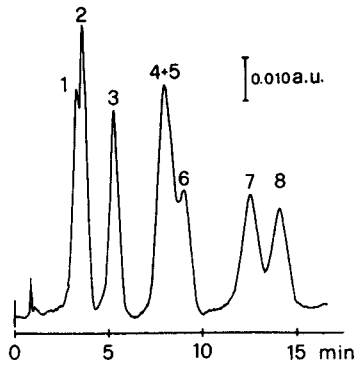

Fig. 3. Chromatogram of (1) cyanazine, (2) simazine, (3) atrazine, (4) propazine, (5) ametryne, (6) terbutylazine, (7) prometryne and (8) terbutryne obtained by LLC. Eluent, acetonitrile–water (45:55, v/v); buffer, pH 7.00; flow-rate, 1.5 ml/min; analytes, 1.0 μg each.

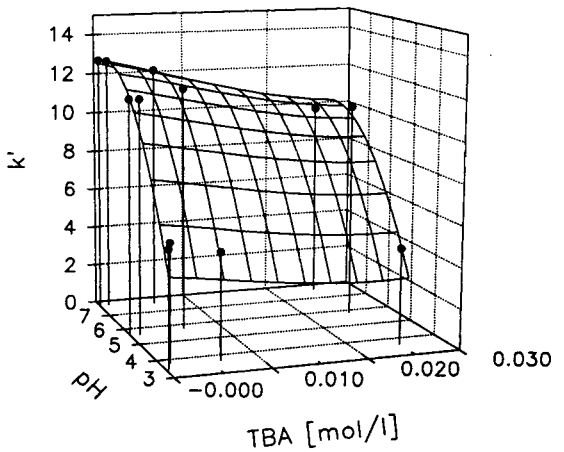

Fig. 4. Retention surface of ametryne (S-triazine) obtained using IIC with analyte and ion interaction reagent having the same positive charge. Eluent, acetonitrile–water (35:65, v/v); buffer pH and TBA concentration as shown.

the elution sequence due to the ionic strength effect is noteworthy. In contrast, for the neutral species the partitioning on the stationary phase is increased in addition to their k' values. For higher pH values (*e.g.*, pH 5) the increase in ionic strength results in greater k' values for all the species.

In addition of the organic modifier, pH and ionic strength effects on k' for triazines, we also investigated the effect of a compound able to modify the polarity of the stationary phase in order to improve the separation of the analytes. To avoid too short elution times and to evidence the effect of a positively charged lipophilic cation, the percentage of acetonitrile in the mobile phase was kept below 35%. Experiments were performed by adding tetrabutylammonium hydroxide (TBA-OH) to the mobile phase, the TBA cation being adsorbed on the surface of the stationary phase, which becomes positive. Fig. 4 shows the retention surface for ametryne as representative of S-triazines. The capacity factors decrease as the TBA concentration increases; this effect may be attributed to the repulsive effect between the positively charged TBA adsorbed on the stationary phase and the analytes in cationic form. Thus the pH of the mobile phase strongly affects the retention of S-triazines whereas Cl-triazines, having lower pK_a values, are not affected in the pH range investigated. On the other hand, the peak resolution does not improve in comparison with the previous LLC procedure when TBA is added to the eluent.

3.2. Ion interaction chromatography (IIC)

By working at a suitable pH, according to the triazine pK_a values, the analytes can be treated as cations and IIC can be applied for their separation. Experiments were carried out in order to optimize the IIC procedure and to evaluate the effectiveness of SDS as a counter ion.

When the eluent contains SDS, the stationary phase assumes a negative charge owing to SDS partitioning, and the strong affinity between the alkyl chain of SDS and the reversed phase modifies the stationary phase with the introduction of dynamic ion-exchange sites and a slight decrease in lipophilic character. The exchange reaction between the protonated triazine compounds ($T-H^+$) in the mobile phase (m) and the SDS adsorbed on the stationary phase (s) can be formally written as

$$T - H^{+}_{(m)} + Na^{+}\ {}^{-}O_3SOC_{12}H_{25(s)} \rightleftharpoons T - H^{+}\ {}^{-}O_3SOC_{12}H_{25(s)} + Na^{+}_{(m)}$$

Under these conditions, the retention of the triazine species increases as much as their partial positive charge is strong. Fig. 5 shows the behaviour of the k' values of the analytes as a function of SDS concentration. According to their pK_a values, S-triazines (ametryne, prometryne and terbutryne) show greater k' increases at higher SDS concentrations. It must be noted that the k' variations as a function of pH are opposite to those in LLC, where an increase in pH does not or only slightly affects k'. The decrease in k' at high pH values, in the presence of SDS, and the more consistent effect on S-triazines gives rise to an inversion in the sequence of elution between ametryne and terbutylazine.

The retention surface as a function of pH and SDS concentration in the eluent, for a generic triazine, changes its slope for either different pH or SDS concentration. Fig. 6 shows, as an example, the cyanazine retention surface. The decrease in k' at high pH indicates a decrease in the lipophilicity in the stationary phase when the SDS concentration increases. This represents an interesting chemometric case of interaction between the two factors (pH and SDS concentration) on the response surface (k').

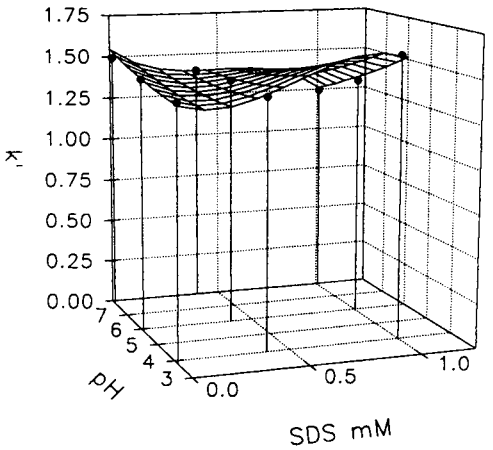

Fig. 6. Retention surface of cyanazine obtained by IIC in the presence of SDS. Eluent, acetonitrile–water (50:50, v/v); buffer pH and SDS concentration as shown.

Fig. 7 shows the separation of atrazines using the optimized IIC procedure, the resolution being better than that for the LLC method.

The ion interaction mechanism investigated in this work allows greater possibilities than LLC

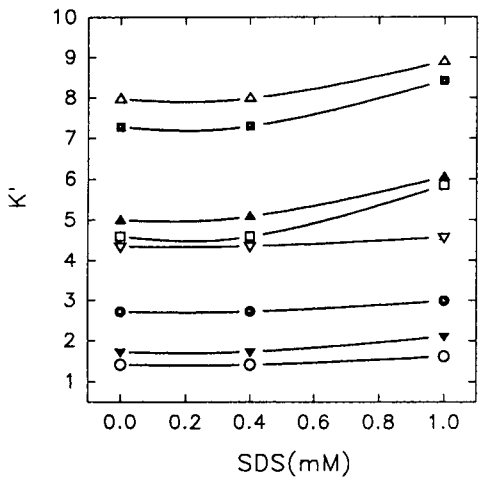

Fig. 5. Effect of SDS concentration on capacity factors in IIC: ○ = cyanazine; ▼ = simazine; ● = atrazine; ▽ = propazine; □ = ametryne; ▲ = terbutylazine; ■ = prometryne; △ = terbutryne. Eluent, acetonitrile–water (50:50, v/v); buffer pH 3.00; SDS concentration as shown.

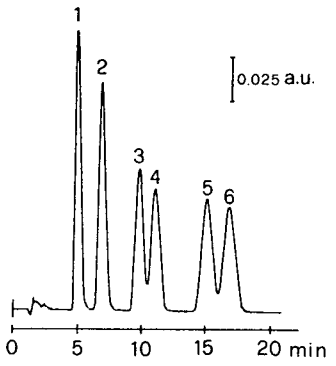

Fig. 7. Chromatogram of (1) simazine, (2) atrazine, (3) propazine, (4) terbutylazine, (5) prometryne and (6) terbutryne obtained by IIC in the presence of SDS. Eluent, acetonitrile–water (50:50, v/v); buffer, pH 7.00; SDS concentration, 1.00 m*M*.

and results in a competitive and more flexible technique for the determination of herbicides and pesticides.

4. Acknowledgements

Financial support from the Ministero dell' Università e della Ricerca Scientifica e Tecnologica (MURST, Rome) and from the Italian National Research Council (CNR, Rome) is gratefully acknowledged.

5. References

[1] J. Sherma, *Anal. Chem.*, 59 (1987) 18.
[2] J.C. Moltó, Y. Picó, G. Font and J. Mañes, *J. Chromatogr.*, 555 (1991) 137.
[3] W. Schüssler, *Chromatographia*, 27 (1989) 431.
[4] D. Barceló, *Org. Mass Spectrom.*, 24 (1989) 898.
[5] G. Durand and D. Barcelò, *J. Chromatogr.*, 502 (1990) 275.
[6] G. Karlaganis, R. Von Arx, H.U. Ammon and R. Camenzind, *J. Chromatogr.*, 549 (1991) 229.
[7] D.S. Owens and P.E. Sturrock, *Anal. Chim. Acta*, 188 (1986) 269.
[8] E.R. Brouwer, I. Liska, R.B. Geerdink, P.C.M. Frintrop, W.H. Mulder, H. Lingeman and U.A.Th. Brinkman, *Chromatographia*, 32 (1991) 445.
[9] V. Coquart and M.C. Hennion, *J. Chromatogr.*, 585 (1991) 67.
[10] W.J. Günther and A. Kettrup, *Chromatographia*, 28 (1989) 209.
[11] J. Lintelmann, C. Mengel and A. Kettrup, *Fresenius' Z. Anal. Chem.*, 346 (1993) 752.
[12] D. Barceló, *Chromatographia*, 25 (1988) 928.
[13] H. Bagheri, J.J. Vreuls, R.T. Ghijsen and U.A.Th. Brinkman, *Chromatographia*, 34 (1992) 5.

ELSEVIER

Journal of Chromatography A, 668 (1994) 371–374

JOURNAL OF CHROMATOGRAPHY A

Preconcentration and determination of 2,4,5-trichlorophenol in air using a wet effluent denuder and high-performance liquid chromatography

Z. Zdráhal*, Z. Večeřa

Institute of Analytical Chemistry, Academy of Sciences of the Czech Republic, Veveří 97, 611 42 Brno, Czech Republic

Abstract

A wet effluent diffusion denuder was used for the preconcentration of gaseous 2,4,5-trichlorophenol (2,4,5-TCP) from air. The wet denuder function is based on capturing gaseous pollutants from air in a film of absorbing liquid that flows continuously down the inner wall of the wet denuder. The air passes through the cylindrical wet denuder under laminar flow conditions. Water (adjusted to pH 8.5) was employed as absorbing liquid. The concentration of 2,4,5-TCP was determined using a liquid picochromatography with a reversed-phase C_{18} stationary phase and UV detection at 218 nm. The detection limit was 685 ng m^{-3}. The measuring systems enables results to be obtained at 7-min intervals.

1. Introduction

Hundreds of different organic substances are emitted into the air and many of them have adverse health effects at trace concentrations. The increasing interest in understanding the distribution and fate of organic compounds in the atmosphere initiated the development of more accurate, sensitive and reliable techniques for their monitoring. An important feature of the techniques is how fast results can be obtained (*i.e.*, the time elapsed between the sample collection and the end of analysis). Filter pack techniques have been widely applied for both gas-phase and gas/particle distribution studies [1–6]. These filter/sorbent systems suffer from artifacts caused by adsorption of gas-phase analytes on the filter or on the collected particles or, on the other hand, by volatilization of analytes from the particles [1,7]. These techniques are often time consuming.

In recent years, diffusion denuders have replaced the commonly used filter packs in some instances to prevent these difficulties. The diffusion denuder is a tube (cylindrical design) or several (usually two) concentric tubes (annular design) through which sample air passes. Under laminar flow conditions, particles pass through the denuder owing to their small diffusion coefficients and then they can be collected downstream of the denuder. Gas molecules diffuse towards the inner tube walls covered with an appropriate sorptive agent in which molecules are accumulated. After sampling, the analyte is usually removed from the surface of the denuder walls by thermal desorption or liquid extraction [8–16]. These procedures, especially liquid extraction, are accompanied by some problems, but the construction of a wet effluent diffusion denuder (wet denuder) [17,18] makes it possible

* Corresponding author.

0021-9673/94/$07.00
SSDI 0021-9673(93)E1130-R

to avoid them. Instead of the fixed film of sorptive agent, a film of absorbing liquid flows continuously down the inner wall of the wet denuder while gas passes countercurrently and, in this way, a continuous stream of concentrated analyte is obtained at the bottom of the denuder. The concentrate can be analysed directly or further treated. The concentration effect is given by the ratio between the liquid flow-rate (hundreds of μl/min) and the gas flow rate (l/min), with an assumed denuder collection efficiency of 100%.

The use of a wet denuder for the preconcentration of gaseous model organic compounds was verified in this work.

2. Experimental

2.1. Wet denuder

The wet denuder was a glass tube (50 cm × 1 cm I.D.), the inner wall of which had been treated by a special procedure [17,18] to maintain a compact film of absorbing liquid (water). The vertical position of the denuder ensured its correct operation. The liquid was fed to the denuder wall through a porous PTFE ring (Porex Technologies, Fairburn, GA, USA) located in the head at the upper end of the denuder. The concentrate was also removed through the head with a PTFE ring at the lower end of the denuder. The concentrate was sucked into a vial by a peristalic pump (laboratory made) and was taken from this vial for analysis. The sampled air entered the denuder through a subduction zone (glass tube, 15 cm × 1 cm I.D.) which ensured adjustment of laminar flow conditions. The air flowed through the denuder in the reverse direction to the absorbing liquid. A membrane pump (JZD, Výčapy, Czech Republic) was located downstream of the denuder.

2.2. HPLC system

A PLC-10 picochromatograph with a glass-fibre UV detection cell (laboratory made) was used [19]. A Jasco (Tokyo, Japan) 875-UV detector was connected to the detection cell and set at 218 nm. A glass column (60 mm × 0.5 mm I.D.) packed with Silasorb C_{18} (5 μm) (Lachema, Brno, Czech Republic) was used, with acetonitrile–water (65:35) as the mobile phase at a flow-rate of 7 μl min^{-1}. The sample volume was usually 10 μl. The principle of sample injection in a non-eluting solvent was applied (sample flow-rate 5 μl min^{-1}) [20].

2.3. Vapour generator

The condenser inside which the solid phase 2,4,5-trichlorophenol (2,4,5-TCP) (Merck, Darmstadt, Germany) was inserted worked as a source of gaseous 2,4,5-TCP at a temperature of 10°C. Nitrogen was passed continuously through the condenser at 0.5 ml min^{-1} and transported 2,4,5-TCP to a T-piece where it was mixed with air that has been cleaned through a charcoal trap. This gas mixture was led to the wet denuder. When dilution was necessary, the part of the nitrogen containing 2,4,5-TCP was withdrawn with a peristaltic pump (Laboratory Equipment, Prague, Czech Republic) before mixing with air. The production of the generator was measured by HPLC (see above) after 2,4,5-TCP had been collected in deionized water. To verify this method, GC with flame ionization detection (Carlo Erba, Milan, Italy; Hewlett-Packard SE-54 capillary column, 30 m × 0.53 mm I.D.; carrier gas nitrogen) was used for the determination of 2,4,5-TCP, after the 2,4,5-TCP had been absorbed in toluene (Lachema). The same volume of solvent (0.5 ml) was always used and the collection times were varied in the range 20–70 min. Both methods gave comparable results. Two collection vials were used in series for the first measurements. No 2,4,5-TCP was found in the second vial and therefore only one vial was used in further experiments. The production of the generator was always determined before denuder experiments.

3. Results and discussion

The simple model system was used to test the wet denuder. 2,4,5-TCP was chosen because of

its relatively good solubility in water, which is why water could be used as the absorbing liquid. 2,4,5-TCP is employed in the manufacture of pesticides, dyes, etc., and is an air pollutant, especially in workplaces.

The length of the denuder was chosen as 50 cm so that the collection efficiency (c/c_0) was at least 99% for an air flow-rate of 0.5 l min^{-1}. It was calculated according to the Gormley and Kennedy equation [21,22], which describes the behaviour of trace amounts of gases in a cylindrical denuder:

$$c/c_0 = 0.819\exp(-14.6272\Delta) + 0.0976\exp(-89.22\Delta) + 0.01896\exp(-212\Delta)$$

$$\Delta = \pi DL/4F$$

where c = mean concentration of the gas trace leaving the denuder, c_0 = concentration of the gas trace entering the denuder, D = diffusion coefficient of the gas trace, L = denuder length and F = gas flow-rate. If Δ is sufficiently low, only the first term of the equation is significant and the equation is simplified.

To verify the expected efficiency of the wet denuder we performed series of repeated experiments at a constant 2,4,5-TCP concentration. The air flow-rate was 0.5 l min^{-1} and the water flow-rate was varied from 100 to 350 μl min^{-1}. During the experiments we found that the liquid flow-rate had to be maintained above 250 μl min^{-1}. Below this flow-rate, the liquid film is probably not compact because the wet denuder wall is slightly rough (tens of μm) after treatment. Water was adjusted to pH 8.5 for better denuder operation. The use of water also restricts the influence of air humidity on denuder operation. Changes in relative humidity cause only various evaporative losses of water, which do not affect the collection procedure when the liquid flow-rate is sufficiently high [17].

Under these conditions, we obtained a collection efficiency of 100.6% with R.S.D. = 5.9% for seven samples taken during 5 h at a 2,4,5-TCP concentration of 21.4 μg m^{-3}. The calculated efficiency was 99.1% if the value of the diffusion coefficient was $6.54 \cdot 10^{-2}$ cm^2 s^{-1} (25°C). It was calculated according to the method of Fuller, Schettler and Giddings [23]. It should be noted there were more sources of errors (not only denuder operation) that contributed to total R.S.D. value, *e.g.*, fluctuation of nitrogen flow through the vapor generator (1.5%), error of LC determination (3.0%) and error of liquid flow-rate determination.

The relationship between collection efficiency and air flow-rate was measured in the range 0.4–1.8 l min^{-1} (Fig. 1). The shape of the curve corresponds to the curve calculated according to the Gormley and Kennedy equation. This confirms that water is a good absorption liquid under the given conditions.

The sets of data obtained in measurements of previous dependences were also used for calculation of the diffusion coefficient of 2,4,5-TCP. It is obvious that the diffusion coefficient can be determined from the slope of a plot of Δ *versus* L/F (Fig. 2). Values of the parameter Δ were calculated from the Gormley and Kennedy equation when known c and c_0 values were substituted. The average value of the diffusion coefficient of 2,4,5-TCP (from five measurements) was $6.13 \cdot 10^{-2}$ cm^2 s^{-1} with R.S.D. = 14.9%. In spite of the experiments performed without holding the air temperature constant (laboratory temperature was 26 ± 1°C), this diffusion coefficient was comparable to the theoretically calculated value of $6.67 \cdot 10^{-2}$ cm^2 s^{-1} at 26°C.

The calibration graph was measured in the

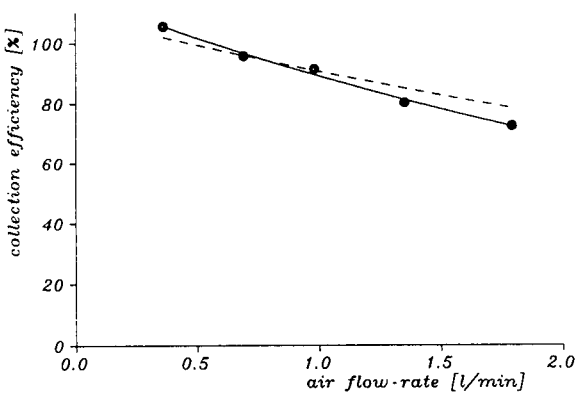

Fig. 1. Relationship between wet denuder collection efficiency and air flow-rate. O = Experimental data; dashed line = theoretical curve according to the Gormley and Kennedy equation.

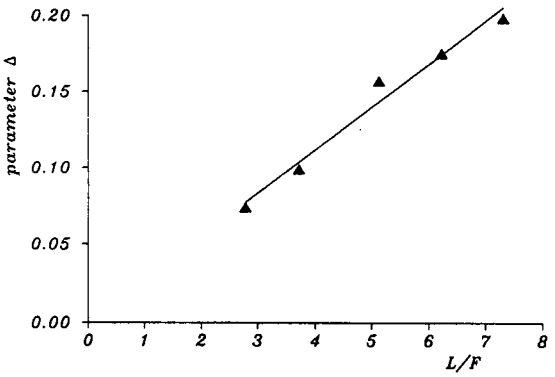

Fig. 2. Plot of parameter Δ *versus* L/F for calculating the diffusion coefficient of 2,4,5-TCP.

range of available concentrations 10–40 μg m^{-3}. The plot of peak area *versus* 2,4,5-TCP concentration was linear ($r = 0.998$) under the given conditions (250 μl min^{-1} liquid and 0.5 l min^{-1} air flow-rates). The estimated detection limit for injection of 10 μl of concentrate was 685 ng m^{-3} (calculated from three times the baseline noise). This limit could be lowered by increasing the sample volume.

The connection of the wet denuder with the picochromatograph allows a result to be obtained every 7 min.

4. Conclusions

The wet denuder proved successful for the collection of gaseous 2,4,5-TCP from air and it could be expected to be applicable also to other classes of organic pollutants if the appropriate absorbing liquid is chosen. The continuously renewed collection surface, the rapidly obtainable concentrate of analytes and the possibility of direct analysis of this concentrate are advantages of the wet denuder.

5. Acknowledgements

This work was supported by a grant (No. 63157) from the Academy of Sciences of the Czech Republic. The authors thank Dr. V. Kahle for technical assistance and for advice.

6. References

[1] E.D. Pellizzari, in L.D. Hansen and D.J. Eatough (Editors), *Organic Chemistry of the Atmosphere*, CRC Press, Boca Raton, FL, 1991, Ch. 1, p. 1.
[2] J. Rudolph, K.P. Muller and R. Koppmann, *Anal. Chim. Acta*, 236 (1990) 197.
[3] M.P. Ligocki and J.F. Pankow, *Anal. Chem.*, 57 (1985) 1138.
[4] H. Rothweiler, P.A. Wager and Ch. Schlatter, *Atmos. Environ.*, 25B (1991) 231.
[5] H. Kaupp and G. Umlauf, *Atmos. Environ.*, 26A (1992) 2259.
[6] T.F. Bidleman, W.N. Billings and W.T. Foreman, *Environ. Sci. Technol.*, 20 (1986) 1038.
[7] M.P. Ligocki and J.F. Pankow, *Environ. Sci. Technol.*, 23 (1989) 75.
[8] Z. Ali, C.L.P. Thomas and J.F. Alder, *Analyst*, 114 (1989) 759.
[9] D.J. Eatough, L.D. Hansen and E.A. Lewis, in D.J. Eatough and L.D. Hansen (Editors), *Organic Chemistry of the Atmosphere*, CRC Press, Boca Raton, FL, 1991, Ch. 2, p. 53.
[10] M. Possanzini, P. Ciccioli, V. Di Palo and R. Draisci, *Chromatographia*, 23 (1987) 829.
[11] J.M. Dasch, S.H. Cadle, K.G. Kennedy and P.A. Mulawa, *Atmos. Environ.*, 23 (1989) 2775.
[12] D.A. Lane, N.D. Johnson, S.C. Barton, G.H.S. Thomas and W.H. Schroeder, *Environ. Sci. Technol.*, 22 (1988) 941.
[13] R.W. Coutant, P.J. Callahan, M.R. Kuhlman and R.G. Lewis, *Atmos. Environ.*, 23 (1989) 2205.
[14] M.S. Krieger and R.A. Hites, *Environ. Sci. Technol.*, 26 (1992) 1551.
[15] R.W. Coutant, P.J. Callahan, J.C. Chuang and R.G. Lewis, *Atmos. Environ.*, 26A (1992) 2831.
[16] C.L.P. Thomas and J.F. Alder, *Anal. Chim. Acta*, 274 (1993) 171.
[17] P.K. Simon, P.K. Dasgupta and Z. Večeřa, *Anal. Chem.*, 63 (1991) 1237.
[18] Z. Večeřa and P.K. Dasgupta, *Anal. Chem.*, 63 (1991) 2210.
[19] M. Krejčí and V. Kahle, *J. Chromatogr.*, 392 (1987) 133.
[20] K. Šlais, D. Kouřilová and M. Krejčí, *J. Chromatogr.*, 282 (1983) 363.
[21] P. Gormley and M. Kennedy, *Proc. R. Ir. Acad., Sect. A*, 52 (1949) 163.
[22] K.M. Adams, S.M. Japar and W.R. Pierson, *Atmos. Environ.*, 20 (1986) 1211.
[23] E.N. Fuller and J.C. Giddings, *J. Gas Chromatogr.*, 3 (1965) 222.

ELSEVIER

Journal of Chromatography A, 668 (1994) 375–383

JOURNAL OF CHROMATOGRAPHY A

Analysis of alkylphenol-based non-ionic surfactants by high-performance liquid chromatography

Dan F. Anghel*[,a], Marieta Balcan[a], Anca Voicu[b], Mihai Elian[b]

[a]*Laboratory of Colloids, Institute of Physical Chemistry, Spl. Independentei 202, 79611 Bucharest, Romania*

[b]*Institute of Organic Chemistry, Spl. Independentei 202A, 71141 Bucharest, Romania*

Abstract

Ethoxylated non-ionic surfactants derived from octyl- and nonylphenols were analyzed by normal-phase HPLC. A silica column (Si-100, 5 μm) with gradient elution and UV detection at 280 nm were used for oligomer determination. Baseline separation of the ethylene oxide adducts of alkylphenols with average ethoxymer numbers as high as 40 was achieved. The elution system and the gradient profile used depend on the average ethoxymer number of the surfactant. The method can provide full information for the quantitative calculation of the oligomer distribution from ethoxylated surfactants. The hydrophobic moiety of the surfactants was characterized by reversed-phase chromatography. An octadecylsilica column (RP-18, 5 μm) and methanol–water (8:2, v/v) as eluent were used. The procedure is useful for the rapid identification of surfactants according to the alkylphenyl chain.

1. Introduction

Ethoxylated non-ionic surfactants are effective, multi-purpose and versatile substances. Commercial products are obtained by reaction of the ethylene oxide with a hydrophobe having an active hydrogen atom (*e.g.*, alkylphenols, fatty acids or fatty alcohols) in the presence of a suitable alkaline catalyst [1]. Alkylphenol polyethoxylates usually contain complex mixtures of compounds that have isomerism in the alkyl chain and in the position of substitution, mono- and dialkyl substitution of the aromatic ring, different ethoxymers and free polyethylene glycol (PEG). When full identification and quantification of the components from ethoxylated alkylphenols are required, the analyst is faced with a difficult task. The terms "ethoxymer" and "oligomer" are equivalent; they are used here for a group of individual adducts containing various numbers of ethylene oxide units.

In the past two decades, separational and instrumental methods have made great strides in the field of non-ionic surfactant analysis. The state-of-the-art of thin-layer and paper chromatography (TLC and PC), gas chromatography (GC) and high-performance liquid chromatography (HPLC) has been reviewed by Cross [2].

HPLC is the most ideal technique for the evaluation of the product composition of non-ionic surfactants [3]. Information about the distribution of ethoxymers [3], the average degree of ethoxylation [4,5], the hydrophobic moiety [6–9] and the PEG content [3,10] of the sample can be readily obtained.

In normal-phase HPLC, the oligomers are separated according to their ethylene oxide con-

* Corresponding author.

0021-9673/94/$07.00
SSDI 0021-9673(93)E1128-M

tent; the hydrophobic chain has virtually no influence on the chromatographic process [6]. The columns used for such a purpose have as packings bare silica gel [3,4] and bonded stationary phases of the amino [3,5,6], diol [10] or cyano [11] types. Reversed-phase chromatography on octyl- or octadecylsilica [3,6,7] allows the surfactant hydrophobic moiety to be investigated. These columns are also suitable for determining the PEG content of the samples.

Polarity gradient elution and UV detection are mostly employed [3–7,11]. However, fluorescence [12] and mass spectrometric [13,14] detection have also been used. Mass spectrometry can reveal interesting structural information and is very suitable for analysing minute amounts of surfactants from streams and lakes.

This paper describes the use of HPLC in the analysis of non-ionic surfactants. Normal-phase HPLC was applied for the separation, identification and determination of oligomers from commercial samples of alkylphenol polyethoxylates. The behaviour of these surfactants in reversed-phase HPLC and the characterization of their hydrophobic moiety were also investigated.

2. Experimental

2.1. Apparatus

The equipment consisted of a Hewlett-Packard (Boeblingen, Germany) Model 1084B, liquid chromatograph fitted with a variable-wavelength UV detector and a fraction collector. The UV detector was set at 280 nm. Analytical columns (200 × 4.6 mm I.D.) packed with irregular silica (Si-100, 5 μm) or octadecylsilica (RP-18, 5 μm) were purchased from Hewlett-Packard (Waldbronn, Germany). The semi-preparative column (250 × 9.4 mm I.D.) was packed with spherical (5–6 μm) porous silica (Zorbax Sil) obtained from DuPont (Wilmington, DE, USA).

The column temperatures were 30°C for the Si-100 column and 40°C for the RP-18 and semi-preparative columns. These temperatures were imposed by the volatility of the eluents used. The flow-rates for analytical and semi-preparative separations were of 1 and 3 ml/min, respectively.

The operating conditions for determining the oligomer distributions of alkylphenol polyethoxylates (APEs) by normal-phase HPLC are given in Table 1. Reversed-phase separations were carried out with methanol–water (80:20, v/v) as eluent.

2.2. Chemicals

HPLC eluents were prepared by careful purification of analytical-reagent grade ethanol, methanol, 2-propanol and diethyl ether (Reactivul, Bucharest, Romania). The alcohols were fractionally distilled. Diethyl ether was washed free from peroxides with iron(II) sulphate solu-

Table 1
Eluents and gradients used to determine the distribution of oligomers in ethoxylated alkylphenol surfactants

No.	Average ethoxy units	Eluent A	Eluent B	Gradient
1	1–10	*n*-Hexane–diethyl ether (80:20, v/v)	*n*-Hexane–diethyl ether–dioxane–2-propanol–water–acetic acid (20:30:40:10:1:0.5, v/v)	5–95% B in 45 min
2	1–20	*n*-Hexane–diethyl ether (80:20, v/v)	*n*-Hexane–diethyl ether–dioxane–ethanol–2-propanol–water–acetic acid (10:15:50:20:5:1:0.25, v/v)	10–95% B in 40 min
3	10–40	*n*-Hexane–2-propanol (40:60, v/v)	Ethanol–water (80:20, v/v)	10–95% B in 45 min

tion, dried over sodium and fractionated prior to use. A narrow-cut hexane fraction was purchased from VEGA Petrochemicals (Ploiesti, Romania). It contained 80% *n*-hexane, the remainder being hexane isomers, *n*- and isopentanes and heptanes. The hexane fraction was submitted to fractional distillation and only the fraction boiling at 61°C was used. Dioxane was obtained from Petrochemical Works Savinesti (Savinesti, Romania). It was kept over potassium hydroxide for 1 week and then fractionally distilled. The fraction boiling at 101°C was employed. The purity of all the solvents was checked by UV spectrophotometry against water, using 1-cm light path cells. *n*-Hexane, methanol, ethanol and 2-propanol were accepted as eluents only if they showed >95% transmission at 280 nm. The threshold transmissions at 280 nm for diethyl ether and dioxane were of 90% and 85%, respectively. Acetic acid was purchased from Reactivul and used as received. Doubly distilled water having a conductivity lower than 1.5 μS was employed. In order to remove the particulate matter, the eluents were passed through 0.7-μm glass microfibre filters (Gelman Science, Ann Arbor, MI, USA).

The surfactants studied were commercial samples of the ethoxylated octylphenol (OPE_n) and nonylphenol (NPE_n) types from Detergentul (Timisoara, Romania) or Petrochemical Works Brazi (Ploiesti, Romania) and were used as received. The alkyl chain of these surfactants is highly branched, being the dimer of isobutene (2-methyl-1-propene) and the trimer of propene, respectively.

2.3. Ethoxymer standards

The oligomers separated during a run were identified with the aid of homogeneously ethoxylated alkylphenol standards. Triethylene glycol monononylphenyl ether ($NPEO_3$), octaethylene glycol monononylphenyl ether ($NPEO_8$) and triethylene glycol monooctylphenyl ether ($OPEO_3$) were obtained by reaction of the corresponding alkylphenol with the appropriate ethylene glycol in the presence of dicyclohexylcarbodiimide. Details of the synthesis and purification have been given elsewhere [15]. As higher ethoxymer standards are difficult to synthesize and purify, they were obtained from the polydisperse ethoxylated alkylphenols by semi-preparative HPLC. *n*-Hexane–2-propanol (40:60, v/v) (eluent A) and ethanol–water (80:20, v/v) (eluent B) were used with a linear gradient from 10 to 95% B in 45 min. Six fractions corresponding to ethoxylation degrees of 10–15 were collected and the products recovered by removing the solvent. All samples were subjected to analytical HPLC, and confirmation of their identity was done by IR and ^{1}H NMR spectrometry. Fig. 1 shows the chromatograms of $NPEO_3$, $OPEO_3$, $NPEO_8$ and $NPEO_{15}$. The compounds are almost free from impurities and

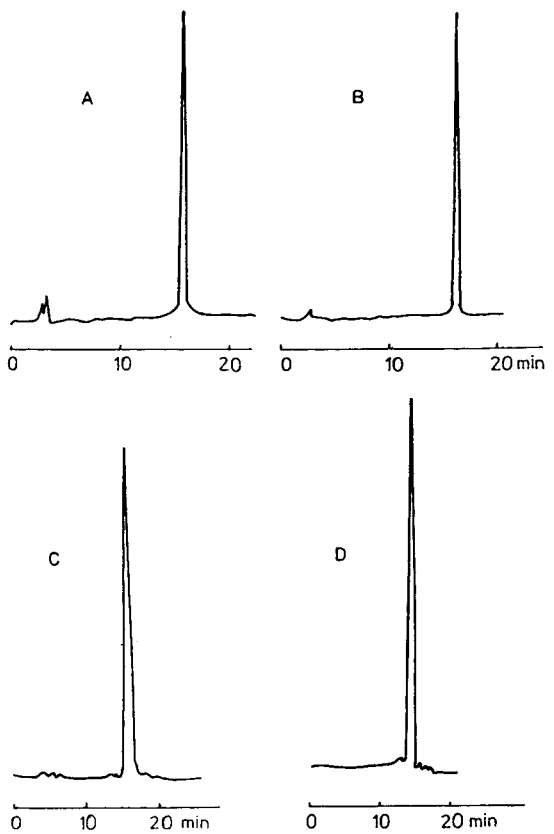

Fig. 1. Gradient elution of ethoxymer standards: (A) $NPEO_3$; (B) $OPEO_3$; (C) $NPEO_8$; (D) $NPEO_{15}$. Eluents and gradients are those in Table 1: for $NPEO_3$ and $OPEO_3$, No. 1; for $NPEO_8$, No. 2; for $NPEO_{15}$, No. 3.

may be used for oligomer identification and determination by HPLC.

2.4. Procedure

Solutions of about 1% (w/v) of commercial surfactant in the less polar solvent A were prepared. For higher ethoxylates, which are not readily soluble in solvent A, small amounts of solvent B were added to assist the dissolution. The volumes injected range from 10 to 50 μl, depending on the ethoxylation degree.

Ethoxymer identification and determination of average ethoxymer numbers were carried out as reported previously [5].

3. Results and discussion

3.1. Ethoxymer separation

In normal-phase chromatography, the most important parameter governing the separation is the adsorbent–solute interaction. The polyoxyethylene chains of non-ionic surfactants interact with the surface hydroxyl groups of silica through hydrogen bonding. The greater the number of oxyethylene units, the tighter will the material be retained and the more molecules of solvent will be required to remove it from the column. This is evident from Fig. 2A, showing the chromatogram of a nonylphenol ethoxylated with 4 mol of ethylene oxide (NPE_4) recorded with isocratic elution. The eluent was a 90:10 (v/v) mixture of eluents A and B listed in the first row of Table 1. The separation has good resolution owing to the column selectivity, but only four ethoxymers are eluted within 1 h. Parameters of the chromatographic process such as capacity factor, selectivity and efficiency are given in Table 2. The selectivity has an almost constant value of 2.2. The capacity factors are 1.63–18.3 and are beyond the optimum range for column efficiency [16]. The column efficiency measured by the height equivalent to a theoretical plate (H) is fairly large. It is evident that with isocratic elution the column operation is not optimum.

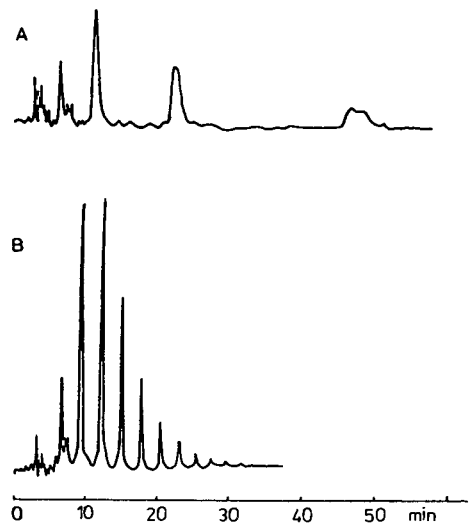

Fig. 2. Separation of NPE_4 ethoxymers with (A) isocratic and (B) gradient elution; Eluent A, *n*-hexane–diethyl ether (80:20, v/v); eluent B, *n*-hexane–diethyl ether–dioxane–2-propanol–water–acetic acid (20:30:40:10:1:0.5, v/v). Isocratic elution, 10% B in A; gradient elution, 5 to 95% B in 45 min.

The column selectivity can be improved by changing the distribution coefficient of the solutes (*i.e.*, during gradient elution). Fig. 2B illustrates the chromatogram obtained on the same NPE_4 sample. It reveals as many as eleven oligomers that are very well separated within 30 min. The parameters of the chromatographic process are considerably improved (see Table 2). The selectivity decreases monotonically and the capacity factor is within the optimum range of values for column efficiency. The height equivalent to a theoretical plate is from several times up to more than an order of magnitude smaller than that obtained under isocratic elution. Although the chromatographic system used was initially proposed for fatty alcohol ethoxylates [17], it provides very good results in the analysis of alkylphenol polyethoxylates also. In addition to NPE_4, several other non-ionic surfactants of the same type were analysed by this method. For example, Fig. 3 shows the chromatogram of NPE_6. The peaks have some inhomogeneities which may be accounted for by nonylphenol isomers. It has been observed that oligomers

Table 2
Selectivity (α), capacity factor (k') and efficiency (H) for isocratic and gradient elution of oligomers from a low ethoxylated nonylphenol (NPE_4)[a]

Oligomer No.	Isocratic[b]				Gradient[c]			
	Retention time (min)	α	k'	H (mm)	Retention time (min)	α	k'	H (mm)
1	6.45	–	1.63	0.169	6.12	–	1.11	0.083
2	11.37	2.22	3.62	0.248	8.69	1.67	1.86	0.093
3	22.55	2.37	8.20	0.142	11.59	1.51	2.81	0.052
4	46.70	2.23	18.37	0.127	14.36	1.35	3.79	0.034
5					17.28	1.28	4.84	0.024
6					20.01	1.22	5.89	0.018
7					22.61	1.17	6.89	0.025
8					24.94	1.13	7.78	0.020
9					26.79	1.10	8.59	0.027
10					29.17	1.08	9.31	0.068
11					30.97	1.08	10.13	0.081

[a] Eluent A, *n*-hexane–diethyl ether (80:20, v/v); eluent B, *n*-hexane–diethyl ether–dioxane–2-propanol–water–acetic acid (20:30:40:10:1:0.5, v/v).
[b] Isocratic elution: 10% eluent B in A.
[c] Gradient elution: 5–95% B in 45 min.

derived from octyl- and nonylphenol show the same chromatographic behaviour. This is additional evidence which supports the previous statement that the hydrophobic moiety does not influence the oligomer separation in normal-phase chromatography [6].

As all the oligomers are baseline separated and removed from the column within a reasonable period of time, the method can be used to determine quantitatively the ethoxymer distribution and the average ethoxylation number of a surfactant sample. Oligomer identifications and detector response factors were obtained with the aid of ethoxymer standards. The case of ethoxylated alkylphenols is the simplest as they bear the chromophore within the molecule. Moreover, they have one chromophore per molecule and the response of the UV detector is independent of the polyoxyethylene chain length [4]. The average ethoxylation numbers of NPE_4, NPE_6 and OPE_6 obtained by HPLC were 4.44, 6.09 and 6.17, respectively. For NPE_6 and OPE_6 samples, good agreement was found between the HPLC results and the ethoxylation degree stated by the producer. For NPE_4 a higher ethoxylation degree was found by HPLC. This demonstrates the ability of HPLC to detect any deficiency appearing during the ethoxylation process.

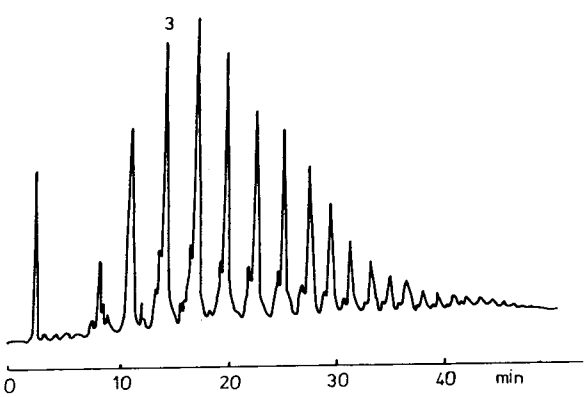

Fig. 3. Chromatogram of NPE_6 using gradient elution. Eluents and gradient as in Fig. 2B.

The method proposed by Vonk *et al.* [17] is very suitable for the analysis of non-ionic surfactants with a low ethoxylation degree. Our attempts to use it for surfactants having average ethoxylation numbers higher than 10 resulted in excessive band widths of the peaks at the end of

chromatogram. This effect denotes strong adsorption of the surfactant molecules on the silica, and makes the eluent less able to remove them from the column. Attempts to improve the polarity of eluent B led to the second elution system in Table 1. The chromatogram obtained with NPE_{10} is presented in Fig. 4. Although more polar, the eluent does not alter the resolution, but it shortens the duration of analysis and removes a larger number of oligomers from the column than the first eluent mixture. The chromatogram is complicated and shows for low ethoxylation degrees (up to 9) a small leading peak accompanying the main peak. On increasing the eluent strength, the large peak of the $(n+1)$th ethoxymer comes closer to the small peak of the nth ethoxymer, and overlaps it at $n=9$.

In normal-phase chromatography, *ortho*-, *meta*- and *para*-isomers elute from the column in the same elution order [16]. The sequence accounts for the strength of interaction between the solute molecules and the active sites on the stationary phase. The *p*-alkylphenol may result from synthesis with a certain amount of *ortho*-isomer. On ethoxylation this material will give a corresponding amount of *ortho*-derivative. The presence of a bulky alkyl group in the *ortho* position hinders the interaction between the hydroxyl active site of silica and the polyoxyethylene chains of the surfactant. Consequently, the *ortho*-isomer is less retained by the column than its *para* counterpart. When submitted to IR analysis, the NPE_{10} sample revealed as much as 30% of *o*-alkylate. Hence the leading peaks were assigned to the *ortho*-isomer.

Often, the formulation chemist needs nonionic surfactants with a certain value of the hydrophile–lipophile balance (HLB). If the respective surfactant is not commonly available, the desired product may be obtained by surfactant blending. As the HLB is an additive property, a range of intermediate HLBs can be obtained by blending appropriate amounts of surfactants with low and high HLB values. HPLC may assist in this search. Fig. 5 shows the chromatogram of the NPE_4 and NPE_{30} mixture and the gradient profile used. NPE_4 shows a good oligomer separation and suggests that the analysis of low-molecular-mass surfactants can be accomplished by suitable matching of the gradient in less than 20 min. At the same time,

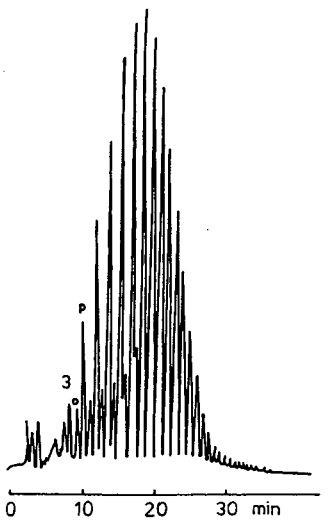

Fig. 4. Chromatogram of NPE_{10}. Eluent A, *n*-hexane–diethyl ether (80:20, v/v); eluent B, *n*-hexane–diethyl ether–dioxane–ethanol–2-propanol–water–acetic acid (10:15:50:20:5:1:0.25, v/v). Gradient: 10–95% B in 40 min.

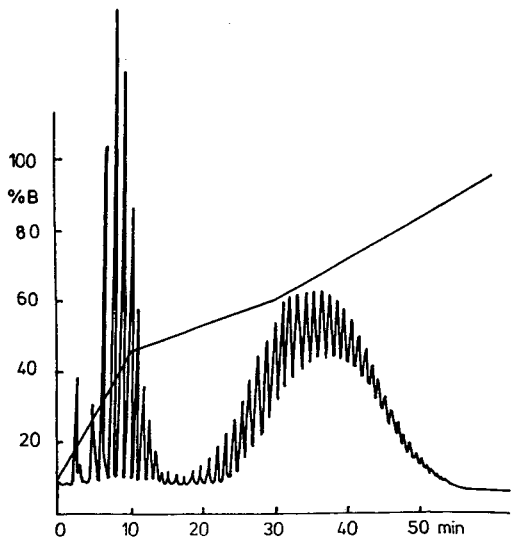

Fig. 5. Chromatographic behaviour of a low (NPE_4) and high (NPE_{30}) ethoxylate mixture. Conditions as in Fig. 4 except for the gradient profile.

lower molecular mass ethoxylates of known ethoxymer distribution such as NPE_4 are useful markers for higher molecular mass surfactants. The approach is very good when highly ethoxylated standards are not available. In the above chromatogram, as many as 50 oligomers are counted. By subtracting the NPE_4 oligomers, for NPE_{30} 39 oligomers result.

Because of poor resolution, the oligomer distribution for NPE_{30} cannot be obtained from the data in Fig. 5. To improve the resolution and obtain a baseline separation of NPE_{30} and higher ethoxylated surfactants, a more polar elution system is necessary. The chromatogram of NPE_{30} obtained with the third elution system in Table 1 is shown in Fig. 6. The sample has 41 ethoxymers, which agrees well with the previously reported number. Peak identification was made with the aid of an $NPEO_{15}$ ethoxymer standard, by using both internal and external standard methods. The most important achievement on elution with this system is the considerable improvement in resolution. Peak areas were used to determine the average ethoxymer numbers of NPE_{30} and NPE_{40} samples. They gave values of 29.00 and 37.20, respectively. For an NPE_{50} sample, poor resolution was obtained and it was not possible to obtain reliable data for calculating the oligomer distribution.

Fig. 7 shows the distribution of oligomers *versus* the ethoxymer number. The data were selected from a large number of examined samples and cover the range of commercially available NPEs with average ethoxymer numbers within the range 4–40. They illustrate the information that can be obtained about the oligomer distribution from ethoxylate samples by using HPLC. The method is currently applied to control the quality of industrially produced non-ionic surfactants. Table 3 presents some average ethoxymer numbers obtained by HPLC. The subscript on each sample abbreviation is the value stated by the producer. Generally, the agreement between the values is fairly good, but sometimes there are serious differences. This demonstrates the capability of HPLC of controlling both the synthesis and the end use of alkylphenol ethoxylates.

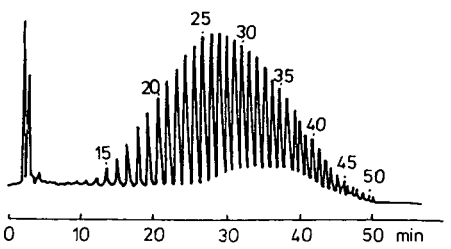

Fig. 6. Gradient elution of the oligomers from NPE_{30}. Eluent A, *n*-hexane–2-propanol (40:60, v/v); eluent B, ethanol–water (80:20, v/v). Gradient: 10–95% B in 45 min.

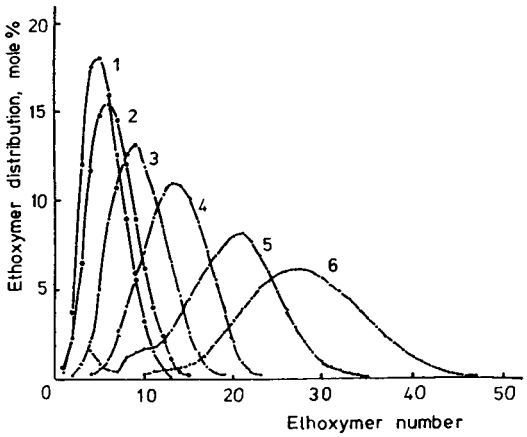

Fig. 7. Distribution of ethoxymers from various nonylphenol-based non-ionic surfactants: (1) NPE_4; (2) NPE_7; (3) NPE_{10}; (4) NPE_{15}; (5) NPE_{20}; (6) NPE_{30}.

Table 3
Average ethoxymer number of alkylphenol-based non-ionic surfactants determined by HPLC

Surfactant	Average ethoxymer No.	Surfactant	Average ethoxymer No.
NPE_3	2.96	NPE_{16}	18.13
NPE_4	4.44	NPE_{20}	19.38
NPE_6	6.09	NPE_{30}	29.00
NPE_7	6.64	NPE_{40}	37.20
NPE_8	8.68	OPE_2	1.79
NPE_{10}	10.22	OPE_3	2.75
NPE_{12}	12.23	OPE_6	6.17
NPE_{15}	13.11	OPE_8	8.05

3.2. Investigation of hydrophobic moiety

Reversed-phase HPLC can give information about the hydrophobic moiety of non-ionic surfactants [6–9,12]. It can be also used for the rapid identification and determination of non-ionic surfactants in technical samples [8,9,13,14], microemulsions for enhanced oil recovery [7], water and waste water samples [6,12–14] and during biodegradation tests [6,12].

We applied this method to the analysis of alkylphenol polyethoxylates. The surfactants under consideration were both homogeneously and polydisperse ethoxylates. The parent alkylphenols were also investigated.

Fig. 8 shows the chromatograms of (A) the parent nonylphenol and of (B) NPE_{30} and (C) NPE_7. The chromatogram of nonylphenol has a main peak that is preceded and succeeded by three and two smaller peaks, respectively. The chromatogram of NPE_{30} shows a similar "fingerprint" (see Fig. 8B). This "fingerprint" is typical of surfactants that show secondary peaks in normal-phase chromatography (see Figs. 3 and 4). The sample of NPE_7 is more homogeneous with respect to the nonylphenyl chain (see Fig. 8C). Here only minor impurities are associated with the main peak, which may be assigned to the *para*-isomer of nonylphenol. It is obvious that the surfactant was obtained from a carefully purified nonylphenol. Irrespective of the ethoxylation degree, all the NPE_n surfactants tested fell into these types of chromatograms.

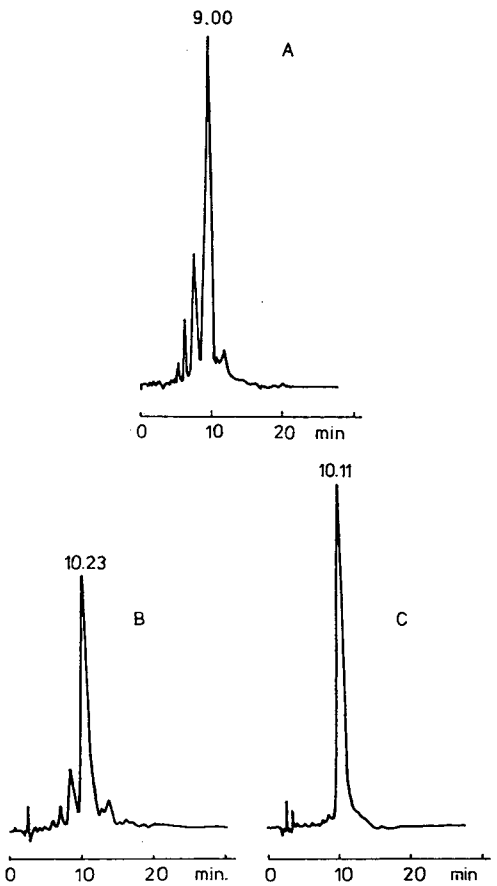

Fig. 8. Reversed-phase chromatogram of (A) nonylphenol, (B) NPE_{30} and (C) NPE_7 on an octadecylsilica column. Eluent: methanol–water (80:20, v/v).

Fig. 9 illustrates the chromatograms of (A) octylphenol and (B) OPE_6. They are simpler than those of nonylphenol and of ethoxylated nonylphenols. As only one peak is present in the sample it seems reasonable to assign it to *p*-octylphenol.

For both OPE_n and NPE_n surfactants the chromatograms show no influence of the ethoxylation degree on retention time. It is interesting that whatever the ethoxylation number, the surfactants are retained more tightly than their parent alkylphenols by the column. The phenomenon is equivalent to an increase in the

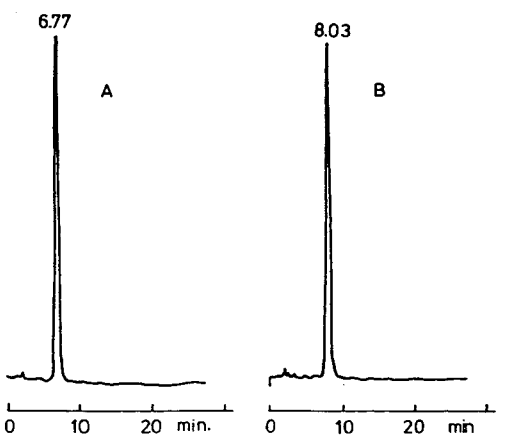

Fig. 9. Chromatogram of (A) octylphenol and (B) OPE_6. Column, octadecylsilica; eluent, methanol–water (80:20, v/v).

hydrophobic character of the alkylphenyl chains due to the presence of polyoxyethylene groups.

4. Conclusions

This work represents an attempt to use HPLC in the determination of ethoxylated octyl- and nonylphenols. The results confirm the power of this method to characterize the polyethoxylates and the possibility of detecting deficiencies appearing in synthesis.

Information about ethoxymer distribution was obtained by normal-phase chromatography on a silica column. The elution systems and the gradient programmes allow the baseline separation, identification and determination of oligomers. Surfactant samples having average ethoxylation numbers as high as 40 can be characterized in this way.

The hydrophobic moiety of the surfactants and the parent hydrophobe were investigated by reversed-phase chromatography. Differences between surfactants produced by alkylphenyl chains were found. The method can be used to distinguish non-ionic surfactants according to their alkylphenyl chains.

5. References

[1] C.R. Enyeart, in M.J. Schick (Editor), *Nonionic Surfactants*, Marcel Dekker, New York, 1967, p. 44.
[2] J. Cross, *Nonionic Surfactants: Chemical Analysis*, Marcel Dekker, New York, 1987.
[3] N. Garti, V.R. Kaufman and A. Aserin, in J. Cross (Editor), *Nonionic Surfactants: Chemical Analysis*, Marcel Dekker, New York, 1987, p. 225.
[4] M.C. Allen and D.E. Linder, *J. Am. Oil Chem. Soc.*, 58 (1981) 950.
[5] D.F. Anghel, M. Balcan, A. Voicu and M. Elian, *Rev. Chim. (Bucharest)*, 38 (1987) 148.
[6] M. Ahel and W. Geiger, *Anal. Chem.*, 57 (1985) 2584.
[7] P.L. Desbene, B. Desmazieres, J.J. Basselier and A. Desbene-Monvernay, *J. Chromatogr.*, 465 (1989) 69.
[8] C. Zhon, A. Bahr and G. Schwedt, *Anal. Chim. Acta*, 236 (1990) 273.
[9] L. Nitsche and L. Huber, *Fresenius' J. Anal. Chem.*, 345 (1993) 585.
[10] I. Zeman, J. Silha and M. Bares, *Tenside Detergents*, 23 (1986) 181.
[11] R.E.A. Escott, S.J. Brinkworth and T.A. Steedman, *J. Chromatogr.*, 282 (1983) 655.
[12] A. Marcomini, S. Capri and W. Giger, *J. Chromatogr.*, 403 (1987) 243.
[13] J. Rivera, J. Caixah, I. Espadaler, J. Romero, F. Ventura, J. Guardiola and J. Om, *Water Supply*, 7 (1989) 97.
[14] H.F. Schroeder, *Water Sci. Technol.*, 23 (1991) 339.
[15] A. Voicu, M. Elian, M. Balcan and D.F. Anghel, *Tenside, Detergents, Surfactants*, in press.
[16] R.E. Majors, *Anal. Chem.*, 45 (1973) 755.
[17] H.J. Vonk, A.J. van Wely, L.G.J. van der Ven, A.J.J. de Breet, M.E.F. Biemond, F.P.B. van der Maeden, A. Venema and W.G.B. Huysmans, in *Proceedings of the VIIth International Congress on Surface Active Substances, Moscow, 1976*, Vol. 1, Nats. Kom. SSSR Poverkhn. Akt. Veshchestvam, Moscow, 1977, p. 435.

ELSEVIER

Journal of Chromatography A, 668 (1994) 385–393

JOURNAL OF CHROMATOGRAPHY A

Improvement of a computer program for the ion chromatographic determination of some anions in natural waters

N. Gros, B. Gorenc*

Department of Chemistry and Chemical Technology, University of Ljubljana, 61000 Ljubljana, Slovenia

Abstract

A previous computer program for the optimum ion chromatographic determination of fluoride, chloride, bromide, sulphate, nitrite, nitrate and hydrogenphosphate in waters was applied to conductivity detection. In this work the abilities of a spectrophotometric detector especially for the determination of bromide, nitrite and nitrate at lower concentrations were systematically examined and incorporated into the program. The new program permits the planning of the analysis with UV detection, and also the prediction of the most appropriate detector for the determination of these three anions in different individual water samples.

1. Introduction

Computer-assisted procedures described in the literature are mostly concerned with the optimization of the eluent composition and separation [1,2], but there are also other parameters that have to be optimized for the successful determination of anions in natural waters. Our previous computer program [3] facilitates the selection of detector output ranges and permits the planning of the determination of fluoride, chloride, nitrite, bromide, nitrate, hydrogenphosphate and sulphate with conductivity detection, and the method development is thus rapid and highly efficient. The measurement of conductivity is the most general method of detection for the ion chromatographic determination of anions. In different types of natural waters (*e.g.*, precipitates, tap water, sea water, mineral waters) these anions appear in different concentrations and different concentration proportions. In many instances the great concentration differences between individual anions prevent the successful determination of all the anions, especially those present at lower concentrations. The use of an additional spectrophotometric detector which permits the detection of nitrite, bromide and nitrate often increases the number of anions that can be successfully determined in natural waters by ion chromatography.

The aim of this work was the adaptation of the previous computer program [3] for the use of two different detectors. The structure of the program was modified and two additional databases were constructed on the basis of statistically evaluated results of several systematic ion

* Corresponding author.

0021-9673/94/$07.00
SSDI 0021-9673(93)E1210-Q

chromatographic experiments with spectrophotometric detection.

2. Experimental

2.1. Apparatus and experimental conditions

All the experiments were carried out on a Dionex 4000i ion chromatographic apparatus with a Dionex variable-wavelength detector (Dionex, Sunnyvale, CA, USA). The system consisted of an AG4A guard column, an AS4A separation column and an anion micromembrane suppressor after which the detector flow cell was inserted. The injection volume was 50 μl, eluent flow-rate 2.0 ml/min, regenerant sulphuric acid concentration 12.5 mmol/l, regenerant flow-rate 2.8 ml/min and applied wavelength 190–217 nm. An SP 4290 integrator (Spectra-Physics, San Jose, CA, USA) was used.

2.2. Reagents and procedures

All solutions and eluents were prepared from analytical-reagent grade chemicals using deionized water obtained from a Milli-Q water purification system (Millipore, Bedford, MA, USA). Sodium hydrogencarbonate was purchased from Merck (Darmstadt, Germany). All other chemicals [Na_2CO_3, $NaNO_2$, $NaNO_3$, NaBr and H_2SO_4 (96%, 1.84 kg/l)] were purchased from Kemika (Zagreb, Croatia). Two stock solutions, 100 mmol/l $NaHCO_3$ and 100 mmol/l Na_2CO_3 were used to prepare the eluent, 1.7 mmol/l $NaHCO_3$–1.8 mmol/l Na_2CO_3.

2.3. Basic experiment

Chromatographic responses at different wavelengths were examined with the aim of building up an experimentally based database and with the aim of checking the maximum absorption for nitrite, bromide and nitrate. The areas and heights of chromatographic peaks of injected solutions with anion concentrations of 1 mg/l were measured for a detector output range of 0.02 absorbance at 23 whole-number wavelengths between 190 and 217 nm. The maximum absorption was obtained at 190 nm for bromide, 203 nm for nitrate and 211 nm for nitrite and the further experiments were performed at these wavelengths.

In the main experiment, six detector output ranges from 0.002 to 0.1 absorbance were examined in order to find usable calibration functions for nitrite, bromide and nitrate. Concentrations of the calibration solutions were selected in accordance with the composition of natural waters and extended from 0.008 to 4.9 mg/l for nitrite, from 0.021 to 4.5 mg/l for bromide and from 0.001 to 6.4 mg/l for nitrate. Approximately 700 experiments were done.

Calibration functions for a selected anion in a selected detector output range were obtained by measuring the areas or heights of the chromatographic peaks from at least seven calibration solutions of different concentrations. Each solution was injected at least twice. Concentrations of the calibration solutions were chosen so that the measured chromatographic peaks extended over the whole detector output range and so that the first and the last calibration solutions would serve as an indication of the anion concentrations that could be determined in a certain detector output range. All the measurements were done at the wavelength of maximum absorption. Under our experimental conditions bromide was not determinable in the lowest detector output range of 0.002 absorbance.

2.4. Statistical evaluation of results

For each set of measurements the regression line $y = a + bx$ and related statistical parameters were calculated, where y is peak area or peak height and x is the concentration of anions.

3. Results and discussion

The improvement of the previous computer program [3] consisted of three stages. In the first stage, two additional experimentally obtained databases connected with UV detection were constructed. Second, the structure of the pro-

gram was adapted to the use of a UV detector. Finally, three new blocks of computer program were added. The operation of the modified program is illustrated on two examples with different natural water samples.

3.1. Computer-assisted procedures

The structure of the first database for a UV detector is similar to existing database for a conductivity detector [3]. It includes eleven statistical parameters for each calibration graph ($y = a + bx$) as follows: n = number of calibration points; x_1 = the lowest concentration of calibration solution; x_n = the highest concentration of calibration solution; $\bar{x}$ = mean of the x values (concentrations); $\bar{y}$ = mean of the y values (peak areas or heights); a = intercept; s_a = standard deviation of the intercept; b = slope; s_b = standard deviation of the slope; r = correlation coefficient; and $s_{y/x}$ = standard error of the estimate. The total number of data points is 374.

The second new database consists of responses of the UV detector for nitrite, bromide and nitrate at different wavelengths between 190 and 217 nm. Variables $y\lambda$ and $y\lambda_{max}$ were introduced. This database was constructed in order to allow the use of the first database for analyses at wavelengths that differ from those with maximum absorption. The reason is that in reality the measurements for nitrite, bromide and nitrate are not always done at the wavelengths of the maximum absorption [4,5] and that different workers quote different λ_{max} values [6,7].

A database with statistical F factors for different degrees of freedom and a 0.05 significance level was also added [8].

The structure of the improved program is shown in Fig. 1. The four real starting positions (four triangles in Fig. 1), known peak area, known peak height, approximately known concentration or the prior choice of a certain detector output range remained the same. There are three new blocks, H, I and J. The main functions of blocks A, B, C, D, E, F and G were described previously [3]. No global changes were made to these blocks, but their detailed structure and also some data inputs shown in Figs. 2–5 were modified. The changes are orientated toward the

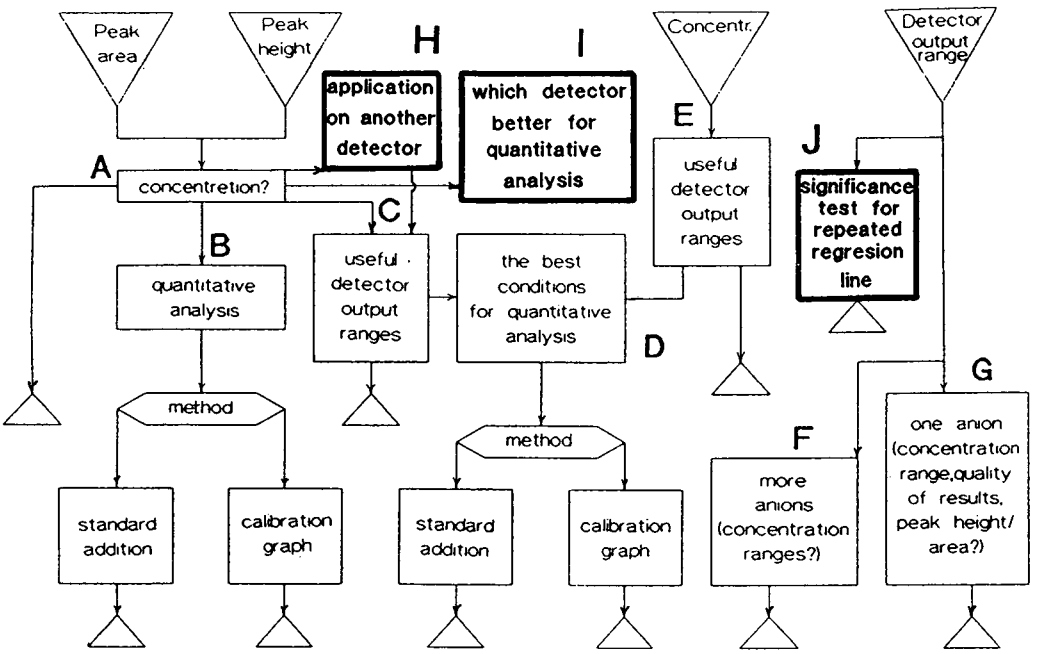

Fig. 1. The main structure of the improved computer program.

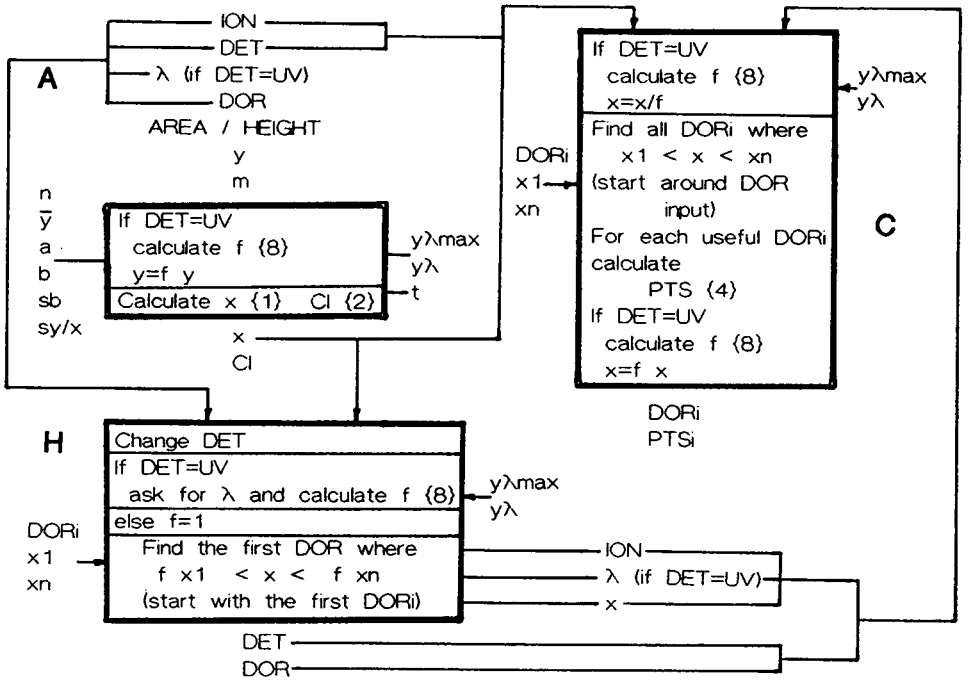

Fig. 2. The main operations, data inputs and data outputs for blocks A, C and H.

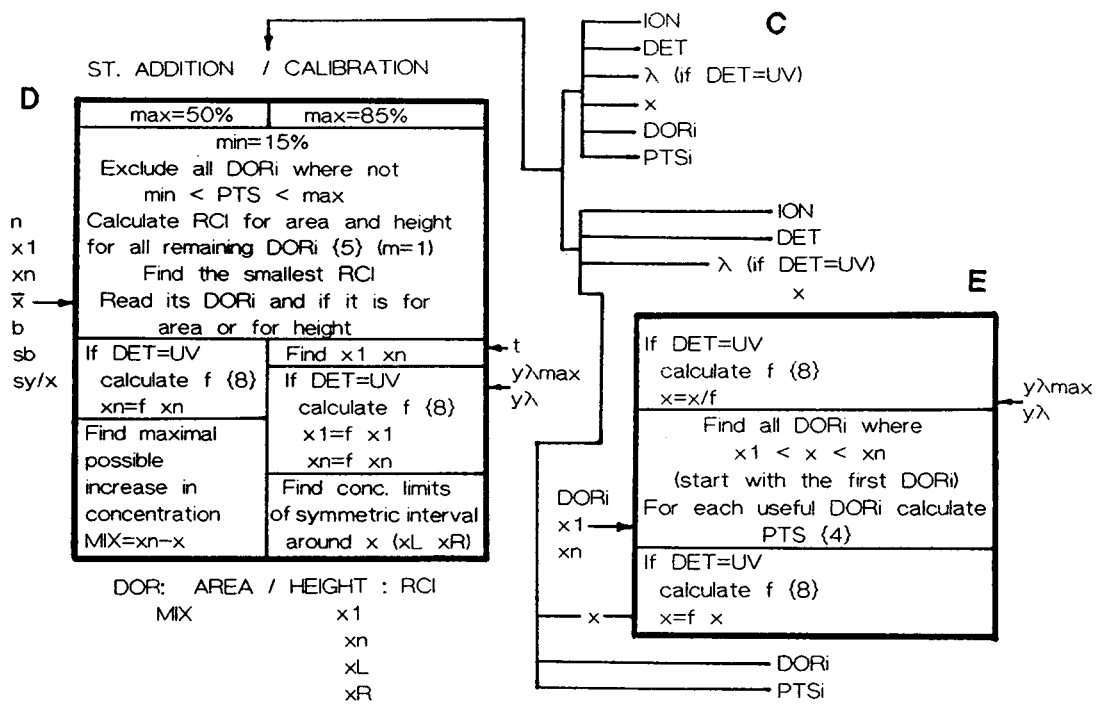

Fig. 3. The main operations, data inputs and data outputs for blocks D and E.

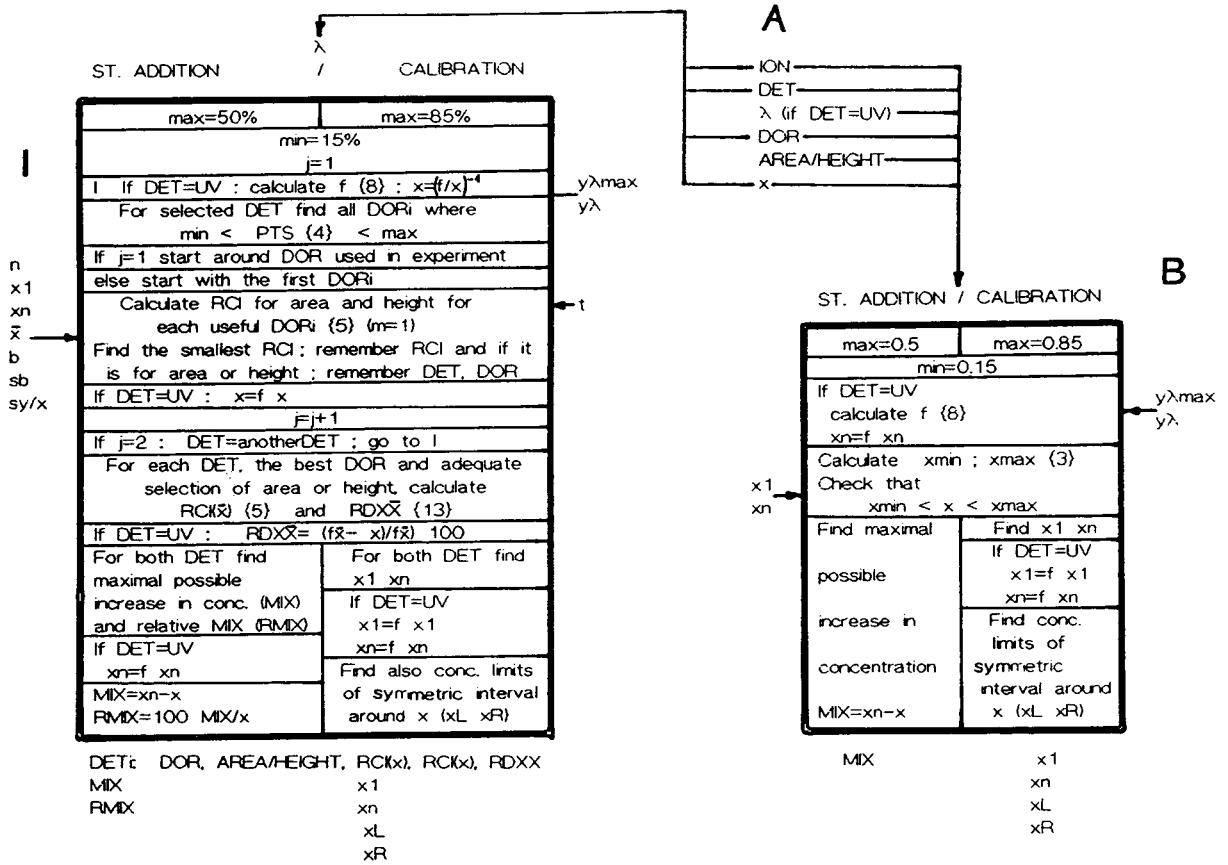

Fig. 4. The main operations, data inputs and data outputs for blocks B and I.

use of another detector also at wavelengths that differ from λ_{max}. The additional variables DET, λ, $y\lambda_{max}$ and correction factor f were used. Relative confidence intervals (RCI) for UV detection were also calculated for λ_{max}.

For understanding the detailed structure of the program, general principles have to be described. Each block is represented by a rectangle. All the data necessary for the operation of the individual blocks are shown in figures. Data from the main two files for UV and conductivity detection are on the left-hand side of the rectangle. The data from the file that allows the corrections of results if the wavelength used differs from λ_{max}, the file with t factors and the file with F factors are on the right-hand side. The user must input the data at the top, and output data are found at the bottom. The main sequences of the operations are described on each rectangle. The numbers of necessary mathematical relationships are stated in brackets.

The list of mathematical relationships used by the program is as follows:

$$\{1\} \quad x = \frac{y - a}{b}$$

$$\{2\} \quad \mathrm{CI} = \frac{s_{y/x} t}{b} \left[\frac{1}{n} + \frac{1}{m} + \frac{(y - \bar{y})^2 s_b^2}{b^2 s_{y/x}^2} \right]^{1/2}$$

$$\{3\} \quad x \text{ min} = \min x_n, \; x \text{ max} = \max x_n$$

$$\{4\} \quad \mathrm{PTS} = \frac{x}{x_n} \cdot 100$$

$$\{5\} \quad \mathrm{RCI} = \frac{s_{y/x} t \cdot 100}{xb} \left[\frac{1}{n} + \frac{1}{m} + \frac{(x - \bar{x})^2 s_b^2}{s_{y/x}^2} \right]^{1/2}$$

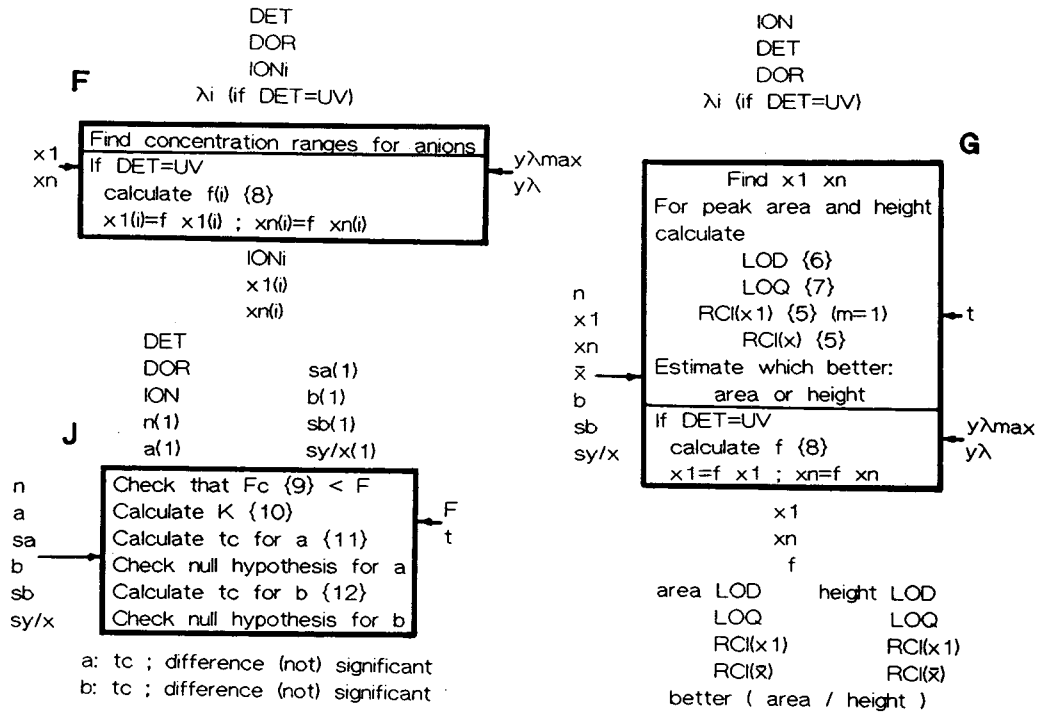

Fig. 5. The main operations, data inputs and data outputs for blocks F, G and J.

$$\{6\} \quad \mathrm{LOD} = \frac{3s_{y/x}}{b}$$

$$\{7\} \quad \mathrm{LOQ} = \frac{10s_{y/x}}{b}$$

$$\{8\} \quad f = \frac{y\lambda_{\max}}{y\lambda}$$

$$\{9\} \quad \mathrm{Fc} = \left(\frac{\text{greater } s_{y/x}}{\text{smaller } s_{y/x}}\right)^2$$

$$\{10\} \quad K = \left[\frac{s^2_{y/x}(n-2) + s^2_{y/x_1}(n_1-2)}{n+n_1-4}\right]^{1/2}$$

$$\{11\} \quad tc = \frac{|a-a_1|}{K\left(\frac{s^2_\alpha}{s^2_{y/x}} + \frac{s^2_{\alpha_1}}{s^2_{y/x_1}}\right)^{1/2}}$$

$$\{12\} \quad tc = \frac{|b-b_1|}{K\left(\frac{s^2_b}{s^2_{y/x}} + \frac{s^2_{b_1}}{s^2_{y/x_1}}\right)^{1/2}}$$

$$\{13\} \quad \mathrm{RDX\bar{X}} = \left|\frac{\bar{x}-x}{\bar{x}}\right| \cdot 100$$

The meanings of the symbols that appear in the above mathematical relationships and in the figures are as follows:

CI = confidence interval;
DET = detector;
DOR = detector output range;
f = correction factor;
Fc = calculated F factor
ION = anion;
LOD = limit of detection;
LOQ = limit of quantification;
m = number of repeated measurements;
MIX = maximum increase in concentration;
PTS = % of total scale on which chromatographic peak appears;
RCI = relative confidence interval;
RDX$\bar{X}$ = relative deviation of x from $\bar{x}$;
RMIX = relative MIX;
tc = calculated t factor

x_L = lower concentration limit of symmetric concentration interval around x;

x_R = upper concentration limit of symmetric concentration interval around x;

$y\lambda$ = response of UV detector for selected anion at selected λ;

$y\lambda_{max}$ = response of UV detector for selected anion at λ_{max}.

The subscript i shows that there are more data of the same type.

The first newly introduced block H is a sort of interface. It is useful when a preliminary experiment was carried out with one detector. The estimation of concentration was made on the basis of this experiment. However, it is evident that this detector does not represent a good solution and we would like to carry out the optimization procedure (blocks C and D) with another detector. Block H changes the value of the variable DET and asks for λ if the detector is a UV type. It finds the first useful detector output range DOR, which is essential for the operation of block C.

With the introduction of block H and with the changes in blocks A–G, the program became suitable for the predictions and planning of the analysis with spectrophotometric detection. However, block I allows the comparison of the abilities of both detectors for the determination of bromide, nitrite or nitrate in a specific water sample (Fig. 4). It also helps in planning the quantitative analysis for both detectors with the method of standard additions (MIX, RMIX) or with a calibration graph (x_1, x_n, x_L, x_R). It predicts the best detector output range and the best conditions (the measurement of area or height) for each detector. The quality criterion is the relative confidence interval (RCI) calculated for the estimated concentration. For an easier and more appropriate decision for one of the two detectors, the program reports some other parameters. The concentration ranges for suggested detector output ranges are not the same for both detectors. Therefore, RCI for $\bar{x}$ are calculated. The relative deviation of estimated concentration from $\bar{x}$ is also important. The new more comparable parameter RMIX was introduced.

Block J offers the possibility of occasional checking of the agreement of repeated calibration functions with data from databases. The significance test for a and b has been described [9]. The equations were modified in such a manner that they permit the calculations with parameters that are saved in computer databases.

3.2. Examples of application

The operation of the modified program is illustrated on examples with different natural water samples. In the first instance we had determined the concentration of bromide in drinking water. The determination of bromide is not always possible with conductivity detection. Therefore, we decided to use a UV detector. The wavelength was 190 nm. A preliminary experiment was carried out at the lowest detector output range (0.005 absorbance). The concentration was estimated from the measured peak area with the aid of block A. The results were $x = 0.054$ mg/l and CI = 0.012 mg/l.

In the next stage the selection of DOR was checked. With block C all useful detector output ranges with related percentages of the total scale on which the chromatographic peaks appear were found. These are 0.005 absorbance (PTS = 30.0%), 0.01 absorbance (PTS = 13.6%) and 0.02 absorbance (PTS = 6.0%). Block D was selected for the planning of quantitative analysis under the optimum experimental conditions. We decided to use the method of calibration function. The computer suggested the DOR 0.005 absorbance and the measurement of height which has a lower confidence interval. The reported value of RCI was 22.7%. Other predictions were $x_1 = 0.021$ mg/l, $x_n = 0.190$ mg/l, $x_L = 0.021$ mg/l and $x_R = 0.087$ mg/l. Quantitative analysis was carried out under predicted conditions. The determined concentration was 0.057 mg/l and it shows very good agreement with the computer estimation (0.054 mg/l).

The prediction that the measurement of peak height offers better results was checked. We calculated RCI for the measurement of peak area and peak height. The former value was 29.8% and the latter 17.2%. The conclusion is the same as in the prediction. This example illustrates the operation of blocks A, C and D which were adapted for the use of a UV detector.

We also wanted to check if the calibration functions (area–concentration, height–concentration) with four calibration points, which was used for the determination of bromide in drinking water, differed significantly from those in the database. Block J was used. For the relationship between peak area and concentration the values of *tc* were 0.18 for *a* and 0.62 for *b*. The related parameters for the measurements of peak height were 1.27 and 0.83. No one value exceeded the critical value of 2.31 for the *t*-test ($p = 0.05$).

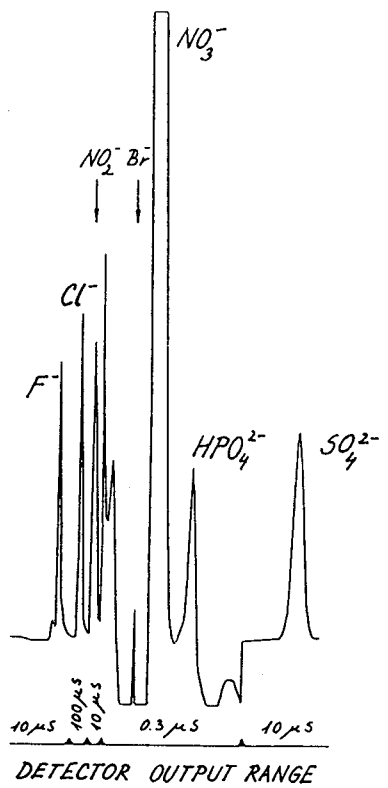

Fig. 6. Chromatogram of mineral water with conductivity detector.

The program reported that there is no significance difference within each pair of calibration functions.

Figs. 6 and 7 show chromatograms of mineral water with conductivity and UV detection, respectively. Also in this instance bromide cannot be successfully determined with a conductivity detector; the baseline is unstable and out of range. In this sample of mineral water the determination of nitrite is possible with both detectors. We would like to know which is better in this situation; block I can help. The concentration estimated with block A was 1.8 mg/l, λ was equal to λ_{max} and the method of standard additions was selected. The report of block I is represented in Table 1.

The program suggests the measurement of peak height with the conductivity detector and peak area with the UV detector. Conductivity detection also permits a greater increase in concentration. Therefore, we decided to use the conductivity detector. We prepared five solutions with different standard additions. The determined concentration of nitrite was 2.8 mg/l. To

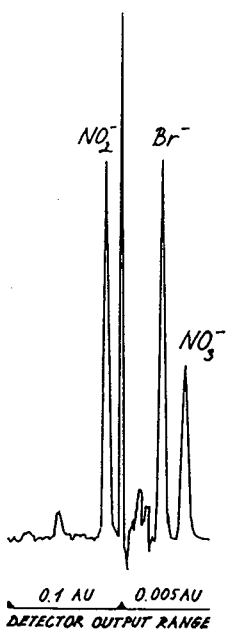

Fig. 7. Chromatogram of the same mineral water as in Fig. 6 with UV spectrophotometric detector.

Table 1
Report of the computer program when block I was used

Parameter	Detector	
	Conductivity	UV
DOR	10 μS	0.1 AU
Area/height	Height	Area
RCI(x)	9.1%	22.3%
RCI($\bar{x}$)	8.9%	22.0%
RDX$\bar{X}$	46.5%	29.3%
MIX	4.6 mg/l	3.1 mg/l
RMIX	256%	172%

check the prediction of the more appropriate detector, the experiment was repeated with the UV detector, and confirmed the prediction. The relative confidence intervals obtained were 62.0% for peak height and 97.7% for peak area.

This example with mineral water also illustrates that the use of the improved program allows more successful planning and more complete analysis of the anions in natural waters. Fig. 6 shows appropriate chromatographic peaks for the determination of fluoride, chloride, nitrite, hydrogenphosphate and sulphate. With the assistance of block B appropriate standard additions were calculated. The quantitative analysis was successful under the predicted conditions and the determined concentrations were 0.66 mg/l for fluoride, 20.9 mg/l for chloride, 0.50 mg/l for hydrogenphosphate and 6.74 mg/l for sulphate.

Determination of nitrate with conductivity detection is possible but not simultaneously with hydrogenphosphate. Detection of nitrate in a more appropriate detector output range requires the switching of the detector output range between the two anions, which results in an unstable baseline, making the successful determination of hydrogenphosphate impossible. The use of UV detection for the determination of nitrate is a very economical solution. Nitrate can be determined at the same time as bromide, for which UV detection represents the only possibility (Figs. 6 and 7).

In the accordance with the predictions of block B, for the determination of nitrate in the detector output range 0.005 absorbance and with the calibration graph method, calibration solutions were prepared in the concentration range 2.4–15.0 mg/l. Bromide was determined in the same detector output range with the method of standard additions. The quantitative analysis was successful for both anions; the results were 6.99 and 0.20 mg/l.

With the combination of both detectors all seven anions were successfully determined. With the use of the improved program the planning of quantitative analysis was more rapid and easier.

4. Conclusions

The improvement of the computer program extends its usability to the spectrophotometric detector and allows the selection of the most appropriate detector for many different water samples. This new program covers different real situations more completely and more successfully.

5. References

[1] P.R. Haddad and C.E. Cowie, *J. Chromatogr.*, 303 (1984) 321.
[2] Q. Xiauren, X. Chong-Yu and W. Baeyens, *J. Chromatogr.*, 640 (1993) 3.
[3] N. Gros and B. Gorenc, *Chromatographia*, 36 (1993) 251.
[4] S. Rokushika, K. Kihara, P.F. Subosa and W.X. Leng, *J. Chromatogr.*, 514 (1990) 355.
[5] J.K. Thomsen and R.P. Cox, *J. Chromatogr.*, 512 (1990) 53.
[6] D. Huiru, J. Meiyu and Z. Qing, *Anal. Lett.*, 24 (1991) 305.
[7] D.L. Milles and C. Espejo, *Analyst*, 102 (1977) 104.
[8] J.C. Miller and J.N. Miller, *Statistics for Analytical Chemistry*, Wiley, New York, 1988, p. 217.
[9] U. Hillebrand, *GIT Fachz. Lab.*, 9 (1991) 1001.

ELSEVIER

Journal of Chromatography A, 668 (1994) 395–402

JOURNAL OF CHROMATOGRAPHY A

Retention behaviour of barbituric acid derivatives on a β-cyclodextrin polymer-coated silica column

Esther Forgács*, Tibor Cserháti

Central Research Institute for Chemistry, Hungarian Academy of Sciences, P.O. Box 17, H-1525 Budapest, Hungary

Abstract

The retentions of 45 barbituric acid derivatives were determined on a β-cyclodextrin (β-CD) polymer-coated silica column using unbuffered methanol–water, ethanol–water, acetonitrile–water, dioxane–water and tetrahydrofuran–water eluent mixtures. Stepwise regression analysis indicated that the retention of barbituric acid derivatives is mainly governed by the lipophilicity, molar refractivity (related to the solute volume) and to a lesser extent by the electronic parameters of substituents in each eluent system, suggesting the significant importance of these physico-chemical parameters in the determination of retention behaviour. The spectral map technique indicated that the solvent strength and selectivity of organic modifiers on a β-CD polymer-coated silica column depended on their bulkiness and electronic parameters, respectively.

1. Introduction

Cyclodextrins (CDs) can form inclusion complexes with a wide variety of compounds [1–3]. As the complex formation modifies the retention characteristics of the guest molecule, CDs have found growing acceptance and application in many fields of chromatography and electrophoresis (gas chromatography, thin-layer chromatography, high-performance liquid chromatography, isotachophoresis and electrophoresis). Both polar [4] and non-polar [5] cyclodextrin derivatives have been used in capillary gas chromatography for enantiomer separations. Reversed-phase thin-layer chromatography has been used to determine the inclusion complex stability of several chlorophenol derivatives [6]. The effective mobilities of various inorganic ions such as iodide, periodate and tetrathionate decreased with increasing concentration of α-, β- and γ-CDs in the isotachophoretic separation of these ions [7]. The application of α- and β-CDs in the capillary electrophoresis of peptides improved the separation [8]. CDs have been used extensively in HPLC either as eluent additives or covalently bonded to a silica surface. CDs added to the eluent modify the retention of aliphatic alcohols [9], drugs [10] and various steroids [11]. The application of a covalently bonded β-CD column for semi-preparative separations has also been reported [12]. Separations on silica columns with covalently bonded CDs are generally carried out in aqueous eluents similarly to the separations on traditional reversed-phase columns; CD derivatives for application to the adsorption separation of enantiomers have also been synthetized [13].

The objectives of these investigations were to determine the retentions of 45 barbituric acid derivatives on a β-CD polymer-coated silica column (β-CD column) using various eluents systems, to evaluate the retention data by multi-

* Corresponding author.

0021-9673/94/$07.00
SSDI 0021-9673(93)E1038-2

variate statistical methods, to find the relationship between retention characteristics and physico-chemical parameters of the barbituric acid derivatives and to determine the influence of organic modifiers on the retention behaviour of barbiturates on a β-CD column.

2. Experimental

Monomeric β-CD polymerized on the surface of silica particles without binding the polymer covalently to the silanol groups, using a slight modification of the preparation method published recently [14]. A column of 250 × 4 mm I.D. was filled with the β-CD polymer-coated silica. The HPLC system consisted of a Liquopump Model 312 pump (LaborMIM, Budapest, Hungary), a Cecil Instruments (Cambridge, UK) CE-212 variable-wavelenth UV detector, a Valco (Houston, TX, USA) injector with a 20-μl sample loop and a Waters Model 740 integrator (Waters–Millipore, Milford, MA, USA). The flow-rate was 0.6 ml/min and the detection wavelength was set at 240 nm. The eluents were methanol–water, acetonitrile–water, ethanol–water, dioxane–water and tetrahydrofuran–water with 50% (v/v) organic modifier concentrations. Buffers were not used.

The structures of the barbituric acid derivatives are shown in Table 1. The barbituric acids were dissolved in each instance in the eluent at a concentration of 0.05 mg/ml. The dead volume of the column was determined by injecting sodium nitrate solution. Each determination was run in quadruplicate. The capacity factors (log k') and asymmetry factors were calculated separately for each barbituric acid derivative in each eluent system [15].

2.1. Determination of the relationship between the physico-chemical parameters of barbituric acid derivatives and their retention characteristics

To find the physico-chemical parameters of solutes that significantly influence their retention behaviour, stepwise regression analysis [16] was applied. In the common multivariate regression analysis the presence of independent variables that exert no significant influence on the dependent variable lessens the significance level of those independent variables which have a significant influence on the dependent variables. To overcome this difficulty, the stepwise regression analysis automatically eliminates from the selected equation the insignificant independent variables. In our calculations the dependent variables were always the logarithm of capacity factors and the independent variables were the different physico-chemical parameters of the barbituric acid derivatives. The acceptance level for the individual independent variables was set to the 95% significance level. Stepwise regression analysis was carried out five times, the log k' values determined in the five eluent systems being separately the dependent variables. The physico-chemical parameters included in the calculation were the following: π, the Hansch–Fujita substituent constant characterizing hydrophobicity; H-AC and H-Do, indicator variables for proton acceptor and proton donor properties, respectively; M-RE, molar refractivity; F and R, the Swain–Lupton electronic parameters characterizing the inductive and resonance effect, respectively; σ, Hammett's constant, characterizing the electron-withdrawing power of the substituent; Es, Taft's constant, characterizing steric effects of the substituent; and B_1 and B_4, Sterimol width parameters (determined by the distance of the substituents at their maximum point perpendicular to attachment bond axis).

2.2. Determination of the influence of organic modifiers on the retention behaviour of barbiturates on a β-CD column

To separate solvent strength and solvent selectivity, the "spectral map" technique [17,18] was applied. The data matrix consisted log k' values of barbituric acid derivatives determined in five eluent systems. Calculations were carried out twice, the eluent systems and barbituric acid derivatives being the variables and observations, respectively. The potency values of the eluent systems and solutes were considered as the solvent strength and retention capacity, respectively. To visualize the spectral characteristics of

Table 1
Structure of barbituric acid derivatives

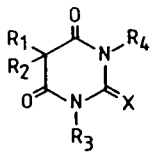

No.	R_1	R_2	R_3	R_4	X
1	H	H	H	H	O
2	Methyl	Methyl	H	H	O
3	3-Pentyl	Methyl	H	H	O
4	Methyl	1-Methylpentyl	H	H	O
5	Ethyl	Ethyl	H	H	O
6	Ethyl	1-Methylbutyl	H	H	O
7	Ethyl	3-Methylbutyl	H	H	O
8	Ethyl	1-Methylpropyl	H	H	O
9	Ethyl	*n*-Pentyl	H	H	O
10	Butyl	1-Methylpropyl	H	H	O
11	Butyl	1-Methylbutyl	H	H	O
12	Butyl	3-Methylbutyl	H	H	O
13	Ethyl	*n*-Octyl	H	H	O
14	Ethyl	3-Dimethyloctyl	H	H	O
15	Allyl	Isopropyl	H	H	O
16	Allyl	Isobutyl	H	H	O
17	Allyl	1-Methylbutyl	H	H	O
18	Allyl	1-Methylcyclohexenyl	H	H	O
19	Allyl	2-Cyclopentyl	H	H	O
20	Ethyl	1-Cyclohexenyl	H	H	O
21	Ethyl	Ethyl	H	H	S
22	Ethyl	1-Methylbutyl	H	H	S
23	Allyl	1-Methylbutyl	H	H	S
24	Ethyl	1,3-Dimethylbutyl	H	H	S
25	Ethyl	Phenyl	H	H	O
26	Ethyl	Ethyl	Phenyl	H	O
27	Ethyl	Ethyl	Benzoyl	H	O
28	Ethyl	Ethyl	Benzoyl	Benzoyl	O
29	Ethyl	Ethyl	*p*-Cl-benzoyl	H	O
30	Ethyl	Ethyl	*p*-NO_2-benzoyl	H	O
31	Ethyl	Ethyl	*p*-NO_2-benzoyl	*p*-NO_2-benzoyl	O
32	Ethyl	Phenyl	Phenyl	H	O
33	Ethyl	Phenyl	Benzoyl	Methyl	O
34	Ethyl	Phenyl	*p*-NH_2-benzoyl	Methyl	O
35	Ethyl	Phenyl	*o*-NO_2-benzoyl	Methyl	O
36	Ethyl	Phenyl	*p*-NO_2-benzoyl	Methyl	O
37	Ethyl	Phenyl	*m*-NO_2-benzoyl	Methyl	O
38	Ethyl	Ethyl	*p*-NO_2-benzoyl	Methyl	O
39	Ethyl	Ethyl	Benzoyl	Methyl	O
40	Methyl	Phenyl	Benzoyl	H	O
41	Methyl	Phenyl	Benzoyl	Methyl	O
42	Ethyl	Phenyl	Benzoyl	H	O
43	Ethyl	Methyl	H	H	O
44	Ethyl	Propyl	H	H	O
45	Methyl	Methyl	Methyl	H	O

Barbituric acid derivatives were synthesized by Professor J. Bojarski and co-workers (Department of Organic Chemistry, Academy of Medicine, Krakow, Poland).

the eluents and solutes, two-dimensional spectral maps [19] of barbituric acid derivatives and eluent systems were separately calculated.

The relationship between the physico-chemical parameters of the organic modifiers and their solvent strength was calculated by stepwise regression analysis. Stepwise regression analysis was carried out three times, as follows. (A) The independent variables were the various physico-chemical parameters of organic modifiers (π, H-Ac, H-Do, M-RE, F, R, σ, Es, B_1 and B_4 and the ratio B_4/M-RE). The inclusion of the combined variable B_4/M-RE was motivated by the assumption that the surface/volume ratio may influence the complex formation of solutes with the CD cavities on the support surface, resulting in a significant impact on the retention. The dependent variable was the solvent strength of the organic modifiers (potency values determined with the "spectral map" technique). (B, C) The independent variables were as in calculation (A) and the dependent variables were (B) the first and (C) the second coordinates of the two-dimensional spectral map of organic modifiers. The other parameters for the calculations were the same as in Section 2.1.

3. Results and discussion

The capacity factors and asymmetry factors of the barbituric acid derivatives are given in Table 2. Blank entries in Table 2 indicate that the corresponding barbiturate either eluted near the dead volume or its retention time was greater than 30 min. Both the quality of the organic modifier and the character of the substituents of the barbiturates considerably influenced the capacity factors, suggesting that the β-CD polymer column can be successfully used for the separation of these type of solutes. In each instance the asymmetry factors were near 1, that is, the tailing of peaks on this column was negligible. This suggests that the covering of the polar silica surface by the β-CD had been carried out satisfactorily.

3.1. Influence of physico-chemical parameters of barbituric acid derivatives on their retention on a β-CD column

The parameters of the correlations describing the relationships between retention parameters and physico-chemical characteristics of barbituric acid derivatives are given in Table 3. The equations fit the experimental data well, the significance level being over 99% (see F values). The physico-chemical parameters of barbituric acid derivatives explain 15–61% of the total variance, indicating that other parameters not included in the calculations may have a considerable influence on the retention.

The lipophilicity values and steric parameters of substituents have the greatest impact on the retention characteristics of barbiturates on the β-CD polymer-coated silica column (see $b_{\%}$ values in Table 3). The preponderant role of solute lipophilicity and steric parameters can be explained by the assumption that the retention of barbiturates on the β-CD support is influenced by the following interactions:

(1) Interactions of solutes with the cyclodextrin cavity: it is generally accepted that these interactions are determined by both the lipophilicity and the size of the guest molecules. The steric parameters define the capacity of the guest molecule to enter the cyclodextrin cavity and the lipophylicity of the guest molecule determines the strength of interaction with the hydrophobic inner surface of the CD cavity. The results in Table 3 demonstrate the importance of these interactions.

(2) Polar interactions between solutes and the polar groups on the β-CD polymer surface or between the polar substructures of the solutes and free silanol groups not covered by the β-CD polymer: these interactions are probably influenced by the electron-withdrawing and electron-donating properties of the polar substructures of the barbituric acid derivatives; however, as seen in Table 2, they are of secondary importance.

We emphasize that the interactions mentioned above can take place not only between the support and solutes but also between the support

Table 2
Log k' values and asymmetry factors (AS) obtained with (I) methanol–water, (II) acetonitrile–water, (III) ethanol–water, (IV) dioxane–water and (V) tetrahydrofuran–water as mobile phases

Compound[a]	I		II		III		IV		V	
	Log k'	AS	Log k'	AS	Log k'	AS	Log k'	AS	Log k'	AS
1	−0.37	1.1	–	–	−0.73	1.2	−0.23	1.1	−0.36	1.2
2	−0.46	1.2	–	–	–	–	−0.42	1.3	−0.37	1.1
3	0.69	1.5	0.02	1.3	0.18	1.2	1.1	1.2	−0.40	1.2
4	0.28	1.3	−0.34	1.2	−0.13	1.2	−0.23	1.3	−0.26	1.2
5	−0.11	1.2	−0.50	1.1	−0.37	1.4	−0.30	1.2	−0.42	1.2
6	0.32	1.1	0.55	1.1	0.01	1.5	−0.31	1.2	−0.29	1.1
7	0.29	1.2	−0.09	1.2	−0.07	1.1	−0.35	1.1	−0.31	1.2
8	0.22	1.2	−0.23	1.0	−0.04	1.2	−0.27	1.2	0.40	1.3
9	0.31	1.2	−0.21	1.1	−0.02	1.1	−0.31	1.2	−0.28	1.1
10	0.33	1.1	−0.17	1.1	0.07	1.1	−0.14	1.1	−0.20	1.2
11	0.34	1.2	−0.17	1.3	0.08	1.1	−0.12	1.2	−0.48	1.3
12	0.45	1.3	−0.14	1.3	0.14	1.2	−0.13	1.24	−0.49	1.5
13	0.67	1.1	0.01	1.2	0.26	1.1	0.05	1.1	−0.39	1.3
14	–	–	0.14	1.1	0.32	1.3	−0.03	1.1	−0.25	1.4
15	−0.40	1.0	−0.33	1.2	−0.18	1.1	−0.12	1.2	−0.14	1.2
16	0.06	1.1	−0.33	1.1	−0.18	1.1	−0.12	1.1	−0.24	1.1
17	0.31	1.1	−0.19	1.2	−0.01	1.2	−0.27	1.2	−0.15	1.1
18	0.14	1.2	−0.39	1.1	−0.18	1.2	−0.20	1.1	−0.26	1.2
19	0.47	1.1	−0.08	1.3	0.10	1.1	−0.34	1.2	−0.55	1.3
20	0.39	1.1	−0.10	1.2	0.01	1.0	−0.40	1.2	−0.61	1.1
21	0.20	1.0	−0.15	1.1	0.01	1.0	−0.31	1.0	−0.44	1.1
22	0.61	1.1	0.10	1.0	0.31	1.0	0.01	1.1	−0.29	1.0
23	0.68	1.0	0.12	1.1	0.40	1.1	0.06	1.2	−0.27	1.2
24	0.40	1.1	−0.14	1.2	0.01	1.0	−0.33	1.0	−0.56	1.1
25	0.47	1.1	−0.11	1.1	0.17	1.2	−0.20	1.3	−0.58	1.2
26	0.00	1.1	−0.30	1.1	−0.20	1.2	−0.19	1.2	−0.63	1.1
27	0.42	1.1	−0.25	1.0	0.06	1.0	−0.23	1.0	−0.56	1.0
28	–	–	0.06	1.1	0.61	1.3	0.16	1.1	−0.40	1.2
29	0.60	1.1	0.06	1.2	0.16	1.0	0.61	1.0	−0.40	1.2
30	0.57	1.1	−0.20	1.1	0.18	1.1	0.00	1.1	0.02	1.1
31	0.80	1.2	0.28	1.1	0.14	1.1	0.00	1.0	0.02	1.2
32	−0.09	1.0	−0.11	1.2	0.42	1.3	0.01	1.1	0.40	1.2
33	0.87	1.1	0.77	1.0	0.44	1.0	0.01	1.1	−0.39	1.0
34	0.98	1.0	−0.07	1.0	0.55	1.0	−0.55	1.1	−0.33	1.2
35	0.85	1.1	−0.12	1.1	−0.12	1.1	0.39	1.0	0.06	1.0
36	1.02	1.1	−0.08	1.0	0.69	1.2	−0.13	1.2	−0.42	1.1
37	0.37	1.2	−0.20	1.2	0.10	1.1	−0.13	1.1	−0.42	1.1
38	0.50	1.1	−0.28	1.2	0.20	1.0	−0.07	1.0	−0.33	1.3
39	0.40	1.1	−0.34	1.1	0.00	1.2	−0.18	1.2	−0.40	1.2
40	0.42	1.2	−0.36	1.2	0.23	1.1	−0.17	1.2	−0.59	1.1
41	−0.07	1.1	−0.18	1.3	0.39	1.1	−0.01	1.1	−0.36	1.1
42	0.88	1.1	−0.01	1.1	0.39	1.2	−0.01	1.1	−0.36	1.2
43	−0.34	1.1	−0.01	1.2	−0.54	1.1	−0.02	1.1	−0.36	1.1
44	−0.20	1.1	−0.55	1.3	−0.43	1.2	−0.71	1.0	−0.77	1.1
45	−0.20	1.0	−0.55	1.1	−0.43	1.1	0.73	1.1	0.74	1.2

Concentrations of organic modifiers were 50% (v/v) in each instance.
[a] See Table 1.

Table 3
Effects of various physico-chemical parameters of barbituric acid derivatives on their retention behaviour on a β-CD column: results of stepwise regression analysis (number of samples = 45): $\log k' = a + b_1x_1 + b_2x_2$

Parameter[a]	Eluent[b]				
	I	II	III	IV	V
a	−0.47	0.98	−0.71	−0.62	−0.69
b_1	0.02	0.19	0.17	0.05	0.06
x_1	M-RE	$\Sigma\pi$	$\Sigma\pi$	$\Sigma\pi$	$\Sigma\pi$
S_{b2}	0.01	0.04	0.903	0.03	0.01
$b_{1\%}$	71.27	–	52.16	34.73	–
b_2	−0.29	–	0.31	0.01	–
x_2	σ	–	H-AC	M-RE	–
S_{b2}	0.12	–	0.05	0.01	–
$b_{2\%}$	28.72	–	47.84	65.24	–
r^2	0.5321	0.3060	0.6127	0.4569	0.1421
F	21.61	18.08	31.64	16.83	6.79

[a] a = Intercept; b_1 and b_2 = regression coefficients; s_{b1} and s_{b2} = standard deviations of regression coefficients b_1 and b_2; $b_{1\%}$ and $b_{2\%}$ = path coefficients (dimensionless numbers indicating the relative impact of the individual independent variables on the dependent variable); r^2 = coefficient of determination (indicates the ratio of variance explained by the independent variables); F = calculated value of the Fisher significance test.

[b] Eluent (1:1, v/v): I = methanol–water; II = acetonitrile–water; III = ethanol–water; IV = dioxane–water; V = tetrahydrofuran–water.

and the molecules of organic modifiers, which explains the slightly different character of the equations in Table 2. It can be assumed that the retention strength and selectivity on the β-CD polymer column are the result of the interplay of the various interactions discussed above.

3.2. *Influence of organic modifiers on the retention behaviour of a β-CD column*

The selectivity map of the barbituric acid derivatives is shown in Fig. 1. When we take into consideration the retention behaviour of barbiturates simultaneously in all five eluent systems, the solutes that have phenyl (32), benzoyl (33), *o*-nitrobenzoyl (35) and *p*-nitrobenzoyl (30) substituents at position R_3 differ in their retention characteristics from the other barbituric acid derivatives. This result indicates that these substituents have a considerable effect in each eluent system. The fact that the lipophilicity and molar refractivity (related to the bulkiness) of these substituents are high explains their marked role in the retention behaviour, and supports the conclusions drawn from data in Table 3.

The parameters of the equations describing the influence of organic modifiers on the retention behaviour of β-CD columns are given in Table 4. The equations fit the experimental data well, the significance level being over 99%. The physico-chemical parameters of the organic modifiers explain 83–90% of the total variance, indicating the good fit of the equations to the experimental values. The solvent strength of the organic modifiers is determined by the surface/volume ratio (see Eq. 1 in Table 4). As the inclusion complex formation depends markedly on the capacity of a guest molecule to enter the CD cavity (that is, on the steric parameters), this result suggests the involvement of inclusion complex formation in the retention mechanism of the β-DE columns. The selectivity of organic modifiers depends on their electronic parameters (σ) and molar refractivity (bulkines) (see Eqs. 2 and 3 in Table 4). These results emphasize again the impact of polar interactions and of inclusion complex formation between the molecules of organic modifiers and the surface of β-CD polymer-coated silica.

The selectivity map of the eluent systems is

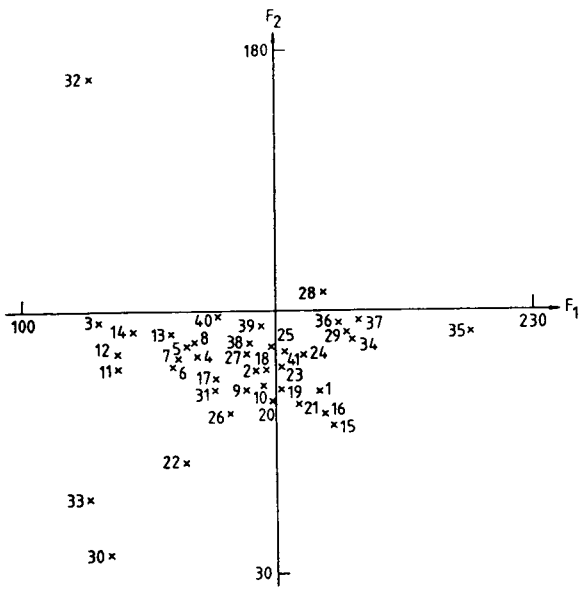

Fig. 1. Selectivity map of barbituric acid derivatives. Number of iterations, 78; maximum error, $2.13 \cdot 10^{-2}$. Numbers refer to barbituric acid derivatives in Table 1.

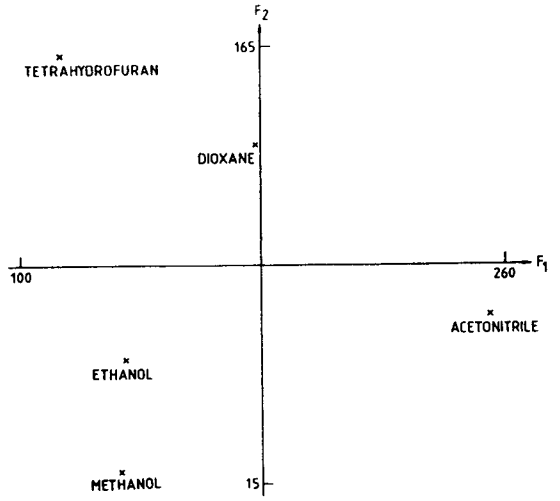

Fig. 2. Selectivity map of eluent systems. Number of iterations, 48; maximum error, $6.02 \cdot 10^{-3}$.

shown in Fig. 2. The organic modifiers form three loose clusters (methanol and ethanol; dioxane and tetrahydrofuran; acetonitrile). The distribution of organic modifiers entirely supports our previous conclusions that the steric characteristics are one of the main determinants of selectivity (bulky dioxane and tetrahydrofuran form separate clusters). As the polarity of –OH is different from that of ≡CN it is understandable that the selectivities of methanol and ethanol differ from that of acetonitrile, indicating again the importance of polar interactions between the molecules of organic modifiers and the surface of the β-CD support.

It can be concluded that babituric acid derivatives can be well separated on a β-CD polymer-coated silica column. Stepwise regression analysis confirmed that the retention of barbituric acid derivatives is mainly governed by the lipophilicity and steric parameters of the substituents. The spectral map technique indicated that the solvent strength and selectivity of organic modifiers on a β-CD polymer-coated silica column depended on their bulkiness and electronic parameters, respectively.

Table 4
Relationships between solvent strength and selectivity of organic modifiers and their physico-chemical parameters: results of stepwise regression analysis: $y = a + bx$

Parameter[a]	Equation No.[b]		
	1	2	3
a	7.05	102.10	−39.91
b	19.63	273.07	8.01
x	B_4/M-RE	σ	M-RE
S_b	5.00	67.93	1.49
r	0.9147	0.9183	0.9516

[a] For symbols, see Table 3.

[b] (1) y = solvent strength of eluent systems (roman numbers refer to eluent systems in Table 3): I, 2.39; II, 1.57; III, 0.19; IV, 1.17; V, 2.83. (2) y = first coordinate of selectivity map of eluent systems. (3) y = second coordinate of selectivity map of eluent systems.

4. Acknowledgement

This work was supported by Grant OTKA 2670 of the Hungarian Academy of Sciences.

5. References

[1] J. Szejtli, in J.L. Atwood, J.E. Davis and D.D. McNicol (Editors), *Inclusion Compounds*, Vol. III, Academic Press, London, 1984.
[2] J. Szejtli, *Cyclodextrins and Their Inclusion Complexes*, Akadémiai Kiadó, Budapest, 1982.
[3] J. Szejtli, B. Zsadon and T. Cserháti, in W.L. Hinze and D.W. Armstrong (Editors), *Ordered Media in Chemical Separation* (*ACS Symposium Series*, No. 342), American Chemical Society, Washington, DC, 1987, pp. 200–217.
[4] D.W. Armstrong, W. Li, C.-D. Chang and J. Pitha, *Anal. Chem.*, 62 (1990) 914–923.
[5] D.W. Armstrong, W. Li and J. Pitha, *Anal. Chem.*, 62 (1990) 215–217.
[6] T. Cserháti, J. Szejtli and M. Szögyi, *J. Chromatogr.*, 509 (1990) 255–262.
[7] K. Fukushi and K. Hiiro, *J. Chromatogr.*, 518 (1990) 189–198.
[8] J. Liu, K.A. Cobb and M. Novotny, *J. Chromatogr.*, 519 (1990) 189–197.
[9] M. Gosselet and B. Sebille, *J. Chromatogr.*, 552 (1991) 563–573.
[10] B. Agnus, B. Sebille and M. Gosselet, *J. Chromatogr.*, 552 (1991) 583–592.
[11] K. Shimada, T. Oe and M. Suzuki, *J. Chromatogr.*, 558 (1991) 1306–1310.
[12] R.R. West and J.H. Cardellina, II, *J. Chromatogr.*, 539 (1991) 15–23.
[13] D.W. Armstrong, A.M. Stalcup, M.L. Hilton, J.D. Duncan, J.R. Faulkner, Jr., and S.C. Chang, *Anal. Chem.*, 62 (1990) 1610–1615.
[14] N. Thuaud, B. Sebille, A. Deratini, B. Popping and C. Pellet, *Chromatographia*, 36 (1993) 373.
[15] L.R. Snyder and J.J. Kirkland, *Introduction to Modern Liquid Chromatography*, Wiley, New York, 1973, pp. 222–224.
[16] H. Mager, *Moderne Regressionsanalyse*, Salle, Sauerlander, Frankfurt/Main, 1982, pp. 135–157.
[17] P.J. Lewi, *Arzneim.-Forsch.*, 26 (1976) 1290.
[18] T. Cserháti and E. Forgács, *Anal. Chim. Acta*, 279 (1993) 107.
[19] J.W. Sammon, Jr., *IEEE Trans. Comput.*, C18 (1969) 401.

ELSEVIER

Journal of Chromatography A, 668 (1994) 403–411

JOURNAL OF CHROMATOGRAPHY A

Determination of alpidem, an imidazopyridine anxiolytic, and its metabolites by column-switching high-performance liquid chromatography with fluorescence detection

L. Flaminio, M. Ripamonti, V. Ascalone*

Synthélabo Recherche (LERS), Department of Chemical and Pharmaceutical Development, Clinical Pharmacokinetics Group, Via N. Rivoltana 35, 20090 Limito (MI), Italy

Abstract

Alpidem, 6-chloro-2-(4-chlorophenyl)-N,N-dipropylimidazo[1,2-*a*]pyridine-3-acetamide, is an anxiolytic imidazopyridine that undergoes a first-pass elimination after oral administration to humans; it is actively metabolized and three circulating metabolites have been identified in plasma due to N-dealkylation, oxidation or a combination of both processes. For the determination of the unchanged drug and its metabolites in human plasma, a column-switching HPLC method was developed. The method, based on solid-phase extraction (performed on-line), involves the automatic injection of plasma samples (200 μl) on to a precolumn filled with C_{18} material, clean-up of the sample with water in order to remove protein and salts and transfer of the analytes to the analytical column (after valve switching) by means of the mobile phase. All the processes were performed in the presence of an internal standard, a compound chemically related to alpidem. During the analytical chromatography, the precolumn was flushed with different solvents and after regeneration with water, it was ready for further injections. The analytical column was a C_8 type and the mobile phase was acetonitrile–methanol–phosphate buffer solution (45:15:45, v/v/v) at a flow-rate of 1.5 ml min^{-1}. The column was connected to a fluorimetric detector operating at excitation and emission wavelengths of 255 and 423 nm, respectively. The limits of quantitation of alpidem and three metabolites were 2.5 and 1.5 ng ml^{-1}, respectively, in human plasma.

1. Introduction

In the last few years, interest in solid-phase extraction (SPE) has grown considerably as an alternative to the traditional liquid–liquid extraction, which has some disadvantages such as low selectivity, emulsion formation, extensive solvent use and waste disposal and non-automation [1]. In particularly, automatic on-line SPE with HPLC, known as column-switching HPLC, offers a simple solution to the complex problem of sample purification and preconcentration of drugs and metabolites in biological fluids [2–5]. The automation allows the sample throughput to be increased [6,7] and human errors to be avoided.

Alpidem, 6-chloro-2-(4-chlorophenyl)-N,N-dipropylimidazo[1,2-*a*]pyridine-3-acetamide, is a non-benzodiazepinic anxiolytic that has an interesting anxiolytic profile at both animal and clinical levels [8,9]. The drug, after oral administration to humans, is actively metabolized, and three circulating metabolites have been identified

* Corresponding author.

0021-9673/94/$07.00
SSDI 0021-9673(93)E1056-6

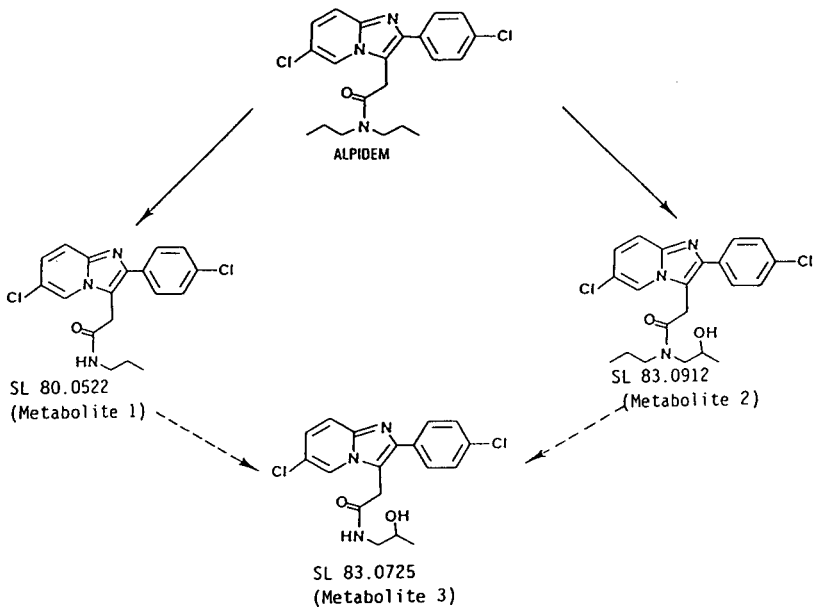

Fig. 1. Metabolic pathway of alpidem in humans and structures of metabolites.

(Fig. 1). They originate from N-dealkylation, with loss of a propyl group to give metabolite 1, oxidation of a propyl group to give metabolite 2 and oxidation of a propyl group and loss of the other propyl group to give metabolite 3. For the determination of alpidem and its metabolites in human plasma a method has been published [10] that is based on liquid–liquid extraction and HPLC with fluorescence detection; here we propose a method based on column-switching HPLC that does not require any manipulation of the biological sample before injection.

2. Experimental

2.1. Chemicals, reagents and standards

Methanol and acetonitrile were of HPLC grade (E. Merck, Darmstadt, Germany) and potassium dihydrogenphosphate was of analytical-reagent grade (E. Merck). The water used for the preparation of the buffer solutions and chromatographic eluent was of HPLC grade, produced from tap water by a two-step process: prepurification through a Milli-RO 60 Plus and then through a Milli-Q4 system (Millipore, Bedford, MA, USA).

The 0.025 *M* phosphate solution used for the preparation of the eluent mixture was prepared by dissolving 137 g of anhydrous potassium dihydrogenphosphate in water and diluting to 1 l, then further diluting 25 ml of this solution to 1 l. The mobile phase was prepared by mixing 450 ml of the 0.025 *M* phosphate solution, 400 ml of acetonitrile and 150 ml of methanol, then filtering through a 0.22-μm filter membrane by means of a solvent clarification kit (Millipore). Alpidem, SL 80.0522 (metabolite 1), SL 83.0912 (metabolite 2), SL 83.0725 (metabolite 3) (Fig. 1) and SL 80.0633, 6-chloro-2-(3,4-dimethoxyphenyl)-N,N-dipropylimidazo[1,2-*a*]pyridine-3-acetamide (Internal Standard), were of pharmaceutical grade and were provided by Synthélabo Recherche (Bagneux, France).

2.2. Standard solutions

Stock standard solutions of alpidem, the metabolites and the internal standard were prepared in methanol at a concentration of 1 mg

ml^{-1}. Fresh stock standard solutions were prepared every 2 months and stored at 0–5°C. Working standard solutions were prepared from the stock standard solutions by suitable dilutions with methanol (see Table 1). Fresh working standard solutions were prepared every 2 weeks and stored at 0–5°C.

The standard solutions were used for the preparation of the plasma standards used for calibration.

2.3. Sample preparation

Aliquots (20 μl) of methanolic standard solutions (Table 1) were added to drug-free plasma (calibration samples), and 20 μl of internal standard solution (Table 1) were added to all samples (calibration samples and unknowns). All the samples were transferred into Eppendorf centrifuge vials (with caps), the vials were centrifuged on an Eppendorf-type centrifuge at 11 000 *g* and the supernatant was transferred to conical autosampler vials for automatic sample injection. The scheme of the operations is illustrated in Fig. 2.

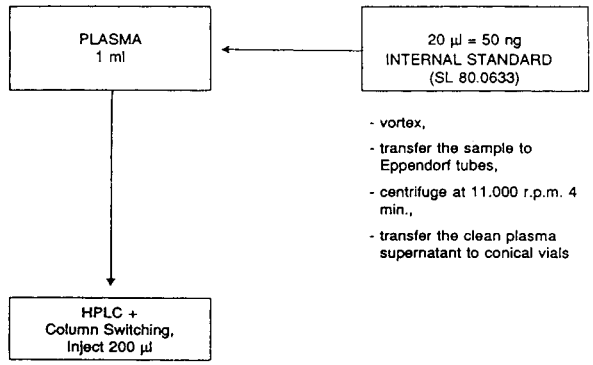

Fig. 2. Scheme of sample preparation. Internal standard = 6-chloro-2-(3,4-dimethoxyphenyl)-N,N-dipropylimidazo[1,2-*a*]pyridine-3-acetamide.

2.4. Basic chromatographic system

The basic chromatographic system consisted of a Model 420 constant-flow pump (Kontron, Milan, Italy), an SFM 23/B spectrofluorimetric HPLC detector (Kontron) operating at excitation and emission wavelengths of 255 and 423 nm respectively, a Model 460 automatic sample injector (Kontron) provided with a six-port automatic valve and an external 250-μl loop and an analytical column (15 cm × 0.46 cm I.D.) packed with 5-μm Hypersil C_8 BDS (Shandon, Runcorn, UK) provided with a guard column (2 cm × 0.46 cm I.D.) packed with 40-μm Pelliguard LC_8 (Supelco, Bellefonte, PA, USA).

The mobile phase was acetonitrile–methanol–0.025 *M* phosphate solution (pH 4.5) (40:15:45, v/v/v) at a flow-rate of 1.5 ml min^{-1}.

2.5. Extended chromatographic system

The apparatus required for automatic column-switching HPLC was obtained by implementing

Table 1
Standard solutions used for daily calibration

Standard solution	Alpidem (ng per 20 μl)	Metabolite 3 (ng per 20 μl)	Metabolite 1 (ng per 20 μl)	Metabolite 2 (ng per 20 μl)	Internal standard (ng per 20 μl)
A	100	200	100	100	–
B	50	100	50	50	–
C	25	50	25	25	–
D	10	20	10	10	–
E	5	10	5	5	–
F	2.5	5	2.5	2.5	–
G	–	–	–	–	50

the basic apparatus with a precolumn (7.5 cm × 0.21 cm I.D.) for on-line purification, dry-packed with 30–40-μm Perisorb C_{18} (Merck), a valve-switching apparatus provided with a Tracer Model MCS-670 six-port solvent selector (Kontron), a programmer for the management of the valves and a Programmer 200 solvent selector (Kontron) and finally a Model 410 HPLC single-piston pump (Kontron) used for the clean-up of the processed plasma samples. The solvents used for precolumn clean-up and back-flushing were water, acetonitrile–water (50:50, v/v), acetonitrile, methanol–water (50:50, v/v) and water, each supplied at a flow-rate of 2 ml min^{-1}. The extended apparatus is shown in Fig. 3.

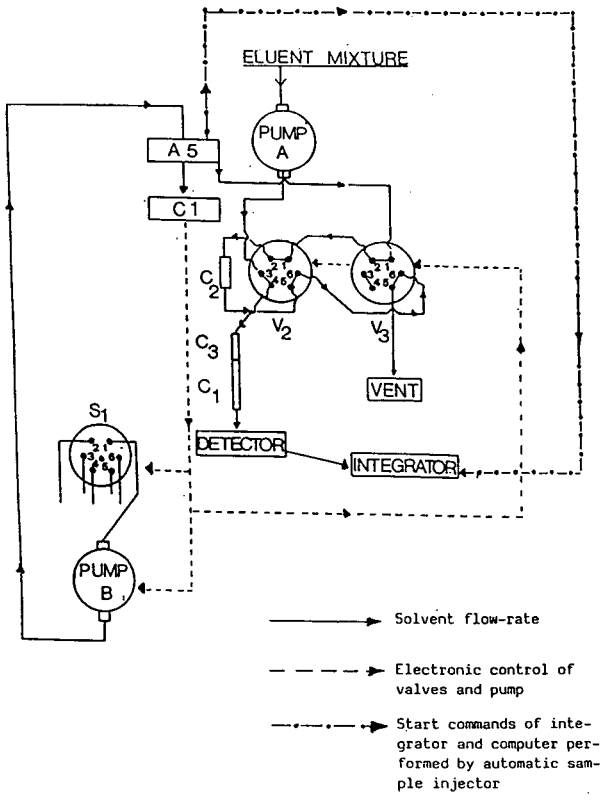

Fig. 3. Scheme of extended chromatographic apparatus. C_1 = Analytical column; C_2 = precolumn; C_3 = guard column; V_2 = valve for back-flushing; S_1 = solvent selector; A 5 = automatic sample injector; C 1 = computer.

2.6. Operating conditions for on-line clean-up and column-switching HPLC

The operations of fluid sampling, clean-up and enrichment on the precolumn, transfer of the analytes from the precolumn to the analytical column and analytical chromatography with simultaneous precolumn back-flushing and regeneration are performed automatically as depicted in Figs. 4–7. The programmes of on-line clean-up and column switching can be summarized as follows: after the injection of a human plasma sample (200 μl) on to the precolumn, the latter is flushed for 2 min with pure water; alpidem, metabolites and internal standard are retained, while proteins and salt are removed, then the precolumn is connected to the analytical column for 1.5 min in order to transfer the

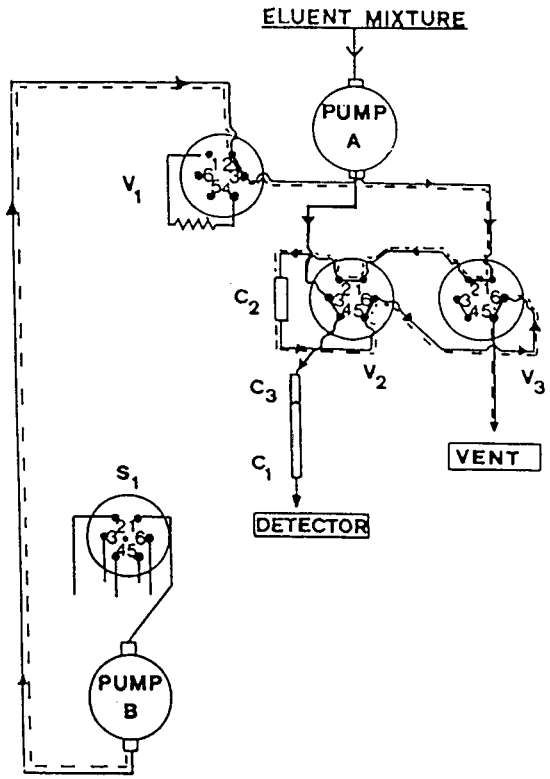

Fig. 4. Equilibrium preceding sample injection.

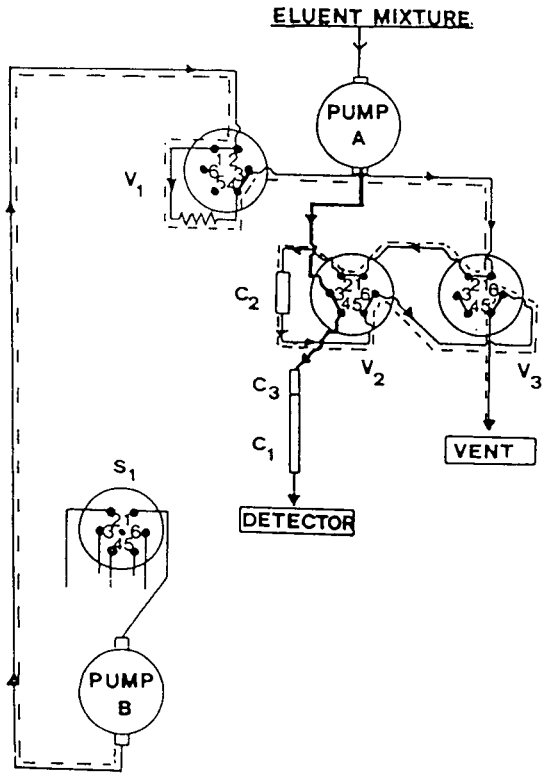

Fig. 5. Loading and clean-up of the sample on the pre-column.

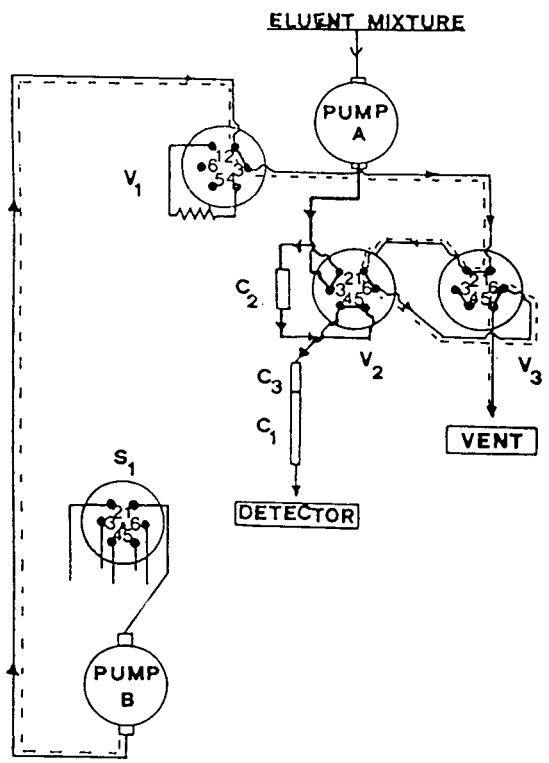

Fig. 6. V_2 switching and elution of sample from the pre-column to the top of the analytical column.

analytes to the analytical column by means of the mobile phase. While the analytical chromatography takes place, the precolumn is back-flushed with acetonitrile–water (50:50, v/v), acetonitrile, methanol–water (50:50, v/v) and water.

3. Results

3.1. Stability

As far as the stability of alpidem and its metabolites in different media is concerned, the results indicate that all the compounds were stable in methanol (stock standard solutions) for at least 2 months if maintained at 0–5°C and the methanolic working standard solutions were stable for at least 2 weeks if maintained under the same conditions.

Concerning the stability of the compounds in human plasma samples, when maintained under ordinary laboratory conditions no variations were found for all the investigated compounds during 24 h in comparison with freshly prepared and immediately analysed plasma samples (processed according to the described method). Also, no significant variations were found in human plasma samples when submitted to three freeze–thaw cycles in comparison with freshly prepared plasma samples that were immediately analysed.

The stability study was performed at levels of 8 and 80 ng ml^{-1} in human plasma for both alpidem and its metabolites, in triplicate, in the presence of 50 ng ml^{-1} of internal standard.

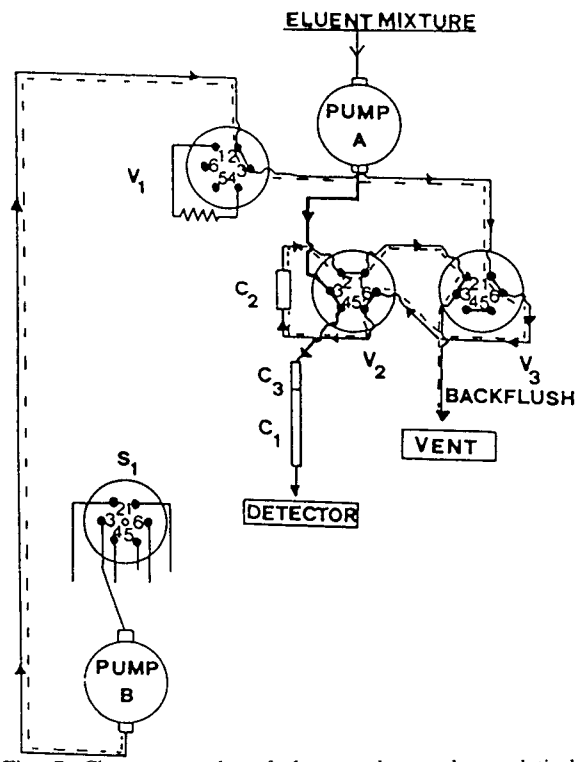

Fig. 7. Chromatography of the sample on the analytical column and back-flushing of the precolumn.

3.2. Selectivity

Several drug-free human plasma samples from different subjects were tested for the absence of interfering compounds; in no case was any chromatographic interference found at the retention times of alpidem, its metabolites and the internal standard (Fig. 8A).

Some drugs that could be co-administered with alpidem were checked for the possibility of giving chromatographic interferences. Diazepam, nordiazepam, lorazepam, nitrazepam, amitriptyline, chlomipramine (and their demethylated metabolites), ranitidine and cemetedine do not interfere chromatographically as they give no response to the fluorescence detector; trazodone responds to the detector but is well separated from the compounds of interest; zolpidem, another imidazopyridine, interferes with the more polar metabolite of alpidem (metabolite 3), but the metabolites of zolpidem do not interfere.

3.3. Recovery

The absolute recovery of alpidem and its metabolites was evaluated by comparing the chromatographic response of aqueous standard solutions (in physiological fluid) directly injected on to the HPLC column (by-passing the precolumn) to the response of plasma standards processed according to the described method. The recovery of alpidem was about 77%, for all three metabolites it was about 80% and for the internal standard it was about 73%.

3.4. Linearity

A linear correlation was found in human plasma between the ratio of peak height of alpidem to that of the internal standard and the concentration of alpidem in the range 2.5–100 ng ml^{-1}, in the same range for metabolites 1 and 2 and in the range 5–200 ng ml^{-1} for metabolite 3 (Fig. 9A–D).

3.5. Limit of quantification

The limit of quantification (LOQ) of the method, calculated on a peak with a signal-to-noise ratio of about 3, was 2.5 and 1.5 ng ml^{-1} in human plasma for alpidem and its metabolites respectively (the limit was calculated from the chromatogram reported in Fig. 8B).

3.6. Precision and accuracy

The method was validated according to an internal protocol that involved two analysts working on the same chromatographic apparatus (on different days); each analyst, after the daily calibration (performed in quadruplicate), analysed five times each two quality control specimens, of low and medium concentrations, over a 2-day period. The precision and accuracy results were evaluated during a day (intra-day) and during different days (inter-day); the cumulative results (Table 2) show that the described method

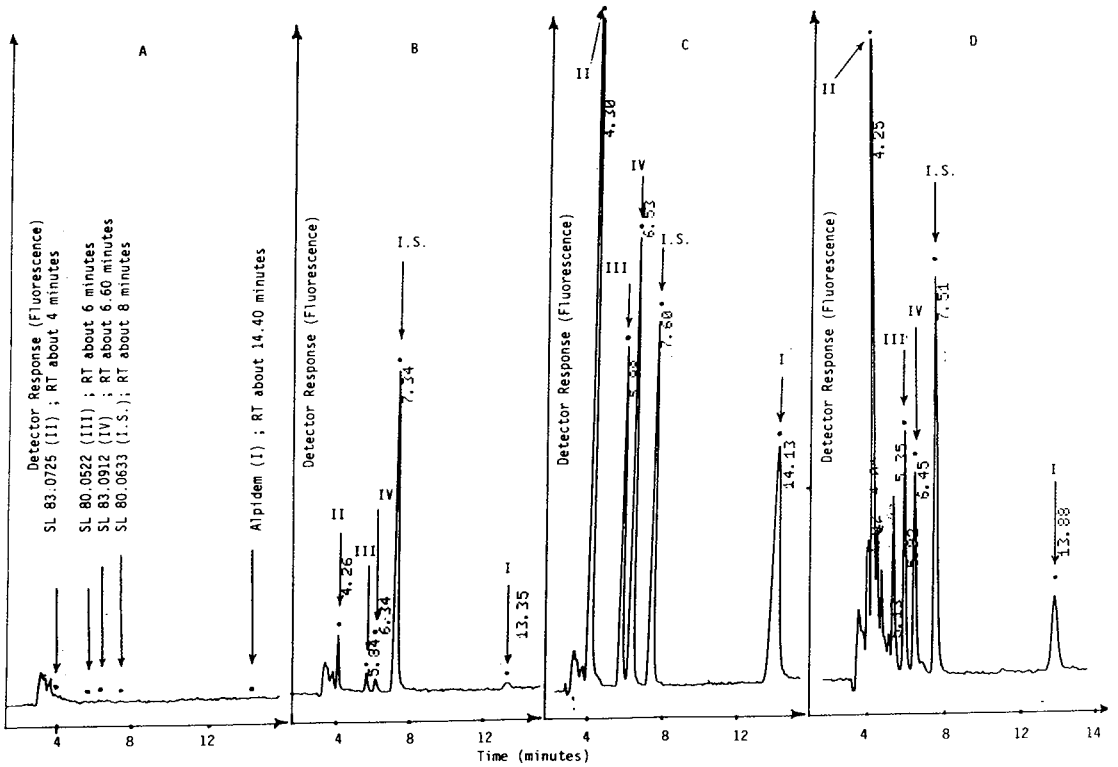

Fig. 8. (A) Chromatogram of drug-free plasma. (B) Chromatogram of a plasma standard containing metabolite 3 at 5 ng ml^{-1}, other compounds at 2.5 ng ml^{-1} and internal standard at 50 ng ml^{-1}. (C) Chromatogram of a plasma standard containing metabolite 3 at 160 ng ml^{-1}, metabolite 1 at 40 ng ml^{-1}, metabolite 2 and alpidem at 80 ng ml^{-1} and internal standard at 50 ng ml^{-1}. (D) Chromatogram of a plasma sample from a subject administered orally with alpidem with a 50-mg dose daily for 8 days; sample taken on day 7, 4 h after drug intake. RT = Retention time.

possesses sufficient precision and accuracy to be used for pharmacokinetic studies in humans. Fig. 8C shows a typical chromatogram.

3.7. Application of the method to specimens from in vivo studies

The proposed method has been extensively used for the determination of alpidem and its active metabolites in plasma from subjects treated orally with alpidem by single and/or repetitive oral administration during pharmacokinetic investigations and in clinical studies (phase 2 to phase 4) for assessing patient compliance. The method gave results comparable to those obtained by the conventional liquid–liquid extraction method [10] but it is simpler, being completely automated. Fig. 8D shows a typical chromatogram.

4. Discussion

The stability study performed on human plasma samples spiked with alpidem and its metabolites confirmed that there was no degradation of any compound, parent drug and/or metabolites, thus allowing us to leave plasma samples on the rack of the automatic sample injector (preinjection conditions) for up to 24 h; this is an extreme condition, since during 24 h it is possible to process 94 plasma samples. The precolumn, the core of the purification and extraction process, is usually replaced after about 250–300 plasma

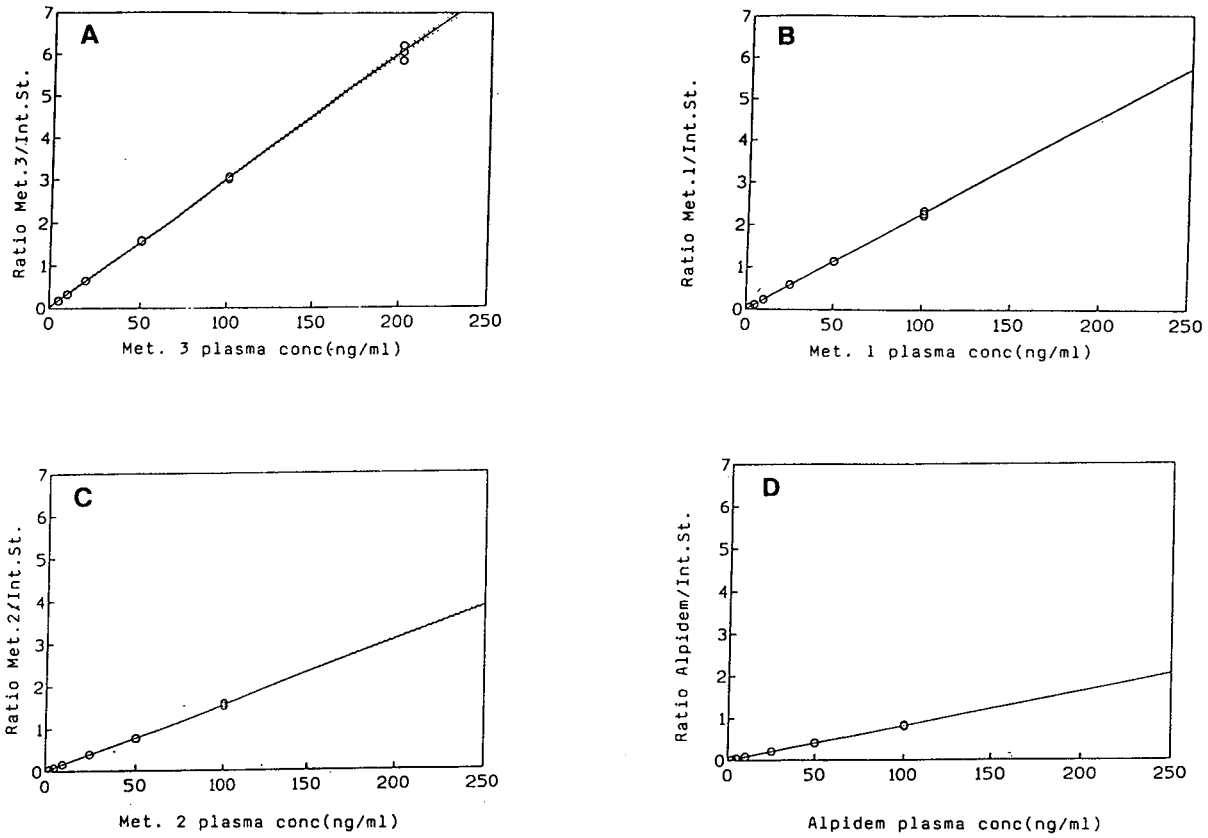

Fig. 9. (A) Regression line for metabolite 3. Equation: $y = 32.978\ x - 0.91$ ($n = 24$, $r = 0.9995$). (B) Regression line for metabolite 1. Equation: $y = 43.599\ x - 0.073$ ($n = 24$, $r = 0.9997$). (C) Regression line for metabolite 2. Equation: $y = 64.839\ x - 0.311$ ($n = 24$, $r = 0.9994$). (D) Regression line for alpidem. Equation: $y = 122.526\ x - 0.228$ ($n = 24$, $r = 0.9994$).

injections (or when the back-pressure exceeds 30 bar).

The efficiency of the analytical column is not affected by the plasma injections on to the precolumn; with the same column it was possible to analyse more than 1500 samples; there is an increase in the throughput of the samples (in comparison with the traditional extraction method) with continuous running outside of the normal working periods, and the extensive automation of the system allows minimum sample handling, removes the need for an extraction solvent and is subject to a minimum of human errors and contamination.

Selectivity with regard to endogeneous compounds and co-administered psychotropic drugs was very good and the sensitivity, precision and accuracy of the method, which has been used routinely without any problems, are high. As the only potentially crucial part of the whole chromatographic system is the precolumn (with the risk of precipitation of biological material and clogging), it was necessary to ensure that in case of an accident and a subsequent high back-pressure of the pump, a simple security apparatus will stop the pump and reset the automatic sample injector.

Finally, for laboratories that do not have a switching apparatus similar to ours, there is the possibility of utilizing the several different devices available on the market or of assembling in-house a cheap system consisting of an isocratic pump, a solvent selector and two six-port switching valves; the valves and solvent selector can be

Table 2
Precision and accuracy results

Parameter	Metabolite 3		Parameter	Metabolite 1	
	160 ng ml^{-1}	16 ng ml^{-1}		40 ng ml^{-1}	4 ng ml^{-1}
Precision:			Precision:		
R.S.D. intra (%)[a]	1.1	1.3	R.S.D. intra (%)[a]	1.0	3.4
R.S.D. inter (%)[b]	0.9	0	R.S.D. inter (%)[b]	0.4	0
R.S.D. total (%)	1.4	1.3	R.S.D. total (%)	1.0	3.4
LS[c]	2.3	1.8	LS[c]	1.5	4.8
Accuracy[d] (%)	98.0 ± 1.0	98.2 ± 0.6	Accuracy[d] (%)	103.0 ± 0.6	100.9 ± 0.5
	Metabolite 2			Alpidem	
	80 ng ml^{-1}	8 ng ml^{-1}		80 ng ml^{-1}	8 ng ml^{-1}
Precision:			Precision:		
R.S.D. intra (%)[a]	1.0	2.7	R.S.D. intra (%)[a]	1.2	4.2
R.S.D. inter (%)[b]	1.0	1.3	R.S.D. inter (%)[b]	1.7	4.0
R.S.D. total (%)	1.4	3.0	R.S.D. total (%)	2.1	5.8
LS[c]	2.5	4.3	LS[c]	4.3	9.9
Accuracy[d] (%)	103.5 ± 1.2	103.5 ± 1.8	Accuracy[d] (%)	102.9 ± 1.9	98.4 ± 4.4

Precision and accuracy of the method for the determination of metabolite 3, metabolite 1, metabolite 2 and alpidem in human plasma evaluated by analysing quality control samples ($n = 20$ for each concentration, for all compounds).
[a] Within-day relative standard deviation.
[b] Between-day relative standard deviation.
[c] 95% upper confidence limit for the R.S.D.
[d] Calculated as (concentration found/nominal concentration) · 100 at the 95% confidence limit.

managed through the "event time" section of an integrator connected by means of an interface, or by the auxiliary outputs, nowadays available, in several automatic sample injectors. If the precolumn cleaning is performed with normal-flush washings, only one switching valve is required; however, in our experience, back-flush washing is more effective in precolumn regeneration.

5. References

[1] N. Simpson, *Int. Chromatogr. Lab.*, 11 (1992) 7.
[2] W. Voelter, K. Zech, P. Arnold and G. Ludwig, *J. Chromatogr.*, 199 (1980) 343.
[3] W. Roth, K. Beschke, R. Jank, A. Zimmer and F.W. Koss, *J. Chromatogr.*, 222 (1981) 475.
[4] R.D. McDowall, G.S. Murkitt and J.A. Walford, *J. Chromatogr.*, 317 (1984) 475.
[5] V. Ascalone and L. Dal Bo', *J. Chromatogr.*, 423 (1987) 239.
[6] M.J. Koenigbour and R.E. Majors, *LC · GC Int.*, 3, No. 9 (1990) 10.
[7] A. Dale, *Eur. Chromatogr. Anal.*, 3 (1991) 5.
[8] M. Dimsdale, J.C. Friedman and B. Zivkovic, *Drugs Future*, 13 (1988) 106.
[9] B. Zivkovic, E. Morel, D. Yoly, G.H. Perrault, D.J. Sanger and K.G. Lloyd, *Pharmacopsychiatry*, 23 (1990) 108.
[10] V. Ascalone, P. Catalani, L. Dal Bo', N. Deschamps and P. Guinebault, *J. Chromatogr.*, 414 (1987) 101.

ELSEVIER

Journal of Chromatography A, 668 (1994) 413–417

JOURNAL OF CHROMATOGRAPHY A

Short Communication

Effect of temperature on separation of norgestrel enantiomers by high-performance liquid chromatography

Henryk Lamparczyk*, Paweł K. Zarzycki, Joanna Nowakowska

Medical Academy, Faculty of Pharmacy, Gen. J. Hallera 107, PL-80-416 Gdańsk, Poland

Abstract

The influence of mobile phase composition, concentration of β-cyclodextrin and temperature on the high-performance liquid chromatographic separation of norgestrel was studied. In studies of the effect of temperature on the enantioselectivity of (±)-norgestrel, acetonitrile–water (25:75, v/v) modified by the addition of β-cyclodextrin (14 m*M*) was applied as the mobile phase. Enantiomers were detected using UV detection at 240 nm. The capacity factors were measured over a wide range of column temperatures from −5 to 70°C.

1. Introduction

Plots of the logarithms of capacity factors against the reciprocal of absolute temperature are usually linear and are known as Van 't Hoff plots [1–3]. Nevertheless, any reversible process that alters the enthalpy or entropy of adsorption in principle gives rise to non-linear Van 't Hoff plots. Among others, changes in conformation and changes in the extent to which the mobile phase interacts with either the analyte or the stationary phase are examples of such reversible behaviour [4,5]. Moreover, the presence of multiple types of retention mechanisms or multiple types of binding sites also leads to non-linearity of the Van 't Hoff plots. Particularly in chiral recognition, multiple types of retention and the importance of conformation can be expected, and therefore the effect of temperature on retention might be very complex.

Cyclodextrins (CDs) are toroidal-shaped cyclic oligomers of α-1,4-D-glucopyranose units and they are well known as chiral selectors [6,7]. The name "cyclodextrins" includes a large group of α-, β- and γ-CDs together with numerous derivatives, but β-cyclodextrin (β-CD) is the most often used cyclodextrin. In HPLC cyclodextrins have been used both chemically bonded to a stationary phase and added to the mobile phase [8,9].

Despite the number of papers dealing with various applications of CDs in chromatography, including chiral separations, the knowledge of the stereoselectivity and structural relationships between CDs and guest molecules is poor. Many factors seems to be responsible for the separation including the type of CD used [10], its concentration in the mobile phase [10,11], the type of mobile phase [10–12] and the temperature of the separation process [10]. In this paper we report the influence of mobile phase composition, concentration of β-CD and temperature on the separation of norgestrel enantiomers, which were chosen as a model compounds. Norgestrel [(±)-13β-ethyl-17-hydroxy-18,19-dinor-17α-pregn-4-en-20-yn-3-one] is an interesting ster-

* Corresponding author.

0021-9673/94/$07.00
SSDI 0021-9673(93)E0039-W

oidal compound with progestogenic activity which is commonly used as a contraceptive agent. Enantiomers of this compound have different intrinsic pharmacological activity [13].

2. Experimental

2.1. Reagents

Norgestrel racemic mixture (Prempak) was supplied by Ayerst Laboratories (Andover, UK) and D-(−)norgestrel (Levonorgestrel) by Sigma (St. Louis, MO, USA).

Acetonitrile (Merck, Darmstadt, Germany) was of HPLC grade. Water was purified by double distillation. Mobile phases were filtered through a 1.5-μm membrane prior to use.

β-Cyclodextrin was supplied by Chinoin (Budapest, Hungary) and was purified by recrystallization from boiling water.

2.2. Chromatography

The liquid chromatograph, consisting of an analytical solvent pump, UV–Vis spectrophotometer and linear recorder, was a product of Knauer. A Rheodyne Model 7125 injection valve was used for sample introduction. Two types of column were used, Knauer ODS-1 (120 × 4.6 mm I.D.) and Supelco ODS (150 × 4.6 mm I.D.). The capacity factors were not influenced by the type of column used.

The flow-rate was varied, depending on the column and cyclodextrin concentration used, from 1 to 3 ml/min and the dead retention time from 0.64 to 0.22 min. The sample size was 20 μl and the concentration of the solutes was 10 μg/ml.

The column temperature was controlled by immersing the column in a stirred constant-temperature bath containing ethanol–water (30:70, w/w) used as a heat-exchange medium. The bath was connected to a thermostat adjustable from −5 to 70°C. Temperature was controlled with an accuracy of ±0.5°C. Additionally, the bottle with mobile phase was thermostated 1 h before the experiment in order to obtain proper temperature equilibrium.

Acetonitrile–water of various compositions was used as the mobile phase.

The void volume was determined by injecting sodium nitrate solution. The UV detector was operated at 240 nm. The capacity factors were calculated in the usual manner and are based on the average of at least five independent determinations of each solute.

3. Results and discussion

A plot of the capacity factors *versus* acetonitrile–water composition for norgesterel racemic mixture is shown in Fig. 1. The mobile phase was used without a chiral selector. As one normally expects, increasing the organic modifier concentration in the mobile phase hastens the elution of the analyte. However, owing to the low solubility of β-CD in mobile phases with a high concentration of organic component, a composition of acetonitrile–water (25:75, v/v) was chosen for further investigations.

The influence of the β-CD concentration on the capacity factors is exemplified in Fig. 2 by

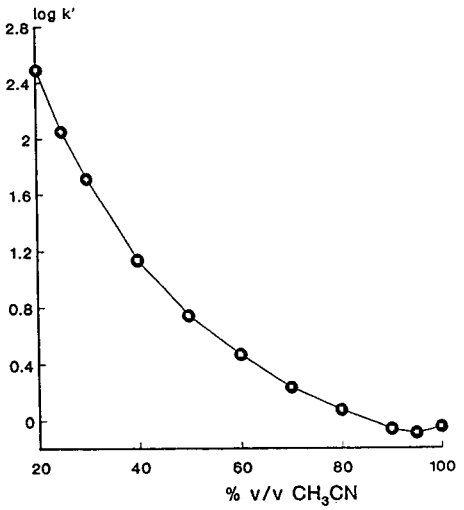

Fig. 1. Plot of log k' *vs.* mobile phase composition for D-(±)-norgestrel racemic mixture. The mobile phase (acetonitrile–water) was used without a chiral selector. Column, Knauer ODS-1 (120 × 4.6 mm I.D.) at 40°C.

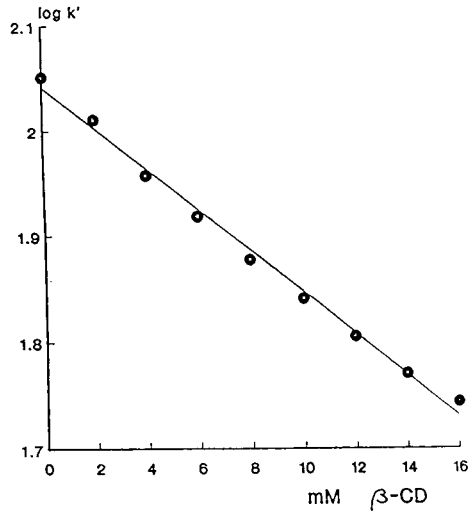

Fig. 2. Plot of log k' *vs.* concentration of β-CD with acetonitrile–water (25:75, v/v) as the mobile phase for D-(±)-norgestrel racemic mixture. Column, Knauer ODS-1 (120 × 4.6 mm I.D.) at 40°C.

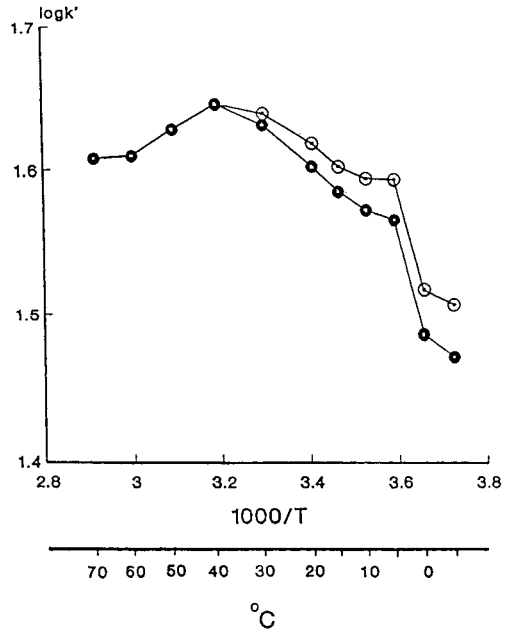

Fig. 3. Plots of log k' *vs.* $1000/T$ for the enantiomers of norgestrel. Column, Supelco ODS (150 × 4.6 mm I.D.). Mobile phase, acetonitrile–water (25:75, v/v) modified with the addition of 14 mM β-cyclodextrin. ○ = D-(−)- and ● = D-(+)-norgestrel.

the behaviour of norgestrel racemic mixture. The measurements were performed at 40°C (313 K) and no chiral resolution was observed over the whole range of β-CD concentrations. It is often observed that an increase in the concentration of β-CD leads to a concomitant decrease in the capacity factor [10–12,14] and, as can be see in Fig. 2, for norgestrel racemic mixture this is also this case. The observed effect suggests that the adsorption of guest–CD complexes on the reversed stationary phase is very close to zero for both enantiomers of norgestrel and that the predominating mechanism for retention is the formation of guest–CD complexes in the mobile phase. The plot is linear over the range of β-CD concentrations investigated. The shortest retention was observed using a 16 mM concentration of β-CD. However, owing to the extreme solubility conditions (the solubility of β-CD in water at 25°C is 16.3 mM) at such a high concentration, a mobile phase with the addition of 14 mM β-CD was chosen for further studies of the temperature effect.

Plots of the logarithms of the capacity factors against the reciprocal of absolute temperature are shown in Fig. 3. A linear Van 't Hoff behaviour is observed in the range between 70 and 40°C. In this region stereoselectivity is not observed. The temperature at which the deviation from linear Van 't Hoff behaviour, together with chiral separation, begins is 40°C. When the temperature decreases down to the sub-ambient region the retention also decreases. The best chiral separation was achieved in the range from −5 to 0°C. Chromatograms obtained at 40, 20 and 0°C are shown in Fig. 4. Although, chiral recognition is maintained at 20°C, baseline separation is observed at 0°C.

The effect of temperature on enantioselectivity in HPLC systems with mobile phases modified with the addition of CDs has not been described previously, with the exception of recent work by Seidel *et al.* [15]. They studied effect of temperature, in a narrow range from 65 to 35°C, on the separation of the mycotoxins ochratoxin A and zearalenone. Both compounds are not enantiomers, but the mobile phase used was modified by the addition of β-CD. The result obtained was a

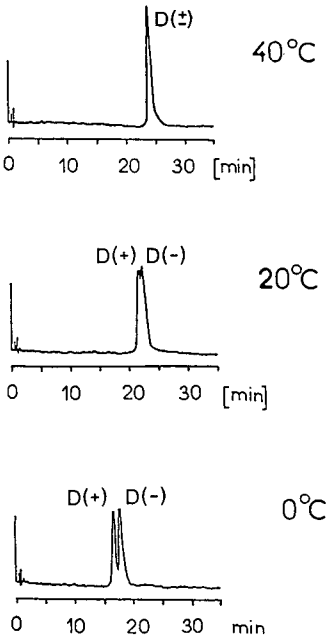

Fig. 4. Separation of D-(±)-norgestrel enantiomers at 40, 20 and 0°C. Other chromatographic conditions as in Fig. 3.

typical Van 't Hoff plot which corresponds to the first part of the plot presented in Fig. 3 from 70 to 40°C. On the other hand, we recently observed that for 1,8-dimethylnaphthalene the retention decreases when the temperature decreases [10], whereas other dimethylnaphthalenes behave typically, *i.e.*, the retention increases when the temperature decreases. These studies were performed in the temperature range 25–70°C. The unusual behaviour of 1,8-dimethylnaphthalene can be explained by considering that an increase in temperature always decreases CD complexation. Moreover, the increase in complexation is followed by a decrease in capacity factors. The second phenomenon can be easily explained by considering the better solubility of guest–CD complexes in the mobile phase. In contrast, the degree of complexation for other dimethylnaphthalenes is much lower and therefore the increase in complexation when the temperature decreases does not influence the k' *vs.* $1/T$ plot in the temperature range studied.

Considering the experimental results described

Table 1
Separation factors (α) and resolutions (R_s) for norgestrel enantiomers at various temperatures

Column temperature (°C)	α	R_s
30	1.02	0.08
20	1.04	0.15
15	1.04	0.23
10	1.05	0.30
5	1.06	0.44
0	1.08	0.60

in both previous papers [10,15], the following suggestions on the separation mechanism of norgestrel enantiomers on a molecular level can be given. In the temperature range 70–40°C the degree of complexation with β-CD for both enantiomers is very low and therefore the typical Van 't Hoff plot in Fig. 3 is observed. The phenomenon that retention decreases with increase in temperature has been observed many times in both HPLC and GC. On a molecular level it can be easily explained by the faster migration of the solute molecules through the chromatographic column and their lower affinity to the stationary phase. With norgestrel enantiomers in this temperature range, the complexation with β-CD is not enantioselective. Below 40°C the inclusion mechanism starts to be important. As evidence, deviation from the Van 't Hoff plot is observed in Fig. 3 and also the norgestrel enantiomers start to differ in their affinity to the β-CD molecule, as exemplified in Fig. 4. Table 1 lists the separation factors α $[\alpha = k'_{(-)}/k'_{(+)}]$ and resolutions defined as $R_s = [t_{R(-)} - t_{R(+)}]/2[\sigma_{(-)} + \sigma_{(+)}]$. On a molecular level, the enantioselectivity in this temperature range, can probably be interpreted as being due to slower rotation of the guest and host molecules and hence a steric fit is possible.

The results presented here also suggest that the predominant mechanism for retention is the formation of guest–CD complexes in the mobile phase.

4. Acknowledgement

This work was supported in part by grant 202429101 from the State Committee for Scientific Research.

5. References

[1] L.R. Snyder, *J. Chromatogr., Sci.*, 8 (1970) 692.
[2] R.P.W. Scott and J.B. Lawrence, *J. Chromatogr. Sci.*, 8 (1970) 619.
[3] J. Chmielowiec and H. Sawatzky, *J. Chromatogr. Sci.*, 17 (1979) 245.
[4] W.R. Melander, A. Nahum and Cs. Horvath, *J. Chromatogr.*, 185 (1979) 129.
[5] W.H. Pirkle, *J. Chromatogr.*, 558 (1991) 1.
[6] W.L. Hinze, *Purif. Sep. Methods*, 10 (1981) 159.
[7] J. Szejtli, *Cyclodextrins and Their Inclusion Complexes*, Akadémiai Kiadó, Budapest, 1982.
[8] D.W. Armstrong and W. DeMond, *J. Chromatogr. Sci.*, 22 (1984) 411.
[9] D. Sybilska, J. Lipkowski and J. Wójcikowski, *J. Chromatogr.*, 253 (1982) 95.
[10] D. Sybilska, M. Asztemborska, A. Bielejewska, J. Kowalczyk, H. Dodziuk, K. Duszczyk, H. Lamparczyk and P. Zarzycki, *Chromatographia*, 35 (1993) 637.
[11] H. Lamparczyk, P. Zarzycki, R.J. Ochocka, M. Asztemborska, and D. Sybilska, *Chromatographia*, 31, (1991) 157.
[12] A. Walhagen and L.E. Edholm, *Chromatographia*, 32 (1991) 215.
[13] H. Lamparczyk, *Analysis and Characterization of Steroids*, CRC Press, Boca Raton, FL, 1992.
[14] H. Lamparczyk, P. Zarzycki, R.J. Ochocka and D. Sybilska, *Chromatographia*, 30 (1990) 91.
[15] V. Seidel, E. Poglits, K. Schiller and W. Lindner, *J. Chromatogr.*, 635 (1993) 227.

ELSEVIER

Journal of Chromatography A, 668 (1994) 419–425

JOURNAL OF CHROMATOGRAPHY A

Determination of panomifene in human plasma by high-performance liquid chromatography

V. Erdélyi-Tóth*,[a], E. Pap[a], J. Kralovánszky[a], E. Bojti[b], I. Klebovich[b]

[a]National Institute of Oncology, Clinical Research Department, Ráth Gy. u. 7–9, H-1525 Budapest, Hungary
[b]EGIS Pharmaceuticals Ltd., Department of Pharmacokinetics, Keresztúri út 30–38, H-1106 Budapest, Hungary

Abstract

An ion-pair HPLC method was developed for the determination of the antiestrogenic drug panomifene, (*E*)-1,2-diphenyl-1-{4-[2-(2-hydroxyethylamino)ethoxy]phenyl}-3,3,3-trifluoropropene, in human plasma. Tamoxifen, 20 ng in 1 ml of plasma, was used as an internal standard. The compounds were isolated from plasma by liquid–solid extraction. Fluorescence detection was achieved by on-line photochemical conversion of the compounds into highly fluorescent phenanthrene derivatives. The sensitivity of the method was 1 ng/ml. The within-day and between-day precision, linearity, extraction recovery and stability of panomifene in plasma and in deproteinized plasma were determined for validation of the method. The method is suitable for measuring plasma levels of panomifene and tamoxifen and for pharmacokinetic studies.

1. Introduction

Panomifene (PAN) (*E*)-1,2-diphenyl-1-{4-[2-(2-hydroxyethylamino)ethoxy]phenyl}-3,3,3-trifluoropropene, is a compound structurally similar to tamoxifen (TMX) (Fig. 1). In preclinical *in vitro* and *in vivo* studies it was found to be a potent antiestrogen with a strong inhibitory effect on estrogen-dependent tumours. The binding affinity to the estrogen receptors of cytosol appeared to be more than double that of TMX. Essential pharmacological activity is associated with proper agonistic and consecutive central (antigonadotropic) actions [1,2]. The favourable properties led to the selection of PAN for a clinical phase I trial.

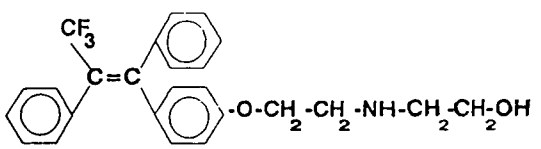

Fig. 1. Structure of panomifene, (*E*)-1,2-diphenyl-1-{4-[2-(2-hydroxyethylamino)ethoxy]phenyl}-3,3,3-trifluoropropene.

Similarly to published HPLC methods for TMX [3–7], an ion-pair chromatographic method was developed for the determination of PAN in human plasma. TMX was used as an internal standard (I.S.). Fluorescence detection was achieved by "on-line" photochemical conversion of the compounds under UV irradiation into highly fluorescent phenanthrene products using a postcolumn photoreactor included in the HPLC system.

* Corresponding author.

0021-9673/94/$07.00
SSDI 0021-9673(93)E1218-O

2. Experimental

2.1. Reagents and chemicals

Panomifene (PAN, EGIS-5650) and tamoxifen citrate (TMX) were kindly provided by EGIS Pharmaceuticals (Budapest, Hungary).

Analytical-reagent grade chemicals were used as received: potassium dihydrogenphosphate and 85% phosphoric acid were purchased from Reanal (Budapest, Hungary), triethylamine from Fluka (Buchs, Switzerland), and 96% sulphuric acid from Rudi Pont (Milan, Italy). 1-Heptanesulphonic acid sodium salt (chromatography grade) was obtained from Supelco (Gland, Switzerland) and acetonitrile (LiChrosolv grade) from Merck (Darmstadt, Germany). AMPREP Phenyl (PH) microcolumns (1 ml) were supplied by Amersham (Aylesbury, UK).

Doubly distilled water was used for the preparation of the solutions. Chromatographic eluents were filtered through a Paraplan membrane filter (0.2 μm) before use.

Polypropylene tubes and vials were used for preparing, storing and measuring the standard solutions of PAN and TMX and the biological samples.

2.2. Instruments and equipment

PT 1200 and R 160 P balances (Sartorius, Göttingen, Germany), an OP 208/1 precision digital pH meter (Radelkis, Budapest, Hungary), a Vibrofix (vortex mixer, Janke et Kunkel, IKA, Staufen, Germany), a K23 refrigerated, time-programmable centrifuge (Janetzki, Engelsdorf, Germany), an MPW-310 time-programmable micro centrifuge (Mechanika Precyzyjna Warszawa, Warsaw, Poland) and a freezer (−24°C) (Lehel Jászberény, Hungary) were used.

Solid-phase extraction was carried out using a laboratory-made processing system. The extracts were evaporated under nitrogen with a laboratory-made sample evaporator equipped with a Block-therm thermostat (Kutesz, Budapest, Hungary).

The HP 1084 B HPLC system (Hewlett-Packard, Palo Alto, CA, USA) consisted of a variable-volume injector (79841 A), an automatic sampling system (79842 A) and a terminal (7985 B). A Shimadzu (Kyoto, Japan) RF-530 fluorescence HPLC monitor was used. A Model C 6808 Beam-Boost photoreactor (ICT, Frankfurt, Germany) was incorporated on-line between the chromatograph and the detector.

2.3. Chromatographic conditions

The chromatographic separation was achieved on a 250 mm × 4.6 mm I.D. Si-100-S 10 Phenyl (10 μm) column equipped with a 20 mm × 4.6 mm I.D. SI-100-S Phenyl precolumn (BST, Budapest, Hungary). The mobile phase consisted of 0.005 *M* heptanesulphonic acid in 0.05 *M* KH_2PO_4–H_3PO_4 buffer (pH 3.0) containing 300 μl of triethylamine (TEA) per litre as A and acetonitrile as B eluent, with the composition A–B (25:75, v/v). The flow-rate was 1.2 ml/min. The temperatures of eluents A and B were 80 and 60°C, respectively. The sample injection volume was 10–30 μl.

The postcolumn photochemical derivatization of PAN and TMX was accomplished on-line in a 10 m × 0.3 mm I.D. reaction coil (PTFE tube) knitted on the mercury lamp (UV wavelength 254 nm) of the Beam Boost photoreactor.

The excitation and emission wavelengths of the fluorescence detector were 257 and 378 nm, respectively.

2.4. Sample preparation

Heparinized plasma samples were used. Plasma was separated from whole blood by centrifugation and was immediately stored frozen at −24°C until processing. Before use the plasma samples were thawed at room temperature. Stock standard solutions of PAN and TMX (10.0 mg in 10.00 ml of methanol) were prepared. Working standard solutions containing 1–100 ng of PAN in 20-μl aliquots were prepared by diluting the stock standard solution with methanol–water (1:1, v/v).

Plasma samples (980 μl) were spiked with 20-μl aliquots of PAN working standard solutions, then 20 ng of TMX [in 10 μl of methanol–

water (1:1, v/v)] was added to each plasma sample as an I.S.

The spiked plasma samples prepared in conical polypropylene tubes were processed with 1000 μl of acetonitrile for deproteinization. The centrifuge tubes were capped, mixed on a vortex mixer for 1 min and centrifuged for 60 min at 5000 rpm (2500 *g*) with a free-swinging rotor at −10°C.

A 1600-μl volume of the supernatant was transferred to a calibrated 2 ml polypropylene vial and diluted to volume with 0.05 *M* phosphate buffer (KH_2PO_4–H_3PO_4) (pH 3.0) containing 2% heptanesulphonic acid. The mixture was extracted by liquid–solid extraction using a phenyl microcolumn (1-ml capacity). The columns were conditioned with 5 × 1 ml of acetonitrile and 1 ml of doubly distilled water, followed by 1 ml of 0.05 *M* phosphate buffer (pH 3.0) containing 250 μl of TEA per 100.00 ml.

The deproteinized sample, containing an ion-pair reagent, was transferred on to the previously activated column. After the column had been washed consecutively with 2 × 100 μl of 0.05 *M* phosphate buffer (pH 3.0) containing 0.005 *M* heptanesulphonic acid–acetonitrile (20:80, v/v), 50 μl of 0.025 *M* sulphuric acid was added to adjust the pH of the column. PAN and TMX were eluted with 5 × 100 μl of 0.05 *M* phosphate buffer (pH 3.0) containing 0.005 *M* heptanesulphonic acid–acetonitrile (20:80, v/v).

The eluate was collected in a polypropylene Eppendorf vial and evaporated under nitrogen at ambient temperature. The residue was dissolved in 100 μl of 0.05 *M* phosphate buffer (pH 3.0) containing 0.005 *M* heptanesulphonic acid–acetonitrile (30:70, v/v) and an aliquot was injected into the chromatographic system.

2.5. Validation

Quantitative analysis was performed by the internal standard method, measuring the area of chromatographic peaks. Factors needed for the calculations were obtained by analysis of blank plasma and standard samples supplemented with known amounts of PAN and the I.S.

Standard samples were prepared by adding a 20-μl aliquot of a working standard solution of PAN and 10 μl of the I.S. (20 ng) in methanol–water (1:1, v/v) to 0.05 *M* phosphate buffer (pH 3.0) containing 0.005 *M* heptanesulphonic acid–acetonitrile (30:70, v/v) mixture to give a final volume of 100 μl.

Calibration graphs were fitted by the computer program Medusa Version 1.5/1.587 (CheMicro, Budapest, Hungary). For statistical evaluations a computer program published by Tallarida and Murray [8] was used.

Precision of the chromatographic system

Repetitive injections ($n = 6$) were made of PAN standard solutions of three different concentrations (100, 20 and 5 ng per 100 μl). Each sample contained 20 ng of TMX as I.S. The injection volume was 10 μl.

Linearity, within-day precision

The linearity of the method was studied in a concentration range corresponding to the expected plasma levels with six independent parallel measurements at each concentration. For standard samples 5, 10, 20, 50 and 100 ng per 100 μl and for spiked plasma samples 1, 2, 5, 10, 20, 50 and 100 ng/ml (final volume 100 μl) of PAN were determined. Each sample contained 20 ng of the I.S.

Calibration graphs were constructed by plotting the concentrations of PAN against the peak-area ratios (PAN/I.S.). Statistical analysis of the results was performed to calculate the within-day precision of the method.

Between-day precision

Calibration graphs were prepared by adding PAN to three independent samples of blank plasma at concentrations of 5, 10, 20, 50 and 100 ng/ml on six consecutive days. The study demonstrated both the within-day and the between-day precision.

Recovery

The extraction recoveries of PAN and the I.S. were calculated by comparing the peak areas obtained with spiked plasma samples after extraction with those obtained with standard sam-

ples at the same concentration (independent samples).

Stability of PAN in human plasma

The stability of PAN was examined in human plasma spiked at concentrations of 100, 50 and 10 ng/ml and stored at −24°C for 4 weeks, determinations being made weekly. The stability of PAN in human plasma spiked with the same PAN concentrations deproteinized with acetonitrile was also studied.

3. Results

Without previous photocyclization when the "on-line" photoreactor was switched off, no peaks could be observed with standard solutions containing PAN and the I.S. Typical chromatograms of blank plasma, a standard sample containing 20 ng per 100 μl of PAN and the I.S. and a spiked plasma containing PAN (20 ng/ml) and the I.S. (20 ng/ml) are shown in Fig. 2. The chromatographic system provided a good separation of PAN and the I.S. from the endogenous components. The chromatogram of blank plasma showed no significant matrix interference peaks.

The reproducibility of the chromatographic conditions (retention time, peak area, ratio of the peak areas) was determined by replicate injections ($n = 6$) of 10 μl of standard samples containing 20 ng of the I.S. and 100, 20 and 5 ng of PAN in 100 μl. This examination also tested the reproducibility of the photoconversion of the compounds by using the "on-line" photoreactor.

In this set, the photocyclization depended on the flow-rate of the mobile phase and the length of the irradiated pathway. Owing to the length of the knitted reaction coil (10 m) in a fixed configuration and the applied flow-rate of 1.2 ml/min, the irradiation period was allowed to be *ca.* 50 s according to the instruction manual for the reactor.

Based on the system suitability test, the relative standard deviations (R.S.D.s) for retention times, peak areas and ratio of peak areas were found less than 0.5%, 6% and 7%, respectively. The reproducibilities of the peak shapes, retention times and the photochemical conversions were acceptable under these conditions. On evaluating 20 consecutive chromatograms, the retention time of PAN varied between 5.65 and 5.80 min (5.73 ± 0.05 min) and that of the I.S. varied between 6.95 and 7.12 min (7.03 ± 0.05 min). The retention times increased slightly with ageing of the chromatographic column.

The minimum detectable concentration was 20 pg/ml and the limit of quantification was 1 ng of PAN in 1 ml of plasma. Calibration graphs were constructed to demonstrate the linear relationship between the peak-area ratio and the concentration of the samples. The range covered 1–100 ng/ml for plasma. The upper limit of

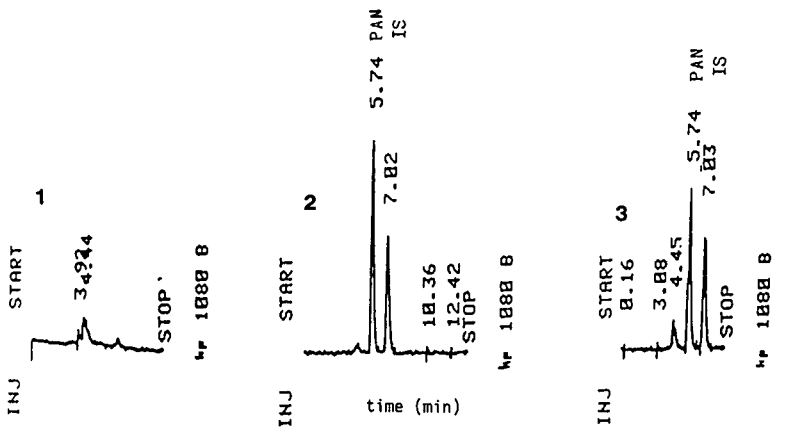

Fig. 2. Typical chromatograms of (1) blank plasma, (2) standard sample containing 20 ng per 100 μl of PAN and I.S. and (3) spiked plasma containing PAN (20 ng/ml) and I.S. (20 ng/ml).

quantification, however, was 300 ng/ml for PAN compared with 20 ng/ml for the I.S. A linear relationship was found in the investigated range with a correlation coefficient (r^2) of 0.999. The intercept was zero. The R.S.D.s (within-day precision) were between 2.89 and 8.90%, which are acceptable values for biological samples.

The reproducibility of the method was demonstrated by the construction of calibration graphs in the concentration range 5–100 ng/ml using three freshly made daily independent parallel plasma samples at each concentration over 6 days. The statistical evaluations of the within-day and the between-day precisions are summarized in Table 1.

Table 1
Within-day and between-day precisions of the assay for panomifene in spiked plasma

Day	n	Concentration found (mean ± S.D.) (ng/ml)	R.S.D. (%)
Within-day precision			
1	3	4.847 ± 0.217	4.47
		9.986 ± 0.625	6.25
		20.546 ± 3.046	14.83
		45.055 ± 2.120	4.70
		100.292 ± 5.913	5.89
2	3	5.598 ± 0.527	9.41
		10.842 ± 1.010	9.31
		23.031 ± 3.980	17.28
		49.321 ± 1.270	2.57
		101.279 ± 1.680	1.66
3	3	6.345 ± 0.856	13.49
		12.051 ± 0.542	4.50
		21.696 ± 2.380	10.97
		47.279 ± 2.162	4.57
		102.039 ± 3.907	3.83
4	3	5.204 ± 0.822	15.78
		10.299 ± 0.336	3.26
		20.782 ± 0.628	3.02
		49.756 ± 1.434	2.88
		100.399 ± 2.193	2.18
5	3	5.486 ± 0.211	3.85
		9.565 ± 0.121	1.26
		19.412 ± 0.761	3.92
		51.273 ± 3.524	6.87
		99.592 ± 2.839	2.85
6	3	5.891 ± 0.629	10.67
		10.026 ± 1.014	9.87
		19.883 ± 1.763	8.86
		52.886 ± 2.107	3.89
		99.610 ± 2.390	2.40
Between-day precision			
–	18	5.584 ± 0.682	12.21
		10.462 ± 1.014	9.69
		20.892 ± 2.370	11.35
		49.262 ± 3.145	6.39
		100.535 ± 3.041	3.02

Table 2
Extraction recoveries of panomifene and the internal standard

Compound	Plasma concentration (ng/ml)	Extraction recovery [mean ± S.D. (n = 6)] (%)
PAN	100	74.36 ± 13.60
	50	77.50 ± 12.37
	20	56.89 ± 8.29
	10	69.41 ± 11.55
	5	67.21 ± 16.68
I.S.	20	76.42 ± 13.70

Data concerning the extraction recoveries of the compounds are presented in Table 2. The extraction of PAN and the I.S. was not complete but was sufficiently high to determine the concentrations of PAN at low ng/ml levels in plasma.

During 4 weeks of storage at −24°C, the concentration of PAN in the plasma decreased by about 50%; however, no degradation product could be seen in the chromatogram. No significant decrease in concentration was observed in plasma deproteinized with acetonitrile (Fig. 3).

The method has proved to be sufficiently sensitive and selective to be used in clinical pharmacokinetic studies. Fig. 4 shows a typical plasma concentration–time curve after oral administration of 24 mg of panomifene to a healthy female volunteer.

4. Discussion

The HPLC method described here for the determination of PAN and TMX (I.S.) is a sensitive and rapid procedure suitable for clinical and research use.

Methods proposed previously to determine TMX and TMX analogues in biological fluids use fluorimetric detection based on measurement of

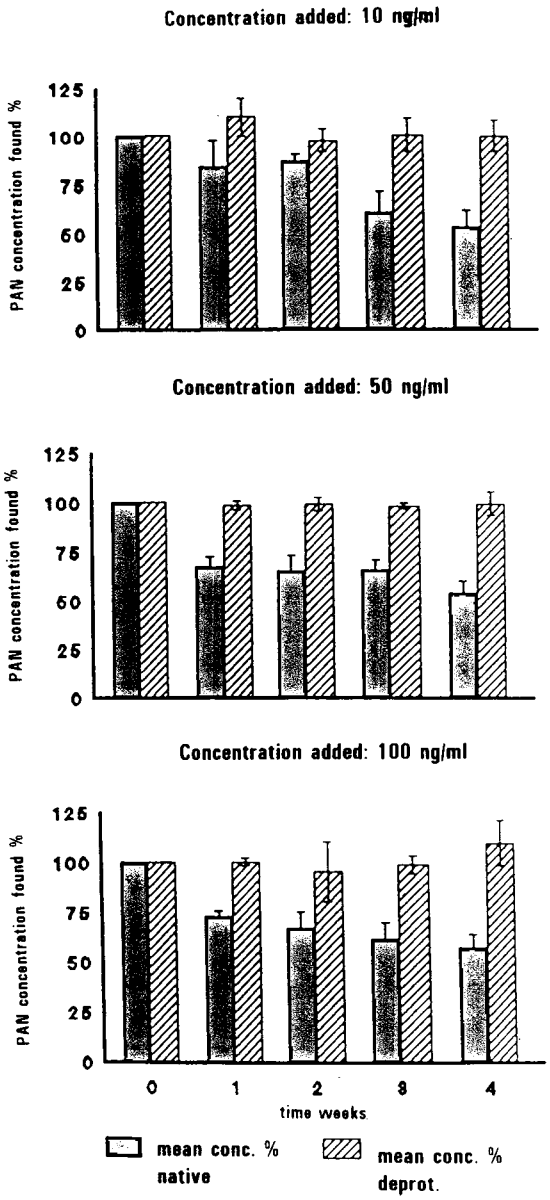

Fig. 3. Stability of PAN in native plasma and in plasma deproteinized with acetonitrile. Time of storage, 4 weeks; temperature of storage, −24°C. A 20 ng/ml concentration of the I.S. was added to each sample before examination.

the fluorescence developed by UV photochemical conversion of the triphenylethylene nucleus to phenanthrenes [3–7]. With "off-line" photolysis and injection of the photocyclization products into the chromatographic system, we were

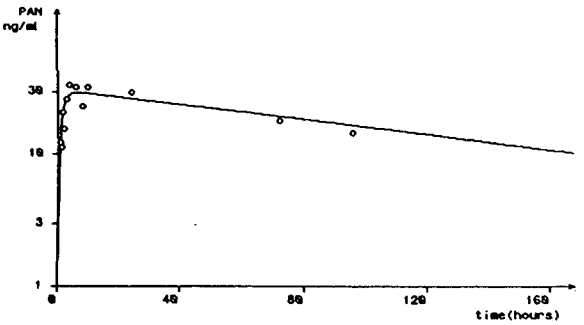

Fig. 4. Plasma concentration–time curve for PAN after oral administration of 24 mg of panomifene to a healthy female volunteer. Plasma half-life of absorption: $t_{1/2}(k_a) = 0.91$, plasma half-life of the elimination of the drug: $t_{1/2}(k_e) = 103.95$, lagtime (time elapsed between drug administration and appearance of the drug in the plasma): $t_{lag} = 0.50$ h. Peak of the plasma concentration: $C_{max} = 29.52$ ng/ml; time to peak = 6.79 h. Area under the plasma concentration–time curve from 0 to ∞ calculated by trapezoidal rule: $AUC_{0-\infty}$ (trap.rule) = 4714.79 (ng/ml)·h; mean residence time: MRT = 153.4 h.

not able to achieve a good resolution for the corresponding PAN phenanthrene derivative. Postcolumn fluorescence activation developed by Brown *et al.* [4] overcame this problem.

Using postcolumn on-line photocyclization, the exposure to UV radiation was dependent only on the stability of the flow-rate and the UV lamp intensity. The geometry of the system was fixed. To achieve the maximum photochemical conversion of PAN, an illumination period of 50 s at a flow-rate of 1.2 ml/min was required, which corresponded to 10 m of illuminated reaction coil. Increasing the illumination period decreased the formation of the fluorescent products.

C_8 and C_{18} reversed-phase columns and mobile phases with a high percentage of organic modifier [3] showed strong peak tailing for the compounds studied. This could be minimized, but not eliminated, by adding an organic amine [4] or an ion-pairing substance [3] to the mobile phase. Similarly to Camaggi *et al.* [5], we were not able to elute TMX from a LiChrosorb 5 RP-18 (Chrompack) column (150 × 4.6 mm I.D.) even by using acetonitrile–0.005 *M* pentanesulphonate (pH 3.0) (80:20) as the mobile phase.

Complete chromatographic separation and resolution of PAN and TMX with a cyano-bonded stationary phase [5] and acidified aqueous acetonitrile containing an ion-pairing reagent as eluent could not be reproduced.

Adequate separation of the analytes and plasma constituents was achieved with a phenyl column eluted isocratically with acetonitrile–phosphate buffer containing heptanesulphonate. As expected, a decrease in pH led to a decrease in the retention times of the basic compounds. The optimum operating pH range in our system was 3.0. TEA could be seen as a tailing-suppressing agent, which improved the elution profile of PAN and TMX.

The observed chromatographic behaviour of PAN and TMX indicated that the retention of the compounds is based not only on a pure reversed-phase mechanism, but additionally on interactions with the polar silica surface of the column. The strong interaction with the polar silica surface caused irreversible adsorption of the compounds, mainly TMX, on any glass surface of sample containers. In order to avoid these problems, polypropylene tubes and vials were used for preparing, storing and measuring the standard solutions of PAN and I.S. and the biological samples.

Simple and reproducible sample processing is important for a high sample output. Extraction with organic solvents as suggested in the literature [3,4] proved unsuitable as the extracts were found to contain impurities that were poorly separable from PAN.

Sample processing was successful using a protein-precipitation procedure with an equal volume of acetonitrile following solid-phase extraction with a phenyl microcolumn. The deproteinization avoided clogging of the extraction column. A plasma sample deproteinized with acetonitrile was stable even on storage for 4 weeks at −24°C. Addition of an ion-pairing reagent to the acetonitrile-containing plasma improved the absorption of the compounds of interest on the column. Satisfactory elution was achieved only if the microcolumn was adjusted to pH 1 with sulphuric acid before extraction. The procedure resulted in a clean extract with minimal co-extraction of plasma components. The extraction recoveries obtained with the phenyl microcolumns were high and reproducible. The method has proved to be sufficiently sensitive and selective to be used in clinical pharmacokinetic studies.

5. Acknowledgements

We gratefully acknowledge the technical assistance of Mrs. Elisabeth Rozsnyay-Czapko and the administrative work of Mrs. Judith Bodi. This work was supported by grant from EGIS Pharmaceuticals, Budapest, Hungary.

6. References

[1] K. Tory, E. Csányi, T. Horváth, G. Ábrahám, J. Borvendég and Gy. Cseh, in S. Eckhardt and S. Kerpel-Fronius (Editors), *CMEA Chemotherapy Symposium 1984*, Akadémiai Kiadó, Budapest, 1985, pp. 509–515.

[2] E. Csányi, K. Tory, S. Elek, S. Nyitray, A. Miklós and Z. Magyar, presented at the *16th International Congress of Chemotherapy, Jerusalem, Israel, 1989*, Abstract 245.

[3] Y. Golander and L.A. Sternson, *J. Chromatogr.*, 181 (1980) 41–49.

[4] R.R. Brown, R. Bain and V.C. Jordan, *J. Chromatogr.*, 272 (1983) 351–358.

[5] C.M. Camaggi, E. Strocchi, N. Canova and F. Panutti, *J. Chromatogr.*, 275 (1983) 436–442.

[6] E.A. Lien, P.M. Ueland, E. Solheim and S. Kvinnsland, *Clin. Chem.*, 33 (1987) 1608–1614.

[7] C.D. Kikuta and R. Schmid, *J. Pharm. Biomed. Anal.*, 7 (1989) 329–337.

[8] R.J. Tallarida and R.B. Murray, *Manual of Pharmacologic Calculations with Computer Programs*, Springer, New York, 1986.

ELSEVIER

Journal of Chromatography A, 668 (1994) 427–433

JOURNAL OF CHROMATOGRAPHY A

Rapid sample preparation technique for the determination of pyrrolizidine alkaloids in plant extracts

R. Chizzola

Institute for Botany and Food Science, Veterinary Medicine University of Vienna, Linke Bahngasse 11, A-1030 Vienna, Austria

Abstract

To determine toxic pyrrolizidine alkaloids from various plant sources, a sample preparation technique is described that affords alkaloid fractions suitable for capillary GC or TLC determination. The procedure includes the reduction of the alkaloid N-oxides with the oxygen-absorbing resin Serdoxit and a clean-up with strong cation-exchange solid-phase columns. If desired an enrichment of the alkaloids can be obtained. The method was tested with methanolic extracts from *Senecio vulgaris*, *Petasites hybridus* and *Symphytum officinale*.

1. Introduction

Pyrrolizidine alkaloids (PAs) are ester alkaloids that occur in a wide range of plants, but especially in Boraginaceae, Asteraceae and Fabaceae. Those PAs with a 1,2-unsaturated pyrrolizidine moiety (see Fig. 4) are hepatotoxic and have shown carcinogenic and mutagenic potency in some animal feeding experiments [1]. PAs from toxic pasture plants have led to loss of cattle and transfer of these alkaloids into milk or honey has been reported [2]. Further, this kind of alkaloid occurs as minor constituents in some medicinal plants. Because of their high toxicity, the use of medicinal plants containing them has been severely restricted in Germany. It must be ensured that the daily contact with toxic PAs from phytopharmaceuticals does not exceed 1 or 100 μg by internal or external application, respectively [3]. Therefore, it is of interest to determine these alkaloids even at low concentrations. The usual techniques, such as capillary GC, HPLC or TLC, require a lengthy sample clean-up and concentration step. The sample preparation method proposed here using solid-phase columns avoids the use of separating funnels and allows an enrichment of the alkaloids.

2. Experimental

2.1. Reagents

Solutions used included the following: ammonia, 12.5% in distilled water; HCl–methanol (1), concentrated HCl–distilled water–methanol (25:135:40); HCl–methanol (2), concentrated HCl–distilled water–methanol (25:75:100); and sodium dithionite, 5% in distilled water. Serdoxit oxygen-absorbing resin was obtained from Serva (Heidelberg, Germany). Varian Bond Elut LRC SCX 1211-3039, 0.5- and 2-g strong cation-exchange solid-phase extraction columns were obtained from ICT (Vienna, Austria). HPTLC plates were silica gel 60 F-254 (10 × 20 cm) from Merck. Dipping solutions (1) was 0.1% *o*-chloranil in toluene and dipping solution (2) was

0021-9673/94/$07.00
SSDI 0021-9673(93)E1298-E

2 g of 4-dimethylaminobenzaldehyde + 85 ml of acetic acid + 15 ml of 32% HCl. The mobile phase was CH_2Cl_2–MeOH–25% ammonia (85:14:1.5). The GC internal standard was 18 mg of caffeine in 100 ml of methanol. PAs used as reference substances were senecionine, seneciphylline, retrorsine and retrorsine-N-oxide, obtained from Roth (Karlsruhe, Germany).

2.2. Extraction of plant material

A 0.2–1-g amount of dry, finely powdered plant material was extracted in a 25-ml flask for 1 h with boiling methanol (65°C). After cooling to room temperature the extracts were diluted to 25 ml and filtered.

2.3. Preparation of extraction columns

The Serdoxit column was prepared by filling 1 g of the resin into an empty solid-phase extraction column fitted with a valve for flow regulation and rinsing intensively with MeOH and distilled water. As Serdoxit also reacts with oxygen from air, it has to be regenerated immediately before use with 4 ml of a solution of the reducing agent sodium dithionite. Serdoxit is provided with an indicator which turns from black to yellow when fully regenerated. Excess of sodium dithionite was washed out with 8 ml of distilled water and 4 ml of MeOH were added to displace the water. The SCX columns were first treated with 8 ml of HCl–MeOH (2) solution and then washed neutral with MeOH.

2.4. Clean-up procedure

The clean-up procedure is summarized in Fig. 1. It consists of three steps: the reduction of the N-oxides in the Serdoxit column, a first clean-up by retention and subsequent elution of the PAs from the SCX column, and extraction of the PAs in the alkaline phase with dichloromethane.

A 3–6-ml volume of the methanolic plant extract was applied to the freshly regenerated Serdoxit column (Fig. 1: 1). The dropping velocity was adjusted to 1 drop in 3 s to ensure a

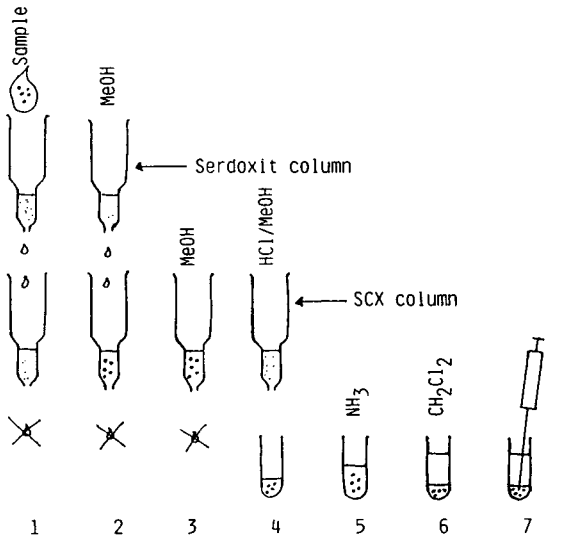

Fig. 1. Scheme for the clean-up of pyrrolizidine alkaloids in plant extracts. 1 = Applying 3–6 ml extract onto the Serdoxit column, reduction of the N-oxides to the free alkaloids; 2 = washing the alkaloids through the Serdoxit column; 3 = retention of the alkaloids, washing out other compounds from the SCX columns; 4 = elution of the alkaloids with HCl–MeOH; 5 = making the eluate alkaline; 6 = extraction of the alkaloids with CH_2Cl_2; 7 = taking the CH_2Cl_2 layer for analysis.

sufficient contact time for complete reduction of the N-oxides. MeOH (5 ml) was added to wash the extract completely through the Serdoxit column (Fig. 1: 2). In this step the Serdoxit column must not run dry. Extract coming from the outlet of the Serdoxit column dropped directly on to the top of the SCX column (with 0.5 g of packing material). The PAs were retained in the SCX column. The extract passed through the SCX column by action of gravity; there was no need for flow control. After all extract had passed through the SCX column, addition of 8 ml of MeOH was necessary to wash out other compounds (Fig. 1: 3).

The PAs were eluted from the SCX resin with 8 ml of HCl–MeOH (1) solution (Fig. 1: 4). This eluate was made alkaline with 3 ml of ammonia solution (Fig. 1: 5) and then mixed with 1.5 ml of dichloromethane (Fig. 1: 6). After vigorous shaking, an aliquot of the CH_2Cl_2 layer was

taken (Fig. 1: 7) and evaporated to dryness. If larger sample volumes had to be analysed and greater enrichment was desired, larger SCX columns containing 2 g of packing material were used. In this event 12 ml of HCl–MeOH (1) solution were necessary to elute the PAs.

2.5. Capillary gas chromatography

The GC apparatus used was a Carlo Erba Vega Series 6000 equipped with a Carlo Erba DP 700 integrator and a Carlo Erba A200S autosampler and flame ionisation detector (Fisons Instruments, Milan, Italy). Various apolar capillary GC columns are suitable. For this work two different columns were employed. One was an SE-54 (Machery–Nagel, Düren, Germany) capillary column (50 m × 0.32 mm I.D.; 0.25-μm film thickness) operated with the following temperature programme: 1 min at 150°C, increased at 6.5°C/min to 260°C, 10 min at 260°C, increased at 10°C/min to 280°C. Most of the PAs eluted in this system at 260°C. Alternatively, an Rtx-5 column (30 m × 0.32 mm I.D.; 0.1-μm film thickness) was used (Restek; obtained from ICT). The temperature programme was 3 min at 120°C, increased at 6°C/min to 230°C, 8 min at 230°C, increased at 10°C/min to 270°C. The PAs eluted at 230°C. Hydrogen was used as the carrier gas for the first column and helium for the second column at the optimal velocity. The detector temperature was set at 280°C and the injector temperature at 260°C with a bottom split of *ca.* 12 ml/s.

The dried sample from the clean-up procedure was taken up to 100 μl of MeOH containing the internal standard caffeine and 1 μl of this solution was injected into the GC system. To establish the calibration graph, 5–150 μl of senecionine solution (7.3 mg in 50 ml) were evaporated to dryness and the residue was dissolved in 100 μl of internal standard solution 0.36 mg/ml. Each of the concentrations was injected at least three times. The ratios of the senecionine peak area to the caffeine peak area were calculated and plotted against the amount of senecionine in micrograms.

2.6. High-performance thin-layer chromatography

The dried PA fraction from the clean-up step was dissolved in 100 μl of MeOH and 2–10 μl of this solution were applied to the TLC plates in 2-mm bands using a Camag (Berlin, Germany) Linomat IV automatic application device. On each plate three spots of 0.15–0.85 μg of a reference alkaloid (senecionine, seneciphylline or retrorsine) were placed for calibration.

The developing chamber was fitted with a filter-paper to ensure better saturation. The plates were removed after 20 min when the front has reached 7 cm. For detection the plates were dipped for 3 s into dipping solution (1) using a DC-Tauchfix dipping device from Baron (Insel Reichenau, Germany). After heating at 100°C for 1 min and cooling to room temperature, the plates were dipped into dipping solution (2) for 3 s and dried in an air stream.

Quantitative evaluation was carried out by scanning the plates with a CS 9000 dual-wavelength flying spot scanner from Shimadzu (Kyoto, Japan). It was operated in the reflection mode at 580 nm with a zig-zag scan amplitude of 5 mm.

2.7. Calculation of pyrrolizidine alkaloid content in the plant material

The PA content in the plant material was calculated according to the following equations which result from sample preparation.

In GC analysis the amount A of PA in the dried plant is given by

$$A = (x g_c v_e)/(g_a v_u p)$$

where A = amount of PA in dried plant (μg/g), x = amount of the individual alkaloid in the cleaned fraction, obtained from the calibration graph, g_c = amount of CH_2Cl_2 used in the clean-up procedure (g) (1.98 g per 1.5 ml), g_a = mass (g) of the aliquot of the CH_2Cl_2 layer which is brought to dryness, v_u = volume (ml) of the plant extract cleaned up, v_e = total volume (ml)

of the plant extract and p = amount (g) of dried plant extracted.

In TLC analysis the equation is

$$A = (xg_c v_e v_a)/(v_t g_a v_u p)$$

where v_a = volume (μl) in which the PA fraction has been taken up after clean-up (100 μl) and v_t = volume (μl) of alkaloid fraction applied to the TLC plate.

3. Results and discussion

The usual clean-up of alkaloid extracts carried out in separating funnels is lengthy and requires large amounts of solvents. This procedure has been replaced by the use of strong cation-exchange columns which at neutral pH bind PAs [4,5]. The addition of methanol to HCl for elution of PAs from the SCX column was necessary to obtain complete recovery. Moreover, the samples usually contain other compounds which also may be retained by ionic or non-specific interactions in the column and can be eluted with HCl. Therefore, an additional cleaning of the HCl eluate is required by making it alkaline and extracting it with dichloromethane.

3.1. Reduction of N-oxides

To determine PAs by GC or TLC they must be present as free alkaloids. As PAs extracted from plants occur at least partly as N-oxides, a reduction step is needed. The prevalent reduction of N-oxides with zinc dust in acidic medium, which requires several hours, has been replaced by the use of the oxygen-absorbing resin Serdoxit, allowing the reduction to be performed in a few minutes. Serdoxit, an adsorbate of indigosulphonate on a highly porous anion exchanger, enables mild reduction conditions to be used [6].

To test the reduction step with Serdoxit, a 2.1-ml portion of methanol containing 22.8 μg (0.0565 μmol) of retrorsine-N-oxide was passed through a Serdoxit column. The eluate containing retrorsine from retrorsine-N-oxide reduction was evaporated to dryness and the residue was dissolved in 200 μl of methanol. Its retrorsine content was determined by HPTLC with authentic retrorsine as a standard. For four replicates a mean of 0.060 ± 0.004 μmol of retrorsine was recorded. This indicates that complete reduction of the N-oxides was achieved.

3.2. Capillary gas chromatography

The determination of PAs by capillary GC is possible without derivatization steps [7] but they elute at fairly high temperatures. To decrease the elution temperature thin-film columns are preferable. A column length of 30–50 m is necessary to separate closely related PAs [7].

The calibration graph was recorded with senecionine and was used to calculate the amounts of all PAs. The typical shape of this graph can be seen in Fig. 2. It shows good linearity between 3 and 25 μg of senecionine in 100 μl of internal standard. At lower concentrations, however, the graph became flatter, indicating decomposition of PAs to a small extent in the GC system, an effect which could be observed on both columns used. The injection of small amounts of senecionine showed that 0.5 μg in 100 μl of internal standard (i.e., 5 ng injected) was still were detected by flame ionization detection. Because of the poor linearity of the calibration graph in this low concentration range, exact quantitative results were difficult to obtain. Nevertheless, working with 6 ml of plant

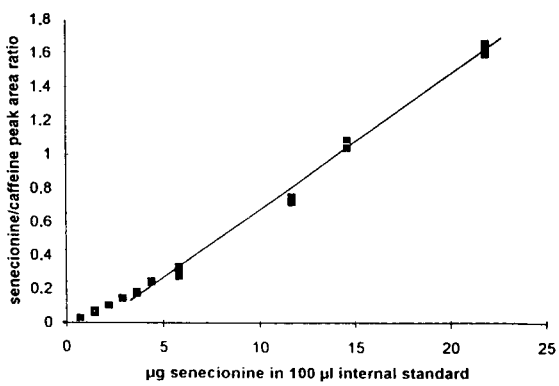

Fig. 2. Calibration graph for GC determination of pyrrolizidine alkaloids.

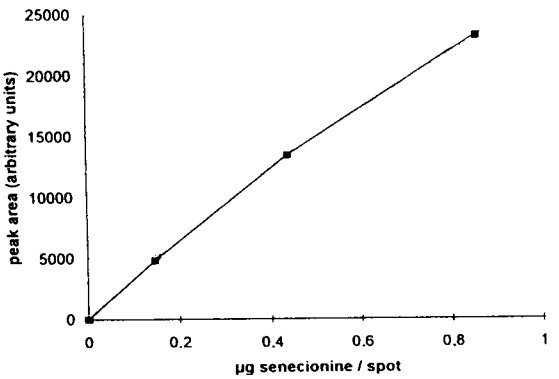

Fig. 3. Calibration graph for TLC determination of pyrrolizidine alkaloids.

extract, corresponding to 0.25 g of dried plant in the clean-up, a detection limit of 1.5–2 μg/g dried plant could be achieved. The use of larger SCX columns (with 2 g of packing material) allowed the preparation of larger sample volumes and greater enrichment. In this instance the detection limit could be decreased to 0.4–0.5 μg/g dried plant. Further enrichment was not appropriate as enriched impurities impaired the clarity of the chromatogram.

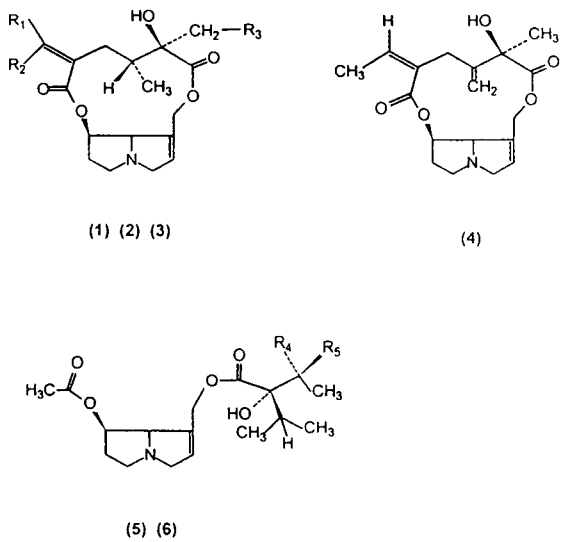

(1) (2) (3) (4)

(5) (6)

Fig. 4. Structures of some toxic pyrrolizidine alkaloids. 1 = Senecionine ($R_1 = R_3 = H$, $R_2 = CH_3$); 2 = integerrimine ($R_1 = CH_3$, $R_2 = R_3 = H$); 3 = retrorsine ($R_1 = H$, $R_2 = CH_3$, $R_3 = OH$); 4 = seneciphylline; 5 = acetyllycopsamine ($R_4 = H$, $R_5 = OH$); 6 = acetylintermedine ($R_4 = OH$, $R_5 = H$).

3.3. High-performance thin-layer chromatography

PAs were detected on the TLC plates through a reaction giving purple spots on a light yellow background. *o*-Chloranil corrects the PAs into pyrrole derivatives, which react with 4-dimethylaminobenzaldehyde to give purple complexes. N-Oxides do not react with *o*-chloranil [8,9]. This detection procedure was easier to carry out than those using H_2O_2 and acetic anhydride to generate the pyrrole derivatives [7].

Fig. 3 presents the calibration graph obtained by TLC scanning. It was necessary to record an individual calibration graph on each plate because the multitude of steps in the detection procedure did not allow exact, reproducible colour formation from plate to plate. The smallest spot that can still be seen or detected by the TLC scanner contained 20 ng of senecionine. With regard to sample clean-up with 0.5-g SCX columns, the detection limit of 2 μg/g dried plant was of the same order of magnitude as for GC analysis. There were, however, some differences between the individual PAs in colour formation on the TLC plate. Senecionine gave a 2.4-fold more intense colour than retrorsine.

3.4. Recovery of the whole pyrrolizidine alkaloid analysis

The equations for calculating the PA content of a plant sample were established on the assumption that quantitative extraction and enrichment of the alkaloids could be achieved. To test if this is so, 17.5 μg of senecionine were added to 5 ml of an extract from *Petasites hybridus* rhizomes. In the original extract 20.8 ± 1.00 μg of senecionine were recorded. After addition of senecionine, its content increased to 37.4 ± 4.6 μg (three replicates). Therefore, a recovery of more than 90% could be achieved.

3.5. Application to pyrrolizidine alkaloid-containing plants

The described sample preparation procedure was used to determine the PA content in *Senecio vulgaris*, a poisonous weed, *Symphytum officinale* and *Petasites hybridus*. The last two are medicinal plants, their use being impaired by the presence of toxic PAs as minor compounds. The structures of the PAs from the plants studied are

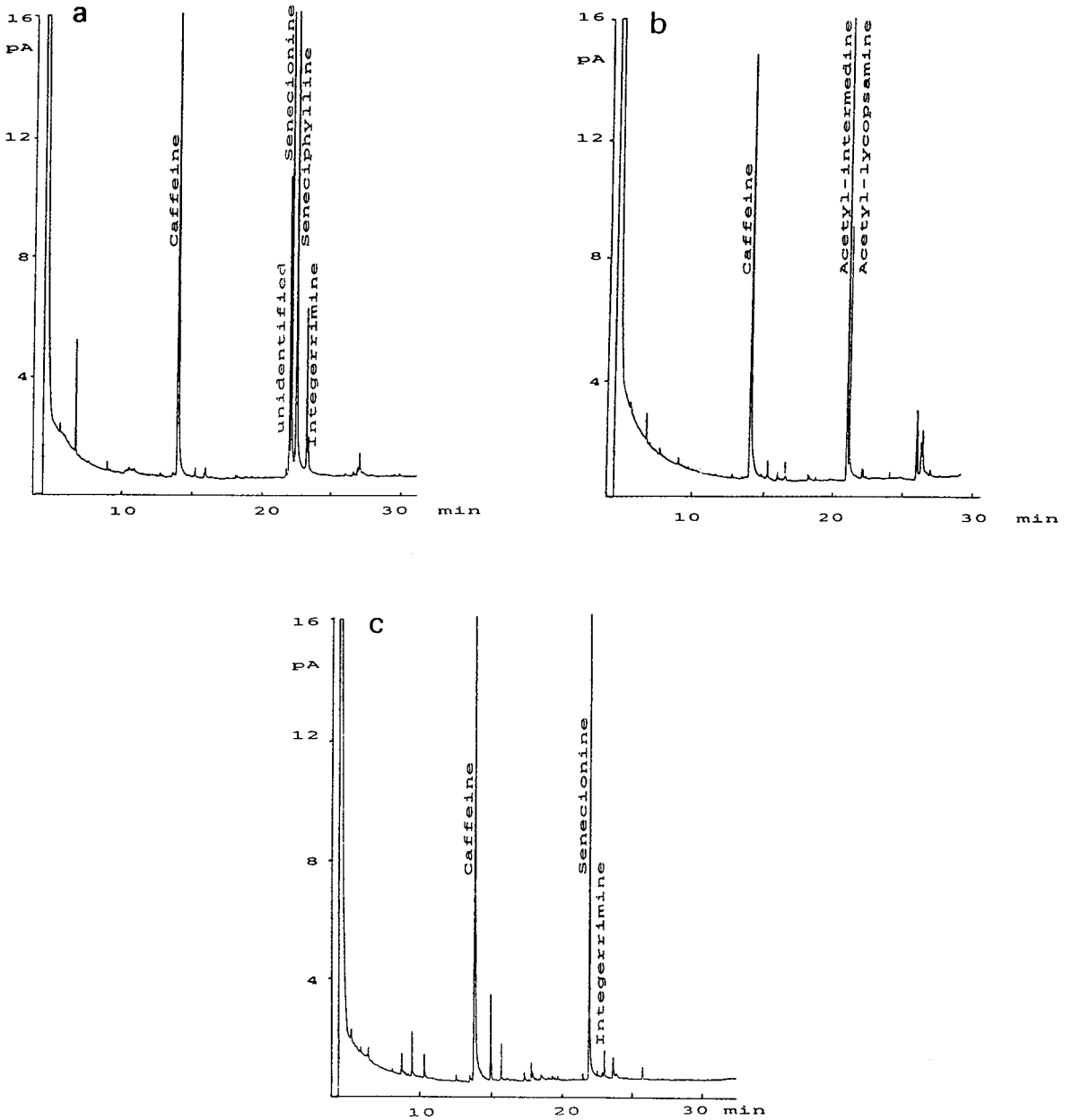

Fig. 5. Gas chromatograms from selected plant extracts after clean-up. (a) *Senecio vulgaris*; (b) *Symphytum officinale*; (c) *Petasites hybridus*.

Table 1
Pyrrolizidine alkaloid content of *Senecio vulgaris*, *Petasites hybridus* and *Symphytum officinale*.

Plant	Method	Compound	Concentration (μg/g)[a]
Senecio vulgaris (above-ground parts)	GC	Senecionine	354 (9.1%)
		Seneciphylline	632 (13.5%)
		Integerrimine	135 (16.7%)
	TLC		Not determined
Petasites hybridus (rhizomes)	GC	Senecionine	104 (4.8%)
		Integerrimine	12.4 (10.8%)
	TLC		161 (5.8%)
Symphytum officinale (roots)	GC	Acetylintermedine	463 (3.7%)
		Acetyllycopsamine	237 (6.8%)
	TLC		590 (6.9%)

[a] Means of 3–5 replicates in μg/g dried plant, with R.S.D. in parentheses.

shown in Fig. 4. The chromatograms shown in Fig. 5 were recorded on the Rtx-5 column, on which the internal standard caffeine eluted at a retention time of 14.00–14.05 min. *Senecio vulgaris* displayed an unidentified PA, senecionine, seneciphylline and integerrimine at retention times of 22.01, 22.16, 22.53 and 23.25 min, respectively (Fig. 5a). These alkaloids could not be separated by TLC. In *Symphytum officinale* the main PAs detected were the stereoisomers acetylintermedine and acetyllycopsamine, with retention times of 21.0 and 21.3 min, respectively (Fig. 5b). *Petasites hybridus* contained mainly senecionine and little integerrimine (Fig. 5c). Table 1 summarizes the amounts of individual PAs in the different plants. The highest PA content was in *Senecio vulgaris* and the lowest in *Petasites hybridus*. The analyses were carried out with 3–5 replicates for each plant. The standard deviation of the calculated PA content ranged from 3.7 to 16.7%. The discrepancies between GC and TLC analysis may arise from the different responses of the alkaloids in the colour formation on the TLC plate.

The proposed method is suitable for determining pyrrolizidine alkaloids from various plants over a wide concentration range.

4. Acknowledgement

This study was partly supported by the Fonds 200 Jahre Veterinärmedizinische Universität Wien.

5. References

[1] Th. Danninger, U. Hagemann, V. Schmidt and P.S. Schönhöfer, *Pharm. Ztg.*, 128 (1984) 289.
[2] A.R. Mattocks, *Chemistry and Toxicology of Pyrrolizidine Alkaloids*, Academic Press, New York, 1986.
[3] *Bundesanzeiger*, June 17th (1992) 4805; *Dt. Apoth. Ztg.*, 132 (1992) 1406.
[4] J.T. Deagen and M.L. Deinzer, *Lloydia*, 40 (1977) 395.
[5] Ch. Mauz, U. Candrian, J. Lüthy, Ch. Schlatter, V. Sery, G. Kuhn and F. Kade, *Pharm. Acta Helv.*, 60 (1985) 256.
[6] H.J. Huizing and T.M. Malingré, *J. Chromatogr.*, 173 (1979) 187.
[7] E. Röder and V. Neuberger, *Dtsch. Apoth.-Ztg.*, 128 (1988) 1991.
[8] R.J. Molyneux and J.N. Roitman, *J. Chromatogr.*, 195 (1980) 412.
[9] H.J. Huizing, F. De Boer and T.M. Malingré, *J. Chromatogr.*, 195 (1980) 407.

ELSEVIER

Journal of Chromatography A, 668 (1994) 435–439

JOURNAL OF CHROMATOGRAPHY A

Limitations of additivity of Kováts retention indices

Janusz Oszczapowicz

Department of Chemistry, Warsaw University, Pasteura 1, 02-093 Warsaw, Poland

Abstract

It is shown that the Kováts retention index is not a fully additive property. For the prediction of retention indices, a correlation method should be used instead of additivity. The value of the additivity parameter for a given group depends on the structure of the remainder of the molecule.

1. Introduction

It is assumed that retention index is an additive property, *i.e.*, the introduction of a certain substituent into molecules of similar structure changes their retention indices by the same value, called the additivity parameter or additivity increment. The additivity method, although not very precise, is often used in chromatographic practice on account on its simplicity. A retention index is calculated by addition of the increment for a substituent to the retention index of the unsubstituted compound.

However, in many instances, considerable differences between calculated and experimental values have been encountered. Budahegyi *et al.* [1], in a review on applications of the retention index system concluded, "Of the various methods available . . . the increment method is one of the most favourable. At present . . . a universal increment method fails for the retention index system, and its elaboration is a task for the near future". Hawkes [2,3] later showed that in some instances, "The rule that addition of a CH_2 group to a molecule increases the retention index by 100 ± 3 is subject to a greater uncertainty". Therefore, a new approach to the problem of retention index prediction was necessary.

2. Retention index prediction

It has been pointed out [4] that the prediction of any parameter for a compound belonging to one group based on the parameter of a corresponding compound belonging to another group is a typical problem of correlation analysis, where the parameters (P^1) of the compounds of one series are expressed as a function, usually linear, of the parameters (P^2) of compounds in another series:

$$P^1(x_i) = aP^2(x_i) + b \tag{1}$$

Any additivity scheme is a very particular case of the linear Eq. 1, namely one in which the slope of the correlation line (a) is by definition equal to unity, and only then does the term b become an additivity parameter. Therefore, before making any attempts at calculating additivity parameters for a group of compounds, an attempt at linear regression should be made, as only when a appears to be equal to unity will the additivity method yield reliable results.

The first attempts at the application of the correlation method instead of additivity rules for the prediction of retention indices were made less than 10 years ago [4–9]. In our laboratory,

0021-9673/94/$07.00
SSDI 0021-9673(93)E1164-U

structure–retention relationships have been investigated for several series of compounds containing amidino (–N=CR–N<) or imino (–N=C<) groups (amidines and imines). The retention indices of these compounds were in the wide range between 800 and 2800 index units (i.u.).

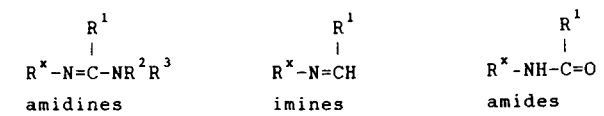

As the variable substituents R^x in the series, C_3–C_{10} *n*-alkyl groups, isopropyl, isobutyl, cyclohexyl and benzyl were chosen, and as aryl groups both *meta* and *para* methyl-, methoxy-, ethoxy-, fluoro-, chloro-, bromo- and nitrophenyl isomers were chosen.

Accordingly to additivity rules, the retention index of a compound containing a given functional group is calculated by addition of the increment of this group to the retention index of the unsubstituted compound. Amidino ($-N=CR^1-NR^2R^3$), imino ($-N=CHR^1$) or acylamino ($-NH-CO-R^1$) groups are the substituents whose increments should be added to the retention indices of the corresponding hydrocarbons R^xH taken as the reference compounds (standards). In the correlation method, retentions of compounds with a given substituent are linearly related to the retention indices of unsubstituted compounds. The relationship has the form

$$I(\mathrm{Cpd}_i) = aI(\mathrm{Std}_i) + b \qquad (2)$$

where I = Kováts retention index, Cpd = compound and Std = reference compound (standard).

In spite of the common practice, the use of hydrocarbons or substituted hydrocarbons R^xH as the basis for the prediction of retention data for compounds containing their moieties in the molecule does not seem to be the best choice, because isomerism is not taken into account. Hence we have assumed that better, more accurate results might be obtained if other simple compounds, containing some functional group at the corresponding carbon atom, were taken as the references. For the studied series, primary amines (R^xNH_2; see formulae) seemed to be the most appropriate, because they are available as the substrates for the synthesis of all the types of compounds studied. Correlation would show the change in the retention index when the NH_2 group is replaced by an amidino, imino or amido group.

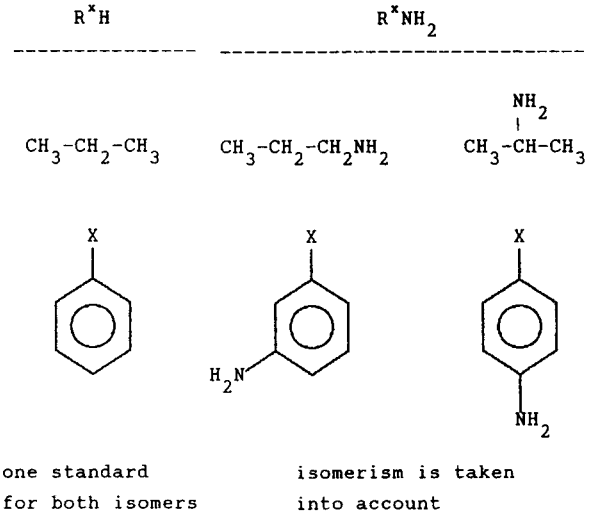

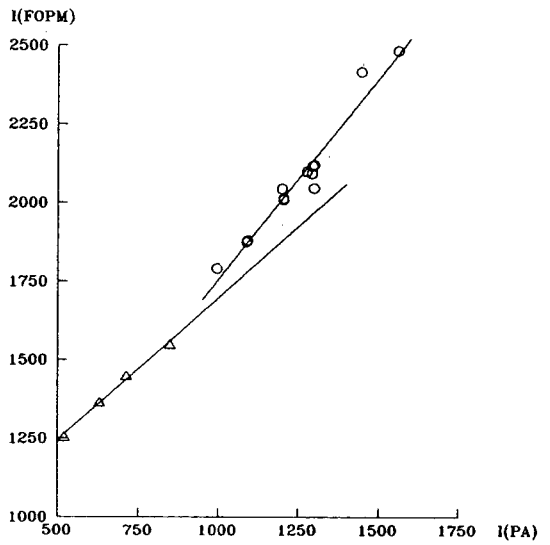

Fig. 1. Correlation of retention indices of N^1,N^1-(3-oxapentamethylene)formamidines (FOPM) with those of corresponding primary amines (PA).

The proper choice of model compounds for the prediction of retention indices appears to be very important. For each series of compounds the correlation with the retention indices of primary amines is of higher quality than that with unsubstituted hydrocarbons, and therefore is of greater predictive value. However, correlations with the retentions of hydrocarbons are still satisfactory.

Attempts at correlation for all the series studied revealed that in each instance there are at least two regression lines, one for compounds containing purely aliphatic substituents and the other for those with a substituted phenyl ring, as shown by the two examples in Figs. 1 and 2. Therefore, for compounds with aliphatic and aromatic substituents separate correlations were calculated. The amidines can be divided into series depending on the substituents at the amidino carbon atom and further at the amino nitrogen atom.

The regression coefficients a with confidence intervals calculated at a significance level of 0.05 for the series with an alkyl group at the amidino carbon atom are given in Table 1. For most of the series the slopes of the correlation lines (a) are not significantly different from unity, but for two series, alkyl derivatives of dimethylacetamidines (ADM) and aryl derivatives of amidines containing a morpholine moiety (FOPM), they are undoubtedly different from unity. The best example is provided by alkyl derivatives of acetamidines, where the correlation is of excellent quality, as shown by the correlation coefficient r.

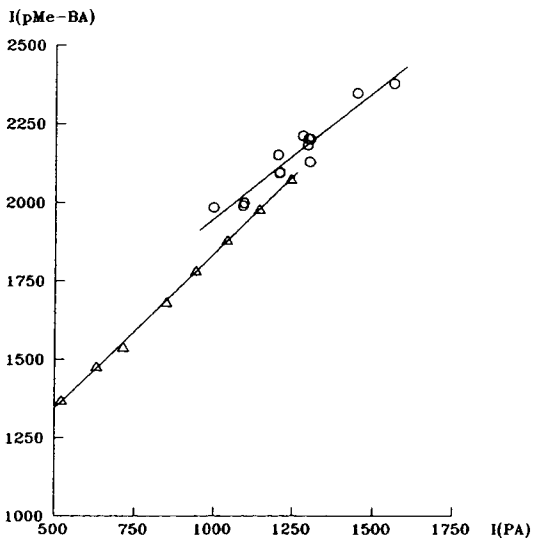

Fig. 2. Correlation of retention indices of p-methylbenzylideneanilines (pMe-BA) with those of corresponding primary amines (PA).

Table 1
Parameters of correlations[a] of retention indices of amidines[b] and tetramethylguanidines[b] with those of primary amines

Series[c]	a	b	r
Alkyl derivatives			
FDM	0.91 ± 0.22	400	0.997
ADM	0.86 ± 0.04	553	0.9999
FTM	0.91 ± 0.30	737	0.994
FPM	0.94 ± 0.23	788	0.997
FHM	0.90 ± 0.23	915	0.997
FOPM	0.92 ± 0.24	782	0.997
TMG	1.07 ± 0.53	462	0.987
Aryl derivatives			
FDM	1.05 ± 0.11	337	0.986
ADM	0.99 ± 0.11	470	0.986
FTM	0.99 ± 0.09	760	0.989
FPM	0.99 ± 0.09	826	0.990
FHM	1.02 ± 0.10	885	0.989
FOPM	1.28 ± 0.19	477	0.976
TMG	1.09 ± 0.13	421	0.982

[a] I(amidine) = aI(amine) + b.
[b] On the basis of refs. 4 and 6.
[c] For abbreviations, see formulae in text.

It should be mentioned that even when a can be taken as equal to unity, the terms b are not identical for alkyl and aryl series. The difference between "additivity parameters" for alkyl and aryl derivatives are as high as 300 i.u. in some instances. In all correlations isoalkyl and cyclohexyl derivatives do not fit the corresponding correlations, and for such compounds other "additivity parameters" are obtained.

Non-additivity is much more evident for benzamidines (Z-BDM) and benzylideneamines (imines, Z-BA) (see formulae). Parameters of the linear regressions for these compounds are summarized in Table 2. For all series of alkyl

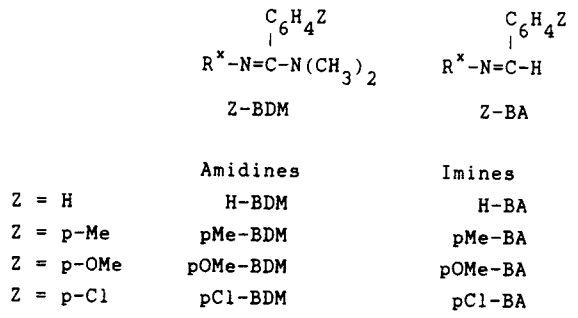

derivatives of dimethylbenzamidines (BDM) and for *p*-methylbenzylideneanilines (pMe-BA), the regression coefficient *a* is distinctly different from unity. For other series, where *a* does not differ significantly from unity, other values of *b* are obtained for alkyl and aryl derivatives.

Non-additivity is observed also for monosubstituted amides of carboxylic acids. Analysis of the parameters of these correlations presented in Tables 3 and 4 lead to similar conclusions.

Amides of butyric acids may serve as a good example of the influence of the structure of an alkyl chain, such as exchange of an *n*-propyl for an isopropyl group, on the values of the retention indices in the series. Correlation of the retention indices of the amides of isobutyric acid with those of the straight-chain isomer (Table 5) clearly indicates that such a change does not involve a change in retention index by a constant value, thus providing further support for the conclusion that retention index is not fully additive property. It seems very likely that the main

Table 2
Parameters of correlations[a] of retention indices of dimethylbenzamidines[b] and corresponding imines[b] with those of primary amines

Series[c]	*a*	*b*	*r*
Alkyl derivatives			
H-BDM	0.84 ± 0.11	1021	0.991
pMe-BDM	0.83 ± 0.14	1098	0.986
pOMe-BDM	0.82 ± 0.11	1257	0.991
pCl-BDM	0.82 ± 0.11	1216	0.991
H-BA	0.97 ± 0.07	751	0.997
pMe-BA	0.99 ± 0.03	851	0.999
pOMe-BA	0.95 ± 0.03	1042	0.9995
pCl-BA	0.98 ± 0.09	1040	0.997
Aryl derivatives			
H-BDM	0.93 ± 0.23	907	0.950
pMe-BDM	0.91 ± 0.21	999	0.956
pOMe-BDM	0.89 ± 0.21	1162	0.954
pCl-BDM	0.91 ± 0.24	1098	0.946
H-BA	0.94 ± 0.24	840	0.948
pMe-BA	0.78 ± 0.24	1171	0.926
pOMe-BA	0.96 ± 0.25	1023	0.946
pCl-BA	0.89 ± 0.15	1224	0.971

[a] $I(\text{amidine}) = aI(\text{amine}) + b$.
[b] On the basis of ref. 5.
[c] BDM = Benzamidines; BA = benzylideneamines.

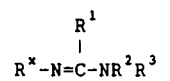

R^1	NR^2R^3	Series	Abbr.
H	NMe_2	N^1,N^1-dimethylformamidines	FDM
CH_3	NMe_2	N^1,N^1-dimethylacetamidines	ADM
H	N□	N^1,N^1-tetramethyleneformamidines	FTM
H	N⬡	N^1,N^1-pentamethyleneformamidines	FPM
H	N⬡	N^1,N^1-hexamethyleneformamidines	FHM
H	N⬡O	N^1,N^1-(3-oxa-pentamethylene)-formamidines	FOPM
NMe_2	NMe_2	N^1,N^1,N^2,N^2-tetramethylguanidines	TMG

Table 3
Parameters of correlations[a] of retention indices of formamides[b], $HCONHR^x$ (FA), and acetamides[b], CH_3CONHR^x (AA), with those of primary amines

Series	a	b	r
Alkyl derivatives			
FA	1.05 ± 0.06	359	0.999
AA	1.04 ± 0.07	665	0.998
Aryl derivatives			
FA	0.89 ± 0.10	588	0.988
AA	1.00 ± 0.07	425	0.995

[a] $I(\text{amide}) = aI(\text{amide}) + b$.
[b] According to ref. 10.

Table 4
Parameters of correlations[a] of retention indices of monosubstituted amides of *n*-butyric acid[b] (A-nBtr) and isobutyric acid[b] (A-iBtr) with those of primary amines (PA)

Series	a	b	r
Alkyl			
A-nBtr	1.05 ± 0.11	509	0.992
A-iBtr	0.94 ± 0.06	569	0.997
Aryl			
A-nBtr	0.84 ± 0.15	746	0.969
A-iBtr	0.97 ± 0.12	506	0.987

[a] $I(\text{amide}) = aI(\text{amine}) + b$.
[b] According to ref. 11.

reason why the retention index system fails for some types of compounds is the assumption of additivity.

Table 5
Parameters of correlations[a] of retention indices of monosubstituted amides of isobutyric acid (A-iBtr) with those of amides of *n*-butyric acid (A-nBtr)

R	Series	a	b	r
Alkyl	A-iBtr	0.82 ± 0.13	238	0.99
Aryl	A-iBtr	0.91 ± 0.13	98	0.99

[a] $I(\text{A-iBtr}) = aI(\text{A-nBtr}) + b$.

3. Conclusions

The Kováts retention index is not a fully additive property. For prediction of the retention indices the correlation method (Eq. 2) should be used instead. The term *b* in this equation is a real additivity parameter only when *a* is equal to unity.

Series of compounds containing *n*-alkyl and aryl groups should be treated separately, because even when *a* is equal to unity, the *b* term for them may appear different, *i.e.*, another "additivity parameter" is obtained for each group.

Compounds with non-linear alkyl groups such as isopropyl, *tert.*-butyl or cyclohexyl do not belong to the same family as *n*-alkyl groups. It is not possible at present to determine whether they belong to one or to more groups, because insufficient experimental data are available.

4. Acknowledgement

This research was supported by project 2 0584 91 01 from the Committee for Scientific Research.

5. References

[1] M.V. Budahegyi, E.R. Lombosi, T.S. Lombosi, S.Y. Mészáros, Sz. Nyiredy, G. Tarján, I. Timar and J.M. Takács, *J. Chromatogr.*, 271 (1983) 213.
[2] S.J. Hawkes, *Chromatographia*, 28, 237 (1989).
[3] S.J. Hawkes, *Chromatographia*, 32, 211 (1991).
[4] J. Oszczapowicz, J. Osek and E. Dolecka, *J. Chromatogr.*, 315 (1984) 95.
[5] J. Oszczapowicz, J. Osek, K. Ciszkowski, W. Krawczyk and M. Ostrowski, *J. Chromatogr.*, 330 (1985) 79.
[6] J. Osek, J. Oszczapowicz and W. Drzewiński, *J. Chromatogr.*, 351 (1986) 177.
[7] J. Oszczapowicz, J. Osek, W. Krawczyk and B. Kielak, *J. Chromatogr.*, 357 (1986) 93.
[8] J. Oszczapowicz, K. Ciszkowski and J. Osek, *J. Chromatogr.*, 362 (1986) 383.
[9] J. Osek, J. Jaroszewska-Manaj, W. Krawczyk and J. Oszczapowicz, *J. Chromatogr.*, 369 (1986) 398.
[10] J. Oszczapowicz, J. Kowalczyk and J. Tykarski, in preparation.
[11] J. Oszczapowicz, D. Weych and K. Weber, in preparation.

ELSEVIER

Journal of Chromatography A, 668 (1994) 441–448

JOURNAL OF CHROMATOGRAPHY A

Relative electron-capture detector response of selected polychlorinated biphenyl congeners Influence of detector temperature and design ☆

M. Cigánek, M. Dressler*, V. Lang☆☆

Institute of Analytical Chemistry, Academy of Sciences of the Czech Republic, Veveří 97, 611 42 Brno, Czech Republic

Abstract

Molar and mass responses for polychlorinated biphenyls (PCBs) IUPAC Nos. 28, 52, 77, 101, 126, 138, 153, 169 and 180 were determined for electron-capture detectors of two different designs, Model 400 (Carlo Erba) and PU 4400/03 (Philips Scientific). The detector temperature influences the response level of different PCB congeners in different ways. The course of the dependences of the molar responses on temperature in the range 150–360°C varies for different congeners. It is also influenced by the design of the detector. The presence of oxygen in the gas passing through the detector influences the response of PCB congeners. The application of the relative responses determined at one detector temperature to another temperature can produce a relative error of several tens per cent. The same is valid for the application of the relative responses from one detector design to another design. The error with different oxygen contents in the carrier gas can also be 100%.

1. Introduction

Polychlorinated biphenyls (PCBs) are prominent environmental contaminants [1] and belong among eleven global chemical pollutants [2]. Owing to their high stability, their effect on the environment and their harmful effects on human health, PCBs are among the most frequently investigated analytes in environmental analytical chemistry. The electron-capture detector (ECD) is the most often used detection system for trace analysis of PCBs. The ECD temperature is known to be an important parameter influencing the detector response; a variation of 3% can result in a 10% error in the evaluation of the capture coefficient [3]. There are a number of tabulated responses both for selected [4–6] PCBs and for all PCB congeners [7,8]. They were measured under different experimental conditions and for different ECD types. Many data on experimental conditions under which the responses were determined are incomplete.

The basic idea of this work was to study the behaviour of selected PCB congeners in ECDs at different detector temperatures. The effects of the detector design and amount of oxygen in the gas on the course of the temperature dependences were also investigated. Six PCB congeners used to follow threshold limits for total PCBs in food [9] with IUPAC designation [10] Nos. 28, 52, 101, 138, 153 and 180 (the standard compounds) and three most toxic congeners with

* Corresponding author.

☆ This study was performed as a part of the project TOCOEN (Toxic Organic Compounds in the Environment), Part XXVII.

☆☆ Present address: MEGA, Department of Analytical Laboratories, 471 27 Stráž pod Rálskem, Czech Republic.

0021-9673/94/$07.00
SSDI 0021-9673(93)E0007-H

IUPAC Nos. 77, 126 and 169 (the toxic compounds) were selected. The standard congeners are used for congener-selective determination of PCBs. The toxic congeners are most important for congener-selective determination with respect to evaluation of the toxic effects of PCBs.

2. Experimental

2.1. Materials

PCBs Nos. 28, 52, 77, 101, 126, 138, 153, 169 and 180 were obtained from Promochem (Germany). The carrier and make-up gas (nitrogen) with a stated content of 6 ppm (v/v) of oxygen was purchased from Linde-Technoplyn (Czech Republic). For some PCB analyses nitrogen as carrier gas can be advantageous. For the preparation of nitrogen containing less than 1 ppm of oxygen, an oxygen scrubber from Hewlett-Packard USA) was used. An HP-5 capillary column (I.D. 0.53 mm) from Hewlett-Packard was employed. For injection of liquid samples, 75SN Grob and 7001N syringes from Hamilton (Bonaduz, Switzerland) were used.

2.2. Apparatus

Two gas chromatographs were used: a PU 4400 (Philips Scientific, Cambridge, UK) with a PU 4400/03 ECD detector and an HRGC 5300 Mega Series (Carlo Erba, Milan, Italy) with a Model 400 ECD. Both detectors are coaxial models.

The experimental conditions for the PU 4400 were as follows: the packed column, 3.1 m × 4.0 mm I.D., Chromosorb W AW (80–100 mesh) with 10% of SE-54; column temperature, 210°C; flow-rates of nitrogen containing 6 ppm of oxygen and nitrogen containing less than 1 ppm of oxygen, 45.0 ± 0.3 ml min^{-1}; injector temperature, 230°C; volume injected, 1 μl of a solution containing 0.5 ng of each PCB congener in hexane; detector temperature, increased from 150°C to 360°C at 30°C min^{-1}; no make-up gas; constant-current mode; detector current 12.

The experimental conditions for the HRGC 5300 were as follows: HP-5 capillary column, length 30 m × 0.53 mm I.D.; film thickness, 0.88 μm; temperature programme, initially 60°C (held for 2 min), increased at 20°C min^{-1} to 200°C, at 5°C min^{-1} to 230°C and at 3°C min^{-1} to 260°C (held for 10 min); flow-rate of nitrogen containing less than 1 ppm of oxygen, 7.8 ± 0.2 ml min^{-1}; on-column injector; volume injected, 1 μl of a solution containing 0.5 ng of each PCB congener in hexane; detector temperature, increased from 150°C to 390°C at 30°C min^{-1}; total flow-rate through the detector, 33.0 ± 0.3 ml min^{-1}; constant-current mode; pulse voltage, 50.0 V; pulse width, 1 μs; reference current, 1.0 nA; attenuation, 128.

The PCB congener responses at each temperature used fall within the linear response range of both detectors.

For processing the signals from the detectors an HP 3393A integrator (Hewlett-Packard) was used. The response values given are the arithmetic averages of three parallel measurements of the peak area.

The congeners used are presented in Table 1. Quantification of the data obtained was performed with the values of the molar (MR) and mass responses (WR): $MR_i = A_i M_i / m_i$ where M_i is the molecular mass of congener i, m_i the amount of congener i injected in grams and A_i the area in digits given by the integrator; $WR = A/m_i$.

Table 1
PCB congeners tested

PCB No.	Substitution pattern	Number of chlorine atoms
28	2,4,4′	3
52	2,2′,5,5′	4
77	3,3′,4,4′	
101	2,2′,4,5,5′	5
126	3,3′,4,4′,5	
138	2,2′,3,4,4′,5	6
153	2,2′,4,4′,5,5′	
169	3,3′,4,4′,5,5′	
180	2,2′,3,4,4′,5,5′	7

Table 2
Molar responses (*MR*) and relative molar responses (*RMR*)

PCB No.	Model 400		PU 4400		RMR_{PU}/RMR_{400}
	$MR \times 10^{-14}$	*RMR*	$MR \times 10^{-14}$	*RMR*	
28	6.7	0.96	11.6	0.58	0.60
52	1.8	0.26	5.1	0.25	0.96
77	5.8	0.83	34.0	1.69	2.04
101	7.0	1.00	20.1	1.00	1.00
126	12.3	1.76	53.3	2.65	1.51
138	16.8	2.40	58.9	2.93	1.22
153	11.5	1.64	79.7	3.98	2.43
169	17.7	2.53	65.1	3.24	1.28
180	26.8	3.83	93.3	4.64	1.21

Detector temperature = 400°C.

3. Results and discussion

3.1. Congener response

Table 2 presents the values of the molar and relative molar responses of PCB congeners at 300°C with the gas containing less than 1 ppm of oxygen. The molar responses on the Model 400 ECD increase in the order of PCBs 52, 77, 28, 101, 153, 126, 138, 169 and 180. The highest molar responses in the group with the same number of chlorine atoms are found for PCB congeners 77, 126 and 169 (toxic congeners). The molar responses on the PU 4400 detector increase in the order of PCBs 52, 28, 101, 77, 126, 138, 169, 153 and 180. As with the Model 400 ECD, congener No. 180 has the highest molar response. The toxic congeners again have the highest responses except for No. 169, which has a lower molar response than No. 153.

Table 3 gives the mass and relative mass responses of individual congeners. The order of the values is similar to that for the molar responses, except that the order of congeners 28 and 101 for the Model 400 ECD and of congeners 126 and 138 for the PU 4400 is changed. Toxic congeners also have the highest mass response. The magnitude of the response depends not only on the number of chlorine atoms in the biphenyl molecule but also on the structure of the congener (see also refs. 4 and 5).

3.2. Influence of ECD temperature on the response of PCBs

For comparison of the courses of the dependences of the response on the ECD temperature, PCB molar responses were related to the molar response of congener No. 28 at a detector temperature of 150°C. Fig. 1 shows the courses

Table 3
Mass responses (*WR*) and relative mass responses (*RWR*)

PCB No.	Model 400		PU 4400		RWR_{PU}/RWR_{400}
	WR	*RWR*	*WR*	*RWR*	
28	2.60	1.21	4.50	0.73	0.60
52	0.62	0.29	1.75	0.28	0.97
77	1.98	0.93	11.60	1.88	2.02
101	2.14	1.00	6.16	1.00	1.00
126	3.76	1.76	16.60	2.69	1.53
138	4.65	2.17	16.3	2.65	1.22
153	3.19	1.49	22.1	3.59	2.41
169	4.90	2.29	18.0	2.92	1.28
180	6.78	3.17	23.6	3.83	1.21

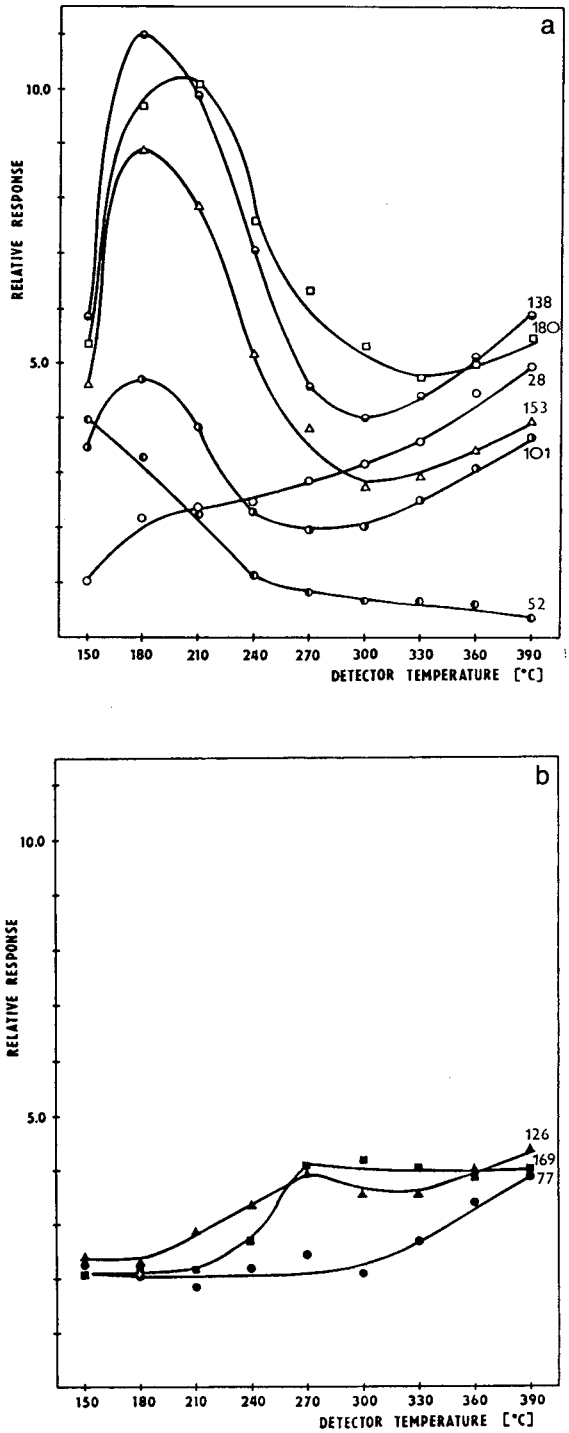

Fig. 1. Relative molar responses of selected PCBs with the Model 400 ECD.

of the congener dependences on the Model 400 ECD with nitrogen containing less than 1 ppm of oxygen and Fig. 2 shows the courses for the PU 4400 ECD with the same oxygen content in the gas. Fig. 3 shows the courses for the PU 4400 ECD with nitrogen containing 6 ppm of oxygen. The dependences are divided into two panels to permit a clear comparison of the dependences of standard and toxic congeners, respectively.

The PCB congener responses change with the ECD temperature in different ways. The order of the magnitudes of the congener relative responses also changes. The effect of the ECD temperature on the response of the PCBs is analysed in greater detail for the Model 400 ECD. At 150°C the magnitudes of the relative responses increase in the order of PCBs 28, 169, 77, 126, 101, 52, 153, 180 and 138 and at 330°C the order is PCBs 52, 101, 77, 153, 28, 126, 169, 138 and 180 (Fig. 1a and b). The change in the detector temperature by 180°C causes an important change in the order of the responses. In the range from 270 to 360°C, to which a detector is heated for the detection of analytes of low volatility, there are various changes in the relative molar responses of PCB congeners. This is important information which must be taken into account when quantifying the data obtained by an ECD. This is also demonstrated by the data in Table 4, giving the relative molar responses of the congeners at 180, 300 and 360°C on both detectors. The response changes are accidental at different temperatures on both detectors. This follows more clearly from the relative errors originating from application of the responses found at one detector temperature to another temperature (300°C). With changes in the detector temperature serious errors in the quantification of congeners may occur. Both positive and negative errors occur for different congeners and they reach up to 370%.

3.3. Influence of congener structure on the course of the response dependence

The influence of the congener structure on the course of the response dependence is analysed in a greater detail for the Model 400 detector. The

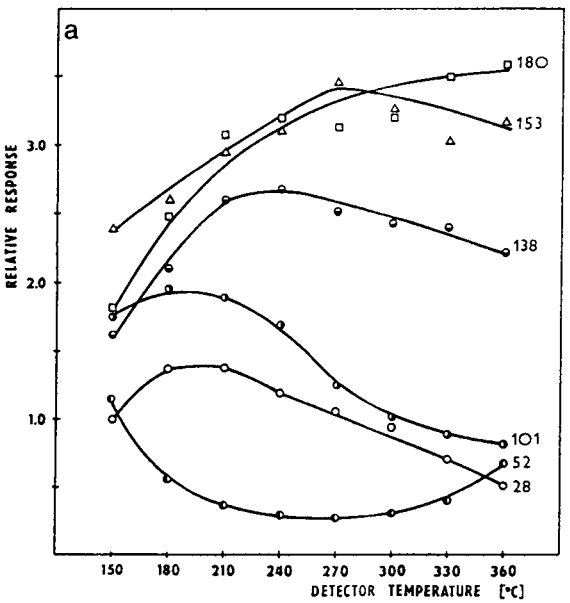

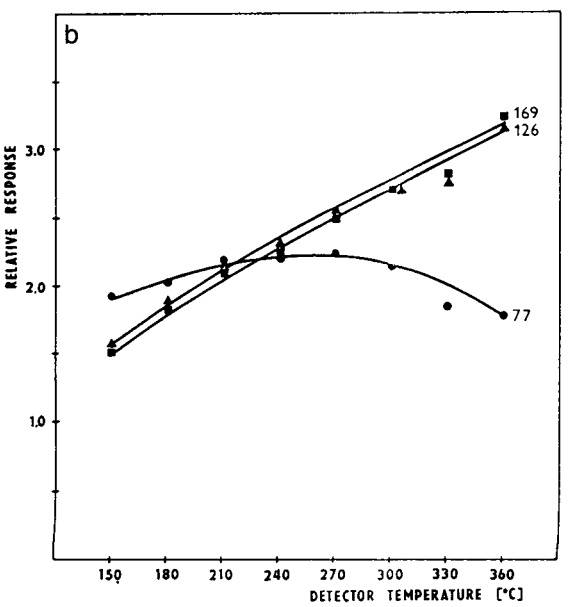

Fig. 2. Relative molar responses of selected PCBs with the PU 4400/03 ECD without oxygen in nitrogen.

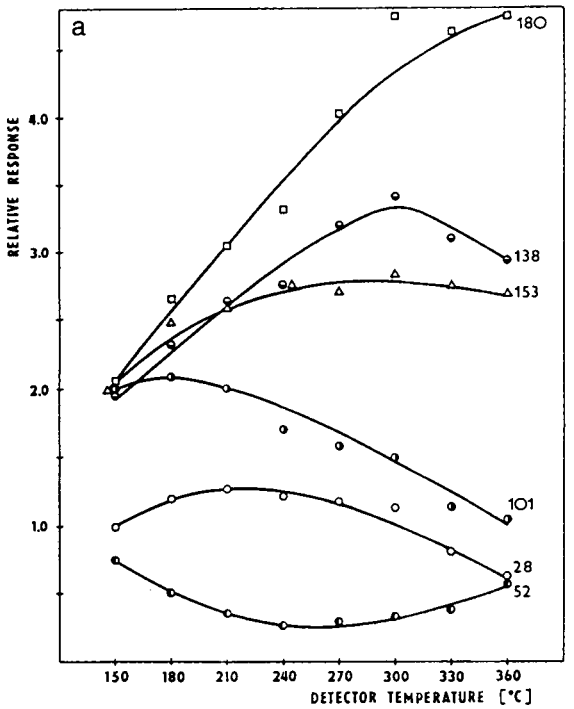

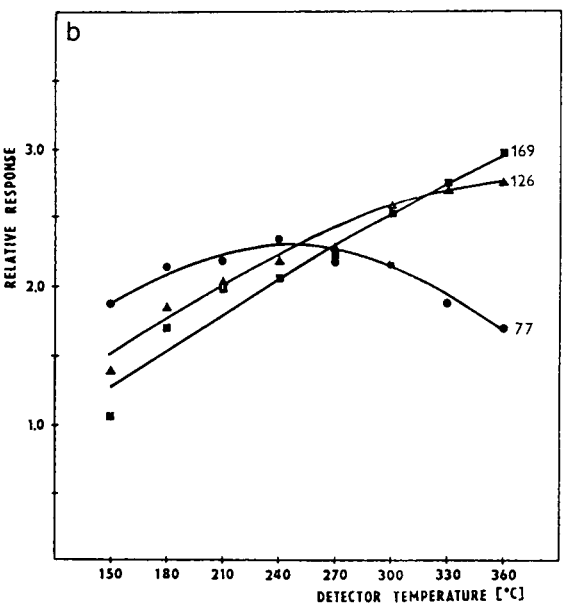

Fig. 3. Relative molar responses of selected PCBs with the PU 4400/03 ECD with 6 ppm of oxygen in nitrogen.

Table 4
Relative molar responses (*RMR*) for different detector temperatures and their relative errors (%) with respect to the *RMR* at 300°C

PCB No.	CE					PU				
	180°C		300°C: *RMR*	360°C		180°C		300°C: *RMR*	360°C	
	RMR	%		*RMR*	%	*RMR*	%		*RMR*	%
28	2.2	−31	3.2	4.5	+41	1.3	+44	0.9	0.5	−44
52	3.3	+371	0.7	0.6	−14	0.6	+100	0.3	0.7	+133
77	2.1	0	2.1	3.4	+62	2.0	−5	2.1	1.8	−14
101	4.7	+153	2.0	3.1	+55	2.0	+102	1.0	0.8	−20
126	2.3	−36	3.6	4.0	+11	1.9	−30	2.7	3.2	+19
138	11.0	+175	4.0	5.1	+28	2.1	−12	2.4	2.2	−8
153	8.9	+230	2.7	3.4	+26	2.6	−22	3.3	3.2	−3
169	2.2	−48	4.2	3.9	−7	1.9	−30	2.7	3.2	+19
180	9.7	+83	5.3	5.0	−6	2.5	−22	3.2	3.6	+13

dependences in Fig. 1a show that congeners Nos. 101, 153, 180 and 138 have maximum responses in the temperature range 180–200°C, No. 28 has the maximum response at 390°C and No. 52 at 150°C. In the given temperature range the response dependences of congeners Nos. 101, 153, 180 and 138 have one maximum and one minimum. The response for congener No. 28 increases monotonically with increase in temperature, whereas that of congener No. 52 decrease. For congeners Nos. 77, 126 and 169 the difference in the response dependences with variation in temperature is not so important (Fig. 1b).

From comparison of the response dependences of the congeners with the same number of chlorine atoms the following conclusions can be drawn.

Tetrachlorobiphenyls

The response of congener No. 52 decreases with increase in temperature and that of No. 77 remains constant in the range 150–300°C and then increases; in the range 150–210°C No. 52 has a higher response whereas above 210°C it is congener No. 77.

Pentachlorobiphenyls

The response of congener No. 126 increases with the increase in temperature with a local maximum at 270°C. No. 101 has the highest response at 180°C; in the range 150–220°C No. 101 has a higher response, whereas above 220°C it is No. 77.

Hexachlorobiphenyls

The responses of congeners Nos. 138 and 153 have the highest value at 180°C and the lowest at 300°C; for congener No. 169 the response increases up to 270°C and then remains constant; No. 169 has a higher response than No. 153 in the temperature range 260–390°C; congener No. 138 has a higher response over the whole range of temperatures.

The changes in the courses of the congener response dependences on ECD temperature are assumed to be due to different electron-capture mechanisms at different detector temperatures [11].

3.4. Dependence of the response on the detector design

The design and dimensions of the ECD cell plays an important role in its performance. The electron-capture coefficients in different ECDs can therefore differ.

The difference between Figs. 1a and 2a and between Figs. 1b and 2b gives an idea of the influence of different ECD designs (Model 400 and PU 4400) on the PCB congener relative responses and on the courses of the temperature dependences. With the Model 400 ECD a capillary column was used. The make-up gas flow-rate was such as to produce an overall gas flow-rate through the detector similar to that in the PU 4400 ECD with a packed column. These overall flow-rates through the ECD were optimized according to the detector design. The dependences of the relative responses have different shapes on the two detectors. The response maxima for PCBs Nos. 101, 138 and 153 are shifted to higher temperatures on the PU 4400. The response of No. 180 increases monotonically with increase in temperature. The response of No. 28 decreases monotonically from 210°C, in contrast to the course on the Model 400 ECD. No. 77 exhibits the maximum response on the PU 4400 at *ca.* 270°C. Congeners Nos. 126 and 169 have different courses of the response dependences, their response increasing almost linearly with increase in temperature.

In Table 5 we compare published data and our results for the mass responses of individual congeners relative to congener No. 101. The differences are large: the difference between the lowest and the highest relative response on different types of ECD (and with different experimental conditions) is almost sevenfold (Nos. 153 and 180). The differences are caused by the experimental conditions, *i.e.*, the detector temperature, flow-rate and purity of the gases, the detector regime (frequency and width of pulses) and the amount of solutes (in consequence of the limited ECD linearity). The PCB responses in the literature are mostly related to octachloronaphtalene (OCN), which should minimize the influences of the experimental conditions and apparatus on the response. However, it follows from Table 5 that in spite of this, considerable differences exist between the published data for the relative responses of PCBs.

Tables 2 and 3 give a comparison of the relative responses we measured on two different ECDs at the same detector temperature, the other experimental conditions being different. The relative response ratio (the ratio of the relative responses of the same congener on the two different types of ECD) does not remain constant for the two types of detector investigated even at the same detector temperature. If congener No. 101 is taken as a basis (relative response = 1), the molar ratio varies in the range from 0.60 (No. 28) to 2.43 (No. 153) and the mass ratio varies from 0.60 (No. 28) to 2.41 (No. 153). The error in the application of both relative molar and mass responses of the congener from one ECD type to another therefore reaches several hundred per cent.

Table 5
Comparison of published relative mass responses with those obtained in this work

Ref.	PCB No.								
	28	52	101	138	153	180	77	126	169
12			1.00	0.82	0.82	0.74			
13		0.72	1.00	1.32	1.74	1.66			
14	0.28	1.15	1.00	1.58	0.90	0.99			
5		0.89	1.00	1.18	1.19				
8[a]	0.78	0.76	1.00	0.62	0.90	0.60	1.10	1.35	0.77
8[a]	0.89	0.81	1.00	0.72	0.60	0.62	0.91	1.44	0.81
8[a]	0.91	0.82	1.00	0.70	0.60	0.62	0.84	1.46	0.82
8[a]	1.17	1.21	1.00	0.92	0.55	1.01	2.01	1.84	1.08
8[a]	1.45	1.17	1.00	0.94	0.52	0.97	2.13	1.89	1.10
This work (Model 400 ECD)	1.21	0.29	1.00	2.17	1.49	3.17	0.93	1.76	2.29
This work (PU 4400 ECD)	0.73	0.28	1.00	2.65	3.59	3.83	1.88	2.69	2.92

[a] Different columns and internal standards were used.

3.5. Influence of oxygen

The effect of different amounts of oxygen in the gas in the ECD on the responses of PCB congeners was studied by using carrier gases with different oxygen contents. The influence of the presence of 6 ppm of oxygen on the relative response and the course of the response dependences on temperature can be seen from Figs. 2a and 3a (without oxygen) and Figs. 2b and 3b (with oxygen). A 6 ppm concentration of oxygen in nitrogen increases the relative responses of Nos. 180 and 138 and decreases those of No. 153 over the whole range of temperature. The relative responses of the other congeners are not significantly affected. The courses of the dependences do not differ significantly. The relative error in the determination of the responses using a gas with different oxygen contents can be up to 100%.

4. Conclusions

With different temperatures of the ECD various changes in the relative molar and mass responses of the selected PCB congeners occur; for this reason relative errors of several tens per cent may occur on application of the values of relative responses from one detector temperature to another.

The temperature course of the responses depends on the type of ECD used and on the content of oxygen in the gas passing through it.

Separation is the main problem in PCB congener analysis. However, accuracy of the quantitative results is also important. The profound differences among the temperature dependences of the various PCB congener responses can have a significant effect on the analytical results. There is a tendency to apply the same relative response factors in all PCB analyses. However, it is not possible to use published relative congener responses for different ECD temperatures and designs. A difference of 60°C above 300°C (the minimum detector temperature that is generally used in PCB analysis) results in errors of several tens per cent.

5. Acknowledgement

The authors thank Pye Unicam (Cambridge, UK) for the loan of the PU 4400 gas chromatograph. This work was supported by Grant No. 63157 by AVCR.

6. References

[1] V. Lang, *J. Chromatogr.*, 595 (1992) 1.
[2] C.C. Travis and S.T. Hester, *Environ. Sci. Technol.*, 25 (1992) 814.
[3] W.E. Wentworth and E. Chen, *J. Gas Chromatogr.*, 5 (1967) 170.
[4] V. Zitko, O. Hutzinger and S. Safe, *Bull. Environ. Contam. Toxicol.*, 6 (1971) 160.
[5] B. Boe and E. Egaas, *J. Chromatogr.*, 180 (1979) 127.
[6] S.D. Cooper, M.A. Moseley and E.D. Pellizzari, *Anal. Chem.*, 57 (1985) 2469.
[7] M.D. Mullin, C.M. Pochin, S. McGrindle, M. Rokes, S.H. Safe and L.M. Safe, *Environ. Sci. Technol.*, 18 (1984) 468.
[8] E.D. Pellizzari, M.A. Moseley and S.D. Cooper, *J. Chromatogr.*, 334 (1985) 277.
[9] *Bundesgesetzblatt*, 1 (1988) 422.
[10] K. Ballschmiter and M. Zell, *Fresenius' Z. Anal. Chem.*, 302 (1980) 20.
[11] W.E. Wentworth and E.C.M. Chen, in A. Zlatkis and C.F. Poole (Editors), *Electron Capture—Theory and Practice in Chromatography*, Elsevier, Amsterdam, 1981, Ch. 3, p. 27.
[12] W.M. Draper and S. Koszdin, *J. Agric. Food Chem.*, 39 (1991) 1457.
[13] F.I. Onuska, R.J. Kominar and K.A. Terry, *J. Chromatogr.*, 279 (1983) 111.
[14] F.I. Onuska and K.A. Terry, *J. High Resolut. Chromatogr. Chromatogr. Commun.*, 9 (1986) 671.

ELSEVIER

Journal of Chromatography A, 668 (1994) 449–453

JOURNAL OF CHROMATOGRAPHY A

Determination of trace amounts of selenium in poultry feedstuffs by gas chromatography

Vekoslava Stibilj*[,a], Marjan Dermelj[a], Anthony R. Byrne[a], Tatjana Šimenc[b], Jasna M. Stekar[b]

[a]*Jožef Stefan Institute, Nuclear Chemistry Department, University of Ljubljana, 61 001 Ljubljana, Slovenia*
[b]*Biotechnical Faculty, Zootechnical Department, University of Ljubljana, Ljubljana, Slovenia*

Abstract

In view of the importance of establishing reliable selenium concentration levels in different kinds of feedstuffs, the purpose of this work was to develop optimum experimental conditions for the isolation and GC determination of selenium as its chelate with 4-nitro-1,2-diaminobenzene. It was shown that ignition of the sample in an oxygen flask followed by reduction of Se(VI) to Se(IV) and the formation of 5-nitro-2,1,3-benzoselenadiazole chelate in HCl medium is a relatively rapid procedure giving a low blank value and allowing the determination of selenium in commercial feedstuffs and similar biological samples. The method was validated by the analysis of suitable certified or standard reference materials.

1. Introduction

Until 1957, selenium was known only as one of the most toxic elements. In that year, Schwarz and Foltz [1] identified selenium as a constituent of cellular glutathione peroxidase (GSH-Px) and since then its presence in enzymes such as plasma GSH-Px, phospholipid hydroperoxide GSH-Px, I iodothyronine-5′-diiodinase and selenoprotein P has been established, thus providing evidence for the involvement of selenium in numerous metabolic processes [2–4].

Symptoms of Se deficiency in poultry are manifested as exudative diathesis, fibrosis of the pancreas, fibrosis of the skeletal musculature and muscular dystrophy, whereas permanent excessive doses of selenium in poultry feed can cause blind staggers, alkali disease and acute toxicity, which are manifested in a decrease in egg laying and flying capability, in different anomalies of the embryo, incidence of paralysis and limping, liver cirrhosis, loss of feathers, etc. [5–7].

According to the Enviromental Health Criteria [8], the daily requirement of selenium in poultry is 30–50 $\mu g\ kg^{-1}$, provided that the amount of vitamin E in the daily ration is adequate. The major part is provided by grains, which are the main component of their feedstuffs and can contain, according to literature data [9], very variable amounts of selenium.

The legal regulation for the quality of different feeds in Slovenia specifies a minimum content of 150 $\mu g\ kg^{-1}$ of Se for dry poultry feedstuffs when added in the form of sodium selenite or selenate. The corresponding regulation for the maximum allowed amounts of harmful constituents in dry poultry feedstuffs permits a limiting value of 500 $\mu g\ kg^{-1}$ of Se. In spite of

* Corresponding author.

0021-9673/94/$07.00
SSDI 0021-9673(93)E0009-J

this, official control methods for selenium are lacking. Also, reliable data on the concentration levels of selenium in natural or industrially prepared feedstuff mixtures are very scarce or do not exist.

For the determination of microgram and nanogram amounts of selenium in biological samples the most often used and sensitive methods (with limits of detection from 0.2 to 50 $\mu g\ kg^{-1}$) are fluorimetry, hydride generation atomic absorption spectrometry, radiochemical neutron activation analysis (RNAA), instrumental NAA and GC with electron-capture detection (ECD) [6,10,11]. Each of these methods has advantages and also disadvantages such as matrix effects, interferences, contamination problems and reagent purity. In spite of the minimum possibilities of sample contamination and of the sensitivity of the RNAA method [12–18], our experience shows that this method is time consuming and too expensive for routine work.

For the determination of such amounts of selenium, the GC method seems to be very attractive [19–23]. In addition to the availability of such equipment in our laboratory, the motives for developing this technique for the determination of selenium in feeds and food products were to reduce costs, obtain rapid and accurate results, and not least to exploit the possibility of checking the results with those obtained for the same samples by RNAA. This required investigation of the optimum experimental conditions for the isolation and GC determination of selenium in the form of its chelate with 4-nitro-1,2-diaminobenzene from HCl medium, in combination with a simple destruction technique giving high recoveries and low blank values. This latter is very important when low concentrations of selenium must be determined. Although the prescribed Se concentrations in feedstuffs, in the range 150–500 $\mu g\ kg^{-1}$, are relatively high, a margin of sensitivity is required and when checking individual components of feeds, such as cereals growing in selenium-deficient areas [6], the levels may be very low (few $\mu g\ kg^{-1}$ range). Oxygen combustion in a closed flask was shown to fulfil these requirements.

The reliability of the method and the results obtained were checked by the analysis of appropriate certified or standard reference materials. Further, a selection of local feedstuffs were analysed and compliance with the regulations was checked.

2. Experimental

2.1. Sample preparation

Samples of mixed commercial poultry feedstuffs with declared supplements of selenium (150 $\mu g\ kg^{-1}$) were homogenized according to a standard method for the preparation of laboratory samples for analytical purposes [24] and ground.

2.2. Reagents

All reagents were of analytical grade or better, namely anhydrous Na_2SeO_4 (Sigma, Deisenhofen, Germany), 4-nitro-1,2-diamino-benzene (4NDB), 30% HCl (Suprapur), $Mg(NO_3)_2$ and urea[$CO(NH_2)_2$] (Merck, Darmstadt, Germany), toluene(Nanograde) (Promochem, Wesel, Germany) and Whatman No. 42 filterpaper (Whatman, Maidstone, UK) for lining the combustion boats.

2.3. Preparation of standard Se solution

The synthesis of 5-nitro-2,1,3-benzoselenadiazole chelate (5NBSeD) from Na_2SeO_4 and 4NDB was performed according to McCarthy *et al.* [21]. Its purity was checked by the determination of its melting point (224–226°C) and by elemental analysis (found, C 31.20, H 1.22, N 18.20; theoretical values, C 31.59, H 1.33, N 18.40%) and also by mass spectrometry (m/z = 229).

For the preparation of a stock standard solution, 1.271 mg of 5NBSeD chelate were weighed and transferred quantitatively with toluene into a 50-ml volumetric flask. A suitable aliquot of this solution, which is stable for more than 1 month, was diluted every 14 days with toluene to obtain working solutions with selenium concentrations

of 5.28, 10.56, 15.84 and 21.12 ng ml^{-1}. The calibration graphs for the standard solutions correlated adequately ($r = 0.998$).

2.4. Destruction of samples and isolation of selenium

Two methods of sample destruction were tested, oxygen combustion and destruction with $Mg(NO_3)_2$, followed by isolation of the Se chelate. The procedure is given in more detail in Fig. 1.

2.5. Recovery of the procedure for GC determination of Se

The recovery of the whole procedure for the GC determination of Se (with oxygen combustion) was obtained by standard additions of known amounts of Se (20–200 ng) via the Se stock solution to the filter-paper and also to some real samples.

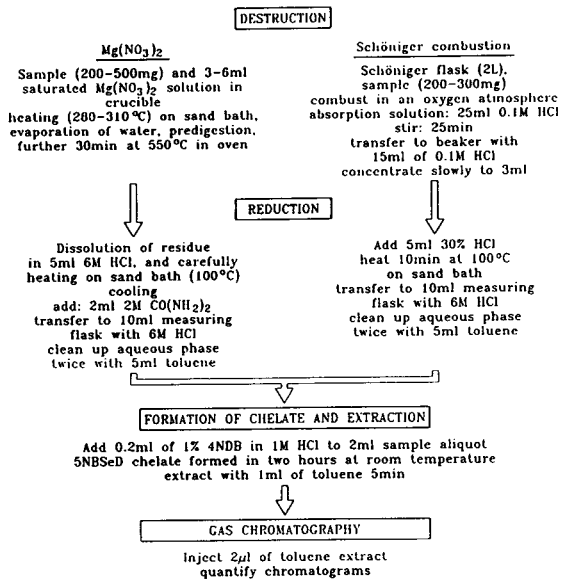

Fig. 1. Scheme for determination of selenium in feedstuffs by GC.

2.6. Apparatus and working conditions

A Hewlett-Packard (Avondale, PA, USA) Model 5890A gas chromatograph with a ^{63}Ni electron-capture detector was used for selenium determination. The temperatures were: column 200°C, injector 260°C and detector 280°C. The carrier gas was nitrogen (99.995%; Ruše, Slovenia) at a flow-rate of 40 ml min^{-1}. An HP 19094A-A28 2.35 m × 0.2 cm I.D. glass column (Hewlett-Packard) packed in our laboratory with 3% OV-17 stationary phase on Chromosorb W HP (0.15–0.20 mm) (Serva, Heidelberg, Germany) was used for the separation of 5-NBSeD. The sensitivity of the recorder was 1 or 10 mV with a charge speed of 0.63 cm min^{-1}, according to the concentration levels.

3. Results and discussion

Samples of plant origin normally contain selenium at the $\mu g\ kg^{-1}$ level. For the determination of such concentrations all analytical methods require prior destruction of the sample.

First, the decomposition of samples with a saturated solution of $Mg(NO_3)_2$ was studied. The advantages of saturated $Mg(NO_3)_2$ solution as a destructive agent are particularly its ease of manipulation, the need for only simple equipment, its suitability for the destruction of both fresh and dry samples and the very small losses of selenium (about 6%, as found by the ^{75}Se tracer technique), in spite of heating the residue at 550°C. However, the RNAA results for the determination of selenium in the saturated $Mg(NO_3)_2$ solution used showed high blank values (30–50 $\mu g\ kg^{-1}$), and the volume necessary for complete destruction of fresh or lyophilized samples was 3–6 ml (depending on the sample mass). A further disadvantage of this destruction technique was the appearance of some unindentified interfering peaks in the chromatograms of the Se chelate, in spite of adding 2 ml of 2 *M* $CO(NH_2)_2$ after reduction of Se(VI) to Se(IV) and cleaning up the toluene extract of

the Se chelate with 6 *M* HCl. Therefore, we decided that this destruction procedure was not practicable for use in combination with GC analysis.

From our previous experience [18] and the above facts, a simple combustion procedure in an oxygen atmosphere seemed to be the most promising in combination with the GC determination of Se. Provided that the concentration of Se in the filter-paper is below 15 $\mu g\ kg^{-1}$ (as was the case with the Whatman No. 42 filter-paper), then with the use of only a small volume of Suprapur 30% HCl as adsorption solution and for reduction of Se(VI) to Se(IV) (6 ml), the total blank value arising from the filter-paper, HCl and 4NDP reagent is minimal. Chromatograms of the solvent, Se standard, 6 *M* HCl, the reagent blank and a real sample are shown in Fig. 2.

The method was tested by the use of the standard addition technique, performed using filter-paper alone and with various matrices carried through the whole procedure, and a mean overall recovery of 88.1 ± 7.8% was routinely obtained.

Using the described method, some commercial poultry feedstuffs were analysed. From the results obtained (Table 1), it is evident that selenium levels are in the range required by the Slovenian regulation for poultry feedstuffs (150–500 $\mu g\ kg^{-1}$).

The sample signal from the chromatogram may be quantified either by immediate injection into the column of a suitable aliquot of standard solution of 5NBSeD in toluene, or from a calibration graph constructed daily. It was found that the response of the detector was constant throughout the day for the same amount of Se chelate.

The reliability of the results was checked by the analysis of appropriate certified or standard reference materials and by comparison with results obtained by RNAA in our laboratory. From the results obtained (Tables 2 and 3), good agreement with both the certified and RNAA values is evident.

The advantageous features of the method, namely the simple and rapid destruction procedure (combustion in oxygen), the low blank value (the contributions only of the filter-paper and Suprapur hydrochloric acid), the non-requirement for a clean-up procedure of the

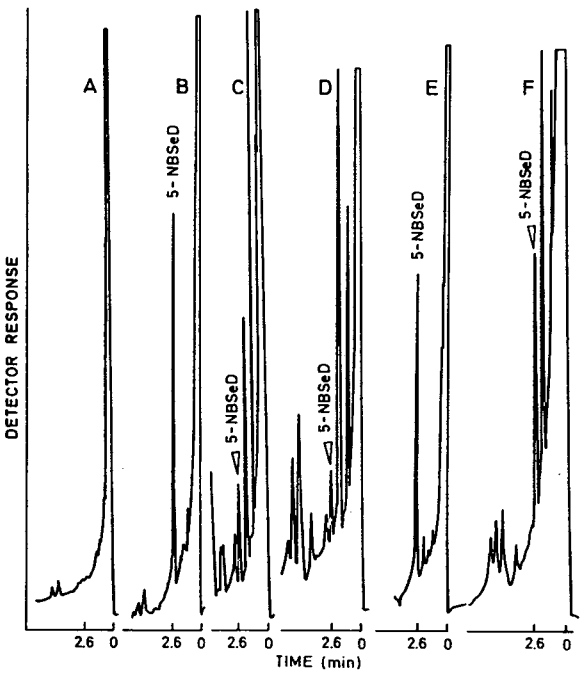

Fig. 2. Chromatograms for (A) solvent, (B) 10.56 pg Se standard, (C) 2.4 pg Se in reagent blank, (D) 2.1 pg Se in 6 *M* HCl, (E) 21.12 pg Se standard and (F) 17.79 pg Se in feedstuff Bro-val 1.

Table 1
Results ($\mu g\ kg^{-1}$ dry mass) for selenium in commercial poultry feedstuffs marketed in Slovenia

Commercial poultry feedstuff	$\bar{x} \pm s$ $(n)^a$
PŠ	276 ± 22 (6)
Bro-val 1	215 ± 22 (6)
Bro-jr	250 ± 33 (6)
Bro-val 2	275 ± 31 (5)
Jr	239 ± 21 (6)
NSK finely ground	264 ± 16 (6)
NSK-2	238 ± 9 (6)
Bro-fin	271 ± 15 (6)

[a] Mean ± standard deviation; n = number of determinations.

Table 2
Results for selenium in certified or standard reference materials (μg kg^{-1} dry mass)

Sample	$\bar{x} \pm s$ $(n)^a$	Certified value
Lucerne 1992 International Analytical Group [25]	105 ± 13 (4)	117 ± 12
Mixed feed 1992 International Analytical Group [25]	432 ± 16 (4)	420 ± 50
BCR CRM 189 Wholemeal Flour	125 ± 9 (4)	132 ± 10
NIST SRM 1568 Rice Flour	362 ± 25 (4)	400 ± 100
NIST SRM 1567a Wheat Flour	973 ± 27 (4)	1100 ± 200

[a] Mean ± standard deviation; n = number of determinations.

Table 3
Comparison of results (μg kg^{-1} dry mass) for selenium in some poultry feedstuffs and BCR CRM 189 Wholemeal Flour determined by GC and RNAA

Sample	$\bar{x} \pm s$ $(n)^a$	
	GC	RNAA
PŠ	276 ± 22 (6)	282 ± 26 (6)
Bro-val	215 ± 22 (6)	236 ± 18 (6)
KIS Feedstuff	291 ± 7 (4)	320 ± 28 (6)
BCR CRM 189 Wholemeal Flour[b]	125 ± 9 (4)	137 ± 10 (3)

[a] Mean ± standard deviation; n = number of determinations.
[b] Certified Se content: 132 ± 10 μg kg^{-1}.

5NBSeD extract in toluene, the high recovery of 88.1 ± 7.8% (determined by standard additions) and the low detection limit (1.2 μg kg^{-1}) make it suitable and convenient for the routine determination of selenium in poultry feedstuffs.

4. References

[1] K. Schwarz and C.M. Foltz, *J. Am. Chem. Soc.*, 39 (1957) 3239.
[2] D. Behne, A. Kyriakopoulos, H. Meinhold and J. Kohrle, *Biochem. Biophys. Res. Commun.*, 173 (1990) 1143.
[3] B.A. Zachara, *J. Trace Elem. Electrolytes Health Dis.*, 6 (1992) 137.
[4] J. Arthur, F. Nicol and J.C. Beckett, *Am. J. Clin. Nutr., Suppl*, 57 (1993) 236S.
[5] *Selenium in Nutrition*, National Academic Press, Washington, DC, revised ed. 1983, p. 174.
[6] J.F. Combs and S.B. Combs, *The Role of Selenium in Nutrition*, Academic Press, New York, 1986, p. 532.
[7] L.R. McDowel, *Minerals in Animal and Human Nutrition*, Academic Press, Orlando, FL, 1992, p. 524.
[8] *Environmental Health Criteria 58, Selenium*, WHO, Geneva, 1987, p. 306.
[9] R. Seeger and H.G. Neuman, *Dtsch. Apoth.-Ztg.*, 131 (1991) 354.
[10] S.E. Raptis, G. Kaiser and G. Tölg, *Fresenius' Z. Anal. Chem.*, 316 (1983) 105.
[11] J. Piwonka, G. Kaiser and G. Tölg, *Fresenius' Z. Anal. Chem.*, 321 (1985) 225.
[12] A.R. Byrne and L. Kosta, *Talanta*, 21 (1974) 1083.
[13] H. Polkowska-Motrenko, M. Dermelj, A.R. Byrne, A. Fajgelj, P. Stegnar and L. Kosta, *Radiochem. Radioanal. Lett.*, 53 (1982) 319.
[14] M. Dermelj, G. Hancman, A. Gosar, A.R. Byrne and L. Kosta, *Vestn. Slov. Kem. Druš.*, 23 (1985) 127.
[15] M. Dermelj, A.R. Byrne, M. Franko, B. Smodiš and P. Stegnar, *J. Radioanal. Nucl. Chem., Lett.*, 106 (1986) 91.
[16] M. Dermelj, M. Horvat, A.R. Byrne and P. Stegnar, *Chemosphere*, 16 (1987) 877.
[17] A. Fajgelj, M. Dermelj, A.R. Byrne and P. Stegnar, *J. Radioanal. Nucl. Chem. Lett.*, 128 (1988) 93.
[18] M. Dermelj, V. Stibilj, J.M. Stekar and A.R. Byrne, *Fresenius' J. Anal. Chem.*, 340 (1991) 258.
[19] C.F. Poole, N.J. Evans and D.C. Wibberley, *J. Chromatogr.*, 136 (1977) 73.
[20] K. Toei and Y. Shimoishi, *Talanta*, 28 (1981) 967.
[21] T.P. McCarthy, B. Brodie, J.A. Milner and R.F. Bevill, *J. Chromatogr.*, 225 (1981) 9.
[22] K.W.M. Siu and S.S. Berman, *Talanta*, 31 (1984) 1010.
[23] K. Johansson and A. Olin, *J. Chromatogr.*, 589 (1992) 105.
[24] *Methodenbuch, Band III, Die Chemische Untersuchung von Futtermitteln*, Neumann, Neudamm, Germany, 1976.
[25] *Ringtest of the International Analytical Group 1992*, Bedrijfslaboratorium voor Grond- en Gewasonderzoek, International Analytical Group, Oosterbeek, Netherlands, 1992, p. 18.

ELSEVIER

Journal of Chromatography A, 668 (1994) 455–462

JOURNAL OF CHROMATOGRAPHY A

Dynamic headspace gas chromatographic method for determining volatiles in virgin olive oil

M.T. Morales*, R. Aparicio, J.J. Rios

Instituto de la Grasa y sus Derivados (CSIC), Avda. Padre García Tejero 4, Seville 41012, Spain

Abstract

Dynamic headspace sampling methods prior to capillary gas chromatography are especially suitable in the determination of volatile compounds at a wide range of concentrations, and numerous methods have been developed and applied to very different kinds of samples. In this work, a simple and rapid dynamic headspace technique was developed to determine volatiles present in virgin olive oil samples. Headspace components were swept from 0.5 g of sample at low temperature (40°C) and concentrated on Tenax TA, thermally desorbed and subsequently trapped in a fused-silica cold trap previously cooled to −110°C. They then passed to the capillary column. This system was connected to a mass spectrometer to identify the most important compounds and a comparative study of the main volatiles identified in virgin olive oil samples using other methods was carried out. Sniffing of the components eluted from the chromatographic column was also performed. Different virgin olive oil samples showing different chromatographic profiles were analysed. The differences were mainly quantitative because most compounds were present in all oils analysed, and only the proportions in which these compounds are present varied. Discriminant analysis of these compounds allowed the origin of each sample to be determined with a probability of greater than 90%.

1. Introduction

The flavour of a sample is normally very complex and the volatile components are responsible for this complex sensation. The concentration range in which these compounds are present is very wide. It used to be difficult to determine all of them using the same method because in many instances the methods used lack sensitivity and those volatiles present at trace levels are not detected.

Dynamic headspace (DHS) methods have been widely used in the determination of the volatile compounds present in foods and they have the great advantage of concentrating the sample so that it is possible to detect compounds present at low concentrations that sometimes contribute significantly to the flavour [1]. DHS–GC methods including thermal desorption are powerful tools for the efficient concentration of numerous flavour and fragance volatiles.

Virgin olive oil is the most highly flavoured of vegetable oils and for this reason it is greatly appreciated by consumers. The volatile components responsible for this flavour have been studied for years and a great number of compounds have been identified [2–4]. Different methods have been used [5]. Most studies used dynamic headspace techniques with solvent desorption, large amounts of samples, long analysis times and, in many instances, packed columns.

The first objective of this work was the identi-

* Corresponding author.

0021-9673/94/$07.00
SSDI 0021-9673(93)E1040-7

fication of the volatile compounds obtained by a new, previously optimized DHS method [6] that allows the determination of the wide range of compounds differing in polarity, volatility, concentration and molecular size that contribute to the complex flavour of virgin olive oil. The method involves the use of Tenax TA as adsorbent material, thermal desorption and cryofocusing prior to capillary GC to avoid undesirable peak broadening. The results were compared with those obtained using other techniques.

The characterization of olive oils by their non-volatile compounds has also been widely studied [7,8], but their characterization by their volatile compounds has scarcely been reported [9], despite the fact that volatiles are related to sensory notes [10] and hence to olive oil quality [11]. Hence the second objective of this work was the characterization of virgin olive oil samples on the basis of their origin.

2. Experimental

2.1. Samples

Thirty-two samples of virgin olive oil collected from Spain, Italy and Greece and corresponding to three stages of maturity were analysed in duplicate. Seven representative samples of the whole set were selected, either on the basis of their profile or the quantitative values of their peaks, for analysis by GC–MS. In this way we ensured that the most important peaks were properly identified. The most suitable sample was selected to be used in odour port assessment (sniffing).

2.2. Dynamic headspace sampling

The isolation of volatiles was carried out using a previously proposed system [6]. A 0.5-g amount of virgin olive oil sample with 3.33 ppm (w/w) of isobutyl acetate added as an internal standard was placed in a vessel, stirred and heated at 40°C to facilitate the removal of the volatiles. The sample surface was swept with nitrogen and volatiles were passed through a reflux condenser kept at 5–10°C to prevent subsequent interference from water. The volatiles were then trapped in a Tenax TA trap (Chrompack) at room temperature. The flow-rate was maintained at 200 ml/min using a rotameter and sampling was performed for 15 min. Adsorbent traps were conditioned prior to use by heating them at 300°C for several hours and again at 220°C with passage of the carrier gas. Blank runs were carried out periodically during the study.

2.3. Desorption method

The desorption of volatiles trapped in the Tenax TA trap was carried out in the opposite direction to adsorption by using a Chrompack thermal desorption cold trap injector (TCT) [12]. The temperatures and time of injection were controlled by an injector control unit. Desorption was carried out by heating the trap at 220°C for 5 min. Volatiles were then transported by the carrier gas with a desorption flow-rate of 7 ml/min to a fused-silica cold trap previously cooled to −110°C with liquid nitrogen for 5 min, where they condensed. Finally, the samples were injected into the capillary GC system by flash heating the cold trap at 170°C. The TCT system was flushed after each run by heating at 300 and 240°C.

2.4. GC analysis

A Hewlett-Packard Model 5890 Series II gas chromatograph equipped with a flame ionization detector and a Model 3396B integrator was employed for quantitative analysis. Helium (99.999%, 103 kPa inlet pressure) was used as the carrier gas and nitrogen as make-up gas. A fused-silica Supelcowax 10 column (60 m × 0.32 mm I.D., 0.5 μm film thickness) was used. The oven temperature was held at 40°C for 4 min, then increased at 4°C/min to 240°C, where it was held for 10 min; the injector temperature was 175°C and the detector temperature was 275°C. The integrator was linked to a Model 80386

computer where chromatograms were held in a relational database.

2.5. GC–MS analysis

The TCT was installed in the GC–MS system. Volatiles were obtained as described above. In order to achieve a more concentrated sample, 25 g of virgin olive oil were placed in the vessel extractor bottle and swept with nitrogen for 30 min. A Hewlett-Packard Model 5890 Series II gas chromatograph coupled with an MS 30/70 mass spectrometer (VG Analytical, Manchester, UK) and a VG Model 11/250 data system was used for mass spectrometric analyses. A J&W DB-WAX fused-silica capillary column (60 m × 0.25 mm I.D., 0.25 μm film thickness) was employed. The column temperature was held at 40°C for 15 min, then increased to 220°C at 1°C/min. The carrier gas (helium) flow-rate was 1 ml/min. The end of the fused-silica column was inserted directly into the ion source block. The spectra were recorded at an ionization voltage of 70 eV and an ion source temperature of 200°C.

Sample components were verified by comparison of the mass spectral data with those of authentic reference compounds. For some compounds, standard samples were not available to confirm positive identifications. In these cases, the sample components were tentatively identified by mass spectrum matching using the NBS mass spectral library collection. In the absence of suitable reference spectra, samples of suspect components were obtained or synthetized and their mass spectra acquired.

2.6. Sniffing

The separated components of the isolate were assessed sensorially at the outlet of the capillary column. Aromas were described by two assessors with more than 10 years experience and by two assessors who, although not experienced, were habitual consumers of virgin olive oil.

3. Results and discussion

3.1. Analysis by GC–MS and sniffing

A gas chromatogram of virgin olive oil is shown in Fig. 1, indicating the presence of over 100 components, 56 of which were identified in this work. Table 1 gives the names, the identification methods and the corresponding odour

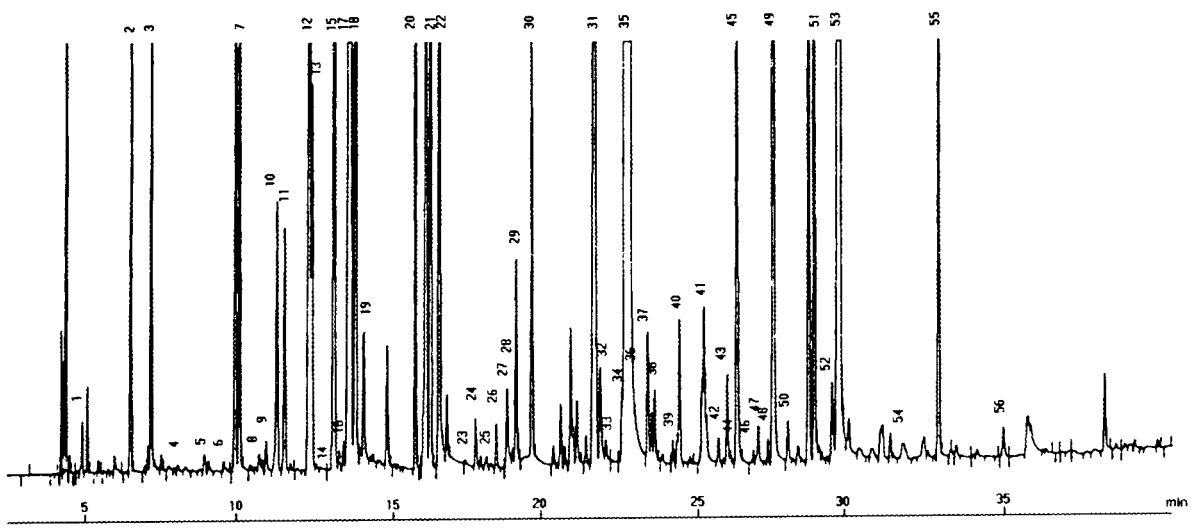

Fig. 1. Chromatogram showing identified peaks. Sample quality level, extra-virgin olive oil; nationality, Spain; variety, Arbequina; ripeness, unripe; extraction system, centrifugation. For peak identification, see Table 1.

Table 1
Volatile compounds identified in virgin olive oil

Peak No.[a]	Compound	Identification method	Sniffing	Ref.
1	Hexene	MS		
2	Acetone	GC, MS		13
3	Methyl acetate	GC, MS		
4	Octene	MS	Solvent-like	14
5	Ethyl acetate	GC, MS	Sweet, aromatic	2, 4, 13–15
6	2-Butanone	MS	Fragrant, pleasant	
7	3-Methylbutanal	MS	Sweet, fruity	2, 16
8	1,3-Hexadien-5-yne	MS		
9	An alcohol		Sweet, apple	
10	Ethylfuran	MS	Rancid	
11	Ethyl propanoate	MS	Sweet, strawberry, apple	2
12	An alcohol + hydrocarbon		Pungent, acid	
13	3-Pentanone	MS	Sweet	2, 4, 13
14	4-Methylpentan-2-one	MS	Sweet	
15	Pent-1-en-3-one	MS	Sweet, strawberry	
16	2-Methylbut-2-enal	MS	Solvent-like	
17	Isobutyl acetate[b]	GC, MS		
18	A hydrocarbon		Sweet, apple	
19	Methylbenzene	MS	Glue, solvent-like	4, 14
20	Butyl acetate	MS	Green, pungent	14, 15
21	Hexanal	GC, MS	Green, apple	2–4, 13, 16
22	A hydrocarbon		Sweet, aromatic	
23	2-Methylbutyl propanoate	MS	Aromatic, ketonic	
24	2-Methyl-1-propanol	GC, MS	Ethyl acetate-like	2, 13
25	(*E*)-2-Pentenal	MS	Green apple	2
26	An alcohol		Grassy	
27	(*Z*)-2-Pentenal	MS	Green, pleasant	2
28	Ethylbenzene	GC, MS	Strong	14, 15
29	An aldehyde		Artichoke, green, flowers	
30	3-Hexenal[c]	GC, MS	Green, green leaves, grassy	14–16
31	1-Penten-3-ol	GC, MS	Wet earth	2, 4, 14
32	3-Methylbutyl acetate	GC, O[d]	Banana	2, 4, 14
33	Heptan-2-one	MS	Fruity	14, 15
34	(*E*)-2-Hexenal	MS	Bitter almonds	2, 4, 14–16
35	(*Z*)-2-Hexenal	GC, MS	Green, fruity, sweet	2, 4, 14, 15
36	2-Methylbutan-1-ol	MS	Fish oil	2, 4
37	3-Methyl-2-butenyl acetate	MS	Putty-like unpleasant	
38	Dodecene or methylundecene	MS		
39	Pentan-1-ol	GC, MS	Pungent	4, 14
40	Ethenylbenzene	MS		4, 14, 15
41	Hexyl acetate	GC, MS	Sweet, fruity	4, 14, 15
42	A C_8 ketone	MS	Fruity, mushroom-like	
43	Octan-2-one	GC, MS	Mouldy	2, 4, 14, 15
44	3-(4-Methyl-3-pentenyl)furan	MS	Paint-like strong	
45	3-Hexenyl acetate	GC, MS	Green, green banana, green leaves	2, 4, 14–16
46	2-Penten-1-ol	GC, MS	Banana	
47	6-Methyl-5-hepten-2-one	MS	Fruity	
48	Nonan-2-one	MS	Fruity	2, 14
49	Hexan-1-ol	GC, MS	Fruity, aromatic, soft	2, 4, 14
50	(*E*)-3-Hexen-1-ol	GC, MS		2, 4, 13, 14
51	(*Z*)-3-Hexen-1-ol	GC, MS	Banana	4, 14, 16

Table 1 *(continued)*

Peak No.[a]	Compound	Identification method	Sniffing	Ref.
52	2,4-Hexadienal	MS		2
53	(*E*)-2-Hexen-1-ol	MS	Green, grassy	4, 14
54	Acetic acid	GC, MS		4, 16
55	Methyl nonanoate	GC, MS	Sweet, floral	
56	Methyl decanoate	MS	Fresh	

[a] Peak numbers refer to the chromatogram in Fig. 1.
[b] Internal standard.
[c] Compound synthesized to verify identification.
[d] Identified by odour quality perceived at the sniffing port.

descriptions. Most of them had been reported in virgin olive oil in previous works as cited, but the proposed method probably gives a greater number of aldehydes, ketones and compounds with fewer carbon atoms than other methods. The volatiles clearly identified corresponded to different chemical families, these being seven hydrocarbons, nine alcohols, nine aldehydes, nine ketones, one acid, twelve esters and two furans.

In flavour and fragance analysis, the identification of all peaks is no longer the main goal, the aim now being to separate and to investigate only those parts of the chromatogram with interesting organoleptic properties [17]. This may be possible by sniffing the effluent, a technique used for determining which components of a complex mixture of volatiles have odour and for evaluating the significance of their aroma.

In other methods [2,15] it is necessary to prefractionate the concentrate prior to GC–MS analysis because the non-polar fraction (hydrocarbons) interferes with the results. In our case the hydrocarbons, which have less significance in the aroma [2], basically appear in the first part of the chromatogram where the aroma compounds are at very low concentrations. For this reason the study of this zone is more difficult. In the rest of the chromatogram direct olfaction of the different compounds is relatively easy because this problem does not exist.

It is well known that the balanced flavour of virgin olive oil is attained by an adequate equilibrium between "green" and "fruity" notes [14], which change with ripeness. To assess the presence of the compounds responsible for these characteristic notes, sniffing of the effluent was carried out. Such a procedure identified a great number of odour descriptions, the most commonly used terms being "green', "fruity", "pleasant", "sweet" and, less commonly, "unpleasant notes". This is logical because the analysed samples correspond to virgin olive oil [18]. All of these odour descriptions have been previously described in virgin olive oil and in the direct olfaction of its isolate [4] and are present in the main sensory attributes that are usually studied in virgin olive oil [11].

The "green" notes formed a group of odour descriptions, as was expected [14]. These corresponded to typically green odour compounds [16] such as aliphatic C_6 compounds and corresponding hexyl esters: hexanal, 3-hexenal, 3-hexenyl acetate, hexyl acetate and 3-hexen-1-ol. It should be noted that 2-hexenal has been previously described as strong, green, bitter almonds [14] and as green, fruity, pleasant [15]. In our case the different *Z* and *E* isomers each showed different descriptions. This seems to be due to the fact that each isomer could be responsible for a different sensation. However, both (*E*)- and (*Z*)-2-pentenal showed green notes in sniffing.

Another large group of odour descriptions was constituted by the "fruity", "sweet" and "floral" notes, esters being mainly responsible for this sensation. Some ketones, especially C_5 ketones, are responsible for the "sweet" notes and C_{7-9}

ketones elicited a "fruity" description. Some alcohols and hydrocarbons also gave this kind of description.

A third, less important, group constituted by unpleasant notes such as "solvent-like", "paint" and "putty" was also obtained in the sniffing of the effluent. Various compounds seem to be responsible for these odour descriptions.

3.2. Characterizing samples on the basis of their origin

Data processing was performed with the BMDP package [19]. All the variables have an almost normal distribution, so that no transformation had to be applied to the data set of 56 volatiles. Analysis of variance (ANOVA) [20] was applied, using countries, Spain, Italy and Greece, as factor variables. Seventeen volatiles (Table 2), showed significant differences among countries at a significance of $F > 95\%$ ($p < 0.050$), six of them with a significance of $F < 0.001$. The seventeen volatiles are basically related to "sweet", "greens" and "fruity" sensory perceptions perceived by sniffing (Table 1), but there is not a definite preponderance of a particular series of compounds among those identified by GC–MS.

Stepwise linear discriminant analysis (SLDA) [20] was applied to the seventeen selected volatiles in order to discriminate the samples on the basis of their origin, and 90.5% of correct classifications were obtained by only three volatiles: 1,3-hexadien-5-yne, 2-methyl-1-propanol and 3-hexenyl acetate (Nos. 8, 24 and 45).

Fig. 2 shows the plot based on the two canonical equations. Three decision rules allow the samples to be characterized: If the first canonical variable has negative values, then the sample was collected in Greece; if the first canonical variable has positive values and the second canonical variable has positive values,

Table 2
Results for the volatile compounds showing significant differences between countries

Peak No.[b]	Peak-area ratio[a]			F	Significance of F
	Spain	Italy	Greece		
8	0.01 ± 0.01	0.28 ± 0.24	2.27 ± 0.69	38.655	<0.001
9	3.27 ± 1.94	0.53 ± 0.18	0.60 ± 0.49	6.417	0.005
10	1.35 ± 0.57	0.33 ± 0.27	1.74 ± 0.45	9.706	0.001
15	6.01 ± 2.43	1.32 ± 0.90	7.95 ± 2.00	11.692	<0.001
18	3.47 ± 1.37	2.51 ± 0.86	8.23 ± 3.08	9.907	0.001
20	2.89 ± 1.06	1.28 ± 0.80	3.82 ± 0.94	7.100	0.003
21	9.21 ± 4.10	2.37 ± 0.92	11.77 ± 3.53	8.436	0.001
23	tr[c] –	0.34 ± 0.22	0.10 ± 0.10	6.801	0.004
24	0.76 ± 0.29	0.40 ± 0.31	1.69 ± 0.57	11.168	<0.001
30	5.66 ± 1.92	7.93 ± 2.65	16.89 ± 2.61	25.816	<0.001
35	127.78 ± 63.79	472.70 ± 236.68	165.54 ± 47.92	7.784	0.002
44	0.68 ± 0.31	1.01 ± 0.41	7.54 ± 2.69	27.616	<0.001
45	0.73 ± 0.73	6.08 ± 3.86	6.44 ± 3.37	5.725	0.008
46	9.95 ± 5.39	6.50 ± 2.88	48.82 ± 22.46	13.659	<0.001
47	tr[c] –	tr[c] –	0.30 ± 0.24	7.154	0.003
51	11.29 ± 3.28	20.81 ± 6.45	18.49 ± 4.08	4.993	0.014
56	0.15 ± 0.10	0.56 ± 0.20	0.76 ± 0.43	5.890	0.007

[a] Peak numbers refer to the chromatogram in Fig. 1.
[b] Ratio of the compound peak area to the internal standard peak area, multiplied by 100. Mean values ±95% confidence interval.
[c] Trace (<0.01).

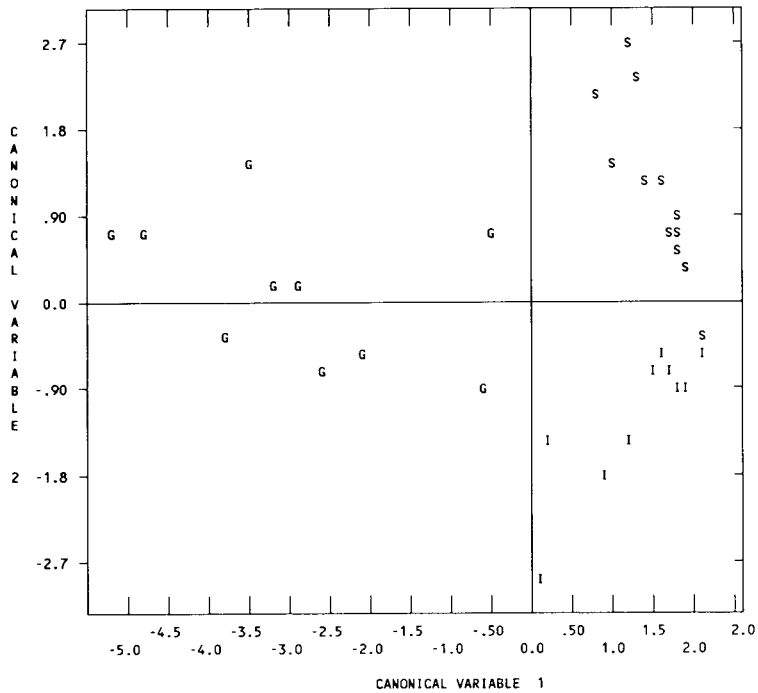

Fig. 2. Two-dimensional plot showing the discrimination obtained by means SLDA of the peaks that showed greater significant differences between samples.

then the sample was collected in Spain; if the first canonical variable has positive values and the second canonical variable has negative values, then the sample was collected in Italy.

4. Conclusions

The system proposed in this work allows the analysis of a large number of polar volatile compounds responsible for the aroma of virgin olive oil without carrying out prefractionation of the sample. Several compounds had not been previously described in this kind of sample and short-chain aliphatic compounds were especially well obtained. The main differences between samples from different origins were well established and a correct characterization was obtained.

5. Acknowledgements

The authors acknowledge their indebtedness to Mr. M. Martin, Mrs. R.G. Cordones, Mrs. A. Guinda and Mrs. M.V. Alonso for the sniffing experiments. This work was supported by CICYT (Spain) ALI-91-0786.

6. References

[1] R.V. Golovnya, *J. Chromatogr.*, 251 (1982) 249.
[2] R.A. Flath, R.R. Forrey and D.G. Guadagni, *J. Agric. Food Chem.*, 21 (1973) 948.
[3] E. Fedeli, *Riv. Ital. Sostanze Grasse*, 54 (1977) 202.
[4] J.M. Olías, M.C. Dobarganes, F. Gutiérrez and R. Gutiérrez, *Grasas Aceites (Seville)*, 29 (1978) 211.
[5] M.T. Morales, R. Aparicio and F. Gutiérrez, *Grasas Aceites (Seville)*, 43 (1992) 164.
[6] M.T. Morales and R. Aparicio, *Anal. Chim. Acta*, 282 (1993) 423.
[7] R. Aparicio, *J. Chemometr.*, 3 (1988) 175.

[8] R. Aparicio and V. Alonso, *Prog. Lipid Res.*, (1993) in press.
[9] M.T. Morales and R. Aparicio, *Grasas Aceites (Seville)*, 44 (1993) 113.
[10] R. Aparicio and M.T. Morales, *Food Qual. Pref.*, (1993) in press.
[11] *Organoleptic Assessment of Olive Oil, COI/T20/Doc. No. 3, Resolution No. RES 5/56-IV/87*, International Olive Oil Council, Madrid, 1987.
[12] R.P.M. Dooper, *Chrompack News*, 10 (1983) 1.
[13] G. Lercker, P. Capella and P. Deserti, *Sci. Tecnol. Alimenti*, 3 (1973) 299.
[14] J.M. Olías, F. Gutiérrez, M.C. Dobarganes and R. Gutiérrez, *Grasas Aceites (Seville)*, 31 (1980) 391.
[15] R. Gutiérrez, M.C. Dobarganes, F. Gutiérrez and J.M. Olías, *Grasas Aceites (Seville)*, 32 (1981) 299.
[16] H. Guth and W. Grosch, *Fat Sci. Technol.*, 93 (1991) 335.
[17] P. Werkhoff and W. Bretschneider, *J. Chromatogr.*, 405 (1987) 87.
[18] *Off. J. Eur. Commun.*, Regulation No. 2568/91, July 11th (1991).
[19] W.J. Dixon, *BMDP Statistical Software*, University of California Press, Los Angeles, 1983.
[20] B.G. Tabachnick and L.S. Fidell, *Using Multivariate Statistics*, Harper & Row, New York, 1983.

ELSEVIER

Journal of Chromatography A, 668 (1994) 463–467

JOURNAL OF CHROMATOGRAPHY A

Separation and identification of stereoisomeric cyclobutanediols by gas chromatography–mass spectrometry

Béla Török*, Zsolt Szegletes, Árpád Molnár

Department of Organic Chemistry, József Attila University, Dóm tér 8, H-6720 Szeged, Hungary

Abstract

A procedure is described for the separation and identification of *cis*- and *trans*-2,2,4,4-tetramethyl-1,3-cyclobutanediol. The separation of the isomeric diols was achieved by gas chromatography on an HP-1 capillary column under optimized conditions. The identification of the isomers was carried out through the mass spectrometric analysis of silyl derivatives prepared by using silylating agents of different steric demands. Striking reactivity differences of the isomers resulted in selective derivatization, permitting the unequivocal identification of the isomers. The results were supported by the analysis of authentic samples.

1. Introduction

The catalytic reduction of dimethylketene dimer resulted in the first synthesis of a mixture of *cis*- and *trans*-2,2,4,4-tetramethyl-1,3-cyclobutanediol [1]. The first separation of the isomers was performed on a preparative scale in the form of their formate esters. This method, however, required a large amount of starting material and provided only an appropriate isomer distribution, which is not satisfactory in most instances.

We were interested in studying the transformations of stereoisomeric cyclobutanediols, which required the reliable identification of the individual isomers. Moreover, the analysis of a large number of samples was expected, and a rapid and accurate analytical method was therefore needed. As substituted cyclic diols are important building blocks in organic synthetic [2], their separation and identification and the determination of their purity are of great general interest.

In this paper, we report the gas chromatographic (GC) separation of the above stereoisomeric cyclobutanediols and their identification by mass spectrometric (MS) analysis of their derivatives.

2. Experimental

2.1. Chemicals

All solvents were of spectroscopic grade (Reanal, Budapest, Hungary). The diol mixture with an isomeric ratio of about 1 was the product of City Chemical (New York, USA). Authentic *cis*-diol for comparison was prepared by treating the diol mixture with dilute sulphuric acid [3]. This treatment results in decomposition of the diols via dehydration. As the *trans* compound reacts much faster, the reaction permits the isolation of pure *cis*-diol. N,N-Diethyltrimeth-

* Corresponding author.

0021-9673/94/$07.00
SSDI 0021-9673(93)E1203-C

ylsilylamine and N *tert.*-butyldimethylsilyl-N-methyltrifluoroacetamide (MTBSTFA) (both from Fluka, Buchs, Switzerland) were used as silylating agents.

2.2. Derivatization

Silyl ethers were prepared according to the conventional method. A 5-mg sample of the diol mixture was dissolved in N,N-dimethylformamide (100 μl) and an excess of the silylating agent (200 μl) was added at room temperature. The reaction was complete within 15 min. A 5-μl volume of this mixture was used for analysis.

2.3. Chromatography

An HP 5890 gas chromatograph coupled with an HP 5970 MSD system (electron impact ionization at 70 eV, Hewlett-Packard, Avondale, PA, USA) was used for GC and MS measurements. Separation was carried out on free fatty acid phase (FFAP) (50 m × 0.2 mm I.D., 0.5 μm) and HP-1 (50 m × 0.2 mm I.D., 0.5 μm) capillary columns (both from Hewlett-Packard). Both columns were operated in the isothermal mode (oven temperatures 160°C for the FFAP and 150°C for the HP-1 column) with helium as carrier gas (flow-rate 0.85 cm^3/min). Calculations were carried out with an HP 59970 Chemstation (Hewlett-Packard).

3. Results and discussion

The GC separation of simple alcohols on packed columns usually gives satisfactory results [4–6]. The analysis of diols, in contrast, is more difficult. Therefore, it was not surprising that the application of packed columns with conventional partition liquids [Carbowax 20M, Apiezon, SE-52, 1,2,3-tris(2-cyanoethoxy)propane] did not result in the separation of the two cyclobutanediol isomers. In contrast, an FFAP capillary column specially designed for the analysis of hydroxy compounds [7] gave an excellent baseline separation of the two isomers. The long analysis time (more than 22 min), however, was inconvenient and further improvements were necessary.

As the stereoisomeric diols are centro- (*trans*) and planesymmetric (*cis*) and the molecular shape of both compounds is nearly spherical, near-zero dipole moments can be expected. We reasoned, therefore, that columns designed for the analysis of non-polar materials should be suitable for the separation of our diol isomers. A faster analysis was also expected owing to the weaker interaction between the partition liquid and the cyclobutanediols. Indeed, analysis on an HP-1 column required only about 10 min with the same excellent separation as on the FFAP column [Fig. 1B: peaks 6 (*cis*) and 7 (*trans*)]. Moreover, the retention indices [8] could easily be determined on HP-1 (Fig. 1A: peaks 1, 2, 3, 4 and 5; Table 1), in contrast with FFAP column, where this required the use of very high-molecular-mass hydrocarbons.

Whereas the above measurements can be carried out by means of simple detectors (flame ionization or thermal conductivity), more sophisticated techniques are needed to identify the individual compounds. Unfortunately, the MS detector used in our study operating at an ionization potential of 70 eV produced almost identical fragmentation patterns for the two diol isomers [Fig. 2A (*trans*) and B (*cis*) and Fig. 3], which is in accordance with literature data [9].

Derivatization of the diols appeared to be the solution to the problem. All our initial efforts with simple derivatives (different esters and ethers) failed to produce mass spectra suitable

Table 1
Retention indices of stereoisomeric cyclobutanediols and some derivatives on an HP-1 column at 150°C

Compound[a]	Retention index[b]
1a	1085.3
1b	1068.7
2a	1164.3
2b	1175.8
3a	1158.0

[a] See Figs. 2 and 3.
[b] *n*-Alkanes used for the determination of retention indices were C_9, C_{10}, C_{11}, C_{12} and C_{13}.

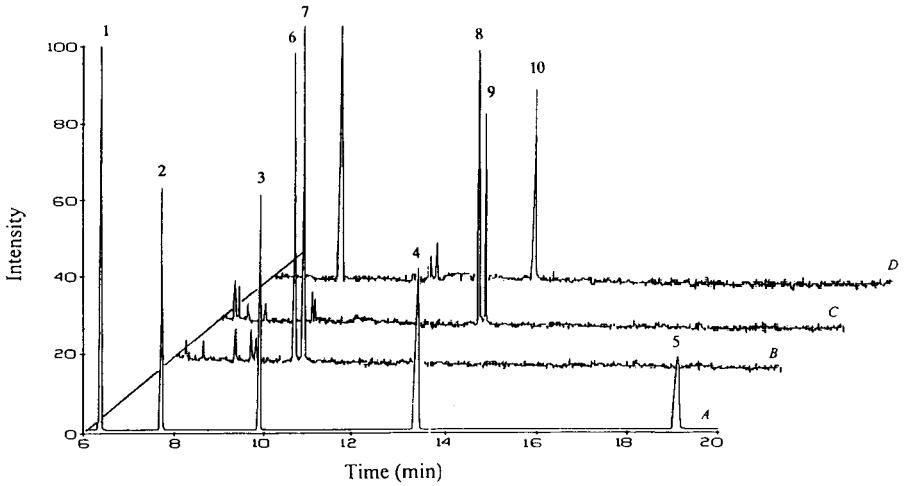

Fig. 1. Total ion chromatograms of the samples investigated. (A) Mixture of *n*-nonane (1), *n*-decane (2), *n*-undecane (3), *n*-dodecane (4) and *n*-tridecane (5); (B) mixture of *cis*- (6) and *trans*-diols (7); (C) mixture of *trans*- (8) and *cis*-bis-TMS (9) derivatives; (D) *trans*-(*tert.*-butyldimethylsilyl) ether (10) derivative.

for identification. Silyl derivatives were therefore prepared in a further attempt to apply them in identification studies [10–12]. The results of MS measurements of the trimethylsilyl and *tert.*-butyldimethylsilyl derivatives are given in Fig. 2. On the basis of these observations, the following main conclusions can be drawn: (i) both diols yield a bistrimethylsilyl derivative; (ii) there are no significant differences in the mass spectra of the trimethylsilyl derivatives at 70 eV (Fig. 3); and (iii) only one of the diol isomers reacts with MTBSTFA under the derivatization condition applied, the other isomer being unreactive (Fig. 1, total ion chromatogram D).

These data, in accordance with our earlier results of a comprehensive study of the derivatization of these isomeric diols [13], can be accounted for as follows. Silylation of diols is certainly a stepwise process. Reaction of sterically demanding silylating agents with these highly

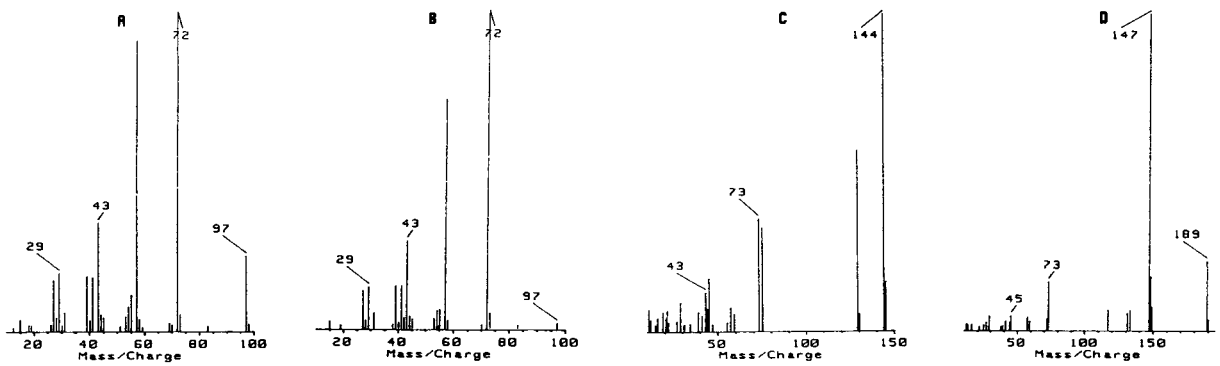

Fig. 2. Mass spectra of the compounds studied. (A) *trans*-2,2,4,4-Tetramethyl-1,3-cyclobutanediol (**1a**); (B) *cis*-2,2,4,4-tetramethyl-1,3-cyclobutanediol (**1b**); (C) *trans*-2,2,4,4-tetramethyl-cyclobutanediol bis-TMS ether (**2a**); (D) *trans*-2,2,4,4-tetramethylcyclobutane-1-*tert.*-butyldimethylsilyloxy-3-ol (**3a**).

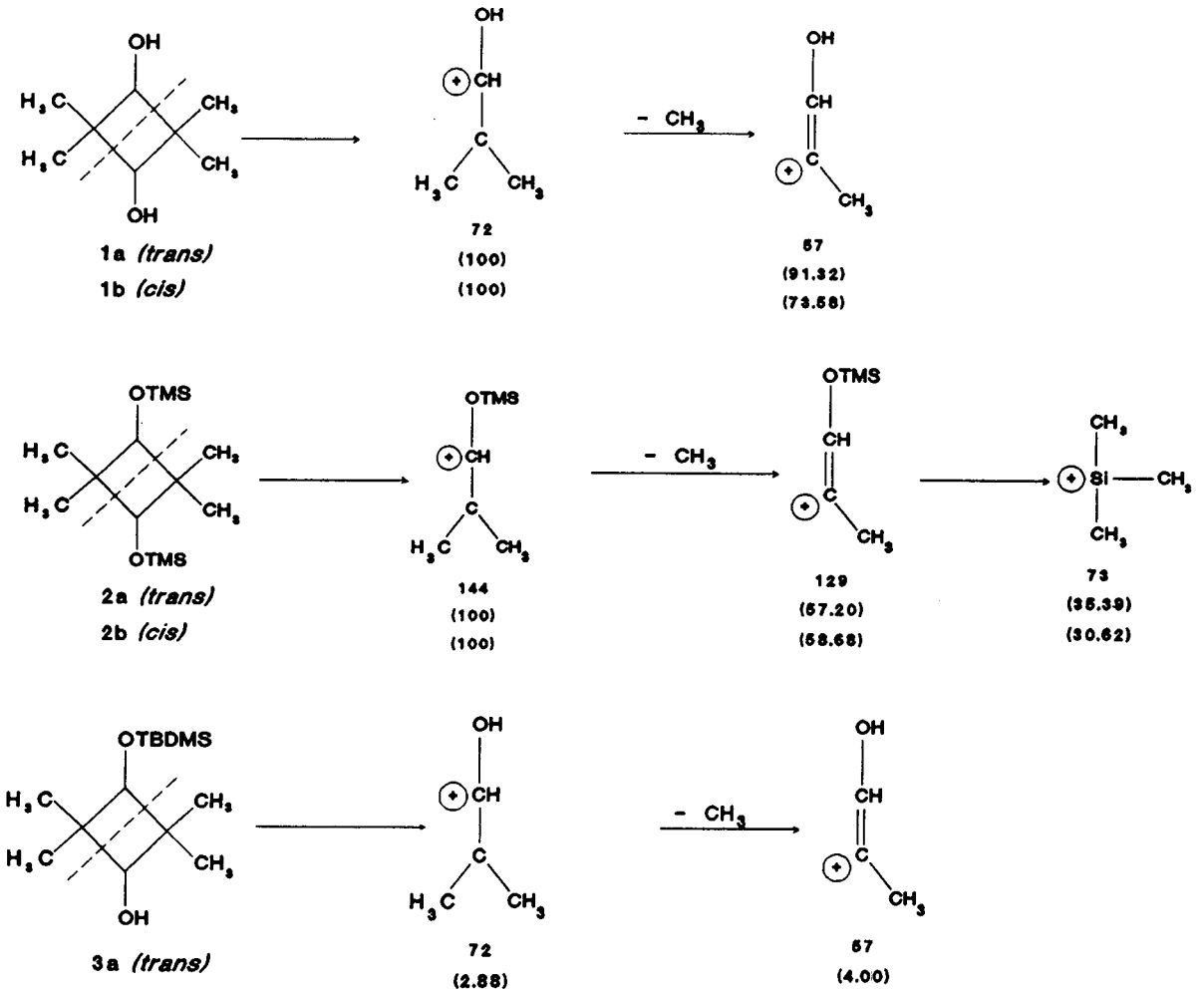

Fig. 3. Fragmentation patterns and the relative intensities of mass peaks of *trans*- (**1a**), and *cis*-2,2,4,4-tetramethyl-1,3-cyclobutanediol (**1b**), *trans*- (**2a**) and *cis*-2,2,4,4-tetramethyl-1,3-cyclobutanediol bis-TMS ether (**2b**) and *trans*-2,2,4,4-tetramethylcyclobutane-1-*tert*.-butyldimethylsilyloxy-3-ol (**3a**).

sterically hindered diols results in striking differences in reactivity. Simple reagents (acid halides, methyl iodide and reagents producing trimethylsilyl derivatives) react readily with both hydroxyl groups in each diol, yielding the corresponding bis derivatives. This does not occur, however, with hindered reagents, which result in severe steric interactions during the derivatization reaction. Neither of the two closely situated hydroxy groups in the *cis*-diol reacts with MTBSTFA, whereas the *trans* compound produces only the monosilylated derivative (Fig. 3). This interpretation was unequivocally confirmed by the attempted silylation of the authentic *cis*-diol sample, which was also unreactive under the reaction conditions employed.

In conclusion, it has been demonstrated that appropriate chromatographic conditions selected on the basis of chemical and steric characteristics permit the GC separation of stereoisomeric 2,2,4,4-tetramethyl-1,3-cyclobutanediols. Unequivocal identification of the individual isomers

was achieved with the utilization of reactivity differences in the silylation of the stereoisomeric diols with sterically demanding reagents.

4. Acknowledgement

We acknowledge support for this research provided by the Hungarian National Science Foundation through grant OTKA 1885/1991 and T 4311.

5. References

[1] R.H. Hasek, E.U. Elam, J.C. Martin and R.G. Nations, *J. Org. Chem.*, 26 (1961) 700.
[2] Á. Molnár, in S. Patai (Editor), *The Chemistry of Functional Groups, Supplement E: the Chemistry of Hydroxyl, Ether and Peroxide groups*, Vol. 2, Wiley, Chichester, 1993.
[3] R.H. Hasek, R.D. Clark and J.H. Chandet, *J. Org. Chem.*, 26 (1961) 3130.
[4] J. Bonastre and P. Greiner, *Bull. Soc. Chim. Fr.*, (1967) 1395.
[5] J. Bonastre and P. Greiner, *Bull. Soc. Chim. Fr.*, (1968) 118.
[6] J. Bonastre and P. Greiner, *Bull. Soc. Chim. Fr.*, (1968) 1292.
[7] *Chromatography Users Catalog*, Hewlett-Packard, Avondale, PA, 1992, p. 78.
[8] J.A. Rijks and C.A. Cramer, *Chromatographia*, 7 (1974) 99.
[9] A. Reinhardt, *Ph. D. Thesis*, Universität Hamburg, Hamburg, 1978, p. 11.
[10] A. Pierce, *Silylation of Organic Compounds*, Chemical, Rockford, IL, 1976, p. 487.
[11] J. Drozd, *J. Chromatogr.*, 113 (1975) 303.
[12] V. Miller and V. Pacakova, *Chem. Listy*, 67 (1973) 1121.
[13] B. Török, K. Felföldi, Á. Molnár and M. Bartók, *J. Organomet. Chem.*, 460 (1993) 111.

ELSEVIER

Journal of Chromatography A, 668 (1994) 469–473

JOURNAL OF CHROMATOGRAPHY A

Short Communication

Evaluation of chromatographic methods for the determination of nifedipine in human serum

Andrzej Jankowski*, Henryk Lamparczyk

Department of Biopharmaceutics, Medical Centre of Postgraduate Education, Debowa 3, 85-626 Bydgoszcz, Poland

Abstract

Gas–liquid chromatography and high-performance liquid chromatography were compared for the identification and determination of nifedipine in biological samples and the elaboration of the optimum liquid–liquid extraction procedure. The determination limits were 2 and 10 ng/ml, respectively, and the detection limits were 1 and 5 ng/ml, respectively. The calibration graphs were linear in the ranges 2–300 and 10–500 ng/ml, respectively. Recoveries based on three different concentrations were 88.7–95.8% and 93.7–104.2%, respectively. Both methods are sensitive, specific and reproducible enough for pharmocokinetic studies and therapeutic drug monitoring.

1. Introduction

Nifedipine [dimethyl 1,4-dihydro-2,6-dimethyl-4-(2-nitrophenyl)pyridine-3,5-dicarboxylate] is a calcium-channel blocking agent, which selectively dilates arteries with little or no effect on other blood vessels. Therefore, nifedipine is used in the treatment of angina pectoris, arterial hypertension and Reynold's phenomenon [1–3].

Nifedipine exhibits large inter-subject variability in absorption, metabolism and excretion. Hence specific, sensitive and rapid measurements of nifedipine in plasma and serum are required for pharmacokinetic studies and to examine the relationship between blood levels and clinical effects. Several methods for the assay of nifedipine in plasma have been described, including a fluorescence method [4], gas chromatography [5–7] and high-performance liquid chromatography [8–10]. Many of these methods, however, are inappropriate for clinical use because they have low sensitivity, are time consuming, need a large amount of plasma and require expensive equipment, which may not be available in clinical laboratories.

The aim of this study was to evaluate two chromatographic methods, gas–liquid (GLC) and high-performance liquid chromatography (HPLC) for the determination of nifedipine in human serum, for the purposes of pharmacokinetic studies and therapeutic drug monitoring.

2. Experimental

2.1. Materials and reagents

Nifedipine and internal standards (nitrazepam and diazepam) were kindly supplied by Pharmaceutical Enterprise "Polfa". Doubly distilled

* Corresponding author.

0021-9673/94/$07.00
SSDI 0021-9673(93)E0038-V

water was used throughout. Other reagents and solvents were of HPLC grade.

2.2. Chromatography

For the HPLC experiments a Kontron Model 400 system consisting of a (Model 420) solvent pump, a (Model 432) UV detector and computer system for acquisition and integration of the data was used. A 250 mm × 4.6 mm I.D. Kontron RP-18 (10-μm) column was used at ambient temperature. The mobile phase was methanol (POCh)–water (70:30, v/v) modified with the addition of 1% glacial acetic acid (POCh). The flow-rate was 1.5 ml/min and the UV detector was operated at 238 nm. Under these conditions the retention time of nifedipine was 4.2 min and that of the internal standard (nitrazepam) was 3.8 min.

Fig. 1 shows typical chromatograms of blank serum and serum spiked with 50 ng/ml of nifedipine and 150 ng/ml of the internal standard.

GLC experiments were performed using a Pye Unicam Model 104 chromatograph with a ^{63}Ni electron-capture detector and a glass column (1.5 m × 4 mm I.D.) packed with 3% OV-17 on Chromosorb W HP (125–150 μm). The operating temperatures were oven 260°C (isothermal), injection port 270°C and detector 300°C. The flow-rate of the carrier gas (argon) was 50 ml/min. Under these conditions, the retention time of nifedipine was 2.7 min and that of diazepam (internal standard) was 4.4 min.

Fig. 2 shows typical chromatograms of blank

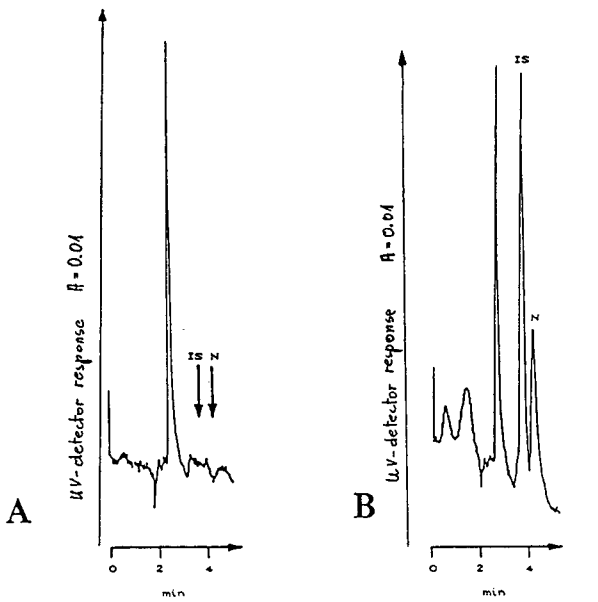

Fig. 1. Typical chromatograms of (A) blank serum and (B) serum spiked with 50 ng/ml of nifedipine (N) and 150 ng/ml of nitrazepam (internal standard, IS). Chromatographic method, HPLC; column, Kontron RP-18 (250 mm × 4.6 mm I.D.); mobile phase, methanol–water (70:30, v/v) modified with the addition of 1% glacial acetic acid.

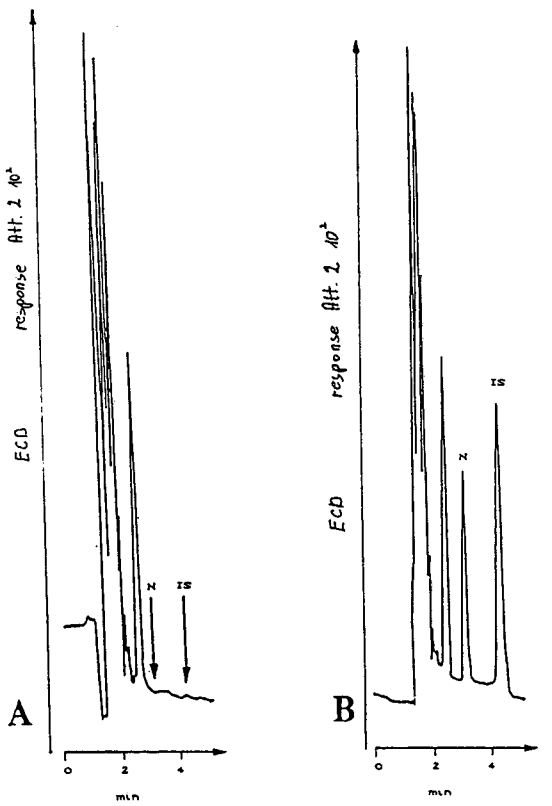

Fig. 2. Typical chromatograms of (A) blank serum and (B) serum spiked with 40 ng/ml of nifedipine (N) and 40 ng/ml of diazepam (IS). Chromatographic method, GLC; column (1.5 m × 4 mm I.D.), packed with 3% OV-17 on Chromosorb W HP (100–120 mesh); column temperature, 260°C; detection, ^{63}Ni electron-capture detector.

serum and serum spiked with 40 ng/ml of nifedipine and 40 ng/ml of the internal standard.

2.3. Extraction procedure

Because nifedipine is very sensitive to light, all samples were stored in complete darkness and analytical operations were done in "gold light". The extraction procedure chosen as the optimum after a number of experiments is described below and was applied for both chromatographic methods considered.

To 1.0 ml of serum sample were added 150 ng of nitrazepam (internal standard for HPLC method) or 40 ng of diazepam (internal standard for GLC method). The sample was then alkalinized with 0.1 ml of 1 *M* NaOH and extracted with 5.0 ml of hexane (POCh)–dichloromethane (Aldrich) (70:30, v/v) by shaking it horizontally for 20 min.

After centrifugation for 10 min, the organic phase was transferred into a conical tube and evaporated to dryness under a stream of nitrogen at 40°C. The residue was dissolved in 120 μl of the mobile phase (for the HPLC method) or 120 μl of benzene (POCh) (for the GLC method). The injection volumes were 20 μl for the HPLC method and 5 μl for the GLC method.

3. Results and discussion

The first stage of the investigation was a search for the optimum pH for nifedipine extraction. The extraction was performed at neutral and alkaline pH, using several organic solvents. It was found that pH does not influence the recovery, but the amount of interfering materials was markedly lower with alkaline extraction.

In order to find the best solvent for extraction of nifedipine from human serum, a number of solvents including chloroform (POCh), dichloromethane and dichloromethane–hexane (30:70, v/v) were tested. Using chloroform and dichloromethane endogenous biological interfering substances were also extracted. The interfering peaks became negligible and nifedipine was well separated from endogenous substances when dichloromethane–hexane (30:70, v/v) was used for extraction. The last solvent system also provided the best recovery, as shown in Table 1. The recovery results were obtained using three different concentrations of nifedipine and HPLC as the detection method.

The determination limits [the lowest concentration that can be determined with a relative standard deviation (R.S.D.) lower than 10%] were 2 and 10 ng/ml for the GLC and HPLC methods, respectively, whereas the detection limits (the lowest measurable concentration that can be distinguished from zero, detected at a signal-to-noise ratio of 3:1) were 1 and 5 ng/ml, respectively.

The calibration graphs were linear in the range of 2–500 ng/ml for the GLC and 10–500 ng/ml for the HPLC method. Recoveries based on three different concentrations and using dichloromethane–hexane as the extraction system were 88.7–95.8% and 93.7–104.2% for the GLC and HPLC methods, respectively.

Table 1
Influence of extraction solvent on recovery of nifedipine from human serum ($n = 6$)

Concentration (ng/ml)	Recovery ± S.D. (%)		
	Chloroform	Dichloromethane	Dichloromethane–hexane (7:3)
25	90.8 ± 8.16	86.4 ± 14.17	104.2 ± 4.13
100	87.6 ± 11.41	81.3 ± 9.21	93.7 ± 4.85
250	84.4 ± 6.12	83.5 ± 8.33	98.1 ± 2.02
150 (IS)	71.4 ± 14.43	68.2 ± 9.13	75.3 ± 7.17

Table 2
Validation of GLC and HPLC methods for nifedipine assay ($n = 6$)

Parameter	Concentration (ng/ml)					
	25		100		250	
	HPLC	GLC	HPLC	GLC	HPLC	GLC
Mean (ng/ml)	26.93	24.43	102.59	94.14	239.24	251.38
S.D.	0.75	2.24	3.09	5.15	2.82	10.97
R.S.D. (%)	2.79	9.20	3.01	5.47	1.18	4.36
Accuracy (%)	7.72	8.66	3.15	4.38	4.30	6.18

For the determination of precision and accuracy, pools of 6 ml of serum were spiked with nifedipine to give concentrations of 25, 100 and 250 ng/ml. Aliquots of 1 ml from each pool were extracted and assayed using the GLC and HPLC methods simultaneously. The results are given in Table 2 and show a slightly better precision and accuracy for the HPLC method. However, the GLC method was slightly more sensitive and the retention time for nifedipine was shorter with the GLC method (2.7 min) than the HPLC method (4.2 min). Nevertheless, the total time of analysis, including elution of the internal standards, was almost the same for both methods. The costs of analysis were also similar for the two methods.

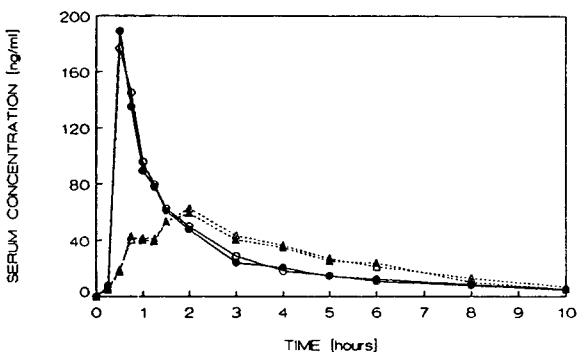

Fig. 3. Concentration *vs.* time profiles for serum from a healthy volunteer after administration of 20 mg of two different forms of nifedipine, determined using GLC and HPLC methods. ● = preparation A (HPLC); ○ = preparation A (GLC); ▲ = preparation B (HPLC); △ = preparation B (GLC).

Hence it can be concluded that both methods are sensitive, specific and reproducible enough for pharmacokinetic studies and therapeutic drug monitoring. In order to confirm these findings, both methods were applied successfully to the determination of nifedipine in human serum. Fig. 3 shows profiles of nifedipine concentration in blood from one healthy volunteer after oral administration of two commercial forms of the drug in a cross-over study, obtained using the two investigated methods. For the same preparation, the curves obtained on the basis of the two methods did not exhibit significant differences. On the other hand, substantial differences were found among two different nifedipine preparations. This finding emphasizes the need for monitoring nifedipine concentrations in blood during therapy.

4. References

[1] S.R. Hamann, M.T. Piascik and R.G. McAllister, Jr., *Biopharm. Drug Dispos.*, 7 (1986) 1.
[2] J.A. Miller, K.A. McLean, D.J. Sumner and J.L. Reid, *Eur. J. Clin. Pharmacol.*, 24 (1983) 315.
[3] J.L. Blackshear, C. Orlandi, G.H. Williams and N.K. Hollenberg, *J. Cardiovasc. Pharmacol.*, 8 (1986) 37.
[4] K. Schlossman, *Arzneim.-Forsch.*, 22 (1972) 60.
[5] S. Kondo, A. Kuchiki, K. Yamamoto, K. Akimoto, K. Takahashi, N. Awata and I. Sugimoto, *Chem. Pharm. Bull.* 28 (1980) 1.

[6] S.R. Hamann and R.G. McAllister, Jr., *Clin. Chem.*, 29 (1983) 158.
[7] L.J. Lesko, A.K. Miller, R.L. Yeager and D.C. Chatterji, *J. Chromatogr. Sci.*, 21 (1983) 415.
[8] K. Miyazaki, N. Kohri, T. Arita, H. Shimono, K. Katoch, A. Nomura and H. Yasuda, *J. Chromatogr.*, 310 (1984) 219.
[9] P. Brummelen and D.D. Breimer, *J. Chromatogr.*, 308 (1984) 209.
[10] M.E. Sheridan, G. Clarke and M.L. Robinson, *J. Pharm. Biomed. Anal.*, 7 (1989) 519.

ELSEVIER

Journal of Chromatography A, 668 (1994) 475–480

JOURNAL OF CHROMATOGRAPHY A

Capillary gas chromatographic determination with nitrogen–phosphorus detection of the calcium antagonist nicardipine and its pyridine metabolite M-5 in plasma

M.T. Rosseel*, R.A. Lefebvre

Heymans Institute of Pharmacology, University of Ghent Medical School, De Pintelaan 185, B-9000 Ghent, Belgium

Abstract

A capillary gas chromatographic method with nitrogen–phosphorus detection for the simultaneous determination of nicardipine and its pyridine metabolite M-5 was developed. The method involves extraction of the plasma with hexane–methylene chloride (1:1, v/v), followed by evaporation of the organic phase. The extract is injected into a fused-silica capillary column coated with cross-linked 5% phenyl–methylsilicone. A temperature gradient (85–285°C) is applied and the two products and the internal standard can be separated within 22 min. The limit of detection is 0.5 ng/ml for both products. The method is suitable for pharmacokinetic studies in humans.

1. Introduction

Nicardipine [2(N-methylbenzylamino)ethyl-methyl-1,4-dihydro-2,6-dimethyl-4-(3-nitrophenyl)-pyridine-3,5-diarboxylate hydrochloride] is a dihydropyridine calcium channel blocker with coronary and peripheral arterial vasodilatory activity used for the treatment of angina pectoris and hypertension [1]. Studies in animals and humans of the metabolism and pharmacokinetics of orally administered nicardipine demonstrated that it was rapidly absorbed, extensively first-pass metabolized to several metabolites (Fig. 1) and rapidly eliminated [1]. The degradation of nicardipine measured in aqueous solution suggests that nicardipine hydrochloride, although light sensitive, is less dramatically modified than nifedipine [2].

Plasma levels of nicardipine have been determined by packed column gas chromatography (GC) with electron-capture detection (ECD) [3]. Using this method, nicardipine was determined following oxidation to a pyridine analogue metabolite [M-5]. A laborious thin-layer chromatographic–GC–mass spectrometric method for the determination of the individual concentrations of nicardipine and its pyridine metabolite has been described [4]. Reported HPLC methods are not sensitive enough [5–7] as the detection limits are >2 ng/ml. Wu *et al.* [8] used a capillary GC method with ECD but the calibration graphs were not linear.

This paper describes a specific and sensitive capillary GC (cGC) method for the simultaneous determination of nicardipine and its metabolite M-5 in the plasma of healthy volunteers.

* Corresponding author.

0021-9673/94/$07.00
SSDI 0021-9673(93)E1113-E

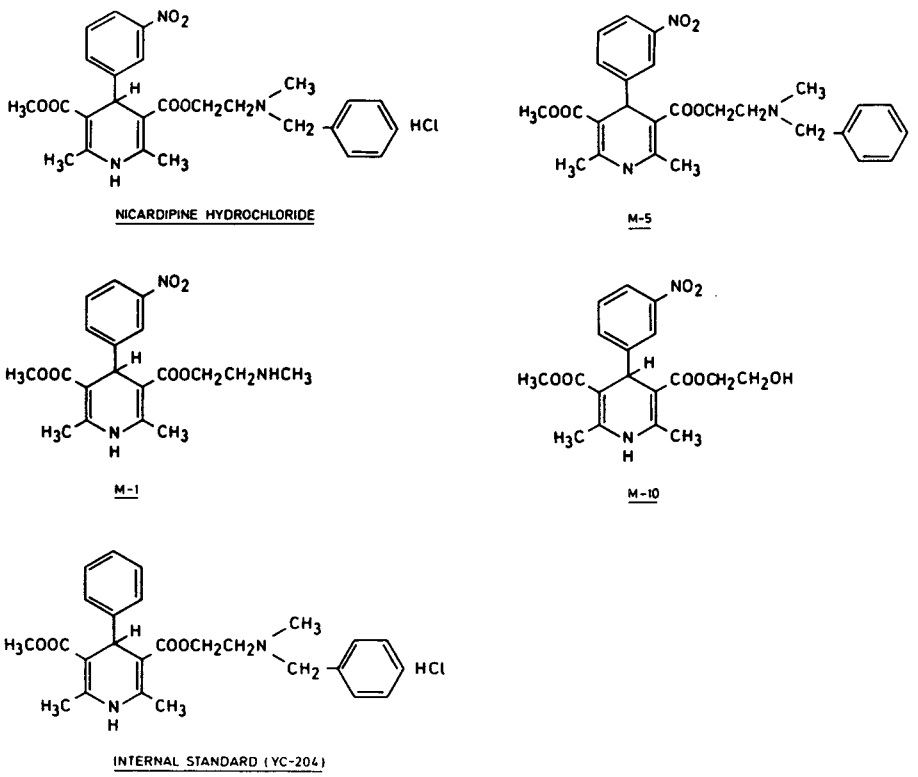

Fig. 1. Structures of nicardipine hydrochloride, its metabolites M-1, M-5 and M-10 and the internal standard (YC-204).

2. Experimental

2.1. Materials

Nicardipine hydrochloride was obtained from Sarva Syntex (Brussels, Belgium). The internal standard (I.S.) YC-204 and the metabolites M-1, M-5 and M-10 were supplied by Yamanouchi Pharmaceutical (Tokyo, Japan).

Hexane and ethyl acetate were of pesticide grade from UCB (Leuven, Belgium) and Carlo Erba (Milan, Italy), respectively. Methylene chloride, sodium hydroxide and triethylamine were of analytical-reagent grade from Merck (Darmstadt, Germany).

Stock solutions

Stock solutions I (technician I) and II (technician II) of nicardipine and the M-5 metabolite were prepared in methanol at a concentration of 1 mg/ml (equivalent to base) and were stored in brown glass tubes at −20°C. Appropriate dilutions were made. A stock solution of the I.S. (1 mg/ml) was prepared in methanol. A 1 μg/ml dilution was made.

Nicardipine and metabolite M-5 standard samples

Plasma samples of 20 ml were spiked with nicardipine and metabolite M-5 (1–50 ng/ml) using stock solution I. These plasma samples were divided into 1.5-ml portions and kept frozen at −20°C until assay.

Nicardipine and metabolite M-5 quality control samples

Plasma samples of 50 ml were spiked with nicardipine and metabolite M-5 (5, 10 and 30

ng/ml) using stock solution II. These plasma samples were divided into 1.5-ml portions and kept frozen at −20°C until assay.

At least three quality control samples (one of each concentration) were used with each set of unknown samples.

2.2. Gas chromatography

A Hewlett-Packard Model 5880 gas chromatograph, equipped with a HP on-column injector, was used. GC was performed on a 12 m × 0.32 mm I.D. Ultra 2 cross-linked 5% phenyl–methylsilicone fused-silica capillary column, with a film thickness of 0.52 μm and a phase ratio of 150 (Hewlett-Packard, Avondale, PA, USA). Samples were injected with a 10-μl Hamilton syringe and a fused-silica needle (0.18 mm O.D.). The oven temperature programme was as follows: initial temperature, 85°C for 1.00 min; programming rate, 20°C/min; final temperature, 285°C, maintained for 17 min. The detector temperature was 300°C. Helium was used as the carrier gas at a flow-rate of 6.0 ml/min and as make-up gas at a flow-rate of 20.0 ml/min. The detector was operated with hydrogen at 3.5 ml/min and with air at 75 ml/min. The peak heights were recorded on a Hewlett-Packard Model 3396A recording integrator.

2.3. Extraction procedure

The internal standard (10 ng in 10 μl of methanol) was added to 1 ml of plasma in a brown, glass-stoppered centrifuge tube. After alkalinization with 0.2 ml of 1.0 *M* Na_2CO_3 and addition of 20 μl of 0.5 *M* triethylamine in hexane–methylene chloride (1:1, v/v), the mixture was extracted twice with 3 ml of hexane–methylene chloride (1:1, v/v) by shaking horizontally for 20 min. The phases were separated by centrifugation (3015 *g*, 20 min, 4°C).

The organic phases were transferred with a Pasteur pipette into a 6-ml brown silanized glass-stoppered conical tube containing 10 μl of 2% triethylamine in ethyl acetate and evaporated to dryness in darkness under a stream of nitrogen at room temperature. The residue was reconstituted in 10 μl of ethyl acetate and 0.5 μl was used for cGC. The samples were stored at −20°C until analysis (within 48 h).

2.4. Calibration

Calibration graphs were constructed by plotting peak-height ratios of product to internal standard against the plasma standard concentration of the product. The best-fit straight line was obtained using the method of least squares and weighing factors of $1/(\text{concentration})^2$. The concentrations of the products in the unknown samples were calculated using this regression line.

2.5. Subjects

Twelve healthy volunteers received a single oral administration of 30 mg of nicardipine. Blood samples were obtained at different intervals after intake and plasma was stored at −20°C until assay.

3. Results and discussion

3.1. Chromatograms

Under the cGC conditions employed, the internal standard, metabolite M-5 and nicardipine are well separated from each other and have retention times of *ca.* 15.06, 15.30 and 21.77 min, respectively. The metabolites, M-1 and M-10, elute together at a retention time of 12.00 min. Representative chromatograms of plasma extracts are shown in Figs. 2 and 3.

3.2. Calibration

Linear relationships were found when the peak-height ratios of nicardipine or metabolite M-5 to the internal standard (y) were plotted against the plasma concentration (x). A typical regression line using $1/(\text{concentration})^2$ as weighing factor for nicardipine is $y = 0.01396 + 0.03546x$, correlation coefficient $(r) = 1.0177$, and for M-5 $y = 0.01529 + 0.06349x$, $r = 0.8518$.

Table 1
Accuracy and reproducibility of the cGC method for the determination of nicardipine and metabolite M-5 in standard plasma samples

Compound	Concentration (ng/ml)	R.S.D. (%)	Accuracy (%)	n
Nicardipine	1	14.0	97.9	9
	2	13.7	106.5	12
	5	12.6	101.9	12
	10	11.9	109.2	12
	20	4.6	98.2	12
	50	5.6	97.6	12
	Mean	10.4	101.8	
Metabolite M-5	1	14.5	98.0	9
	2	15.8	105.8	12
	5	12.7	101.0	12
	10	6.9	97.3	12
	20	9.8	98.5	12
	50	9.9	106.3	12
	Mean	11.6	101.1	

3.3. Accuracy and precision

The accuracy and precision of the method could be derived from back-calculated plasma standard concentrations and by replicate analysis of quality control samples. The results for the back-calculated plasma standards are summarized in Table 1. Results for the independently prepared quality control samples are summarized in Table 2.

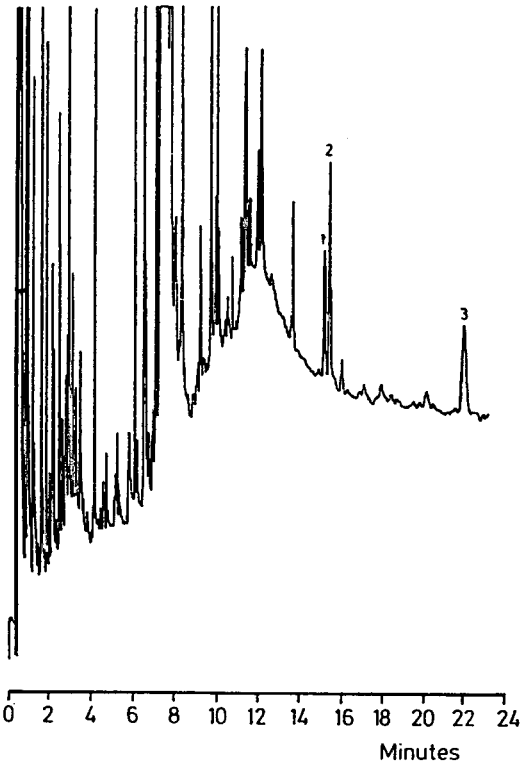

Fig. 2. Chromatogram of an extract of control human plasma spiked with 20 ng/ml of nicardipine (3), 20 ng/ml of metabolite M-5 (2) and 10 ng/ml of internal standard (1).

3.4. Detection limit

At a signal-to-noise ratio of 3, the minimum detectable concentration of both products in

Table 2
Accuracy and reproducibility of the results for quality control samples of nicardipine and metabolite M-5

Compound	Concentration added (ng/ml)	Within-day			Between-day		
		R.S.D. (%)	Accuracy (%)	n	R.S.D. (%)	Accuracy (%)	n
Nicardipine	5	10.9	104.4	5	12.4	96.1	12
	10	5.7	93.0	5	9.4	98.9	13
	30	6.7	100.5	5	8.0	104.0	13
Metabolite M-5	5				11.4	99.5	12
	10				10.0	101.1	13
	30				11.9	109.3	13

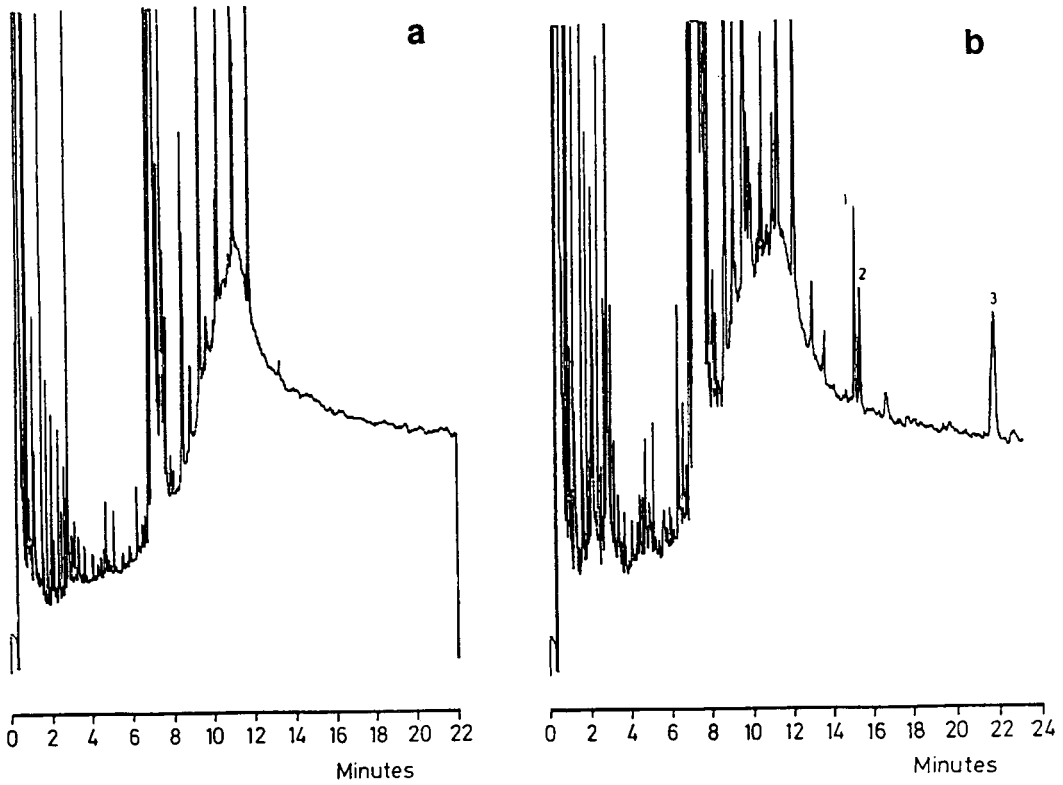

Fig. 3. Chromatograms of extracts. (a) Control human plasma from volunteer 1; (b) plasma from the same volunteer 1.5 h after a single oral dose of 30 mg of nicardipine containing 17.5 ng/ml of nicardipine (3), 7.9 ng/ml of metabolite M-5 (2) and 10 ng/ml of internal standard (1).

plasma under the conditions used was *ca.* 0.5 ng/ml.

3.5. Subjects

Mean (± S.E.M.) concentration–time profiles for nicardipine and metabolite M-5 in twelve healthy volunteers after a single oral dose of 30 mg of nicardipine are shown in Fig. 4.

4. Conclusions

Using a cross-linked 5% phenyl–methylsilicone fused-silica capillary column with on-column injection and nitrogen–phosphorus detection, a specific, sensitive and reproducible method for the determination of nicardipine and its pyridine metabolite M-5 in plasma is possible.

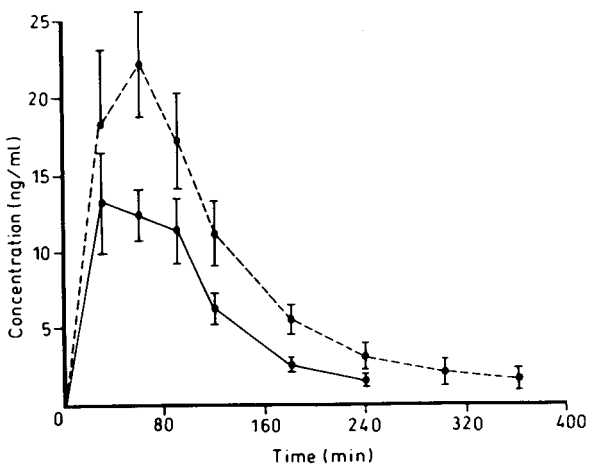

Fig. 4. Mean (± S.E.M.) concentration–time profiles for nicardipine (dashed line) and its metabolite M-5 (solid line) in twelve healthy volunteers following a single oral dose of 30 mg of nicardipine.

5. Acknowledgements

The authors thank Mrs. M. De Meulemeester for technical assistance. They also thank Professor Dr. A. Dupont, Vrije Universiteit Brussel, Brussels, for providing the human plasma samples and Apr. M. Pauwels, Sarva-Syntex, Brussels, for supplying nicardipine hydrochloride.

6. References

[1] E.M. Sorkin and S.P. Clissold, *Drugs*, 33 (1987) 296.
[2] M.C. Bonferoni, G. Mellerio, P. Giunchedi, C. Caramella and U. Conte, *Int. J. Pharm.*, 80 (1992) 109.
[3] S. Higuchi, H. Sasaki and T. Sado, *J. Chromatogr.*, 110 (1975) 301.
[4] S. Higuchi and S. Kawamura, *J. Chromatogr.*, 223 (1981) 341.
[5] T. Wu, I.J. Massey and S. Kushinsky, *J. Pharm. Sci.*, 73 (1984) 1444.
[6] G.C. Visor, E. Bajka and E. Benjamin, *J. Pharm. Sci.*, 75 (1986) 44.
[7] S.I. Kobayashi, *J. Chromatogr.*, 420 (1987) 439.
[8] A.T. Wu, I.J. Massey and S. Kushinsky, *J. Chromatogr.*, 415 (1987) 65.

ELSEVIER

Journal of Chromatography A, 668 (1994) 481–484

JOURNAL OF CHROMATOGRAPHY A

Short Communication

Chromatography of methyl derivatives of 5-ethyl-5-phenyl-2-thiobarbituric acid

Jacek Bojarski*, Maria Kubaszek, Henryk Bartoń, Elżbieta Chmiel

Department of Organic Chemistry, School of Medicine, Jagiellonian University, 30-048 Kraków, Poland

Abstract

Methylation of 5-ethyl-5-phenyl-2-thiobarbituric acid yields two pairs of monomethyl and dimethyl derivatives which are constitutional isomers differing in the N- *vs.* S-methyl substitution. These products were separated by column chromatography on silica gel and also by TLC and HPLC. The chiral methyl derivatives and closely related compounds were resolved using β-cyclodextrin in the mobile phase as a selector. The order of the eluted enantiomers was established by chemical transformation and correlation with enantiomers of known configuration.

1. Introduction

Several 5,5-disubstituted barbituric acids [2,4,6(1H,3H,5H)-pyrimidinetriones] and their 2-thio analogues are well known drugs with hypnotic and antiepileptic activity. Their N-methyl derivatives also show biological activity and are used in the pharmaceutical and toxicological gas chromatographic analysis of parent compounds [1]. Recently we investigated the methylation of 5-ethyl-5-phenyl-2-thiobarbituric acid (2-thiophenobarbital-5-ethyl-5-phenyl-2-thioxo-4,6-(1H,3H,5H)-pyrimidinedione, **1**) using methyl halides and a base (sodium hydride, tetra-*n*-butylammonium hydroxide or potassium hydroxide) [2]. All possible methylation products, *i.e.* N- (**2**), S- (**3**) monomethyl and N,N'- (**4**) and N,S- (**5**) dimethyl derivatives of 1 were obtained (Fig. 1). Compounds **2–4** were obtained previously by other methods [3,4]; **5** has not been described in the literature. We used various chromatographic methods to separate and identify these products. Compounds **2**, **3** and **5** are chiral, and we used chiral chromatography to resolve their enantiomers, as well as the enantiomers of closely related compounds (**6–9**).

2. Experimental

2.1. Reagents and materials

Compound **1**, **7** and **8** were obtained by condensation of diethyl ethylphenylmalonate with thiourea, N-ethylurea and N-ethylthiourea, respectively; compounds **2–5** were obtained by methylation of **1** [2]; compound **9** was obtained by oxidation of N-methyl-2-(N-methyl-thiocarbamyl)-imino-5-ethyl-5-phenylbarbituric acid [5]. Pure enantiomers of **6** with known configuration were kindly donated by Professor J. Knabe (Saarbrücken, Germany), β-cyclodextrin was obtained from Chinoin (Budapest, Hungary). Other reagents and solvents were of analytical

* Corresponding author.

SSDI 0021-9673(93)E0024-O

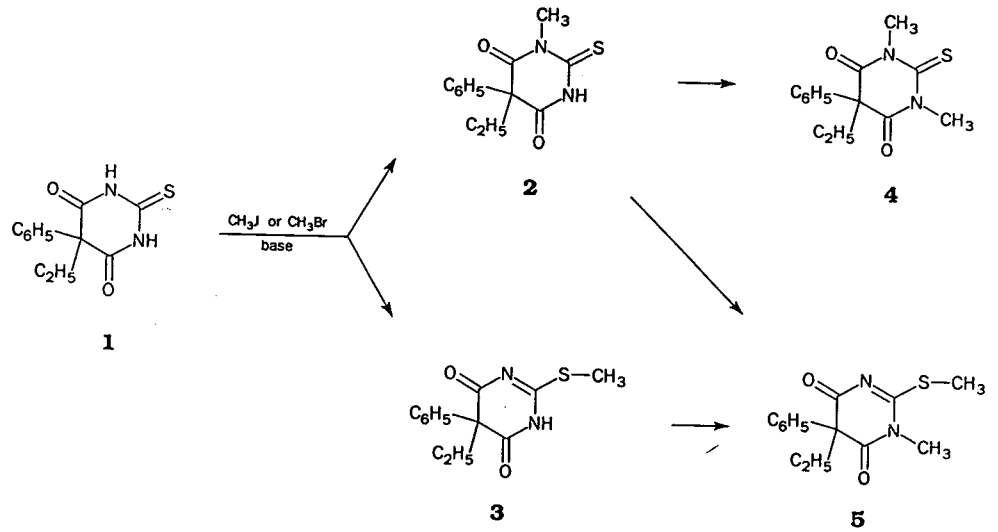

Fig. 1. Methylation of 5-ethyl-5-phenyl-2-thiobarbituric acid (1).

grade (POCh) and were used without purification.

2.2. Chromatography

Column chromatography was carried out in a glass column of diameter 4 cm. Silica gel was used as the adsorbent for chromatography, with 70–325 mesh (Merck). The eluents used were cyclohexane–ethyl acetate [(A) 4:1, (B) 2:1, (C) 1:1]. The volume of collected samples was 5 ml and sample content was determined by TLC.

TLC was performed on precoated TLC aluminium sheets using silica gel 60 F_{254} (Merck). The solvent systems used were: (D) chloroform, (E) chloroform–toluene–acetone (2:2:1) and (F) cyclohexane–ethyl acetate (4:1). Visualization was with UV light at 254 nm.

A Liquochrom OE 312/1 chromatograph equipped with an OE 308 UV detector (Labor MIM, Budapest, Hungary) was used for HPLC. Compounds **2–5** were chromatographed in normal mode using a Sil 10-μm column (250 mm × 4.6 mm I.D.), 4% anhydrous ethanol in *n*-hexane as a mobile phase, a flow-rate of 3 ml/min and UV detection at 240 and 260 nm. Chiral chromatography was carried out in reversed-phase mode using a Chromsil C_{18} 10-μm column (250 mm × 4.6 mm I.D.). The mobile phase was composed of aqueous saturated solution of β-cyclodextrin, 96% ethanol, 0.1 *M* NaH_2PO_4 and 0.1 *M* Na_2HPO_4 (80:10:7.5:2.5) and the flow-rate was 1.5 ml/min. UV detection was at 240 nm and the temperature of chromatographic runs was 25°C.

For configuration assignment the collected eluates of the second-eluted enantiomer of compounds **2**, **5** and **7** were desulphurized to the enantiomers of the corresponding 2-oxo analogues, **6** and **8**, by intensive stirring with 100 mg

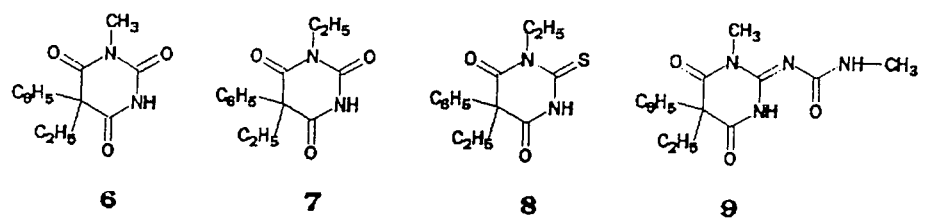

of red HgO for 3 h at room temperature. Then the solvent was evaporated, the residue was extracted with 1 ml of ethanol, and the extract was concentrated to 20–30 μl and co-chromatographed under conditions described above with the enantiomer of **6**. The eluate with the second-eluted enantiomer of compound **9** was transformed into the enantiomer of **6** by heating with concentrated HCl for 1 h, storing for 24 h at room temperature, evaporating the solvent, extracting with ethanol (1 ml) and concentrating of the sample and chromatography under conditions given above.

3. Results

Liquid chromatography of products **2–5** is exemplified by the results of elution after chromatography of the reaction mixture obtained after methylation of **1** (0.94 g) on 150 g of silica gel:

Eluent A: 165 ml + 145 ml (compound **4**, 0.1 g) + 60 ml, eluent change.

Eluent B: 80 ml + 100 ml (compound **2**, 0.23 g) + 110 ml + 65 ml (compounds **5**, 0.13 g) + 50 ml (compound **5** and **1**, 0.10 g) + 65 ml (compound **1**, 0.06 g) + 90 ml; eluent change.

Eluent C: 135 ml + 125 ml (compound **3**, 0.35 g).

The results of TLC and HPLC separations for compounds **2–5** are presented in Table 1, while

Table 1
Results of TLC and HPLC (normal-phase mode) separations of methyl derivatives of 2-thiophenobarbital

Compound	TLC (R_F values)			HPLC (t_R, min)
	Solvent system			
	D	E	F	
1	0.13	0.60	0.29	–
2	0.25	0.69	0.44	1.5
3	0.04	0.56	0.13	7.8
4	0.51	0.74	0.58	1.1
5	0.13	0.66	0.21	3.1

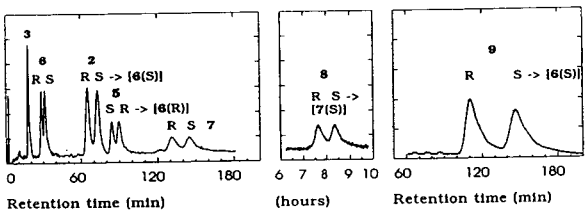

Fig. 2. Resolution of enantiomers of methyl derivatives of 5-ethyl-5-phenyl-2-thiobarbituric acid and closely related compounds. For conditions see the Experimental section. For compound designation and structures see Fig. 1 and the text.

those of chiral chromatography are given in Fig. 2 and Table 2.

4. Discussion

The results presented above show that the chromatographic methods used are well suited for separation and identification of all products of methylation of 2-thiophenobarbital, which are two pairs of constitutional isomers. In each pair the N-CH_3-substituted compound migrated faster than its S-CH_3-substituted counterpart in all chromatographic systems used with the exception of chiral chromatography. The fastest migration was observed for the N,N′-dimethyl derivative.

Of the three chiral methyl derivatives of 2-thiophenobarbital (compounds **2**, **3** and **5**) and four other closely related compounds (**6–9**), only one (**3**) was not resolved into enantiomers with

Table 2
Retention times and enantioseparation factors for chiral products of methylation of 2-thiophenobarbital and related compounds

Compound	t_R (min)		α
	R	*S*	
2	65.5	74.0	1.13
3	18.0	18.0	1.0
5	90.1	84.8	1.06
6	28.8	31.5	1.10
7	132.5	146.5	1.12
8	457.0	501.0	1.10
9	112.0	148.0	1.32

β-cyclodextrin in the mobile phase used as the chiral selector. For all but one resolved compounds the first eluted was the enantiomer with the *R* configuration. For the N,S-dimethyl derivative of **1** (compound **5**) the first eluted was the (*S*)-enantiomer, probably because of the C_2–N_3 double bond in the ring —the structural feature unique among the resolved compounds.

The elution order and configuration were confirmed by transformation of the second-resolved enantiomer of compounds **2**, **5** and **8** to the corresponding 2-oxo analogue (compound **6**), of which the elution order and configuration under similar conditions were determined previously [6] based on synthetic specimens of individual enantiomers of **6** [7].

The elution order of the enantiomers of compound **7** was assumed to be the same as that of compound **6**. The elution order of the enantiomers of compound **9** was correlated with that of **6** by hydrolytic splitting of the exocyclic N-methylurea moiety.

5. References

[1] D.N. Pillai and S. Dilli, *J. Chromatogr.*, 220 (1981) 253.
[2] M. Kubaszek, M. Paluchowska, E. Chmiel and J. Bojarski, *Pol. J. Chem.*, submitted for publication.
[3] F.S. Crossley, E. Miller, W.H. Hartung and M.L. Moore, *J. Org. Chem.*, 5 (1940) 238.
[4] W.R. Boon, H.C. Carrington, N. Greenhalgh and C.H. Vasey, *J. Chem. Soc.*, (1954) 3263.
[5] K. Hesse, H. Goldhahn and H. Fürst, *Arch. Pharm.*, 295 (1962) 598.
[6] J. Zukowski, D. Sybilska and J. Bojarski, *J. Chromatogr.*, 364 (1986) 225.
[7] J. Knabe, H. Junginger and W. Geismar, *Liebigs Ann. Chem.*, 739 (1970) 15.

ELSEVIER

Journal of Chromatography A, 668 (1994) 485–494

JOURNAL OF CHROMATOGRAPHY A

Reversed-phase retention characteristics of some bioactive heterocyclic compounds

Yassin Darwish, Tibor Cserháti*, Esther Forgács

Central Research Institute for Chemistry, Hungarian Academy of Sciences, P.O. Box 17, 1525 Budapest, Hungary

Abstract

The lipophilicities and specific hydrophobic surface areas of sixteen bioactive heterocyclic compounds were determined by reversed-phase thin-layer chromatography using various eluent systems. The data were evaluated by principal component analysis (PCA), separately calculated from the correlation and covariance matrices, and by cluster analysis. The ratio of the variances explained by the first PC component was high and was very similar for both PCA methods, suggesting that the eluents have common elution characteristics. The lipophilicities and specific hydrophobic surface areas of the compounds are well separated on the two-dimensional non-linear maps of PC variables, indicating the different information contents of the two physico-chemical parameters. The information contents of cluster analysis and two-dimensional non-linear mapping techniques were found to be similar but not identical.

1. Introduction

In recent years, quantitative structure–activity relationship (QSAR) studies have found growing acceptance and application in the design of new bioactive compounds [1,2]. Many molecular parameters have been correlated with the biological activity, and many of them can be readily determined by various chromatographic techniques [3]. Chromatographic methods have some advantages, *e.g.*, they are simple and rapid and require minute amounts of substances which need not necessarily be very pure.

Lipophilicity is a frequently used molecular parameter in QSAR studies [4]. Reversed-phase thin-layer chromatography (RP-TLC) has been extensively applied to determine lipophilicity [5,6]. However, in RP-TLC the apparent lipophilicity (R_M value) depends on the chromatographic conditions, mainly on the organic phase concentration in the eluent [7–9]. The support particles partially retain their original adsorptive characteristics even after coating [10], and the R_M value changes with the amount [11] and quality [12,13] of the coating substance. When the compound contains one or more dissociable polar substituents, the pH of the eluent [14,15] and the salt concentration [16–18] also modify the lipophilicity. It has been established that not only the R_M value extrapolated to zero organic phase concentration (R_{M0}) but also the slope (b) of the plot between the R_M values and the organic phase concentration of the eluent (C) characterizes the molecular lipophilicity [19,20]. For a homologous series of compounds, the slope and the R_{M0} value exhibit a significant linear correlation [20], but for a non-homologous

* Corresponding author.

0021-9673/94/$07.00
SSDI 0021-9673(93)E1037-Z

series of solutes both parameters are needed to describe the lipophilicity accurately [21]. The slope has been regarded as a characteristic of the specific hydrophobic surface area of the compounds [22].

The application of computer-assisted multivariate mathematical–statistical methods makes possible the simultaneous evaluation of an almost unlimited number of variables (chromatographic parameters), which greatly facilitates the solution of theoretical and practical problems. Principal component analysis (PCA) has been applied in chromatography to identify basic factors that influence solute–solvent interactions and to classify solutes and solvents into groups having similar characteristics [23]. The advantages of PCA are that it clusters the variables according to their relationship (clustering chromatographic systems or solutes on the basis of their retention behaviour) and the clusters can be easily visualized by a non-linear mapping technique [24]. In addition, PCA offers the possibility of the extraction of one or more background variables having a concrete physicochemical meaning for the theory and practice of chromatography and it decreases the number of variables to the minimum number required for the solution of a problem [25]. PCA is suitable not only for the calculation of two–two variable relationship (PC variables), but also for the study of all variables of a linear correlation system. PCA can be carried out on both the correlation and covariance matrices of the original data set but the results can sometimes be different [26].

Recently, cluster analysis has found broad application in various fields [27]. In chemistry, cluster analysis has been used for the classification of compounds based on their properties. Cluster analysis belongs to the class of procedures that seek to separate the component data into groups by uncovering the interrelationships that exist among them [28,29].

The objectives of this study were to determine the lipophilicities and specific hydrophobic surface areas of some bioactive heterocyclic compounds for future QSAR studies by reversed-phase chromatography, to compare the physicochemical parameters determined in various chromatographic systems, to evaluate the relationships between retention characteristics by various multivariate mathematical–statistical methods such as PCA, two-dimensional non-linear mapping and cluster analysis and to assess the similarities and dissimilarities between the information content of the methods.

2. Experimental

The structures of the compounds are compiled in Table 1. The imines (group A) were the starting materials for further synthetic work and the phenoxy (group B) and benzothiazole derivatives (group C) were synthesized as promising insecticides and antibacterial agents, respectively. The compounds were dissolved in acetone (0.5 mg/ml) and 2 μl of each solution were spotted on Silcoplate F-254 plates (Reanal Fine Chemicals, Budapest, Hungary) impregnated by overnight predevelopment with *n*-hexane–paraffin oil (95:5, v/v). The plates were developed in a sandwich chamber at room temperature using different organic modifiers at various concentrations, and neutral, salt-containing, basic and acidic aqueous phases. The following solvent systems were applied: I, methanol–water; II, methanol–aqueous NaCl; III, methanol–aqueous CH_3COONa; IV, methanol–aqueous CH_3COOH; V, ethanol–water; VI, ethanol–aqueous NaCl; VII, methanol–aqueous CH_3COONa; and VIII, methanol–aqueous CH_3COOH [methanol and ethanol were used in the concentration range 30–50% (v/v) in steps of 5%, and the end concentration of additives in the eluent was 0.25 *M* in each instance]; IX, acetone; X, tetrahydrofuran and XI, dioxane [20–40% (v/v) in steps of 5%]; XII, 1-propanol; and XIII, 2-propanol [10–20% (v/v) in steps of 2.5%]; XIV, acetonitrile [15–35% (v/v) in steps of 5%]; and XV, glycerol [80–95% (v/v) in steps of 2.5%].

After development, the plates were dried at 105°C and the spots were detected under a UV lamp and with iodine vapour. Four independent parallel determinations were carried out in each

Table 1
Structures of heterocyclic compounds studied

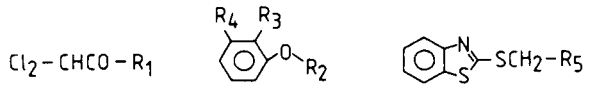

A B C

General formula

Compound No.	General formula	R_1	R_2	R_3	R_4	R_5
1	A	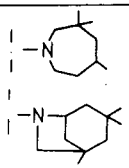	–	–	–	–
2			–	–	–	–
3	B	–	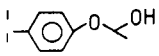	CH_3	CH_3	–
4		–		CH_3	CH_3	–
5		–	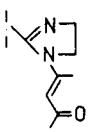	CH_3	CH_3	–
6		–	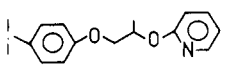	H	H	–
7		–	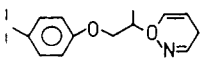	H	H	–
8	C	–	–	–	–	$-COOC_2H_5$
9		–	–	–	–	
10		–	–	–	–	$-CONHNH_2$
11		–	–	–	–	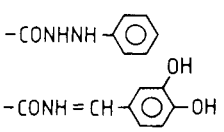
12		–	–	–	–	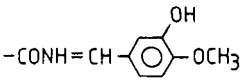
13		–	–	–	–	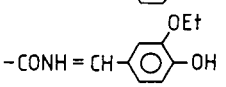
14		–	–	–	–	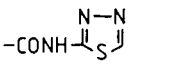
15		–	–	–	–	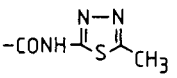
16		–	–	–	–	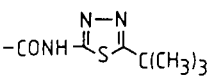

The heterocyclic compounds were synthesized by Dr. Y. Darwish (Mansoura University, Mansoura, Egypt).

instance. The data were omitted from the calculations when the spot of the solute remained at the start or was very near to the front or the relative standard deviation of the four parallel determinations was above 8%. The R_M values of the compounds were determined according to the equation

$$R_M = \log (1/R_F - 1) \quad (1)$$

To increase the accuracy of the lipophilicity determination and to determine the specific hydrophobic surface area, linear correlations were calculated between the R_M values of the compounds and the concentration of organic solvent (C) in the eluent:

$$R_M = R_{M0} + bC \quad (2)$$

where R_M is the actual R_M value of a compound determined at a concentration C of organic modifier in the eluent, R_{M0} (intercept) is the R_M value of a compound extrapolated to zero organic phase concentration in the eluent and b (slope) is the lipophilicity change of a compound caused by unit concentration change of the organic phase. The R_{M0} and b values in eqn. 2 were considered to be the best indicator of the lipophilicity and the specific hydrophobic surface area of the compounds, respectively.

The calculation was carried out separately for each compound and for each eluent system.

To compare the retention behaviour of the compounds, the data (parameters of eqn. 2) were evaluated by multivariate mathematical–statistical methods, as follows.

2.1. Principal component analysis

PCA has been used to assess the similarities and dissimilarities both between the RP-TLC systems and solutes. PCA was carried out on the retention data matrix consisting of the lipophilicity and specific hydrophobic surface area values of solutes. The RP-TLC systems were the variables and the solutes were the observations. To elucidate the effect of normalization required for the calculation of the correlation matrix on the results of PCA, PCA was carried both on the correlation and on the covariance matrix. The limit of the variance explained was set to 99.9% in both instances.

2.2. Non-linear mapping technique

For easier visualization of the distribution of RP-TLC systems and solutes, the two-dimensional non-linear maps of PC loadings and variables obtained by both PCAs were calculated. The iteration was carried out to the point where the difference between the two last iterations was lower than 10^{-8}.

2.3. Cluster analysis

Cluster analysis has been used to elucidate the similarities between RP-TLC systems. To study the effect of PCA on the cluster formation, calculations were carried out on the original data matrix and on the PC variables calculated both from the correlation and the covariance matrices.

2.4. Comparison of the various multivariate methods

To compare the information content of the two PCA methods, linear correlations were calculated between the corresponding coordinates of the two-dimensional non-linear maps. Dependent variables were always those calculated from the covariance matrix:

PC loadings:

$$Y_{\text{cov1}} = a + bX_{\text{corr1}} \quad (3)$$

$$Y_{\text{cov2}} = a + bX_{\text{corr2}} \quad (4)$$

PC variables:

$$Y_{\text{cov3}} = a + bX_{\text{corr3}} \quad (5)$$

$$Y_{\text{cov4}} = a + bX_{\text{corr4}} \quad (6)$$

where X and Y are the coordinates of the corresponding non-linear maps of PC loadings and variables calculated from the correlation and covariance matrices, respectively.

Cluster analysis and non-linear mapping techniques are theoretically similar, and therefore

the distances between the units (in this instance RP-TLC systems) have to be similar. To verify the validity of the hypothesis outlined above, linear correlations were calculated between the corresponding distances on the cluster dendograms (the dependent variable being in both instances the distances on the cluster dendogram calculated from the original data matrix). Linear correlations were also calculated between the distances on the cluster dendogram (dependent variables) of the original data matrix and the distances on both two-dimensional non-linear maps. To facilitate calculations only the neighbouring distances were included.

3. Results and discussion

Each compound showed normal retention behaviour, that is, the retention decreased monotonously with increasing concentration of organic modifier and no anomalous retention behaviour was observed to make questionable the application of eqn. 2. The relationships between the R_M values and the concentration of organic phase in the eluent were in each instance highly significant, as shown on some examples in Table 2. The r values indicate that the change in the organic solvent concentration explains 82–99% of the change in compound retention, proving again the applicability of eqn. 2. It was found that the slope values for glycerol–water eluents are the lowest, a finding in good accordance with the solvent strength theory that a less lipophilic solvent exerts a weaker effect on retention. The high R_{M0} values indicate that the compounds are hydrophobic and they show very low mobility in water as eluent, that is, the use of a relatively high concentration of organic modifier is needed for their effective reversed-phase separation. The R_{M0} values differ slightly according to the character of the organic modifier, although they have to be identical as theoretical values extrapolated to zero organic phase concentration. This discrepancy can be tentatively explained by the inherent low reproducibility of RP-TLC and the possible non-linearity of extrapolation. However, R_{M0} values of similar magnitude have been successfully used in previous QSAR studies and we strongly believe that the discrepancies discussed above will not influence their further application.

3.1. Principal component analysis

Results of PCA carried out on the correlation and covariance matrices are summarized in Table 3. The first principal component explains most of the total variance, indicating that the retention characteristics of the fifteen eluent systems can be described by only one background variable. This result suggests that the eluents have common elution characteristics. In other words, a single chromatographic system should be sufficient to obtain most of the information content of all RP-TLC systems. Unfortunately, PCA does not define this system as a concrete physico-chemical unit, but only indicates its mathematical possibility. The ratio of the variance explained for both PCA methods is very similar, that is, the PCAs calculated from the correlation and covariance matrices extract similar amounts of information from the original data matrix. This finding indicates that the normalization required for the calculation of the correlation matrix does not modify markedly the variance explained by the principal components.

3.2. Non-linear mapping technique

The two-dimensional non-linear maps of PC loadings calculated from the correlation and covariance matrices are very similar (Figs. 1 and 2). Except for glycerol, all the eluent systems form one cluster. This finding supports our previous quantitative conclusion that the retention characteristics of glycerol differ considerably from those of the other organic modifiers. The eluents containing salt, acidic and alkaline additives are not separated from the corresponding neutral eluent systems, that is, the pH value and sodium chloride content have negligible effects on the retention behaviour of these heterocyclic derivatives. This finding is surprising because the compounds are alkaline and therefore the pH of the eluent should modify their retention. The

Table 2
Parameters of linear correlations between the R_M value of pesticides and the concentration of organic modifier (C) in the mobile phase

Compound No.	No. of eluent system																	
	I			II			III			IV			IX			XV		
	R_{M0}	$-b \cdot 10^2$	r	R_{M0}	$-b \cdot 10^2$	r	R_{M0}	$-b \cdot 10^2$	r	R_{M0}	$-b \cdot 10^2$	r	R_{M0}	$-b \cdot 10^2$	r	R_{M0}	$-b \cdot 10^2$	r
1	2.17	3.81	0.9844	2.13	3.72	0.9708	2.11	3.72	0.9658	2.36	4.20	0.9761	1.66	2.90	0.9764	3.04	2.24	0.9882
2	2.50	4.14	0.9883	2.35	3.82	0.9708	2.48	4.16	0.9917	2.36	3.86	0.9942	1.81	2.26	0.9598	2.38	1.41	0.9649
3	2.82	4.42	0.9766	2.93	4.70	0.9744	2.71	4.26	0.9695	3.17	5.44	0.9806	2.36	4.30	0.9593	3.21	2.37	0.9873
4	2.12	2.55	0.8511	2.73	3.32	0.9960	1.13	2.24	0.9608	1.12	2.62	0.9559	2.19	3.86	0.9647	2.32	1.45	0.9709
5	2.74	3.83	0.9117	2.26	3.28	0.9367	2.35	3.64	0.9036	1.38	3.20	0.9776	2.45	5.10	0.9729	3.41	2.51	0.9470
6	2.26	4.13	0.9672	2.09	3.62	0.9942	2.33	4.42	0.9516	2.28	4.26	0.9774	2.12	4.00	0.9651	6.47	5.68	0.9623
7	2.94	4.71	0.9878	2.92	4.64	0.9803	3.05	5.00	0.9781	3.06	5.08	0.9882	2.59	5.04	0.9837	3.14	2.19	0.9854
8	2.51	3.89	0.9797	2.51	3.88	0.9969	2.51	3.94	0.9674	2.68	4.36	0.9614	2.24	3.88	0.9598	3.00	2.18	0.9371
9	2.07	3.74	0.9874	1.94	3.50	0.9846	2.30	4.40	0.9698	1.61	3.08	0.9480	1.28	3.02	0.9942	2.23	2.07	0.9810
10	2.57	4.27	0.9931	2.73	4.58	0.9859	2.79	4.84	0.9594	2.87	5.06	0.9615	2.55	5.22	0.9210	2.32	1.75	0.9603
11	2.84	5.13	0.9930	2.69	4.56	0.9674	3.00	5.48	0.9569	3.02	5.50	0.9925	2.11	5.10	0.9835	2.42	2.04	0.9784
12	3.14	5.18	0.9649	2.34	3.34	0.9579	2.70	4.26	0.9933	3.18	5.36	0.9886	2.50	5.56	0.9686	3.56	2.81	0.9960
13	2.84	4.11	0.8209	3.39	5.42	0.9992	3.85	6.52	0.9746	3.71	6.16	0.9955	2.72	5.62	0.9847	2.83	1.72	0.9915
14	2.73	4.39	0.9905	2.38	3.45	0.9915	2.81	4.56	0.9621	2.49	3.86	0.9952	2.19	3.72	0.9955	3.42	2.54	0.9914
15	2.48	3.86	0.9155	2.57	4.04	0.9919	2.24	3.22	0.9603	2.65	3.36	0.9705	2.72	5.52	0.9749	3.03	2.10	0.9686
16	2.53	3.93	0.9914	2.50	3.80	0.9935	2.47	3.84	0.9608	2.91	4.92	0.9740	2.20	3.66	0.9690	2.82	1.95	0.9919

Roman numbers refer to the reversed-phase chromatographic systems in Experimental and arabic numbers refer to solutes in Table 1. Equation: $R_M = R_{M0} + bC$.

Table 3
Similarities and dissimilarities between the retention characteristics of RP-TLC systems

No. of principal component	Variance explained (%)		Total variance explained (%)	
	CORR	COVA	CORR	COVA
1	80.15	84.53	80.15	84.53
2	6.69	5.53	86.84	90.06
3	3.92	3.17	90.77	93.24

Results of principal component analysis using the correlation (CORR) and the covariance matrix (COVA).

elucidation of this phenomenon needs further investigation.

The two-dimensional non-linear maps of PC variables are shown in Figs. 3 and 4. As for the two-dimensional non-linear map of PC loadings, similar conclusions can be drawn from both maps: the hydrophobicity (R_{M0}) and specific hydrophobic surface area (b) of the compounds are well separated from each other, indicating that the two physico-chemical parameters have different information contents and both of them can be included in QSAR studies as separate

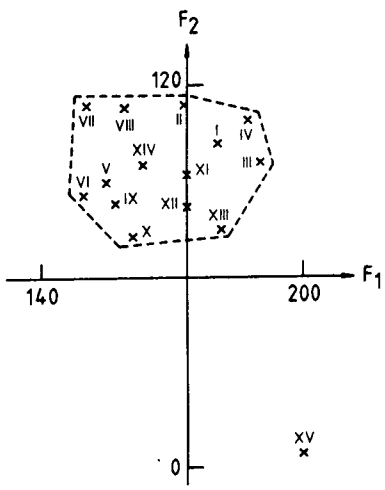

Fig. 1. Two-dimensional non-linear map of PC loadings calculated from the correlation matrix. Number of iterations, 485; maximum error, $2.87 \cdot 10^{-2}$. Numbers refer to eluent systems in Experimental.

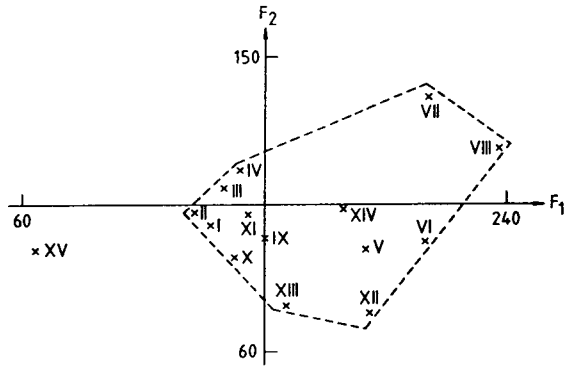

Fig. 2. Two-dimensional non-linear map of PC loadings calculated from the covariance matrix. Number of iterations, 68; maximum error, $1.67 \cdot 10^{-2}$. Numbers refer to eluent systems in Experimental.

independent variables. The compounds do not form separate clusters according to their chemical structures, which makes it probable that each substructure has a similar impact on the retention characteristics.

3.3. Cluster analysis

The cluster dendogram calculated from the original data matrix is shown in Fig. 5. The distribution of RP-TLC systems represented by distances proves again that the retention characteristics of glycerol (system XV) deviate the most strongly from the retention characteristics of other systems. The dendograms of clusters calcu-

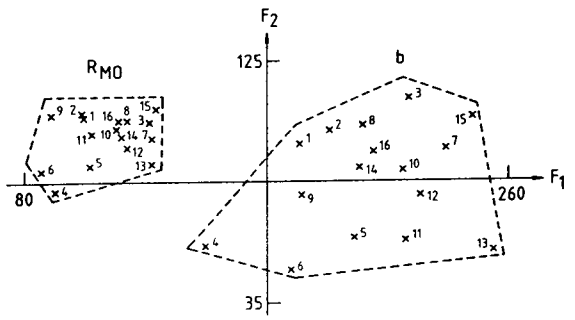

Fig. 3. Two-dimensional non-linear map of PC variables calculated from the correlation matrix. Number of iterations, 288; maximum error, $1.00 \cdot 10^{-2}$. Numbers refer to heterocyclic compounds in Table 1. R_{M0} = lipophilicity; b = specific hydrophobic surface area.

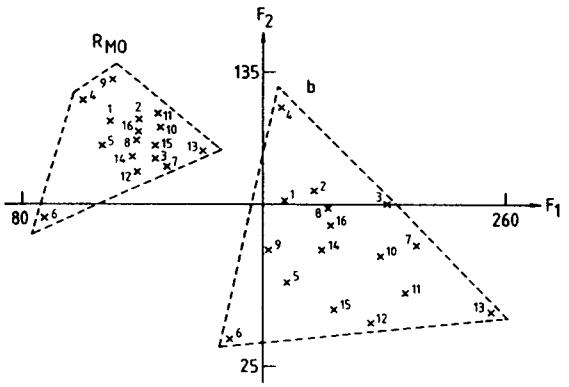

Fig. 4. Two-dimensional non-linear map of PC variables calculated from the covariance matrix. Number of iterations, 109; maximum error, $7.95 \cdot 10^{-3}$. Numbers refer to heterocyclic compounds in Table 1. R_{M0} = lipophilicity; b = specific hydrophobic surface area.

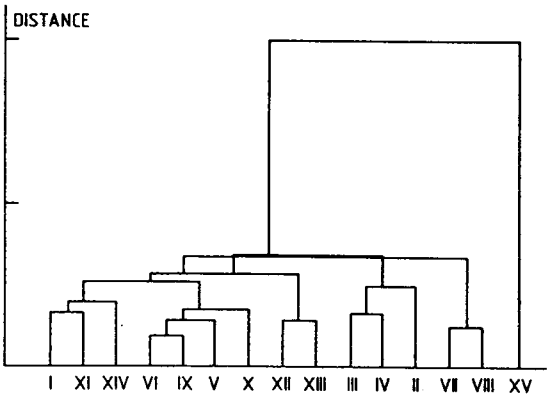

Fig. 6. Cluster dendogram of eluent systems calculated from PCA loadings (correlation matrix). Numbers refer to eluent systems in Experimental.

lated from the PC loadings are shown in Figs. 6 and 7. The clusterings of chromatographic parameters are appreciably different on both dendograms. These results indicate that the use of PCA considerably modifies the distribution of eluent systems, and the results of PCA and cluster analysis may be different. We must stress that this conclusion is based only on experimental data and is not supported by theoretical considerations. It is reasonable to assume that the conclusions are valid only for this data matrix and each generalization may lead to severe misinterpretation.

3.4. Comparison of the various multivariate methods

The parameters of linear correlations between the corresponding coordinates of the two-dimensional non-linear maps of PC loadings and variables calculated from the correlation and covariance matrices are compiled in Table 4. The significant correlations between the coordinates

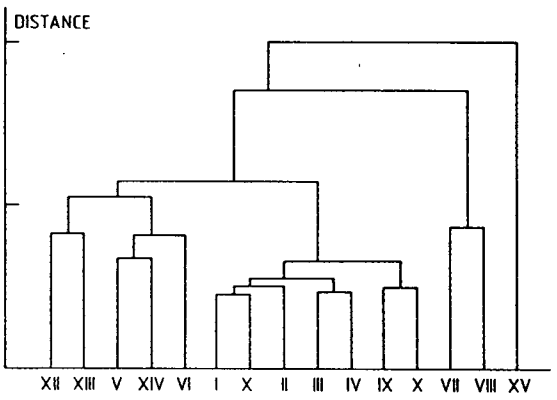

Fig. 5. Cluster dendogram of eluent systems calculated from the original data matrix. Numbers refer to eluent systems in Experimental.

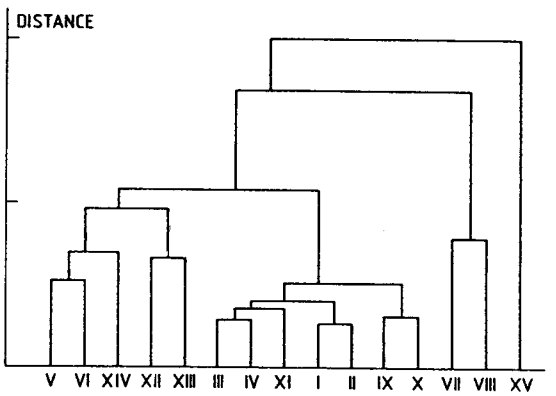

Fig. 7. Cluster dendogram of eluent systems calculated from the PCA loadings (covariance matrix). Numbers refer to eluent systems in Experimental.

Table 4
Comparison of the information content of PCAs carried out on the correlation and on the covariance matrix

Equation No.	Parameter				
	n	a	b	S_b	r
3	15	421.41	−1.63	0.38	0.7682
4	15	51.34	0.42	0.18	0.5401
5	32	−30.89	1.19	0.06	0.9659
6	32	57.46	0.35	0.10	0.5422

Parameters of the linear correlations between the corresponding coordinates of the two-dimensional non-linear maps of PC loadings and variables:

PC loadings:

$$Y_{cov1} = a + bX_{corr1} \quad (3)$$

$$Y_{cov2} = a + bX_{corr2} \quad (4)$$

PC variables:

$$Y_{cov3} = a + bX_{corr3} \quad (5)$$

$$Y_{cov4} = a + bX_{corr4} \quad (6)$$

Table 5
Comparison of the information content of non-linear mapping technique and cluster analysis both carried out on the PCA loadings

Equation No.	Parameter				
	n	a	b	S_b	r
7	7	26.88	0.54	0.11	0.9116
8	7	10.55	0.87	0.10	0.9656

Parameters of significant linear correlations[a]:

$$Y = a + bX_1 \quad (7)$$

$$Y = a + bX_2 \quad (8)$$

[a] Y = distances between the nearest neighbouring RP-TLC systems on the cluster dendogram calculated from the original data matrix; X_1 = distances between the same RP-TLC systems on the two-dimensional non-linear map of PC variables calculated from the covariance matrix; X_2 = distances between the same RP-TLC systems on the two-dimensional non-linear map of PC variables calculated from the correlation matrix.

support our previous conclusions drawn from the comparison of the variances explained that in our case the information content of PCAs computed from different matrices is similar. However, the ratio of variance explained is fairly low in the case of the second coordinates, suggesting the existence of small differences between the PCA methods.

No significant linear correlation was found between the distances of RP-TLC systems on the various cluster dendograms. This finding supports our previous qualitative conclusion that the use of PCA modifies the group formation of RP-TLC systems. The parameters of significant linear correlations between the corresponding distances on various maps are compiled in Table 5. The results suggest that the information contents of non-linear mapping and cluster analysis are similar.

It can be concluded that both PCA and CA can be successfully applied for the evaluation of the similarities in the retention behaviour of reversed-phase chromatographic systems and solutes. We assume that PCA followed by two-dimensional non-linear mapping is superior to cluster analysis, because the non-linear mapping technique has a higher dimensionality than cluster analysis.

4. Acknowledgements

Y.D. expresses his gratitude to the Ministry of Culture and Public Education of Hungary for supporting his work. This work was supported by grant OTKA T6436 from the Hungarian Academy of Sciences.

5. References

[1] C. Hansch, in C.J. Cavallito (Editor), *Structure–Activity Relationships*, Pergamon Press, Oxford, 1973, p. 57.
[2] J. Andrew, W.E. Stuper, P. Brugger and S. Jurs, *Computer Assisted Studies of Chemical Structure and Biological Function*, Wiley, New York, 1979.
[3] R. Kaliszan, *Quantitative Structure–Chromatographic Retention Relationships*, Wiley, New York, 1987.
[4] R. Franke, in J.K. Seydel (Editor), *QSAR and Strategies in the Design of Bioactive Compounds*, VCH, Weinheim, 1985, p. 59.

[5] C.B.C. Boyce and B.B. Milborrow, *Nature*, 208 (1965) 537.
[6] G.L. Biagi, A.M. Barbaro and M.C. Guerra, *J. Chromatogr.*, 41 (1969) 371.
[7] P. Jandera, J. Churacek and H. Colin, *J. Chromatogr.*, 214 (1981) 35.
[8] I.D. Wilson, C.R. Bielby and E.D. Morgan, *J. Chromatogr.*, 238 (1982) 97.
[9] E. Janos and T. Cserhati, *Acta Phytopathol. Acad. Sci. Hung.*, 17 (1982) 343.
[10] W.F. Giesen and L.H.M. Janssen, *J. Chromatogr.*, 237 (1982) 199.
[11] T. Cserhati, Y.M. Darwish and Gy. Matolcsy, *J. Chromatogr.*, 270 (1983) 97.
[12] M.C. Guerra, A.M. Barbaro, G. Cantelliforti, M.T. Folfani, G.L. Biagi and P.A. Borea, *J. Chromatogr.*, 216 (1981) 93.
[13] L. Ogierman and A. Siloviecki, *J. High. Resolut. Chromatogr. Chromatogr. Commun.*, 4 (1981) 357.
[14] B. Rittich, M. Polster and O. Kralik, *J. Chromatogr.*, 197 (1980) 43.
[15] Gy. Vigh, J. Varga-Puhony, J. Hlavay and E. Pap, *J. Chromatogr.*, 236 (1982) 51.
[16] T. Cserhati, Y.M. Darwish and Gy. Matolcsy, *J. Chromatogr.*, 241 (1982) 107.
[17] E. Pap and Gy. Vigh, *J. Chromatogr.*, 259 (1983) 49.
[18] T. Cserhati, B. Bordas, E. Fenyvesi and F. Szejtli, *J. Chromatogr.*, 259 (1983) 107.
[19] T. Cserhati, *Chromatographia*, 18 (1984) 18.
[20] T. Cserhati, *Chromatographia*, 18 (1984) 318.
[21] K. Valko, *J. Liq. Chromatogr.*, 7 (1984) 1405.
[22] C. Horvath, W. Melander and I. Molnar, *J. Chromatogr.*, 125 (1976) 129.
[23] T. Cserhati and H.E. Hauck, *J. Chromatogr.*, 514 (1990) 45.
[24] J.W. Sammon, Jr., *IEEE Trans. Comput.*, C18 (1969) 401.
[25] K.V. Mardia, J.T. Kent and J.M. Bibby, *Multivariate Analysis*, Academic Press, London, 1979, p. 213.
[26] T. Cserhati and Z. Illes, *J. Pharm. Biomed. Anal.*, 9 (1991) 685.
[27] W.R. Dillon, *Multivariate Analysis*, Wiley, New York, 1984.
[28] P. Willett, *Similarity and Clustering in Chemical Information Systems*, Research Studies Press, New York, 1987.
[29] V.S. Rose, I.F. Croall and J.H. MacFie, *Quant. Struct.–Act. Relat.*, 10 (1991) 350.

ELSEVIER

Journal of Chromatography A, 668 (1994) 495–500

JOURNAL OF CHROMATOGRAPHY A

Relationship between the high-performance liquid and thin-layer chromatographic retention of non-homologous series of pesticides on an alumina support

Tibor Cserháti*, Esther Forgács

Central Research Institute for Chemistry, Hungarian Academy of Sciences, P.O. Box 17, H-1525 Budapest, Hungary

Abstract

The retentions of 26 commercial pesticides were determined on an alumina HPLC column and in TLC carried out on alumina layers using *n*-hexane–dioxane mixtures as eluents. Both the log k'_0 and R_{M0} values of the pesticides decreased linearly with increasing concentration of dioxane in the eluent and they were strongly intercorrelated. The prediction power of TLC for HPLC was low, probably owing to the different pH of the alumina surface. The hydrophilic retention parameters of pesticides determined on alumina supports have a negligible effect on the type of their biological activity (herbicidal, fungicidal, acaricidal or insecticidal).

1. Introduction

In the last decade, alumina supports have gained growing acceptance and application in high-performance liquid chromatography (HPLC) [1,2]. A possible advantage for the use of alumina instead of silica supports is the greater pH stability of the former [3,4]. The characteristics and applications of alumina [5] and modified alumina supports [6] have recently been discussed. Alumina supports have been used successfully for the separation of transition metal ions [7] and alkyl- and phenylnaphthalenes [8] and for the preconcentration of sulphate from complex matrices [9]. Many efforts have been devoted to the development of modified alumina support coated with hydrophobic ligands [10,11]. Polybutadiene-coated alumina has been used for the determination of the lipophilicity of organic bases [12] and imidazol(in)e drugs [13], and for the separation of proteins [14]. However, octadecylsilica was better than octyl-coated alumina for peptide separations [15].

Thin-layer chromatography (TLC) is a rapid and inexpensive method suitable for the separation of many organic and inorganic compounds. As many HPLC sorbents are also applied in TLC [16–18], the use of TLC as a pilot method for the development of HPLC separation procedures offers considerable advantages. The predictive power of TLC for HPLC depends strongly on the type of solutes [19] and on the experimental conditions [20].

The objectives of this work were the determination of the retention of some pesticides frequently used in agricultural practice on both

* Corresponding author.

0021-9673/94/$07.00
SSDI 0021-9673(93)E1131-I

HPLC and TLC alumina supports, the evaluation of the predictive power of TLC for HPLC and the elucidation of the relationship between the biological activity and retention characteristics of pesticides [21].

2. Experimental

2.1. High-performance liquid chromatography

A 25 cm × 4 mm I.D. alumina column was used in each experiment. The alumina support was the experimental product of the research team of Dr. L. Zsembery (Hungarian Alumina Trust, Research and Development Laboratory, Budapest, Hungary). The retention characteristics of the column have been reported previously [22]. The HPLC equipment consisted of a Liquopump Type 312 (Labor MIM, Budapest, Hungary), a Cecil (Cambridge, UK) CE-212 spectrophotometer used as the detector, a 20-μl injector (Valco, Houston, TX, USA) and a Waters (Milford, MA, USA) Model 740 integrator. The flow-rate was 1 ml/min and the detection wavelength 240 nm. The column was not thermostated. Each HPLC measurement was run in triplicate.

2.2. Thin-layer chromatography

DC-Alufolien F_{254} precoated plates (Merck, Darmstadt, Germany) were used without any pretreatment. The developments were carried out in sandwich chambers (22 × 22 × 3 cm) at room temperature and the running distance was *ca.* 15 cm. The chambers were not presaturated. After development the plates were dried at 105°C and the spots were detected under UV light or with iodine vapour. Each determination was run in quadruplicate. When the relative standard deviation (R.S.D.) between parallel determinations was higher than 5%, the data were omitted from the calculations.

The pesticides studied are listed in Table 1. The pesticides were dissolved in dioxane at concentrations of 5 and 0.1 mg/ml for TLC and HPLC investigations, respectively. The eluents were *n*-hexane–dioxane mixtures (10–60% (v/v) dioxane in steps of 5% (v/v) for HPLC and 5–60% (v/v) dioxane in steps of 5% (v/v) for TLC).

Linear correlations were calculated between the logarithm of the capacity factor and the dioxane concentration (C) in the eluent (Eq. 1) and between the R_M value and the dioxane concentration in the eluent (Eq. 2) separately for each pesticide:

$$\log k' = \log k'_0 + b_1 C \quad (1)$$

where k' is the actual retention value of a pesticide at C% (v/v) dioxane concentration and k'_0 is the theoretical retention value of a pesticide at 0% (v/v) dioxane concentration (pure *n*-hexane),

$$R_M = R_{M0} + b_2 C \quad (2)$$

where R_M is the actual R_M value of a pesticide determined at C% (v/v) dioxane concentration and R_{M0} is the theoretical R_M value extrapolated to zero dioxane concentration.

To elucidate the validity of the hypothesis that for homologous series of solutes the slope and intercept values are strongly intercorrelated [23,24], the homologous or inhomogeneous character of pesticides as solutes in adsorption chromatography was assessed by calculating linear correlations between the slope (b_1 and b_2) and intercept value ($\log k'_0$ and R_{M0}) of Eqs. 1 and 2. To find the relationship between the HPLC and TLC retention data the slope and intercept values of Eq. 1 were correlated with the corresponding value of Eq. 2.

To assess the similarities and dissimilarities between the chromatographic parameters and biological activites of pesticides, principal component analysis (PCA) was applied [25]. The adsorption capacities (intercept values of Eqs. 1 and 2) and the specific hydrophilic surface areas (slope values of Eqs. 1 and 2) of pesticides were taken as variables and the pesticides were the observations. Only pesticides with each physicochemical parameter determined were included in the calculations. The two-dimensional non-linear map of PC loadings and variables was also calculated [26]. Iteration was carried out to the

point when the differences between the two last iterations was smaller than 10^{-8}.

3. Results and discussion

Pesticides separate well on an alumina column and they give symmetrical peaks with each eluent system. Their retention times differ considerably, hence an alumina column can be used successfully for the separation of pesticides.

The parameters of Eq. 1 are given in Table 1. The relationship between log k' and dioxane concentration is linear and the correlation coefficient in most instances is higher than 0.99, confirming the applicability of Eq. 1. The slope and intercept values differ considerably from each other, supporting the previous qualitative conclusion that an alumina column is suitable for the separation of commercial pesticides. The parameters in Table 1 make possible the calculation of retention time differences for each pair of pesticides at each eluent composition:

$$t_1 - t_2 = t_0(10^{a_1+b_2C} - 10^{a_2+b_2C}) \quad (3)$$

where a and b are intercept and slope values for pesticides 1 and 2 at dioxane concentration C. The eluent composition corresponding to the maximum retention time difference can also be calculated: the first derivative of Eq. 3 must be zero and the dioxane concentration expressed accordingly:

$$C = [a_1 - a_2 + \log(b_1/b_2)]/(b_2 - b_1) \quad (4)$$

As in HPLC, the TLC retention of pesticides decreases linearly with increasing concentration of dioxane in the eluent, and no anomalous retention behaviour was observed. However, the correlation coefficients were markedly lower,

Table 1
Parameters of linear correlations between log k' and dioxane concentration (C) in the eluent: $\log k' = \log k'_0 + b_1 C$

No.	Pesticide	Log k'_0	$-b_1 \cdot 10^{-2}$	$S_{b_1} \cdot 10^{-3}$	r
1	Bromoxynil	0.78	2.47	1.80	0.9947
2	Isoproturon	1.30	3.62	2.48	0.9930
3	Chlorotoluron	1.30	3.61	2.39	0.9935
4	Methiocarb	0.98	3.35	2.94	0.9924
5	Chlorbromuron	0.72	3.09	0.88	0.9992
6	Linuron	0.75	3.32	2.37	0.9949
7	Bromopropylate	1.06	4.59	3.41	0.9978
8	*p,p'*-DDT	−0.22	2.14	1.81	0.9892
9	Diphenamid	0.97	3.61	2.41	0.9956
10	Carboxin	0.97	3.46	3.50	0.9850
11	Buprofezin	0.07	3.12	2.31	0.9919
12	Binacapryl	0.36	2.87	1.50	0.9959
13	Iodphenphos	0.06	2.34	1.21	0.9960
14	Oxadixyl	1.56	1.84	1.60	0.9925
15	Fuberidazol	1.46	3.06	3.79	0.9850
16	Iprodione	1.16	3.57	4.60	0.9838
17	Ethofumasate	0.93	3.28	1.06	0.9990
18	Oxabetrinil	0.53	3.00	2.42	0.9904
19	Oxadiazon	0.04	2.94	2.40	0.9901
20	Lenacil	1.71	3.37	0.88	0.9997
21	Terbacil	1.72	3.39	0.94	0.9996
22	Atrazine	0.79	3.03	4.18	0.9815
23	Terbutylazine	0.97	4.31	8.30	0.9486
24	Aziprotryne	0.32	2.84	3.08	0.9828
25	Terbutryn	0.33	2.91	2.95	0.9849
26	Clofentezine	0.46	2.88	1.07	0.9979

indicating the inherent lower reproducibility of TLC.

The correlation between the slope and intercept values of Eq. 1 was fairly weak:

$$\log k'_0 = -0.29 + 0.35b_1$$
$$n = 26,\ r_{calc.} = 0.3907,\ r_{95\%} = 0.3889 \qquad (5)$$

and no significant correlation was found between the corresponding parameters of Eq. 2. This finding indicates that from the chromatographic point of view pesticides cannot be regarded as a homologous series of solutes.

A good significant correlation was found between the log k'_0 and R_{M0} values:

$$\log k'_0 = -0.37 + 0.90R_{M0}$$
$$n = 25,\ r_{calc.} = 0.8060,\ r_{99.9\%} = 0.6177 \qquad (6)$$

The result indicates that in this instance TLC is suitable for the prediction of the retention behaviour of pesticides in HPLC. However, it must be emphasized that both the log k'_0 and R_{M0} values are theoretical constructions describing the retention of pesticides in pure *n*-hexane, in which they hardly elute.

No significant linear correlation was found between the slope values of Eqs. 1 and 2. The discrepancy can be tentatively explained by the supposition that the surface pH and the adsorption capacity of active centres on the alumina surface may be different, modifying the contact surface between solute and support. This finding also indicates that the predictive power of TLC is fairly low. Although TLC results may predict the theoretical retention behaviour of pesticides in *n*-hexane in HPLC, owing to the absence of a correlation between the slope values of Eqs. 1 and 2 they are inadequate for the prediction of the retention behaviour in *n*-hexane–dioxane mixtures in which the pesticides really elute.

The results of PC analysis are given in Table 2. The first two components account for about 80% of the total variance. This means that two background variables include most of the information content of the four chromatographic parameters. It must be emphasized that the two hypothetical variables need not to have any concrete physical (or chromatographic) meaning. PC analysis only proves the mathematical possibility. The adsorption capacities of HPLC (log k'_0) and TLC (R_{M0}) aluminas have high loadings in the first PC. This result indicates that the first PC can be regarded as a parameter related to the adsorption strength of the supports. The second PC contains the corresponding slope values b_1 and b_2. As the slope values can be regarded as quantities related to the surface of solutes in

Table 2
Relationship between the HPLC and TLC retention behaviours of pesticides: results of principal component analysis

No. of PC component	Eigenvalue	Variance explained (%)	Total variance explained (%)
1	1.99	49.76	49.76
2	1.23	30.48	80.24
3	0.69	17.28	97.53

Retention parameters[a]	Principal component loadings		
	1	2	3
Log k'_0 (adsorption capacity in HPLC)	0.96	−0.16	−0.03
b_1 (specific hydrophilic surface area in HPLC)	0.53	0.63	−0.57
R_{M0} (adsorption capacity in TLC)	0.88	−0.08	0.43
b_2 (specific hydrophilic surface area in TLC)	−0.12	0.89	0.43

[a] See Eqs. 1 and 2.

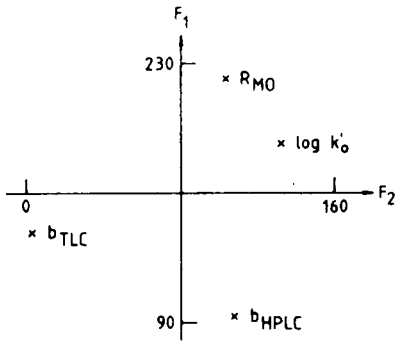

Fig. 1. Two-dimensional non-linear map of principal component loadings. No. of iterations, 29; maximum error, $9.89 \cdot 10^{-4}$.

contact with the support [27], the second PC characterizes the specific hydrophilic surface area of pesticides.

The capacity values of alumina supports (log k'_0 and R_{M0}) are nearer to each other on the two-dimensional non-linear map of PC loadings than the corresponding slope values (Fig. 1). This finding entirely supports the results of Eq. 6 that the adsorption capacities of HPLC and TLC alumina supports are similar.

Pesticides do not form separate clusters according to the type of their biological activity (herbicidal, fungicidal, acaricidal or insesticidal) on the two-dimensional non-linear map of PC variables (Fig. 2). This finding indicates that the hydrophilic retention parameters determined on an alumina support have a negligible impact on the type of biological activity of pesticides.

It can be concluded that a wide variety of commercial pesticides can be successfully separated on alumina supports both in HPLC and TLC using *n*-hexane–dioxane eluents. However, the predictive power of TLC for HPLC is relatively low.

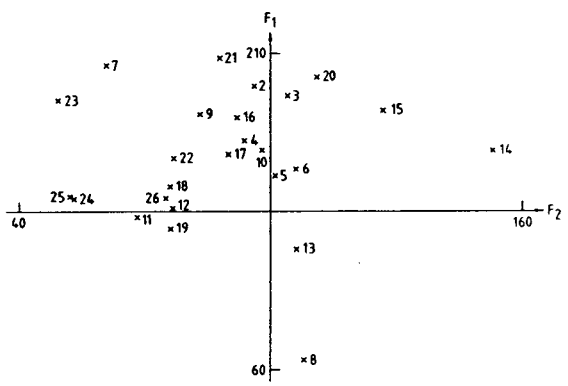

Fig. 2. Two-dimensional non-linear map of principal component variables. No. of iterations, 91; maximum error, $1.15 \cdot 10^{-2}$. Numbers refer to pesticides in Table 1.

4. Acknowledgement

This work was supported by Grant OTKA 2670 of the Hungarian Academy of Sciences.

5. References

[1] J.E. Haky, S. Vemulapalli and L.F. Wieserman, *J. Chromatogr.*, 505 (1990) 307.
[2] J.E. Haky and S. Vemulapalli, *J. Liq. Chromatogr.*, 15 (1990) 3111.
[3] R. Kaliszan, J. Petrusewitz, R.W. Blain and R. Hartwick, *J. Chromatogr.*, 458 (1988) 395.
[4] A. Berthod, *J. Chromatogr.*, 549 (1991) 1.
[5] K. Cabdera, D. Lubda and G. Jung, *Kontakte (Darmstadt)*, (1992) 12.
[6] K. Cabdera, D. Lubda and G. Jung, *Kontakte (Darmstadt)*, (1992) 32.
[7] D.K. Singh and P. Mehrotra, *Chromatographia*, 23 (1987) 747.
[8] J. Puncochárová, J. Vareka, L. Vodicka and J. Kriz, *J. Chromatogr.*, 498 (1989) 248.
[9] W. Buchberger and K. Winsauer, *J. Chromatogr.*, 482 (1989) 505.
[10] J.J. Pesek and H.D. Lin, *Chromatographia*, 28 (1989) 565.
[11] J.E. Haky, N.D. Ramdial, A.R. Raghani and L.F. Wieserman, *J. Liq. Chromatogr.*, 14 (1991) 2859.
[12] G. Yilinkou and R. Kaliszan, *Chromatographia*, 30 (1990) 277.
[13] R.-G. Yilinkou and R. Kaliszan, *J. Chromatogr.*, 550 (1991) 573.
[14] J.E. Haky, A. Raghani and B.M. Dunn, *J. Chromatogr.*, 541 (1991) 303.
[15] J.E. Haky, N.D. Ramdial, B.M. Dunn and L.F. Wieserman, *J. Liq. Chromatogr.*, 15 (1992) 1831.
[16] L. Witherow, R.J. Thorp, I.D. Wilson and A. Warrander, *J. Planar Chromatogr.*, 3 (1990) 169.
[17] M. Mack, H.E. Hauck and H., Herbert, *GIT Fachz. Lab.*, 34 (1990) 276.

[18] W. Fischer, H.E. Hauck and W. Jost, in F.A.A. Dallas (Editor), *Recent Advances in Thin-Layer Chromatography (Proceedings of Chromatographic Society International Symposium, 1987)*, Plenum Press, New York, 1988, p. 139.
[19] T. Cserháti and T. Bellay, *Acta Phytopathol. Entomol. Hung.*, 23 (1988) 257.
[20] J.K. Rozylo and M. Janicka, *J. Planar Chromatogr.*, 4 (1991) 241.
[21] R. Kaliszan, *Quantitative Structure–Chromatographic Retention Relationships*, Wiley, New York, 1987.
[22] T. Cserháti, *Chromatographia*, 29 (1990) 593.
[23] T. Cserháti, *Chromatographia*, 18 (1984) 18.
[24] K. Valkó, *J. Liq. Chromatogr.*, 7 (1984) 1405.
[25] A.R. Dillon and M. Goldstein, *Multivariate Analysis*, Wiley, New York, 1984, p. 23.
[26] J.W. Sammon, Jr., *IEEE Trans. Comput.*, C18 (1969) 401.
[27] C. Horvath, W. Melander and I. Molnár, *J. Chromatogr.*, 125 (1976) 129.

ELSEVIER

Journal of Chromatography A, 668 (1994) 501–507

JOURNAL OF CHROMATOGRAPHY A

Extraction and *in situ* densitometric determination of alkaloids from *Catharanthus roseus* by means of overpressured layer chromatography on amino-bonded silica layers I. Optimization and validation of the separation system

A. Nagy-Turák, Z. Végh*

Chemical Works of Gedeon Richter Ltd., P.O. Box 27, 1475 Budapest 10, Hungary

Abstract

A simple, rapid and efficient method was developed for the separation and spectrodensitometric determination of bis-indole alkaloids, minor components of *Catharanthus roseus*. Separation was performed on amino-bonded silica gel layers using one-dimensional overpressured layer chromatographic development. Optimization of the eluent was performed by the PRISMA model followed by a factorial experimental design using the geometric mean of the normalized resolution as a response function. Peak purity test and validation data verified that the method was sufficient for separation of these closely related alkaloids.

1. Introduction

Vinblastine (VLB) and vincristine (VCR) are the most important bis-indole alkaloids of *Catharanthus roseus*, having high anti-neoplastic activity, but their determination is very difficult as they are only minor components of the plant. To determine these alkaloids in a plant extract, several closely related compounds must be separated from each other in a highly complex matrix. The industrial isolation of these important alkaloid components requires reliable and rapid analytical methods.

HPLC is often used for the purity testing of bulk drug substances of *Catharanthus* alkaloids (VLB, VCR) [1] and for measuring them in biological fluids for pharmacokinetic studies [2]. VLB and VCR of plant origin have been determined by HPLC either from cell cultures of *Catharanthus roseus* or from the plant extract itself after purification by solid-phase [3,4] or ion-pair extraction [5].

Quantitative TLC methods described for *Catharanthus roseus* cannot separate VLB and related compounds in the drug extract in a single development. These methods involve two-dimensional developments (with 2–4 runs) and elution–spectrophotometric [6,7] or densitometric [7] determination of these components.

HPLC methods used for these tasks require thorough sample pretreatment and highly purified solvents. Multi-dimensional TLC methods are laborious, time consuming and need large amounts of sorbents and solvents.

Our aim was to develop a rapid and simple liquid chromatographic method for the determination of bis-indole alkaloids, with special emphasis on VLB, from extracts of *Catharanthus*

* Corresponding author.

0021-9673/94/$07.00
SSDI 0021-9673(93)E1220-T

roseus drug. It seemed that overpressured layer chromatography (OPLC) using spectrodensitometry was suitable for this task owing to its simplicity, flexibility and modest sample pretreatment demands. This technique has been successfully applied in our laboratory for different kinds of separations on various sorbents [8–12] utilizing its higher efficiency compared with conventional TLC [13].

In this work, amino-bonded silica gel HPTLC layers were used, utilizing the different selectivity of the sorbent compared with silica gel [12]. An amino-bonded (NH_2) sorbent offers the possibility of the one-dimensional OPLC separation of *Catharanthus* alkaloids of interest.

In this first part, the optimization and validation of the separation system are presented. The second part will deal with the optimization of the extraction of VLB from the plant material utilizing the one-dimensional OPLC separation system described here.

2. Experimental

All solvents and chemicals were of analytical-reagent grade. Authenthic alkaloid standards were prepared at the Chemical Works of Gedeon Richter (Budapest, Hungary).

Amino-bonded silica gel was obtained from Merck (Darmstadt, Germany) (HPTLC precoated plate NH_2, Cat. No. 15647) or prepared by amino modification of silica gel sheets (HPTLC Aluminium sheets silica gel 60 F_{254}, Merck, Cat. No. 5548) according to Mincsovics [14] (some other sorbents from Merck were used only in preliminary experiments). For preparing dual-phase sorbents, only a section of the HPTLC silica sheet was modified by the reagent. Four edges of the sorbent layers were sealed with Impres emulsion (Laberté, Budapest, Hungary) for OPLC development [15].

Chromatograms were developed in normal unsaturated chambers (Desaga, Heidelberg, Germany) and in a Chrompres-10 overpressured layer chromatograph (Laberté, Budapest, Hungary) at room temperature. The OPLC conditions were as follows: membrane pressure, 1 MPa; linear velocity of eluent, 0.8 cm/min; and running distance, 16 cm.

The chromatograms were evaluated by spectrodensitometry at 298 nm with a computer-controlled TLC Scanner II (CAMAG, Muttenz, Switzerland) using CATS software (version 3.04).

3. Results and discussion

3.1. Preliminary experiments

A model mixture of authentic alkaloid standards (Table 1) and a plant extract were chromatographed on different sorbents (bare silica and octyl-, octadecyl-, cyanopropyl- and amino-bonded silica gel) in a normal unsaturated chamber (N_{us}) for the selection of a suitable stationary phase. Comparing the different sorbents tested, the resolution and spot shape of the alkaloids were the best on amino-bonded silica gel. Simple eluents gave promising separations of the standard mixture on these plates.

3.2. Optimization of eluent for OPLC developments by the PRISMA model

On the basis of preliminary experiments, hexane–dichloromethane (a), hexane–acetone (b) and hexane–2-propanol (c) mixtures were used as mobile phases in the initial OPLC systems for optimization by the PRISMA model [16]. The solvent strength of eluents used for preliminary experiments in N_{us} chambers had to be decreased for OPLC development. Relatively good separations are illustrated in Fig. 1. These densitograms show, nevertheless, that the separation of alkaloids is not yet satisfactory either for the standard mixture or for the plant extract. To improve the selectivity of separation, different combinations of the initial eluents were tested as marked in Fig. 2A by the circles. At the selectivity points 1–1–8, 8–1–1 and 3–4–3 in the triangle diagram, spots migrated to the β- or γ-front, owing to the solvent-demixing effect. Hence chromatograms obtained with these eluent combinations could not be evaluated. The chromatogram obtained with a 1:8:1 mixture of

Table 1
Structure of the alkaloids investigated

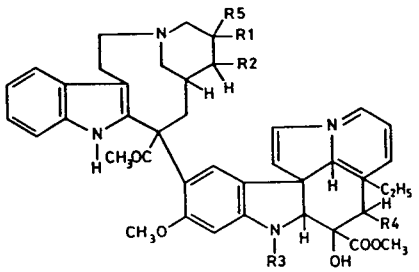

No.	Name	R1	R2	R3	R4	R5
I	Deacetylvinblastine	Et	H	Me	OH	OH
II	Vincristine	Et	H	CHO	$OCOCH_3$	OH
III	N-Demethylvinblastine	Et	H	H	$OCOCH_3$	OH
IV	Vinblastine	Et	H	Me	$OCOCH_3$	OH
V	Deacetoxyvinblastine	Et	H	Me	H	OH
VI	Leurosine	-O-		Me	$OCOCH_3$	Et

eluents a, b and c (point 1–8–1) was promising, and further experiments were therefore carried out in the neighbourhood of point 1–8–1 in the triangle as marked in Fig. 2B with circles.

Fig. 3 shows the densitogram of the best separation achieved by PRISMA at the selectivity point 2–7–1. It can be seen that the separation of the model mixture is good but with the drug extract the peak of VLB is disturbed by two slightly overlapping peaks (marked with arrows). This separation, therefore, is not suitable for the quantitative determination of the VLB content of *Catharanthus* drug extracts.

3.3. Optimization of eluent with factorial experimental design

As the OPLC PRISMA optimization system resulted in good resolution only for the compounds in the standard mixture, the separation of the plant extract components was further improved by a factorial experimental design method [17]. The 'normalized resolution' of peak pairs introduced by Gazdag *et al.* [18] for HPLC was used for characterizing the separations. The peak resolution (R_s) can also be divided to two parts as follows:

$$R_s = 1/4\sqrt{N}(\alpha - 1)/\alpha \cdot k_2'/(k_2' + 1) = 1/4\sqrt{N}D \quad (1)$$

From Eq. 1, D can be expressed as a function of capacity factors:

$$D = (k_2' - k_1')/(k_2' + 1) \quad (2)$$

Using the equation

$$R_F = 1/(1 + k') \quad (3)$$

the normalized peak resolution can be expressed with R_F values:

$$D = (R_{F_2} - R_{F_1})/R_{F_2} \quad (4)$$

where $R_{F_2} > R_{F_1}$, *i.e.*, in the case of planar liquid chromatography (*e.g.*, TLC, OPLC) the normalized resolution (D) can be regarded as the relative difference in R_F values. The use of the D value is advantageous because it can easily be determined and characterizes the separation better than the ΔR_F value. The geometric mean of the normalized resolution values was used as the response function (Y) [19] in the experimental design for characterizing the separations of different chromatograms:

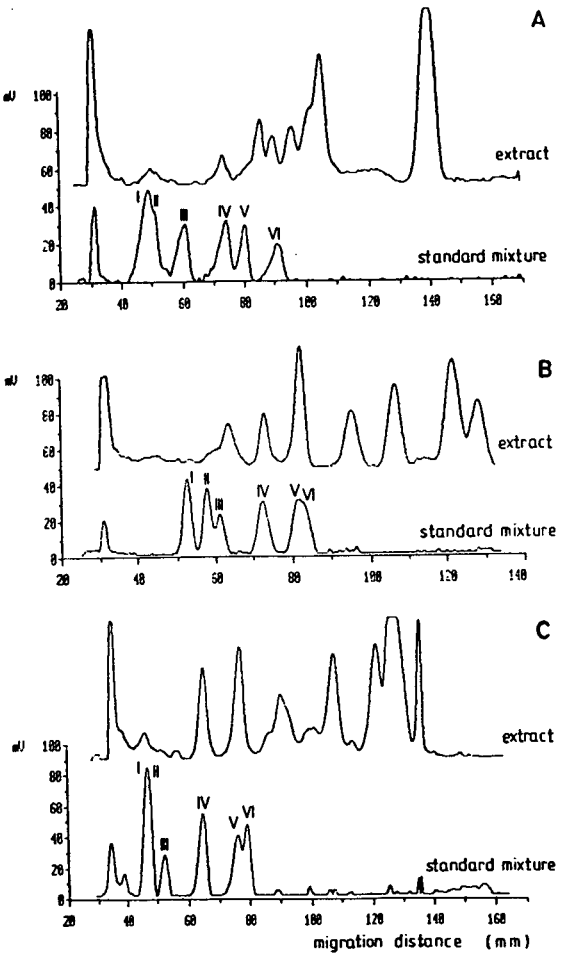

Fig. 1. Separation of alkaloids in a model mixture and a drug extract by the initial OPLC systems (a, b and c) used for optimization by the PRISMA model. Sorbent: amino-bonded silica (laboratory-modified). Eluent: (A) hexane–dichloromethane (30:70, v/v); (B) hexane–acetone (70:30, v/v); (C) hexane–2-propanol (85:15, v/v). Compound numbers as in Table 1.

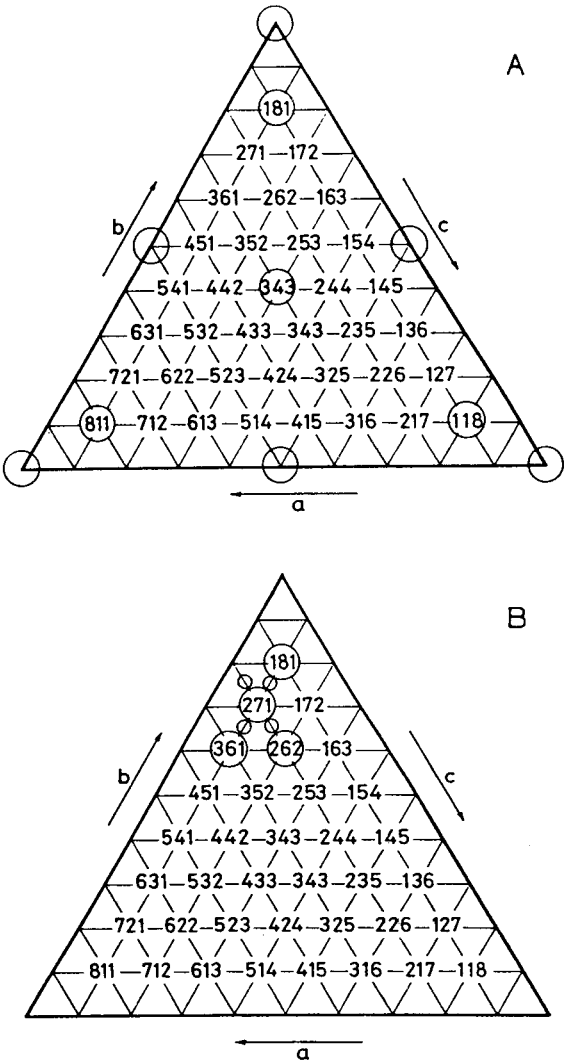

Fig. 2. Triangle diagrams of eluent compositions tried in PRISMA optimization. Vertices of the triangle correspond to the initial eluents (a, b and c). (A) Experiments in the first step; (B) experiments in the second step.

$$Y = \sqrt[n]{\prod_{i=1}^{n} D_i} \qquad (5)$$

which should be maximized in order to improve the separation. By using this function the disturbances caused by unknown adjacent peaks of VLB in drug extracts can also be taken into account.

The experimental design matrix applied and its results, *i.e.*, the values of the response function (Y) and the fitted model, are given in Table 2(A). The signs and values of the coefficients in the fitted model show that the separation of compounds can be improved by increasing the volume fraction of dichloromethane and/or decreasing that of 2-propanol. After evaluating the effects of different factors, based on the fitted model, further chromatograms were developed

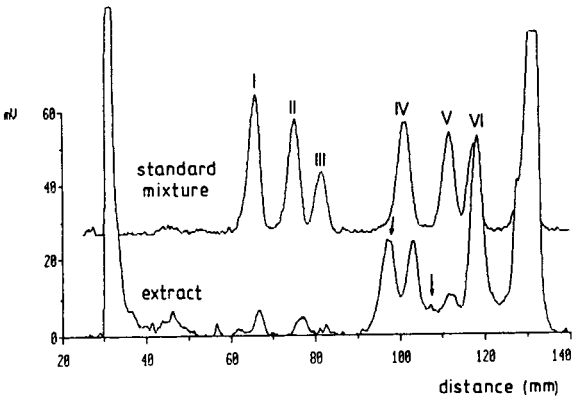

Fig. 3. Separation of compounds resulting from PRISMA optimization. The arrows show the unidentified peaks adjacent to VLB in the plant extract. Eluent: hexane–dichloromethane–acetone–2-propanol (64.5:14:21:1.5, v/v). Sorbent and other conditions as in Fig. 1. Compound numbers as in Table 1.

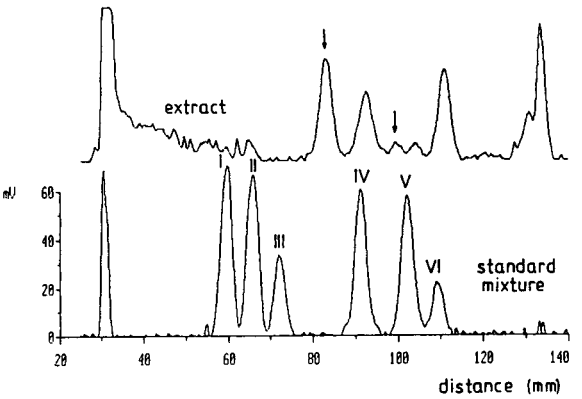

Fig. 4. Separation of compounds using the optimum eluent composition achieved by factorial experimental design. Eluent: hexane–dichloromethane–acetone–2-propanol (65:13:21:0.9, v/v). Other conditions as in Fig. 3. Compound numbers as in Table 1.

[Table 2(B)]. The best separation is illustrated in Fig. 4. It is clearly demonstrated that a baseline separation of components has been achieved both for the standard mixture and the *Catharanthus* extract (peaks adjacent to VLB in the drug extract are marked with arrows).

3.4. Check of peak purity

As VLB was separated from drug extract in a single run by one-dimensional OPLC development, the examination of the selectivity of separation is of great importance. *In situ* spectral comparison for the peak purity test was insuffi-

Table 2
Factorial experimental design matrix for eluent optimization and the response function (Y)

Serial No.	x_1	x_2	x_3	Hexane	CH_2Cl_2	Acetone	2-Propanol	$Y=\sqrt[n]{\prod_{i=1}^{n} D_i}$
(A) Initial experiments								
1	+	+	+	63	11	24	2	0.0717
2	−	+	+	67	7	24	2	0.0000
3	+	−	+	69	11	18	2	0.0708
4	−	−	+	73	7	18	2	0.0773
5	+	+	−	64	11	24	1	0.0801
6	−	+	−	67	7	24	1	0.0886
7	+	−	−	70	11	18	1	0.1106
8	−	−	−	74	7	18	1	0.0000
Fitted model: $Y = 0.0624 + 0.0181x_1 + 0.0001x_2 - 0.0096x_3$								
(B) Further experiments based on the fitted model								
9				66	11.7	21	1.1	0.123
10				65	12.6	21	1.0	0.128
11				65	13.5	21	0.9	0.125
12				64	14.4	21	0.8	0.094

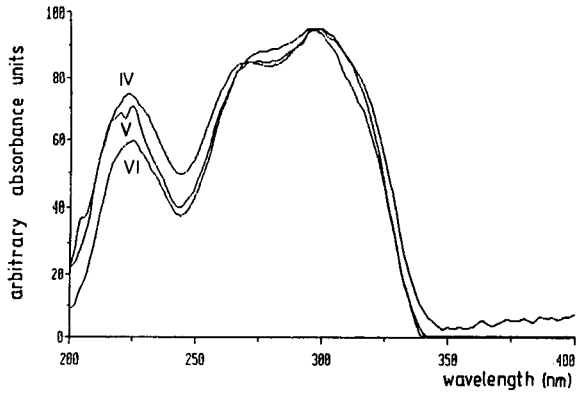

Fig. 5. UV reflectance spectra of VLB (IV), deacetoxy-VLB (V) and leurosine (VI). Chromatographic conditions as in Fig. 4.

cient because the UV reflectance spectra of the alkaloids examined are almost identical (Fig. 5).

A peak homogeneity test of the separated spots was therefore performed by two-(perpendicular)-dimensional development of the chromatograms on amino-bonded (Fig. 6A) and on laboratory-made dual-phase layers (Fig. 6B). *Catharanthus* extract containing *ca.* 3 μg of VLB was applied on the chromatoplates. The optimized eluent had been used for the first development by OPLC on amino-bonded silica. Development in the second direction was carried out either on the NH_2 phase with hexane–2-propanol (8:2, v/v) as eluent by OPLC (Fig. 6A), or on silica with ethyl acetate–benzene–ethanol–ammonia (100:5:18:1.6, v/v) as eluent [7] in a saturated normal chamber (Fig. 6B). Fig. 6 shows that no additional spot was observed in densitograms of the track of VLB in the second direction. Hence the spot of VLB is pure, *i.e.*, a single OPLC run is suitable for the determination of VLB.

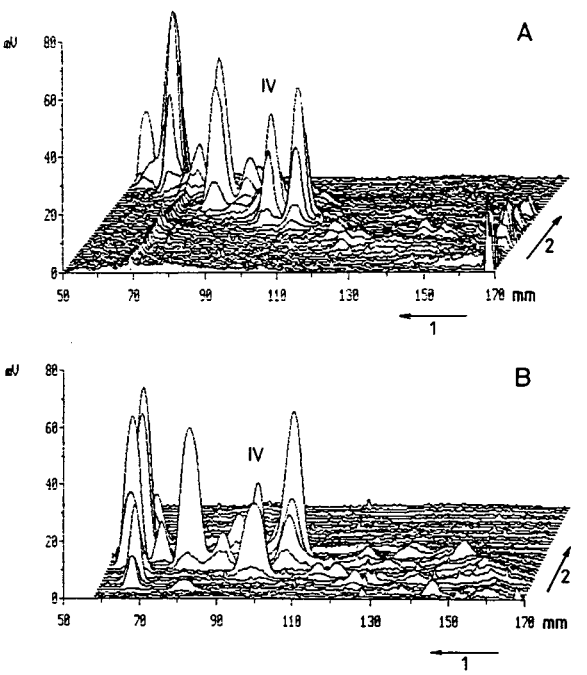

Fig. 6. Two-dimensional chromatograms of drug extract for peak purity test. Chromatographic conditions are described in the text. The arrows show the directions of developments.

3.5. Validation of the method

To apply this method for quality control purposes, it is necessary to prove its effectiveness by a validation process.

Stability tests were performed as described elsewhere [20,21]. The components of the drug extracts are stable during chromatographic development when using the optimized eluent. The drug extract was stable in methanolic solution for 3 h and also for 30 min standing on the sorbent layer before chromatography.

The calibration graph based on the peak area of VLB (y) is linear within the range 100–1000 ng of spots applied (x), as expressed by the fitted linear regression function $y = 1.51x + 41.57$. No trend was observed in the plot of residuals. Linearity of the fitted function was also verified by the F-test.

The limit of detection (LOD) for VLB was determined as described elsewhere [20] and was found to be about 50 ng.

The repeatibility of the chromatographic measurements was determined from five parallel applications of the same drug extract to the same chromatoplate: x(VLB content) = 246.8 mg/kg; S.D. = 7.1 mg/kg; R.S.D. = 2.9%.

In the ruggedness test, the effects of slight changes in the following parameters on the result of VLB determinations were studied [22]: the quality of the sorbent layer (ready-made or

laboratory-modified), volume fractions of eluent composition and OPLC equipment. Measurements were carried out with a factorial experimental design. It was found that the equipment and small changes in eluent composition have no influence on the results of measurements, but the quality of the sorbent has a moderate influence on the determination of VLB content.

4. Conclusions

Important alkaloids of *Catharanthus roseus* could be separated by a single one-dimensional OPLC development. By means of this method, the time of analysis and the sorbent and solvent consumption can be dramatically decreased compared with earlier two-dimensional methods. Vinblastine and related compounds are highly polar basic substances, therefore the amino-bonded HPTLC sorbent proved to be useful for their separation. OPLC development gave the possibility of utilizing the high resolving power of HPTLC plates over a long development distance. As the OPLC PRISMA optimization system resulted in good resolution only for the compounds in the standard mixture, the separation of the plant extract components was further improved by a factorial experimental design method. Separation of the spots in the chromatograms could be well characterized by the normalized resolution. The geometric mean of the normalized resolution values of peak pairs was successfully applied as a response function for the optimization process.

Peak purity tests were based on two-dimensional developments because there was no difference in the UV spectra of the alkaloids separated. Validation data showed that the method is suitable for routine measurements.

5. Acknowledgements

The authors thank Mrs. Anna Kassai for providing the alkaloid standards and Mr. Emil Mincsovics (Laberté, Budapest, Hungary) for the amino modification method of silica layers.

6. References

[1] *The United States Pharmacopeia XXII Revision*, US Pharmacopeial Convention, Rockville, MD, 1989.
[2] D.E.M. Vendrig, J. Teeuwsen and J.J.M. Holthuis, *J. Chromatogr.*, 424 (1988) 83.
[3] J.P. Renaudin, *J. Chromatogr.*, 291 (1984) 165.
[4] K. Hirata, M. Asada, E. Yatani, K. Miyamoto and Y. Miura, *Planta Med.*, 59 (1993) 46.
[5] P. Morris, *Planta Med.*, 52 (1986) 121.
[6] A.N. Masoud, N.R. Farnsworth, L.A. Sciuchetti, R.N. Blomster and W.A. Meer, *Lloydia*, 31 (1968) 202.
[7] P. Horváth and G. Iványi, *Acta Pharm. Hung.*, 52 (1982) 150.
[8] E. Mincsovics, T. Székely, M. Hoznek, Z. Végh, I. Zámbó, G. Szepesi and E. Tyihák, in S. Görög (Editor), *Advances in Steroid Analysis*, Elsevier, Amsterdam, 1982, p. 427.
[9] G. Szepesi, K. Dudás, A. Pap, Z. Végh, E. Mincsovics and E. Tyihák, *J. Chromatogr.*, 237 (1982) 137.
[10] G. Szepesi, Z. Végh, Zs. Gyulai and M. Gazdag, *J. Chromatogr.*, 290 (1984) 127.
[11] M. Gazdag, G. Szepesi, M. Hernyes and Z. Végh, *J. Chromatogr.*, 290 (1984) 135.
[12] K. Ferenczi-Fodor, I. Kovács and G. Szepesi, *J. Chromatogr.*, 392 (1987) 464.
[13] E. Tyihák and E. Mincsovics, *J. Planar Chromatogr.*, 1 (1988) 309.
[14] E. Mincsovics, personal communication.
[15] K. Ferenczi-Fodor, E. Mincsovics and E. Tyihák, in J. Sherma and B. Fried (Editors), *Handbook of Thin-Layer Chromatography*, Marcel Dekker, New York (1990).
[16] K. Dallenbach-Toelke, Sz. Nyiredy, B. Meier and O. Sticher, *J. Chromatogr.*, 365 (1986) 63.
[17] E. Morgan, *Chemometrics: Experimental Design*, Wiley, Chichester, 1991.
[18] M. Gazdag, G. Szepesi and E. Szelecki, *J. Chromatogr.*, 454 (1988) 83.
[19] S. Kemény and A. Deák, *Mérések Tervezése és Eredményeik Értékelése*, Műszaki, Budapest, 1991.
[20] K. Ferenczi-Fodor, Z. Végh and Zs. Pap-Sziklay, *J. Planar Chromatogr.*, 6 (1993) 198.
[21] Z. Végh, *J. Planar Chromatogr.*, 6 (1993) 228.
[22] A. Nagy-Turák and Z. Végh, in preparation.

ELSEVIER

Journal of Chromatography A, 668 (1994) 509–517

JOURNAL OF CHROMATOGRAPHY A

Use of cyclodextrins and cyclodextrin derivatives in high-performance liquid chromatography and capillary electrophoresis

Julianna Szemán*,[a], Katalin Ganzler[b]

[a]CYCLOLAB Cyclodextrin Research and Development Laboratory Ltd., Budapest, Hungary
[b]Central Research Institute for Chemistry of the Hungarian Academy of Sciences, Budapest, Hungary

Abstract

Carboxymethyl- and carboxyethyl-β-cyclodextrin have proved to be effective chiral mobile phase additives in HPLC for the resolution of enantiomers of hexobarbital, ephedrine and an aminomethylbenzodioxane derivative. The separations are influenced by a combination of hydrophobic and electrostatic interactions. The type and concentration of the cyclodextrin derivative and the pH and type of base used to adjust the pH can be varied in order to optimize the method. In addition, a coating procedure was developed for capillary electrophoresis. The enantiomers of epinephrine were resolved on a γ-cyclodextrin-coated capillary. The length of the capillary has a significant effect on the resolution. β-Cyclodextrin was found to give no resolution.

1. Introduction

Cyclodextrins (CDs) can be very effective for enantiomer separations in a variety of separation methods. When CDs are used as chiral mobile phase additives in liquid chromatography, at least three factors control the enantioselective separation: differences in the stability constants of the CD complexes, differences in the adsorption of CD complexes on the surface of stationary phase and differences in the adsorption of free solute molecules on the cyclodextrin layer that is adsorbed on the surface [1]. In addition to the hydrophobic complex-forming interaction between the CD cavity and the guest molecule in the case of ionic guests, electrostatic interaction is also involved when using ionic CD derivatives [2]. In previous work we studied the use of ionic CD derivatives as mobile phase additives [3]. We now report on the effect of two statistically substituted ionic β-CD derivatives, namely carboxymethyl-β-CD (CMBCD) and carboxyethyl-β-CD (CEBCD), on the enantiomeric separation of some cationic guests.

Cyclodextrins are also used in capillary electrophoresis. Enantiomeric separation in capillary electrophoresis is usually achieved by the addition of a chiral selection to the buffer solution [4–6]. Using this approach, the chiral selector has to be replaced after each electrophoretic run. Immobilization of cyclodextrins can offer an advantage, in that the chiral selector is bound to the surface of the capillary, thus avoiding the need to replace it. Recently, an immobilized cyclodextrin stationary phase has been developed for coating fused-silica capillaries using

* Corresponding author.

0021-9673/94/$07.00
SSDI 0021-9673(93)E0041-R

GLC stationary phases [7]. Here, we report another approach for the immobilization of cyclodextrins.

2. Coating theory

Grafting vinyl monomers to cellulose or other hydroxyl-containing polymers using Ce(IV) or Co(IV) salts or redox catalysts is a well known technique in the textile industry [8–11]. Coating capillaries with cyclodextrins involves a similar mechanism, the difference being that an acrylamide layer is bound to the capillary wall prior to the cyclodextrin coating, to minimize electroosmotic flow and solute–wall interaction. The polymerization of acrylamide is a free radical polymerization, where chain termination is performed either by chain elongation or by charge disproportionation [12]. During acrylamide polymerization, owing to the chain termination step several double bonds develop, thus providing binding sites for the cyclodextrins:

Chain termination of acrylamide:

$$AA(n)^* + AA(m)^* \rightarrow AA(n+m)$$

$$AA(n)^* + AA(m)^* \rightarrow AA(n) + AA(m-1){=}A$$

where $AA(n)$ and $AA(m)$ denote polyacrylamide from n or m segments, respectively, and $AA(m-1){=}A$ represents polyacrylamide with m segments, containing a vinyl group at the end of the chain. During polymerization both termination steps occur, but their ratio is different depending on the conditions [12].

In this coating procedure a cyclodextrin layer is grafted to the double bonds present in the linear acrylamide [13] coating:

Coating reactions:

Initiation:

$$CD{-}OH + Ce^{4+} \rightarrow Complex \rightarrow CD{-}O^* + Ce^{3+} + H^+$$

Propagation:

$$CD{-}O^* + AA(m-1){=}A \rightarrow CD{-}O{-}AA(m)^*$$

Termination:

$$CD{-}O{-}AA(m)^* + Ce^{4+} \rightarrow CD{-}O{-}AA(m) + Ce^{3+} + H^+$$

3. Experimental

3.1. Reagents

Cyclodextrins, CMBCD [Degree of substitution (DS): 3, CY-2006], CEBCD (DS: 3.5, CY-2012) and soluble γ-cyclodextrin polymer (CY-3009) are commercial products of CYCLOLAB (Budapest, Hungary). The racemic solutes tested (Fig. 1) were of pharmaceutical grade. Epinephrine samples [(−)- and (±)-] were purchased from Aldrich (Steinheim, Germany). Eluents were prepared from HPLC-grade solvents (CHEMOLAB). Triethylamine (TEA) was purchased from Carlo Erba (Milan, Italy), cerium(IV) sulphate from Fluka (Buchs, Switzerland) and acrylamide, ammonium peroxodisulphate and TEMED from Bio-Rad Labs. (Hercules, CA, USA). Fused-silica capillaries (50 μm I.D.) were purchased from Polymicro Technologies (Phoenix, AZ, USA). All other reagents were of analytical-reagent grade.

3.2. Apparatus and procedures

HPLC

A Hewlett-Packard HP 1050 HPLC system with multiple wavelength detector and a HPLC

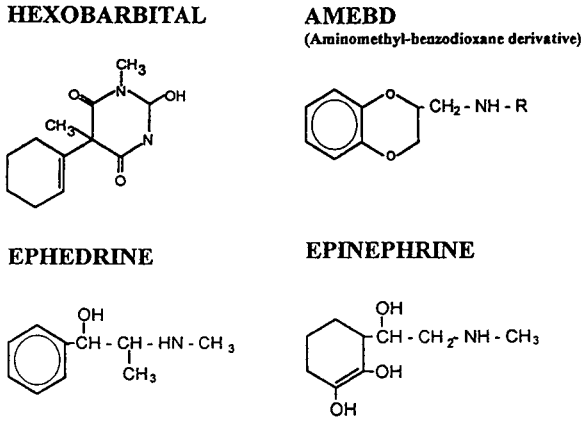

Fig. 1. Structures of the drugs studied.

ChemStation (DOS series) were used. The detector wavelength was 220 nm (band width 4 nm) and the reference wavelength was 350 nm (band width 80 nm). Experiments were carried out using a Nucleosil 300-5 C_4 cartridge column (100 × 4 mm I.D.) (Macherey–Nagel, Düren, Germany). The mobile phase was usually 5 mg/ml aqueous CD solution–ethanol (90:10, v/v); the flow-rate was 1 ml/min.

Capillary electrophoresis

Electrocoating and the electrophoretic runs were performed using a simple laboratory-made capillary electrophoresis system [14] consisting of a power supply and a UV detector (ISCO, Lincoln, NE, USA). Detection was performed at 214 nm.

Coating procedure. Fused-silica capillaries were coated with linear acrylamide (LA) according to the procedure of Hjertén [13] with a slight modification [15]. After polymerization, the excess of LA was pushed out from the capillaries and replaced with 5–10% (w/v) CD solution. CDs were dissolved in the separation buffer. The Ce^{4+} ions were caused to migrate electrophoretically into the capillary to provide the highest grafting ratio (Fig. 2). (Ce solution should be freshly prepared each day.) The coating procedure was completed overnight. The capillary should be washed extensively with the running buffer prior to a run. The stability of the coating was checked under the conditions in ref. 15.

Separation conditions. Electrophoretic separation was performed at room temperature in borate–phosphate buffer (0.02 *M*, pH 7.0) containing 10% of 2-propanol, using a 200 V/cm electric field in each instance. The samples were injected hydrodynamically.

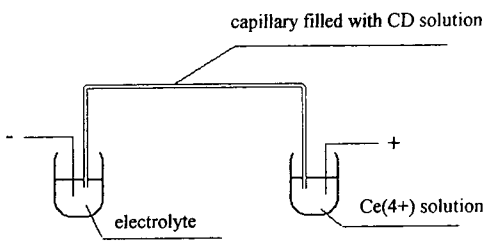

Fig. 2. Electrocoating of the capillary. Conditions: fused-silica capillary filled with CD solution. Applied electric field, 50 V/cm; for other parameters, see Experimental.

4. Results and discussion

4.1. HPLC

Effect of pH and the type of base used to adjust pH on capacity factor and resolution

Hexobarbital enantiomers are resolved using 5 mg/ml CEBCD in the mobile phase at pH 3.3 without using any base to adjust the pH (Fig. 3A

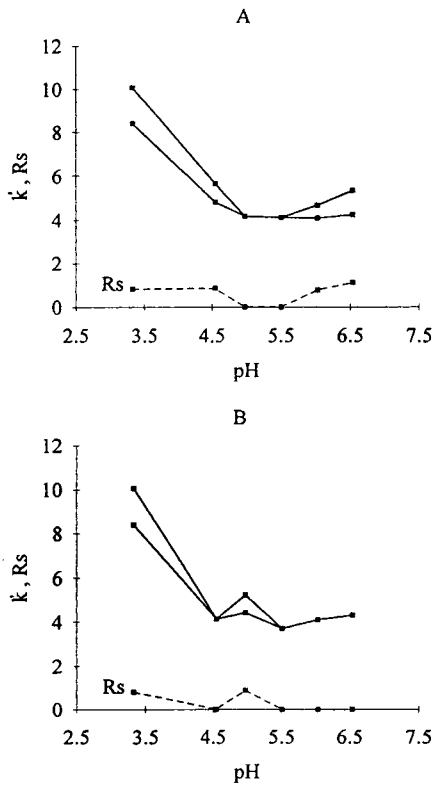

Fig. 3. Effects of pH and the type of base used to adjust pH on the capacity factor and resolution of hexobarbital using CEBCD as mobile phase additive. Mobile phase, 5 mg/ml aqueous CEBCD solution–ethanol (90:10, v/v); pH adjusted with (A) TEA and (B) NaOH. Solid lines, capacity factor of the two enantiomers, dashed lines, resolution.

and B). The capacity factor of hexobarbital decreases on increasing the pH to 5 and increases with further increase in pH when the pH is adjusted with TEA (Fig. 3A). A similar tendency can be observed for resolution. Using NaOH to adjust the pH, enantiomeric separation is observed at pH 5.0. The best resolution, R_s = 1.11, was achieved at pH 6.5 with the CEBCD–TEA eluent (Fig. 4).

Hexobarbital enantiomers could not be resolved using CMBCD when the pH was not adjusted with any base. The use of NaOH to adjust the pH resulted in good enantiomeric resolution at pH 4.5 and 5.5 (Fig. 5B). Although in the literature TEA is usually recommended as a buffer component when chemically bonded CD columns are used, in our experiments the separation of hexobarbital enantiomers cannot be achieved when the pH of CMBCD solution is adjusted with TEA (Fig. 5A).

The enantiomers of another basic guest molecule, an aminomethylbenzodioxane derivative, AMEBD, could also be resolved using 5 mg/ml

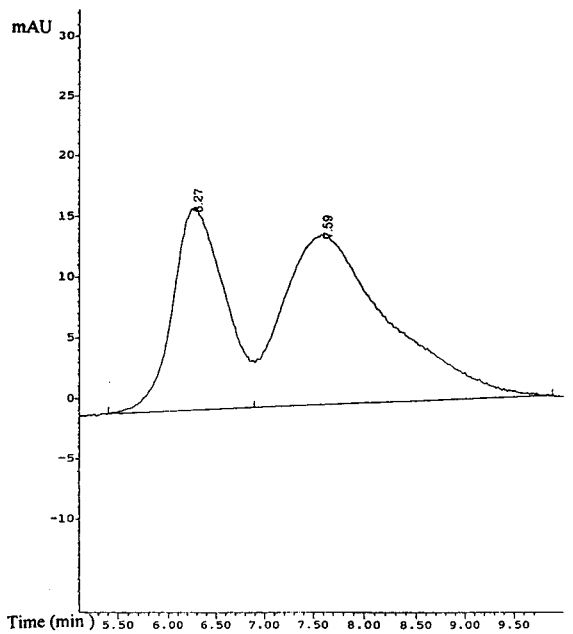

Fig. 4. Separation of hexobarbital enantiomers. Mobile phase, 5 mg/ml aqueous CEBCD solution–ethanol (90:10, v/v); pH = 6.5, adjusted with TEA.

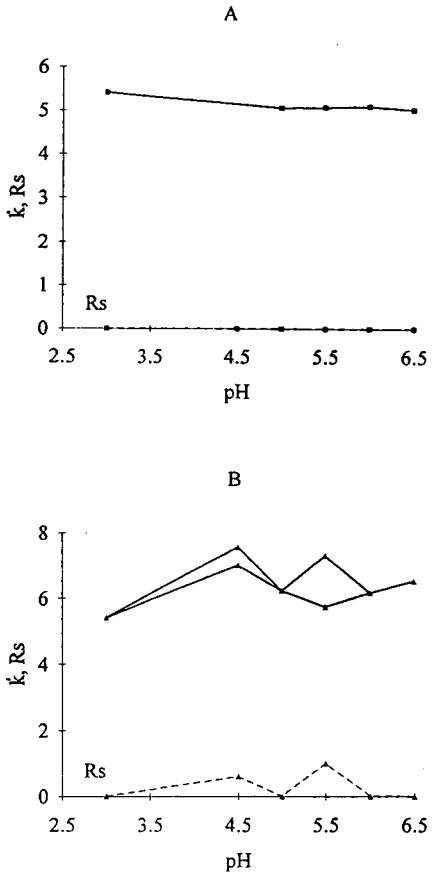

Fig. 5. Effects of the pH and the type of base used to adjust pH on the capacity factor and resolution of hexobarbital using CMBCD as mobile phase additive. Mobile phase, 5 mg/ml aqueous CMBCD solution–ethanol (90:10, v/v); pH adjusted with (A) TEA and (B) NaOH. Solid lines, capacity factor of enantiomers; dashed lines, resolution.

CEBCD at pH 3.3 without using base to adjust the pH. The capacity factor decreases with increasing pH in CEBCD–TEA mobile phases (Fig. 6A); with this, reasonable resolution (R_s = 1.10) was obtained at pH 5.5 (Fig. 7). Resolution could hardly be achieved at all when using NaOH to adjust the pH of CEBCD solution (Fig. 6B). Similarly to the results obtained with hexobarbital, when CMBCD was used as a mobile phase additive, only when NaOH was used as the pH modifier could the resolution of enantiomers of AMEBD be achieved (Fig. 8B).

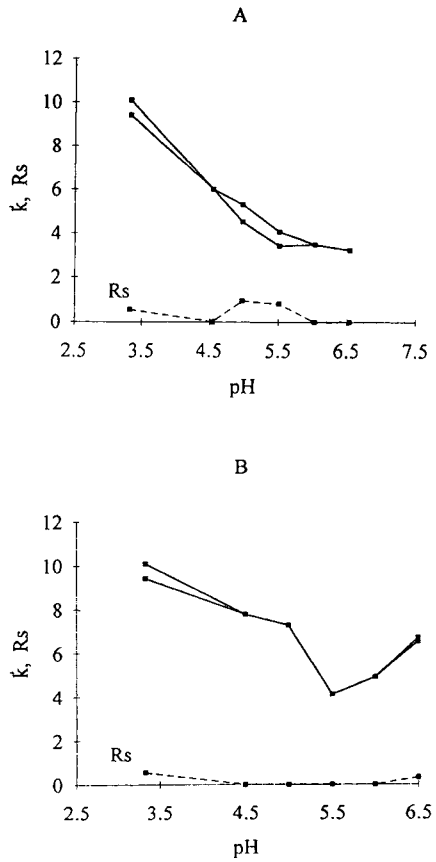

Fig. 6. Effects of the pH and the type of base used to adjust pH on the capacity factor and resolution of AMEBD using CEBCD as mobile phase additive. Mobile phase, 5 mg/ml aqueous CEBCD solution–ethanol (90:10, v/v); pH adjusted with (A) TEA and (B) NaOH. Solid lines, capacity factor of enantiomers; dashed lines, resolution.

The optimum pH is 5.5, where the resolution is 1.11.

The enantiomers of ephedrine were also separated in CEBCD–TEA systems (Fig. 9A) in the pH range 3.3–5.5 (at pH 3.3 no base was added to the CEBCD solution), whereas the CEBCD–NaOH-containing eluents were found not to be effective (Fig. 9B). The capacity factors of ephedrine are lower than 2 when CMBCD is used in the mobile phase; probably the use of a more apolar stationary phase (C_8 or C_{18}) would give better results.

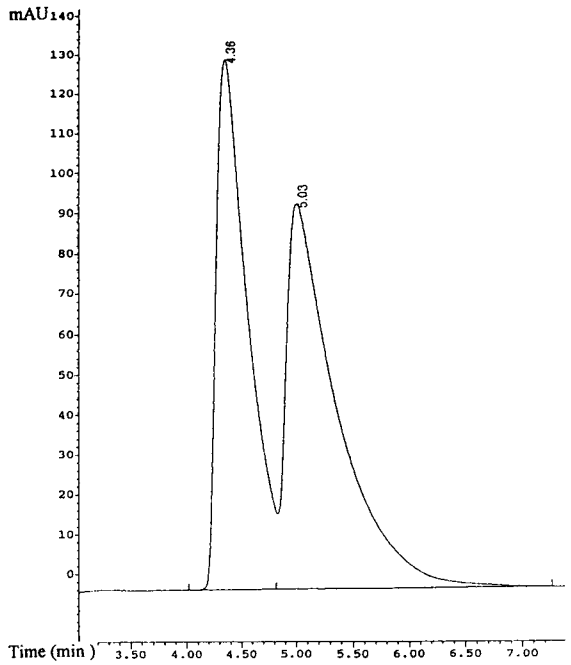

Fig. 7. Separation of AMEBD enantiomers. Mobile phase, 5 mg/ml aqueous CEBCD solution–ethanol (90:10, v/v); pH 5.5, adjusted with TEA.

Effect of CD concentration on capacity factor and resolution

The enantioselectivity generally improves with increasing CD concentration in the mobile phase. However, enhancement of the ionic CD concentration also results in an increase in the ionic strength of the solution. In oppositely charged host–guest systems, electrostatic attractive interactions are weakened by an increase in ionic strength, whereas hydrophobic interactions are strengthened [2]. The resultant of these effects influences the chromatographic behaviour of basic drugs in anionic CD-containing mobile phase systems.

Table 1 summarizes the resolution obtained with different eluent systems. Usually no enantiomeric separation was achieved at 2.5 mg/ml CMBCD or CEBCD concentration. Increasing the CD concentration resulted in a decrease in capacity factor and in an increase in the resolution of enantiomers. However, no enantio-

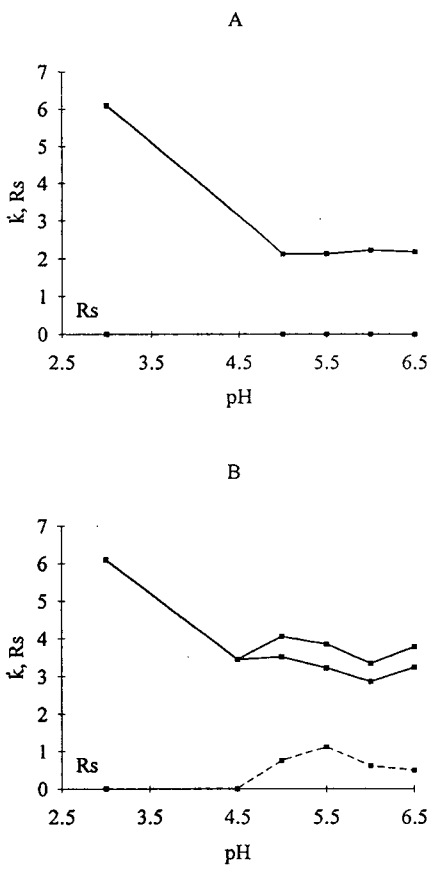

Fig. 8. Effects of the pH and the type of base used to adjust pH on the capacity factor and resolution of AMEBD using CMBCD as mobile phase additive. Mobile phase, 5 mg/ml aqueous CMBCD solution–ethanol (90:10, v/v); pH adjusted with (A) TEA and (B) NaOH. Solid lines, capacity factor of enantiomers; dashed lines, resolution.

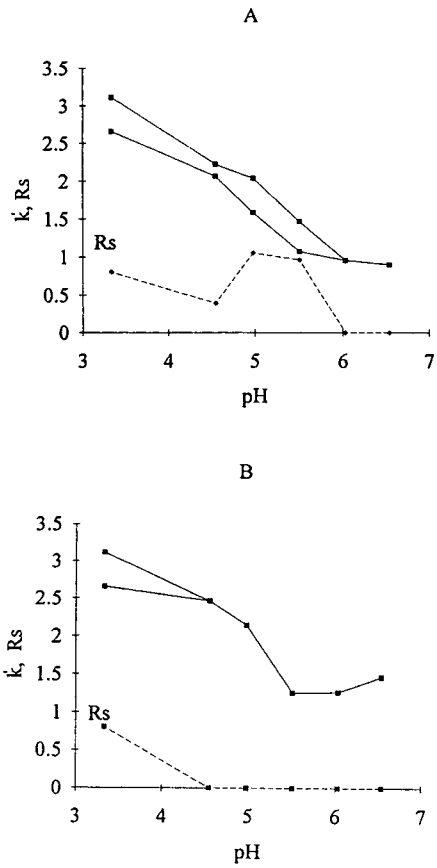

Fig. 9. Effects of the pH and the type base used to adjust pH on the capacity factor and resolution of ephedrine using CEBCD as mobile phase additive. Mobile phase, 5 mg/ml aqueous CEBCD solution–ethanol (90:10, v/v); pH adjusted with (A) TEA and (B) NaOH. Solid lines, capacity factor of enantiomers; dashed lines, resolution.

Table 1
Dependence of resolution on CD concentration in the mobile phase

Solute	Mobile phase	CD (mg/ml)				
		2.5	5	10	20	5 (in 0.05 *M* NaCl)
Hexobarbital	CMBCD–NaOH (pH 5.5)	0	1.01	0.53	0	0
	CEBCD–TEA (pH 5.0)	0	0	0.93	0.87	–
AMEBD	CMBCD–NaOH (pH 5.5)	0.67	0.71	0.61	0	0.43
	CEBCD–TEA (pH 5.0)	0	0.94	0.85	0	–
Ephedrine	CEBCD–TEA (pH 5.0)	0	1.05	0.36	0	–

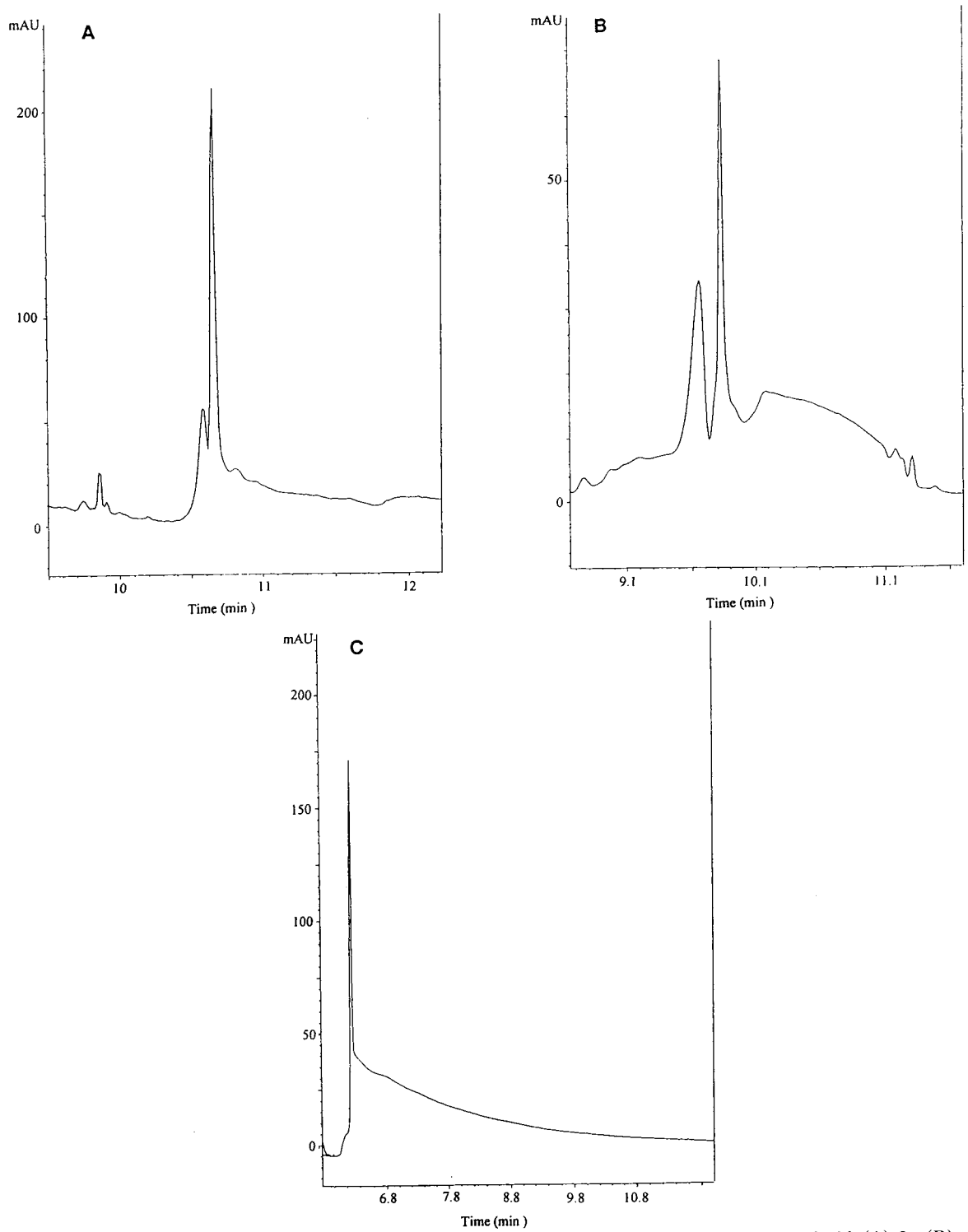

Fig. 10. Effect of CD type on the separation of (±)-epinephrine. Conditions: fused-silica capillary coated with (A) β-, (B) γ- or (C) γ-CD polymer. The effective length of the capillary was 14 cm in each instance. For other parameters, see Experimental.

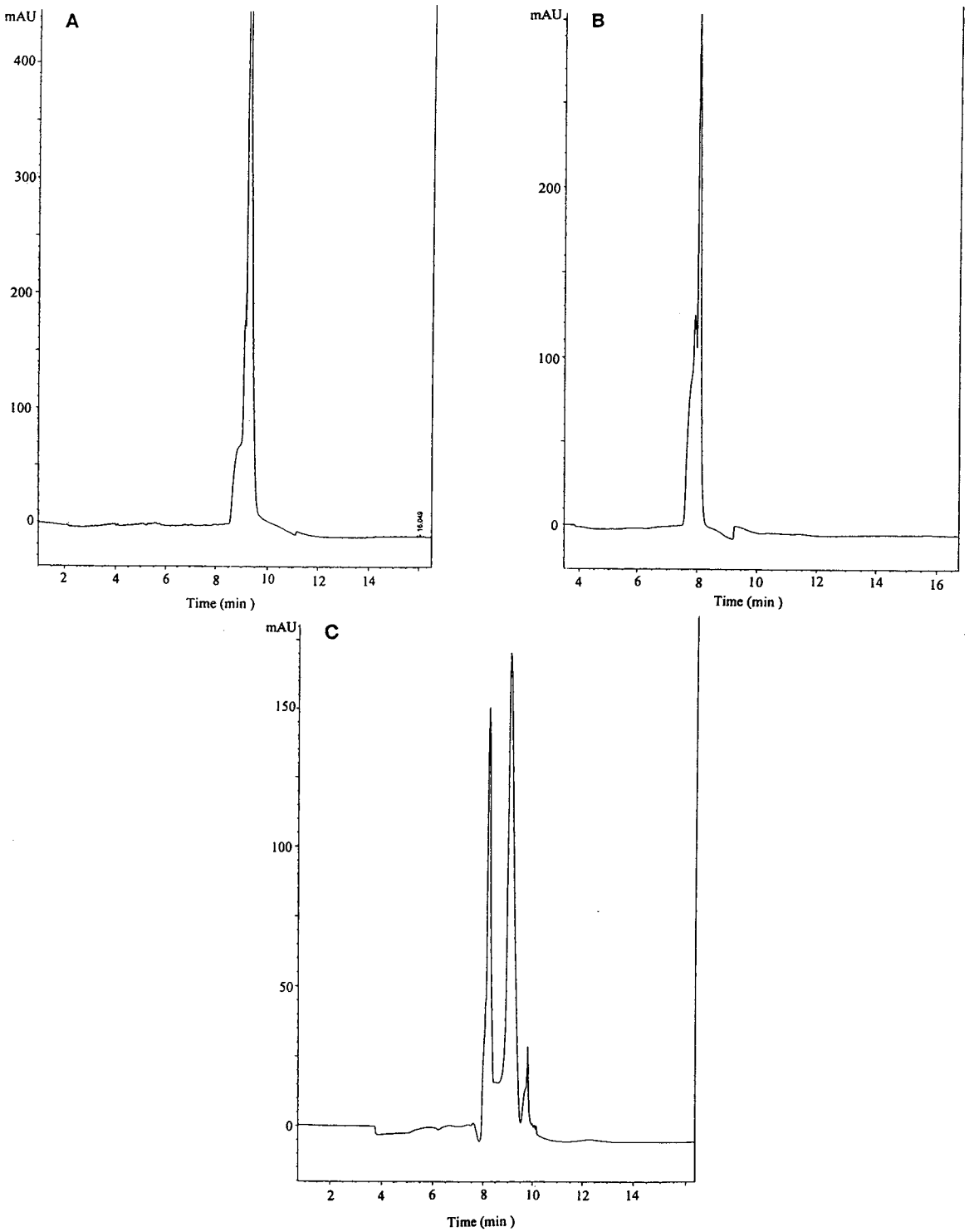

Fig. 11. Effect of the capillary length on the separation of (±)-epinephrine. Conditions: fused-silica capillary coated with γ-CD. Effective length: (A) 5 cm; (B) 8 cm; (C) 18 cm. For other parameters, see Experimental.

meric separation was observed at 20 mg/ml CD concentration. The optimum CD concentration was usually 5–10 mg/ml, except for hexobarbital in the CEBCD–TEA system, where a 10 mg/ml CD concentration was necessary for the resolution of enantiomers. On increasing the ionic strength with NaCl (0.05 *M*), the resolution also decreased.

Effect of the ethanol concentration of mobile phase

The capacity factor, as usual, showed a tendency to decrease with increase in ethanol content of the mobile phase, whereas there were only slight differences in the resolution of enantiomers at different ethanol concentrations.

4.2. Capillary electrophoresis

The effect of the type of CD coating on the separation of epinephrine was studied using β- and γ-CD and water-soluble γ-CD polymer-coated capillaries. As shown in Fig. 10B, a γ-CD coating seems to be the best for the separation of epinephrine enantiomers.

The effect of the capillary length was studied with a γ-CD coating using capillaries with effective lengths of 5, 8 and 18 cm. The resolution increases with increasing capillary length (Fig. 11).

5. Conclusions

Ionic CD derivatives are useful chiral mobile phase additives in HPLC methods. The combination of hydrophobic and ionic interactions offers a wide range of possibilities for optimizing separations. In addition to the usual conditions, such as concentration of CD derivatives and pH, the type of ionic substituents on the CD ring (*e.g.*, carboxymethyl or carboxyethyl) also influences enantiomeric separations. The type of base used to adjust the pH is also an important factor. The effect of TEA, which is a widely used additive in RP-HPLC, was unfavourable when CMBCD was used as a chiral selector.

Chiral-selective capillary coatings were prepared by modifying the coating procedure [15] for enantiomeric separations in capillary electrophoresis. The CD coating proved to be stable at neutral pH for up to 50 injections. The length of the capillary has a significant effect on the resolution of enantiomers. Also, the type of chiral selector plays a significant role in the performance of the capillary. Further studies are planned on the use of other CD derivatives and to test the stability of the column over a wider pH range.

6. Acknowledgement

The authors are grateful to Ms. Mráz-Lakó Adél for technical assistance.

7. References

[1] M.L. Hilton and D.W. Armstrong, in D. Duchene (Editor), *New Trends in Cyclodextrins and Derivatives*, Editions de Santé, Paris, 1991, Ch. 15, p. 536.
[2] Y. Matsui, K. Ogawa, S. Mikami, M. Yoshimoto and K. Mochida, *Bull. Chem. Soc. Jpn.*, 60 (1987) 1219.
[3] J. Szemán and J. Szejtli, in D. Duchene (Editor), *Minutes of the 5th International Symphosium on Cyclodextrins*, Editions de Santé, Paris, 1990, p. 672.
[4] E. Gassmann, J. Kuo and R.N. Zare, *Science*, 230 (1985) 813.
[5] K. Otsuka, S. Terabe and T. Ando, *J. Chromatogr.*, 332 (1985) 219.
[6] T. Schmidt and H. Engelhardt, presented at *HPLC '93 Hamburg, 1993.*
[7] S. Mayer and V. Schurig, *J. High Resolut. Chromatogr.*, 15 (1992) 129.
[8] S. Kaizermann and G. Mino, *J. Polym. Sci.*, 31 (122) (1958) 242.
[9] H. Narita, S. Okamoto and S. Machida, *Macromol. Chem.*, 125 (1969) 15.
[10] P.L. Nayak, H.K. Das and B.C. Singh, *Angew. Makromol. Chem.*, 75 (1979) 2391.
[11] T. Graczyk, *J. Macromol. Sci. Chem.*, A27 (1990) 23.
[12] G. Odian, *Principles of Polymerization*, Wiley-Interscience, New York, 2nd ed., 1981.
[13] S. Hjertén, *J. Chromatogr.*, 347 (1985) 191.
[14] J.W. Jorgenson and K.D. Lukács, *Anal. Chem.*, 53 (1981) 1298.
[15] K. Ganzler, K.S. Greve, A.S. Cohen and B.L. Karger, *Anal. Chem.*, 64 (1992) 2665.

ELSEVIER

Journal of Chromatography A, 668 (1994) 519–527

JOURNAL OF CHROMATOGRAPHY A

Short Communication

Reversed-phase high-performance liquid chromatography of the stereoisomers of some sweetener peptides with a helical nickel(II) chelate in the mobile phase

Grzegorz Bazylak

Biochromatographic Laboratory, Human Nutrition Division, Hygienics Department, Medical University of Łodz, Jaracza 63, 90 251 Łodz, Poland

Abstract

The use of a chiral mobile phase additive in the form of the helically distorted, square-planar, chiral nickel(II) chelate *dl*-[4,4′-(1-methyl-2-propylethane-1,2-diyldiimino)bis(pent-3-en-2-onato)]nickel(II) was investigated for the resolution of optical isomers of dipeptide-type sweeteners, *viz.*, aspartame, alitame and antiaspartame, and some of their decomposition products, *e.g.*, diketopiperazines. The chiral discrimination mechanism for the solutes was elucidated. The proposed chiral RP-HPLC system was applied to the stereoselective determination of aspartame impurities in samples of its commercial dietetic and pharmaceutical formulations.

1. Introduction

The sweetness of non-nutritive dipeptide-type sweeteners (see Fig. 1), *e.g.*, N-aspartylphenylalanine methyl ester (aspartame, **1**), aspartyl-N-(tetramethyl-3-thietanyl)alaninamide (alitame, **2**) and N-acetylphenylalanyllysine (antiaspartame, **3**), is strictly related to only the single

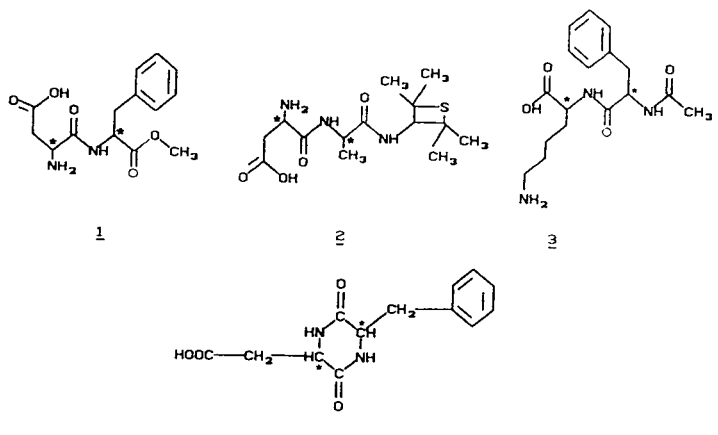

Fig. 1. Structural formulae of the compounds studied: **1** = α-L,L-aspartame; **2** = α-L,D-alitame; **3** = α-L,L-antiaspartame; **4** = diketopiperazine (DKP).

0021-9673/94/$07.00
SSDI 0021-9673(94)00067-J

stereoisomeric and conformationally stable form that enables them to adopt the particular three-point arrangements of chemical groups with respect to the human sweet taste receptors [1]. However, there is lack of reports concerning any possible racemization of the individual intense sweet isomers of synthetic dipeptide-type sweeteners, *viz.*, α-L,L-aspartame [1], α-L,D-alitame [2] and α-L,L-antiaspartame [3], during syntheses or decomposition processes which can lead to the formation of one or more of the three other undesirable, non-sweet stereoisomers, *e.g.*, D,D, D,L- and L,D- for aspartame. Moreover, until now our knowledge about metabolic disorders caused by the consumption of such useless forms of these sweeteners or their β-conformers (identified in stored aspartame-sweetened products [4,5]) has been limited [6,7].

Using high-performance liquid chromatographic (HPLC) methods, stereoselective analyses of unmodified [4,8,9] or protected [10] aspartame isomers have been achieved on achiral [8] and chiral chromatographic columns containing immobilized α-chymotrypsin [9], a crown ether coated on a polymeric support [4] and cellulose tris-3,5-dimethylphenylcarbamate coated on a silica gel surface [10].

For the partial separation of protected aspartame diasteromers, thin-layer chromatography (TLC) using octadecylsilica layers impregnated with (2*S*,4*R*,2′*RS*)-N-(2′-hydroxy-*n*-dodecyl)-4-hydroxyproline and copper (II) ion has also been reported [10]. Some years ago Cooke *et al.* [11] and Lindner *et al.* [12] described the baseline enantioselective separation of dansyldipeptides by reversed-phase (RP) HPLC using chiral metal chelates, *i.e.*, (4-dodecyldiethylenetriamine)zinc(II) and (L-2-isopropyl-4-octyldiethylenetriamine)nickel(II), as chiral mobile phase additives. The results indicated that with a properly designed chiral selector in the form of a transition metal chelate, superior HPLC resolution of free diastereomeric dipeptides could be achieved with high selectivity comparable to the efficiency of HPLC systems employing one of the chiral stationary phases [4,9,10] previously mentioned.

In this study, a direct stereoselective separation of structurally related sweeteners, *i.e.*, underivatized aspartame, alitame and antiaspartame, was developed, employing RP-HPLC on an octadecylsilane stationary phase and a chiral eluent containing the recently synthesized, helically distorted nickel(II) Schiff base chelate *dl*-[4,4′-(1-methyl-2-propylethane-1,2-diyldiimino)bis(pent-3-en-2-onato)]nickel(II) [13,14], which has already been successfully applied to the HPLC assay of diastereomers and enantiomers of aliphatic mono- and diamines [15,16] and amino alcohols [17]. The separation efficiency of the proposed method was also demonstrated by the analysis of aspartame decomposition products, especially the separation of the stereoisomers of cyclic dipeptides [diketopiperazines (DKPs)].

2. Experimental

2.1. Reagents and samples

The crystalline chelate *dl*-[4,4′-(1-methyl-2-propylethane-1,2-diyldiimino)bis(pent-3-en-2-onato)]nickel(II) [Ni(MPA); see Fig. 2], applied as the chiral additive to the mobile phase in RP-HPLC experiments, was prepared as described previously [13,14] with a tetradentate Schiff base derived from the condensation *in situ* (in a 2:1 molar ratio) of (*S*,*S*)-2,3-diaminohexane with 2,4-pentanedione, and nickel(II) acetate pentahydrate in acetone solution. The identity and the helically distorted structure of the synthesized Ni(MPA) chelate was checked by spectral methods [13,14].

All stereoisomeric samples of α-aspartame and

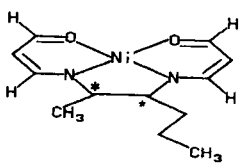

5

Fig. 2. Structure of Ni(MPA) chelate used as the mobile phase additive in the developed HPLC system. The chiral centres are indicated by asterisks (some hydrogen atoms have been omitted for clarity).

α-alitame and their β-conformers were obtained as a gift from NutraSweet (Skokie, IL, USA) and Pfizer (Sandwich, Kent, UK), respectively. The α-antiaspartame samples and all stereoisomers of α- and β-aspartylphenyl (Asp–Phe) dipeptide and pure D- and L-enantiomers of phenylalanine (Phe) were supplied by Sigma (St. Louis, MO, USA). L-Phenylalanine methyl ester was obtained from Aldrich (Milwaukee, WI, USA). All stereoisomers of cyclic Asp–Phe [5-benzyl-3,6-dioxo-2-piperazineacetic acid; diketopiperazine (DKP)] were supplied by NutraSweet. Individual solutions (100 μM) of stereoisomers of the compounds studied were prepared in doubly distilled water and 10-μl volumes were injected directly into the HPLC column.

Commercially available samples of sweetener formulations, containing aspartame as the main ingredient, were supplied from five different Polish manufacturers. An amount of the powdered sample equivalent to about 50 mg of aspartame was extracted with 25 ml of acetonitrile–20 mmol/l potassium phosphate buffer (85:15, v/v) (pH 3.5). An aliquot (1.0 ml) of the extracted solution was added to 2.5 ml of the internal standard (3-hydroxybenzoic acid) solution (0.1 mg/ml) and the final mixture was diluted to 10 ml with the solution used previously in the extraction stage.

2.2. Chromatographic conditions

RP-HPLC analyses were performed on an LDC–Milton Roy Model 3000 high-performance liquid chromatograph equipped with a multi-wavelength UV detector operating at 210 nm and at a sensitivity of 0.05 AUFS. An octadecylsilane reversed-phase Polsil ODS column (25 × 0.4 cm I.D.; $d_p = 7$ μm) (ZOCh, Lublin, Poland) was used. The mobile phase, consisting of acetonitrile (85 ml), 20 mmol/l potassium phosphate buffer (15 ml) and dissolved 2 mmol/l of Ni(MPA) chelate, adjusted to pH 3.5 with 0.1 mol/l potassium hydroxide, was filtered through a 0.45-μm membrane filter and degassed ultrasonically under vacuum before use. The flow-rate was 0.8 ml/min. Prior to sample injection the chromatographic column was equilibrated with 22.5 ml of freshly prepared mobile phase. All measurements were made at 25°C and repeated four times to calculate the capacity factor (k') values.

2.3. Molecular model calculations

The molecular modelling program PCMODEL (Serena Software, Bloomington, IN, USA), implemented on an IBM 386/SX microcomputer, was applied for creation of the proposed structure of associates formed between solutes and Ni(MPA) during chiral recognition in the developed HPLC system.

3. Results and discussion

3.1. Characterization of Ni(MPA)

In the synthesized Ni(MPA) chelate (see Fig. 2), the central nickel(II) ion is surrounded by the coordinated imine and carbonyl groups defining a nearly square-planar surface [18]. However, the non-equivalence of alkyl substitution of the two stereogenic centres, localized in the ethylene bridge connecting imine nitrogen atoms, by methyl and *n*-propyl groups, leads to the formation of the two conformational isomers of the Ni(MPA) molecule [13,14,18]. The steric and energetic factors imply greater stability and population of the (λ–Λ)-isomer in which the more bulky *n*-propyl substituent occupies the axial position with respect to the plane formed by nitrogen and oxygen donor atoms [17,18]. This situation leads to an antiperiplanar configuration and a *trans* orientation of alkyl substituents on the chiral centres, stabilizing the helical distortion of the Ni(MPA) molecule [13,14]; this also means non-planarity of the six-membered chelate rings in the Ni(MPA) molecule [13,18]. The axial position of the *n*-propyl substituent also causes steric hindrance around the coordinatively unsaturated central nickel(II) ion acting as the Lewis acid site [18]. Most of the partial negative charge in the Ni(MPA) chelate is localized on the oxygen carbonyl atoms. However, the surface area of Ni(MPA) is mostly

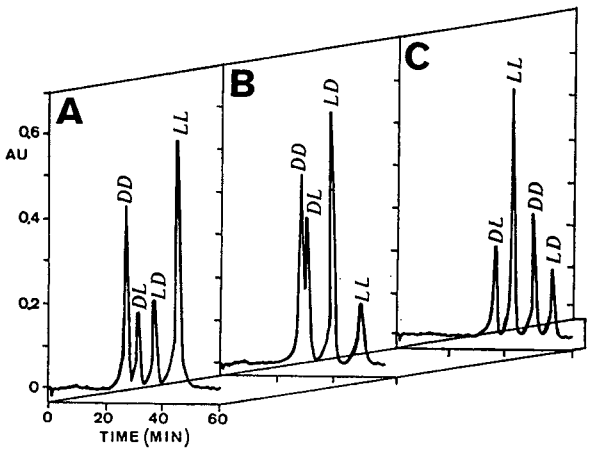

Fig. 3. Stereoselective separation of (A) aspartame, (B) alitame and (C) antiaspartame isomers by RP-HPLC with Ni(MPA) chelate as chiral additive in the mobile phase (see Experimental).

non-polar, *viz.*, it occupied nearly 212 $Å^2$ of the 283 $Å^2$ total surface area of the chelate. As was postulated previously based on measured adsorption isotherm data [16], the Ni(MPA) chelate can be partly sorbed on the octadecylsilane stationary phase in a chromatographic column with an axial *n*-propyl substituent by involving specific hydrophobic interactions.

3.2. Retention of sweetener stereoisomers

Typical chromatograms of stereoisomer mixtures of each sweetener studied with the developed chiral mobile phase are shown in Fig. 3. Table 1 given a detailed comparison of capacity factors and parameters of the separation efficiency calculated for the respective diastereoisomers and enantiomers of individual sweeteners. The data in Fig. 3 and Table 1 show that the retention orders of aspartame and alitame isomers in the proposed chiral HPLC system are identical. One can suggest that the configuration of the analogous aspartyl moiety present in the aspartame and alitame molecules is the main factor controlling the diastereomeric retention order for these solutes. However, replacing the N-terminal residue of esterified phenylalanine, as in aspartame, with a non-aromatic substituent in the form of tetramethyl-3-thietanylalaninamide, as in alitame (see Fig. 1), leads to a non-baseline resolution ($R_s = 0.7$) of the pair of D,D/D,L-diastereomers of the latter sweetener.

Table 1
Values of capacity factors (k'), separation factors (α) and resolution factors (R_s) of isomers of sweeteners obtained with the proposed chiral RP-HPLC system

Sweetener	Stereoisomer	k'	α	R_s
α-Aspartame	D,D[a]	2.7		
	D,L	3.2	1.20[b]	1.4[b]
	L,D	3.9	1.23	2.0
	L,L	5.1	1.31	2.5
α-Alitame	D,D[a]	2.9		
	D,L	3.1	1.07	0.7
	L,D	4.3	1.38	2.5
	L,L	5.7	1.35	2.8
α-Antiaspartame	D,D[c]	3.7		
	L,L	4.5	1.21	2.3
	D,L	5.5	1.22	2.8
	L,D	6.3	1.15	2.3

Mobile phase flow-rate, 0.8 ml/min; $t_0 = 7.2$ min.
[a] First letter assigns the Asp configuration in the sweetener molecule.
[b] Calculated for successive pairs of peaks.
[c] First letter assigns the Lys configuration in the sweetener molecule.

Comparing the retentions of aspartame and antiaspartame isomers, which contain an analogous phenylalanine part in their molecules but differ in the N- and O-terminal residues (see Fig. 1), large retention and selectivity increases associated with the drastic change in the elution sequence of the antiaspartame isomers can be observed. On the chromatograms of antiaspartame isomers the peaks of the enantiomer pairs D,D/L,L and D,L/L,D were registered in close proximity, whereas on the aspartame chromatograms the diastereomer pairs D,D/D,L and L,D/L,L eluted one after the other. Probably, the proposed chiral RP-HPLC system with Ni(MPA) in the mobile phase is more selective during the separation of phenylalanine-containing dipeptides when the highly hydrophobic fragment (*e.g.*, lysine instead of a methyl group) is introduced at the O-terminus of such solutes.

For sweeteners containing peptide and amide bonds, *i.e.*, alitame and antiaspartame, the observed increase in their retention and selectivity accompanied by a reversed vicinity of their stereoisomeric pairs can be partly explained by the increasing flatness of the antiaspartame molecule caused by the phenyl substituent connected to the second chiral centre located between the flat amide bonds of this sweetener. Probably this factor also has a great impact on the differences in the observed retentions and separation efficiencies of antiaspartame and aspartame isomers, where the flatness increase is caused by the presence of a terminal methyl amide group instead of a methyl ester group, respectively.

3.3. Chiral discrimination mechanism

The formation of unstable associates with 1:1 stoichiometry between the square-planar nickel(II) chelates and electron-donor compounds, including di- and tripeptides, was intensively studied as a model of enzyme active site reactivity [18]. The equatorial position of the dipeptide molecule in relation to the planar nickel(II) chelate forced by its helical structure was suggested on the basis of results of *ab initio* molecular calculations [19].

The observed stereospecific separation and retention order of stereoisomers of dipeptide-type sweeteners in the proposed HPLC system can be explained by the occurrence of association processes on the basis of the "three-point-interactions" rule of Dalgliesh [20]. Molecular models of Ni(MPA)–dipeptide associates (see Fig. 4) indicate that chiral discrimination of

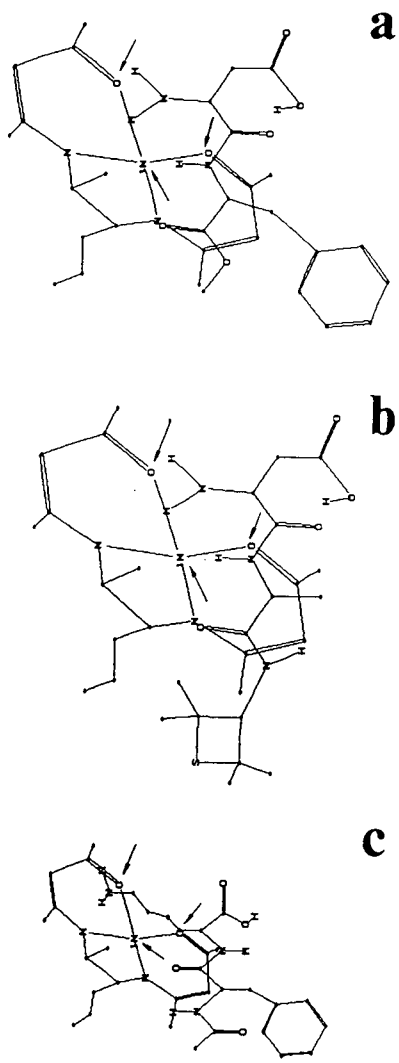

Fig. 4. Views of proposed structures of diastereomeric associates formed between Ni(MPA) and (a) α-L,L-aspartame, (b) α-L,L-alitame and (c) α-L,D-antiaspartame in the developed chiral HPLC system (some hydrogen atoms have been omitted for clarity). Arrows indicate positions of the possible interaction sites.

aspartame (Fig. 4a) an alitame (Fig. 4b) stereoisomers in the developed HPLC system occurs predominantly by electrostatic interactions of the carbonyl group in the vicinity of the chiral carbon atom localized in the phenylalanine moiety of the solute and the central nickel(II) ion in the Ni(MPA) chelate molecule. At a second interaction point, weak hydrogen bond formation between the amide hydrogen of the solute and one of the coordinated carbonyl groups in the chelate molecule can be postulated. With the applied acidic pH of the mobile phase the primary aspartyl amino group of such dipeptide-type sweeteners is protonated [21], leading to electrostatic interactions with the second coordinated carbonyl group of the Ni(MPA) chelate. Hence in this way the third interaction site is formed.

For the L,L-isomer of aspartame or alitame, all three proposed interactions points are "saturated", increasing the relative stability of the associates and thus leading to their stronger retention (see Table 1). For the D,L-isomer the protonated aspartyl amino group in the aspartame or alitame molecule is situated above the peptide bond plane so its distance from the coordinated carbonyl groups of Ni(MPA) is increased, hindering the possible electrostatic interactions, diminishing the stability of the associate and thus reducing the observed HPLC retention of such a solute. The active role of the aspartyl primary amine group in controlling the chiral recognition mechanism of free aspartame isomers in their temperature-gradient HPLC separation with a chiral crown ether stationary phase was also stressed by Motellier and Wainer [4].

For antiaspartame stereoisomers the configuration of the lysine chain with charged primary amino group is essential for the observed enantioselectivity of their separation using the RP-HPLC system described here. However, in this case probably the configuration of the phenylalanine moiety also partly influences the stability of the formed associates (see Fig. 4c) by diminution of interactions between the carbonyl group in the peptide bond of antiaspartame and the coordinatively unsaturated nickel(II) ion in the Ni(MPA) chelate molecule.

3.4. Retention of aspartame decomposition products

The process of aspartame decomposition under acidic conditions leads to the formation of the stereoisomers of species such as the cyclic 5-benzyl-3,6-dioxo-2-piperazineacetic acid [diketopiperazine (DKP); **4** in Fig. 1], aspartylphenylalanine (Asp–Phe), phenylalanine methyl ester (Phe methyl ester), free phenylalanine (Phe) and β-conformers of aspartame and Asp–Phe dipeptide [1,21]. To test the usefulness of the developed HPLC system for the direct, one-run stereoselective separation of the aspartame degradation products the L,L-isomer of α-aspartame was dissolved in acidified water (pH 3) and stored at ambient temperature. The composition of the solution was determined chromatographically after 72 h under HPLC conditions identical with those used previously for the sweetener isomer separation studies. The results of this investigation are illustrated in Table 2 and Fig. 5A.

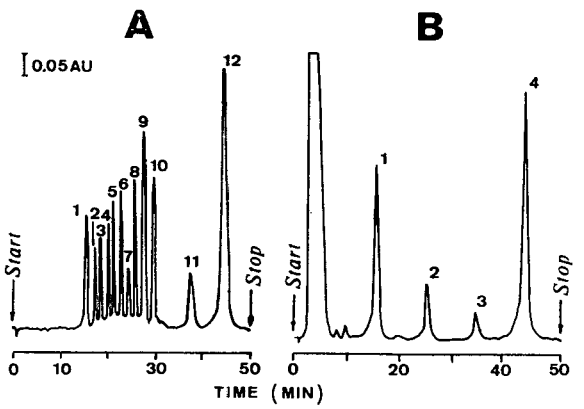

Fig. 5. Chromatograms showing the separation of (A) α-L,L-aspartame decomposition products and (B) α-L,L-aspartame impurities in a commercial product (third sample in Table 3) with the developed HPLC system with Ni(MPA) as chiral additive to the mobile phase. Peaks: (A) 1 = D-phenylalanine; 2 = L-phenylalanine; 3 = D-phenylalanine methyl ester; 4 = L-phenylalanine methyl ester; 5 = D,D-aspartylphenylalanine; 6 = D,L-aspartylphenylalanine; 7 = L,D-aspartylphenylalanine; 8 = L,L-aspartylphenylalanine; 9 = L,L + D,D-diketopiperazine (DKP); 10 = L,D + D,L-diketopiperazine (DKP); 11 = β-L,L-aspartame; 12 = α-L,L-aspartame; (B) 1 = 3-hydroxybenzoic acid (internal standard); 2 = L,L + D,D-diketopiperazine (DKP); 3 = α-L,D-aspartame; 4 = α-L,L-aspartame.

Table 2
Values of capacity factors (k'), separation factors (α) and resolution factors (R_s) of aspartame decomposition products obtained with the proposed chiral RP-HPLC system

Product	Stereoisomer	k'	α	R_s
Phe	D	1.2		
			1.20[a]	2.5[a]
	L	1.4		
Phe methyl ester	D	1.5		
			1.10	1.6
	L	1.6		
Asp–Phe	D,D	1.7		
			1.17	2.2
	D,L	2.0		
			1.05	1.5
	L,D	2.1		
			1.09	2.3
	L,L	2.3		
DKP	L,L	2.5		
			1.00	0.0
	D,D	2.5		
			1.04	1.6
	L,D	2.6		
			1.00	0.0
	D,L	2.6		

Mobile phase flow-rate, 0.8 ml/min; $t_0 = 7.2$ min.
[a] Calculated for successive pairs of peaks.

Using the proposed RP-HPLC system with Ni(MPA) chelate as a chiral additive to the mobile phase, all the diastereomers and enantiomers of Asp–Phe dipeptide, Phe amino acid and Phe methyl ester were satisfactorily resolved with high separation factors (α values). For Asp–Phe dipeptide the chromatographic system is rather diastereoselective because its D,D/D,L- and L,D/L,L-diastereomers eluted as successive peaks (see Table 2).

However, for DKP stereoisomers, two of its enantiomeric pairs, L,L/D,D and L,D/D,L, were not separated ($\alpha = 1$). Again, only the diastereoselectivity of the proposed chiral RP-HPLC system was manifested ($\alpha = 1.04$). It can be assumed that the apical association of the cyclic DKP isomer molecule with the Ni(MPA) chelate through single attractive interactions involve one of the DKP carbonyl groups and the coordinated nickel(II) ion. The enantiospecificity of such a "one-point interaction" chiral recognition mechanism [17,22] is significantly diminished compared with the "three-point interaction" mechanism postulated in this work for the separation of dipeptide-type sweetener stereoisomer mixtures using the chiral RP-HPLC approach.

The peak of β-L,L-aspartame with capacity factor $k' = 4.2$ was recognized on the chromatogram of α-L,L-aspartame degradation products (see Fig. 5A) by injection of an appropriate standard solution. Probably owing to the weaker association with Ni(MPA) chelate in the mobile phase, β-L,L-aspartame is eluted before α-L,L-aspartame with a high value of the separation factor α of the conformers of *ca.* 1.20.

3.5. *Analysis of commercial aspartame formulations*

Commercial preparations of aspartame were analysed using the developed RP-HPLC method

Table 3
Amounts of impurities in aspartame commercial formulations as determined with the proposed chiral RP-HPLC method

Sample	Aspartame[a,b] (%)				DKP[b,c] (%)	
	L,L	L,D	D,D	D,L	L,L/D,D	L,D/D,L
Dietetic	98.5	–[d]	–	–	0.28	–
Dietetic	96.4	–	–	–	0.32	–
Dietetic	97.8	1.2[b]	–	–	0.15	–
Dietetic	95.9	–	–	–	0.63	–
Pharmaceutical[e]	99.1	–	–	–	0.73	–

[a] The results are averages of four determinations (R.S.D. < 3%) and are expressed as a percentage of the claimed content of α-L,L-aspartame.
[b] In aspartame formulations the D,D- and D,L-isomers were not detected. Also not detected was L,D/D,L in the DKP sample.
[c] The results are expressed as values relative to the α-L,L-aspartame content.
[d] Dashes indicate not detected.
[e] Other ingredient: mannitol.

with a chiral eluent containing Ni(MPA) chelate for the determination of the potential presence of aspartame isomers or synthesis impurities (see Fig. 5B). These compounds were identified on the basis of their peak retention times and peak-height ratios at 210, 215 and 230 nm. The results in Table 3 indicate that all the commercial solid samples of aspartame (stored for 1 year at ambient temperature and humidity) analysed contained DKP in the form of an L,L/D,D-isomer mixture (eluted as a single peak) as a minor contaminant. In one sample of commercial aspartame the presence of traces of α-L,D-aspartame, which is non-active to human sweet taste receptors, was determined but this can probably be attributed in part to initiation of racemization processes of α-L,L-aspartame [23] owing to the low dielectric constant ($\varepsilon = 42.7$) of the applied extraction solution (see Experimental).

4. Conclusions

The RP-HPLC method with a chiral mobile phase containing a helically distorted Ni(MPA) chelate allows the selective determination of non-derivatized diastereomers and enantiomers of most common dipeptide-type sweeteners, permitting the effective monitoring of their un-desirable racemization processes in special kinds of dietary formulations.

5. References

[1] S. Salminen and A. Hallikainen, in A.L. Branen, P.M. Davidson and S. Salminen (Editors), *Food Additives* (*Food Science and Technology Series*, Vol. 35), Marcel Dekker, New York, 1990, p. 297.
[2] D.B. Ott, C.L. Edwards and S.J. Palmer, *J. Food Sci.*, 56 (1991) 535.
[3] W. Worthy, *Chem. Eng. News*, 68 (1990) 25.
[4] S. Motellier and I.W. Wainer, *J. Chromatogr.*, 516 (1990) 365.
[5] J. Lawrence and J.R. Iyengar, *J. Chromatogr.*, 404 (1987) 261.
[6] W.E. Lipton, Y.N. Li, M.K. Younoszi and L.D. Stegnik, *Metabolism*, 40 (1991) 1337.
[7] E.G. Burton, G.L. Schoenhard, J.A. Hill, R.E. Schmidt, J.D. Hribar, F.N. Kotsonis and J.A. Oppermann, *J. Nutr.*, 119 (1989) 713.
[8] S.M. Gaines and J.L. Bada, *J. Chromatogr.*, 389 (1987) 219.
[9] P. Jadaud and I.W. Wainer, *Chirality*, 2 (1990) 32.
[10] S.L. Lin, S.T. Chen, S.H. Wu and K.T. Wang, *J. Chromatogr.*, 540 (1991) 392.
[11] N.H.C. Cooke, R.L. Viavattene, R. Eksteen, W.S. Wong, G. Davies and B.L. Karger, *J. Chromatogr.*, 149 (1978) 391.
[12] W. Lindner, J.N. LePage, G. Davies, D.E. Seitz and B.L. Karger, *J. Chromatogr.*, 185 (1979) 323.
[13] M. Bukowska-Strzyzewska, M. Maniukiewicz and G. Bazylak, *J. Crystallogr. Spectrosc. Res.*, 21 (1991) 157.

[14] G. Bazylak, *Pol. J. Chem.*, 66 (1992) 639.
[15] G. Bazylak, *Analyst*, 117 (1992) 1429.
[16] G. Bazylak, *Analusis*, 20 (1992) 611.
[17] G. Bazylak, *Ann. Acad. Med. Lodz*, 32 (1992) 25.
[18] E.G. Jager, B. Kirchhof, E. Schmidt, B. Remde, A. Kipke and R. Muller, *Z. Anorg. Alg. Chem.*, 485 (1982) 141.
[19] B. Jezowska-Trzebiatowska, G. Formicka-Kozlowska and H. Kozlowski, *Chem. Phys. Lett.*, 42 (1976) 242.
[20] C. Dalgliesh, *J. Chem. Soc.*, 137 (1952) 3940.
[21] L.N. Bell and T.P. Labuza, in H. Levine and L. Slade (Editor), *Water Relationships in Food*, Plenum Press, New York, 1991, p. 337.
[22] C.H. Lochmuller and H.H. Hangac, *J. Chromatogr. Sci.*, 20 (1982) 171.
[23] S. Sanyude, R.A. Locock and L.A. Pagliaro, *J. Pharm. Sci.*, 80 (1991) 674.

Author Index

PUBLICATION SCHEDULE FOR THE 1994 SUBSCRIPTION

Journal of Chromatography A and *Journal of Chromatography B: Biomedical Applications*

MONTH	O 1993	N 1993	D 1993	J	F	M	A	
Journal of Chromatography A	652/1 652/2 653/1	653/2 654/1 654/2 655/1	655/2 656/1 + 2 657/1 657/2	658/1 658/2 659/1 659/2	660/1 + 2 661/1 + 2 662/1 662/2	663/1 663/2 664/1	664/2 665/1 665/2 666/1 + 2 667/1 + 2	The publication schedule for further issues will be published later.
Bibliography Section						681/1		
Journal of Chromatography B: Biomedical Applications				652/1	652/2 653/1	653/2 654/1	654/2 655/1	

INFORMATION FOR AUTHORS

(Detailed *Instructions to Authors* were published in *J. Chromatogr. A*, Vol. 657, pp. 463–469. A free reprint can be obtained by application to the publisher, Elsevier Science B.V., P.O. Box 330, 1000 AH Amsterdam, Netherlands.)

Types of Contributions. The following types of papers are published: Regular research papers (full-length papers), Review articles, Short Communications and Discussions. Short Communications are usually descriptions of short investigations, or they can report minor technical improvements of previously published procedures; they reflect the same quality of research as full-length papers, but should preferably not exceed five printed pages. Discussions (one or two pages) should explain, amplify, correct or otherwise comment substantively upon an article recently published in the journal. For Review articles, see inside front cover under Submission of Papers.

Submission. Every paper must be accompanied by a letter from the senior author, stating that he/she is submitting the paper for publication in the *Journal of Chromatography A* or *B*.

Manuscripts. Manuscripts should be typed in **double spacing** on consecutively numbered pages of uniform size. The manuscript should be preceded by a sheet of manuscript paper carrying the title of the paper and the name and full postal address of the person to whom the proofs are to be sent. As a rule, papers should be divided into sections, headed by a caption (*e.g.*, Abstract, Introduction, Experimental, Results, Discussion, etc.) All illustrations, photographs, tables, etc., should be on separate sheets.

Abstract. All articles should have an abstract of 50–100 words which clearly and briefly indicates what is new, different and significant. No references should be given.

Introduction. Every paper must have a concise introduction mentioning what has been done before on the topic described, and stating clearly what is new in the paper now submitted.

Experimental conditions should preferably be given on a *separate* sheet, headed "Conditions". These conditions will, if appropriate, be printed in a block, directly following the heading "Experimental".

Illustrations. The figures should be submitted in a form suitable for reproduction, drawn in Indian ink on drawing or tracing paper. Each illustration should have a caption, all the *captions* being typed (with double spacing) together on a *separate sheet*. If structures are given in the text, the original drawings should be provided. Coloured illustrations are reproduced at the author's expense, the cost being determined by the number of pages and by the number of colours needed. The written permission of the author and publisher must be obtained for the use of any figure already published. Its source must be indicated in the legend.

References. References should be numbered in the order in which they are cited in the text, and listed in numerical sequence on a separate sheet at the end of the article. Please check a recent issue for the layout of the reference list. Abbreviations for the titles of journals should follow the system used by *Chemical Abstracts*. Articles not yet published should be given as "in press" (journal should be specified), "submitted for publication" (journal should be specified), "in preparation" or "personal communication".

Vols. 1–651 of the *Journal of Chromatography*; *Journal of Chromatography, Biomedical Applications* and *Journal of Chromatography, Symposium Volumes* should be cited as *J. Chromatogr.* From Vol. 652 on, *Journal of Chromatography A* (incl. Symposium Volumes) should be cited as *J. Chromatogr. A* and *Journal of Chromatography B: Biomedical Applications* as *J. Chromatogr. B.*

Dispatch. Before sending the manuscript to the Editor please check that the envelope contains four copies of the paper complete with references, captions and figures. One of the sets of figures must be the originals suitable for direct reproduction. Please also ensure that permission to publish has been obtained from your institute.

Proofs. One set of proofs will be sent to the author to be carefully checked for printer's errors. Corrections must be restricted to instances in which the proof is at variance with the manuscript.

Reprints. Fifty reprints will be supplied free of charge. Additional reprints can be ordered by the authors. An order form containing price quotations will be sent to the authors together with the proofs of their article.

Advertisements. The Editors of the journal accept no responsibility for the contents of the advertisements. Advertisement rates are available on request. Advertising orders and enquiries can be sent to the Advertising Manager, Elsevier Science B.V., Advertising Department, P.O. Box 211, 1000 AE Amsterdam, Netherlands; courier shipments to: Van de Sande Bakhuyzenstraat 4, 1061 AG Amsterdam, Netherlands; Tel. (+31-20) 515 3220/515 3222, Telefax (+31-20) 6833 041, Telex 16479 els vi nl. *UK*: T.G. Scott & Son Ltd., Tim Blake, Portland House, 21 Narborough Road, Cosby, Leics. LE9 5TA, UK; Tel. (+44-533) 753 333, Telefax (+44-533) 750 522. *USA and Canada*: Weston Media Associates, Daniel S. Lipner, P.O. Box 1110, Greens Farms, CT 06436-1110, USA; Tel. (+1-203) 261 2500, Telefax (+1-203) 261 0101.

Chiral HPLC Column

Application Guide for Chiral HPLC Column Selection

SECOND EDITION!

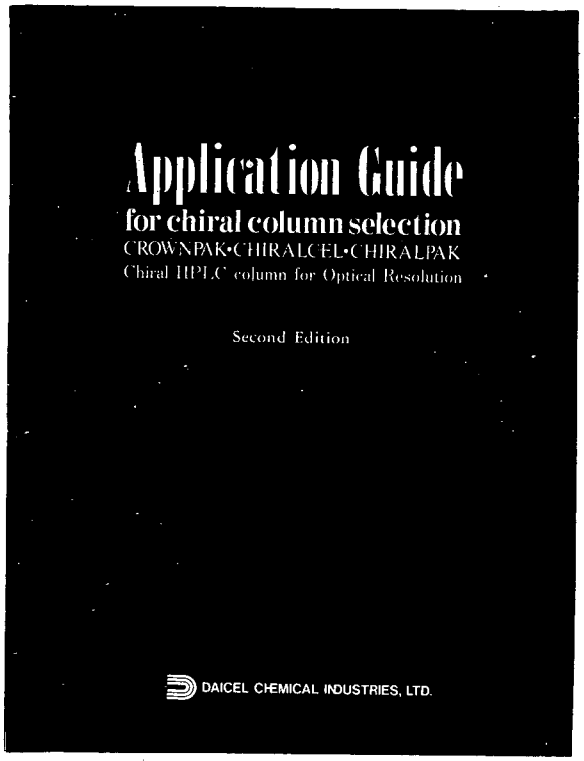

GREEN BOOK

The 112-page green book contains chromatographic resolutions of over 350 chiral separations, cross-indexed by chemical compound class, structure, and the type of chiral column respectively. This book also lists chromatographic data together with analytical conditions and structural information. A quick reference guide for column selection from a wide range of DAICEL chiral HPLC columns is included.

To request this book, please let us know by fax or mail.

DAICEL CHEMICAL INDUSTRIES, LTD.

AMERICA

CHIRAL TECHNOLOGIES, INC.

730 Springdale Drive, P.O. Box 564, Exton, PA 19341
Phone: +1-215-594-2100
Facsimile: +1-215-594-2325

EUROPE

DAICEL (EUROPA) GmbH

Oststr. 22
D-40211 Düsseldorf, Germany
Phone: +49-211-369848
Facsimile: +49-211-364429

ASIA/OCEANIA

DAICEL CHEMICAL INDUSTRIES, LTD.
CHIRAL CHEMICALS NDD
8-1, Kasumigaseki 3-chome,
Chiyoda-ku, Tokyo 100, JAPAN
Phone: +81-3-3507-3151
Facsimile: +81-3-3507-3193